EXPLORATION OF FIVE MEMBERED CYCLIC SULFAMIDATE IMINES AS NUCLEOPHILES IN VARIOUS ORGANIC TRANSFORMATIONS

Ph.D. Thesis

By

DEBASHIS MAJEE

DISCIPLINE OF CHEMISTRY

INDIAN INSTITUTE OF TECHNOLOGY INDORE

JULY 2017

EXPLORATION OF FIVE MEMBERED CYCLIC SULFAMIDATE IMINES AS NUCLEOPHILES IN VARIOUS ORGANIC TRANSFORMATIONS

A THESIS

Submitted in partial fulfillment of the

requirements for the award of the degree

of

DOCTOR OF PHILOSOPHY

by

DEBASHIS MAJEE



DISCIPLINE OF CHEMISTRY

INDIAN INSTITUTE OF TECHNOLOGY INDORE

JULY 2017

INDIAN INSTITUTE OF TECHNOLOGY INDORE

CANDIDATE'S DECLARATION

I hereby certify that the work which is being presented in the thesis entitled "**EXPLORATION OF FIVE MEMBERED CYCLIC SULFAMIDATE IMINES AS NUCLEOPHILES IN VARIOUS ORGANIC TRANSFORMATIONS"** in the partial fulfillment of the requirements for the award of the degree of **DOCTOR OF PHILOSOPHY** and submitted in the **DISCIPLINE OF CHEMISTRY, INDIAN INSTITUTE OF TECHNOLOGY INDORE**, is an authentic record of my own work carried out during the time period from JANUARY 2012 to JULY 2017 under the supervision of **Dr. SAMPAK SAMANTA**, Associate Professor, Discipline of Chemistry, Indian Institute of Technology Indore.

The matter presented in this thesis has not been submitted by me for the award of any other degree of this or any other institute.

Signature of the student with date

(DEBASHIS MAJEE)

This is to certify that the above statement made by the candidate is correct to the best of my/our knowledge.

Signature of thesis supervisor with date

Dr. SAMPAK SAMANTA

Mr. DEBASHIS MAJEE has successfully given his/her Ph.D. Oral Examination held on **19th June 2017.**

Signature(s) of Thesis Supervisor(s) Convener, DPGC

Date: Date:

Signature of PSPC Member #1 Signature of PSPC Member #2 Signature of External

Date: Date: Date:

Signature of the Chairperson (OEB) Signature of Head of Discipline

ACKNOWLEDGEMENT

“Interdependence is a higher value than independence.”

This work done for my Ph.D. thesis is not my sole contribution but is a synergistic product of efforts of numerous people. Here, I wish to take the opportunity to acknowledge them and extend my sincere gratitude for helping me and making this Ph.D. thesis possible.

It is a great pleasure for me to express my deepest sense of gratitude and respect to *Dr. Sampak Samanta,* Associate professor, Discipline of Chemistry, IIT Indore for associating me in his excellent group of Synthetic Organic Chemistry. His constant guidance, encouragement and help throughout the whole course of the thesis work are inexpressible. Being embowered always by his graceful behavior, I feel proud that I have enjoyed the full freedom while carrying out my research work with him.

Besides my advisor, I am thankful to my PSPC members *Dr. Tridib Kumar Sarma* and *Dr. Antony Vijesh* for their valuable and helpful suggestion and encouragement.

I would like to express my sincere thanks to *Prof. Pradeep Mathur*, the Director, IIT Indore for his continuous support in every aspect and providing excellent infrastructure and facilities at our institute.

My sincere thanks also goes to *Dr. Satya S. Bulusu*, Head, Discipline of Chemistry and other faculty members of Discipline of Chemistry which include *Dr. Suman Mukhopadhyay, Dr. Rajneesh Misra, Dr. Apurba K. Das, Dr. Anjan Chakraborty, Dr. Tushar Kanti Mukherjee, Dr. Shaikh M. Mobin, Dr. Biswarup Pathak, Dr. Chelvam Venkatesh, Dr. Sanjay Kumar Singh* and *Dr. Amarendra Singh* for creating a healthy environment in the department.

I would like to extend my deepest gratitude to all my teachers *Dr. Alakananda Hazra, Dr. Bidhan Ch. Bag, Dr. Pranab Sarkar, Dr. Asim Kr. Das,* and *Dr. Gautam Bramhachari* who have taught me during my school and college. Without their blessings, advice and support, I would have never been able to come so far.

I personally extend my heartfelt thanks to *Dr. Anvita Srivastava* for her constant help and support in lab work. I convey my deep regards to my dear group members *Dr. Shivendra Singh Mr. Soumen Biswas, Ms. Anuradha Dagar, Ms. Anubha Yadav, Mr. Soumitra Guin, Ms. Monika Ahuja, Mr. Abhik Paul, Mr. Raman Gupta, Ms. Isha Yadav, Dr. Sanjeeva Kumar Arupula, Dr. Santosh Kumar Gudimella, Dr. Subhendu Chakarbarty* and *Dr. Pradeep Kr. Jaiswal* for their selfless co-operation and help in my lab work. Their presence built the positive vibes to work efficiently in the lab.

It has been a wonderful experience to work with many friends during my Ph.D. who really helped me in many aspects. I would like to record my thanks to *Dr. Rajendra Nasani, Dr. Bhausaheb Kashinath Dhokale, Dr. Raina Thakur, Dr. Dnyaneshwar Rasale* and other fellowmates *Dr. Bhagwati Sharma, Dr. Tamalika Bhattacharya, Dr. Indrajit Maity, Dr. Prabhat Gautam, Dr. Veenu Mishra, Dr. Thaksen Jadhav, Dr. Maruti Konda, Dr. Surajit Chatterjee, Mr. Sagnik Sengupta, Mr. Sagar Biswas, Mr. Anoop Kumar Saini, Md. Akbar, Mr. Ajeet Singh, Ms. Navpreet Kaur, Mr. Arup Mahata, Mr. Anurag, Mr. Sourabh Kumar, Dr. Rohit Rai, Dr. Deepika Tyagi, Mr. Arpan Bhattacharya, Ms. Roopali Prajapati, Dr. Mriganka Das, Dr. Chandan Adhikari, Ms. Nishu Kanwa, Ms. Daisy Sarma, Mr. Kuber Singh Rawat, Mr. Siddharth Jain, Mr. Sayan Miati, Ms. Madhurima Poddar, Ms. Neha Thakur, Ms. Anupama Ekbote* for their generosity, kind support and for providing cooperative environment throughout my Ph.D. work.

I express my heartiest gratitude to my fantastic roommates, *Dr. Anupam Das, Mr. Biju Majumdar* and *Mr. Soumen Biswas, Mr. Soumya Kanti De, Mr. Mirajuddin Ahamed* who have been with me and encouraged during ups and downs of my professional and personal life.

A special thanks to my dear friend *Dr. Sonam Mandani*, who is my Indore city guide. I would also like to express gratitude to my friends *Dr. Partha Goswami, Dr. Satyapriya Bhandari, Dr. Deb Kr. Das* and *Dr. Mrigendra Dubey* who taught me how to cope with the Ph.D. life.

The PhD work could have never been complete without the support of non-teaching staff members. I want to express special thanks to *Mr. Kinny Pandey* and others staff members, *Ms. Sarita Batra, Mr. Ghanshyam Bhavsar, Dr. Ravinder Kumar, Mr. Manish Kushwaha* and *Ms. Vinita Kothari* for their help. I would also like to thank *Ms. Anjali Bandiwadekar, Mr. Gati Krishna Nayak, Mr. Rajesh Kumar, Mr. Lala Ram Ahiwar* and other library staff and *Mr. Prahlad Singh Panwar, Mr. Manoj Pal, Mr. Nitin Bhate* and other technical and non-technical staff for their unswerving help whenever required. Without them, life at IIT Indore would not be so simple.

I owe gratitude to *Mr. Sandeep Maheswari*, a great entrepreneur and motivational speaker for giving me unstoppable motivation and positive energy.

A special thanks to my beloved brother *DICO* who's motivated and pure soul is always with me as an encouragement for lifetime.

I am really lucky to have a wonderful family besides me all the time. I am very much thankful to my grandmother *Mrs. Dasibala Majee* and *Mrs. Junubala Layek*, grandfather Late *Mr. Ankur Ch. Majee* and *Mr. Hiralal Layek*, my parents, *Mrs. Chapa Majee* and *Mr. Paresnath Majee*, my aunties *Mrs. Shyamali Baishnab, Mrs. Shyamali Majee*, *Mrs. Pratima Majee* and *Mrs. Kabita Majee*, my uncles *Mr. Dinanath Majee, Dr. Sanatan Majee, Dr. Adinath Majee, Mr. Lokesh Majee* and *Mr. Dipak Kr. Majee*, my sisters *Mrs. Mousumi Mandal, Ms. Suknya Majee* and *Ms. Sudeshna Majee*, my brothers *Dr. Balaji P. Mandal, Mr. Subhashis Majee, Mr. Anirban Majee, Mr. Sayantan Majee, Mr. Snehasish Majee* and little master *Shreyam*. Last but not the least I would like to express my heartfelt love and regards to *Ms. Prativa Majee* for her care and affection. Without the unconditional support, care and love of all of them, it would have been impossible for me to reach here.

I would like to express my thanks to CSIR-HRDG, New Delhi for my JRF as well as SRF fellowship which fortified me to perform my work comfortably.

Debashis Majee
IIT Indore

Dedicated to my dear brother

DICO

TABLE OF CONTENTS

ABSTRACT **XIX-XX**

LIST OF PUBLICATIONS **XXI-XXII**

LIST OF ABBREVIATIONS **XXIII-XXVI**

LIST OF FIGURES **XXVII-XL**

LIST OF SCHEMES **XLI-XLV**

LIST OF TABLES **XLVI**

Chapter 1 1-24

1.1	General Introduction	1
1.2	Background	2
1.3	Synthesis	2-4
1.4	Properties	5-14
1.4.1	Asymmetric hydrogenation of C=N bond	5-8
1.4.2	Enantioselective alkylation or arylation	8-12
1.4.3	Aziridination	13-14
1.5	Synthetic application of cyclic sulfamidates through nucleophilic ring-opening reaction	14-19
1.6	Conclusion	19
1.7	References	20-24

Chapter 2 25-108

L-Proline catalyzed highly efficient synthesis of *Z*-5-alkylidene cyclic sulfamidate imines: an easy access to 5-alkyl-substituted cyclic sulfamidate imines

2.1	Introduction	25
2.2	Review of literature	25-27
2.2.1	Conclusion	27
2.3	Present work	28-40
2.3.1	Result and discussions	29-40
2.3.1.1	Screening of solvents and bases	29-32
2.3.1.2	Plausible mechanism	32
2.3.1.3	Generality and substrate scope	32-36
2.3.1.4	Synthesis of 2-hydroxy pyrrolidine derivative	37-40
2.4	Conclusion	40
2.5	Experimental section	41-60
2.5.1	General information	41
2.5.2	Materials	41
2.6	Copies of ^{1}H and ^{13}C NMR spectra of reported compounds	61-103
2.7	References	104-107

Chapter 3 109-178

Stereoselective synthesis of functionalized spiro-sulfamidate imine fused δ-lactone scaffold via a one-pot sequential three-component reaction.

3.1	Introduction	109
3.2	Review of literature	110-112
3.2.1	Conclusion	112-113
3.3	Present work	113-123
3.3.1	Result and discussions	114-123
3.3.1.1	Screening of solvents and bases	114-117
3.3.1.2	Plausible mechanism	117-118
3.3.1.3	Generality and substrate scope	118-120
3.3.1.4	Enantioselective synthesis of spirosulfamidate imine fused δ-lactone moiety	121
3.3.1.5	Synthesis of *trans-cis*-β-amino-α-azido derivative	121-122
3.4	Conclusion	123
3.5	Experimental section	123-138
3.5.1	General information	123-124
3.5.2	Materials	124
3.6	Copies of ^{1}H and ^{13}C NMR spectra of reported compounds	139-171
3.7	References	171-178

Chapter 4 179-254

Unprecedented synthesis of 4,6-diarylpicolinates *via* a domino reaction of cyclic sulfamidate imines with Morita-Baylis-Hillman acetates of nitroolefins /nitrodienes

4.1 Introduction 179

4.2 Review of literature 180-184

4.2.1 Conclusion 184

4.3 Present work 185-193

4.3.1 Result and discussions 186-193

4.3.1.1 Screening of solvents and bases 186-187

4.3.1.2 Plausible mechanism 188

4.3.1.3 Generality and substrate scope 188-192

4.3.1.4 Synthesis of 2-(2-(4-chlorophenyl)-5,7-diphenylimidazo [1,2-*a*]pyridine-3-yl)-*N*,*N*-dipropylacetamide 192-193

4.4 Conclusion 193

4.5 Experimental section 194-213

4.5.1 General information 194

4.5.2 Materials 194

4.6 Copies of ^{1}H and ^{13}C NMR spectra of reported compounds 214-248

4.7 References 249-254

Chapter 5 255-362

DABCO promoted domino reaction of cyclic sulfamidate imines with Morita-Baylis-Hillman acetates: a metal-free approach to functionalized nicotinic acid derivatives.

5.1	Introduction	255
5.2	Review of literature	256-263
5.2.1	Conclusion	263
5.3	Present work	264-274
5.3.1	Results and discussion	265-274
5.3.1.1	Screening of solvents and bases	265-266
5.3.1.2	Plausible mechanism	267
5.3.1.3	Generality and substrate scope	267-273
5.3.1.4	Synthesis of triazolopyridine derivative	274
5.4	Conclusion	274
5.5	Experimental section	275-303
5.5.1	General information	275
5.6	Copies of ^{1}H and ^{13}C NMR spectra of reported compounds	304-353
5.7	References	354- 361

Chapter 6 363-454

One-pot sequential reaction of cyclic sulfamidate imine with β-substituted acroleins to access 2,4-disubstituted pyridine by a metal-free new approach

6.1	Introduction	363
6.2	Review of literature	364-371
6.2.1	Conclusion	371
6.3	Present work	372-381
6.3.1	Result and discussions	373-381
6.3.1.1	Screening of solvents and bases	373-376
6.3.1.2	Plausible mechanism	376
6.3.1.3	Generality and substrate scope	376-380
6.3.1.4	Synthesis of 2-arylisonicotinic acid derivatives	380-381
6.4	Conclusion	381
6.5	Experimental section	382-399
6.5.1	General information	382
6.5.2	Materials	382
6.6	Copies of ^{1}H and ^{13}C NMR spectra of reported compounds	400-447
6.7	References	448-453

Chapter 7

7.1 Conclusion and future outlook 455

ABSTRACT

This thesis presents for the first time use of five membered cyclic sulfamidate imines as powerful nucleophiles. 5-alkylidene/alkyl-substituted cyclic sulfamidate imines/aza-heterocyclic scaffolds have been prepared by utilizing this unique reactivity of five membered cyclic sulfamidate imines in an efficient, cost-effective and eco-friendly manner.

To begin with a general introduction of the synthetic application of five membered cyclic sulfamidate imines which exclusively focused on the nucleophilic addition or hydrogenation to the azomethine functionality of the titled compounds.

The next chapter illustrates a very simple, mild and robust method for the synthesis of exclusively *Z*-trisubstituted 5-alkylidene cyclic sulfamidate imines in good to excellent yields *via* a condensation reaction of 4-aryl-5*H*-1,2,3-oxathiazole-2,2-dioxides with several aryl/alkyl-substituted aldehydes using 10 mol% of L-proline as a cheap, nontoxic and naturally available organocatalyst in DMF at room temperature. In addition, the syntheses of 5-alkyl substituted cyclic sulfamidate imines, *trans*-β-amino-α-azido/triazole and 2-hydroxy-4-triazole-5-phenylpyrrolidine derivatives have been achieved from corresponding 5-alkylidene cyclic sulfamidate imines through our developed method.

The third chapter describes a stereoselective synthesis of functionalized spiro-sulfamidate imine fused δ-lactone scaffold *via* a one-pot three-component sequential reaction between 4-aryl-5*H*-1,2,3-oxathiazole-2,2-dioxides, *trans*-β-aryl/alkyl-substituted acroleins and paraformaldehyde in CH_2Cl_2 at room temperature in the presence of commercially available L-proline and DBU as the organocatalysts. Moreover, highly enantioselective synthesis of the above title compounds were achieved by using (*S*)-(-)-α,α-diphenyl-2-pyrrolidinemethanol trimethylsilyl ether as a catalyst instead of L-proline. Furthermore, the obtained Michael adduct was converted into the synthetically valuable intermediate β-amino-α-azido derivative through some efficient steps.

Chapter four demonstrates an unprecedented synthesis of pharmacologically interesting 4,6-diarylpicolinates in high to excellent yields *via* a domino reaction of cyclic sulfamidate imines with Morita-Baylis-Hillman acetates of nitroolefins/nitrodienes in the presence of DABCO as an organic base at 55 °C. Furthermore, the biologically interesting imidazo[1,2-*a*]pyridine (alpidem derivative) has been prepared in high chemical yield through a unique procedure.

In chapter five, a facile, green, metal-free new one-pot synthetic strategy has been developed for the easy access to a wide array of functionalized pyridines having an ester, a nitrile or an acetyl group at the C-3 position in good to excellent yields *via* a domino S_N2/elimination/6π-aza-electrocyclization/aromatization reaction of several 4-aryl/hetero-aryl-substituted 5-membered cyclic sulfamidate imines with a broad range of MBH acetates of acrylate/acrylonitrile/MVK in 2-MeTHF promoted by DABCO as an organobase under an O_2 atmosphere. Finally, a potential PDE10A inhibitor14 triazolopyridine derivative was prepared in 81% yield from 4,6-diphenyl nicotinonitrile using some reported method.

This sixth chapter unfolds a novel L-proline catalyzed Michael reaction between 4-aryl/ heteroaryl-substituted cyclic sulfamidate imines and a range of β-styryl/aryl-substituted acroleins at room temperature, where resultant Michael adducts subsequently undergo in situ elimination/ cyclization/aromatization under the influence of DABCO as an organobase to generate an important class of 2-aryl-4-(*E*)-styrylpyridines/2,4-diarylpyridines in good to high yields. Interestingly, commercially available 2-arylisonicotinic acids as useful intermediates for the synthesis of highly active CypA inhibitors were prepared by the oxidation of alkene double bonds 2-aryl-4-styrylpyridines using $KMnO_4$ as a strong oxidizing agent.
The final chapter of the thesis focuses on the future prospect of the developments as reported in this thesis, many effective methods can be designed for the development of various heterocyclic scaffolds involving cyclic sulfamidate imines as powerful nucleophiles taking several readily available starting materials.

LIST OF PUBLICATIONS

1. Majee D., Srivastava A., Mobin S. M., Samanta S. (2013), L-proline catalyzed highly efficient synthesis of *Z*-5-alkylidene cyclic sulfamidate imines: an easy access to 5-alkyl-substituted cyclic sulfamidate imines, *RSC Adv.*, *3*, 11502-11506 (**DOI**:10.1039/C3RA40299A)
2. Majee D., Biswas S., Mobin S. M., Samanta S. (2014), An expedient one-pot sequential three-component reaction for the stereoselective synthesis of functionalized spiro-sulfamidate imine fused δ-lactone scaffold, *Tetrahedron Lett.*, *55*, 4553-4558 (**DOI**: 10.1016/j.tetlet.2014.06.088)
3. Majee D., Biswas S., Mobin S. M., Samanta S. (2016), Access to 4,6-diarylpicolinates via a domino reaction of cyclic sulfamidate imines with Morita-Baylis-Hillman acetates of nitroolefins/nitrodienes, *J. Org. Chem.*, 81, 4378-4385 (**DOI:** 10.1021/acs.joc.6b00472)
4. Majee D., Biswas S., Mobin S. M., Samanta S. (2017), Domino reaction of cyclic sulfamidate imines with Morita-Baylis-Hillman acetates promoted by DABCO: a metal-free approach to functionalized nicotinic acid derivatives, *Org. Biomol. Chem.*, *15*, 3286-3297 (**DOI**: 10.1039/C7OB00240H)
5. Majee D., Guin S., Biswas S., Samanta S. (2017) A metal-free based new approach to 2,4-disubstitutedpyridines via one-pot sequential Reaction of Cyclic Sulfamidate Imines with β-Substituted Acroliens, *ChemSelect*, *2*, 3423-3427 (**DOI**: 10.1002/slct.201700733)
6. Biswas S., Majee D., Mobin S. M., Samanta S. (2014), Metal-free one-pot protocol for the preparation of unexpected carbazole derivative in water: easy access to pyrimidocarbazole and pyridocarbazolone derivatives, *Synlett*, *25*, 2115-2120 (**DOI**: 10.1055/s-0034-1378446)
7. Biswas S., Majee D., Guin S., Samanta S. (2017), A metal-and solvent-free approach to diversely substituted picolinates via domino reaction of cyclic sulfamidate imines with β,γ-unsaturated α-ketocarbonyls, *J. Org. Chem.*, 82, 10928-10938 (**DOI**: 10.1021/acs.joc.7b01792)

CONFERENCES

1. Poster presentation at the "XII J-NOST Conference for Research Scholars" held at CSIR-Central Drug Research Institute, Lucknow, during 24^{th}-27^{th} Nov, 2016.
2. Participated in "Frontier lecture series in Chemistry (FLSC-2014)" held at Indian Institute of Technology Indore, India, 30^{th}-31^{st} January, 2014.
3. Participated in "Frontiers in Inorganic Chemistry and Organometallics" organized by Discipline of Chemistry, IIT Indore, Indore, 14^{th}-15^{th} April, 2016.
4. Participated in "Laboratory Health and Safety Workshop" organized by Royal Society of Chemistry at IIT Indore, Indore, November 4, 2014.

LIST OF ABBREVIATIONS

Acetone-d_6	Deuterated acetone
Ag_2CO_3	Silver carbonate
AIBN	Azobisisobutyronitrile
$ArB(OH)_2$	Arylboronic acid
AcOH	Acetic acid
$AlCl_3$	Aluminium chloride
ACCN	1,1′-Azobis(cyclohexanecarbonitrile)
$AuCl_3$	Gold (III) chloride
$BnEt_3N^+Cl^-$	Benzyltriethylammonium chloride (BTEAC)
Bn	Benzyl
Bz	Benzoyl
Boc	*t*-Butyloxycarbonyl
$B(C_6F_5)_3$	Tris(pentafluorophenyl)borane
Cbz	Carboxybenzyl
CH_2Cl_2	Dichloromethane
$CHCl_3$	Chloroform
CH_3CN	Acetonitrile
CH_3NO_2	Nitromethane
$Cu(OTf)_2$	Copper (II) trifluoromethanesulfonate
CBr_4	Carbon tetrabromide
$CeCl_3$	Cerium (III) chloride
Cs_2CO_3	Caesium carbonate
$CDCl_3$	Deuterated chloroform
COE	Cyclooctene

$Cu(OAc)_2$	Copper (II) acetate
CuI	Copper (I) iodide
DABCO	1,4-diazabicyclo[2.2.2]octane
DBU	1,8-Diazabicycloundec-7-ene
DCE	Dichloroethane
DMAP	4-Dimethylaminopyridine
DMSO-d_6	Deuterated dimethyl sulfoxide
DMF	Dimethylformamide
dr	Diastereomeric ratio
ee	Enantiomeric excess
EDDA	Ethylenediaminediacetate
ESI-MS	Electrospray ionization mass spectrometry
Et_3N	Triethylamine
Et_2O	Diethyl ether
EtOH	Ethanol
FC	Friedel-Crafts
GABA	γ-Aminobutyric acid
$Gd(OTf)_3$	Gadolinium (III) trifluoromethanesulfonate
HFIP	Hexafluoroisopropanol
Hünig's base	N,N-diisopropylethylamine
IBX	Iodoxybenzoic acid
$InCl_3$	Indium trichloride
*i*PrOH	Isopropyl alcohol
KCN	Potassium cyanide
K_2CO_3	Potassium carbonate

LDA	Lithium diisopropylamide
$LiAlH_4$	Lithium aluminium hydride
LiOAc	Lithium acetate
LiOH	Lithium hydroxide
MCR	Multicomponent reaction
MeOH	Methanol
$MgSO_4$	Magnesium sulfate
MsCl	Methanesulfonyl chloride
MW	Microwave
NaSH	Sodium hydrosulfide
$NaBH_4$	Sodium borohydride
$NiCl_2$	Nickel (II) chloride
NH_4HCO_2	Ammonium formate
NBS	N-Bromosuccinimide
NaN_3	Sodium azide
NaHMDS	Sodium bis(trimethylsilyl)amide
$n Bu_3SnH$	Tributyltin hydride
$PhCO_2H$	Benzoic acid
$Pd(PPh_3)_4$	Tetrakis(triphenylphosphine)palladium (0)
$Pd(OAc)_2$	Palladium (II) acetate
$PdCl_2(PPh_3)_2$	Bis(triphenylphosphine)palladium(II)dichloride
PPh_3	Triphenylphosphine
pTSA	*p*-Toluenesulfonic acid
$PhNHNH_2$	Phenylhydrazine
psi	Pounds per square inch

$Pb(OAc)_4$	Lead (IV) acetate
SeO_2	Selenium dioxide
SDS	Sodium dodecyl sulfate
$Sc(OTf)_3$	Scandium (III) trifluoromethanesulfonate
TCA	Trichloroacetic acid
THF	Tetrahydrofuran
TFA	Trifluoroacetic acid
TMS	Trimethylsilyl
TfOH	Trifluoromethanesulfonic acid
TBAB	Tetra-*n*-butylammonium bromide
TOF-MS	Time-of-flight mass spectrometry
$Ti(OEt)_4$	Titanium ethoxide
$Yb(OTf)_3$	Ytterbium (III) trifluoromethanesulfonate
$Zn(OTf)_2$	Zinc (II) trifluoromethanesulfonate

LIST OF FIGURES

Figure 1.1	Common structures of 5-membered cyclic sulfamidate and sulfamidate imine	1
Figure 1.2	Different sulfamidate bioactive compounds	1
Figure 1.3	Reactive profile of 5*H*-1,2,3-oxathiazole-2,2-dioxides	19
Figure 2.1	5-Alkylidine/alkyl substituted cyclic sulfamidate imine	27
Figure 2.2	Molecular structure of compound **3aa**	30
Figure 2.3	Molecular structures of compound **13**	38
Figure 2.4	Molecular structure of compound **15**	39
Figure 2.5	400 MHz ^{1}H NMR spectrum of **3aa** in $CDCl_3$	62
Figure 2.6	100 MHz ^{13}C NMR spectrum of **3aa** in $CDCl_3$	62
Figure 2.7	400 MHz ^{1}H NMR spectrum of **3ab** in $CDCl_3$	63
Figure 2.8	100 MHz ^{13}C NMR spectrum of **3ab** in $CDCl_3$	63
Figure 2.9	400 MHz ^{1}H NMR spectrum of **3ac** in $CDCl_3$	64
Figure 2.10	100 MHz ^{13}C NMR spectrum of **3ac** in $CDCl_3$	64
Figure 2.11	400 MHz ^{1}H NMR spectrum of **3ad** in $CDCl_3$	65
Figure 2.12	100 MHz ^{13}C NMR spectrum of **3ad** in $CDCl_3$	65
Figure 2.13	400 MHz ^{1}H NMR spectrum of **3ae** in $CDCl_3$	66
Figure 2.14	100 MHz ^{13}C NMR spectrum of **3ae** in $CDCl_3$	66
Figure 2.15	400 MHz ^{1}H NMR spectrum of **3af** in $CDCl_3$	67
Figure 2.16	100 MHz ^{13}C NMR spectrum of **3af** in $CDCl_3$	67
Figure 2.17	400 MHz ^{1}H NMR spectrum of **3ag** in $CDCl_3$	68
Figure 2.18	100 MHz ^{13}C NMR spectrum of **3ag** in $CDCl_3$	68
Figure 2.19	400 MHz ^{1}H NMR spectrum of **3ah** in $CDCl_3$	69
Figure 2.20	100 MHz ^{13}C NMR spectrum of **3ah** in $CDCl_3$	69
Figure 2.21	400 MHz ^{1}H NMR spectrum of **3ai** in $CDCl_3$	70
Figure 2.22	100 MHz ^{13}C NMR spectrum of **3ai** in $CDCl_3$	70
Figure 2.23	400 MHz ^{1}H NMR spectrum of **3aj** in $CDCl_3$	71
Figure 2.24	100 MHz ^{13}C NMR spectrum of **3aj** in $CDCl_3$	71
Figure 2.25	400 MHz ^{1}H NMR spectrum of **3ak** in $CDCl_3$	72

Figure 2.26 100 MHz ^{13}C NMR spectrum of **3ak** in $CDCl_3$ 72
Figure 2.27 400 MHz ^{1}H NMR spectrum of **3al** in $CDCl_3$ 73
Figure 2.28 100 MHz ^{13}C NMR spectrum of **3al** in $CDCl_3$ 73
Figure 2.29 400 MHz ^{1}H NMR spectrum of **3am** in $CDCl_3$ 74
Figure 2.30 100 MHz ^{13}C NMR spectrum of **3am** in $CDCl_3$ 74
Figure 2.31 400 MHz ^{1}H NMR spectrum of **3an** in $CDCl_3$ 75
Figure 2.32 100 MHz ^{13}C NMR spectrum of **3an** in $CDCl_3$ 75
Figure 2.33 400 MHz ^{1}H NMR spectrum of **3ao** in $CDCl_3$ 76
Figure 2.34 100 MHz ^{13}C NMR spectrum of **3ao** in $CDCl_3$ 76
Figure 2.35 400 MHz ^{1}H NMR spectrum of **3ap** in $CDCl_3$ 77
Figure 2.36 100 MHz ^{13}C NMR spectrum of **3ap** in $CDCl_3$ 77
Figure 2.37 400 MHz ^{1}H NMR spectrum of **3be** in $CDCl_3$ 78
Figure 2.38 100 MHz ^{13}C NMR spectrum of **3be** in $CDCl_3$ 78
Figure 2.39 400 MHz ^{1}H NMR spectrum of **3bo** in $CDCl_3$ 79
Figure 2.40 100 MHz ^{13}C NMR spectrum of **3bo** in $CDCl_3$ 79
Figure 2.41 400 MHz ^{1}H NMR spectrum of **3ca** in $CDCl_3$ 80
Figure 2.42 100 MHz ^{13}C NMR spectrum of **3ca** in $CDCl_3$ 80
Figure 2.43 400 MHz ^{1}H NMR spectrum of **3cj** in $CDCl_3$ 81
Figure 2.44 100 MHz ^{13}C NMR spectrum of **3cj** in $CDCl_3$ 81
Figure 2.45 400 MHz ^{1}H NMR spectrum of **3da** in $CDCl_3$ 82
Figure 2.46 100 MHz ^{13}C NMR spectrum of **3da** in $CDCl_3$ 82
Figure 2.47 400 MHz ^{1}H NMR spectrum of **3di** in $CDCl_3$ 83
Figure 2.48 100 MHz ^{13}C NMR spectrum of **3di** in $CDCl_3$ 83
Figure 2.49 400 MHz ^{1}H NMR spectrum of **3eb** in $CDCl_3$ 84
Figure 2.50 100 MHz ^{13}C NMR spectrum of **3eb** in $CDCl_3$ 84
Figure 2.51 400 MHz ^{1}H NMR spectrum of **3eo** in $CDCl_3$ 85
Figure 2.52 100 MHz ^{13}C NMR spectrum of **3eo** in $CDCl_3$ 85
Figure 2.53 400 MHz ^{1}H NMR spectrum of **3fs** in $CDCl_3$ 86
Figure 2.54 100 MHz ^{13}C NMR spectrum of **3fs** in $CDCl_3$ 86
Figure 2.55 400 MHz ^{1}H NMR spectrum of **3fn** in $CDCl_3$ 87
Figure 2.56 100 MHz ^{13}C NMR spectrum of **3fn** in $CDCl_3$ 87

Figure 2.57 400 MHz ^{1}H NMR spectrum of **3ga** in $CDCl_3$ 88
Figure 2.58 100 MHz ^{13}C NMR spectrum of **3ga** in $CDCl_3$ 88
Figure 2.59 400 MHz ^{1}H NMR spectrum of **3ha** in $CDCl_3$ 89
Figure 2.60 100 MHz ^{13}C NMR spectrum of **3ha** in $CDCl_3$ 89
Figure 2.61 400 MHz ^{1}H NMR spectrum of **3hb** in DMSO-d6 90
Figure 2.62 100 MHz ^{13}C NMR spectrum of **3hb** in DMSO-d6 90
Figure 2.63 400 MHz ^{1}H NMR spectrum of **4aa** in $CDCl_3$ 91
Figure 2.64 100 MHz ^{13}C NMR spectrum of **4aa** in $CDCl_3$ 91
Figure 2.65 400 MHz ^{1}H NMR spectrum of **4ab** in $CDCl_3$ 92
Figure 2.66 100 MHz ^{13}C NMR spectrum of **4ab** in $CDCl_3$ 92
Figure 2.67 400 MHz ^{1}H NMR spectrum of **8** in $CDCl_3$ 93
Figure 2.68 100 MHz ^{13}C NMR spectrum of **8** in $CDCl_3$ 93
Figure 2.69 400 MHz ^{1}H NMR spectrum of **9** in $CDCl_3$ 94
Figure 2.70 100 MHz ^{13}C NMR spectrum of **9** in $CDCl_3$ 94
Figure 2.71 400 MHz ^{1}H NMR spectrum of **10** in $CDCl_3$ 95
Figure 2.72 100 MHz ^{13}C NMR spectrum of **10** in $CDCl_3$ 95
Figure 2.73 400 MHz ^{1}H NMR spectrum of **11** in $CDCl_3$ 96
Figure 2.74 100 MHz ^{13}C NMR spectrum of **11** in $CDCl_3$ 96
Figure 2.75 400 MHz ^{1}H NMR spectrum of **12** in $CDCl_3$ 97
Figure 2.76 100 MHz ^{13}C NMR spectrum of **12** in $CDCl_3$ 97
Figure 2.77 400 MHz ^{1}H NMR spectrum of **13** in $CDCl_3$ 98
Figure 2.78 100 MHz ^{13}C NMR spectrum of **13** in $CDCl_3$ 98
Figure 2.79 400 MHz ^{1}H NMR spectrum of **14** in $CDCl_3$ 99
Figure 2.80 100 MHz ^{13}C NMR spectrum of **14** in $CDCl_3$ 99
Figure 2.81 400 MHz ^{1}H NMR spectrum of **15** in $CDCl_3$ 100
Figure 2.82 100 MHz ^{13}C NMR spectrum of **15** in $CDCl_3$ 100
Figure 2.83 400 MHz ^{1}H NMR spectrum of **16** in $CDCl_3$ 101
Figure 2.84 100 MHz ^{13}H NMR spectrum of **16** in $CDCl_3$ 101
Figure 2.85 400 MHz ^{1}H NMR spectrum of **17** in $CDCl_3$ 102
Figure 2.86 100 MHz ^{13}C NMR spectrum of **17** in $CDCl_3$ 102
Figure 2.87 400 MHz ^{1}H NMR spectrum of **18** in $CDCl_3$ 103

Figure 2.88	100 MHz ^{13}C NMR spectrum of **18** in $CDCl_3$	103
Figure 2.89	400 MHz ^{1}H NMR spectrum of **19** DMSO-d6	104
Figure 2.90	100 MHz ^{13}C NMR spectrum of **19** in DMSO-d6	104
Figure 3.1	Respective examples containing spiro fused δ-lactone moieties	109
Figure 3.2	spiro-δ-lactone fused cyclic sulfamidate imine scaffold	113
Figure 3.3	Crystal data and structure refinement for **5aa**	115
Figure 3.4	ORTEP diagram of compound **14**	122
Figure 3.5	400 MHz ^{1}H NMR spectrum of **5aa** in $CDCl_3$	139
Figure 3.6	100 MHz ^{13}C NMR spectrum of **5aa** in $CDCl_3$	139
Figure 3.7	400 MHz ^{1}H NMR spectrum of **6aa** in $CDCl_3$	140
Figure 3.8	100 MHz ^{13}C NMR spectrum of **6aa** in $CDCl_3$	140
Figure 3.9	400 MHz ^{1}H NMR spectrum of **5ab** in $CDCl_3$	141
Figure 3.10	100 MHz ^{13}C NMR spectrum of **5ab** in $CDCl_3$	141
Figure 3.11	400 MHz ^{1}H NMR spectrum of **6ab** in $CDCl_3$	142
Figure 3.12	400 MHz ^{1}H NMR spectrum of **5ac** in $CDCl_3$	143
Figure 3.13	100 MHz ^{13}C NMR spectrum of **5ac** in $CDCl_3$	143
Figure 3.14	400 MHz ^{1}H NMR spectrum of **5ad & 6ad** in $CDCl_3$	144
Figure 3.15	100 MHz ^{13}C NMR spectrum of **5ad & 6ad** in $CDCl_3$	144
Figure 3.16	400 MHz ^{1}H NMR spectrum of **5ae** in $CDCl_3$	145
Figure 3.17	100 MHz ^{13}C NMR spectrum of **5ae** in $CDCl_3$	145
Figure 3.18	400 MHz ^{1}H NMR spectrum of **6ae** in $CDCl_3$	146
Figure 3.19	400 MHz ^{1}H NMR spectrum of **5af** in $CDCl_3$	147
Figure 3.20	100 MHz ^{13}C NMR spectrum of **5af** in $CDCl_3$	147
Figure 3.21	400 MHz ^{1}H NMR spectrum of **6af** in $CDCl_3$	148
Figure 3.22	400 MHz ^{1}H NMR spectrum of **5ag** in $CDCl_3$	149
Figure 3.23	100 MHz ^{13}C NMR spectrum of **5ag** in $CDCl_3$	149
Figure 3.24	400 MHz ^{1}H NMR spectrum of **6ag** in $CDCl_3$	150
Figure 3.25	400 MHz ^{1}H NMR spectrum of **5ah** in $CDCl_3$	151
Figure 3.26	100 MHz ^{13}C NMR spectrum of **5ah** in $CDCl_3$	151
Figure 3.27	400 MHz ^{1}H NMR spectrum of **5ai** in $CDCl_3$	152

Figure 3.28 100 MHz ^{13}C NMR spectrum of **5ai** in $CDCl_3$ 152
Figure 3.29 400 MHz ^{1}H NMR spectrum of **6ai** in $CDCl_3$ 153
Figure 3.30 400 MHz ^{1}H NMR spectrum of **5aj** in $CDCl_3$ 154
Figure 3.31 100 MHz ^{13}C NMR spectrum of **5aj** in $CDCl_3$ 154
Figure 3.32 400 MHz ^{1}H NMR spectrum of **6aj** in $CDCl_3$ 155
Figure 3.33 400 MHz ^{1}H NMR spectrum of **5ba & 6ba** in $CDCl_3$ 156
Figure 3.34 100 MHz ^{13}C NMR spectrum of **5ba & 6ba** in $CDCl_3$ 156
Figure 3.35 400 MHz ^{1}H NMR spectrum of **5ca & 6ca** in $CDCl_3$ 157
Figure 3.36 100 MHz ^{13}C NMR spectrum of **5ca & 6ca** in $CDCl_3$ 157
Figure 3.37 400 MHz ^{1}H NMR spectrum of **5da** in $CDCl_3$ 158
Figure 3.38 100 MHz ^{13}C NMR spectrum of **5da** in $CDCl_3$ 158
Figure 3.39 400 MHz ^{1}H NMR spectrum of **6da** in $CDCl_3$ 159
Figure 3.40 400 MHz ^{1}H NMR spectrum of **5ea** in $CDCl_3$ 160
Figure 3.41 100 MHz ^{13}C NMR spectrum of **5ea** in $CDCl_3$ 160
Figure 3.42 400 MHz ^{1}H NMR spectrum of **6ea** in $CDCl_3$ 161
Figure 3.43 400 MHz ^{1}H NMR spectrum of **5ed** in $CDCl_3$ 162
Figure 3.44 100 MHz ^{13}C NMR spectrum of **5ed** in $CDCl_3$ 162
Figure 3.45 400 MHz ^{1}H NMR spectrum of **5ej** in $CDCl_3$ 163
Figure 3.46 100 MHz ^{13}C NMR spectrum of **5ej** in $CDCl_3$ 163
Figure 3.47 400 MHz ^{1}H NMR spectrum of **6ej** in $CDCl_3$ 164
Figure 3.48 400 MHz ^{1}H NMR spectrum of **5fc** in $CDCl_3$ 165
Figure 3.49 100 MHz ^{13}C NMR spectrum of **5fc** in $CDCl_3$ 165
Figure 3.50 400 MHz ^{1}H NMR spectrum of **12** in $CDCl_3$ 166
Figure 3.51 100 MHz ^{13}C NMR spectrum of **12** in $CDCl_3$ 166
Figure 3.52 400 MHz ^{1}H NMR spectrum of **13** in $CDCl_3$ 167
Figure 3.53 400 MHz ^{1}H NMR spectrum of **14** in $CDCl_3$ 168
Figure 3.54 100 MHz ^{13}C NMR spectrum of **14** in $CDCl_3$ 168
Figure 3.55 400 MHz ^{1}H NMR spectrum of **15** in $CDCl_3$ 169
Figure 3.56 100 MHz ^{13}C NMR spectrum of **15** in $CDCl_3$ 169
Fig 3.57 HPLC data of racemic **5aa** 170
Fig 3.58 HPLC data of **5aa** 170

Fig 3.59	HPLC data of **5aa**	171
Figure 4.1	Some natural product and biologically active compounds containing picoline moiety	179
Figure 4.2	Picolinic acid derivative	184
Figure 4.3	ORTEP diagram of compound **3bd (CCDC)**	189
Figure 4.4	400 MHz ^{1}H NMR spectrum of **3aa** in $CDCl_3$	214
Figure 4.5	100 MHz ^{13}C NMR spectrum of **3aa** in $CDCl_3$	214
Figure 4.6	400 MHz ^{1}H NMR spectrum of **3ab** in $CDCl_3$	215
Figure 4.7	100 MHz ^{13}C NMR spectrum of **3ab** in $CDCl_3$	215
Figure 4.8	400 MHz ^{1}H NMR spectrum of **3ac** in $CDCl_3$	216
Figure 4.9	100 MHz ^{13}C NMR spectrum of **3ac** in $CDCl_3$	216
Figure 4.10	400 MHz ^{1}H NMR spectrum of **3ad** in $CDCl_3$	217
Figure 4.11	100 MHz ^{13}C NMR spectrum of **3ad** in $CDCl_3$	217
Figure 4.12	400 MHz ^{1}H NMR spectrum of **3ae** in $CDCl_3$	218
Figure 4.13	100 MHz ^{13}C NMR spectrum of **3ae** in $CDCl_3$	218
Figure 4.14	400 MHz ^{1}H NMR spectrum of **3af** in $CDCl_3$	219
Figure 4.15	100 MHz ^{13}C NMR spectrum of **3af** in $CDCl_3$	219
Figure 4.16	400 MHz ^{1}H NMR spectrum of **3ag** in $CDCl_3$	220
Figure 4.17	100 MHz ^{13}C NMR spectrum of **3ag** in $CDCl_3$	220
Figure 4.18	400 MHz ^{1}H NMR spectrum of **3ah** in $CDCl_3$	221
Figure 4.19	100 MHz ^{13}C NMR spectrum of **3ah** in $CDCl_3$	221
Figure 4.20	400 MHz ^{1}H NMR spectrum of **3ai** in $CDCl_3$	222
Figure 4.21	100 MHz ^{13}C NMR spectrum of **3ai** in $CDCl_3$	222
Figure 4.22	400 MHz ^{1}H NMR spectrum of **3aj** in $CDCl_3$	223
Figure 4.23	100 MHz ^{13}C NMR spectrum of **3aj** in $CDCl_3$	223
Figure 4.24	400 MHz ^{1}H NMR spectrum of **3ak** in $CDCl_3$	224
Figure 4.25	100 MHz ^{13}C NMR spectrum of **3ak** in $CDCl_3$	224
Figure 4.26	400 MHz ^{1}H NMR spectrum of **3bb** in $CDCl_3$	225
Figure 4.27	100 MHz ^{13}C NMR spectrum of **3bb** in $CDCl_3$	225
Figure 4.28	400 MHz ^{1}H NMR spectrum of **3bc** in $CDCl_3$	226
Figure 4.29	100 MHz ^{13}C NMR spectrum of **3bc** in $CDCl_3$	226

Figure 4.30 400 MHz ^{1}H NMR spectrum of **3bd** in $CDCl_3$ 227
Figure 4.31 100 MHz ^{13}C NMR spectrum of **3bd** in $CDCl_3$ 227
Figure 4.32 400 MHz ^{1}H NMR spectrum of **3bf** in $CDCl_3$ 228
Figure 4.33 100 MHz ^{13}C NMR spectrum of **3bf** in $CDCl_3$ 228
Figure 4.34 400 MHz ^{1}H NMR spectrum of **3bg** in $CDCl_3$ 229
Figure 4.35 100 MHz ^{13}C NMR spectrum of **3bg** in $CDCl_3$ 229
Figure 4.36 400 MHz ^{1}H NMR spectrum of **3bj** in $CDCl_3$ 230
Figure 4.37 100 MHz ^{13}C NMR spectrum of **3bj** in $CDCl_3$ 230
Figure 4.38 400 MHz ^{1}H NMR spectrum of **3bk** in $CDCl_3$ 231
Figure 4.39 100 MHz ^{13}C NMR spectrum of **3bk** in $CDCl_3$ 231
Figure 4.40 400 MHz ^{1}H NMR spectrum of **3ca** in $CDCl_3$ 232
Figure 4.41 100 MHz ^{13}C NMR spectrum of **3ca** in $CDCl_3$ 232
Figure 4.42 400 MHz ^{1}H NMR spectrum of **3cg** in $CDCl_3$ 233
Figure 4.43 100 MHz ^{13}C NMR spectrum of **3cg** in $CDCl_3$ 233
Figure 4.44 400 MHz ^{1}H NMR spectrum of **3da** in $CDCl_3$ 234
Figure 4.45 100 MHz ^{13}C NMR spectrum of **3da** in $CDCl_3$ 234
Figure 4.46 400 MHz ^{1}H NMR spectrum of **3ea** in $CDCl_3$ 235
Figure 4.47 100 MHz ^{1}H NMR spectrum of **3ea** in $CDCl_3$ 235
Figure 4.48 400 MHz ^{1}H NMR spectrum of **3ej** in $CDCl_3$ 236
Figure 4.49 100 MHz ^{13}C NMR spectrum of **3ej** in $CDCl_3$ 236
Figure 4.50 400 MHz ^{1}H NMR spectrum of **3fa** in $CDCl_3$ 237
Figure 4.51 100 MHz ^{13}C NMR spectrum of **3fa** in $CDCl_3$ 237
Figure 4.52 400 MHz ^{1}H NMR spectrum of **3fl** in $CDCl_3$ 238
Figure 4.53 100 MHz ^{13}C NMR spectrum of **3fl** in $CDCl_3$ 238
Figure 4.54 400 MHz ^{1}H NMR spectrum of **3ga** in $CDCl_3$ 239
Figure 4.55 100 MHz ^{13}C NMR spectrum of **3ga** in $CDCl_3$ 239
Figure 4.56 400 MHz ^{1}H NMR spectrum of **3gd** in $CDCl_3$ 240
Figure 4.57 100 MHz ^{13}C NMR spectrum of **3gd** in $CDCl_3$ 240
Figure 4.58 400 MHz ^{1}H NMR spectrum of **3gg** in $CDCl_3$ 241
Figure 4.59 100 MHz ^{13}C NMR spectrum of **3gg** in $CDCl_3$ 241
Figure 4.60 400 MHz ^{1}H NMR spectrum of **3gk** in $CDCl_3$ 242

Figure 4.61	100 MHz ^{13}C NMR spectrum of **3gk** in $CDCl_3$	242
Figure 4.62	400 MHz ^{1}H NMR spectrum of **3am** in $CDCl_3$	243
Figure 4.63	100 MHz ^{13}C NMR spectrum of **3am** in $CDCl_3$	243
Figure 4.64	400 MHz ^{1}H NMR spectrum of **3an** in $CDCl_3$	244
Figure 4.65	100 MHz ^{13}C NMR spectrum of **3an** in $CDCl_3$	244
Figure 4.66	400 MHz ^{1}H NMR spectrum of **3bm** in $CDCl_3$	245
Figure 4.67	100 MHz ^{13}C NMR spectrum of **3bm** in $CDCl_3$	245
Figure 4.68	400 MHz ^{1}H NMR spectrum of **7** in $CDCl_3$	246
Figure 4.69	100 MHz ^{13}C NMR spectrum of **7** in $CDCl_3$	246
Figure 4.70	400 MHz ^{1}H NMR spectrum of **8** in $CDCl_3$	247
Figure 4.71	100 MHz ^{13}C NMR spectrum of **8** in $CDCl_3$	247
Figure 4.72	400 MHz ^{1}H NMR spectrum of **9** in $CDCl_3$	248
Figure 4.73	100 MHz ^{13}C NMR spectrum of **9** in $CDCl_3$	248
Figure 5.1	Several biologically active natural products having a nicotinic scaffold	255
Figure 5.2	Functionalized nicotinate	263
Figure 5.3	ORTEP diagram of compound **3ai (CCDC** 1522097**)**	268
Figure 5.4	400 MHz ^{1}H NMR spectrum of **5** in $CDCl_3$	304
Figure 5.5	100 MHz ^{13}C NMR spectrum of **5** in $CDCl_3$	304
Figure 5.6	400 MHz ^{1}H NMR spectrum of **8** in $CDCl_3$	305
Figure 5.7	100 MHz ^{13}C NMR spectrum of **8** in $CDCl_3$	305
Figure 5.8	400 MHz ^{1}H NMR spectrum of **3aa** in $CDCl_3$	306
Figure 5.9	100 MHz ^{13}C NMR spectrum of **3aa** in $CDCl_3$	306
Figure 5.10	400 MHz ^{1}H NMR spectrum of **3ac** in $CDCl_3$	307
Figure 5.11	100 MHz ^{13}C NMR spectrum of **3ac** in $CDCl_3$	307
Figure 5.12	400 MHz ^{1}H NMR spectrum of **3ad** in $CDCl_3$	308
Figure 5.13	100 MHz ^{13}C NMR spectrum of **3ad** in $CDCl_3$	308
Figure 5.14	400 MHz ^{1}H NMR spectrum of **3af** in $CDCl_3$	309
Figure 5.15	100 MHz ^{13}C NMR spectrum of **3af** in $CDCl_3$	309
Figure 5.16	400 MHz ^{1}H NMR spectrum of **3ag** in $CDCl_3$	310
Figure 5.17	100 MHz ^{13}C NMR spectrum of **3ag** in $CDCl_3$	310

Figure 5.18 400 MHz ^{1}H NMR spectrum of **3ah** in $CDCl_3$ 311
Figure 5.19 100 MHz ^{13}C NMR spectrum of **3ah** in $CDCl_3$ 311
Figure 5.20 400 MHz ^{1}H NMR spectrum of **3ai** in $CDCl_3$ 312
Figure 5.21 100 MHz ^{13}C NMR spectrum of **3ai** in $CDCl_3$ 312
Figure 5.22 400 MHz ^{1}H NMR spectrum of **3ba** in $CDCl_3$ 313
Figure 5.23 100 MHz ^{13}C NMR spectrum of **3ba** in $CDCl_3$ 313
Figure 5.24 400 MHz ^{1}H NMR spectrum of **3bd** in $CDCl_3$ 314
Figure 5.25 100 MHz ^{13}C NMR spectrum of **3bd** in $CDCl_3$ 314
Figure 5.26 400 MHz ^{1}H NMR spectrum of **3be** in $CDCl_3$ 315
Figure 5.27 100 MHz ^{13}C NMR spectrum of **3be** in $CDCl_3$ 315
Figure 5.28 400 MHz ^{1}H NMR spectrum of **3bf** in $CDCl_3$ 316
Figure 5.29 100 MHz ^{13}C NMR spectrum of **3bf** in $CDCl_3$ 316
Figure 5.30 400 MHz ^{1}H NMR spectrum of **3bg** in $CDCl_3$ 317
Figure 5.31 100 MHz ^{13}C NMR spectrum of **3bg** in $CDCl_3$ 317
Figure 5.32 400 MHz ^{1}H NMR spectrum of **3cd** in $CDCl_3$ 318
Figure 5.33 100 MHz ^{13}C NMR spectrum of **3cd** in $CDCl_3$ 318
Figure 5.34 400 MHz ^{1}H NMR spectrum of **3cg** in $CDCl_3$ 319
Figure 5.35 100 MHz ^{13}C NMR spectrum of **3cg** in $CDCl_3$ 319
Figure 5.36 400 MHz ^{1}H NMR spectrum of **3ci** in $CDCl_3$ 320
Figure 5.37 100 MHz ^{13}C NMR spectrum of **3ci** in $CDCl_3$ 320
Figure 5.38 400 MHz ^{1}H NMR spectrum of **3dg** in $CDCl_3$ 321
Figure 5.39 100 MHz ^{13}C NMR spectrum of **3dg** in $CDCl_3$ 321
Figure 5.40 400 MHz ^{1}H NMR spectrum of **3eb** in $CDCl_3$ 322
Figure 5.41 100 MHz ^{13}C NMR spectrum of **3eb** in $CDCl_3$ 322
Figure 5.42 400 MHz ^{1}H NMR spectrum of **3eg** in $CDCl_3$ 323
Figure 5.43 100 MHz ^{13}C NMR spectrum of **3eg** in $CDCl_3$ 323
Figure 5.44 400 MHz ^{1}H NMR spectrum of **3hg** in $CDCl_3$ 324
Figure 5.45 100 MHz ^{13}C NMR spectrum of **3hg** in $CDCl_3$ 324
Figure 5.46 400 MHz ^{1}H NMR spectrum of **3ia** in $CDCl_3$ 325
Figure 5.47 100 MHz ^{13}C NMR spectrum of **3ia** in $CDCl_3$ 325
Figure 5.48 400 MHz ^{1}H NMR spectrum of **3id** in $CDCl_3$ 326

Figure 5.49 100 MHz ^{13}C NMR spectrum of **3id** in $CDCl_3$ 326
Figure 5.50 400 MHz ^{1}H NMR spectrum of **3ig** in $CDCl_3$ 327
Figure 5.51 100 MHz ^{13}C NMR spectrum of **3ig** in $CDCl_3$ 327
Figure 5.52 400 MHz ^{1}H NMR spectrum of **3ak** in $CDCl_3$ 328
Figure 5.53 100 MHz ^{13}C NMR spectrum of **3ak** in $CDCl_3$ 328
Figure 5.54 400 MHz ^{1}H NMR spectrum of **3al** in $CDCl_3$ 329
Figure 5.55 100 MHz ^{13}C NMR spectrum of **3al** in $CDCl_3$ 329
Figure 5.56 400 MHz ^{1}H NMR spectrum of **3am** in $CDCl_3$ 330
Figure 5.57 100 MHz ^{13}C NMR spectrum of **3am** in $CDCl_3$ 330
Figure 5.58 400 MHz ^{1}H NMR spectrum of **3an** in $CDCl_3$ 331
Figure 5.59 100 MHz ^{13}C NMR spectrum of **3an** in $CDCl_3$ 331
Figure 5.60 400 MHz ^{1}H NMR spectrum of **3ao** in $CDCl_3$ 332
Figure 5.61 100 MHz ^{13}C NMR spectrum of **3ao** in $CDCl_3$ 332
Figure 5.62 400 MHz ^{1}H NMR spectrum of **3ap** in $CDCl_3$ 333
Figure 5.63 100 MHz ^{13}C NMR spectrum of **3ap** in $CDCl_3$ 333
Figure 5.64 400 MHz ^{1}H NMR spectrum of **3aq** in $CDCl_3$ 334
Figure 5.65 100 MHz ^{13}C NMR spectrum of **3aq** in $CDCl_3$ 334
Figure 5.66 400 MHz ^{1}H NMR spectrum of **3ar** in $CDCl_3$ 335
Figure 5.67 100 MHz ^{13}C NMR spectrum of **3ar** in $CDCl_3$ 335
Figure 5.68 400 MHz ^{1}H NMR spectrum of **3bm** in $CDCl_3$ 336
Figure 5.69 100 MHz ^{13}C NMR spectrum of **3bm** in $CDCl_3$ 336
Figure 5.70 400 MHz ^{1}H NMR spectrum of **3bp** in $CDCl_3$ 337
Figure 5.71 100 MHz ^{13}C NMR spectrum of **3bp** in $CDCl_3$ 337
Figure 5.72 400 MHz ^{1}H NMR spectrum of **3bq** in $CDCl_3$ 338
Figure 5.73 100 MHz ^{13}C NMR spectrum of **bq** in $CDCl_3$ 338
Figure 5.74 400 MHz ^{1}H NMR spectrum of **3ck** in $CDCl_3$ 339
Figure 5.75 100 MHz ^{13}C NMR spectrum of **3ck** in $CDCl_3$ 339
Figure 5.76 400 MHz ^{1}H NMR spectrum of **3fk** in $CDCl_3$ 340
Figure 5.77 100 MHz ^{13}C NMR spectrum of **3fk** in $CDCl_3$ 340
Figure 5.78 400 MHz ^{1}H NMR spectrum of **3gk** in $CDCl_3$ 341
Figure 5.79 100 MHz ^{13}C NMR spectrum of **3gk** in $CDCl_3$ 341

Figure 5.80 400 MHz ^{1}H NMR spectrum of **3hm** in $CDCl_3$ 342
Figure 5.81 100 MHz ^{13}C NMR spectrum of **3hm** in $CDCl_3$ 342
Figure 5.82 400 MHz ^{1}H NMR spectrum of **3hp** in $CDCl_3$ 343
Figure 5.83 100 MHz ^{13}C NMR spectrum of **3hp** in $CDCl_3$ 343
Figure 5.84 400 MHz ^{1}H NMR spectrum of **3hr** in $CDCl_3$ 344
Figure 5.85 100 MHz ^{13}C NMR spectrum of **3hr** in $CDCl_3$ 344
Figure 5.86 400 MHz ^{1}H NMR spectrum of **3ik** in $CDCl_3$ 345
Figure 5.87 100 MHz ^{13}C NMR spectrum of **3ik** in $CDCl_3$ 345
Figure 5.88 400 MHz ^{1}H NMR spectrum of **3im** in $CDCl_3$ 346
Figure 5.89 100 MHz ^{13}C NMR spectrum of **3im** in $CDCl_3$ 346
Figure 5.90 400 MHz ^{1}H NMR spectrum of **3as** in $CDCl_3$ 347
Figure 5.91 100 MHz ^{13}C NMR spectrum of **3as** in $CDCl_3$ 347
Figure 5.92 400 MHz ^{1}H NMR spectrum of **3at** in $CDCl_3$ 348
Figure 5.93 100 MHz ^{13}C NMR spectrum of **3at** in $CDCl_3$ 348
Figure 5.94 400 MHz ^{1}H NMR spectrum of **3es** in $CDCl_3$ 349
Figure 5.95 100 MHz ^{13}C NMR spectrum of **3es** in $CDCl_3$ 349
Figure 5.96 400 MHz ^{1}H NMR spectrum of **3et** in $CDCl_3$ 350
Figure 5.97 100 MHz ^{13}C NMR spectrum of **3et** in $CDCl_3$ 350
Figure 5.98 400 MHz ^{1}H NMR spectrum of **3fs** in $CDCl_3$ 351
Figure 5.99 100 MHz ^{13}C NMR spectrum of **3fs** in $CDCl_3$ 351
Figure 5.100 400 MHz ^{1}H NMR spectrum of **3it** in $CDCl_3$ 352
Figure 5.101 100 MHz ^{13}C NMR spectrum of **3it** in $CDCl_3$ 352
Figure 5.102 400 MHz ^{1}H NMR spectrum of **9** in $CDCl_3$ 353
Figure 5.103 100 MHz ^{13}C NMR spectrum of **9** in $CDCl_3$ 353
Figure 6.1 Representative molecules containing pyridine moiety 363
Figure 6.2 2,4-diaryl/2-aryl-4-styrylpyridine derivatives 372
Figure 6.3 400 MHz ^{1}H NMR spectrum of **3aa'** in $CDCl_3$ 400
Figure 6.4 100 MHz ^{13}C NMR spectrum of **3aa'** in $CDCl_3$ 400
Figure 6.5 400 MHz ^{1}H NMR spectrum of **3aa** in $CDCl_3$ 401
Figure 6. 6 100 MHz ^{13}C NMR spectrum of **3aa** in $CDCl_3$ 401
Figure 6.7 400 MHz ^{1}H NMR spectrum of **3ab** in $CDCl_3$ 402

Figure 6.8 100 MHz ^{13}C NMR spectrum of **3ab** in $CDCl_3$ 402
Figure 6.9 400 MHz ^{1}H NMR spectrum of **3ac** in $CDCl_3$ 403
Figure 6.10 100 MHz ^{13}C NMR spectrum of **3ac** in $CDCl_3$ 403
Figure 6.11 400 MHz ^{1}H NMR spectrum of **3ad** in $CDCl_3$ 404
Figure 6.12 100 MHz ^{13}C NMR spectrum of **3ad** in $CDCl_3$ 404
Figure 6.13 400 MHz ^{1}H NMR spectrum of **3ae** in $CDCl_3$ 405
Figure 6.14 100 MHz ^{13}C NMR spectrum of **3ae** in $CDCl_3$ 405
Figure 6.15 400 MHz ^{1}H NMR spectrum of **3af** in $CDCl_3$ 406
Figure 6.16 100 MHz ^{13}C NMR spectrum of **3af** in $CDCl_3$ 406
Figure 6.17 400 MHz ^{1}H NMR spectrum of **3ag** in $CDCl_3$ 407
Figure 6.18 100 MHz ^{13}C NMR spectrum of **3ag** in $CDCl_3$ 407
Figure 6.19 400 MHz ^{1}H NMR spectrum of **3ah** in $CDCl_3$ 408
Figure 6.20 100 MHz ^{13}C NMR spectrum of **3ah** in $CDCl_3$ 408
Figure 6.21 400 MHz ^{1}H NMR spectrum of **3ai** in $CDCl_3$ 409
Figure 6.22 100 MHz ^{13}C NMR spectrum of **3ai** in $CDCl_3$ 409
Figure 6.23 400 MHz ^{1}H NMR spectrum of **3ba** in $CDCl_3$ 410
Figure 6.24 100 MHz ^{13}C NMR spectrum of **3ba** in $CDCl_3$ 410
Figure 6.25 400 MHz ^{1}H NMR spectrum of **3be** in $CDCl_3$ 411
Figure 6.26 100 MHz ^{13}C NMR spectrum of **3be** in $CDCl_3$ 411
Figure 6.27 400 MHz ^{1}H NMR spectrum of **3bg** in $CDCl_3$ 412
Figure 6.28 100 MHz ^{13}C NMR spectrum of **3bg** in $CDCl_3$ 412
Figure 6.29 400 MHz ^{1}H NMR spectrum of **3bh** in $CDCl_3$ 413
Figure 6.30 100 MHz ^{13}C NMR spectrum of **3bh** in $CDCl_3$ 413
Figure 6.31 400 MHz ^{1}H NMR spectrum of **3bj** in $CDCl_3$ 414
Figure 6.32 100 MHz ^{13}C NMR spectrum of **3bj** in $CDCl_3$ 414
Figure 6.33 400 MHz ^{1}H NMR spectrum of **3cd** in $CDCl_3$ 415
Figure 6.34 100 MHz ^{13}C NMR spectrum of **3cd** in $CDCl_3$ 415
Figure 6.35 400 MHz ^{1}H NMR spectrum of **3ce** in $CDCl_3$ 416
Figure 6.36 100 MHz ^{13}C NMR spectrum of **3ce** in $CDCl_3$ 416
Figure 6.37 400 MHz ^{1}H NMR spectrum of **3cf** in $CDCl_3$ 417
Figure 6.38 100 MHz ^{13}C NMR spectrum of **3cf** in $CDCl_3$ 417

Figure 6.39 400 MHz ^{1}H NMR spectrum of **3cg** in $CDCl_3$ 418
Figure 6.40 100 MHz ^{13}C NMR spectrum of **3cg** in $CDCl_3$ 418
Figure 6.41 400 MHz ^{1}H NMR spectrum of **3da** in $CDCl_3$ 419
Figure 6.42 100 MHz ^{13}C NMR spectrum of **3da** in $CDCl_3$ 419
Figure 6.43 400 MHz ^{1}H NMR spectrum of **3dk** in $CDCl_3$ 420
Figure 6.44 100 MHz ^{13}C NMR spectrum of **3dk** in $CDCl_3$ 420
Figure 6.45 400 MHz ^{1}H NMR spectrum of **3ea** in $CDCl_3$ 421
Figure 6.46 100 MHz ^{13}C NMR spectrum of **3ea** in $CDCl_3$ 421
Figure 6.47 400 MHz ^{1}H NMR spectrum of **3eg** in $CDCl_3$ 422
Figure 6.48 100 MHz ^{13}C NMR spectrum of **3eg** in $CDCl_3$ 422
Figure 6.49 400 MHz ^{1}H NMR spectrum of **3eh** in $CDCl_3$ 423
Figure 6.50 100 MHz ^{13}C NMR spectrum of **3eh** in $CDCl_3$ 423
Figure 6.51 400 MHz ^{1}H NMR spectrum of **3fg** in $CDCl_3$ 424
Figure 6.52 100 MHz ^{13}C NMR spectrum of **3fg** in $CDCl_3$ 424
Figure 6.53 400 MHz ^{1}H NMR spectrum of **3ga** in $CDCl_3$ 425
Figure 6.54 100 MHz ^{13}C NMR spectrum of **3ga** in $CDCl_3$ 425
Figure 6.55 400 MHz ^{1}H NMR spectrum of **3gc** in $CDCl_3$ 426
Figure 6.56 100 MHz ^{13}C NMR spectrum of **3gc** in $CDCl_3$ 426
Figure 6.57 400 MHz ^{1}H NMR spectrum of **3ge** in $CDCl_3$ 427
Figure 6.58 100 MHz ^{13}C NMR spectrum of **3ge** in $CDCl_3$ 427
Figure 6.59 400 MHz ^{1}H NMR spectrum of **3gg** in $CDCl_3$ 428
Figure 6.60 100 MHz ^{13}C NMR spectrum of **3gg** in $CDCl_3$ 428
Figure 6.61 400 MHz ^{1}H NMR spectrum of **3gk** in $CDCl_3$ 429
Figure 6.62 100 MHz ^{13}C NMR spectrum of **3gk** in $CDCl_3$ 429
Figure 6.63 400 MHz ^{1}H NMR spectrum of **3gl** in $CDCl_3$ 430
Figure 6.64 100 MHz ^{13}C NMR spectrum of **3gl** in $CDCl_3$ 430
Figure 6.65 400 MHz ^{1}H NMR spectrum of **3hi** in $CDCl_3$ 431
Figure 6.66 100 MHz ^{13}C NMR spectrum of **3hi** in $CDCl_3$ 431
Figure 6.67 400 MHz ^{1}H NMR spectrum of **3am** in $CDCl_3$ 432
Figure 6.68 100 MHz ^{13}C NMR spectrum of **3am** in $CDCl_3$ 432
Figure 6.69 400 MHz ^{1}H NMR spectrum of **3an** in $CDCl_3$ 433

Figure 6.70 100 MHz ^{13}C NMR spectrum of **3an** in $CDCl_3$ 433
Figure 6.71 400 MHz ^{1}H NMR spectrum of **3ap** in $CDCl_3$ 434
Figure 6.72 100 MHz ^{13}C NMR spectrum of **3ap** in $CDCl_3$ 434
Figure 6.73 400 MHz ^{1}H NMR spectrum of **3aq** in $CDCl_3$ 435
Figure 6.74 100 MHz ^{13}C NMR spectrum of **3aq** in $CDCl_3$ 435
Figure 6.75 400 MHz ^{1}H NMR spectrum of **3as** in $CDCl_3$ 436
Figure 6.76 100 MHz ^{13}C NMR spectrum of **3as** in $CDCl_3$ 436
Figure 6.77 400 MHz ^{1}H NMR spectrum of **3at** in $CDCl_3$ 437
Figure 6.78 100 MHz ^{13}C NMR spectrum of **3at** in $CDCl_3$ 437
Figure 6.79 400 MHz ^{1}H NMR spectrum of **3cm** in $CDCl_3$ 438
Figure 6.80 100 MHz ^{13}C NMR spectrum of **3cm** in $CDCl_3$ 438
Figure 6.81 400 MHz ^{1}H NMR spectrum of **3cn** in $CDCl_3$ 439
Figure 6.82 100 MHz ^{13}C NMR spectrum of **3cn** in $CDCl_3$ 439
Figure 6.83 400 MHz ^{1}H NMR spectrum of **3cq** in $CDCl_3$ 440
Figure 6.84 100 MHz ^{13}C NMR spectrum of **3cq** in $CDCl_3$ 440
Figure 6.85 400 MHz ^{1}H NMR spectrum of **3cr** in $CDCl_3$ 441
Figure 6.86 100 MHz ^{13}C NMR spectrum of **3cr** in $CDCl_3$ 441
Figure 6.87 400 MHz ^{1}H NMR spectrum of **3gm** in $CDCl_3$ 442
Figure 6.88 100 MHz ^{13}C NMR spectrum of **3gm** in $CDCl_3$ 442
Figure 6.89 400 MHz ^{1}H NMR spectrum of **3gn** in $CDCl_3$ 443
Figure 6.90 100 MHz ^{13}C NMR spectrum of **3gn** in $CDCl_3$ 443
Figure 6.91 400 MHz ^{1}H NMR spectrum of **3hm** in $CDCl_3$ 444
Figure 6.92 100 MHz ^{13}C NMR spectrum of **3hm** in $CDCl_3$ 444
Figure 6.93 400 MHz ^{1}H NMR spectrum of **3hs** in $CDCl_3$ 445
Figure 6.94 100 MHz ^{13}C NMR spectrum of **3hs** in $CDCl_3$ 445
Figure 6.95 400 MHz ^{1}H NMR spectrum of **4aa** in DMSO-d_6 446
Figure 6.96 100 MHz ^{13}C NMR spectrum of **4aa** in DMSO-d_6 446
Figure 6.97 400 MHz ^{1}H NMR spectrum of **4ga** in DMSO-d_6 447
Figure 6.98 100 MHz ^{13}C NMR spectrum of **4ga** in DMSO-d_6 447

LIST OF SCHEMES

Scheme 1.1	Synthesis of six-membered cyclic sulfamidate imines	2
Scheme 1.2	Synthesis of 1,2,3-benzoxathiazine 2,2-dioxide by using of chlorosulfonylisocyanate	3
Scheme 1.3	Synthesis of 5-membered cyclic sulfamidate imines	4
Scheme 1.4	Synthesis of cyclic sulfamidate imines using sulfuric diamide	4
Scheme 1.5	Pd-catalyzed asymmetric hydrogenation of five membered cyclic imines	5
Scheme 1.6	Rh-catalyzed asymmetric hydrogen transfer of cyclic imines	6
Scheme 1.7	Rh-catalyzed transfer hydrogenation of 5*H*-[1,2,3]-oxathiazole-2,2-dioxide derivatives	7
Scheme 1.8	Preparation of Norephedrine form 4-methyl-5-phenyl-5*H*-1,2,3-oxathiazole-2,2-dioxide	8
Scheme 1.9	Grignard addition to cyclic sulfamidate imines	9
Scheme 1.10	Rhodium-catalyzed asymmetric arylation of cyclic ketimines	9
Scheme 1.11	Reaction scope for the Rhodium-catalyzed asymmetric arylation of cyclic *N*-sulfamidate imines	10
Scheme 1.12	Rhodium-catalyzed asymmetric arylation of cyclic ketimines	11
Scheme 1.13	Reactions of 3,5-difluorophenylketimine with different arylboronic acids	12
Scheme 1.14	Reactions of different cyclic ketimines with arylboronic acids	12
Scheme 1.15	Stereoselective aziridination of cyclic imines	13
Scheme 1.16	Stereoselective aziridination of benzofusedcyclic imines	14
Scheme 1.17	Reaction of sulfamidate with thiocyanate and thioacetates	15

Scheme 1.18 Synthesis of β-N-protected amino alcohols 15
Scheme 1.19 Opening of cyclic sulfamidates using nitrogen electrophiles 16
Scheme 1.20 Opening of cyclic sulfamidates using NaCN 17
Scheme 1.21 Ring opening of cyclic sulfamidate with halide 17
Scheme 1.22 Ring opening of cyclic sulfamidate with phosphorous nucleophile 18
Scheme 1.23 Ring opening of cyclic sulfamidate with selenium nucleophile 19
Scheme 2.1 Domino reaction between cyclic *N*-sulfonylimines and simple aldehydes 26
Scheme 2.2 Cycloaddition reaction between 4-cyclohexenyl cyclic sulfamidate imines and α,β-unsaturated aldehydes 26
Scheme 2.3 Cycloaddition reaction between 4-alkenyl cyclic sulfamidate imines and α,β-unsaturated aldehydes 27
Scheme 2.4 Retrosynthetic part for the functionalization of 5-position of cyclic sulfamidate imine 28
Scheme 2.5 Condensation reaction between 5-membered cyclic sulfamidate imine and aldehydes 29
Scheme 2.6 Plausible mechanism of the condensation reaction 32
Scheme 2.7 Condensation reaction of cyclic imine **1h** with aldehydes 36
Scheme 2.8 1,4-addition reaction of **1a** with α,β-unsaturated aldehydes 36
Scheme 2.9 Chemoselective reduction of C=C bond 37
Scheme 2.10 Reduction of prochiral C=N bond 38
Scheme 2.11 Syntheses of *trans*-β-amino-α-azido/triazoles. 39
Scheme 2.12 synthesis of 2-hydroxy pyrrolidine derivative 40
Scheme 2.13 Synthesis of *Z*-5-alkylidene-4-aryl-1,2,3-oxathiazole-2,2-dioxide 42
Scheme 2.14 Boc protection of cyclic sulfamidates 54
Scheme 3.1 Reaction between alkynyl aldehydes and oxindoles 110
Scheme 3.2 Stereoselective synthesis of oxa-spirocyclic indanone derivatives 111
Scheme 3.3 Synthesis of spiro-δ-lactone by Michael hemiacetalization 111

reaction
Scheme 3.4 HAD reaction of Brassard type diene with isatin derivatives 112
Scheme 3.5 Formation of spiro-sulfamidate imine fused δ-lactone derivatives 114
Scheme 3.6 Probable mechanism for the formation of spiro-δ-lactones 118
Scheme 3.7 One-pot enantioselective synthesis of spiro-δ-lactone 121
Scheme 3.8 Stereoselective synthesis of *trans*-*cis*-β-amino-α-azido compounds 122
Scheme 4.1 Synthesis of 3-hydroxy picolinates from unsymmetrical alkynes 180
Scheme 4.2 One-pot synthesis of highly functionalized picolinates 181
Scheme 4.3 DBU promoted synthesis of substituted picolinates 181
Scheme 4.4 Formation of substituted picolinates by using different α,β-unsaturated *O*-pivaloyl oximes 182
Scheme 4.5 Synthesis of poly-substituted picolinates 182
Scheme 4.6 Synthesis of substituted 4-amino-5-fluoro-6-alkylpicolinaldehydes by cascade cyclization 183
Scheme 4.7 Cyclization reaction between β,γ-unsaturated α-ketoesters, and cyclohexanone 183
Scheme 4.8 Cyclization reaction between β,γ-unsaturated α-ketoesters, and and ketones 184
Scheme 4.9 DABCO mediated domino reaction between 4-phenyl-5*H*-1,2,3-oxathiazole-2,2-dioxide and MBH acetate of *trans*-β-nitrostrene 185
Scheme 4.10 Plausible mechanism for this domino reaction 188
Scheme 4.11 One pot synthesis of (*E*)-6 aryl-4-styryl-substituted picolinates 192
Scheme 4.12 Synthesis of 2-amino-4,6-diphenylpyridine (**7**) and Alpidem derivative (**9**) 193
Scheme 5.1 Synthesis of nitotinic acid 256

Scheme 5.2	Synthesis of nicotinate derivative *via* Hantzsch's type synthesis	256
Scheme 5.3	The original Bohlmann-Rahtz pyridine synthesis (1957)	257
Scheme 5.4	Brønsted acid promoted synthesis of functionalized nicotinates	257
Scheme 5.5	Lewis acid promoted synthesis of functionalized nicotinates	258
Scheme 5.6	Multicomponent synthesis of polyfunctionalized nicotinate derivatives.	259
Scheme 5.7	Three component reaction for the synthesis of polysubstituted nicotinate	259
Scheme 5.8	Formation of highly substituted nicotinates from α, β-unsaturated ketones	260
Scheme 5.9	Synthesis of substituted nicotinate from 1,3-dicarbonyls	260
Scheme 5.10	Multi-component approach towards the synthesis of trisubstituted nicotinates.	261
Scheme 5.11	Synthesis of poly-substituted nicotinates using MBH acetates of MVK	261
Scheme 5.12	Synthesis of substituted nicotinate with various oxime acetates and active methylene compounds	262
Scheme 5.13	Multicomponent fashion for the synthesis of 2-aminonicotinonitriles	263
Scheme 5.14	DABCO mediated domino reaction of MBH acetates with cylic sulfamidate imines.	264
Scheme 5.15	Possible mechanism of this domino reaction	267
Scheme 5.16	Synthesis of trizolopyridine derivative **9**	274
Scheme 6.1	Synthesis of pyridine by Rasamay and Chelucci	364
Scheme 6.2	Classical Hantzsch synthesis for the symmetrical pyridine	365
Scheme 6.3	One-pot synthesis of 2,4-diphenylpyridines form (*N*-vinyimino)- phosphoranes	365
Scheme 6.4	Solid support synthesis of 2,4-disubstituted pyridines	366

Scheme 6.5 Synthesis of 2,4-diarylpyridines from 1-substituted ethanones 366

Scheme 6.6 Synthesis of 2,4-diaryl pyridines from α,β,γ,δ-unsaturated aldehydes 367

Scheme 6.7 2,4-disubstituted pyridines by [3+3] cyclization of oximes and enals 367

Scheme 6.8 Scope of 2,4- substituted pyridines by the reaction between enone and allyltrimethylsilane 368

Scheme 6.9 Ru-catalyzed synthesis of 2,4-diarylpyridines 369

Scheme 6.10 Fe catalyzed cyclization of ketooxime acetates and *N*,*N*-dimethyl aniline 369

Scheme 6.11 Synthesis of styryl bipyridine ligand 370

Scheme 6.12 Preparation of substituted or electron donating substituted styryl pyridine 370

Scheme 6.13 Preparation of electron withdrawing substituted styryl pyridine 371

Scheme 6.14 Preparation of functionalized 2-aryl-4-(*E*)-styrylpyridines using cyclic sulfamidate imine as precursor 372

Scheme 6.15 Plausible mechanism for the formation of 2-aryl-4-(*E*)-styrylpyridine 376

Scheme 6.16 Synthesis of 2-arylisonicotinic acid derivatives 381

LIST OF TABLES

Table 2.1	Optimization table of this condensation reaction	31
Table 2.2	Synthesis of *Z*-5 alkylidene-4-aryl-1,2,3-ozathiazole-2,2-dioxides	34
Table 2.3	Crystal data and structure refinement for **3aa**	59
Table 2.4	Crystal data of compound **13**	60
Table 2.5	Crystal data of compound **15**	61
Table 3.1	Optimization of Michael-condensation-hemiacetalization sequence process	116
Table 3.2	One-pot stereoselective synthesis of 4,10-disubstituted-1,7-dioxa-2-thia-3-azaspiro[4.5]dec-3-en-8-one-2,2-dioxides	120
Table 3.3	Crystal data for compound **5aa**	137
Table 3.4	Crystal data for compound **14**	138
Table 4.1	Optimization of the domino reaction	187
Table 4.2	Substrate Scope of 4,6-diarylpicolinate synthesis	190
Table 4.3	Crystal data of compound **3bd**	213
Table 5.1	Optimization of the reaction conditions	266
Table 5.2	Substrate scope of 4,6-diarylnicotinate synthesis	269
Table 5.3	Substrate scope of 4,6-diarylnicotinonitriles	272
Table 5.4	Substrate scope of 3-acetyl-4,6-diarylpyridines	273
Table 5.5	Crystal data for compound **3ai**	303
Table 6.1	Optimization of the reaction conditions	375
Table 6.2	One-pot synthesis of 2-aryl-4-styrylpyridines (**3aa-3ij**)	378
Table 6.3	Synthesis of 2,4-disubstitutedpyridines (**3am-3hs**)	380

Chapter 1

1.1 General Introduction

The design and development of a highly efficient new synthetic protocol for the access to a series of synthetically as well as biologically useful molecules from simple and easily accessible starting materials, under metal-free conditions is the central theme of contemporary organic chemistry.

In past few decades, 5-membered cyclic sulfamidate imines and their derivatives (**Figure 1.1**) have received considerable interest in chemical community because of their useful application in medicinal chemistry in addition to their traditional roles as important reactive intermediates in organic synthesis(**Figure 1.2**).[1-6]

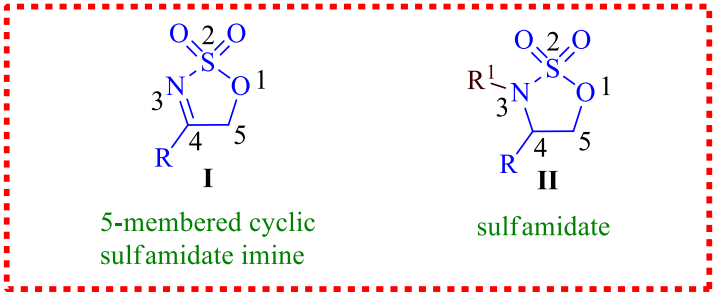


Figure 1.1 Common structures of 5-membered cyclic sulfamidate and sulfamidate imine

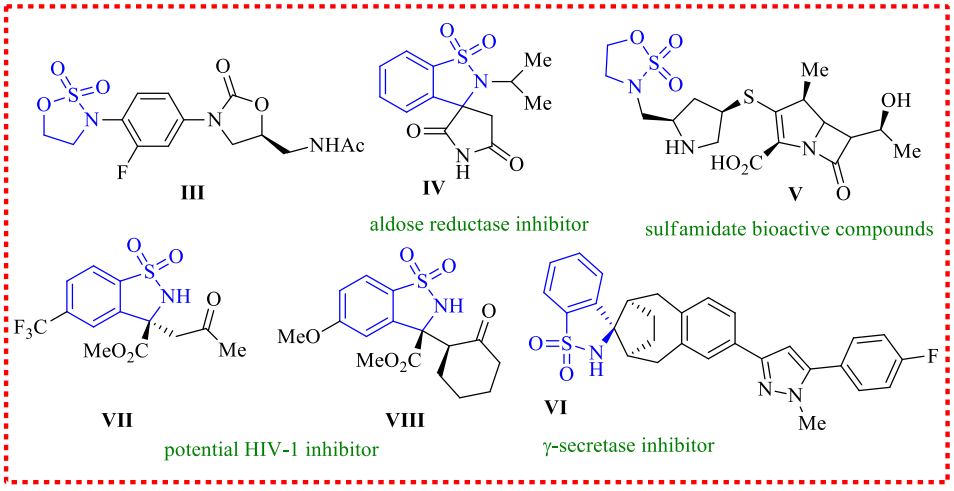


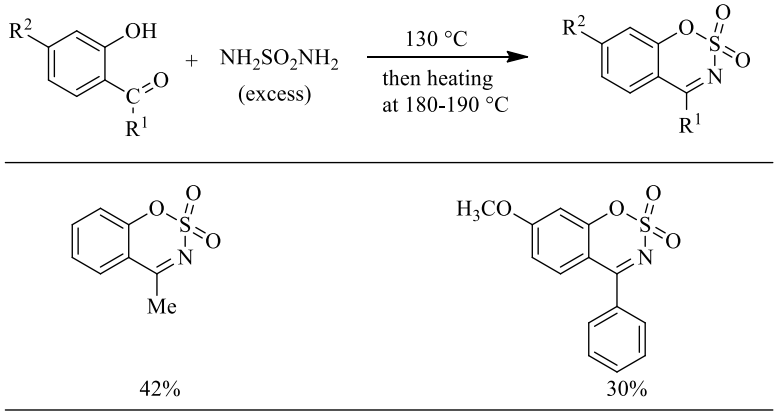
Figure 1.2 Different sulfamidate bioactive compounds

1.2 Background

Cyclic sulfamidate imines and their derivatives represent a very broad family of reagents with a variety of applications in organic synthesis. Importantly, the reduction of a prochiral C=N bond of cyclic sulfamidate imine can be easily performed by using common reducing agents to produce a synthetically attractive chiral 4,5-cyclic sulfamidate. A literature study revealed that enormous works have been carried out for the enantioselective reduction of a prochiral C=N bond of cyclic sulfamidate imines to access the optically active chiral sulfamidates catalysed by transition metal-salts through asymmetric transfer hydrogenation.[7-11] On the other hand, nucleophilic addition to imine bond of cyclic sulfamidate imines is an alternative powerful route to the synthyesis of cyclic sulfamidate with a α-tertiary amines.[12-19] Furthermore, the obtained cyclic sulfamidate can be converted into a variety of chemically and biologically important molecules by using appropriate nucleophiles like N/C/P/S/O/halides/Se-containing molecules.[20-32][37-40]

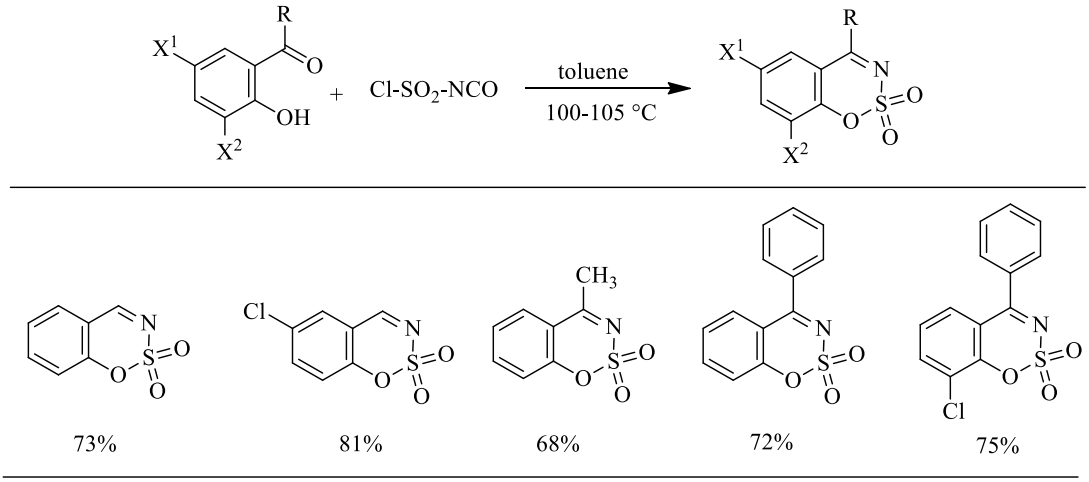
1.3 Synthesis

To the best of our knowledge, in 1965, Prof. J. B. Wright group first synthesized cyclic sulfamidate imine by the reaction of *o*-hydroxy ketones with excess sulfamide upon heating at 180-190 ºC, leading to good yield of 1,2,3-benzothiazine 2,2-dioxide as a heterocyclic system as described in **Scheme 1.1**.[33]



Scheme 1.1 Synthesis of six-membered cyclic sulfamidate imines

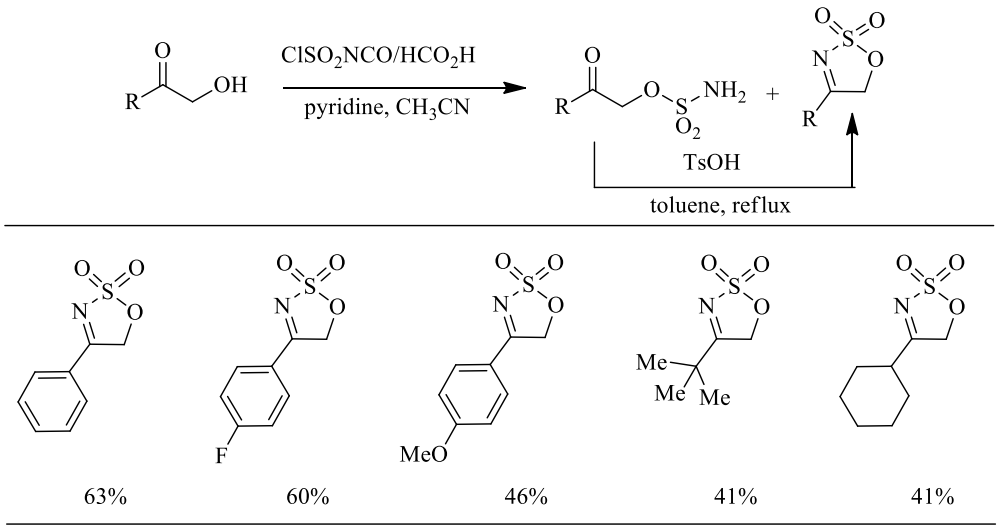
In 1981, Kamal group developed a novel reaction of chlorosulfonylisocyanate as a powerful electrophile with several substituted 2-hydroxybenzaldehydes/ 2-hydroxyacetophenones at 100-105 ºC in toluene for the synthesis of six membered cyclic sulfamidate imines in good yields (66-83%) as described in **Scheme 1.2**.[34]



Scheme 1.2 Synthesis of 1,2,3-benzoxathiazine 2,2-dioxide by using of chlorosulfonylisocyanate

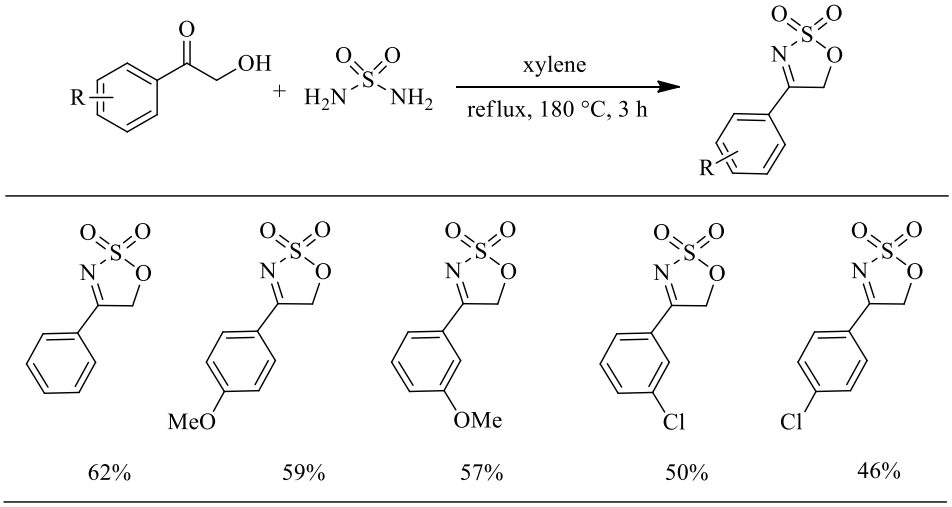
In 2000, Okada *et al.* modified the sulfamoylation reaction of a hydroxyl group and they took DMA or NMP as the best solvent for the same reaction.[35]

For the first time, in 2008, Zhou *et al.* disclosed the preparation of five membered cyclic sulfamidate imines by reacting α-hydroxy ketone and pyridine with a neat mixture of formic acid with chlorosulfonylisocyanate in acetonitrile at room temperature followed by the azeotropic removal of the crude mixture with 10 mol% of p-TSA.[8] Some of the examples are described in **Scheme 1.3**.



Scheme 1.3 Synthesis of 5-membered cyclic sulfamidate imines

To bypass the above drawbacks, α-hydroxyketones were heated with sulfuric diamide ($H_2NSO_2NH_2$) in refluxing xylene to produce oxathiazole in good yields as reported by Lee group in 2011.[9] Some of the good results are summarized in **Scheme 1.4**.



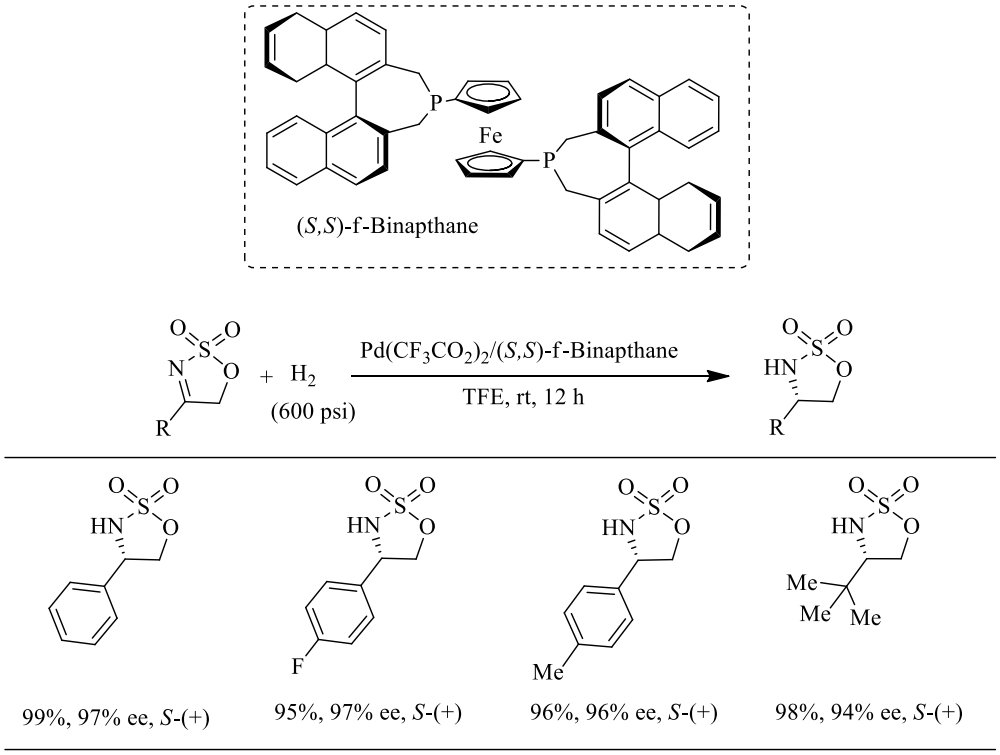
Scheme 1.4 Synthesis of cyclic sulfamidate imines using sulfuric diamide

1.4 Properties

A number of reactions have been performed by utilizying cyclic sulfamidate imines as electrophiles in a variety of novel reactions such as asymmetric hydrogenation, enantioselective alkylation/arylation reaction promoted by transition-metal-salts. Some of them are summarized in **Section 1.4.1-1.4.3**.

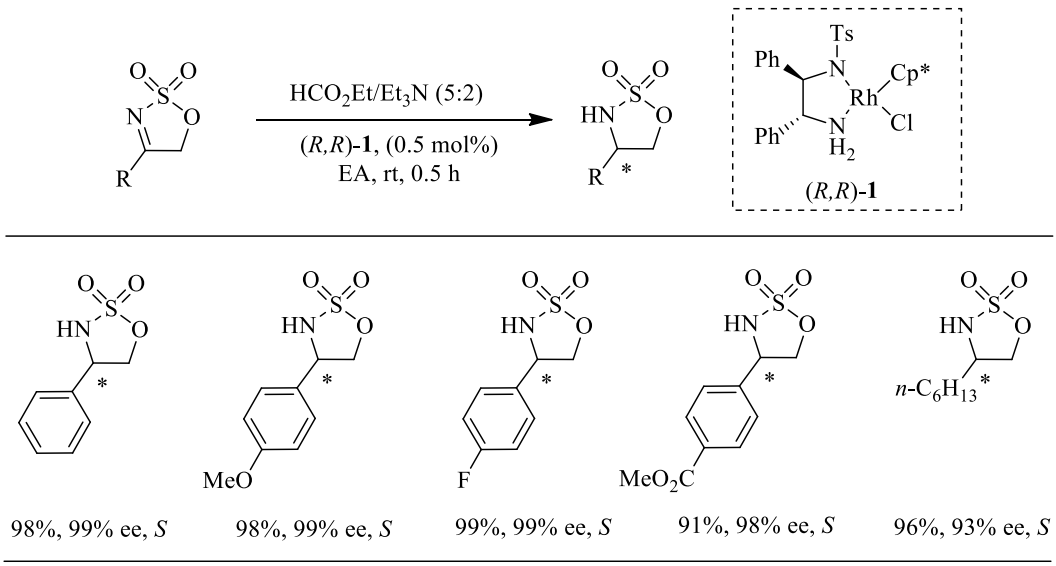
1.4.1 Asymmetric hydrogenation of C=N bond

In 2008, Zhou group has reported an asymmetric hydrogenation of cyclic imines using $Pd(CF_3CO_2)_2$/(*S*,*S*)-f-binaphane as a catalyst in 2,2,2-trifluoroethanol to efficiently synthesize cyclic sulfamidates with high enantioselectivities (upto 99% ee) as described in **Scheme 1.5**.[7]



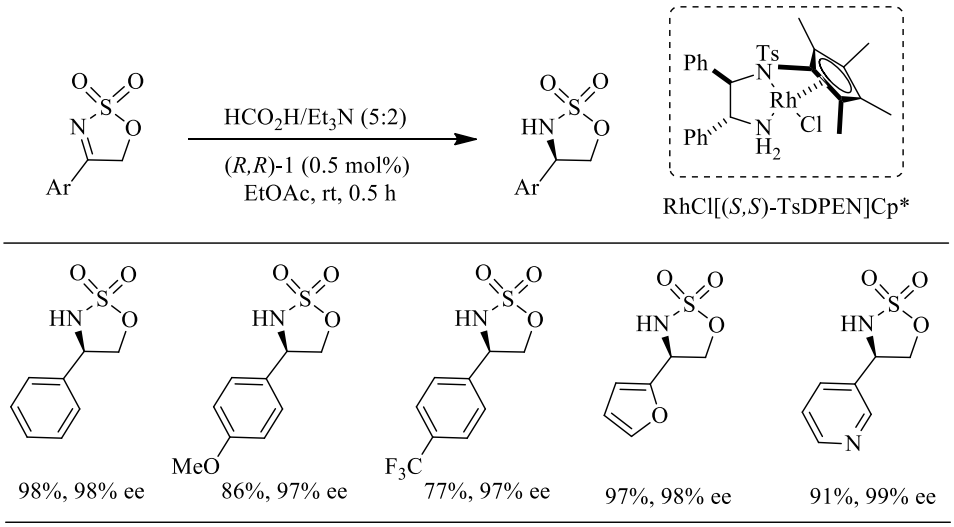
Scheme 1.5 Pd-catalyzed asymmetric hydrogenation of five membered cyclic imines

In 2010, Lee *et al.* unfolded a highly efficient and practical ATH-based procedure for the synthesis of chiral cyclic sulfamidates from the corresponding cyclic imines in presence of chiral Rh catalysts (*S*,*S*)- or (*R*,*R*)-2, Cp*RhCl(TsDPEN) (Cp* = pentamethylcyclopentadienyland (TsDPEN = (1*S*,2*S*)- or (1*R*,2*R*)-*N*-*p*-toluenesulfonyl- 1,2-diphenylethylenediamine) taking 5:2 mixture of HCO_2H and Et_3N as the hydrogen source as described in **Scheme 1.6**.[8]



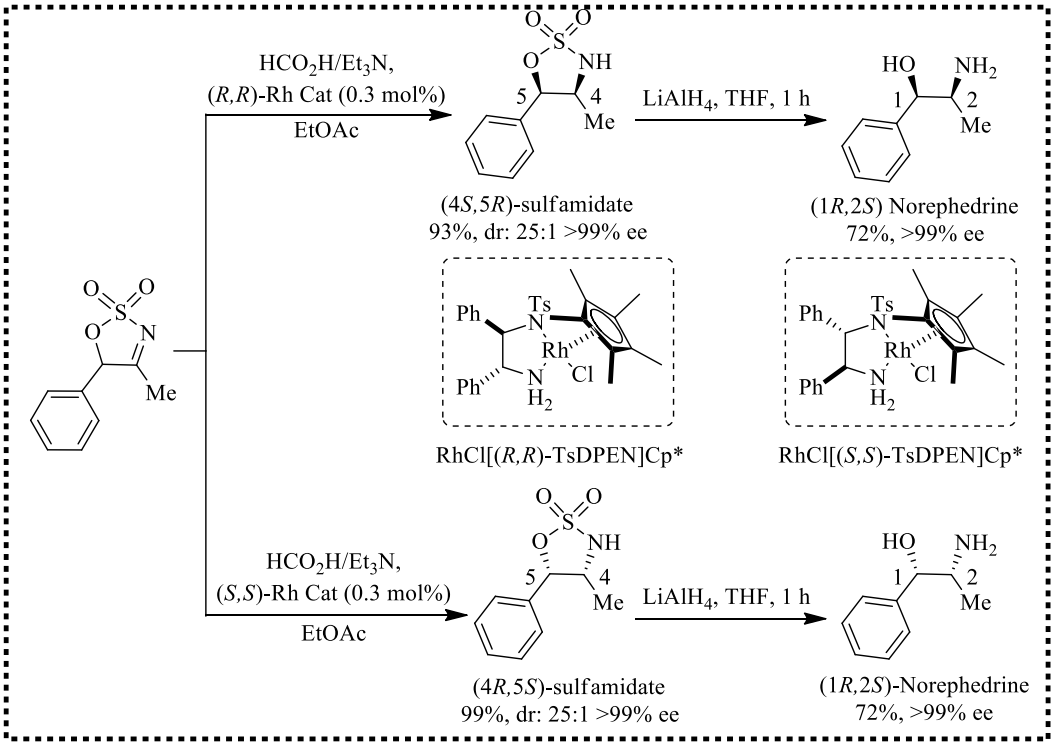
Scheme 1.6 Rh-catalyzed asymmetric hydrogen transfer of Cyclic Imines

In 2011, Lee and his co-workers successfully achieved a highly enantioselective synthesis of 4,5-cyclic sulfamidates through asymmetric transfer hydrogenation (ATH) of the corresponding cyclic sulfamidate imines using chiral Rh catalysts (*S, S*)-Cp*RhCl(TsDPEN) (TsDPEN = *N*-*p*- Ts-1,2-diphenylethylenediamine, Cp* = pentamethylcyclopentadienyl) in the presence of HCO_2H/Et_3N mixture as a well-defined hydrogen source at room temperature.[9] Some of the examples are summarized in **Scheme 1.7**.



Scheme 1.7 Rh-catalyzed transfer hydrogenation of 5*H*-[1,2,3]-oxathiazole-2,2-dioxide derivatives

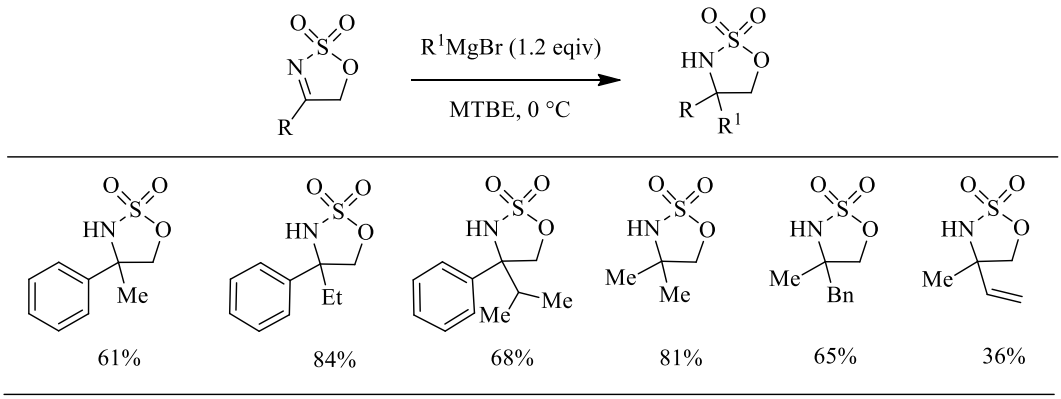
In 2011, Lee group explored cyclic sulfamidate imines in the asymmetric transfer hydrogenation reaction accompanied by dynamic kinetic resolution to afford chiral cyclic sulfamidate with high enantiomeric excess which further furnished Norephedrine as described in **Scheme 1.8**. The ATH process was catalyzed by the well-defined chiral Rh-complexes, (*S*,*S*)- or (*R*,*R*)-Cp*RhCl(TsDPEN) in the presence of HCO_2H/Et_3N as the hydrogen source under mild reaction conditions (rt,15min).[11]



Scheme 1.8 Preparation of Norephedrine form 4-methyl-5-phenyl-5*H*-1,2,3-oxathiazole-2,2-dioxide

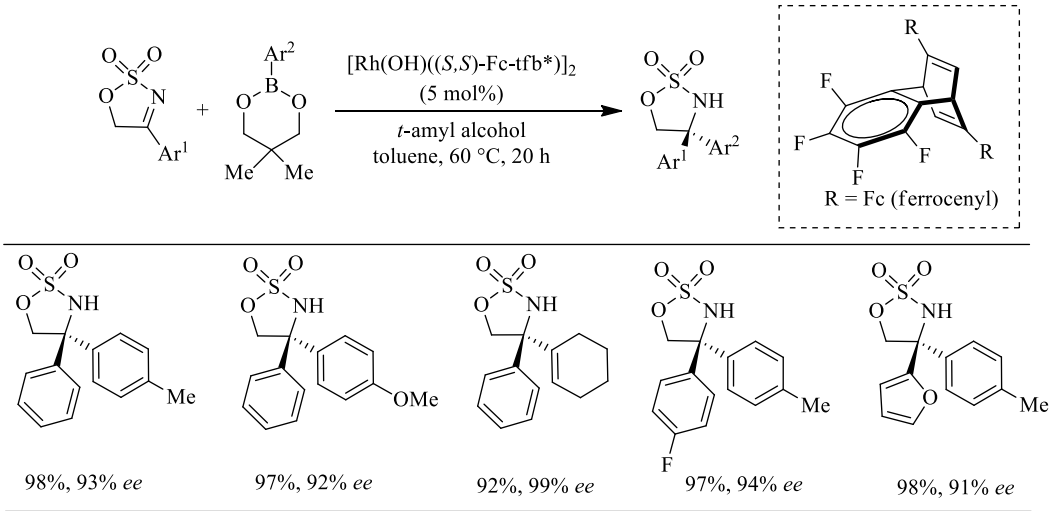
1.4.2 Enantioselective alkylation or arylation

In 2010, Lee group has demonstrated a Grignard addition of alkylmagnesium bromide to cyclic sulfamidate imines at 0 °C, affording a variety of *N*-substituted quaternary sulfamidates in high yields (upto 86%).[12] Some of the interesting results are discussed in **Scheme 1.9**.



Scheme 1.9 Grignard addition to cyclic sulfamidate imines

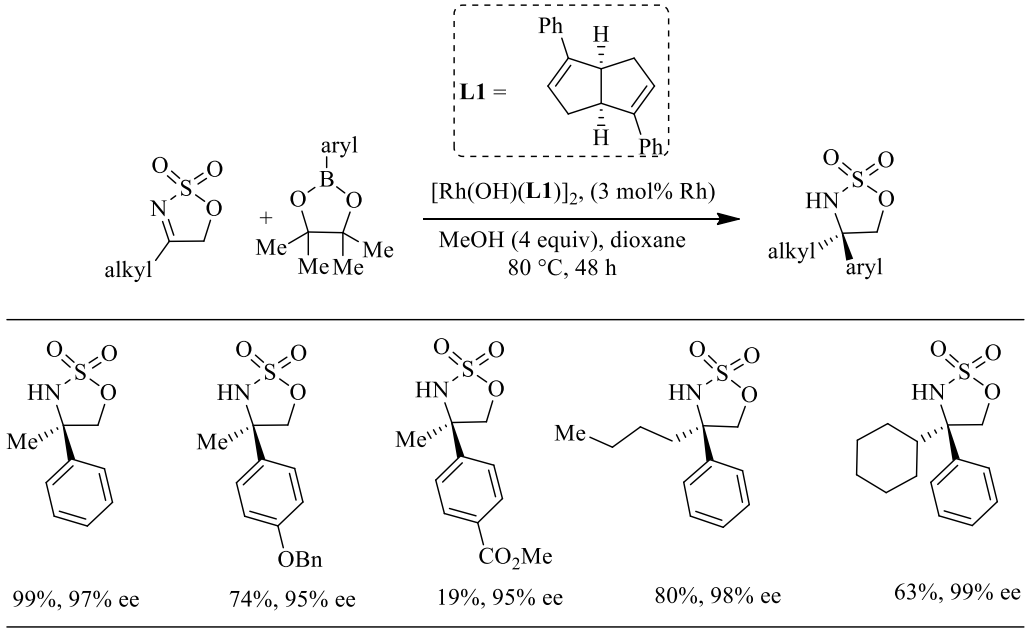
In 2013, Hayashi group revealed a new rhodium-catalyzed asymmetric addition of arylboronates to cyclic ketimines in the presence of ferrocenyl-substituted chiral tetrafluoro-benzobarrelene(tfb) (Fc-tfb*) in a solvent system of 1:1 mixture of *t*-amyl alcohol and toluene at 60 ºC to obtain corresponding sulfamidates in high yields (upto 99%) with high to excellent enantioselectivity (upto 99% ee).[13] Some of the important examples are depicted in **Scheme 1.11**.



Scheme 1.10 Rhodium-catalyzed asymmetric arylation of cyclic ketimines

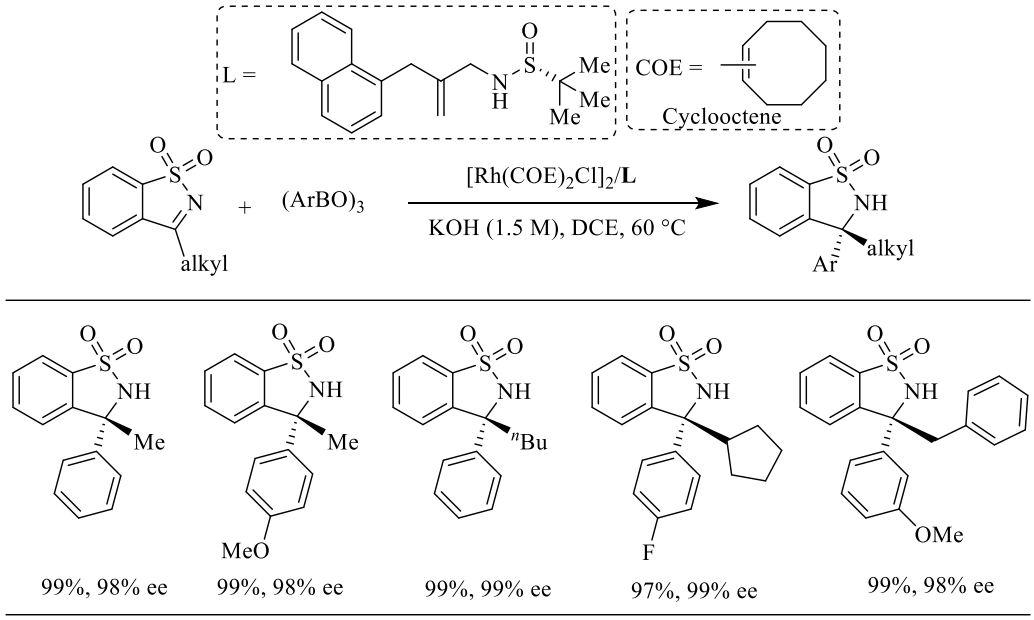
Another highly enantioselective 1,2 addition of arylboronates to cyclic *N*-sulfamidate alkylketimine taking 3 mol% of rhodium/diene complex as a catalyst and MeOH as additive in dioxane at 80 ºC to provide corresponding sulfamidates

in good to excellent yields 98% with excellent enantioselectivity (upto 99%) was established by Feng and Lin groups in 2014.[15] Some interesting examples are summarized in **Scheme 1.11**.



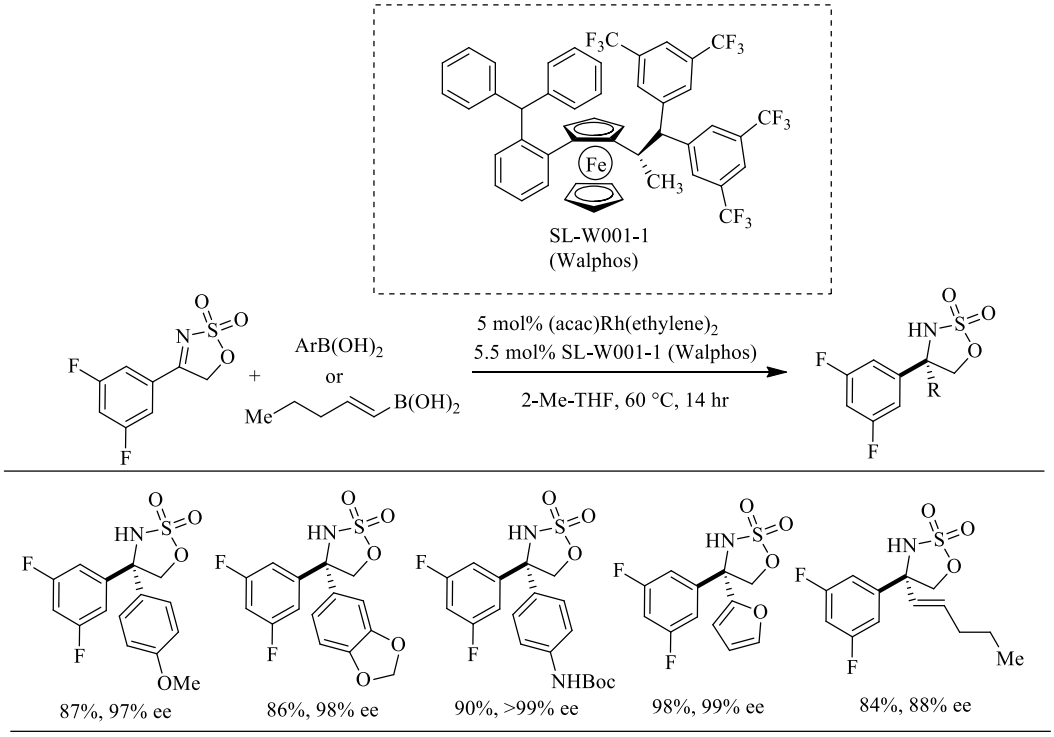
Scheme 1.11 Reaction scope for the Rhodium-catalyzed asymmetric arylation of cyclic *N*-sulfamidate imines

In 2014, Hu group achieved a highly enantioselective rhodium/sulfur olefin complex catalyzed 1,2-addition of arylboroxines/arylboronic acids to cyclic N-sulfonyl aryl alkyl ketimines in DCE at 60 ºC for the access of optically active α-arylalkylsubstituted benzosultams and benzosulfamidates in high yields (upto 99%) with good to excellent enantioselectivity (upto 99%).[16] Some of the promising results are summarized in **Scheme 1.12**.



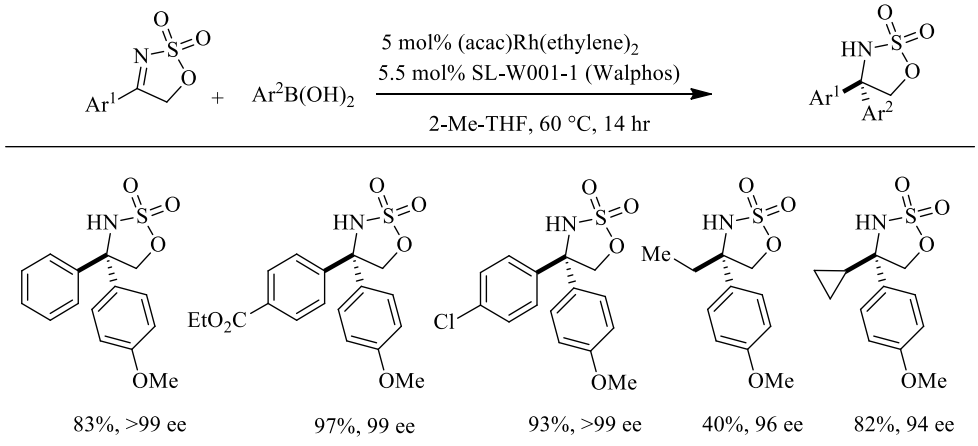
Scheme 1.12 Rhodium-catalyzed asymmetric arylation of cyclic ketimines

In addition to this work, in 2015, Mondschein *et al*. reported a method for the synthesis of chiral *α*-tertiary amines *via* Rh-catalyzed 1,2-addition of arylboronicacids to cyclic ketimines. The desired chiral *α*-tertiary amines were effectively accessed to good yields with excellent enantioselectivities using a commercially available chiral ligand SL-W001-1 (Walphos). The reactions gave best result when they used 2 equivalents of arylboronic acids, 5 mol% Rh salt, 5.5 mol% ligand in presence of 2Me-THF at 60ºC. First they have studied the scope of the reaction using 3,5-difluorophenylketimine with different arylboronic acids (**Scheme 1.13**).*[18]*



Scheme 1.13 Reactions of 3,5-difluorophenylketimine with different arylboronic acids

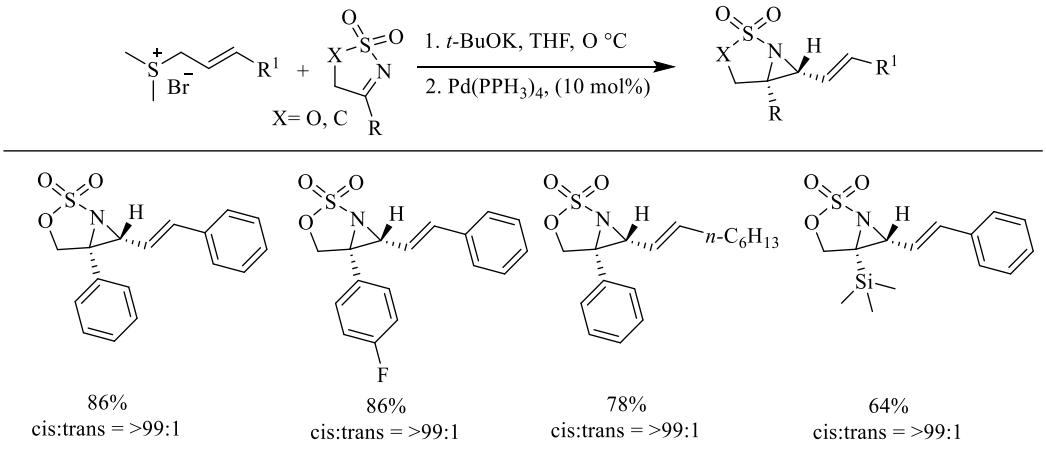
Furthermore, for the enrichment of the generality of the reported reaction they studied the scope of cyclic ketimine substrates against several arylboronic acids. The total reaction scope includes vinyl, aryl, and heteroarylboronic acids with good to excellent yield (40-99%) and excellent enantiomeric excess (88-99% *ee*) (**Scheme 1.14**).



Scheme 1.14 Reactions of different cyclic ketimines with arylboronic acids

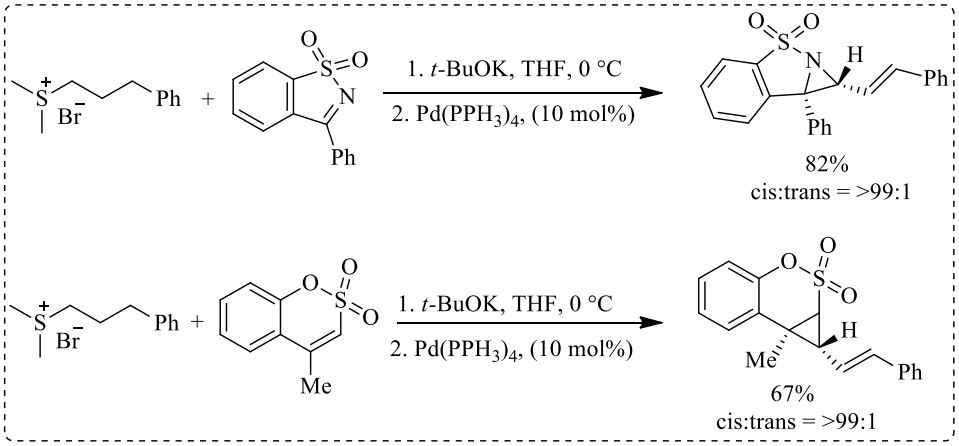
1.4.3 Aziridination

In 2010, Tang group unfolded a highly diastereoselective synthesis of *cis*-vinylaziridines containing a quaternary cabon center *via* sulfurylide-mediated aziridination of cyclic ketimines followed by Pd(0)-catalyzed isomerization. The reactions of sulfur ylide and ketimines underwent in presence of 10 mol% of *t*-BuOK as base in THF.[36] For the isomerization step, 10 mol% loading of $Pd(PPh_3)_4$ was optimum. The optimal condition was not only applicable for various aryl substituents with different electronic and steric characteristics but alkyl substituents also reacted well with excellent diastereoselectivity in moderate to good yields. These reactions provided an easy access to *cis*-trisubstitutedvinylaziridines as describes in **Scheme 1.15**.



Scheme 1.15 Stereoselective aziridination of cyclic imines

In addition to the five membered ketimines, they have investigated about the reactivity of some benzo-fused five and six membered ketimines under identical conditions. Also, in all these cases, the reactions performed well with the satisfactory outcomes (**Scheme 1.16**)



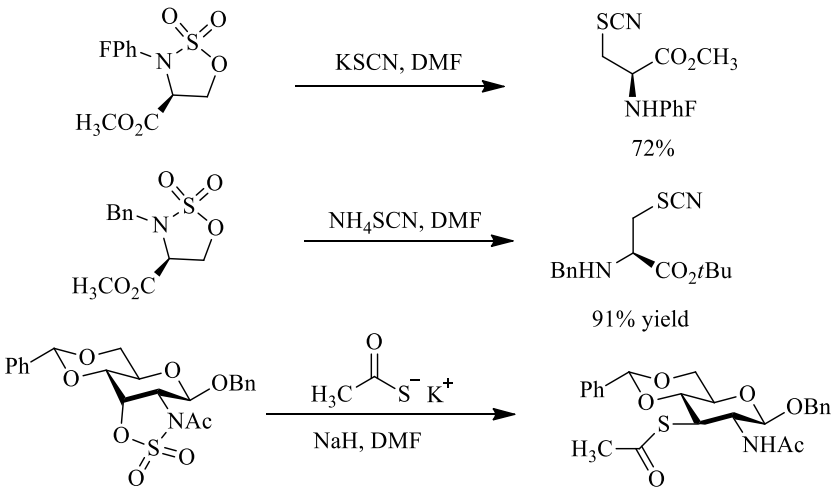
Scheme 1.16 Stereoselective aziridination of benzofusedcyclic imines

1.5 Synthetic application of cyclic sulfamidates through nucleophilic ring-opening reaction

Cyclic Sulfamidates are also very interesting molecules which undergo ring-opening reactions in the presence of a variety of suitable nucleophiles (S, O, N, C, halide, P, Se) to produce a novel class of corresponding chiral amino products.

Sulfur nucleophiles:

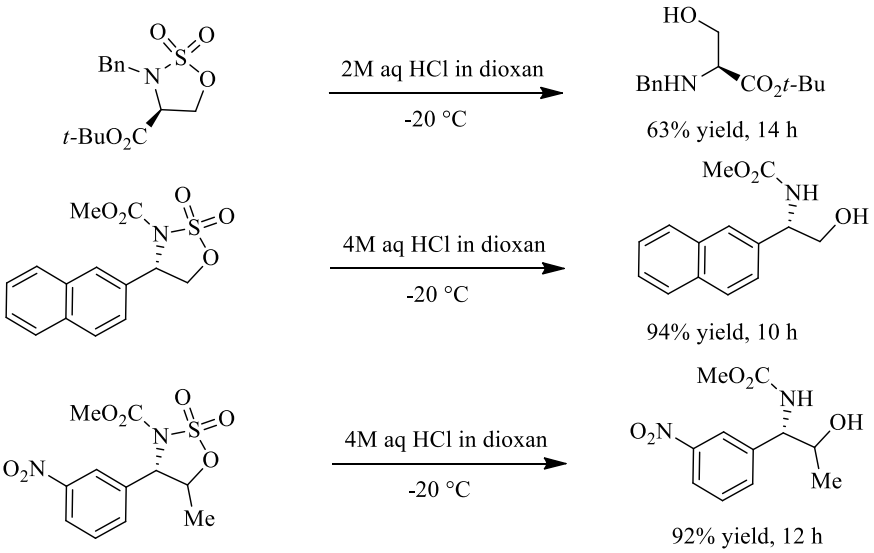
Treatment of sulfamidates with thiocyanate ion in DMF at room temperature gave S-cyanocysteines with 68-91% yields. D-allosamine-derived sulfamidate reacted with thioacetate ion in DMF at room temperature to provide thioester in 82% yield.[20-24] All the reactions are summarized in **Scheme 1.17**.



Scheme 1.17 Reaction of sulfamidate with thiocyanate and thioacetates

Oxygen nucleophiles:

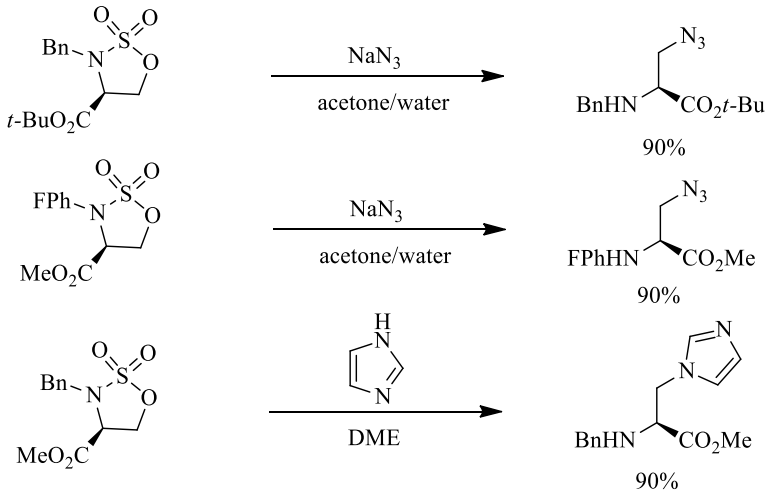
Hydrolysis of N-benzyl protected sulfamidate with 4 M HCl in dioxane produced corresponding N-benzyl protected β-amino alcohol. In the same condition,*N*-(alkyloxycarbonyl)sulfamidates was hydrolyzed to produce corresponding β-aryl-β-carbamato-alcohols with good yield (≥ 90%)(**Scheme 1.18**).[20,24-26]



Scheme 1.18 Synthesis of β-N-protected amino alcohols

Nitrogen nucleophiles:

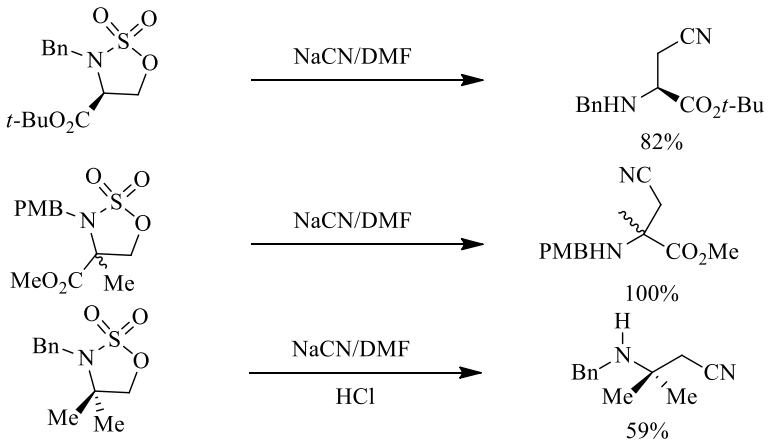
Azide, pyrazole or imidazole can effectively attack at C-5 position of cyclic sulfamidates to provide corresponding β-amino analogues in high yields at room temperature upon heating (60-80 ºC).[20,21,24,27] All the reactions are summarized in **Scheme 1.19**.



Scheme 1.19 Opening of cyclic sulfamidates using nitrogen electrophiles

Carbon nucleophiles:

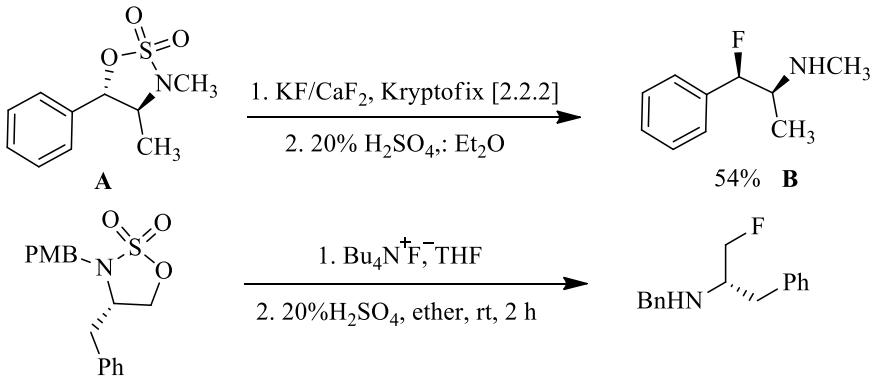
A very efficient well-known carbon nucleophile is cyanide ion (NaCN), which reacted with cyclic sulfamidates in DMF at room temperature to afford the corresponding nitrile counterparts in good yields (82-100%) as discussed in **Scheme 1.20**.[20,24,28,29]



Scheme 1.20 Opening of cyclic sulfamidates using NaCN

Halogen atom as a nucleophile:

Fluoride ion can act as a nucleophile for the ring-opening of five membered cyclic sulfamidates to get a variety of β-amino fluorides by using 1:4 KF/CaF_2 or tetrabutylammonium fluoride.[30-32] Some of the important reactions are summarized in **Scheme 1.21**.

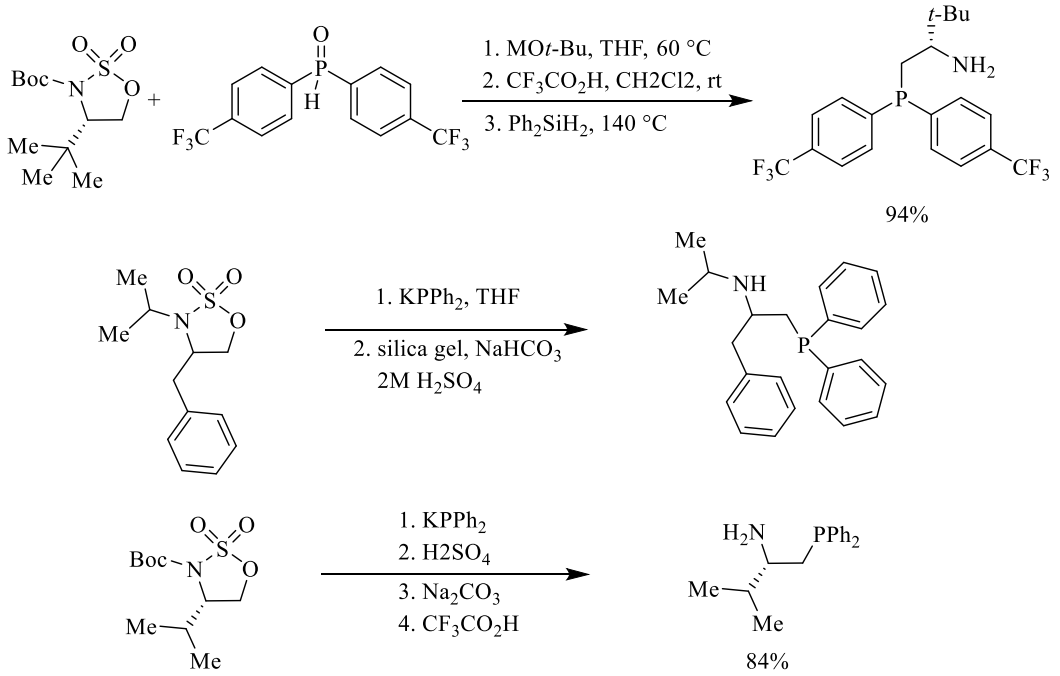


Scheme 1.21 Ring opening of cyclic sulfamidate with halide

Phosphorous nucleophile:

Ring-opening of N-protected cyclic sulfamidates with appropriate phosphorous nucleophile is an efficient alternative route for the synthesis of chiral aminophosphines. Metal phosphides like Potassium diphenylphosphide ($KPPh_2$)

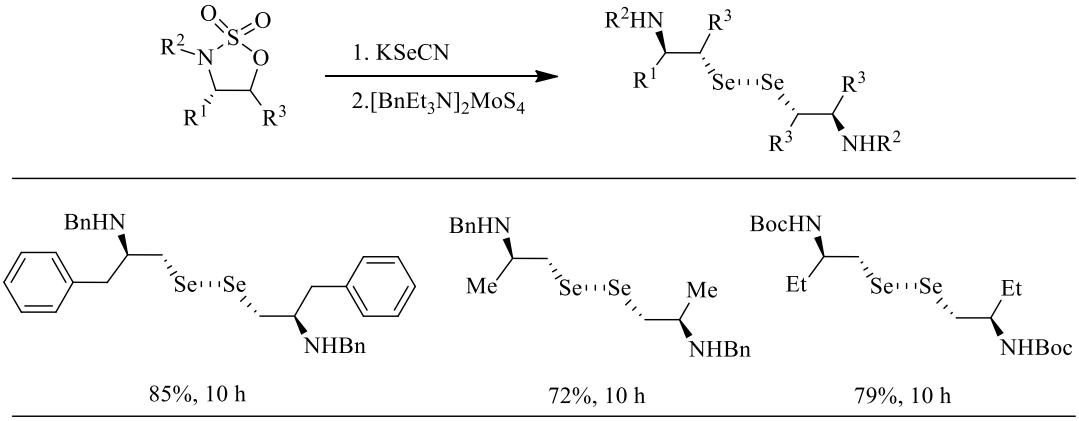
or metal diarylphosphinites are commonly used as phosphorous nucleophiles as discussed in **Scheme 1.22**.[37-39]



Scheme 1.22 Ring opening of cyclic sulfamidate with phosphorous nucleophile

Selenium nucleophile:

In 2010, Chandrasekaran *et al.* synthesized *N*-alkyl-β-aminodiselenides derivatives in high yield by reacting sulfamidates with potassium selenocyanate and benzyltriethylammoniumtetrathiomolybdate ($[BnNEt_3]_2MoS_4$) *via* a sequential one-pot multicomponent reaction. A few representative examples are summarized in **Scheme 1.23**.[40]



Scheme 1.23 Ring opening of cyclic sulfamidate with selenium nucleophile

1.6 Conclusion

A systematic perusal of literature survey reveals that enormous works have been documented for the syntheses of cyclic sulfamidate imines and their derivatives which mainly focused on transition metal-catalyzed asymmetric transfer hydrogenation or nucleophilic attack on prochiral C=N bond. However, there is no successful report in the literature for the direct functionalization on cyclic sulfamidate imine at its C-5 position due to lack of synthetic method available. Moreover, we surprised that 5-membered cyclic sulfamidate imine as a nucleophile has highly overlooked. Therefore, it is a meaningful idea to explore cyclic sulfamidate imine as a nucleophile in a variety of reactions under metal-free conditions to provide aforesaid compounds as well as other interesting biologically active compounds.

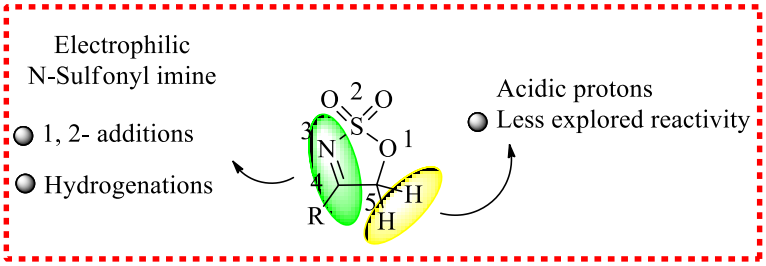


Figure 1.3 Reactivity profile of 5*H*-1,2,3-oxathiazole-2,2-dioxides

1.7 References

1. Meléndez R. E., Lubell W. D. (2003), Synthesis and reactivity of cyclic sulfamidites and sulfamidates, *Tetrahedron*, 59, 2581-2616 (DOI: 10.1016/S0040-4020(03)00284-9)
2. Nicolaou K. C., Snyder S. A., Longbottom D. A., Nalbandian A. Z., Huang X. (2004), New uses for the Burgess reagent in chemical synthesis: Methods for the facile and stereoselective formation of sulfamidates, glycosylamines and sulfamides, *Chem.-Eur. J.*, 10, 5581-5606 (DOI: 10.1002/chem.200400503)
3. Nicolaou K. C., Huang X., Snyder S.A., Rao P. B., Bella M., Reddy M. V., (2002), A novel regio- and stereoselective synthesis of sulfamidates from 1,2-diols using Burgess and related reagents: a facile entry into β -amino alcohols, *Angew. Chem. Int. Ed.*, 41, 834-838 (DOI: 10.1002/1521-3773(20020301)41:5<834::AID-ANIE834>3.0.CO;2-V)
4. Bower J. F., Sÿvenda J, Williams A.J., Charmant J. P. H., Lawrence R. M., Szeto P., Gallagher T. (2004), Cyclic sulfamidates as vehicles for the synthesis of substituted lactams, *Org. Lett.*, 6, 4727-4730 (DOI: 10.1021/ol048036+)
5. Galaud F., Lubell D.W. (2005), Homoserine-derived cyclic sulfamidate as chiral educt for the diversity-oriented synthesis of lactam-bridged dipeptides, *Biopolymers (Peptide Science)*, 80, 665-674 (DOI: 10.1002/bip.20223)
6. Bower F. J., Szeto P.,and Gallagher T. (2007), Enantiopure 1,4-benzoxazines via 1,2-cyclic sulfamidates. synthesis of Levofloxacin, *Org. Lett.*, 9, 3283-3286 (DOI: 10.1021/ol0712475)
7. Wang Y. -Q., Yu C. -B., Wang D. -W., Wang X. -B., Zhou Y. -G. (2008), Enantioselective synthesis of cyclic sulfamidates via Pd-catalyzed hydrogenation, *Org. Lett.*, 10, 2071-2074 (DOI: 10.1021/ol800591u)
8. Kang S., Han J., Lee E.S., Choi E.B., Lee -K. H. (2010), Enantioselective synthesis of cyclic sulfamidates by using chiral rhodium-catalyzed

asymmetric transfer hydrogenation, *Org. Lett.*, 12, 4184-4187 (DOI: 10.1021/ol1017905)

9. Lee S. A., Kwak S.H., Lee K. -I. (2011), Highly enantioselective synthesis of cyclic sulfamidates and sulfamides via rhodium-catalyzed transfer hydrogenation, *Chem. Commun.*, 47, 2372-2374 (DOI:10.1039/C0CC04166A)
10. Han J., Kangab S., Lee K. -I, (2011), Dynamic kinetic resolution in the stereoselective synthesis of 4,5-diaryl cyclic sulfamidates by using chiral rhodium-catalyzed asymmetric transfer hydrogenation, *Chem. Commun.*, 47, 4004 (DOI: 10.1039/c0cc05289b)
11. Lee -K. H., Kang S., Choi E. B. (2012) Stereoselective synthesis of Norephedrine and Norpseudoephedrine by using asymmetric transfer hydrogenation accompanied by dynamic kinetic resolution, *J. Org. Chem*., 77 , 5454-5460 (DOI: 10.1021/jo300867y)
12. Chang S., Lee E. E. (2010), Grignard additions to cyclic sulfamidate imines: synthesis of N-substituted quaternary sulfamidate building blocks, *Synthesis* 14, 2361-2366 (DOI: 10.1055/s-0029-1218778)
13. Nishimura T., Ebe Y., Fujimotoa H., Hayashi T. (2013), Asymmetric synthesis of gem-diaryl substituted cyclic sulfamidates and sulfamides by rhodium-catalyzed arylation of cyclic ketimines, *Chem. Commun.*, 49, 5504-5506 (DOI:10.1039/C3CC42071J)
14. Chen Y. -J., Chen Y. -H., Feng C. -G., Lin G. -Q. (2014) Enantioselective rhodium-catalyzed arylation of cyclic N-sulfamidate alkylketimines: a new access to chiral β-alkyl-β-aryl amino alcohols, *Org. Lett.*, 16 3400-3403 (DOI: 10.1021/ol501464e)
15. Chen Y. -J., Chen Y. -H., Chen-Guo Feng C. -G., Lin G. -Q. (2014) Enantioselective rhodium-catalyzed arylation of cyclic N-sulfamidate alkylketimines: a new access to chiral β-alkyl-β-aryl amino alcohols, *Org. Lett.*, 16, 3400-3403 (DOI: 10.1021/ol501464e)
16. Jiang T., Wang Z., Xu M. -H. (2015) Rhodium-catalyzed asymmetric arylation of cyclic N-sulfonyl aryl alkyl ketimines: efficient access to

highly enantioenriched α-tertiary amines, *Org. Lett.*, 17, 528-531 (DOI: 10.1021/ol503537w)

17. Arigala P., Sadu V. S., Hwang I. -T., Hwang J. -S., Kim C. -U., Lee K. -I. (2015) Copper-catalyzed regio- and stereoselective ring-opening of cyclic sulfamidates with grignard reagents assisted by lithium chloride, *Adv. Synth. Catal.*, 357, 2027-2032 (DOI: 10.1002/adsc.201400850)
18. Kong J., McLaughlin M., Belyk K., Mondschein R. (2015) Enantioselective Rh(I)-catalyzed addition of arylboronic acids to cyclic ketimines, *Org. Lett.*, 17, 5520-5523 (DOI: 10.1021/acs.orglett.5b02032)
19. Zhang Y. -F, Chen D., Wen-Wen Chen W. -W., Xu M. -H. (2016) Construction of cyclic sulfamidates bearing two gem-diaryl stereocenters through a Rhodium-catalyzed stepwise asymmetric arylation protocol, *Org. Lett.*, 18, 2726-2729 (DOI: 10.1021/acs.orglett.6b01183)
20. Baldwin J. E, Spivey A. C., Schofield C. J. (1990) Cyclic sulphamidates: New synthetic precursors for β-functionalised α-amino acids, *Tetrahedron: Asymmetry*, 1, 881-884 (DOI: 10.1016/S0957-4166(00)82279-X)
21. Wei L., Lubell W. D.(2001) Scope and limitations in the use of N-(PhF)serine-derived cyclic sulfamidates for amino acid synthesis, *Can. J. Chem.*, 79, 94-100 (DOI: 10.1139/v00-176)
22. Aguilera B., Ferna´ndez-Mayoralas A. (1996), Nucleophilic displacements on a cyclic sulfamidate derived from allosamine: application to the synthesis of thiooligosaccharides, *Chem. Commun.* 1996, 127-128 (DOI: 10.1039/CC9960000127)
23. Aguilera B., Fernández-Mayoralas A., Jaramillo C. (1997), Use of cyclic sulfamidates derived from D-allosamine in nucleophilic displacements: Scope and limitations, *Tetrahedron*, 53, 5863-5876 (DOI: 10.1016/S0040-4020(97)00246-9)
24. Boulton L. T., Stock H. T., Raphy J., Horwell D. C. (1999) Generation of unnatural α,α-disubstituted amino acid derivatives from cyclic

sulfamidates, *J. Chem. Soc., Perkin Trans.1*, 1421-1430 (DOI: 10.1039/A901667H)

25. Nicolaou K. C., Huang X., Snyder S. A., Rao P. B., Bella M., Reddy M. V. (2002), A novel regio- and stereoselective synthesis of sulfamidates from 1,2-diols using burgess and related reagents: A facile entry into β-amino alcohols, *Angew. Chem. Int. Ed.*, 41, 834-838 (DOI: 10.1002/1521-3773(20020301)41:5<834).
26. Andersen K. K., Kociolek M. G. (1995), Acidity of cyclic sulfamates: Study of substituted 1,2,3-benzoxathiazole 2,2-dioxides and theoretical investigation of the effect of conformation on acidity, *J. Org. Chem.*, 60, 2003-2007 (DOI: 10.1021/jo00112a022).
27. Kim B. M., So S. M. (1998), Efficient hydrolysis of β-aminosulfamic acids using a Lewis acid and a thiol for the synthesis of 2,3-diaminopropanoate derivatives, *Tetrahedron Lett.*, 39, 5381-5384 (DOI: 10.1016/S0040-4039(98)01079-X).
28. White G. J., Garst M. E. (1991), Cyclic sulfamate from N-substituted 2-amino-3-phenyl-1-propanol and its nucleophilic reactions, *J. Org. Chem.*, 56, 3177-3178 (DOI: 10.1021/jo00009a045).
29. Posakony J. J., Tewson T. J. (2002), Substitution reactions of hindered cyclic sulfamidates, *Synthesis*, 7, 859-864 (DOI: 10.1055/s-2002-28509).
30. Posakony J. J., Tewson T. J. (2002), Fluoroamines via chiral cyclic sulfamidates, *Synthesis*, 2002, 766-770 (DOI: 10.1055/s-2002-25766).
31. Ok D., Fisher M. H., Wyvratt M. J., Meinke P. T. (1999) Improved syntheses of fluorinated tertiary butylamines, *Tetrahedron Lett.*, 40, 3831-3834 (DOI: 10.1016/S0040-4039(99)00633-4)
32. Van Dort M. E., Jung Y.-W., Sherman P. S., Kilbourn M. R., Wieland D. M. (1995), Fluorine for hydroxy substitution in biogenic amines: Asymmetric synthesis and biological evaluation of fluorine-18-labeled .beta.-fluorophenylalkylamines as model systems, *J. Med. Chem.*, 38, 810-815 (DOI: 10.1021/jm00005a008).

33. John B. Wright, (1965), The synthesis of 2,1,3-benzothiadiazine 2,2-dioxides and 1,2,3-benzoxathiazine 2,2-dioxides, *J. Org. Chem*., 30, 3960-3962 (DOI: 10.1021/jo01022a521)
34. Kamal A., Sattur P. B., (1981), A Facile synthesis of 1,2,3-benzoxathiazine 2,2-dioxides, *Synthesis*, 4, 272-273 (DOI: 10.1055/s-1981-29410)
35. Okada M., Iwashita S., Koizumi N. (2000), Efficient general method for sulfamoylation of a hydroxyl group, *Tetrahedron Letters*, 41, 7047-7051 (DOI: 10.1016/S0040-4039(00)01130-8)
36. Zhu B. -H., Zheng J. -C., Yu C. -B, Sun X. -L., Zhou Y. -G., Shen Q., Tang Y. (2010), One-pot highly diastereoselective synthesis of cis-vinylaziridines via the sulfur ylide-mediated aziridination and palladium(0)-catalyzed isomerization, *Org. Lett*., 12, 504-507 (DOI: 10.1021/ol9027072)
37. Rönnholm P., Södergren M., Hilmersson G. (2007), Improved and efficient synthesis of chiral N,P-ligands via cyclic sulfamidates for asymmetric addition of butyllithium to benzaldehyde, *Org. Lett*., 9 , 3781-3783 (DOI: 10.1021/ol701504c)
38. Guo R., Lu S., Chen X., Tsang C. -W, Jia W., Sui-Seng C., Amoroso D., Abdur-Rashid K. (2010), Synthesis of chiral aminophosphines from chiral aminoalcohols *via* cyclic sulfamidates, *J. Org. Chem*., 75, 937-940 (DOI: 10.1021/jo902302c)
39. Su H. Y., Song Y., Taylor M. S. (2016), A versatile synthesis of chiral β-aminophosphines, *Org. Biomol. Chem*., 14, 5665-5672 (DOI: 10.1039/c5ob02439k)
40. Baig N., Baig R., Chandrakala R. N., Sudhir V. S., Chandrasekaran S. (2010), Synthesis of unnatural selenocystines and β-aminodiselenides *via* regioselective ring-opening of sulfamidates using a sequential, one-pot, multistep strategy, *J. Org. Chem.*, 75, 2910-2921 (DOI: 10.1021/jo1001388)

Chapter 2

L-Proline catalyzed highly efficient synthesis of *Z*-5-alkylidene cyclic sulfamidate imines: an easy access to 5-alkyl-substituted cyclic sulfamidate imines

2.1 Introduction

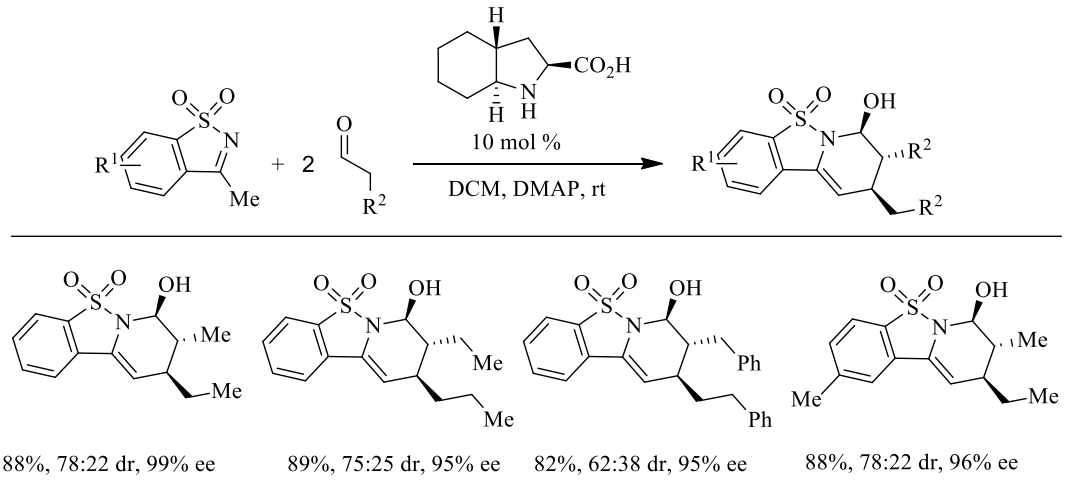
The synthesis of five-membered cyclic sulfamidate imines and their derivatives have been rapidly growing interest in recent years, because of their applications as important reactive intermediates and in medicinal chemistry as discussed profoundly in **Section 1.1**. Over the intervening years, a number of methods have been developed for the synthesis of 5-membered cyclic sulfamidate imines.

Recent progress on the synthesis of 5-membered cyclic sulfamidate imines and their applications are described in **Section 1.3-1.4**.

2.2 Review of literature

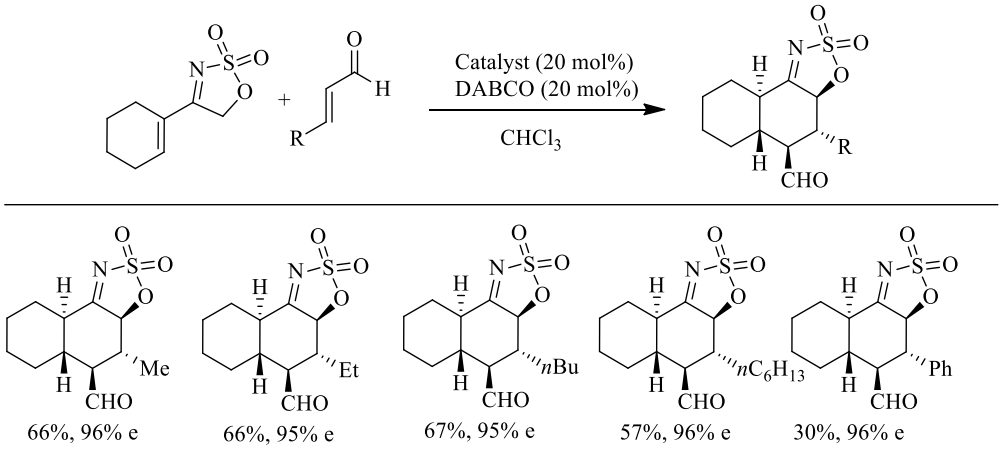
A few methods are available for the synthesis 5-membered cyclic sulfamidate imines as described in **Section 1.3**.[1-5] Most of the reports found in the literatures regarding the synthetic application of five membered cyclic sulfamidate imines have exclusively focused on the reactivity of the prochiral C=N bond.[4-10] In addition, recently very few reports have been published taking sulfamidate imine as a nucleophile.

In 2014, Zhang group developed an asymmetric pseudo three component domino reaction utilizing readily available cyclic *N*-sulfonylimines and simple aldehydes in the presence of *trans*-perhydroindolic acid as an efficient organocatalyst for the preparation of piperidine derivatives consisting of three contiguous stereocenters in excellent yields with good diastereoselectivity and excellent enantioselectivity (up to 89% yield, 80:20 dr, and 99% ee) as shown in **Scheme 2.1**.[11]



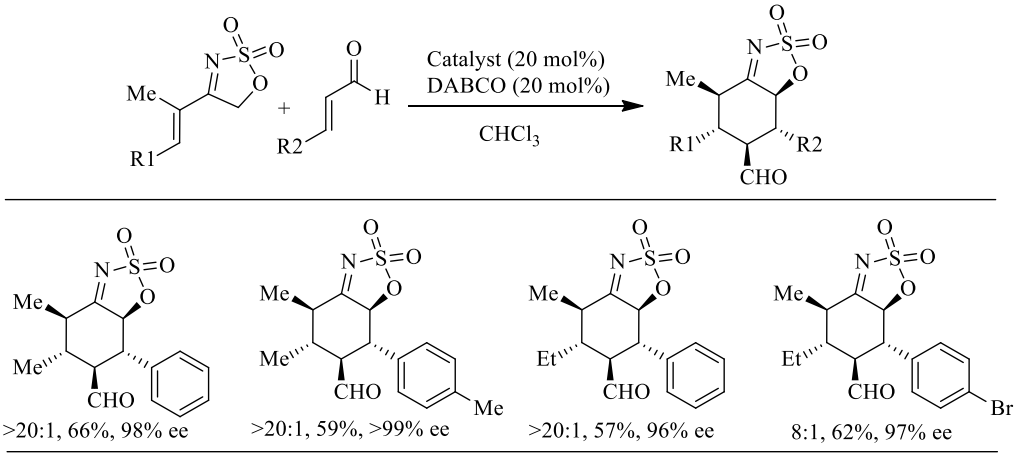
Scheme 2.1 Domino reaction between cyclic *N*-sulfonylimines and simple aldehydes

In 2015, Vicario group had used the concept of the reactivity of C-5 acidic proton by performing [4 + 2] cycloaddition reaction of *in situ* generated electron-rich diene intermediate from 4-alkenyl-5*H*-1,2,3-oxathiazole 2,2-dioxides with α,β-unsaturated aldehydes through the iminium/enamine activation mechanism. The reaction proceeds in presence of 20 mol% *O*-TMS diphenylprolinol as catalyst and 20 mol% of Brønsted base DABCO as co-catalyst to produce highly substituted cyclohexene adduct with five contiguous stereogenic centres (**Scheme 2.2**).[12]



Scheme 2.2 Cycloaddition reaction between 4-cyclohexenyl cyclic sulfamidate imines and α,β-unsaturated aldehydes

Furthermore, they surveyed the performance of their reported procedure by taking more conformationally flexible cyclic sulfamidate imines and acrolein derivatives. All of these reactions ended up in good to high yields with excellent enantio-and high diastereo-slectivites (**Scheme 2.3**).



Scheme 2.3 Cycloaddition reaction between 4-alkenyl cyclic sulfamidate imines and α,β-unsaturated aldehydes

2.2.1 Conclusion

From all the review works, it is clear that five membered cyclic sulfamidate imines are very important in terms of both synthetically as well as pharmaceutically and there are a numbers of procedures available for their synthesis and their applications. Surprisingly, even with considerable progress, there is no successful report to directly functionalize the 5-position of five membered cyclic sulfamidate imines. So it is an open challenge to directly functionalize C-5position of our titled compound.

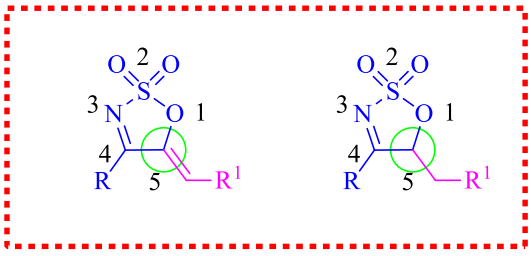
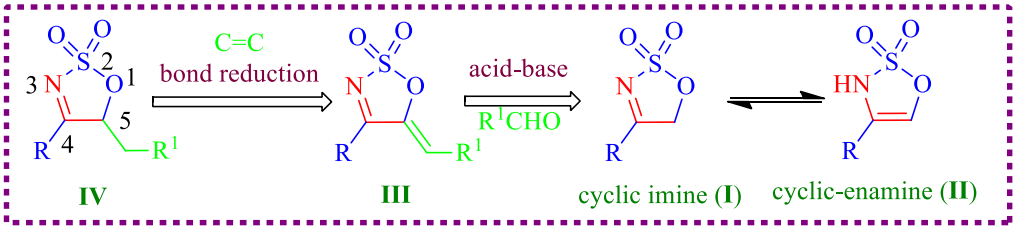


Figure 2.1 5-Alkylidine/alkyl substituted cyclic sulfamidate imine

2.3 Present work

From review work, we have seen that five-membered cyclic sulfamidate imines are useful precursors for the synthesis of a variety of organic molecules. Owing to their great synthetic importance, several methods have been developed for the synthesis of 5-membered cyclic sulfamidate imines. Even with such a progress, the synthesis of 5-alkyl-substituted cyclic sulfamidate imines is still less explored due to poor synthetic method available in the literature. Thus, it will be an interesting idea to functionalize the five membered cyclic sulfamidate imine directly at C-5 position in order to explore the more chemistry. Therefore, we are interested to synthesize the 5-alkylidene/alkyl-substituted cyclic sulfamidate imines in a more practical and efficient manner.

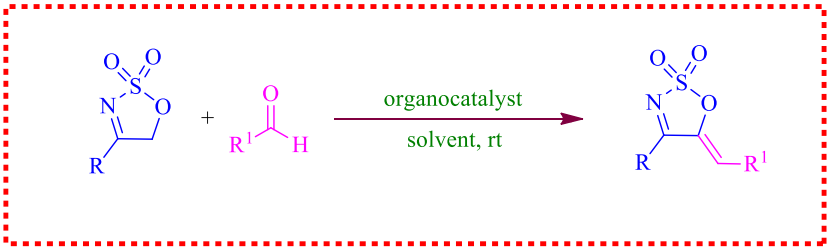
The retro-synthetic path (**Scheme 2.13**) illustrates that the active methylene protons of cyclic sulfamidate imine (**I**) is in equilibrium form of cyclic enamine (**II**) which may be efficiently involved in the condensation reaction with aldehyde in the presence of catalytic amount of a mild acids and bases to access the compound **III**.



Scheme 2.4 Retrosynthetic part for the functionalization of 5-position of cyclic sulfamidate imine

In recent years, naturally available, inexpensive L-proline has emerged as a potent bi-functional (acid-base) organocatalyst for various organic transformations.[13-19] As a part of our continued interest towards the development of organocatalytic mediated new synthetic transformations in an environment friendly manner, we wish to report a clean, organocatalytic, mild and highly efficient synthesis of *Z*-5-

alkylidene cyclic sulfamidate imines through a condensation reaction of 4-aryl-5*H*-1,2,3-oxathiazole-2,2-dioxides with enolizable/non-enolizable aldehydes using L-proline as the catalyst (**Scheme 2.5**).



Scheme 2.5 Condensation reaction between 5-membered cyclic sulfamidate imine and aldehydes

2.3.1 Results and discussions

2.3.1.1 Screening of solvents and catalysts

To find out the best conditions, we initiated the optimization reaction by using 4-phenyl-5*H*-1,2,3-oxathiazole-2,2-dioxide **(1a)** and benzaldehyde **(2a)** as model substrate in the presence of L-proline as an organocatalyst (10 mol%) in EtOH (1.0 mL). Despite less conversion, after 12 h we were able to isolate the desired product **3aa** in 25% yield. The product was well characterized by its spectroscopic data (^{1}H, ^{13}C NMR and HRMS data). Disappearance of ^{1}H NMR peak at δ 5.59 ppm indicates the total consumption of **1a** and appearance of a new peak at δ 6.66 ppm which belongs to the benzylidine C-H proton. Total number of carbon peaks in the ^{13}C spectrum are 11 which perfectly match with our desired compound **3aa.** The HRMS data shows the presence of molecular ion peak $[M+Na]^{+}$ at 308.0409 which corresponds to the molecular weight of **3aa**. The stereochemistry of exo-cyclic C=C bond of **3aa** was exclusively *Z*-configuration which was assigned by single crystal X-ray diffraction analysis data (**Figure 2.2**). All these significant results prompted us to investigate the condensation reaction of **1a** in detail.

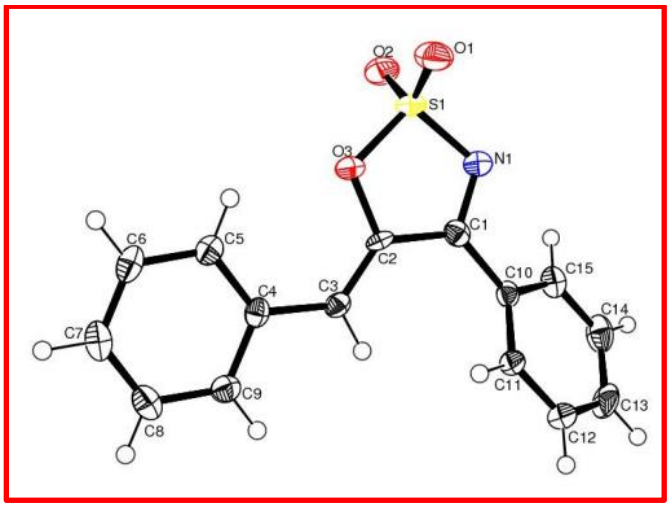
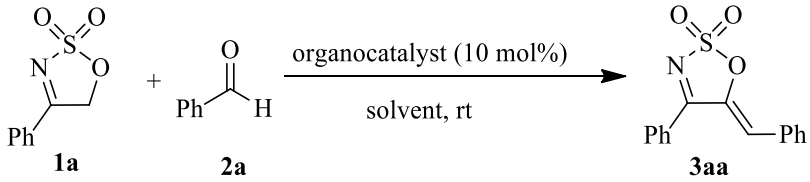


Figure 2.2 Molecular structure of compound **3aa**

Screening of solvents revealed that common organic solvents led to inferior results (10-45% yields), except polar aprotic solvent DMSO (86% yield, entry 4, **Table 2.1**) and DMF (95% yield, entry 3, **Table 2.1**). Interestingly single diastereomer was observed in all these cases as determined by the ^{1}H NMR data of crude reaction mixture. With respect to yield, DMF was chosen as best solvent for this condensation reaction. Further catalysts screening have been done by taking some commercially available catalyst, such as α-amino acids (glycine, L-phenylalanine, L-aspartic acid) and ammonium acetate in DMF. In all these cases reaction proceeds smoothly (except entry 11, L-aspartic acid) leading to the product **3aa** in good yields (66-83%). As we have seen that L-proline is a superior catalyst for this condensation reaction, we assumed that this reaction may require a catalyst which contains both acid and basic nature. To verify our assumption we performed the condensation reaction in presence of only acids (pTSA and $PhCO_2H$) and bases (DABCO and pyrrolidine) in which no reaction took place (entries 13-16) in the same conditions. We are pleased to inform that when we carried out the same reaction in presence of secondary amine salts (entries 17 and 18) we observed our desired product **3aa** in high yield. It is worth mentioning here that tertiary amine salts were ineffective (entries 19 and 20) for this reaction. All these optimization data have been summarized in **Table 2.1** and L-proline and

DMF has been chosen as the best catalyst and solvent (entry 3 in **Table 2.1**) respectively for this reaction.

Table 2.1 Optimization table of this condensation reaction.[a,b]

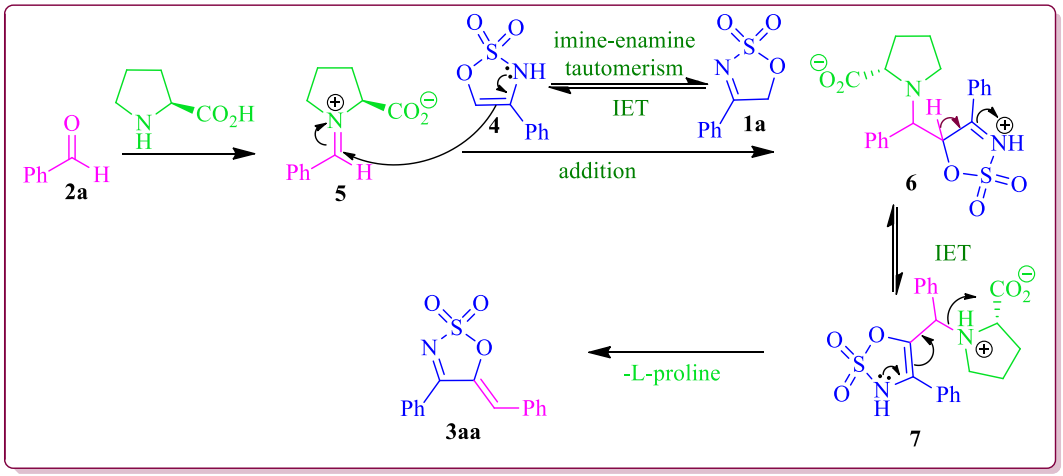


entry	catalyst (10 mol%)	Solvent	time (h)	yield (%)[c]
1	L-Proline	EtOH	12	25
2	L-Proline	MeOH	12	45
3	L-Proline	DMF	12	95
4	L-Proline	DMSO	12	86
5	L-Proline	Hexane	12	10
6	L-Proline	MeCN	12	23
7	L-Proline	THF	12	17
8	L-Proline	DCM	12	20
9	Glycine	DMF	12	83
10	L-Phenylalanine	DMF	12	66
11	L-Aspartic acid	DMF	12	17
12	NH_4OAc	DMF	12	73
13	DABCO	DMF	6	NR
14	Pyrrolidine	DMF	6	NR
15	pTSA	DMF	6	NR
16	$PhCO_2H$	DMF	6	NR
17[d]	Pyrrolidine-$PhCO_2H$	DMF	12	79
18[d]	Et_2NH-$PhCO_2H$	DMF	12	72
19[d]	Et_3N-$PhCO_2H$	DMF	48	10
20[d]	DABCO-$PhCO_2H$	DMF	48	17

[a]Unless otherwise specified, all reactions were carried out with 4-phenyl-5*H*-1,2,3-oxathiazole-2,2-dioxide (0.5 mmol, **1a**), benzaldehyde (0.55 mmol, **2a**) and catalysts (10 mol%) in solvent (1.0 mL) at room temperature under argon atmosphere. [b]Only single diastereomer was observed in all these cases. [c]Isolated product after column chromatography. [d](1:1) ratio of amine and $PhCO_2H$ was used. [e]NR = no reaction.

2.3.1.2 Plausible mechanism

On the basis of above results, we propose the following plausible mechanism for the formation of product **3aa,** summarized in **Scheme 2.6**. In the first step the adduct **5** was generated by nucleophilic reaction of L-proline and benzaldehyde (**2a**), which is subsequently attacked by cyclic enamine **4** to form intermediate **6**. After that intermediate **6** underwent imine-enamine tautomerization (IET) to form intermediate **7**. Finally, the nitrogen lone pair of cyclic enamine **7** pushed proline out and the desired product **3aa** was formed.



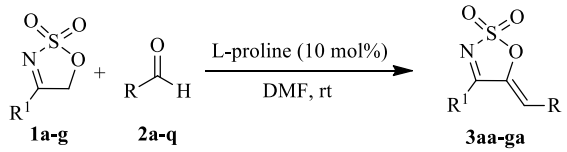
Scheme 2.6 Plausible mechanism of the condensation reaction

2.3.1.3 Generality and substrate scope

Having the optimal reaction conditions in hand, we studied the generality and scope of this novel condensation reaction by treating various imines (**1a-g**) and aldehydes (**2a-q**) under our standard conditions. All the results are compiled in

Table 2.2. It is evident from **Table 2.2** that aromatic aldehyde with various substituents such as Me, MeO, OH, OBn, Cl, Br on the phenyl ring gives excellent yields (90-97%, **3ab-ah**) with cyclic imine **1a** at our optimal condition. Strong electron withdrawing group (NO_2, CN) containing aromatic aldehyde gave the condensation product with lower yield (55-65%, **3ak** and **3al**) in compared to others. Not only aromatic aldehydes but also hetero-aryl aldehydes were good enamine acceptors for these reactions, the excellent yields (93-96%) of **3ai** and **3aj** were isolated (entries 9-10). It is worth mentioning that enolizable aldehydes, such as propanal (**2m**), butanal (**2n**), pentanal (**2o**) and 2,2-dimethoxyacetaldehyde (**2p**) are known to be very challenging substrate for cross aldol reaction. Most interestingly aliphatic aldehydes reacted efficiently with cyclic imine **1a** at 0 °C, isolated the desired products with excellent yields (82-94%, **3am-ap**) in this procedure. Similarly, several structurally diverse aryl and heteroaryl substituted cyclic sulfamidate imines (**1b-g**) gave clean and complete condensations with several aromatic, hetero-aromatic and aliphatic aldehydes by this procedure, provided the corresponding anticipated products in high to excellent yields (85-97%, **3be-ga**).

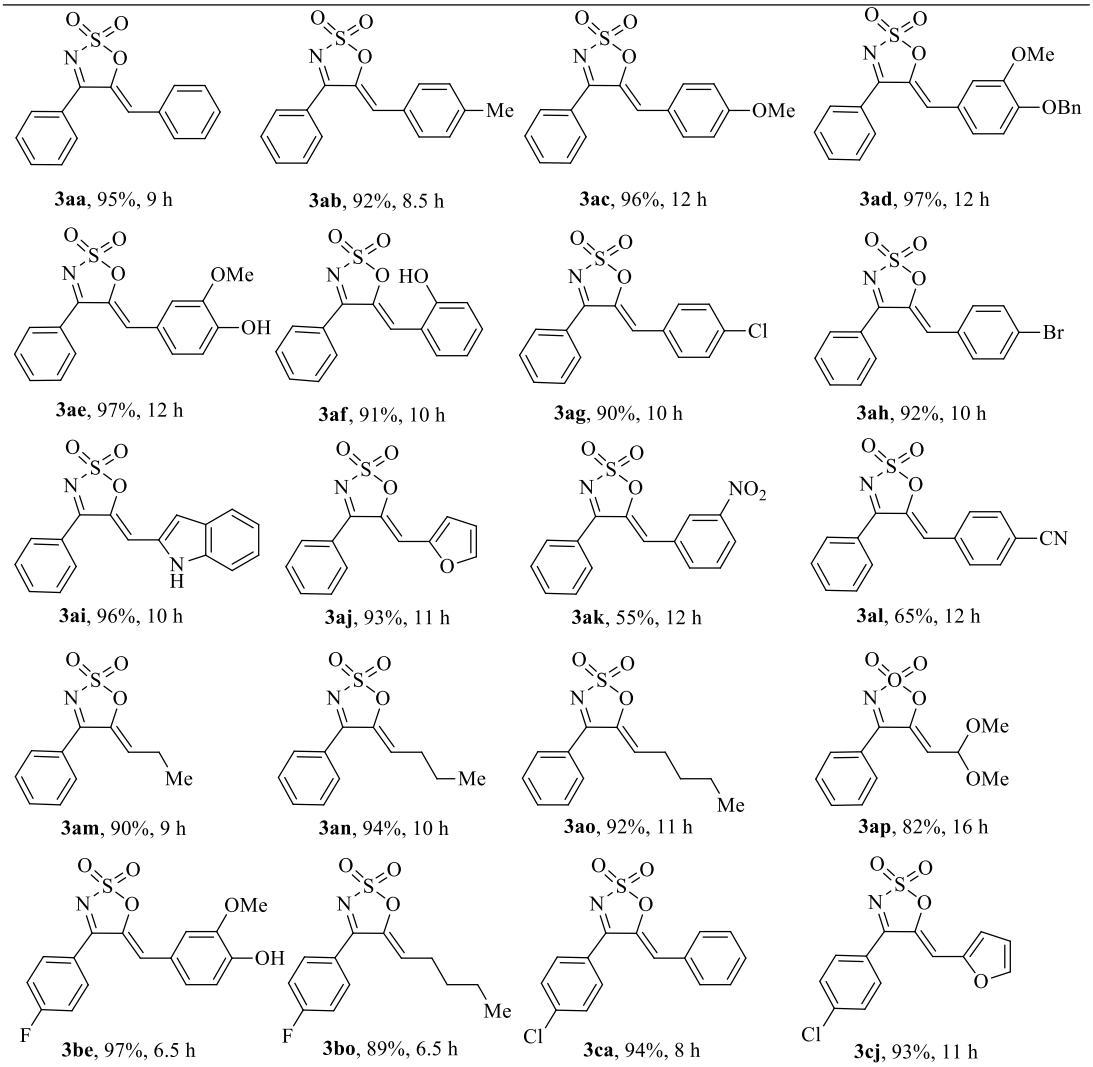
Table 2.2 Synthesis of *Z*-5 alkylidene-4-aryl-1,2,3-ozathiazole-2,2-dioxides[a,b]



1a-g **2a-q** **3aa-ga**

1a: $R^1 = C_6H_5$
1b: $R^1 = 4\text{-}FC_6H_4$
1c $R^1 = 4\text{-}ClC_6H_4$
1d $R^1 = 2\text{-}ClC_6H_4$
1e $R^1 = 4\text{-}BrC_6H_4$
1f $R^1 = 4\text{-}MeC_6H_4$
1f R^1 = 2-Furyl

2a: R = C_6H_5
2b: R = $4Me\text{-}C_6H_4$
2c: R = $4MeOC_6H_4$
2d: R = $4\text{-}OBn\text{-}3MeO\text{-}C_6H_3$
2e: R = $4\text{-}OH\text{-}3MeO\text{-}C_6H_3$
2f: R = $2\text{-}OHC_6H_4$
2g: R = $4\text{-}ClC_6H_4$
2h: R = $4\text{-}BrC_6H_4$
2i: R = 2-Indolyl
2j: R = 2-Furyl
2k: R = $3\text{-}NO_2C_6H_4$
2l: R = $4\text{-}CNC_6H_3$
2m: R = $MeCH_2$
2n: R = $MeCH_2CH_2$
2o: R = $MeCH_2CH_2CH_2$
2p: R = $(MeO)_2CH$
2q: R = $2\text{-}ClC_6H_4$



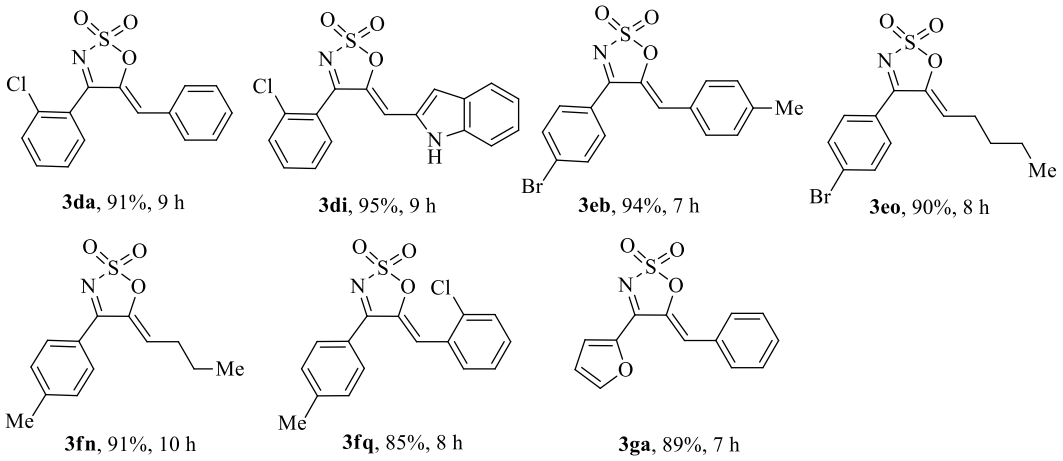
3aa, 95%, 9 h **3ab**, 92%, 8.5 h **3ac**, 96%, 12 h **3ad**, 97%, 12 h

3ae, 97%, 12 h **3af**, 91%, 10 h **3ag**, 90%, 10 h **3ah**, 92%, 10 h

3ai, 96%, 10 h **3aj**, 93%, 11 h **3ak**, 55%, 12 h **3al**, 65%, 12 h

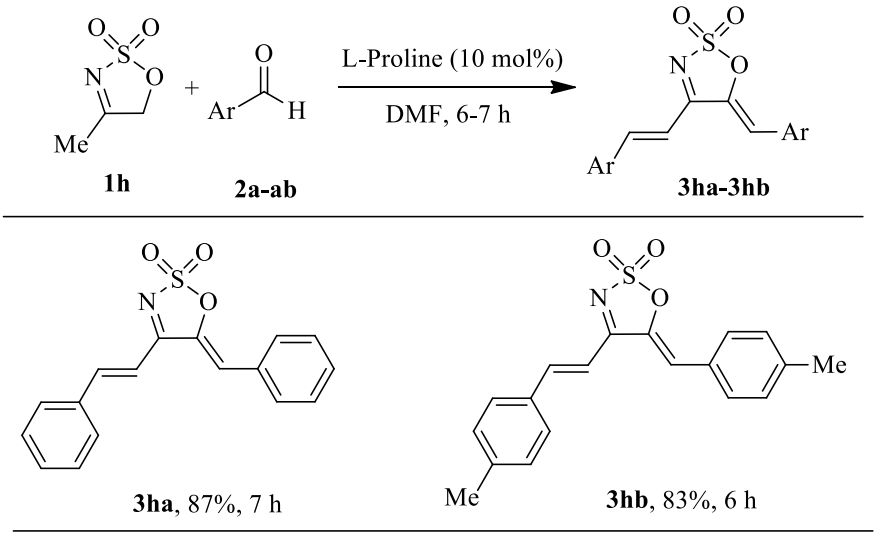
3am, 90%, 9 h **3an**, 94%, 10 h **3ao**, 92%, 11 h **3ap**, 82%, 16 h

3be, 97%, 6.5 h **3bo**, 89%, 6.5 h **3ca**, 94%, 8 h **3cj**, 93%, 11 h



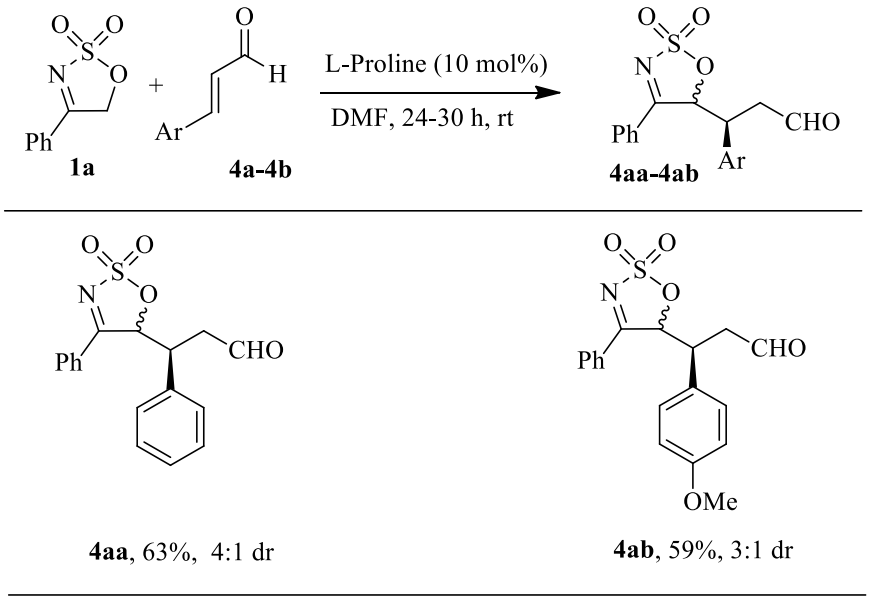
[a]Unless otherwise specified, all reactions were carried out with 4-aryl-5*H*-1,2,3-oxathiazole-2,2-dioxides (0.5 mmol, **1a-g**), aldehydes (0.55 mmol, **2a-q**) and L-proline (10 mol%) in dry DMF (1.0 mL) at room temperature under argon. [b]Only single diastereomer (*Z*) was observed by ^{1}H NMR of the crude products in all these cases. [c]Isolated product after column chromatography. [d]Reactions were performed with aldehydes (1.5 mmol) at 0 ºC. [e]70% aqueous solution of 2,2-dimethoxy acetaldehyde was used.

However, when 4-methyl substituted cyclic sulfamidate (**1h**) was used as an enamine donor, the condensation reactions with aromatic aldehydes (2 equiv.) occurred not only at the 5 position but also at the methyl position, resulting in dialkylidene products in high yields (83-87%, **3ha** and **3hb**, **Scheme 2.16**). Our present conditions are mild enough to tolerate several sensitive functional groups like OH, $CH(OMe)_2$, OBn, Cl, Br, F, CN, NO_2, furyl, indolyl etc



Scheme 2.7 Condensation reaction of cyclic imine **1h** with aldehydes

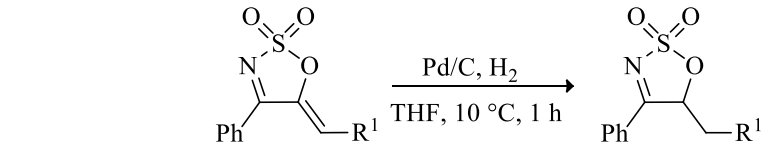
Interestingly, when we treat α,β-unsaturated aldehyde (**4a** and **4b**) with cyclic imine **1a** in our present condition, the afforded 1,4-adduct (**4aa** and **4ab**) as major product with moderate yields (59-63%) and good diastereomeric ratio values (3:1 to 4:1). This reaction offers a direct route for the synthesis of 5-alkyl-substituted cyclic sulfamidate imines (**Scheme 2.8**).



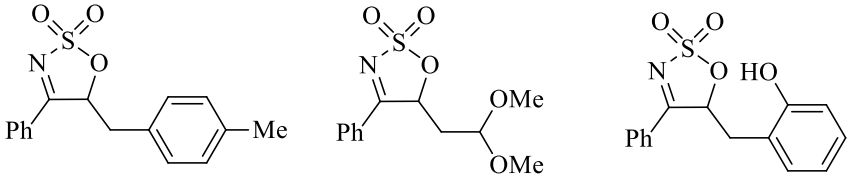
Scheme 2.8 1,4-addition reaction of **1a** with α,β-unsaturated aldehydes

2.3.1.4 Synthesis of 2-hydroxy pyrrolidine derivative

To investigate the application potential of our current methodology, we extended the synthesis of 5-alkylidene cyclic imine into a novel access of 5-alkyl substituted cyclic sulfamidate imines (**8**-**10**) in high yield *via* the chemoselective reduction of the *exo*-cyclic C=C bonds of the corresponding condensation product **3ab**, **3af** and **3an** using 10% Pd/C in THF (**Scheme 2.9**).



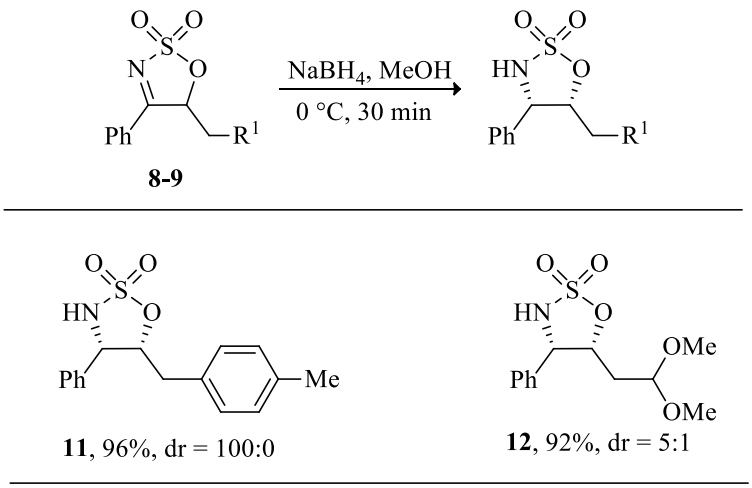
3ab, 3ap, 3af **8-10**



8, 88% **9**, 86% **10**, 91%

Scheme 2.9 Chemoselective reduction of C=C bond

After that highly diastereoselective synthesis of *cis*-cyclic sulfamidate **11** (only *cis* isomer) and **12** (*cis*:*trans* = 5:1) were ensued with excellent yields (92-96%) through the reductions of sterically less hindered side of prochiral C=N bonds of the corresponding cyclic imines (**8** and **9**) using $NaBH_4$ in MeOH at 0 ºC (**Scheme 2.10**). The relative configuration of the product **11** was assigned using the ORTEP data of its Boc protected from **13** as shown in **Figure 2.3**.



Scheme 2.10 Reduction of prochiral C=N bond

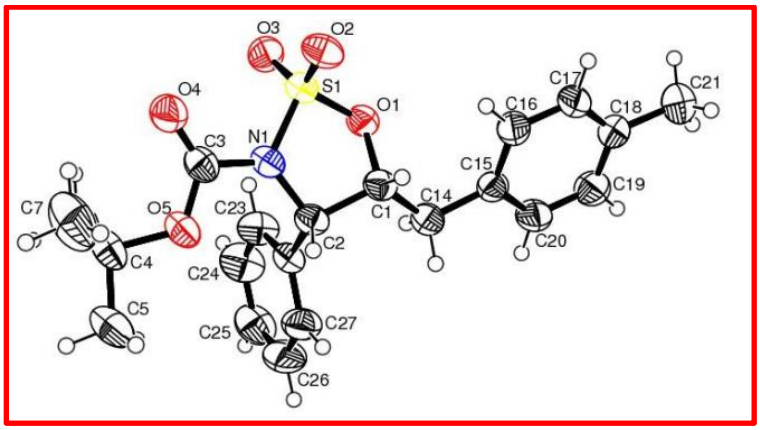
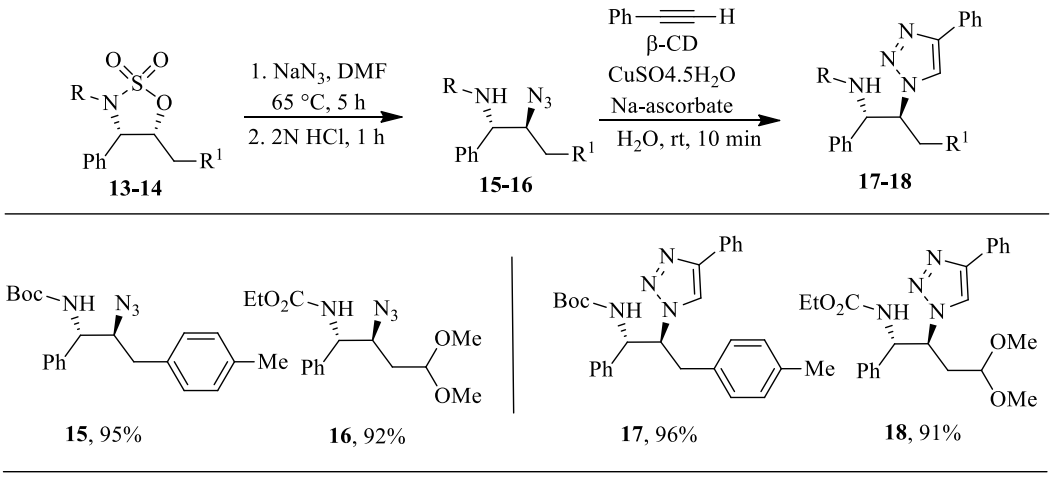


Figure 2.3 Molecular structures of compound **13**

Next the cyclic sulfamidates **13** and **14** were subjected to nucleophilic substitution reaction with NaN_3 in DMF at 65 °C for 4-5 h following known procedure [24] to obtain corresponding *trans*-β-amino-α-azido compounds **15** and **16** in stereospecific manner. The relative configuration of the product **15** was confirmed by its ORTEP data as shown in **Figure 2.4**. Further, the synthesis of highly biologically significant *trans*-β-amino-α-triazoles[20-23]**17** and **18** were achieved (**Scheme 2.11**) in a 1,4-substituted fashion from the corresponding azido compounds **15** and **16** using literature procedure[24-29].



Scheme 2.11 Syntheses of *trans*-β-amino-α-azido/triazoles.

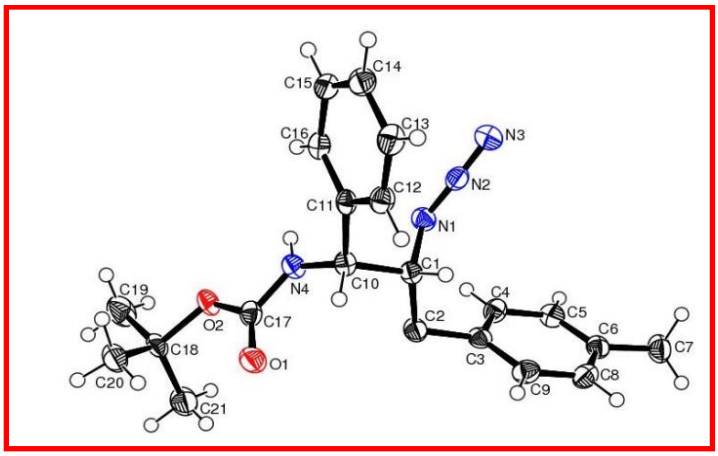
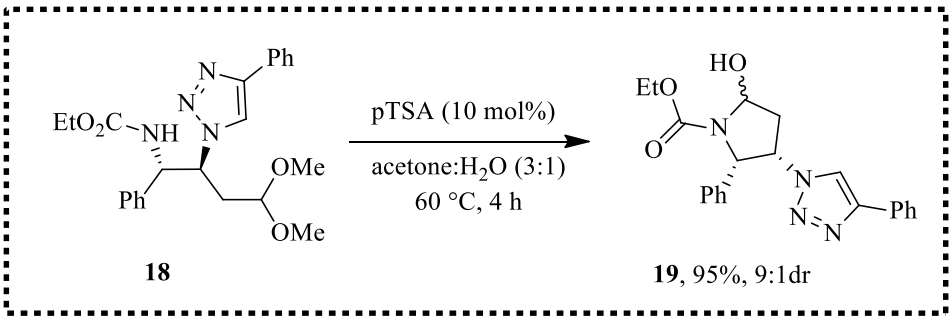


Figure 2.4 Molecular structure of compound **15**

The resulting compound **18,** which possesses a dimethoxy group, is a very important synthetic precursor for further elaboration. For example, a novel access of 2-hydroxy-4-triazole-5-phenylpyrrolidine derivative **19** was achieved in excellent yield (95%) *via* the deprotection of the dimethoxy group using a catalytic amount of pTSA in a mixture of aqueous acetone at 60 ºC and followed by cyclization (**Scheme 2.12**).



18 **19**, 95%, 9:1dr

Scheme 2.12 Synthesis of 2-hydroxy pyrrolidine derivative

2.4 Conclusion

A simple, mild (room temperature), new method for the synthesis of exclusively *Z*-5-alkylidene-4-aryl-1,2,3-oxathiazole-2,2-dioxides through a condensation reaction of 4-aryl-5*H*-1,2,3-oxathiazole-2,2-dioxides with both enolizable and non-enolizable aldehydes using L-proline as an efficient organocatalyst has been developed. Moreover, this condensation reaction provides in good to excellent yields of title compounds with excellent substrate scope. In addition, the chemoselective hydrogenation of exo-cyclic C=C double bonds of cyclic sulfamidate imines can be achieved in THF medium using 10 % Pd/C, offering an efficient new synthetic strategy for the easy access of 5-alkyl-4-aryl-5*H*-1,2,3-oxathiazole-2,2-dioxides. Furthermore, the synthesis of *trans*-β-amino-α-azido/triazole derivatives has been developed through this methodology.

2.5 Experimental section

2.5.1 General Information

All reactions were carried out under air and monitored by TLC using Merck 60 F_{254} pre coated silica gel plates (0.25 mm thickness) and the products were visualized by UV detection. Flash chromatography was carried out with silica gel (200-300 mesh). FT-IR spectra were recorded on a Bruker Tensor-27 spectrometer. ^{1}H and ^{13}C NMR spectra were recorded on a Bruker Avance (III) 400 MHz spectrometer. Data for ^{1}H NMR are reported as a chemical shift (δ ppm), multiplicity (s = singlet, d = doublet, q = quartet, m = multiplet), coupling constant *J* (Hz), integration, and assignment, data for ^{13}C are reported as a chemical shift. High resolutions mass spectral analyses (HRMS) were carried out using ESI-TOF-MS. Single crystal X-ray structural studies were performed on a CCD Agilent Technologies (Oxford Diffraction) SUPER NOVA diffractometer. Data were collected at 293(2) K using graphite-monochromoated Mo Kα radiation (λ_α = 0.71073 Å). The strategy for the Data collection was evaluated by using the CrysAlisPro CCD software. The data were collected by the standard 'phi-omega scan techniques, and were scaled and reduced using CrysAlisPro RED software. The structures were solved by direct methods using SHELXS-97 and refined by full matrix least-squares with SHELXL-97, refining on F^2.[30]

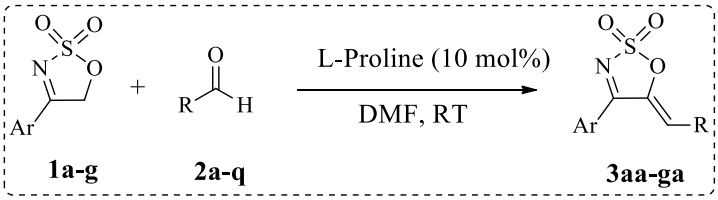
The positions of all the atoms were obtained by direct methods. All non-hydrogen atoms were refined anisotropically. The remaining hydrogen atoms were placed in geometrically constrained positions and refined with isotropic temperature factors, generally 1.2U_{eq} of their parent atoms.

2.5.2 Materials

All these starting materials and catalysts were either purchased from commercial sources or synthesized by literature known procedures.[1-5] *N*,*N*-dimethylformamide was dried over calcium hydride under argon atmosphere and distilled under reduced pressure before prior used.

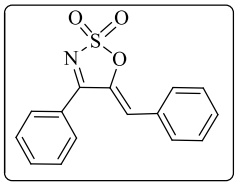
General procedure for the synthesis of *Z*-5-alkylidene-4-aryl-1,2,3-oxathiazole-2,2-dioxide:

To a stirred solution of 4-aryl-5*H*-1,2,3-oxathiazole-2,2-dioxides (0.5 mmol, **1a-g**), aldehydes (0.55 mmol, **2a-q**) and L-proline (10 mol% yield) in dry DMF (1.0 mL) at room temperature under argon atmosphere as shown in **Scheme 2.22**. The progress of the reaction was monitored by TLC. After completion of the reaction, the mixture was extracted with ethyl acetate (3 × 10 mL), washed with water and brine respectively and dried with Na_2SO_4. The organic phase was evaporated by rotary evaporator under reduced pressure to give the crude product. The crude product was purified by column chromatography over silica gel to furnish the pure product. The product was characterized by corresponding spectroscopic data (IR, NMR, HRMS).



Scheme 2.13 Synthesis of *Z*-5-alkylidene-4-aryl-1,2,3-oxathiazole-2,2-dioxide

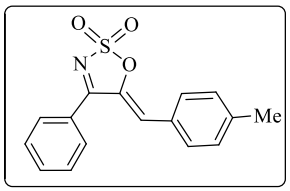
(*Z*)-5-Benzylidene-4-phenyl-1,2,3-oxathiazole-2,2-dioxide (3aa): yellow solid;



mp: 132 °C; 95% yield; **IR** (KBr): ν 2925, 2854, 1638, 1599, 1519, 1491, 1449, 1372 cm^{-1}; **^{1}H NMR** (400 MHz, $CDCl_3$): δ 7.82-7.85 (m, 2H), 7.77-7.79 (m, 2H), 7.70-7.74 (m, 1H), 7.60-7.64 (m, 2H), 7.46-7.48 (m, 3H), 6.66 (s, 1H); **^{13}C NMR** (100 MHz, $CDCl_3$): δ 172.2, 143.6, 134.0, 131.9, 131.7, 131.3, 130.2, 129.7, 129.5, 128.3, 121.0; **HRMS** (ESI) m/z calculated for $C_{15}H_{11}NO_3S$ $[M+Na]^+$: 308.0352, found 308.0409.

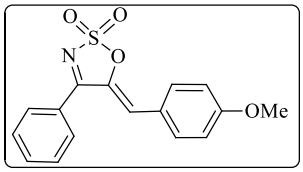
The stereochemistry of *exo*-cyclic C=C double bond of compound **3aa** was assigned by ORTEP data as shown **Figure 2.2.**

(*Z*)-5-(4-Methylbenzylidene)-4-phenyl-1,2,3-oxathiazole-2,2-dioxide (3ab):



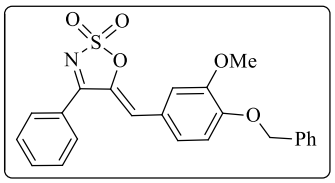
greenish yellow solid; **mp**: 140 °C; 92% yield; **IR** (KBr): ν 2921, 2854, 1635, 1603, 1517, 1487, 1448, 1372, 1346 cm^{-1}; **^{1}H NMR** (400 MHz, $CDCl_3$): δ 7.81-7.84 (m, 2H), 7.66-7.74 (m, 3H), 7.58-7.63 (m, 2H), 7.27 (d, *J* = 7.2 Hz, 2H), 6.65 (s, 1H), 2.41 (s, 3H); **^{13}C NMR** (100 MHz, $CDCl_3$): δ 172.2, 143.1, 142.9, 133.9, 131.8, 130.3, 130.1, 129.6, 128.5, 128.4, 121.4, 22.1; **HRMS** (ESI) m/z calculated for $C_{16}H_{13}NO_3S$ $[M+Na]^+$: 322.0508, found 322.0645.

(*Z*)-5-(4-Methoxybenzylidene)-4-phenyl-1,2,3-oxathiazole-2,2-dioxide (3ac):

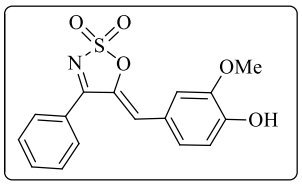


yellowish solid; **mp**: 138 °C; 96% yield; **IR** (KBr): ν 2960, 2925, 2853, 2840, 1598, 1512, 1487, 1363, 1340, 1308 cm^{-1}; **^{1}H NMR** (400 MHz, $CDCl_3$): δ 7.79-7.83 (m, 2H), 7.74-7.78 (m, 2H), 7.68-7.73 (m, 1H), 7.57-7.63 (m, 2H), 6.94-7.00 (m, 2H), 6.63 (s, 1H), 3.88 (s, 3H); **^{13}C NMR** (100 MHz, $CDCl_3$): δ 172.0, 162.7, 142.4, 133.9, 133.7, 130.1, 129.6, 128.5, 124.0, 121.4, 115.1, 55.9 ; **HRMS** (ESI) m/z calculated for $C_{16}H_{13}NO_4S$ $[M+Na]^+$: 338.0457, found 338.0513.

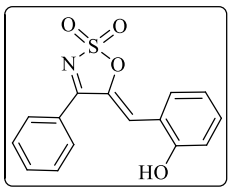
(*Z*)-5-(4-Benzyloxy-3-Methoxybenzylidene)-4-phenyl-1,2,3-oxathiazole-2,2-dioxide (3ad):



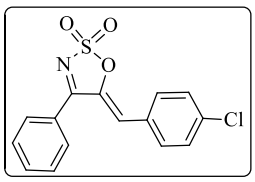
light yellow solid; **mp**: 157 °C; 97% yield; **IR** (KBr): ν 2957, 2923, 1628, 1596, 1510, 1487, 1424, 1369, 1350 cm^{-1}; **^{1}H NMR** (400 MHz, $CDCl_3$): δ 7.76-7.80 (m, 2H), 7.66-7.72 (m, 1H), 7.55-7.61 (m, 2H), 7.34-7.44 (m, 5H), 7.24-7.32 (m, 2H), 6.91 (d, *J* = 8.6 Hz, 1H), 6.58 (s, 1H), 5.20 (s, 2H), 3.92 (s, 3H); **^{13}C NMR** (100 MHz, $CDCl_3$): δ 172.0, 151.7, 150.0, 142.4, 136.4, 133.7, 130.1, 129.6, 129.0, 128.5, 128.4, 127.5, 126.7, 124.5, 121.6, 114.0, 113.6, 71.1, 56.4; **HRMS** (ESI) m/z calculated for $C_{23}H_{19}NO_5S$ $[M+Na]^+$: 444.0876, found 444.1051.

(*Z*)-5-(4-Hydroxy-3-Methoxybenzylidene)-4-phenyl-1,2,3-oxathiazole-2,2-dioxide (3ae): 

yellowish solid; **mp**: 138 °C; 93% yield; **IR** (KBr): ν 3441, 1639, 1598, 1515, 1487, 1463, 1433, 1371 cm^{-1}; **^{1}H NMR** (400 MHz, $CDCl_3$): δ 7.80-7.82 (m, 2H), 7.68-7.73 (m, 1H), 7.58-7.62 (m, 2H), 7.43-7.44 (m, 1H), 7.22-7.24 (m, 1H), 6.96 (d, *J* = 8.3 Hz, 1H), 6.60 (s, 1H), 6.12 (s, 1H), 3.97 (s, 3H); **^{13}C NMR** (100 MHz, $CDCl_3$): δ 172.1, 149.7, 147.2, 142.2, 133.7, 130.1, 129.6, 128.5, 127.8, 123.9, 121.9, 115.3, 112.8, 56.5; **HRMS** (ESI) m/z calculated for $C_{16}H_{13}NO_5S$ $[M+Na]^+$: 354.0407, found 354.0504.

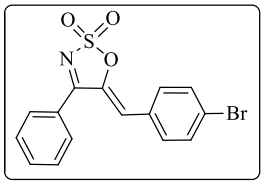
(*Z*)-5-(2-Hydroxybenzylidene)-4-phenyl-1,2,3-oxathiazole-2,2-dioxide (3af): 

yellow solid; **mp**: 190 °C; 91% yield; **IR** (KBr): ν 3447, 3076, 2925, 2854, 1633, 1603, 1520, 1484, 1460, 1365, 1332 cm^{-1}; **^{1}H NMR** (400 MHz, $CDCl_3$): δ 8.11 (d, *J* = 8.0 Hz, 1H), 7.85 (d, *J* = 7.6 Hz, 2H), 7.68-7.71 (m, 1H), 7.57-7.61 (m, 2H), 7.29-7.31 (m, 1H), 7.24 (s, 1H), 7.02-7.06 (m, 1H), 6.81 (d, *J* = 8.3 Hz,1H), 5.50 (s, 1H); **^{13}C NMR** (100 MHz, $CDCl_3$): δ 172.3, 155.5, 143.3, 133.9, 133.4, 131.9, 130.3, 129.6, 128.5, 122.0, 119.0, 115.9, 115.0; **HRMS** (ESI) m/z calculated for $C_{15}H_{11}NO_4S$ $[M+Na]^+$: 324.0301, found 324.0611.

(*Z*)-5-(4-Chlorobenzylidene)-4-phenyl-1,2,3-oxathiazole-2,2-dioxide (3ag): 

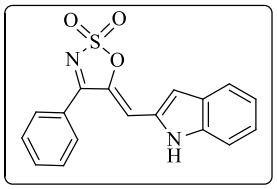
white solid; **mp**: 172 °C; 90% yield ; **IR** (KBr): ν 2923, 1683, 1586, 1523, 1491, 1448, 1411, 1375, 1349 cm^{-1}; **^{1}H NMR** (400 MHz, $CDCl_3$): δ 7.80-7.84 (m, 2H), 7.70-7.76 (m, 3H), 7.60-7.64 (m, 2H), 7.42-7.46 (m, 2H), 6.62 (s, 1H); **^{13}C NMR** (100 MHz, $CDCl_3$): δ 172.1, 143.7, 138.0, 134.1, 132.8, 130.1, 129.9, 129.7, 128.1, 119.4; **HRMS** (ESI) m/z calculated for $C_{15}H_{10}ClNO_3S$ $[M]^+$: 319.0064, found 319.0123.

(*Z*)-5-(4-Bromobenzylidene)-4-phenyl-1,2,3-oxathiazole-2,2-dioxide (3ah):



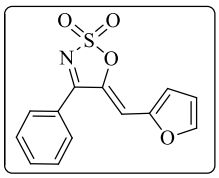
pale yellow solid; **mp**: 180 °C; 92% yield ; **IR** (KBr): ν 2925, 1643, 1582, 1533, 1491, 1447, 1384, 1347, 1330 cm^{-1}; **^{1}H NMR** (400 MHz, $CDCl_3$): δ 7.81-7.83 (m, 2H), 7.71-7.75 (m, 1H), 7.56-7.67 (m, 6H), 6.60 (s, 1H); **^{13}C NMR** (100 MHz, $CDCl_3$): δ 172.0, 143.8, 134.1, 132.9, 132.8, 130.1, 129.7, 128.0, 126.5, 119.5; **HRMS** (ESI) m/z calculated for $C_{15}H_{10}BrNO_3S$ $[M+Na]^+$: 385.9457, found 385.9532.

(*Z*)-5-(2-indolylmethylidene)-4-phenyl-1,2,3-oxathiazole-2,2-dioxide (3ai):



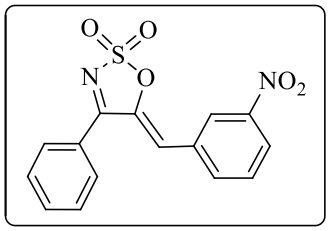
reddish solid; **mp**: 250 °C; 96% yield; **IR** (KBr): ν 3431, 2924, 1626, 1612, 1479, 1342 cm^{-1}; **^{1}H NMR** (400 MHz, acetone-d_6): δ 10.90 (s, 1H, NH), 7.98-8.02 (m, 2H), 7.78-7.82 (m, 1H), 7.66-7.72 (m, 3H), 7.54-7.57 (m, 1H), 7.24-7.31 (m, 3H), 7.09-7.13 (m, 1H); **^{13}C NMR** (100 MHz, acetone-d_6): δ 170.8, 141.5, 139.6, 133.6, 130.0, 129.9, 129.4, 128.3, 128.2, 125.7, 121.8, 120.8, 113.1, 112.2, 112.1; **HRMS** (ESI) m/z calculated for $C_{17}H_{12}N_2O_3S$ $[M+Na]^+$: 324.0563, found 324.0642.

(*Z*)-5-(2-Furylmethylidene)-4-phenyl-1,2,3-oxathiazole-2,2-dioxide (3aj): light



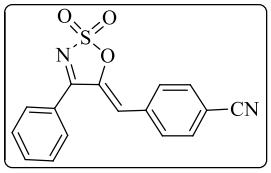
yellowish solid; **mp**: 90 °C; 93% yield; **IR** (KBr): ν 2924, 2853, 1641, 1526, 1491, 1462, 1380, 1349 cm^{-1}; **^{1}H NMR** (400 MHz, $CDCl_3$): δ 7.78-7.84 (m, 2H), 7.68-7.74 (m, 1H), 7.57-7.64 (m, 3H), 7.25 (d, *J* = 3.8 Hz, 1H), 6.71 (s, 1H), 6.63-6.67 (m, 1H); **^{13}C NMR** (100 MHz, $CDCl_3$): δ 170.9, 147.8, 147.0, 141.3, 134.1, 129.9, 129.7, 128.0, 119.6, 114.2, 108.5; **HRMS** (ESI) m/z calculated for $C_{13}H_9NO_4S$ $[M+Na]^+$: 298.0144, found 298.0225.

(*Z*)-5-(4-Nitrobenzylidene)-4-phenyl-1,2,3-oxathiazole-2,2-dioxide (3ak):



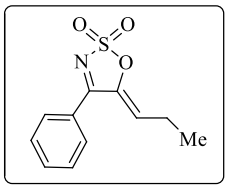
yellowish solid; **mp**: 158 °C; 55% yield; **IR** (KBr): ν 2923, 2853, 1612, 1528, 1490, 1449, 1381, 1353, 1332 cm^{-1}; **^{1}H NMR** (400 MHz, $CDCl_3$): δ 8.50-8.51 (m, 1H), 8.28-8.31 (m, 1H), 8.19-8.21 (m, 1H), 7.83-7.88 (m, 2H), 7.74-7.80 (m, 1H), 7.62-7.71 (m, 3H), 6.71 (s, 1H); **^{13}C NMR** (100 MHz, $CDCl_3$): δ 171.9, 148.9, 144.8, 136.4, 134.5, 132.8, 130.6, 130.2, 129.9, 127.6, 126.1, 125.7, 117.4; **HRMS** (ESI) m/z calculated for $C_{15}H_{10}N_2O_5S$ $[M+Na]^+$: 353.0203, found 353.0234.

(*Z*)-5-(4-Cyanobenzylidene)-4-phenyl-1,2,3-oxathiazole-2,2-dioxide (3al): pale



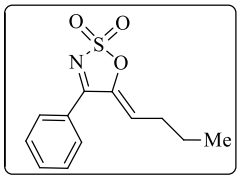
yellowish solid; **mp**: 190 °C; 65% yield; **IR** (KBr): ν 3058, 2924, 2221, 1648, 1600, 1538, 1491, 1447, 1386, 1331 cm^{-1}; **^{1}H NMR** (400 MHz, $CDCl_3$): δ 7.82-7.89 (m, 4H), 7.71-7.78 (m, 3H), 7.61-7.66 (m, 2H), 6.65 (s, 1H); **^{13}C NMR** (100 MHz, $CDCl_3$): δ 171.9, 145.0, 135.4, 134.5, 133.0, 131.7, 130.2, 129.9, 127.7, 118.3, 117.8, 114.5; **HRMS** (ESI) m/z calculated for $C_{16}H_{10}N_2O_3S$ $[M+Na]^+$: 333.0337 found 333.0409.

(*Z*)-5-Propylidene-4-phenyl-1,2,3-oxathiazole-2,2-dioxide (3am): colourless



liquid; 90% yield ; **IR** (KBr): ν 2931, 2365, 1656, 1631, 1538, 1376, 1344 cm^{-1}; **^{1}H NMR** (400 MHz, $CDCl_3$): δ 7.74-7.78 (m, 2H), 7.66-7.70 (m, 1H), 7.53-7.58 (m, 2H), 5.96 (t, *J* = 7.8 Hz, 1H), 2.43-2.51 (m, 2H), 1.15 (t, *J* = 7.5 Hz); **^{13}C NMR** (100 MHz, $CDCl_3$): δ 170.8, 145.8, 134.1, 130.1, 129.6, 128.2, 126.2, 21.4, 13.1; **HRMS** (ESI) m/z calculated for $C_{11}H_{11}NO_3S$ $[M+H]^+$: 238.0532, found 238.1668.

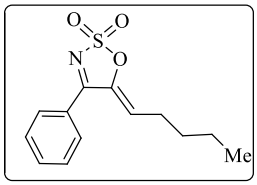
(*Z*)-5-Butylidene-4-phenyl-1,2,3-oxathiazole-2,2-dioxide (3an): colourless



liquid; 94% yield; **IR** (KBr): ν 2963, 2874, 1719, 1660, 1543, 1493, 1454, 1384, 1345 cm^{-1}; **^{1}H NMR** (400 MHz, $CDCl_3$): δ 7.74-7.78 (m, 2H), 7.66-7.70 (m, 1H), 7.54-7.58

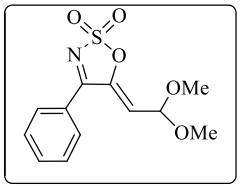
(m, 2H), 5.95 (t, *J* = 7.8 Hz, 1H), 2.39-2.45 (m, 2H), 1.53-1.60 (m, 2H), 0.95 (t, *J* = 7.6 Hz, 3H); **^{13}C NMR** (100 MHz, $CDCl_3$): δ 170.7, 146.2, 134.1, 130.0, 129.6, 128.1, 124.9, 29.7, 22.0, 14.1; **HRMS** (ESI) m/z calculated for $C_{12}H_{13}NO_3S$ $[M+K]^+$: 290.0248, found 290.0343.

(**Z)-5-Pentylidene-4-phenyl-1,2,3-oxathiazole-2,2-dioxide (3ao):** colourless



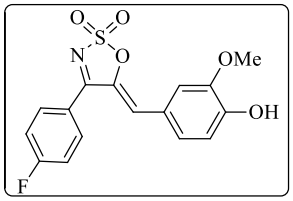
liquid; 92% yield; **IR** (KBr): ν 2959, 2867, 1660, 1542, 1492, 1449, 1383, 1346 cm^{-1}; **^{1}H NMR** (400 MHz, $CDCl_3$): δ 7.73-7.77 (m, 2H), 7.65-7.71 (m, 1H), 7.53-7.58 (m, 2H), 5.98 (t, *J* = 7.8 Hz, 1H), 2.41-2.47(m, 2H), 1.46-1.55 (m, 2H), 1.32-1.43 (m, 2H), 0.93 (t, *J* =7.3 Hz, 3 H); **^{13}C NMR** (100 MHz, $CDCl_3$): δ 170.7, 146.1, 134.1, 130.1, 129.6, 126.1, 125.2, 30.7, 27.6, 22.7, 14.0; **HRMS** (ESI) m/z calculated for $C_{13}H_{15}NO_3S$ $[M+Na]^+$: 288.0665, found 288.0683.

(*Z*)-5-(1,1-Dimethoxyethylidene)-4-phenyl-1,2,3-oxathiazole-2,2-dioxide



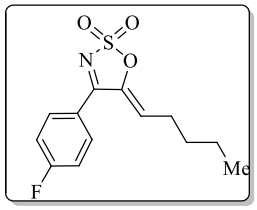
(3ap): colourless liquid; 82% yield; **IR** (KBr): ν 2927, 2831, 1603, 1546, 1493, 1451, 1383 cm^{-1}; **^{1}H NMR** (400 MHz, $CDCl_3$): δ 7.78-7.81 (m, 2H), 7.68-7.73(m, 1H), 7.55-7.60 (m, 2H), 5.92 (d, *J* = 6.8 Hz, 1H), 5.27 (d, *J* = 7.0 Hz, 1H), 3.43 (s, 6 H); **^{13}C NMR** (100 MHz, $CDCl_3$): δ 171.0, 145.7, 134.6, 130.2, 129.7, 127.4, 117.6, 99.14, 54.5; **HRMS** (ESI) m/z calculated for $C_{12}H_{13}NO_5S$ $[M+Na]^+$: 306.0407, found 306.0465.

(*Z*)-5-(4-Hydroxy-3-methoxybenzylidene)-4-(4-fluorophenyl)-1,2,3-



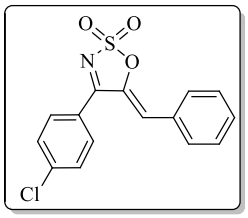
oxathiazole-2,2-dioxide (3be): yellowish solid; **mp**: 197 °C; 97% yield; **IR** (KBr): ν 3435, 2957, 2924, 2853, 1637, 1598, 1513, 1463, 1433 cm^{-1}; **^{1}H NMR** (400 MHz, acetone-d_6): δ 8.70 (s, 1H), 8.07-8.11 (m, 2H), 7.43-7.54 (m, 4H), 6.98-7.02 (m, 2H), 3.91 (s, 3H); **^{13}C NMR** (100 MHz, acetone-d_6): δ 171.0, 167.1, 164.6, 150.7, 147.8, 141.6, 133.0, 132.9, 126.9, 124.8, 124.7, 123.4, 122.3, 116.6, 116.4, 115.9, 114.6, 55.5; **HRMS** (ESI) m/z calculated for $C_{16}H_{12}FNO_5S$ $[M+Na]^+$: 372.0312, found 372.0405

(*Z*)-5-(Pentylidene)-4-(4-fluorophenyl)-1,2,3-oxathiazole-2,2-dioxide (3b):



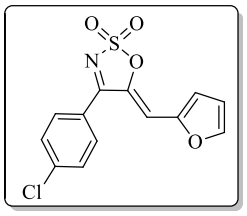
colourless liquid; 89% yield; **IR** (KBr): ν 2960, 2932, 2873, 1660, 1605, 1544, 1506, 1414, 1383 cm^{-1}; **^{1}H NMR** (400 MHz, $CDCl_3$): δ 7.77-7.84 (m, 2H), 7.22-7.29 (m, 2H), 5.95 (t, *J* =7.8 Hz, 1H), 2.42-2.48 (m, 2 H), 1.47-1.56 (m, 2 H), 1.32-1.43 (m, 2 H), 0.93 (t, *J* = 7.3 Hz, 3 H); **^{13}C NMR** (100 MHz, $CDCl_3$): δ 169.5, 167.7, 165.2, 146.0, 132.7, 132.6, 125.2, 124.4, 124.3, 117.2, 117.0, 30.7, 27.6, 22.8, 14.0; **HRMS** (ESI) m/z calculated for $C_{13}H_{14}FNO_3S$ $[M+Na]^+$: 306.0571, found 306.0571.

(*Z*)-5-(Benzylidene)-4-(4-chlorophenyl)-1,2,3-oxathiazole-2,2-dioxide (3ca):



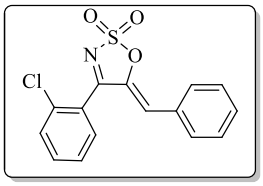
yellowish solid; **mp**: 190 °C; 94% yield; **IR** (KBr): ν 3094, 3067, 1638, 1593, 1517, 1488, 1449, 1403, 1374, 1335 cm^{-1}; **^{1}H NMR** (400 MHz, $CDCl_3$): δ 7.75-7.81 (m, 4H), 7.57-7.63 (m, 2H), 7.45-7.50 (m, 3H), 6.63 (s, 1H); **^{13}C NMR** (100 MHz, $CDCl_3$): δ 171.1, 143.3, 140.8, 132.1, 131.8, 131.5, 131.1, 130.1, 129.5, 126.6, 121.0; **HRMS** (ESI) m/z calculated for $C_{15}H_{10}ClNO_3S$ $[M+Na]^+$: 341.9962, found 342.0030.

(*Z*)-5-(2-furylmethylidene)-4-(4-chlorophenyl)-1,2,3-oxathiazole-2,2-dioxide



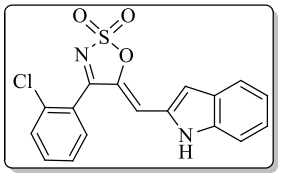
(3cj): yellowish solid; **mp**: 140 °C; 90% yield; **IR** (KBr): ν 3093, 2920, 1628, 1591, 1489, 1407, 1345 cm^{-1}; **^{1}H NMR** (400 MHz, $CDCl_3$): δ 7.78-7.80 (m, 1H), 7.75-7.77 (m, 1H), 7.65-7.67 (m, 1H), 7.59-7.61 (m, 1H), 7.56-7.58 (m, 1H), 7.27 (d, *J* = 8.8 Hz, 1H), 6.68 (s, 1H), 6.65-6.67 (m, 1H); **^{13}C NMR** (100 MHz, $CDCl_3$): δ 169.8, 147.7, 147.2, 141.1, 140.8, 131.2, 131.2, 126.4, 120.0, 114.3, 108.5 ppm; **HRMS** (ESI) m/z calculated for $C_{13}H_8ClNO_4S$ $[M+Na]^+$: 331.9755, found 331.9875.

(*Z*)-5-Benzylidene-4-(2-chlorophenyl)-1,2,3-oxathiazole-2,2-dioxide (3da):



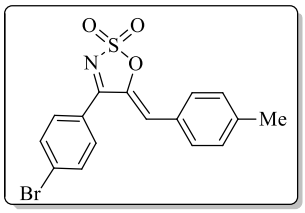
pale yellowish solid; **mp**: 119 °C; 91% yield; **IR** (KBr): ν 3048, 1652, 1597, 1548, 1468, 1383, 1338 cm^{-1}; **^{1}H NMR** (400 MHz, $CDCl_3$): δ 7.72-7.75 (m, 2H), 7.59-7.62 (m, 2H), 7.48-7.55 (m, 2H), 7.41-7.47 (m, 3H), 6.27 (s, 1H); **^{13}C NMR** (100 MHz, $CDCl_3$): δ 171.1, 143.8, 133.5, 133.4, 132.1, 131.8, 131.2, 130.9, 130.9, 129.5, 127.6, 127.5, 120.6; **HRMS** (ESI) m/z calculated for $C_{15}H_{10}ClO_3S$ $[M+Na]^+$: 341.9962, found 342.0050.

(*Z*)-5-(2indolylmethylidene)-4-(2-chlorophenyl)-1,2,3-oxathiazole-2,2-dioxide



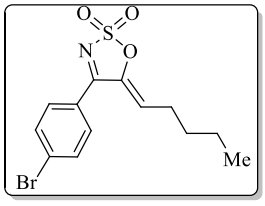
(3di): reddish solid; **mp**: 190 °C; 95% yield; **IR** (KBr): ν 3418, 1634, 1613, 1523, 1509, 1467, 1439, 1375 cm^{-1}; **^{1}H NMR** (400 MHz, $CDCl_3$): δ 9.18 (br s, 1 H), 7.59-7.65 (m, 3 H), 7.45-7.58 (m, 3 H), 7.33-7.39 (m, 1H), 7.12-7.18 (m,1 H), 6.94 (s, 1 H), 6.45 (s, 1 H); **^{13}C NMR** (100 MHz, $CDCl_3$): δ 169.5, 142.0, 139.7, 133.5, 131.3, 131.0, 129.6, 128.1, 127.6, 127.5, 122.4, 121.7, 114.8, 112.2, 111.3; **HRMS** (ESI) m/z calculated for $C_{17}H_{11}ClN_2O_3S$ $[M+ Na]^+$: 381.0071, found 381.0121.

(*Z*)-5-(4-Methylbenzylidene)-4-(4-bromophenyl)-1,2,3-oxathiazole-2,2-dioxide



(3eb): yellowish solid; **mp**: 156 °C; 94% yield; **IR** (KBr): ν 2922, 2853, 1637, 1585, 1512, 1481, 1371 cm^{-1}; ; **^{1}H NMR** (400 MHz, $CDCl_3$): δ 7.74-7.77 (m, 2H), 7.65-7.72 (m, 4H), 7.26-7.30 (m, 2H), 6.59 (s, 1H), 2.42 (s, 3H); **^{13}C NMR** (100 MHz, $CDCl_3$): δ 171.2, 143.2, 142.8, 133.1, 131.9, 131.5, 130.4, 129.1, 128.4, 127.2, 121.3, 22.1;

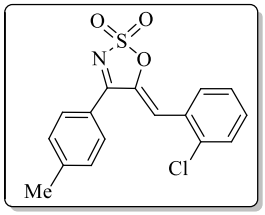
(*Z*)-5-(Pentylidene)-4-(4-bromophenyl)-1,2,3-oxathiazole-2,2-dioxide (3eo):



colourless liquid; 90% yield; **IR** (KBr): ν 3072, 2954, 2929, 2866, 1600, 1588, 1530, 1482, 1371 cm^{-1}; **^{1}H NMR** (400 MHz, $CDCl_3$): δ 7.71-7.73 (m, 2H), 7.69-7.71 (m, 2 H), 5.94 (t, *J* = 7.8 Hz, 1 H), 2.45 (q, *J* = 7.5 Hz, 2H),

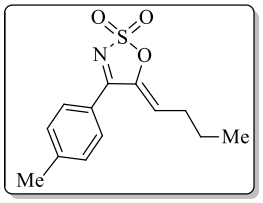
1.46-1.55 (m, 2 H), 1.33-1.43 (m, 2 H), 0.93 (t, *J* = 7.3 Hz, 3 H); **^{13}C NMR** (100 MHz, $CDCl_3$): δ 169.7, 145.9, 133.0, 131.4, 129.4, 126.9, 125.2, 30.6, 27.6, 22.8, 14.0; **HRMS** (ESI) m/z calculated for $C_{13}H_{14}BrNO_3S$ $[M+Na]^+$: 365.9770, found 365.9743.

(*Z*)-5-(4-Methylbenzylidene)-4-(2-chlorophenyl)-1,2,3-oxathiazole-2,2-dioxide



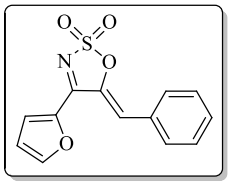
(3fs): yellowish solid; **mp**: 134 °C; 85% yield**; IR** (KBr): ν 2924, 2362, 2344, 1636, 1608, 1522, 1498, 1469, 1440, 1390, 1349 cm^{-1}; **^{1}H NMR** (400 MHz, $CDCl_3$): δ 8.18-8.21 (m, 1H), 7.79-7.81 (m, 2H), 7.36-7.48 (m, 5H), 7.23 (s, 1H), 2.51 (s, 3H) ; **^{13}C NMR** (100 MHz, $CDCl_3$): δ 172.1, 145.6, 144.3, 136.1, 132.4, 132.0, 130.5, 130.5, 130.4, 130.3, 129.3, 127.9, 125.2, 22.1; **HRMS** (ESI) m/z calculated for $C_{16}H_{12}ClNO_3S$ $[M+Na]^+$: 356.0119, found 356.0192.

(*Z*)-5-Butylidene-4-(4-methylphenyl)-1,2,3-oxathiazole-2,2-dioxide (3fn):



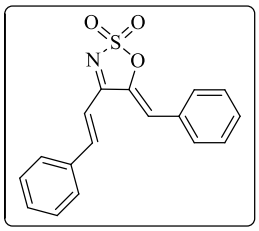
colourless liquid; 91% yield; **IR** (KBr): ν 3069, 3037, 2937, 2877, 2361, 2342, 1659, 1610, 1574, 1533, 1507, 1467, 1428, 1372, 1345, 1304, 1200, 1161, 1103, 1048 cm^{-1}; **^{1}H NMR** (400 MHz, $CDCl_3$): δ 7.66-7.69 (m, 2H), 7.34-7,37 (m, 2H), 5.98 (t, *J* = 7.8 Hz, 1H), 2.46 (s, 3H), 2.42 (q, *J* = 7.8 Hz, 1H), 1.51-1.60 (m, 2H), 0.98 (t, *J* = 7.3 Hz, 3H); **^{13}C NMR** (100 MHz, $CDCl_3$): δ 170.6, 146.2, 145.4, 130.3, 130.2, 125.3, 124.6, 29.7, 22.1, 22.0 14.1; **HRMS** (ESI) m/z calculated for $C_{13}H_{15}NO_3S$ $[M+Na]^+$: 288.0665, found 288.1004.

(*Z*)-5-Benzylidene-4-(2-furyl)-1,2,3-oxathiazole-2,2-dioxide (3ga): light



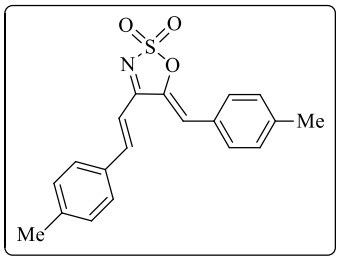
greenish solid; **mp**: 150 °C; 89% yield; **IR** (KBr) ν 2924, 2853, 1638, 1577, 1513, 1467, 1370, 1331 cm^{-1}; **^{1}H NMR** (400 MHz, $CDCl_3$): δ 7.88-7.90 (m, 1H), 7.82-7.86 (m, 2H), 7.64-7.66 (m, 1H), 7.43-7.49 (m, 4H), 6.75-6.78 (m, 1H); **^{13}C NMR** (100 MHz, $CDCl_3$): δ 158.0, 149.9, 145.3, 141.7, 132.0, 131.7, 131.6, 129.4, 123.2, 120.6, 114.2; **HRMS** (ESI) m/z calculated for $C_{13}H_9NO_4S$ $[M+Na]^+$: 298.0144, found 298.0242.

(*Z*)-5-Benzylidene-4-(*trans*-2-phenylethylene)-1,2,3-oxathiazole-2,2-dioxide



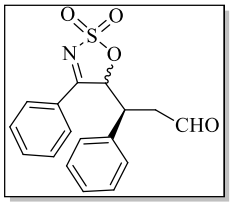
(3ha): 87% yield; **^{1}H NMR** (400 MHz, $CDCl_3$): δ 8.16 (d, *J* = 15.28 Hz, 1H), 7.82-7.84 (m, 2H), 7.69 (d, *J* = 7.6 Hz, 2H), 7.47-7.50 (m, 6H), 7.08 (d, *J* = 15.28 Hz, 1H), 6.73 (s, 1H); **^{13}C NMR** (100 MHz, $CDCl_3$): δ 167.1, 148.7, 143.8, 133.9, 132.1, 131.4 (2C), 130.9, 129.3, 129.2, 129.1, 115.5, 110.9; **HRMS** (ESI) m/z calculated for $C_{17}H_{13}NO_3S$ $[M+Na]^+$: 334.0508, found 334.0563

(*Z*)-5-(4-methylbenzylidene)-4-[*trans*-2-(4-methylphenylethylene)]-1,2,3-



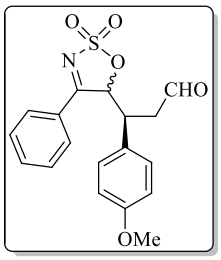
oxathiazole-2,2-dioxide (3hb): 83% yield; **^{1}H NMR** (400 MHz, DMSO-d_6): δ 8.14 (d, *J* = 15.6 Hz, 1H), 7.87 (d, *J* = 8.0Hz, 2H), 7.76 (d, *J*= 8.0 Hz, 2H), 7.67-7.71 (m, 2H), 7.39 (d, *J* = 8.0Hz, 2H), 7.35 (d, *J* = 8.0 Hz, 2H), 2.38 (s, 6H); **^{13}C NMR** (100 MHz, DMSO-d_6): δ 168.0, 148.0, 142.9, 142.5, 141.9, 131.5, 131.2, 130.0, 129.7 (2C), 128.5, 117.2, 114.4, 21.2; **HRMS** (ESI) m/z calculated for $C_{19}H_{17}NO_3S$ $[M+K]^+$: 378.0561, found 378.0328.

5-(3-phenylpropanal)-4-phenyl-5*H*-1,2,3-oxathiazole-2,2-dioxide(**4aa**):



trans:cis = 80:20; orange solid; **mp** 58 °C; 63% yield; **IR** (KBr): ν 3064, 2943, 2863, 1714, 1598, 1569, 1496, 1450, 1369 cm^{-1}; **^{1}NMR** (400 MHz, $CDCl_3$): δ (*major diastereomer*) 9.92 (s, 1H), 7.95-7.98 (m, 2H), 7.72-7.77 (m, 1H), 7.59-7.64 (m, 2H), 7.20-7.25 (m, 1H), 7.14-7.18 (m, 2H), 6.76-6.79 (m, 2H), 6.28 (d, *J* = 2.4 Hz, 1H), 4.04-4.08 (m, 1H), 3.49-3.57 (m, 1H), 2.99-3.04 (m, 1H); **^{13}C NMR** (100 MHz, $CDCl_3$): δ (*major diastereomer*) 200.5, 178.1, 135.5, 134.2, 129.9, 129.8, 129.2, 128.9, 128.8, 128.4, 89.5, 46.3, 41.7; **HRMS** (ESI) m/z calculated for $C_{17}H_{15}NO_4S$ $[M+Na]^+$: 352.0614, found 352.0700.

5-[3-(4-methoxyphenyl)propanal]-4-phenyl-5*H*-1,2,3-oxathiazole-2,2-dioxide

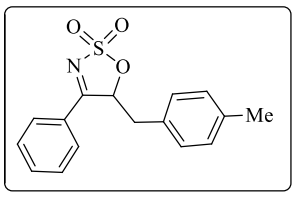


(4ab): orange solid; **mp**: 62 °C; 59% yield; **IR** (KBr): ν 2928, 2841, 1720, 1601, 1569, 1514, 1451, 1370 cm^{-1}; **^{1}H NMR** (400 MHz, $CDCl_3$): δ (*mixture of diastereoisomers, trans:cis* = 75: 25) 9.87 (s, 0.75 H), 9.49-9.50 (m, 0.25H), 7.93-7.96 (m, 1.5H), 7.86-7.90 (m, 0.5H), 7.71-7.76 (m, 1.5H), 7.57-7.63 (m, 2.5H), 7.25-7.28 (m, 0.7H), 6.88-6.91 (m, 0.7H), 6.65-6.70 (m, 4H), 6.25 (d, *J* = 2.5 Hz, 0.75 H), 6.00 (d, *J* = 2.24 Hz, 0.25H), 3.99-4.03 (m, 0.75H), 3.89-3.93 (m, 0.25 H), 3.80 (s, 0.75H), 3.71 (m, 2.25H), 3.42-3.50 (m, 0.75H), 2.93-3.02 (m, 1H), 2.75-2.82 (m, 0.25H); **^{13}C NMR** (100 MHz, $CDCl_3$): δ *(major diastereomer)* 200.6, 178.2, 159.8, 135.4, 130.3, 129.9, 129.8, 129.3, 126.1, 114.1, 89.8, 55.4, 46.6, 41.0 **HRMS** (ESI) m/z calculated for $C_{18}H_{17}NO_5S[M+Na]^+$: 382.0720, found 382.0720.

General experimental procedure for the synthesis of 5-alkyl-4-phenyl-5*H*-1,2,3,-oxathiazole-2,2-dioxides:

5-Alkylidene-4-phenyl-1,2,3-oxathiazole-2,2-dioxide was hydrogenated in the presence of 10% yield Pd/C in THF medium at 10 °C for 1 h (**Scheme 2.18**). The reaction was monitored by TLC. After completion of the reaction, the reaction mixture was filtered through Celite and washed with EtOAc. The filtrate was concentrated under reduced pressure to leave the crude product which was purified by column chromatography over silica-gel to furnish the desired product. The product was fully characterized by spectroscopic data (IR, NMR, HRMS).

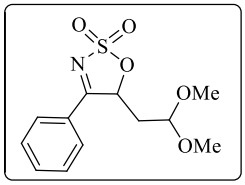
5-(4-Methylbenzyl)-4-Phenyl-5*H*-1,2,3-oxathiazole-2,2-dioxide (8): 88%



yield**; IR** (KBr): ν 2925, 1596, 1568, 1514, 1449, 1362 cm^{-1}; **^{1}H NMR** (400 MHz, $CDCl_3$): δ 7.89-7.92 (m, 2H), 7.71-7.76 (m, 1H), 7.57-7.61 (m, 2H), 7.05-7.13 (m, 4H), 5.98-6.01 (m, 1H), 3.27-3.32 (m, 1H), 3.12-3.18 (m, 1H),

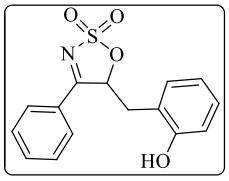
2.33 (s, 3H); **^{13}C NMR** (100 MHz, $CDCl_3$): δ 178.5, 137.9, 135.7, 131.2, 129.9 (2C), 129.8, 129.6, 127.8, 88.6, 39.9, 21.4; **HRMS** (ESI) m/z calculated for $C_{16}H_{15}NO_3S$ $[M+Na]^+$: 340.0404, found 340.0786.

5-(1,1-dimethoxyethyl)-4-Phenyl-5*H*-1,2,3-oxathiazole-2,2-dioxide (9):



colourless gummy liquid; 86% yield; **IR** (KBr): ν 2931, 2364, 2340, 1634, 1600, 1570, 1452, 1355 cm^{-1}; **^{1}H NMR** (400 MHz, $CDCl_3$): *δ* 7.91-7.92 (m, 1H), 7.89-7.90 (m, 1H), 7.67-7.72 (m, 1H), 7.54-7.59 (m, 2H), 5.99 (dd, *J* = 8.8, 2.8 Hz),4.63 (dd, 6.8, 4.2 Hz, 1H), 3.48 (s, 3H), 3.33 (s, 3H), 2.28-2.34 (m, 1H), 2.14-2.21 (m, 1H); **^{13}C NMR** (100 MHz, $CDCl_3$): *δ* 179.2, 135.6, 129.8, 127.6, 102.1, 85.0, 55.8, 54.7, 38.2**;** **HRMS** (ESI) m/z calculated for $C_{12}H_{15}NO_5S$ $[M+Na]^+$: 308.0563, found 308.0691.

5-(2-Hydroxylbenzyl)-4-Phenyl-5*H*-1,2,3-oxathiazole-2,2-dioxide (10): light



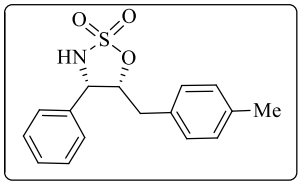
greenish solid**;** 91% yield; **IR** (KBr): ν 3493, 2924, 1598, 1567, 1502, 1456, 1368 cm^{-1}; **^{1}H NMR** (400 MHz, $CDCl_3$): δ 8.10-8.13 (m, 2H), 7.69-7.74 (m, 1H), 7.55-7.60 (m, 2H), 7.17-7.22 (m, 2H), 6.90-6.95 (m, 1H), 6.80-6.82 (m, 1H), 6.17-6.21 (m, 1H), 5.30 (s, 1H), 3.56-3.61 (m, 1H), 2.86-2.93 (m, 1H); **^{13}C NMR** (100 MHz, $CDCl_3$): δ 179.2, 153.7, 135.8, 132.5, 130.3, 129.8, 129.6, 127.6, 121.8, 115.6, 87.4, 36.6; **HRMS** (ESI) m/z calculated for $C_{15}H_{13}NO_4S$ $[M+Na]^+$: 326.0457, found 326.0471.

General experimental procedure for the synthesis of 5-alkyl-4-phenyl-1,2,3,-oxathiazolidine-2,2-dioxide:

To a stirred solution of 5-alkyl-4-phenyl-5*H*-1,2,3,-oxathiazole-2,2-dioxide in MeOH was added $NaBH_4$ at 0 ºC. The stirring was continued for 30 min (**Scheme 2.19**). Then MeOH was evaporated before being quenched with 1N HCl. After that the reaction mixture was extracted with EtOAc, washed with brine and dried with Na_2SO_4. Evaporation of the solvent left the crude product which was purified column chromatography over silica gel to provide the pure product. All

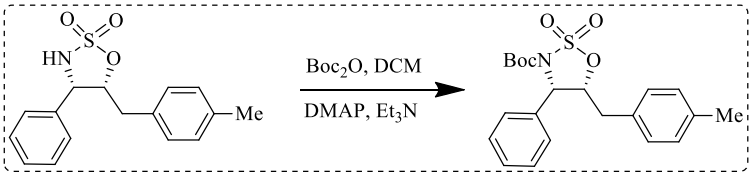
the products were characterized by their spectroscopic data (IR, NMR and HRMS).

***cis*-4-Phenyl-5-(4-methylbenzyl)-1,2,3-oxathiazolidine-2,2-dioxide (11)** white



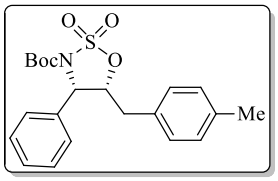
solid; 96% yield; **IR** (KBr): ν 3285, 2923, 1515, 1457, 1402, 1375, 1332 cm^{-1}; **^{1}H NMR** (400 MHz, $CDCl_3$): δ *(cis isomer)* 7.38-7.46 (m, 5H), 7.05-7.08 (m, 2H), 6.91-6.96 (m, 2H), 5.24-5.30 (m, 1H), 5.05 (d, *J* = 4.0 Hz, 1H), 4.96 (dd, *J* = 5.6, 4.0 Hz, 1H), 2.68-2.76 (m, 1H), 2.41-2.47 (m, 1H), 2.31 (s, 3H); **^{13}C NMR** (100 MHz, $CDCl_3$): δ *(cis isomer)* 137.1, 135.3, 132.3, 129.7, 129.6, 129.4, 129.3, 128.0, 86.7, 63.7, 36.5, 21.4; **HRMS** (ESI) m/z calculated for $C_{16}H_{17}NO_3S$ $[M+Na]^+$: 326.0821, found 326.0903

The relative configuration (*cis*) of the product was assigned by the coupling constant of vicinal hydrogen ($J_{H\text{-}5,H\text{-}4}$ = 4.4 Hz), which was further confirmed by single crystal x-ray diffraction data of its Boc protected form (**Figure 2.3**).



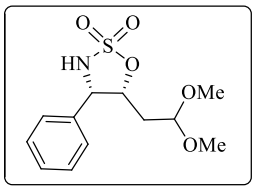
Scheme 2.14 Boc protection of cyclic sulfamidates

***Cis*-N-Boc-4-Phenyl-5-(4-methylbenzyl)-1,2,3-oxathiazolidine-2,2-dioxide**



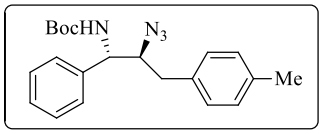
(13): white solid; **mp**: 125 °C; yield; **IR** (KBr) ν 2984, 2935, 1731, 1633, 1519, 1374, 1323 cm^{-1}; **^{1}H NMR** (400 MHz, $CDCl_3$): *δ* 7.37-7.46 (m, 5H), 7.06-7.10 (m, 2H), 6.89-6.92 (m, 2H), 5.27-5.32 (m, 1H), 5.17 (d, *J* = 4.4 Hz, 1H), 2.49-2.63 (m, 2H), 2.32 (s, 3H), 1.43 (s, 9H); **^{13}C NMR** (100 MHz, $CDCl_3$): *δ* 148.5, 139.5, 137.4, , 131.4, 129.7, 129.6, 129.2(2C), 128.3, 85.8, 83.5, 65.1, 36.1, 28.2, 21.4; **HRMS** (ESI) m/z calculated for $C_{21}H_{25}NO_5S$ $[M+Na]^+$: 426.1346, found 426.1387.

***Cis*-4-Phenyl-5-(1,1-dimethoxyethyl)-1,2,3-oxathiazolidine-2,2-dioxide (12):**



***syn : anti* = 5:1**; colourless gummy liquid; 92% yield; **IR** (KBr): ν 2925, 2854, 1632, 1461 cm^{-1}; **^{1}H NMR** (400 MHz, $CDCl_3$): δ (*major diastereomer)* 7.34-7.42 (m, 5H), 5.45-5.55 (m, 1H), 5.19-5.24 (m, 1H), 5.13 (br s, 1H), 4.97 (dd, *J* = 6.0, 4.8 Hz, 1H), 4.36-4.39 (m, 1H), 3.34 (s, 3H), 3.23 (s, 3H), 1.62-1.69 (m, 1H), 1.45-1.52 (m, 1H); **^{13}C NMR** (100 MHz, $CDCl_3$): δ *(major diastereomer)* 135.2, 129.6, 129.5, 127.6, 102.2, 83.2, 63.4, 54.2, 54.1, 34.7; **HRMS** (ESI) m/z calculated for $C_{12}H_{17}NO_5S$ $[M+Na]^+$: 310.0720, found 310.0815.

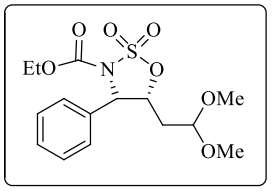
***Trans*-N-Boc-2-Azido-1-phenyl-3-(4-methylphenyl)-1-aminopropane (15):**



white crystalline solid; 95% yield **IR** (KBr): ν 3394, 2978, 2925, 2856, 2117, 2082, 1689, 1509, 1456, 1350, 1319, 1241, 1161 cm^{-1}; **^{1}H NMR** (400 MHz, $CDCl_3$): δ 7.32-7.37 (m, 2H), 7.23-7.30 (m, 3H), 7.14 (s, 4H), 5.29 (br s, 1H), 4.83 (br s, 1H), 3.84-3.89 (m, 1H), 2.84-2.95 (m, 2H), 2.34 (s, 3H), 1.46 (s, 9H); **^{13}C NMR** (100 MHz, $CDCl_3$): δ 155.6, 140.7, 136.9, 134.3, 129.8, 129.5, 129.0, 128.0, 126.7, 80.3, 69.8, 56.4, 38.7, 28.7, 21.4; **HRMS** (ESI) m/z calculated for $C_{21}H_{26}N_4O_2$ $[M+Na]^+$: 389.1948, found 389.1985.

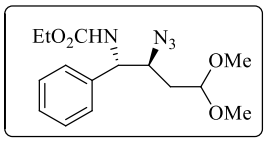
The relative configuration (*trans*) of the product was confirmed by single crystal x-ray diffraction data (**Figure 2.4**).

***Cis*-N-Ethoxycarbonyl-4-phenyl-5-(1,1-dimethoxyethyl)-1,2,3-oxathiazolidine -2,2-dioxide (14):**



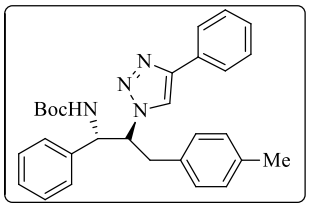
colourless gummy liquid; **IR** (KBr): ν 2986, 2940, 2838, 1742, 1633, 1460, 1378, 1313 cm^{-1}; **^{1}H NMR** (400 MHz, $CDCl_3$): δ *(major)* 7.37 (s, 5H), 5.24-5.29 (m, 1H), 5.22 (d, *J* = 5.6 Hz, 1H), 4.39 (dd, *J* = 7.5, 3.5 Hz, 1H), 4.20-4.24 (m, 2H), 3.32 (s, 3H), 3.23 (s, 3H), 1.59-1.66 (m, 1H), 1.44-1.52 (m, 1H), 1.17-1.24 (m, 3H); **^{13}C NMR** (100 MHz, $CDCl_3$): δ (major) 149.7, 134.2, 129.2, 127.9, 101.5, 80.6, 65.3, 64.4, 54.9, 53.8, 34.1, 14.2; **HRMS** (ESI) m/z calculated for $C_{15}H_{21}ClNO_7S$ $[M+Na]^+$: 382.0931, found 382.1012.

***Trans*-1-*N*-Ethoxycarbonyl-3-azido-4-phenyl-1,1-dimethoxy-4-aminobutane**



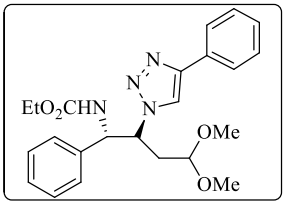
(16): colourless gummy liquid; 92% yield; **IR** (KBr): ν 2928, 2853, 2108, 1701, 1531, 1428, 138 cm^{-1}; **^{1}H NMR** (400 MHz, $CDCl_3$): δ 7.27-7.38 (m, 5H), 5.46 (d, J = 9.2 Hz), 4.84 (m, 1H), 4.55 (dd, J = 6.8, 4.8 Hz, 1H), 4.07-4.13 (m, 2H), 3.83-3.88 (m, 1H), 3.34 (s, 3H), 3.33 (s, 3H), 1.80-1.94 (m, 2H), 1.19-1.25 (m, 3H); **^{13}C NMR** (100 MHz, $CDCl_3$): δ 156.5, 140.0, 129.1, 128.2, 126.7, 102.4, 64.5, 62.7, 61.6, 53.8, 35.8, 14.8; **HRMS** (ESI) m/z calculated for $C_{15}H_{22}N_4O_4$ $[M+Na]^+$: 345.1533, found 345.1600.

***Trans*-1-(4-Methylphenyl)-1-*N*-Boc-amino-2-(4-phenyltriazole)-1-**



phenylpropane (17): white solid compound; 96% yield; **IR** (KBr): ν 3393, 3270, 3119, 3054, 3031, 2962, 2926, 2856, 1705, 1516, 1458, 1365 cm^{-1}; **^{1}H NMR** (400 MHz, $CDCl_3$): δ 7.59-7.62 (m, 2H), 7.34-7.38 (m, 2H), 7.28-7.30 (m, 1H), 7.16-7.23 (m, 3H), 6.98-7.02 (m, 4H), 6.94 (s, 1H), 6.87-6.91(m, 2H), 6.42 (d, J = 8.7 Hz, 1H), 5.26-5.31 (m, 1H), 4.68-4.74 (m, 1H), 3.49-3.56 (m,1H), 3.33-3.38 (m, 1H), 2.25 (s, 3H), 1.43 (s, 9H); **^{13}C NMR** (100 MHz, $CDCl_3$): δ 155.8, 146.8, 139.7, 137.0, 133.8, 130.6, 129.8, 129.1, 129.0, 129.0, 128.4, 128.1, 126.3, 125.9, 122.1, 80.3, 69.3, 53.7, 39.0, 31.3, 21.3;**HRMS** (ESI) m/z calculated for $C_{29}H_{32}N_4O_2[M+H]^+$: 469.2598, found: 469.2616.

ethyl ((1*S*,2*R*)-4,4-dimethoxy-1-phenyl-2-(4-phenyl-1*H*-1,2,3-triazol-1 yl)butyl) carbamate (18): white solid compound; 91% yield; **IR** (KBr): ν 3297,



3123, 3061, 2949, 2634, 1708, 1541, 1461, 1370 cm^{-1}; **^{1}NMR** (400 MHz, $CDCl_3$): δ 7.67-7.71 (m, 2H), 7.36-7.41(m, 2H), 7.29-7.33 (m, 1H), 7.18-7.23 (m, 4H), 6.98-7.01 (m, 2H), 6.42-6.44 (m, 1H), 5.23-5.25 (m, 1H), 4.80-4.85 (m, 1H), 4.05-4.14 (m, 2H), 3.30 (s, 3H), 3.25 (s, 3H), 2.59-2.66 (m, 1H), 2.35-2.40 (m, 1H), 1.20-1.25 (m, 3H); **^{13}C NMR** (100 MHz, $CDCl_3$): δ 156.6, 147.1, 139.2, 130.5, 129.2, 129.1, 128.6, 128.3, 126.3, 126.0, 121.9, 102.0,

63.1, 61.6, 54.2, 53.9, 35.9, 14.8; **HRMS** (ESI) m/z calculated for $C_{23}H_{28}N_4O_4[M+H]^+$: 425.2183, found: 425.2266.

Synthesis of 1-Ethoxycarbonyl-2-hydroxy-4-(4-phenyltriazole)-5-phenylpyrrolidine (19):

To a stirred solution of compound **18** (0. 1 mmol) in acetone/water (3: 1) medium was added pTSA (0.01 mmol). The reaction mixture was heated at 60 °C for 4 h (**Scheme 2.21**). The progress of the reaction was monitored by TLC. After completion of the reaction, the mixture was extracted with ethyl acetate (3 × 10 mL), washed with water and brine respectively and dried with Na_2SO_4. The organic phase was evaporated by rotary evaporator under reduced pressure to give the crude product. The crude product was purified by column chromatography over silica gel to furnish the pure product (95% yield). The product was characterized by corresponding spectroscopic data (IR, NMR, HRMS).

(**19**) White Solid; 95% yield ; **IR** (KBr): ν 3447, 3133, 2985, 2911, 1698, 1433, 1384 cm^{-1}; **^{1}H NMR** (400 MHz, DMSO-d6, mixture of diastereomer = 90:10): δ *(major diastereomer)* 8.20 (s, 1H), 7.62-7.64 (m, 2H), 7.38-7.43 (m, 2H), 7.29-7.33 (m, 1H), 7.10-7.18 (m, 5H), 6.69 (br s), 5.77-5.81 (m, 1H), 5.59-5.65 (m, 1H), 5.38 (d, *J* = 7.8 Hz, 1H), 4.05-4.08 (m, 2H), 2.80-2.87 (m, 1H), 2.56-2.62 (m, 1H), 1.18-1.21 (m, 3H) ; **^{13}C NMR** (100 MHz, DMSO-d6): δ (*major diastereomer*)154.1, 145.7, 137.2, 130.6, 128.8, 127.8, 127.7, 127.6, 127.1, 126.7, 124.9, 121.0, 79.7, 63.9, 60.7, 59.4, 35.8 14.5; **HRMS** (ESI) m/z calculated for $C_{21}H_{22}N_4O_3$ $[M+K]^+$: 417.1323, found 417.1426.

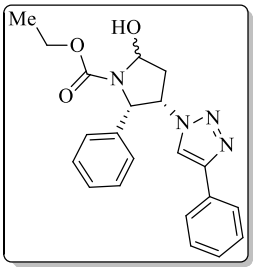


Table 2.3 Crystal data and structure refinement for **3aa**

Compound	**Compound 3aa**
Empirical formula	$C_{15}H_{11}NO_3S$
Molecular weight	285.31
Temperature	150(2) K
Wavelength (Å)	0.71073
Crystal system, space group	Monoclinic, P 21/c
a (Å)	12.6212(3)
b (Å)	6.9825(2)
c (Å)	15.3469(9)
α (°)	90
β (°)	101.991(3)
γ (°)	90
Volume ($Å^3$)	1322.97(9)
Z, Calculated density (mg/m^3)	4, 1.432
Absorption coefficient (mm^{-1})	0.250
F(000)	592
Crystal size (mm)	0.23 × 0.18 × 0.13
θ range (deg)	3.22 to 24.99
Limiting indices	-13<=h<=15, -8<=k<=8, -18<=l<=11
Reflections collected / unique	8823 / 2319 [R(int) = 0.0227]
Completeness to θ = 25.00	99.9 % yield
Max. and min. transmission	0.9682 and 0.9446
Data / restraints / parameters	2319 / 0 / 181
Goodness-of-fit on F^2	1.032
Final R indices [I>2sigma(I)]	R1 = 0.0338, wR2 = 0.0861
R indices (all data)	R1 = 0.0377, wR2 = 0.0896
Largest diff. peak and hole ($e.A^{-3}$)	0.164 and -0.411
CCDC	**913688**

Table 2.4 Crystal data of compound **13**

Compound	**Compound 13**
Empirical formula	C_{21} H_{25} N O_5 S
Molecular weight	403.48
Temperature	150(2) K
Wavelength (Å)	0.71073
Crystal system, space group	Monoclinic, P21/n
a (Å)	9.8446(3)
b (Å)	14.2440(3)
c (Å)	15.0095(3)
α (^{o})	90
β (^{o})	97.378(2)
γ (^{o})	90.
Volume (Å^3)	2087.30(9)
Z, Calculated density (mg/m^3)	4, 1.284
Absorption coefficient (mm^{-1})	0.186
F(000)	856
Crystal size (mm)	0.23 × 0.18 × 0.12
θ range (deg)	3.00 to 24.99
Limiting indices	-11<=h<=9, -16<=k<=16, -17<=l<=1
Reflections collected / unique	17195 / 3671 [R(int) = 0.0243]
Completeness to θ = 25.00	99.8 % yield
Max. and min. transmission	0.9780 and 0.9584
Data / restraints / parameters	3671 / 0 / 257
Goodness-of-fit on F^2	1.094
Final R indices [I>2sigma(I)]	R1 = 0.0393, wR2 = 0.1062
R indices (all data)	R1 = 0.0448, wR2 = 0.1111
Largest diff. peak and hole (e.A^{-3})	0.262 and -0.320
CCDC	**913689**

Table 2.5 Crystal data of compound **15**

Compound	**Compound 15**
Empirical formula	C_{21} H_{26} N_4 O_2
Molecular weight	366.45
Temperature	293(2) K
Wavelength (Å)	0.71073
Crystal system, space group	monoclinic, P 21/c
a (Å)	5.47870(10)
b (Å)	21.0779(6)
c (Å)	16.8942(4)
α (^{o})	90
β (^{o})	93.526(2)
γ (^{o})	90
Volume (Å^3)	1947.24(8)
Z, Calculated density (mg/m^3)	4, 1.243
Absorption coefficient (mm^{-1})	0.082
F(000)	776
Crystal size (mm)	0.08 x 0.05 x 0.02
θ range (deg)	3.09 to 25.00
Limiting indices	-6<=h<=6, -25<=k<=24, -17<=l<=20
Reflections collected / unique	13935 / 3431 [R(int) = 0.0367]
Completeness to θ = 25.00	99.9 % yield
Max. and min. transmission	0.9984 and 0.9935
Data / restraints / parameters	3431 / 0 / 248
Goodness-of-fit on F^2	1.068
Final R indices [I>2sigma(I)]	R1 = 0.0501, wR2 = 0.1321
R indices (all data)	R1 = 0.0634, wR2 = 0.1427
Largest diff. peak and hole (e.A^{-3})	0.752 and -0.203
CCDC	**913690**

2.6 Copies of ^{1}H and ^{13}C NMR spectra of some important compounds described in Chapter 2

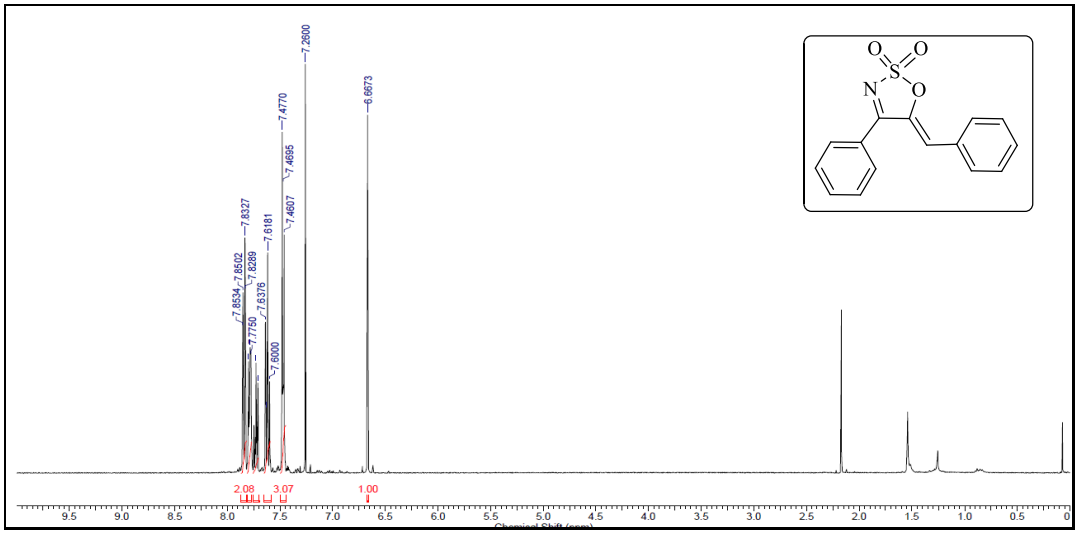


Figure 2.5 400 MHz ^{1}H NMR spectrum of **3aa** in $CDCl_3$

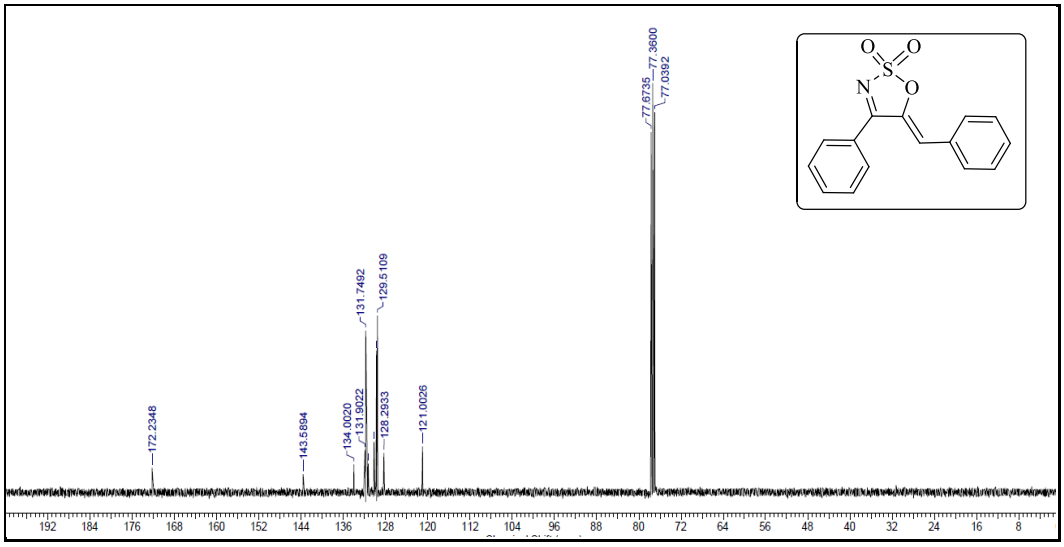


Figure 2.6 100 MHz ^{13}C NMR spectrum of **3aa** in $CDCl_3$

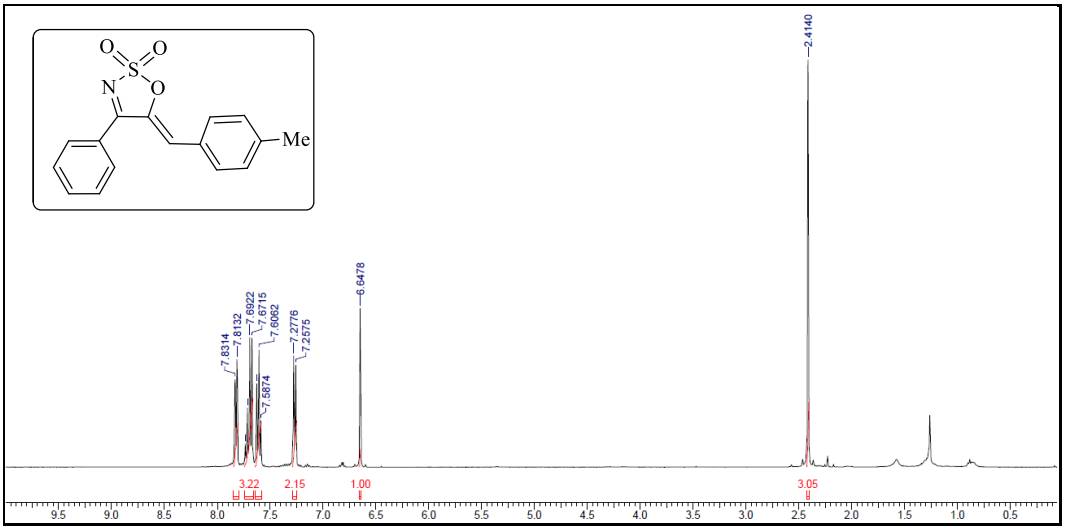


Figure 2.7 400 MHz ^{1}H NMR spectrum of **3ab** in $CDCl_3$

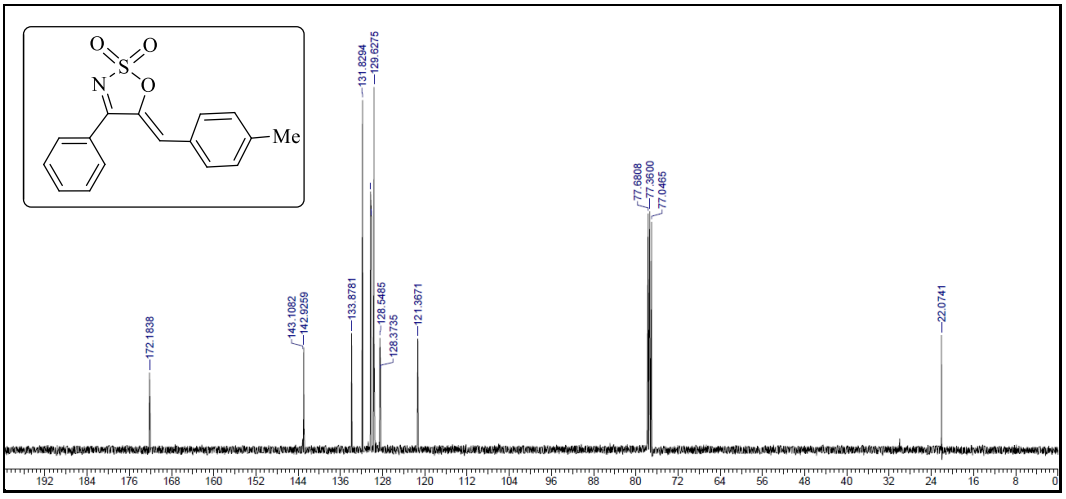


Figure 2.8 100 MHz ^{13}C NMR spectrum of **3ab** in $CDCl_3$

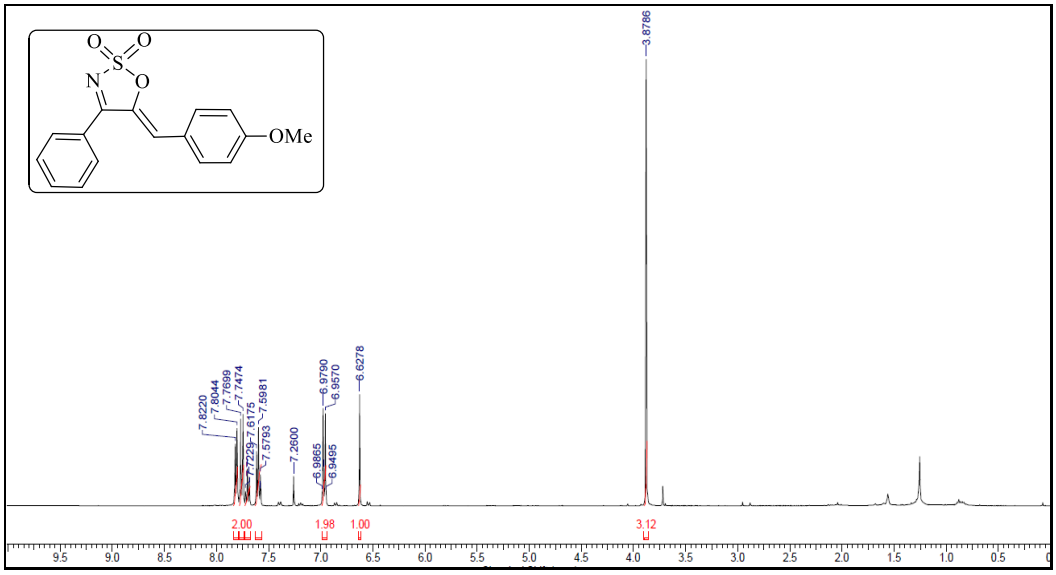


Figure 2.9 400 MHz ^{1}H NMR spectrum of **3ac** in $CDCl_3$

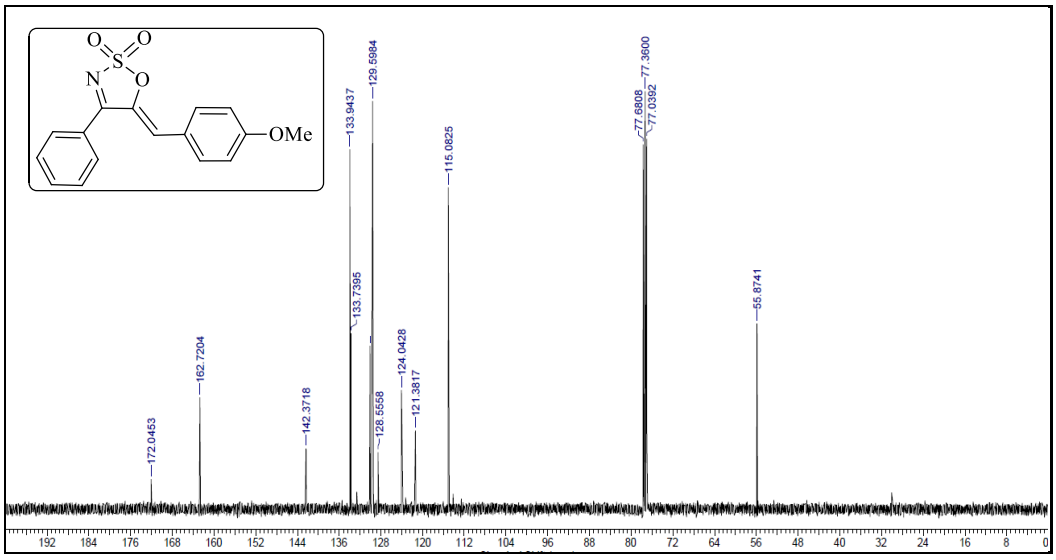


Figure 2.10 100 MHz ^{13}C NMR spectrum of **3ac** in $CDCl_3$

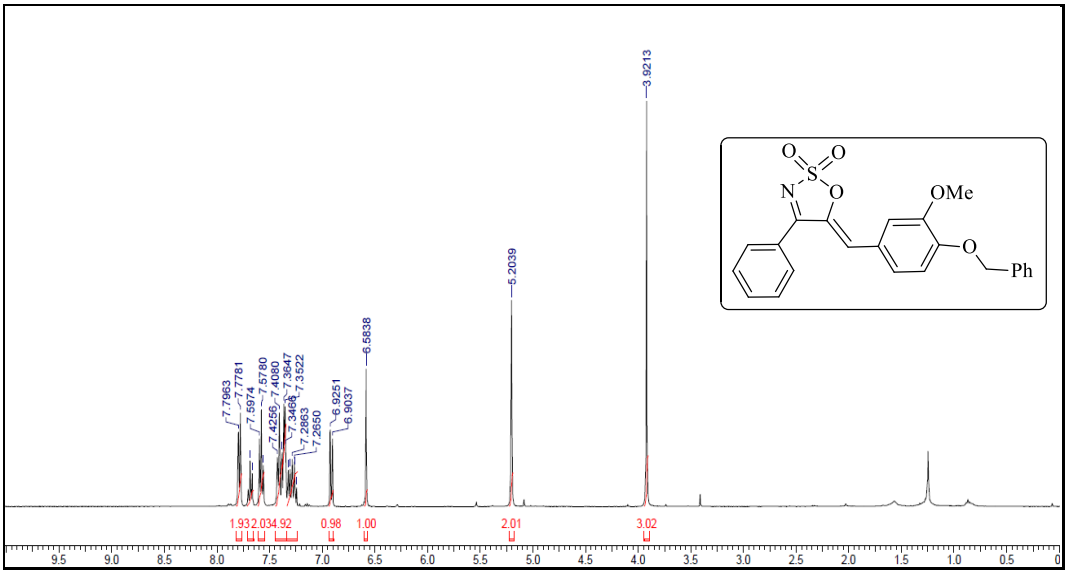


Figure 2.11 400 MHz ^{1}H NMR spectrum of **3ad** in $CDCl_3$

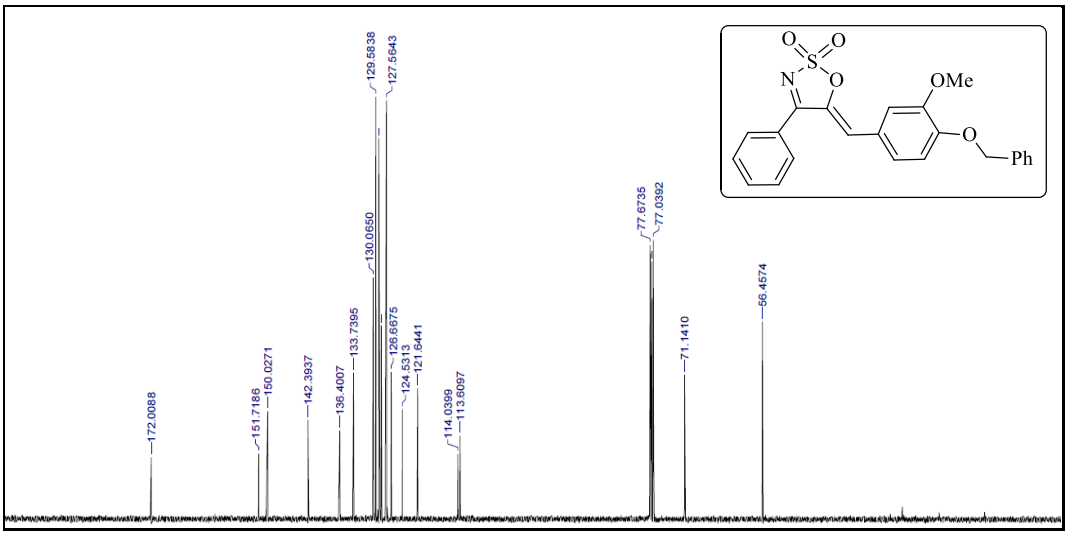


Figure 2.12 100 MHz ^{13}C NMR spectrum of **3ad** in $CDCl_3$

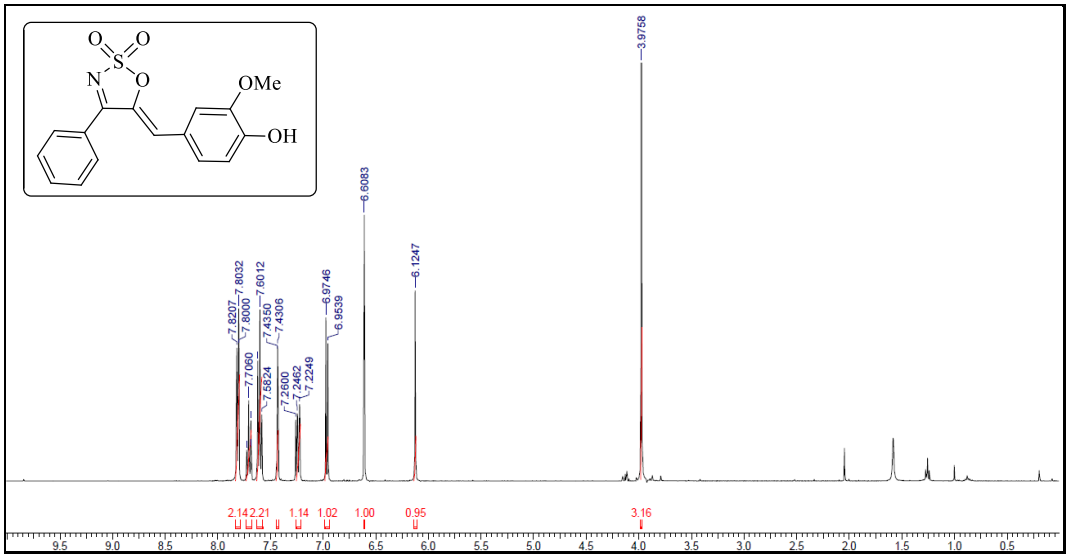


Figure 2.13 400 MHz ^{1}H NMR spectrum of **3ae** in $CDCl_3$

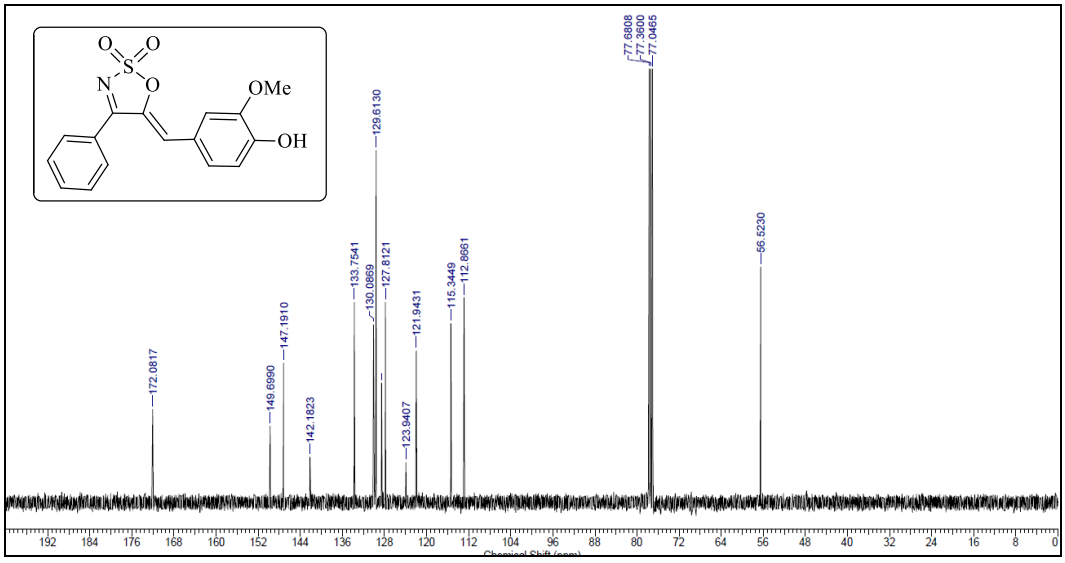


Figure 2.14 100 MHz ^{13}C NMR spectrum of **3ae** in $CDCl_3$

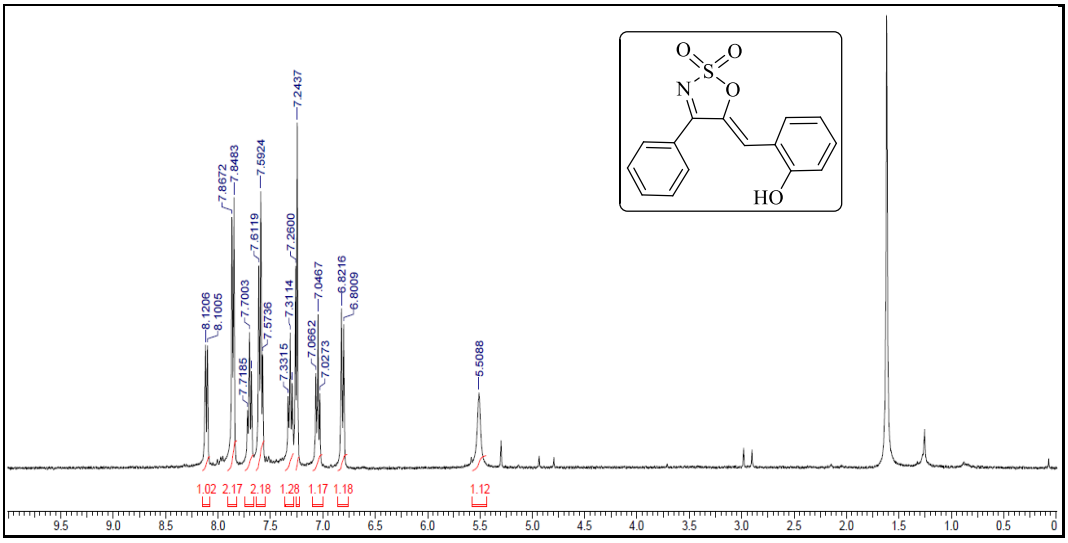


Figure 2.15 400 MHz ^{1}H NMR spectrum of **3af** in $CDCl_3$

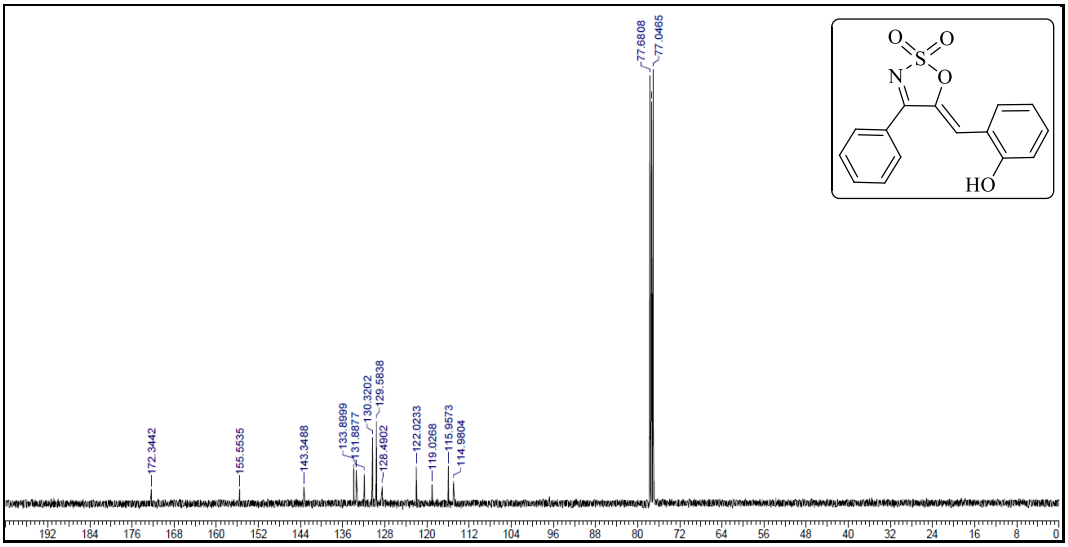


Figure 2.16 100 MHz ^{13}C NMR spectrum of **3af** in $CDCl_3$

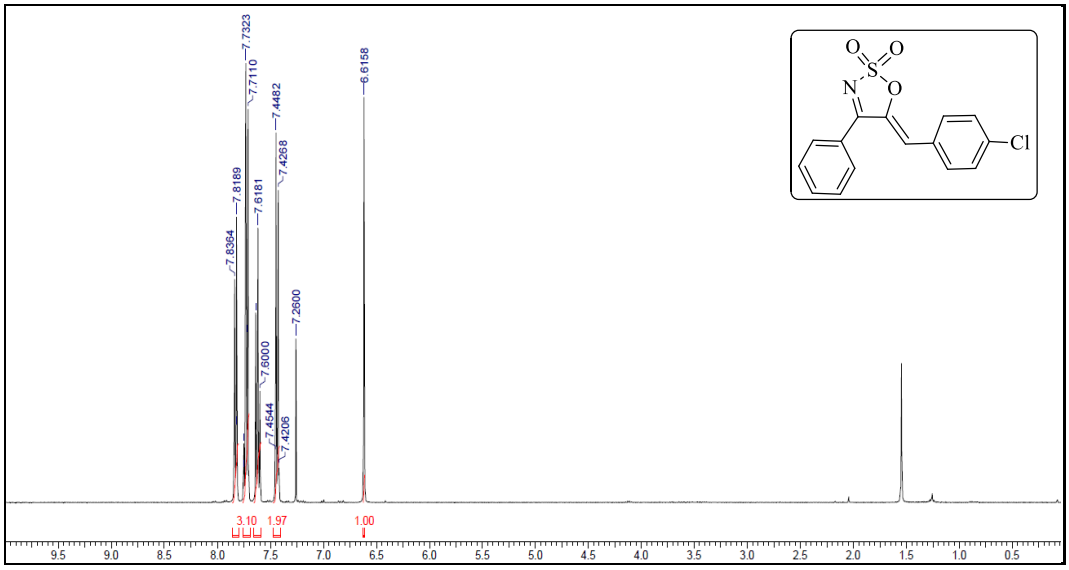


Figure 2.17 400 MHz ^{1}H NMR spectrum of **3ag** in $CDCl_3$

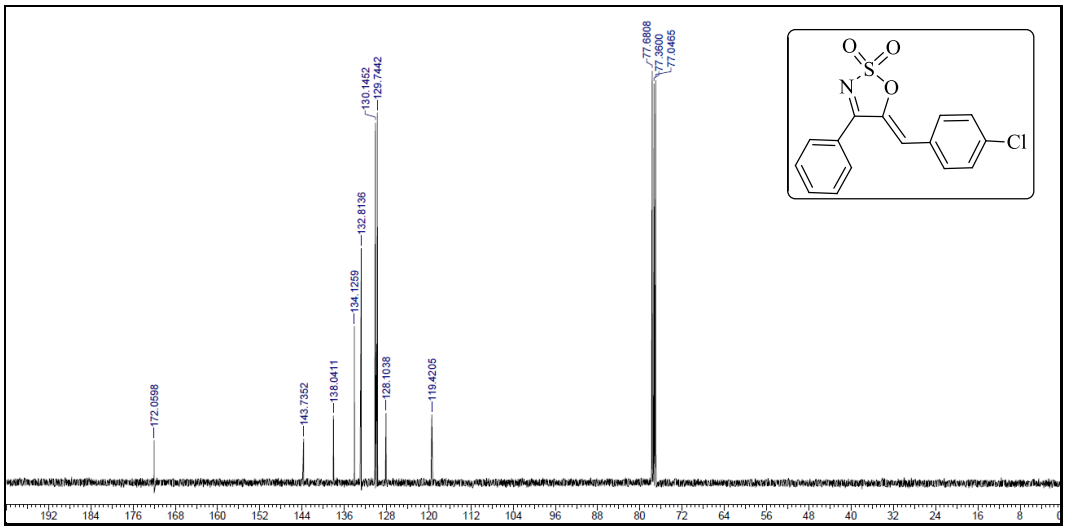


Figure 2.18 100 MHz ^{13}C NMR spectrum of **3ag** in $CDCl_3$

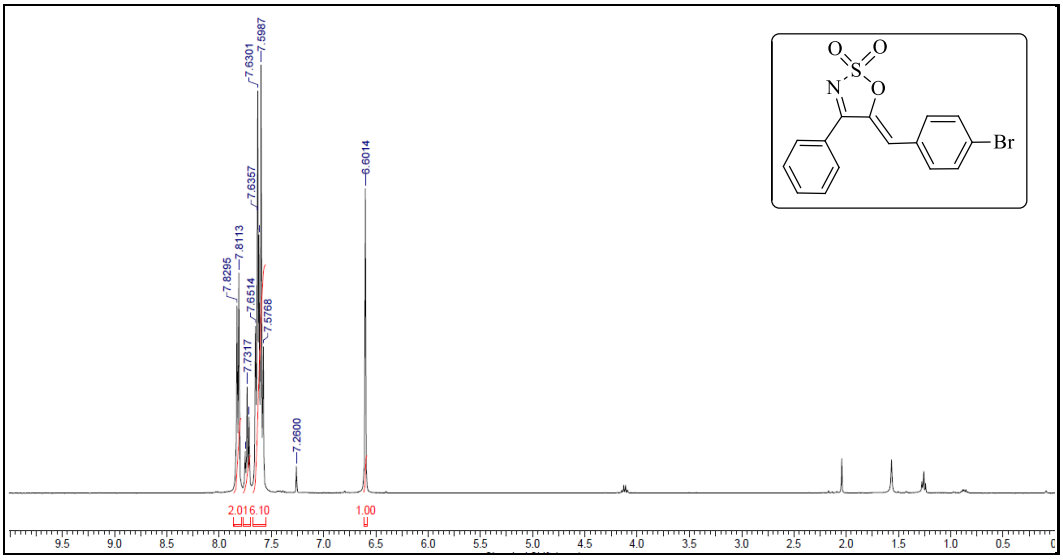


Figure 2.19 400 MHz ^{1}H NMR spectrum of **3ah** in $CDCl_3$

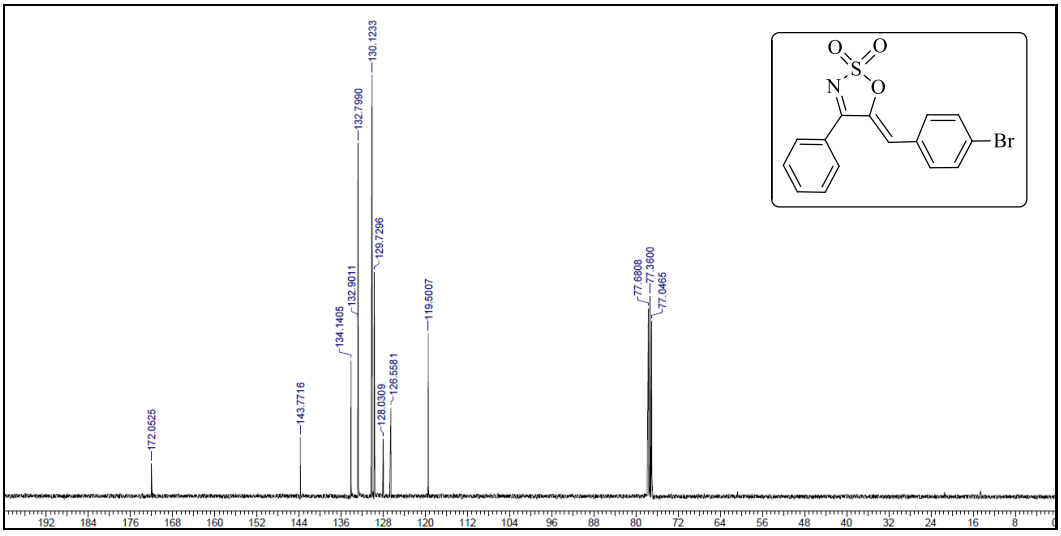


Figure 2.20 100 MHz ^{13}C NMR spectrum of **3ah** in $CDCl_3$

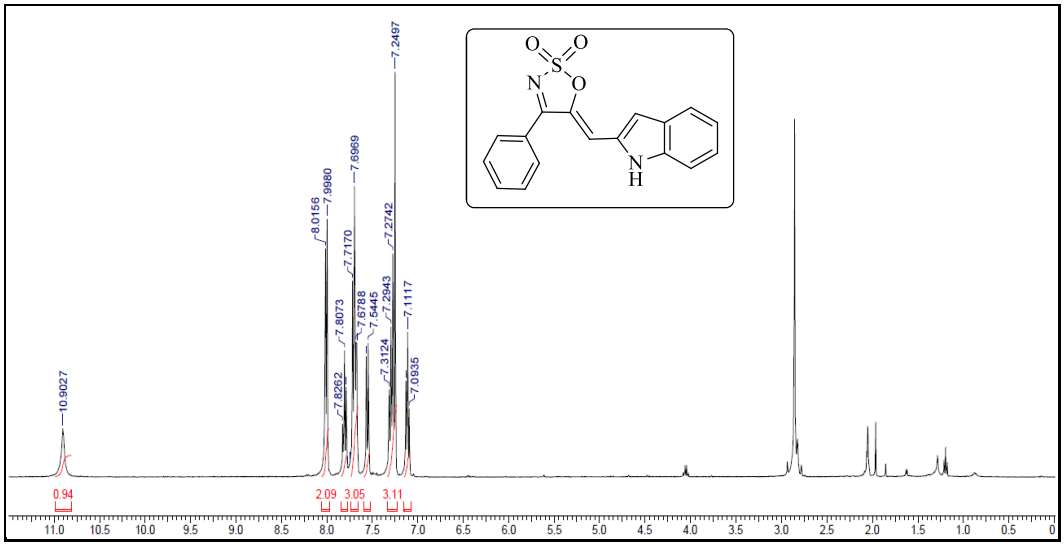


Figure 2.21 400 MHz ^{1}H NMR spectrum of **3ai** in $CDCl_3$

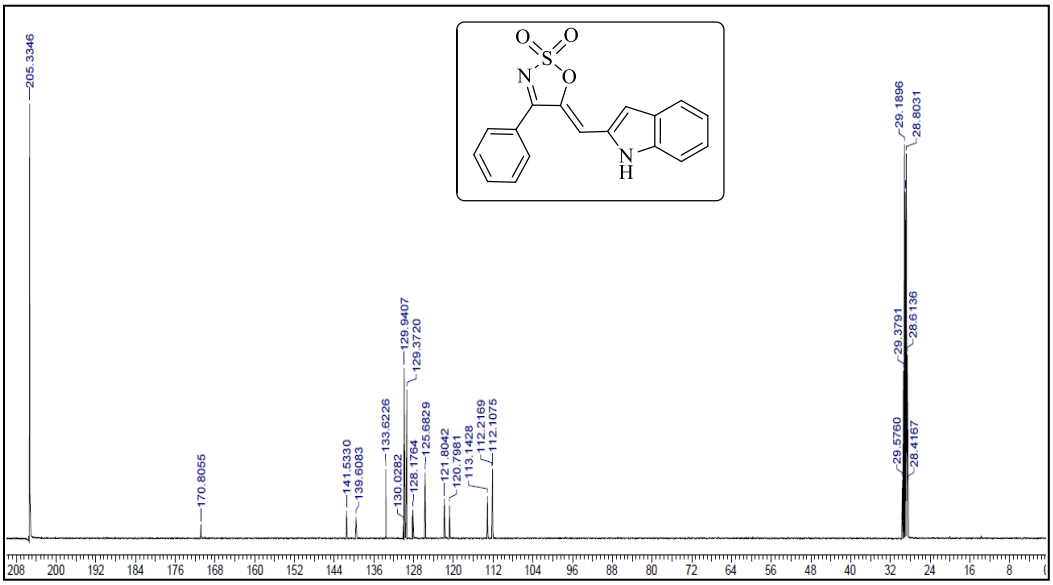


Figure 2.22 100 MHz ^{13}C NMR spectrum of **3ai** in $CDCl_3$

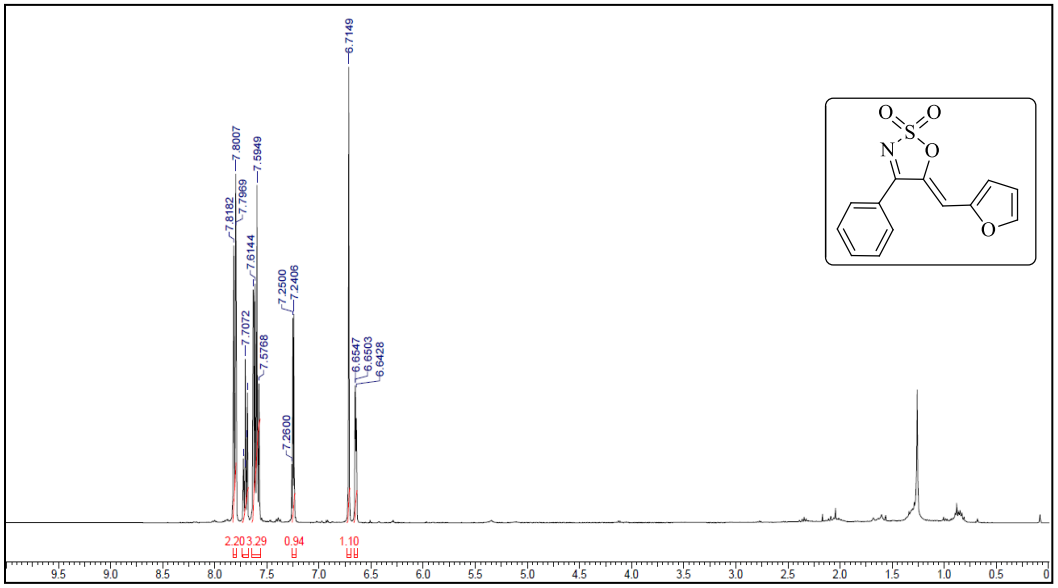


Figure 2.23 400 MHz ^{1}H NMR spectrum of **3aj** in $CDCl_3$

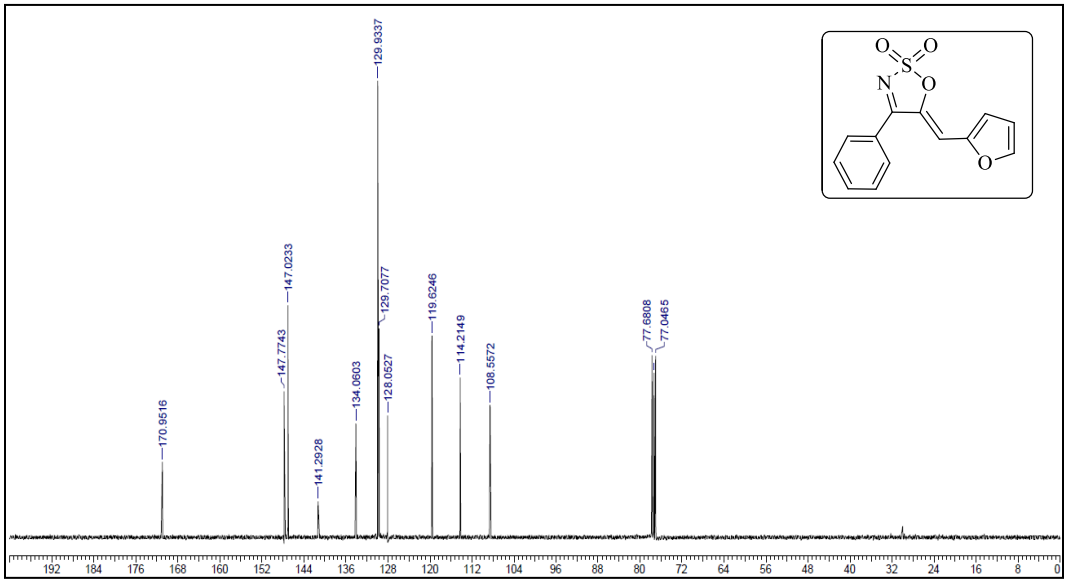


Figure 2.24 100 MHz ^{13}C NMR spectrum of **3aj** in $CDCl_3$

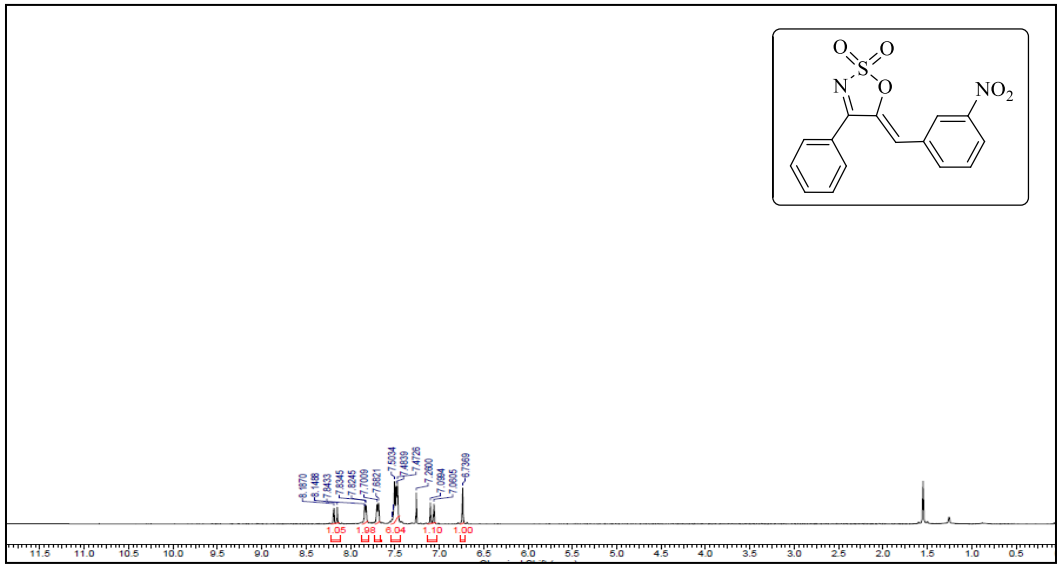


Figure 2.25 400 MHz ^{1}H NMR spectrum of **3ak** in $CDCl_3$

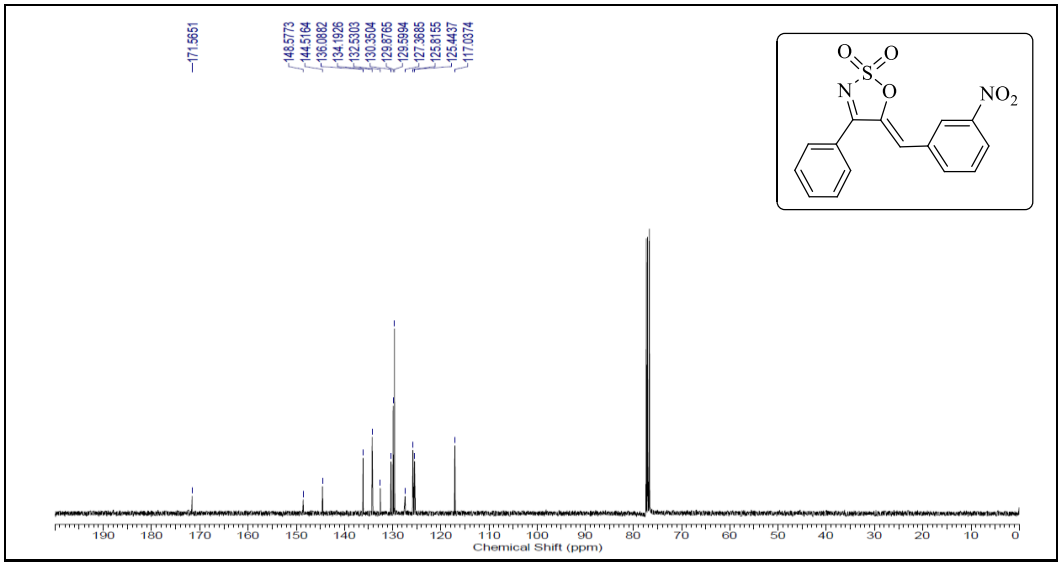


Figure 2.26 100 MHz ^{13}C NMR spectrum of **3ak** in $CDCl_3$

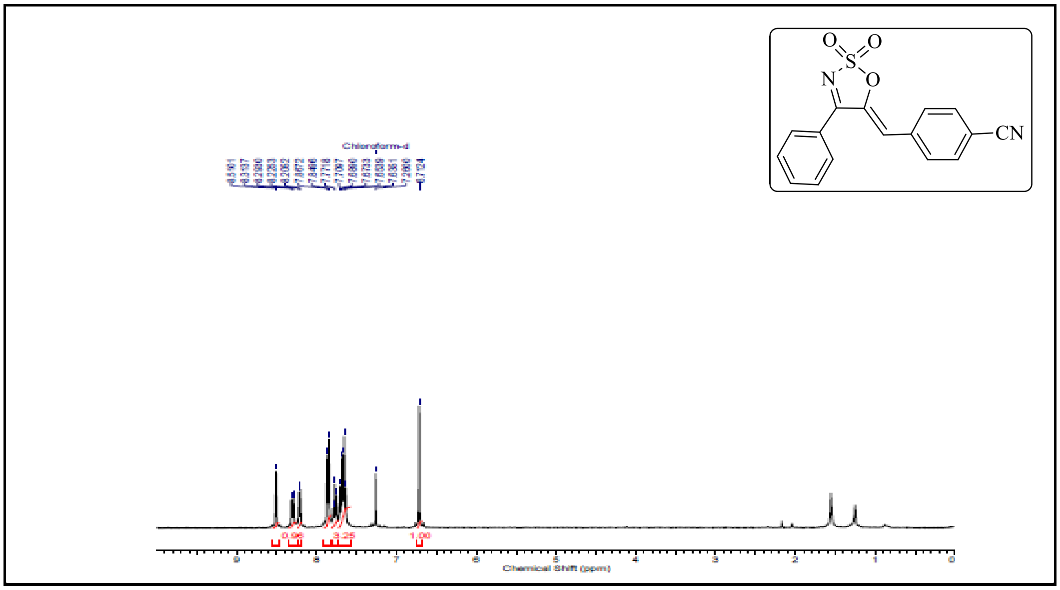


Figure 2.27 400 MHz ^{1}H NMR spectrum of **3al** in $CDCl_3$

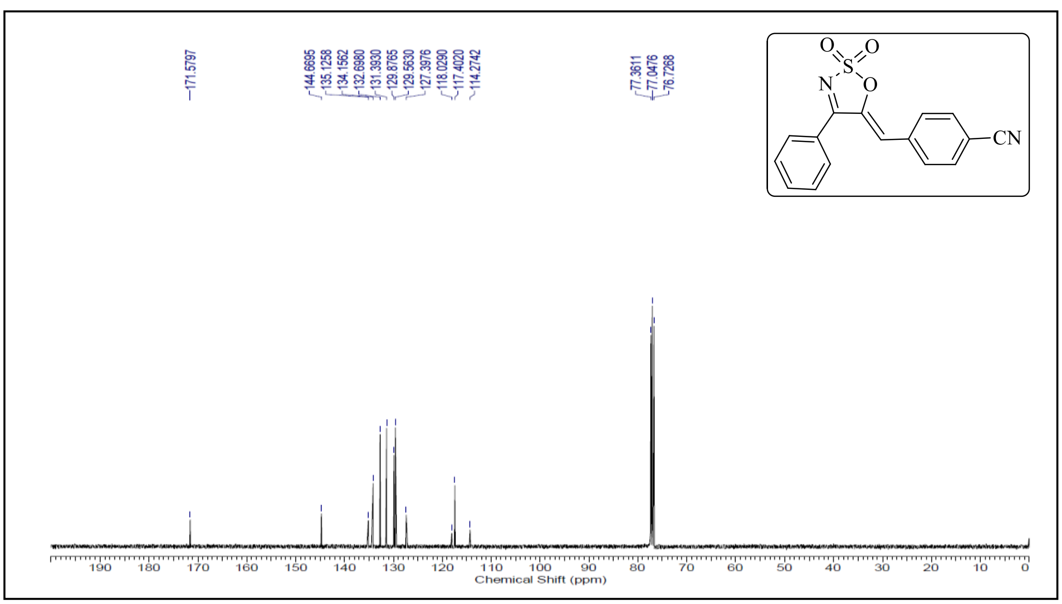


Figure 2.28 100 MHz ^{13}C NMR spectrum of **3al** in $CDCl_3$

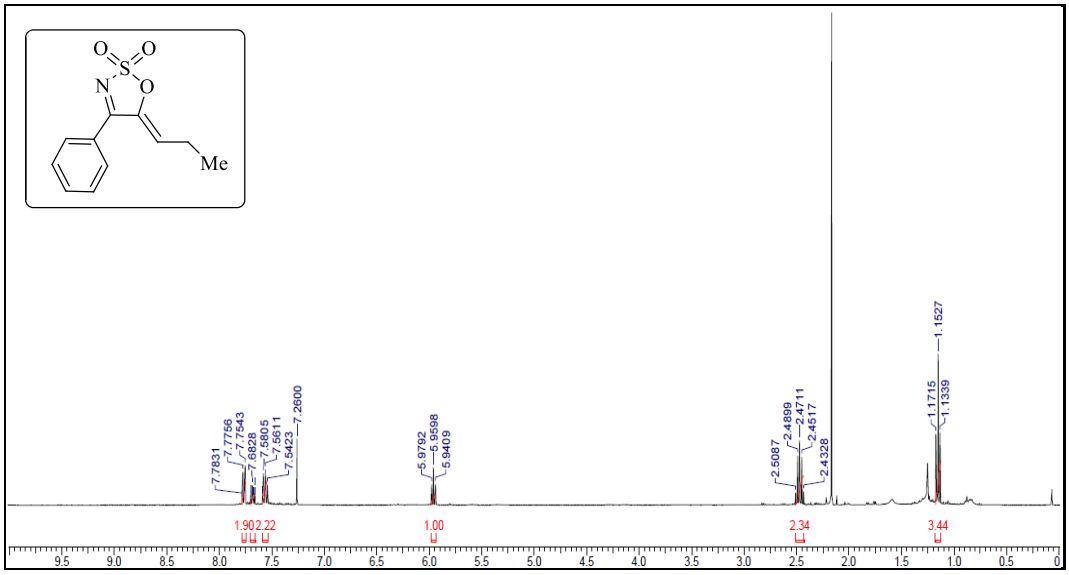


Figure 2.29 400 MHz ^{1}H NMR spectrum of **3am** in $CDCl_3$

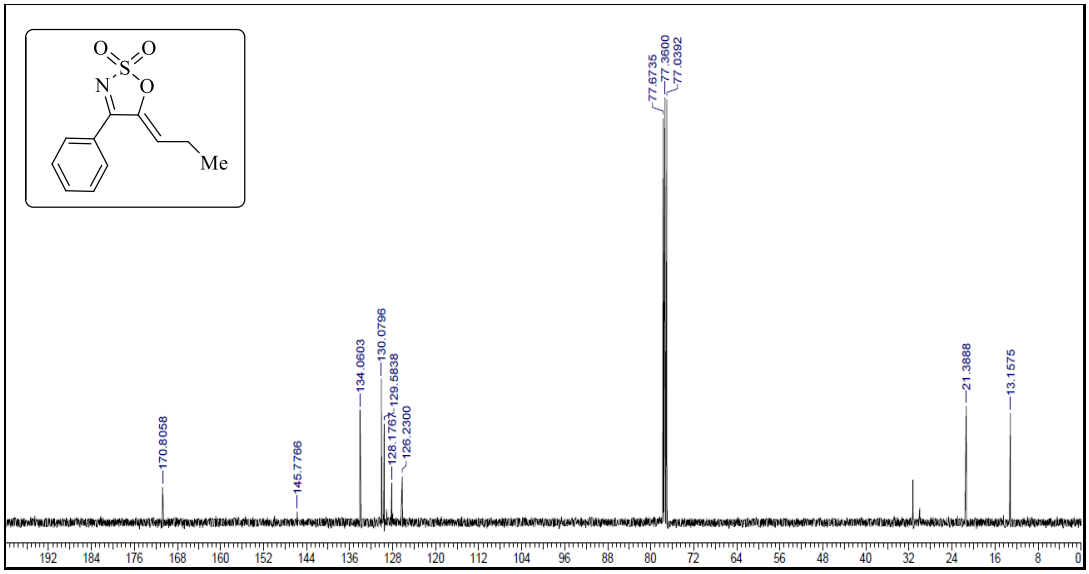


Figure 2.30 100 MHz ^{13}C NMR spectrum of **3am** in $CDCl_3$

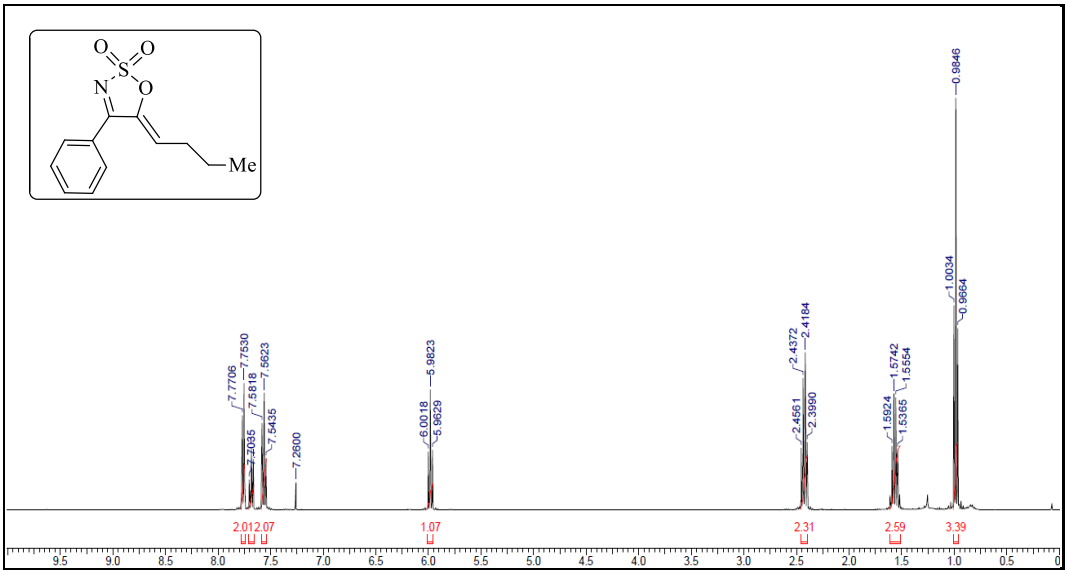


Figure 2.31 400 MHz ^{1}H NMR spectrum of **3an** in $CDCl_3$

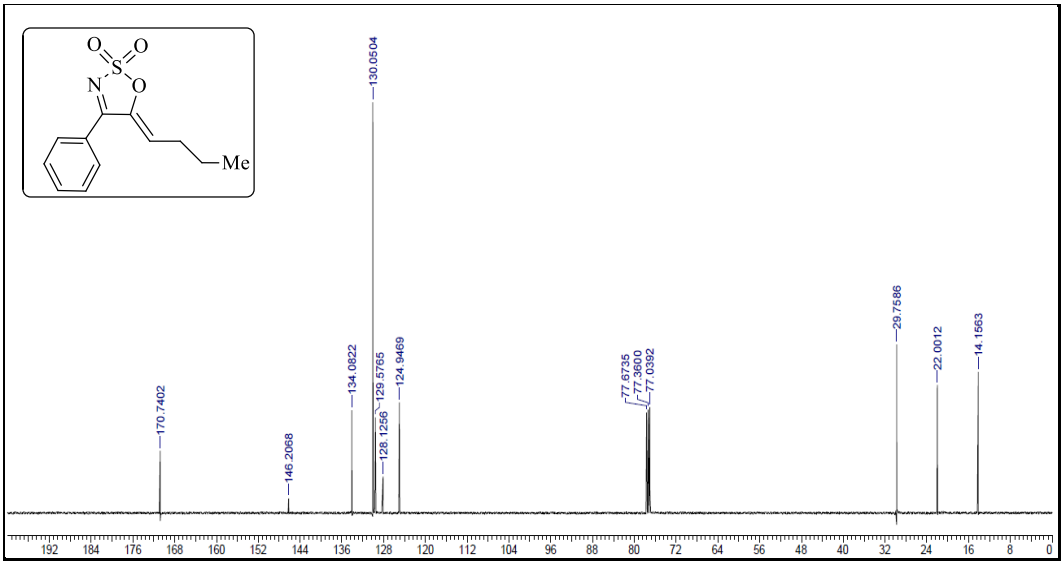


Figure 2.32 100 MHz ^{13}C NMR spectrum of **3an** in $CDCl_3$

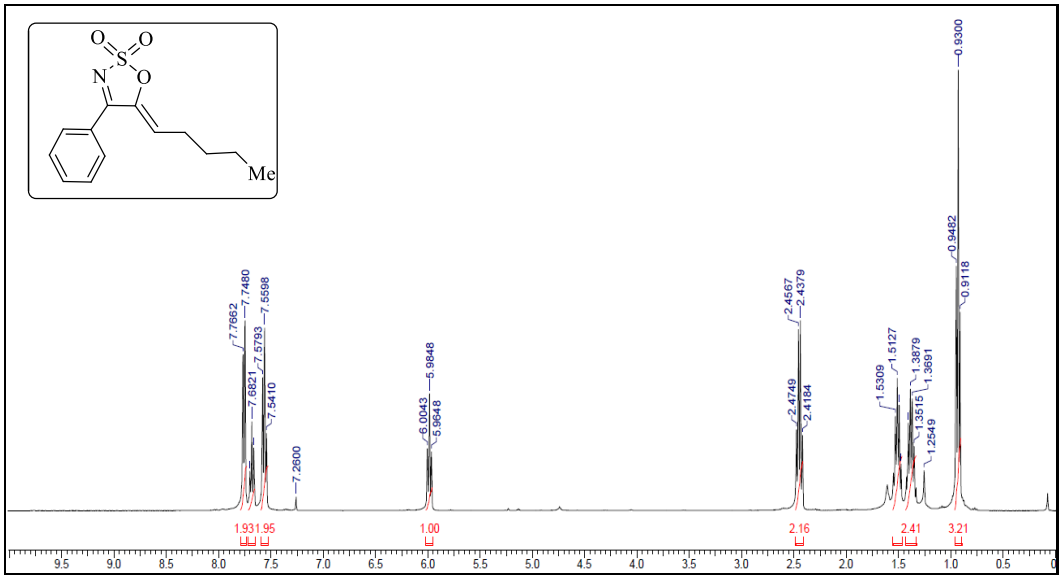


Figure 2.33 400 MHz ^{1}H NMR spectrum of **3ao** in $CDCl_3$

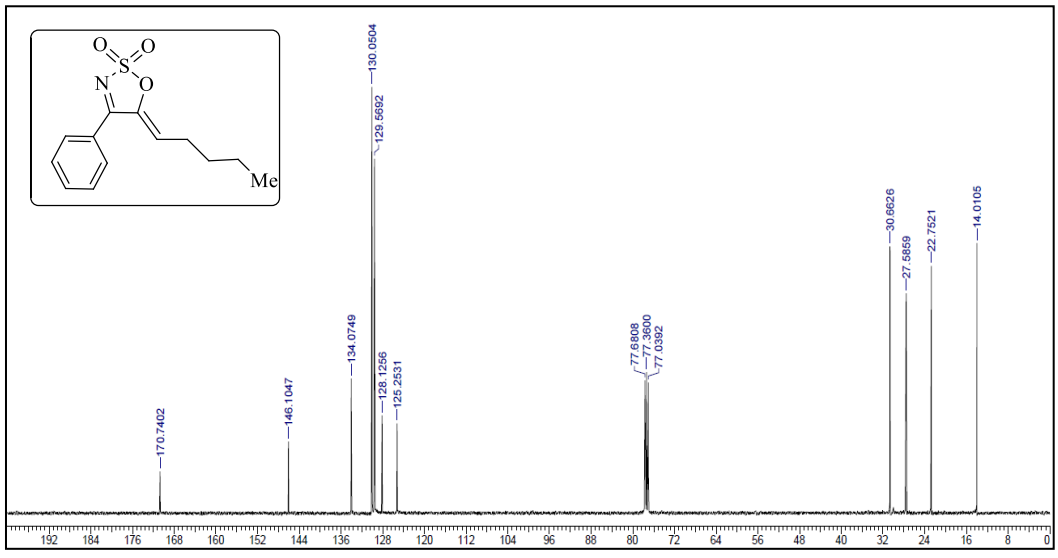


Figure 2.34 100 MHz ^{13}C NMR spectrum of **3ao** in $CDCl_3$

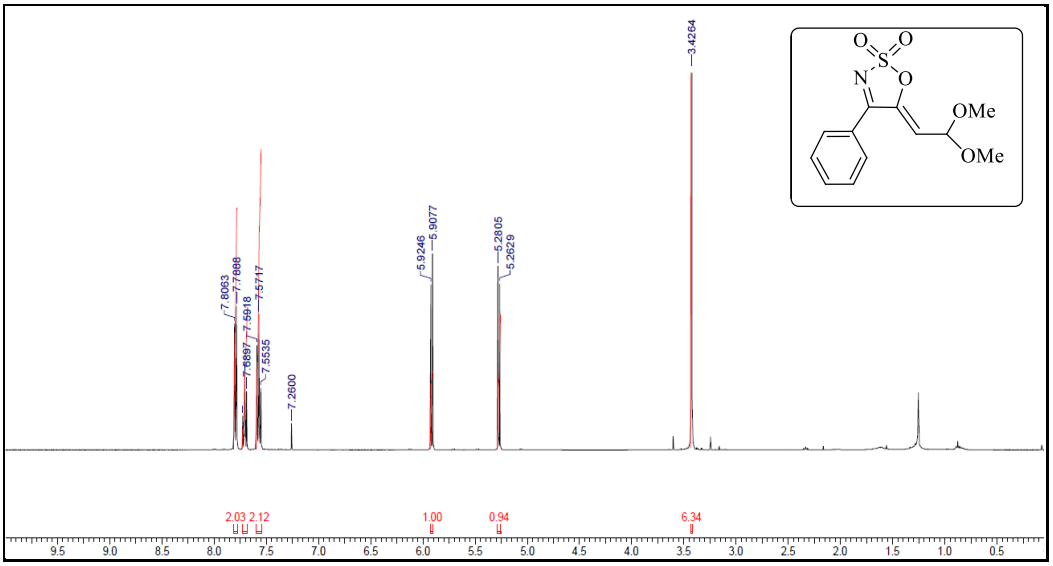


Figure 2.35 400 MHz ^{1}H NMR spectrum of **3ap** in $CDCl_3$

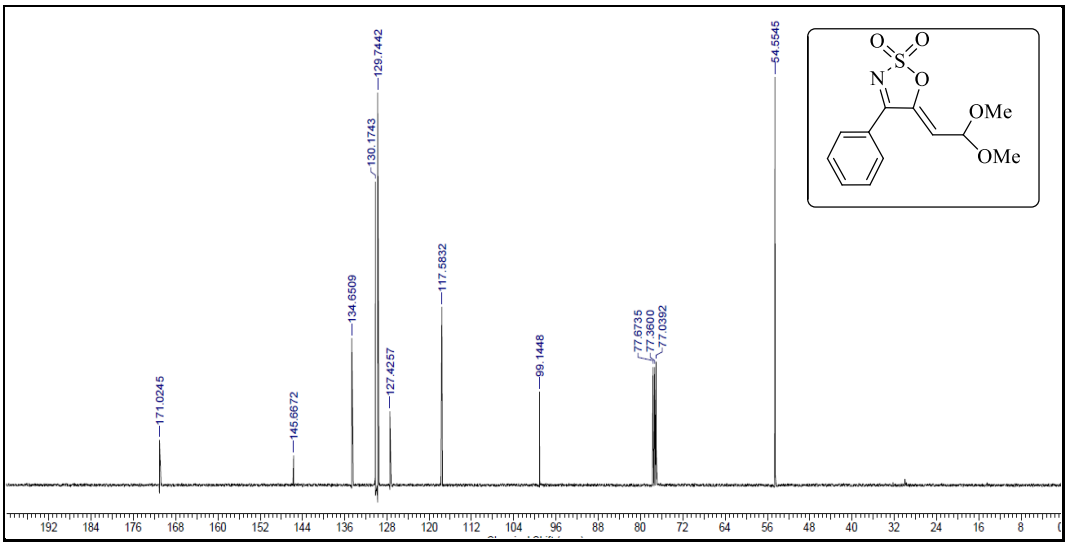


Figure 2.36 100 MHz ^{13}C NMR spectrum of **3ap** in $CDCl_3$

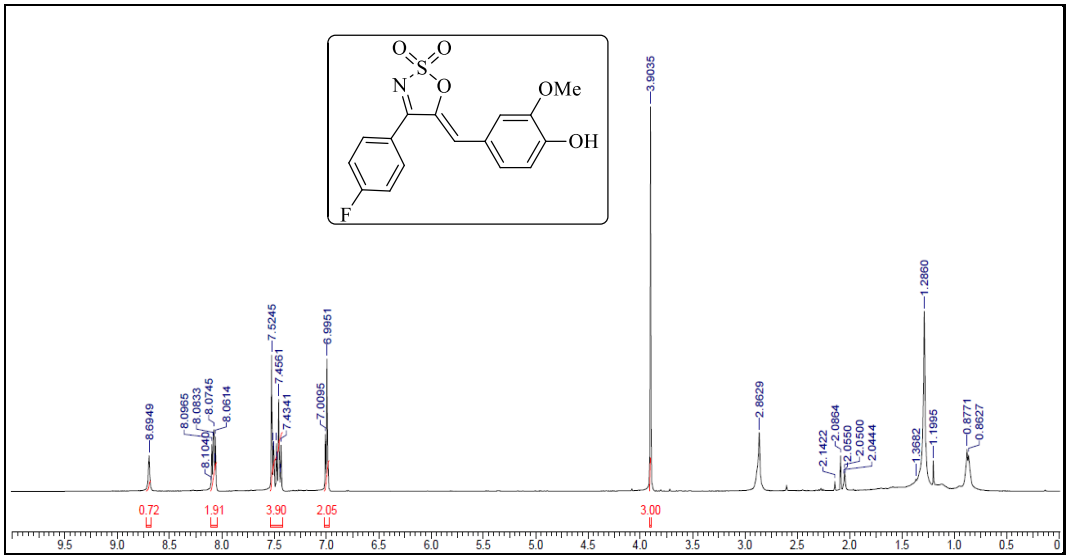


Figure 2.37 400 MHz ^{1}H NMR spectrum of **3be** in $CDCl_3$

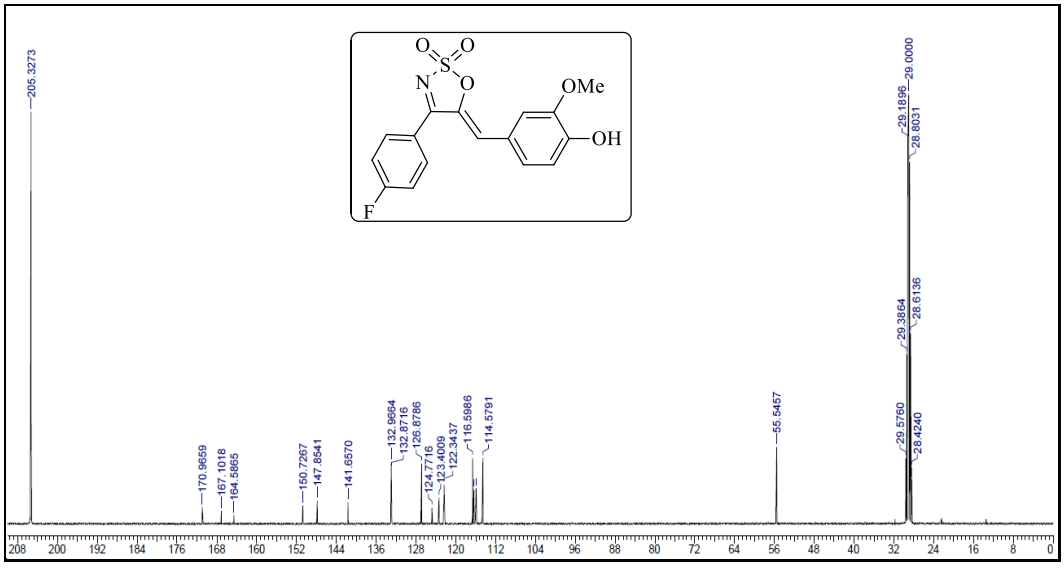


Figure 2.38100 MHz ^{13}C NMR spectrum of **3be** in $CDCl_3$

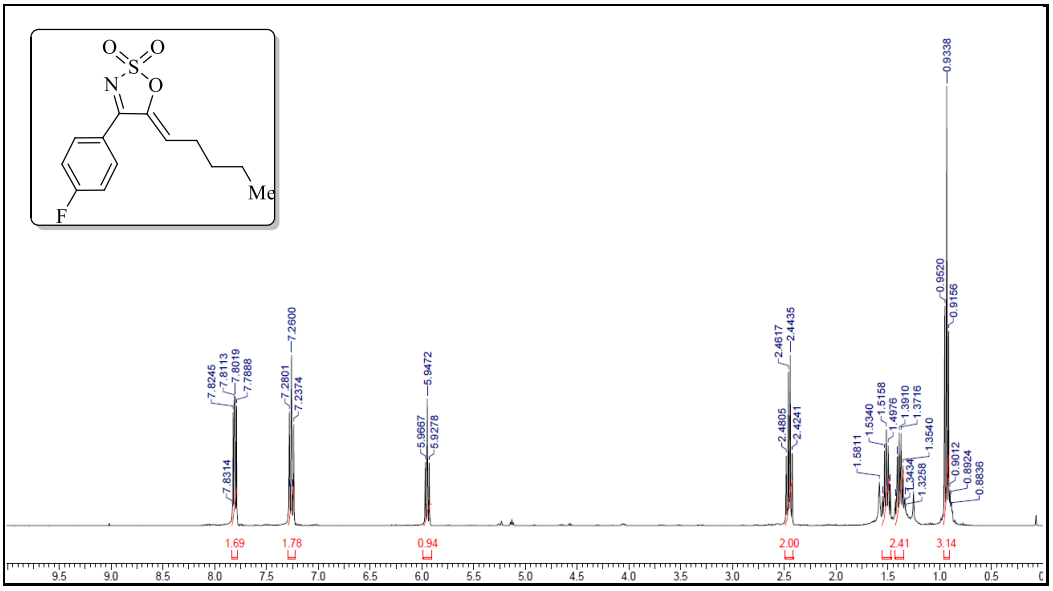


Figure 2.39 400 MHz ^{1}H NMR spectrum of **3bo** in $CDCl_3$

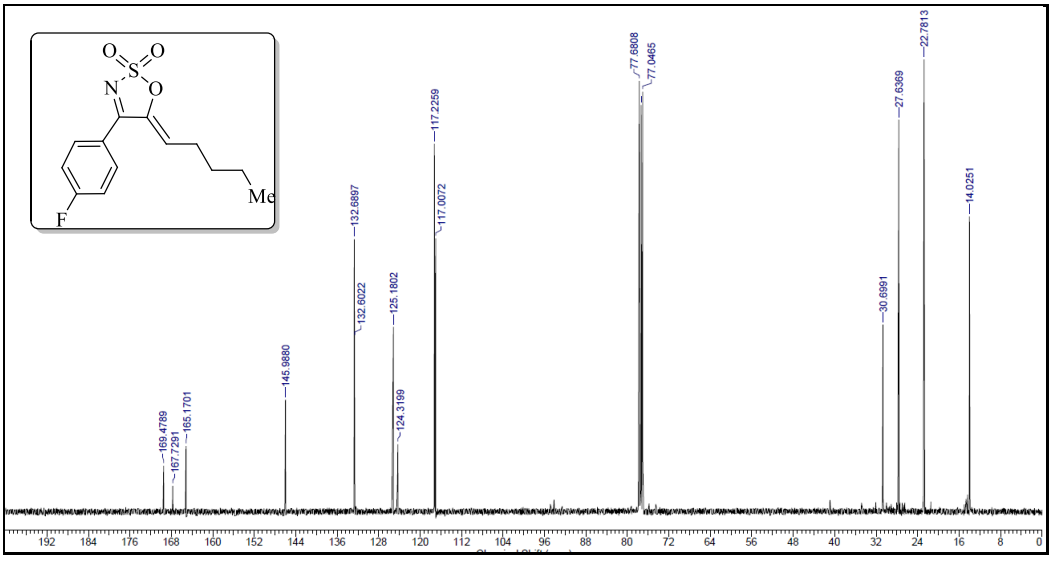


Figure 2.40 100 MHz ^{13}C NMR spectrum of **3bo** in $CDCl_3$

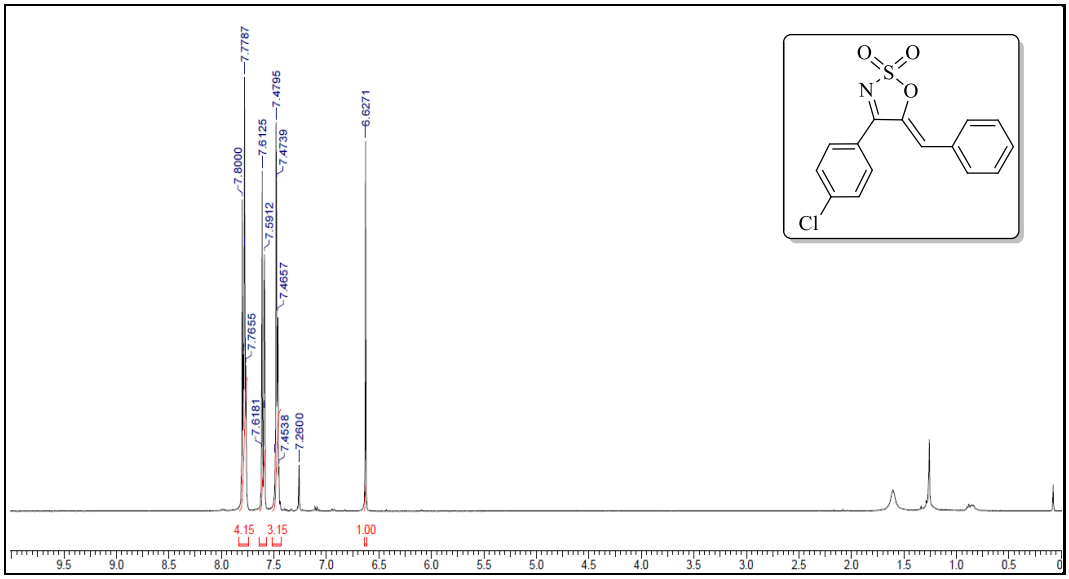


Figure 2.41 400 MHz ^{1}H NMR spectrum of **3ca** in $CDCl_3$

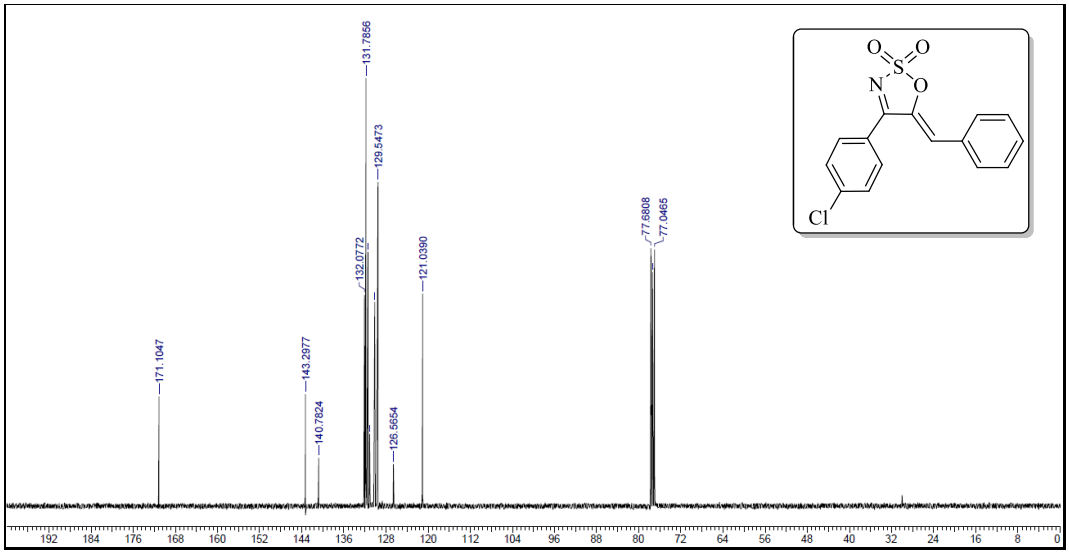


Figure 2.42 100 MHz ^{13}C NMR spectrum of **3ca** in $CDCl_3$

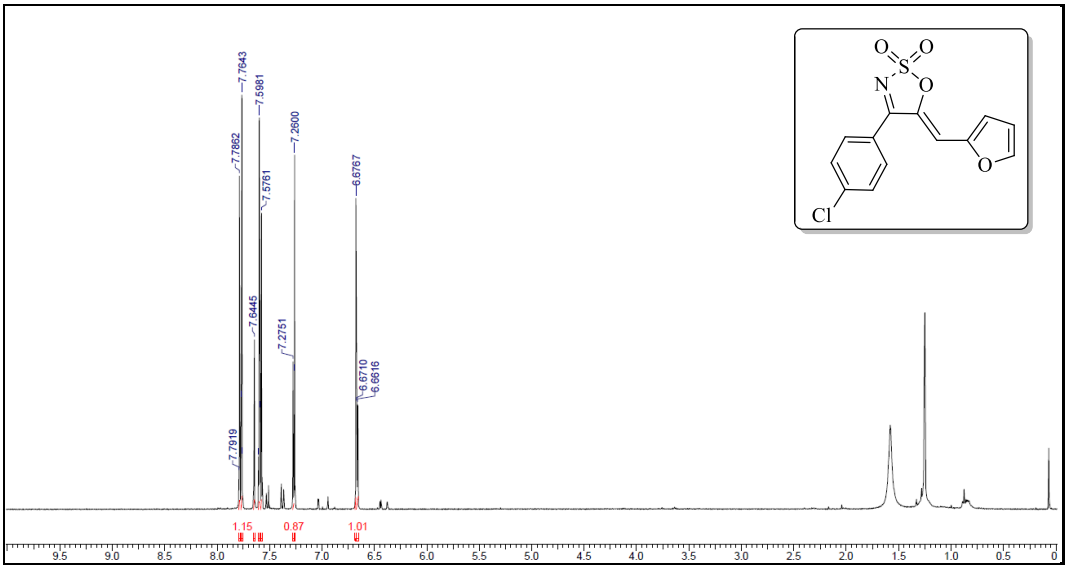


Figure 2.43 400 MHz ^{1}H NMR spectrum of **3cj** in $CDCl_3$

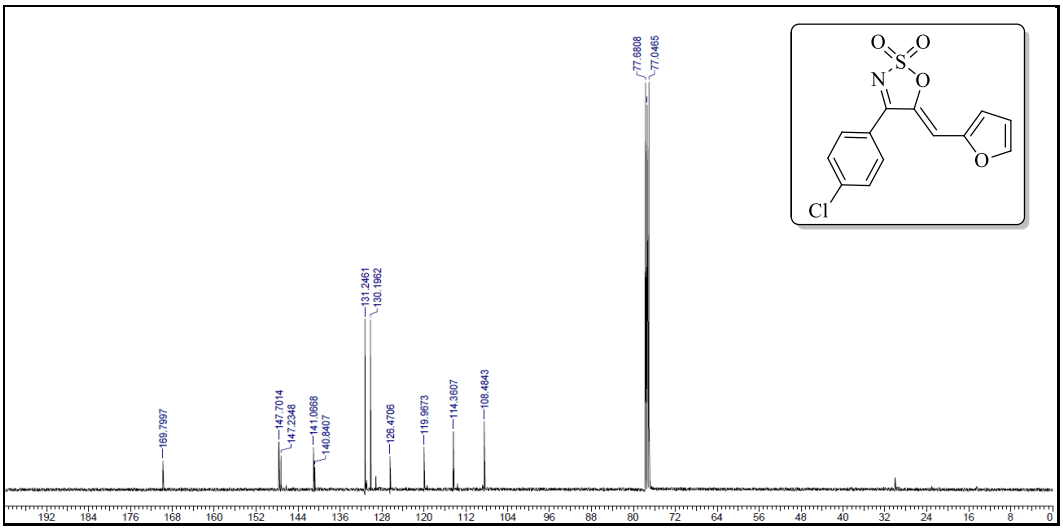


Figure 2.44 100 MHz ^{13}C NMR spectrum of **3cj** in $CDCl_3$

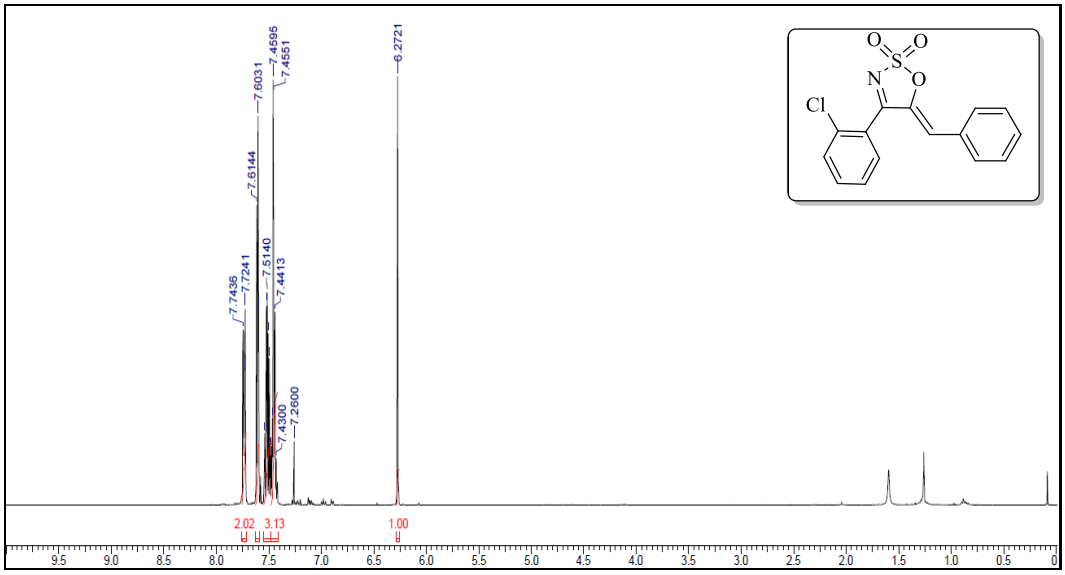


Figure 2.45 400 MHz ^{1}H NMR spectrum of **3da** in $CDCl_3$

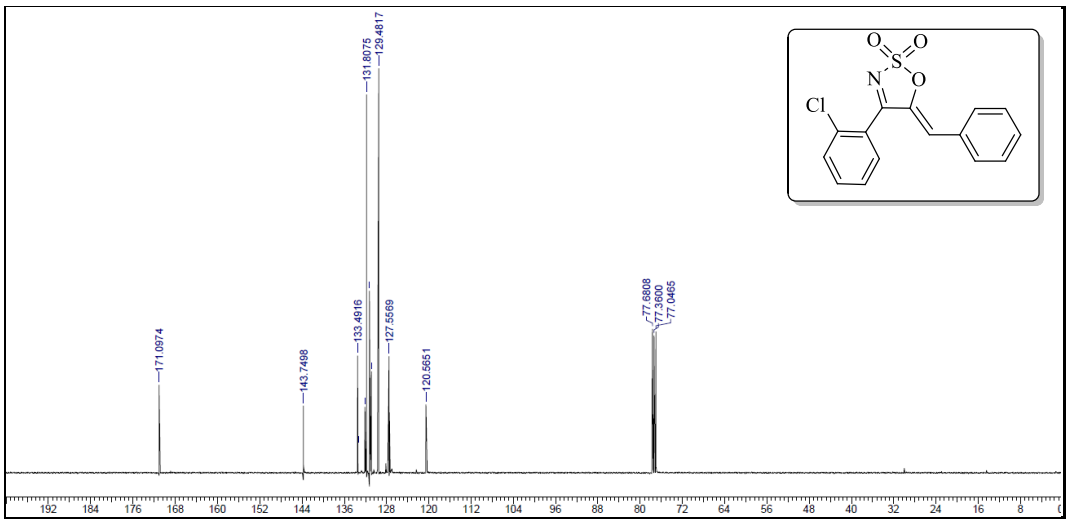


Figure 2.46 100 MHz ^{13}C NMR spectrum of **3da** in $CDCl_3$

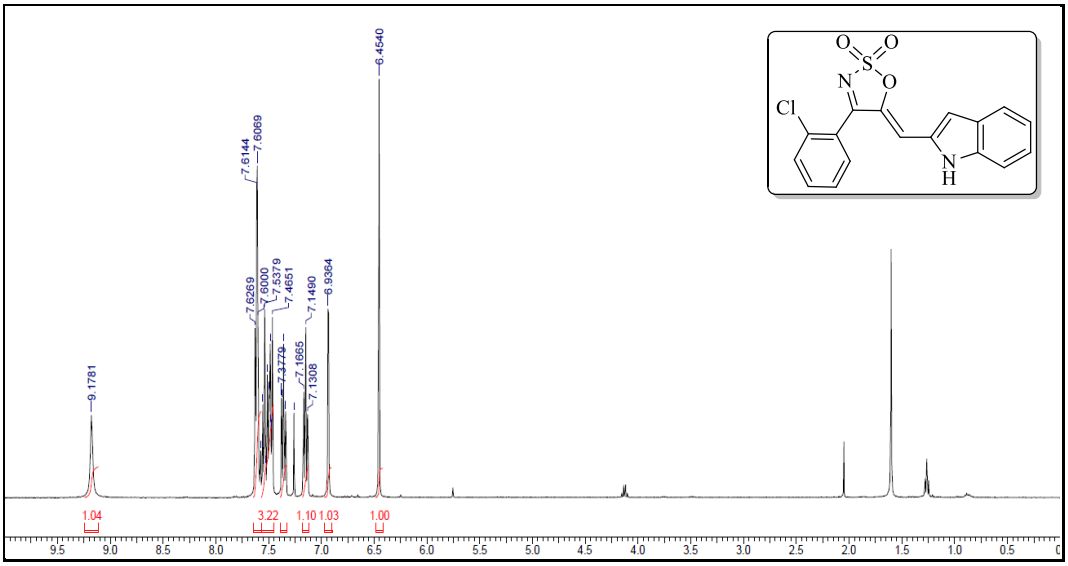


Figure 2.47 400 MHz ^{1}H NMR spectrum of **3di** in $CDCl_3$

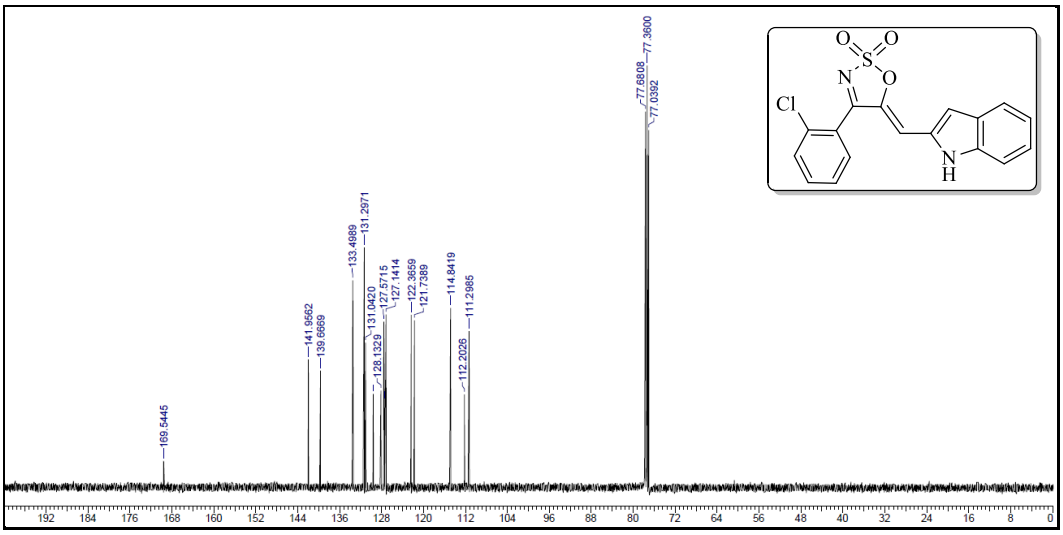


Figure 2.48 100 MHz ^{13}C NMR spectrum of **3di** in $CDCl_3$

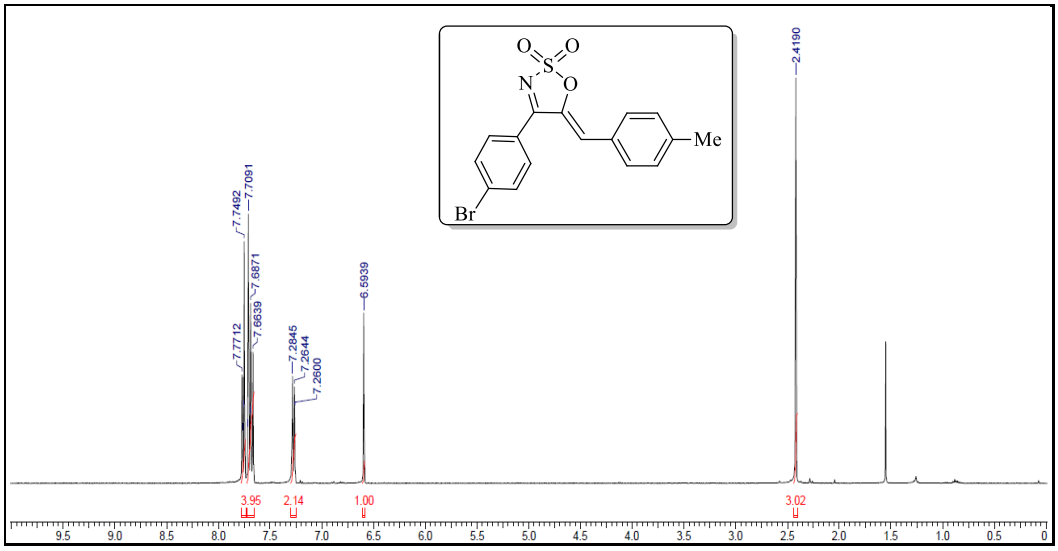


Figure 2.49 400 MHz ^{1}H NMR spectrum of **3eb** in $CDCl_3$

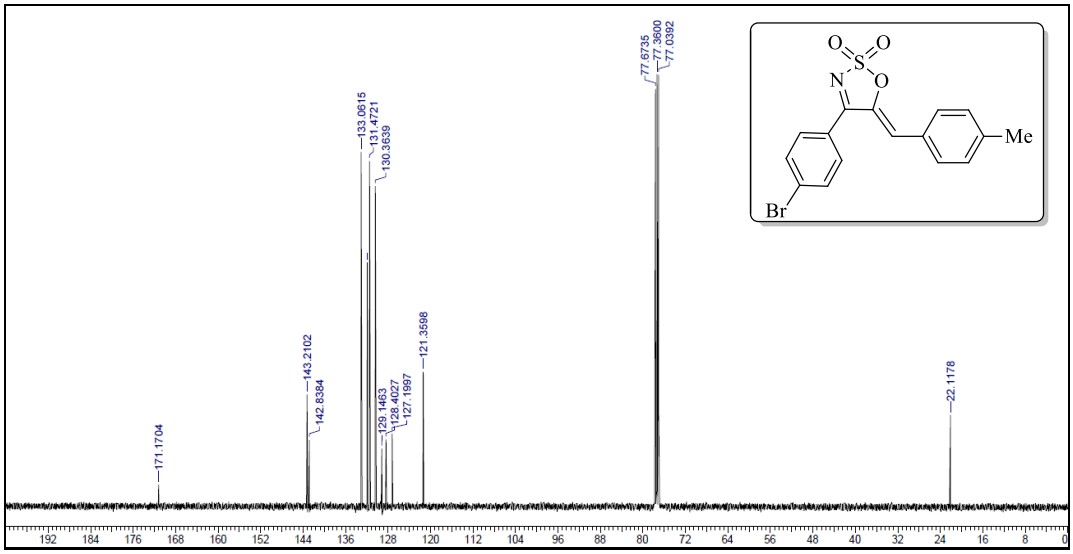


Figure 2.50 100 MHz ^{13}C NMR spectrum of **3eb** in $CDCl_3$

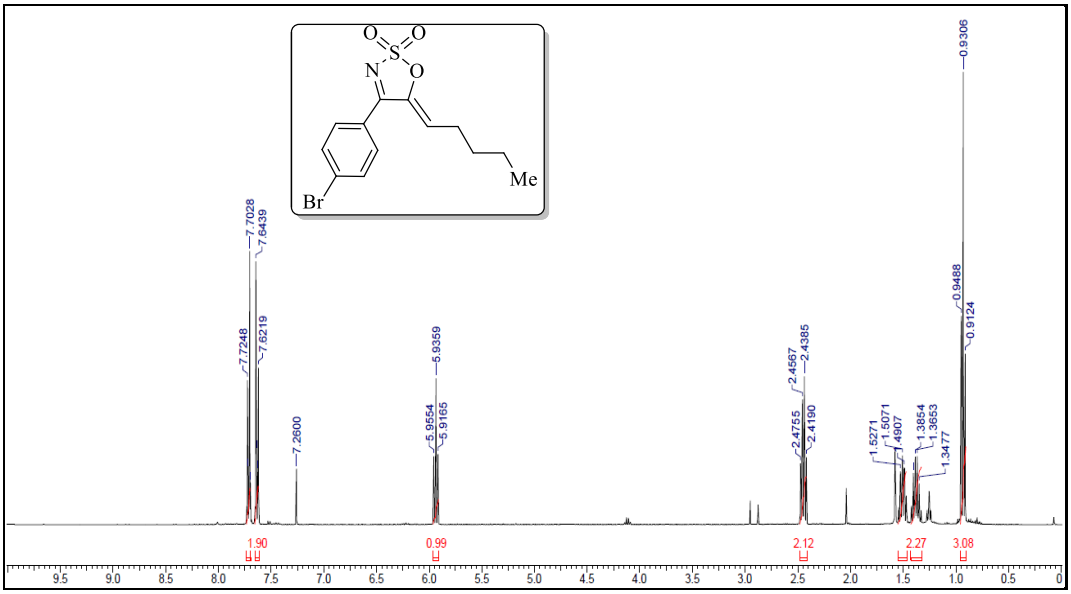


Figure 2.51 400 MHz ^{1}H NMR spectrum of **3eo** in $CDCl_3$

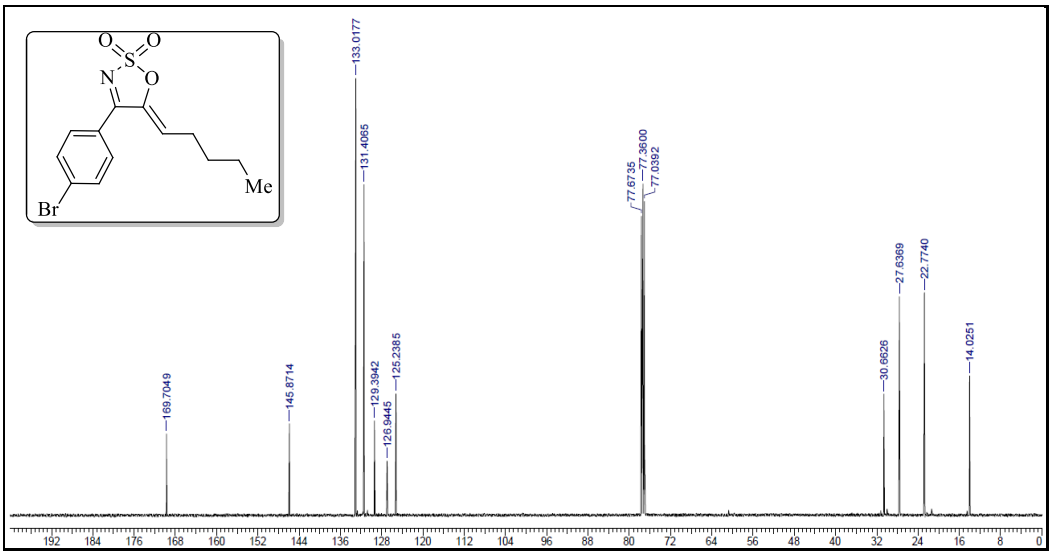


Figure 2.52 100 MHz ^{13}C NMR spectrum of **3eo** in $CDCl_3$

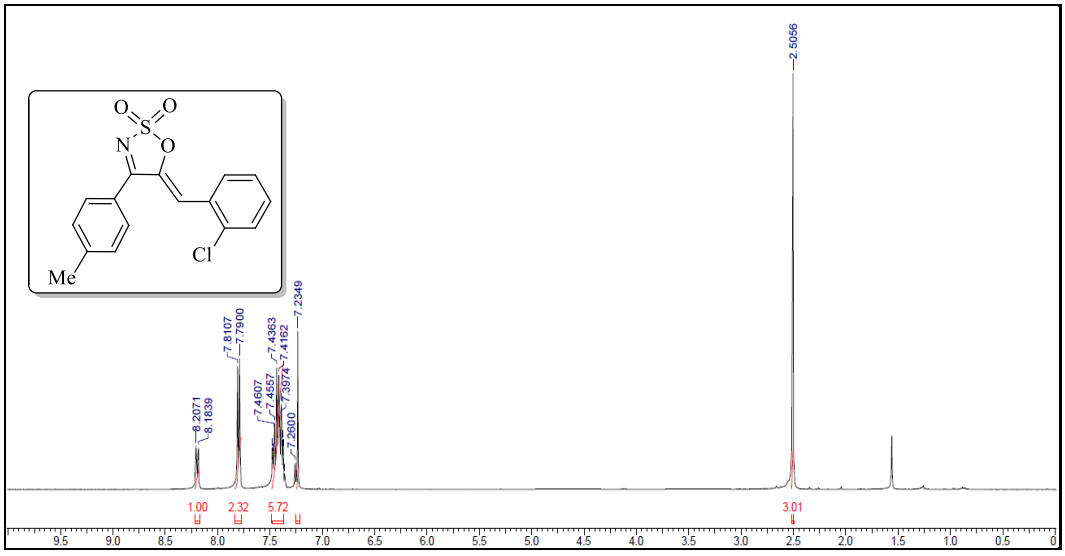


Figure 2.53 400 MHz ^{1}H NMR spectrum of **3fs** in $CDCl_3$

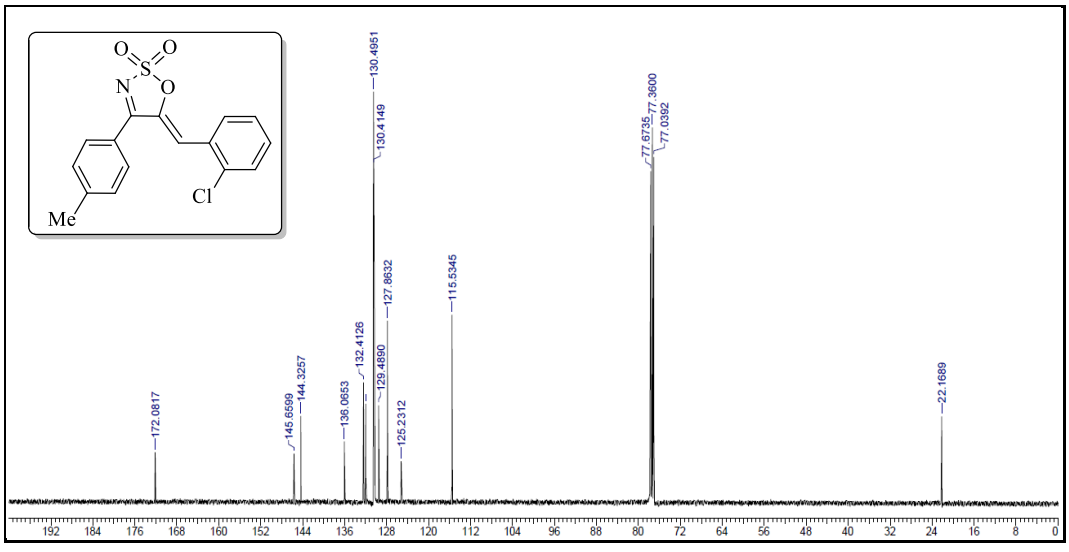


Figure 2.54 100 MHz ^{13}C NMR spectrum of **3fs** in $CDCl_3$

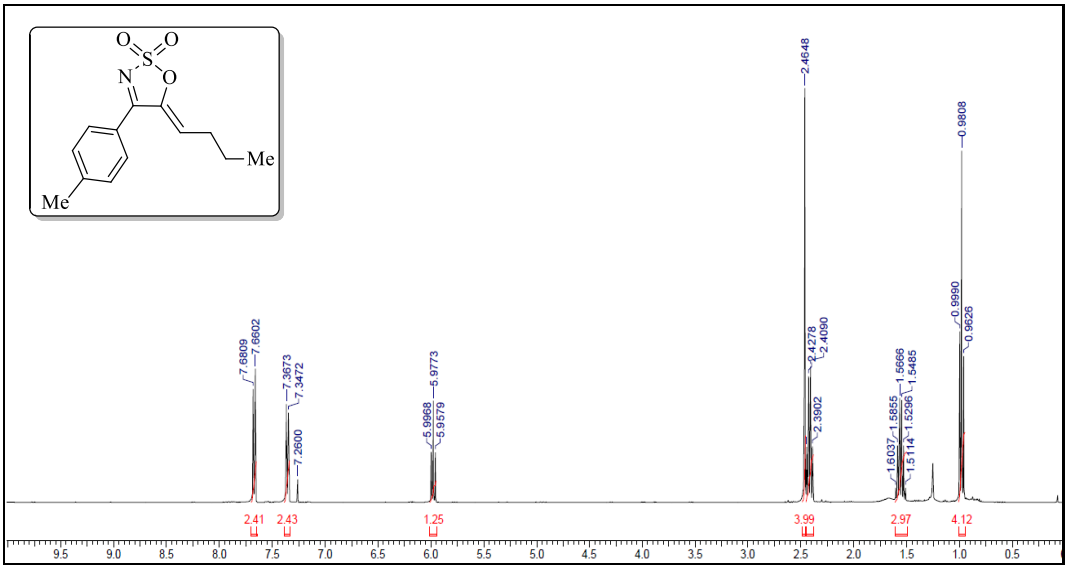


Figure 2.55 400 MHz ^{1}H NMR spectrum of **3fn** in $CDCl_3$

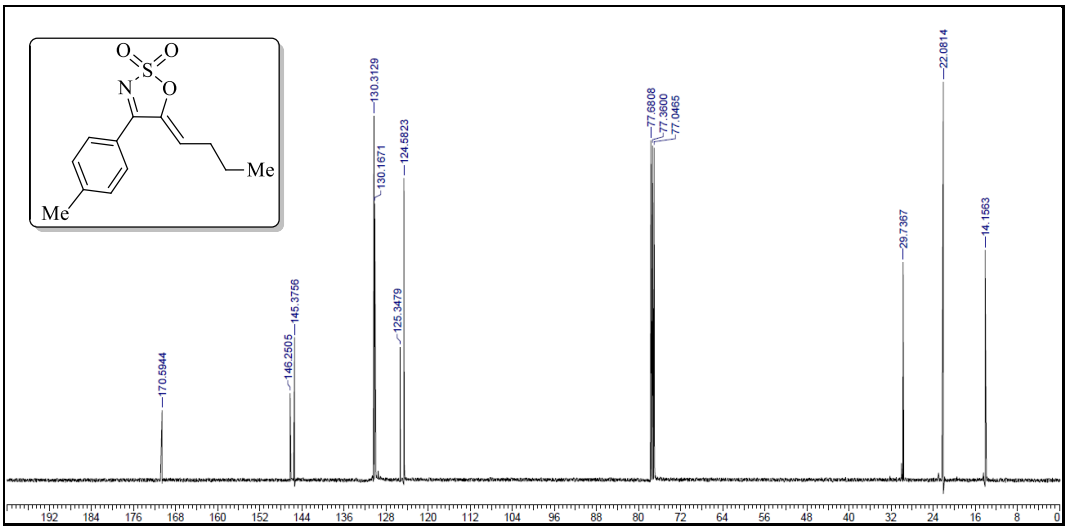


Figure 2.56 100 MHz ^{13}C NMR spectrum of **3fn** in $CDCl_3$

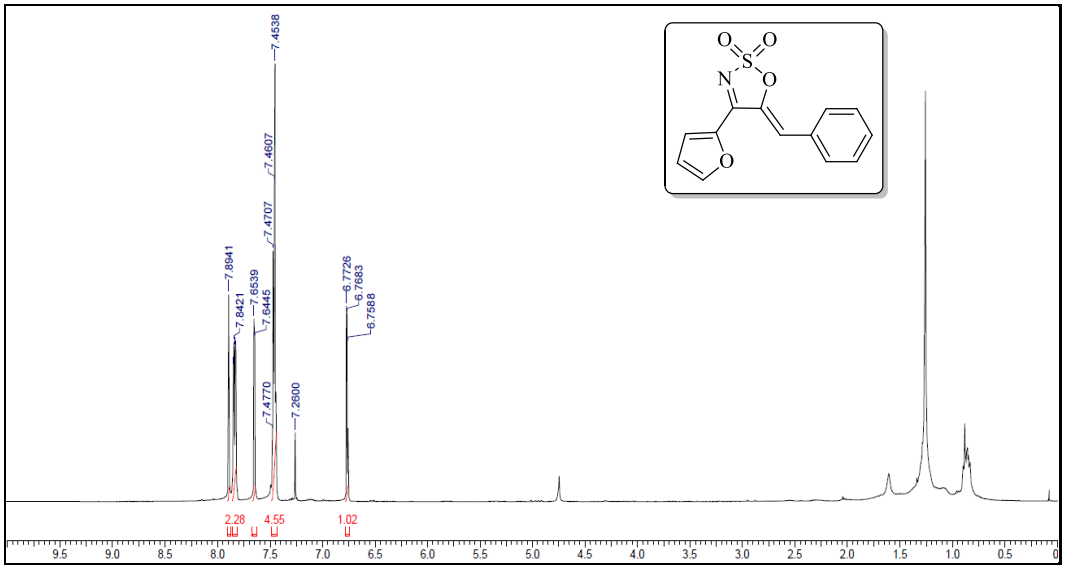


Figure 2.57 400 MHz ^{1}H NMR spectrum of **3ga** in $CDCl_3$

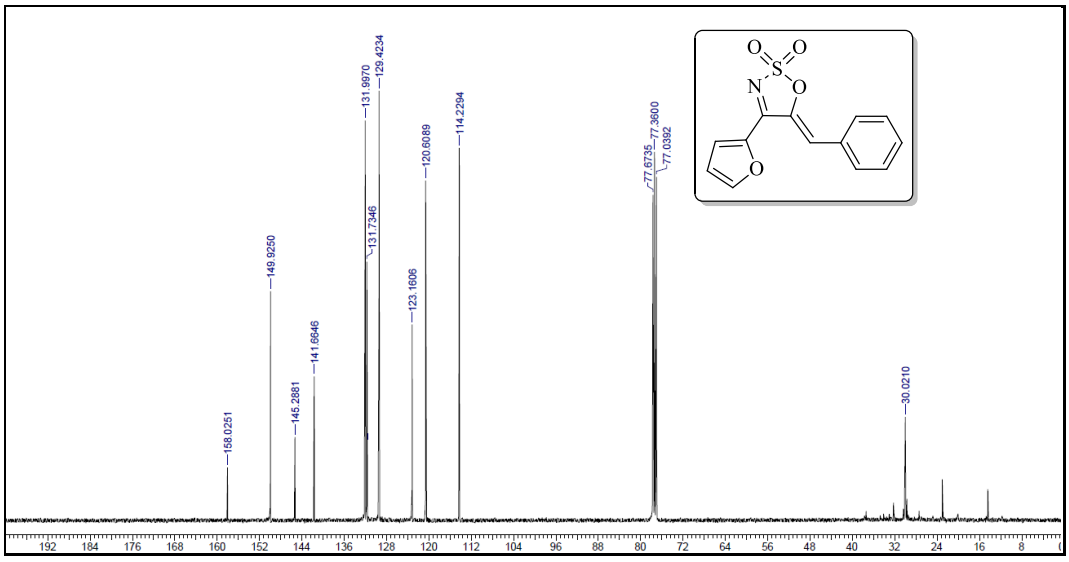


Figure 2.58 100 MHz ^{13}C NMR spectrum of **3ga** in $CDCl_3$

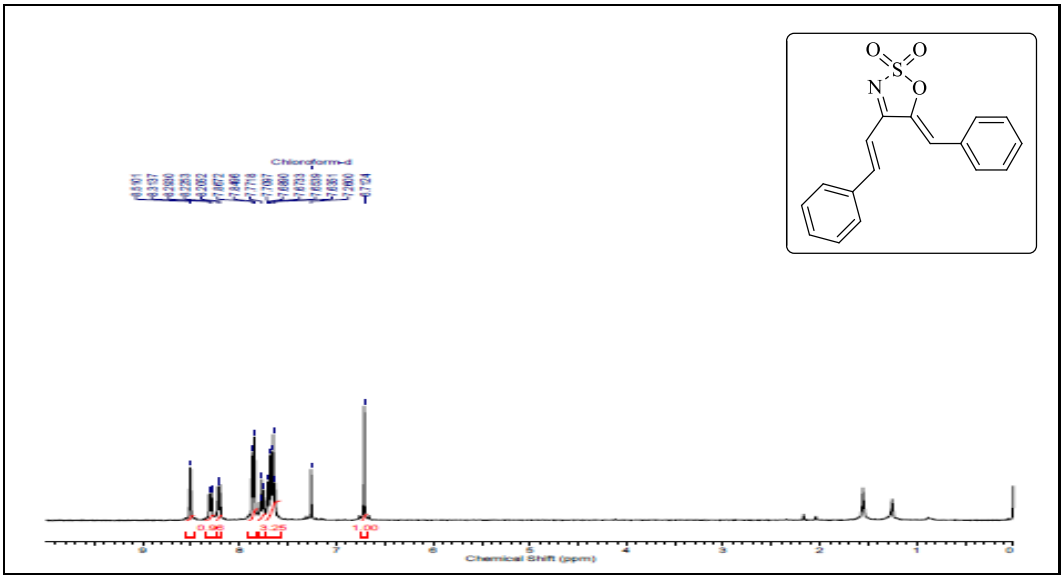


Figure 2.59 400 MHz ^{1}H NMR spectrum of **3ha** in $CDCl_3$

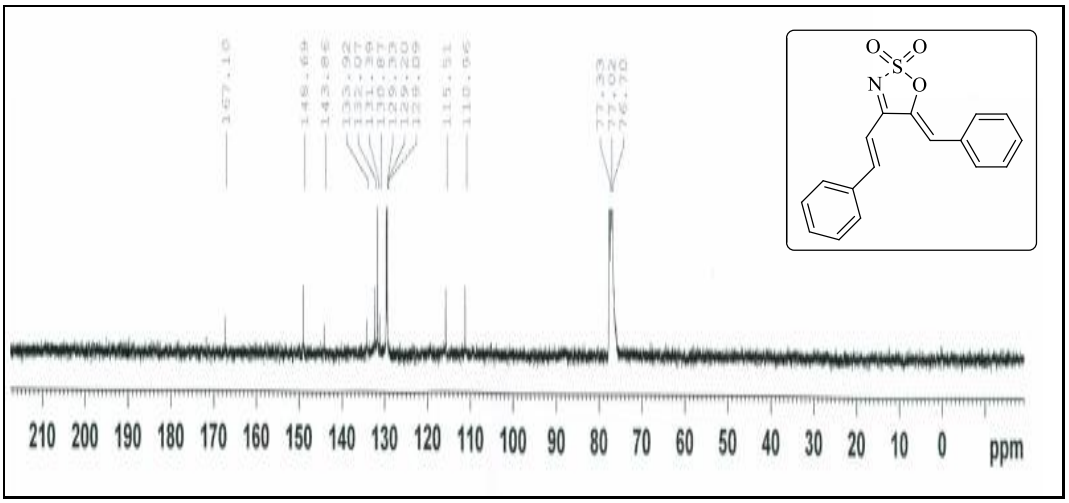


Figure 2.60 100 MHz ^{13}C NMR spectrum of **3ha** in $CDCl_3$

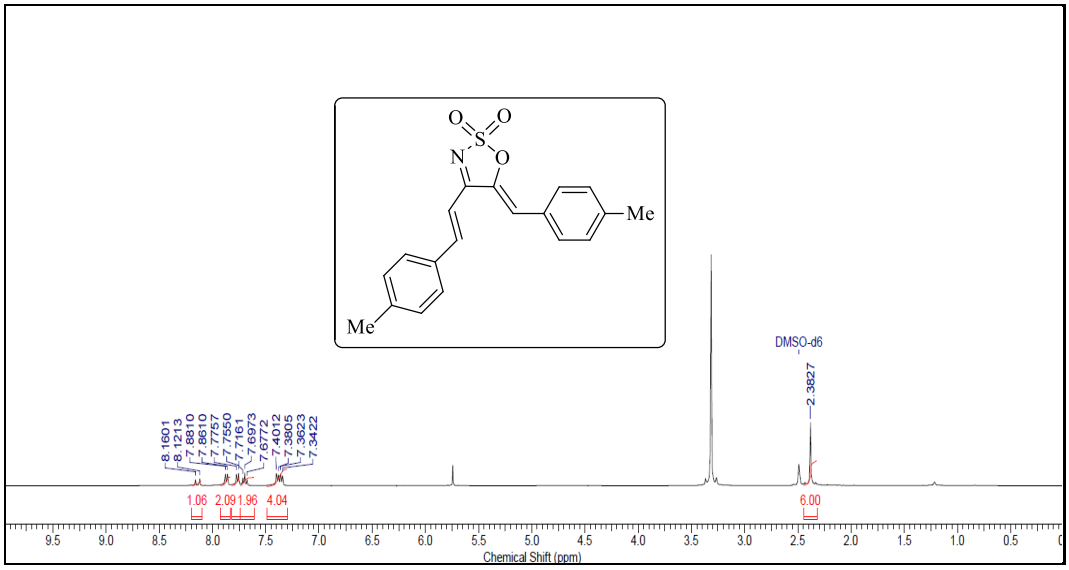


Figure 2.61 400 MHz ^{1}H NMR spectrum of **3hb** in DMSO-d_6

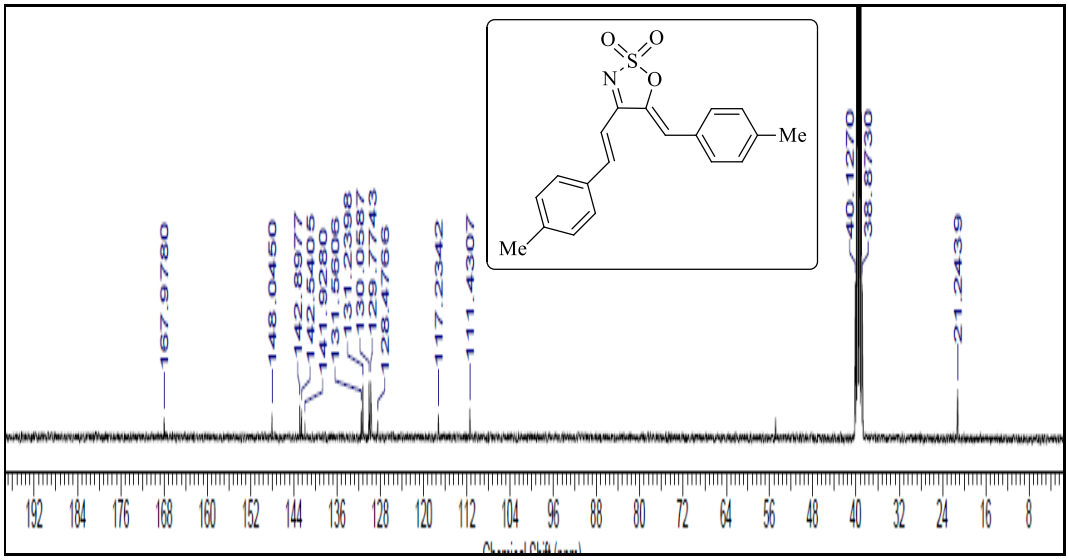


Figure 2.62 100 MHz ^{13}C NMR spectrum of **3hb** in DMSO-d_6

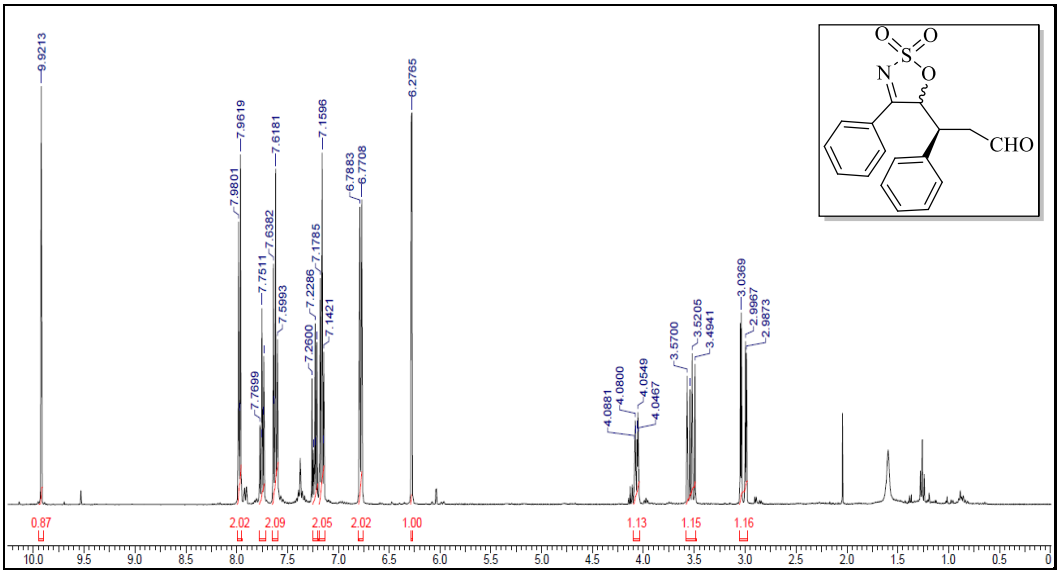


Figure 2.63 400 MHz ^{1}H NMR spectrum of **4aa** in $CDCl_3$

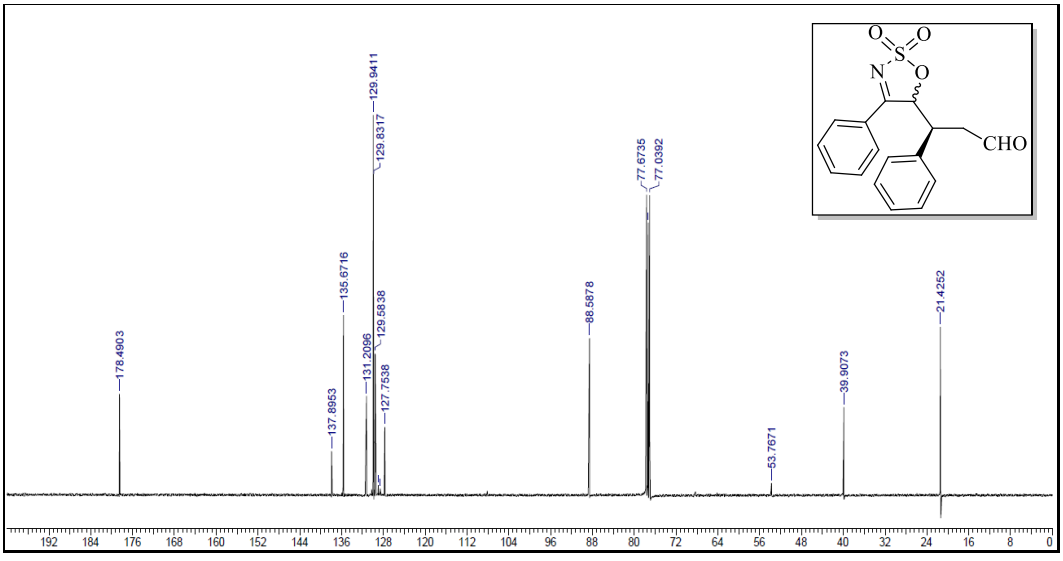


Figure 2.64 100 MHz ^{13}C NMR spectrum of **4aa** in $CDCl_3$

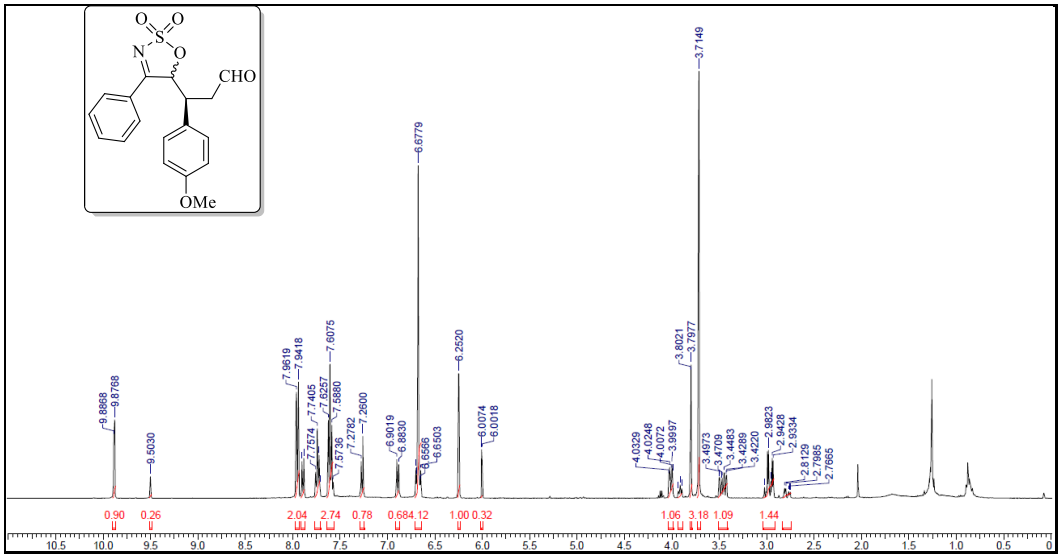


Figure 2.65 400 MHz ^{1}H NMR spectrum of **4ab** in $CDCl_3$

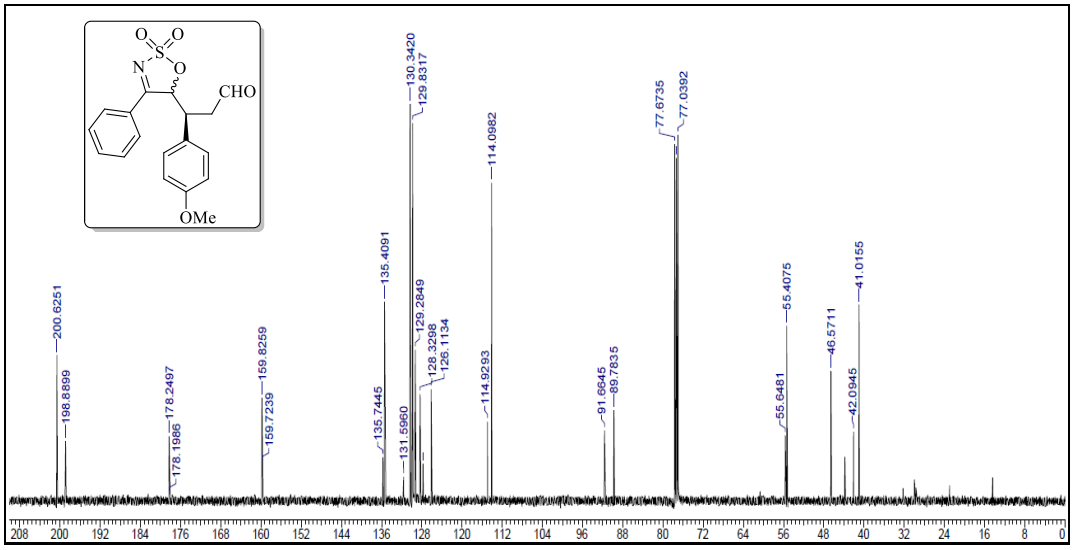


Figure 2.66 100 MHz ^{13}C NMR spectrum of **4ab** in $CDCl_3$

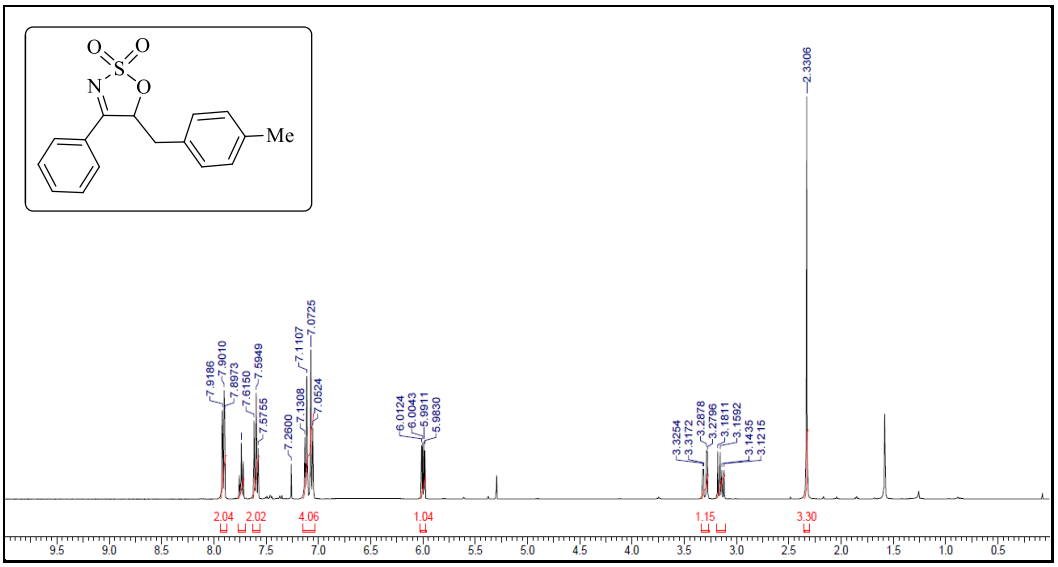


Figure 2.67 400 MHz ^{1}H NMR spectrum of **8** in $CDCl_3$

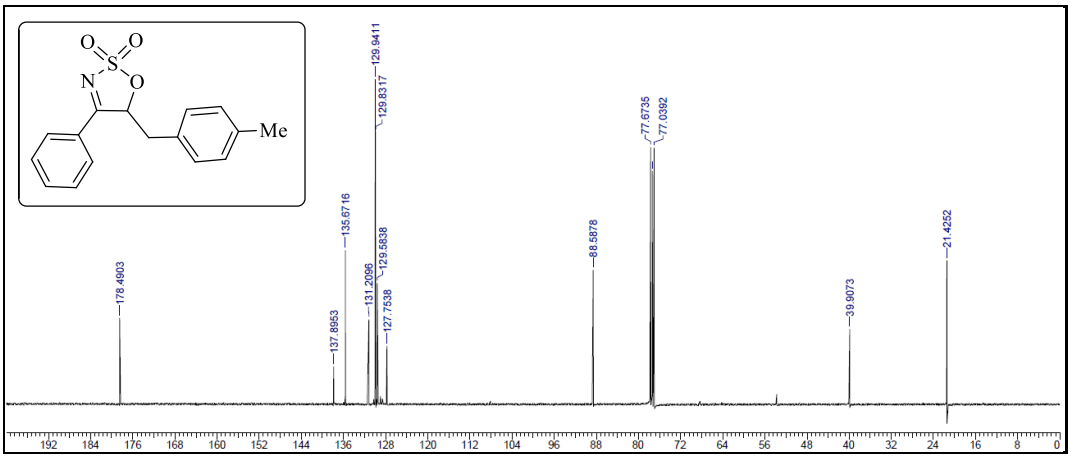


Figure 2.68 100 MHz ^{13}C NMR spectrum of **8** in $CDCl_3$

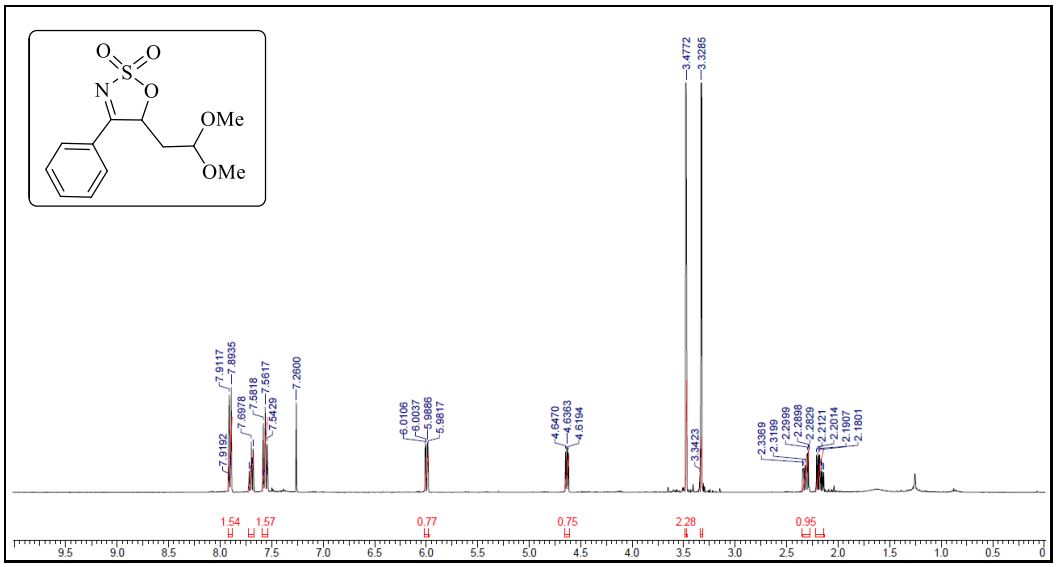


Figure 2.69 400 MHz ^{1}H NMR spectrum of **9** in $CDCl_3$

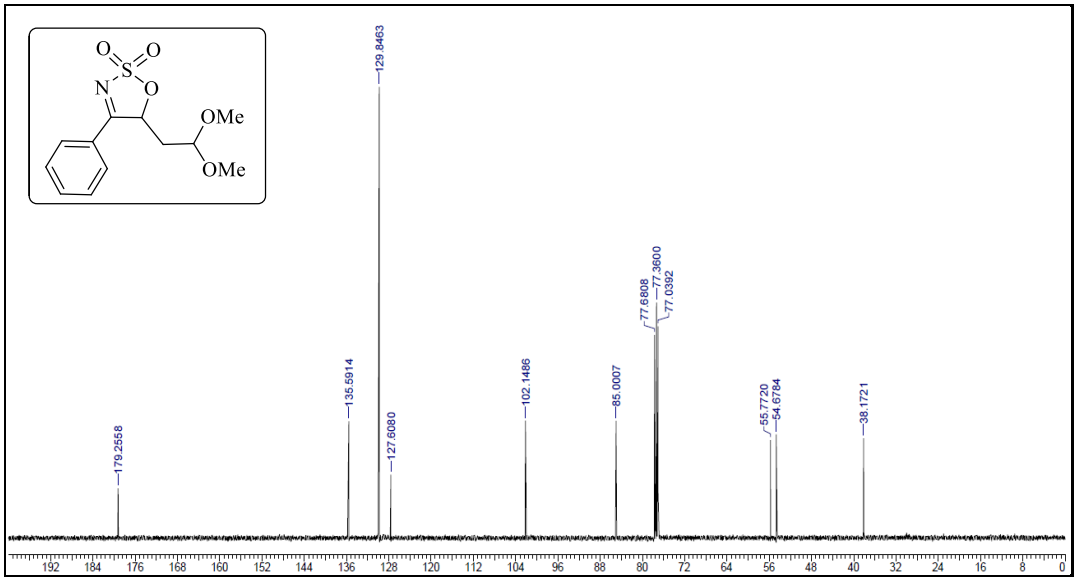


Figure 2.70 100 MHz ^{13}C NMR spectrum of **9** in $CDCl_3$

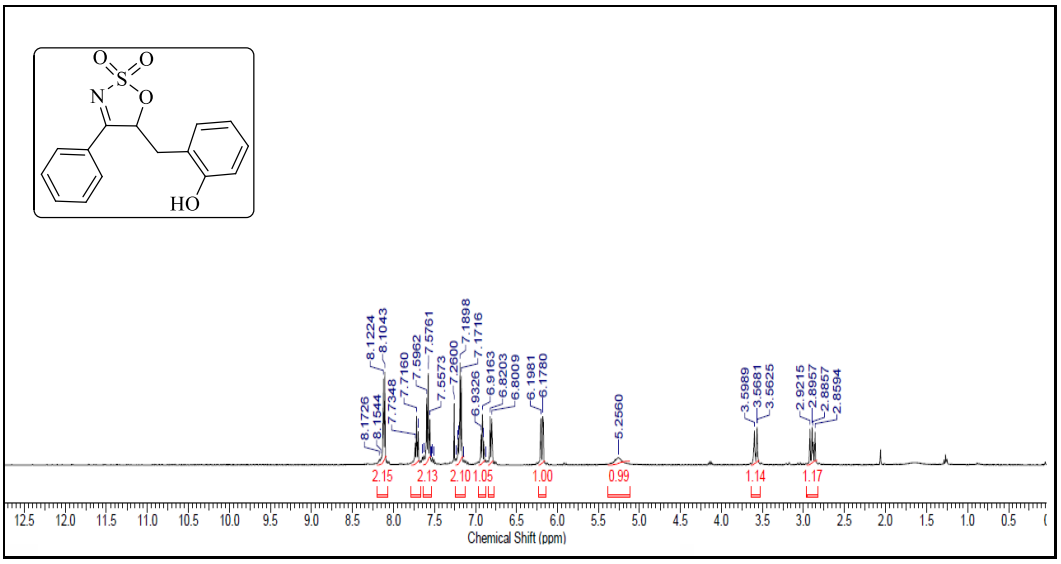


Figure 2.71 400 MHz ^{1}H NMR spectrum of **10** in $CDCl_3$

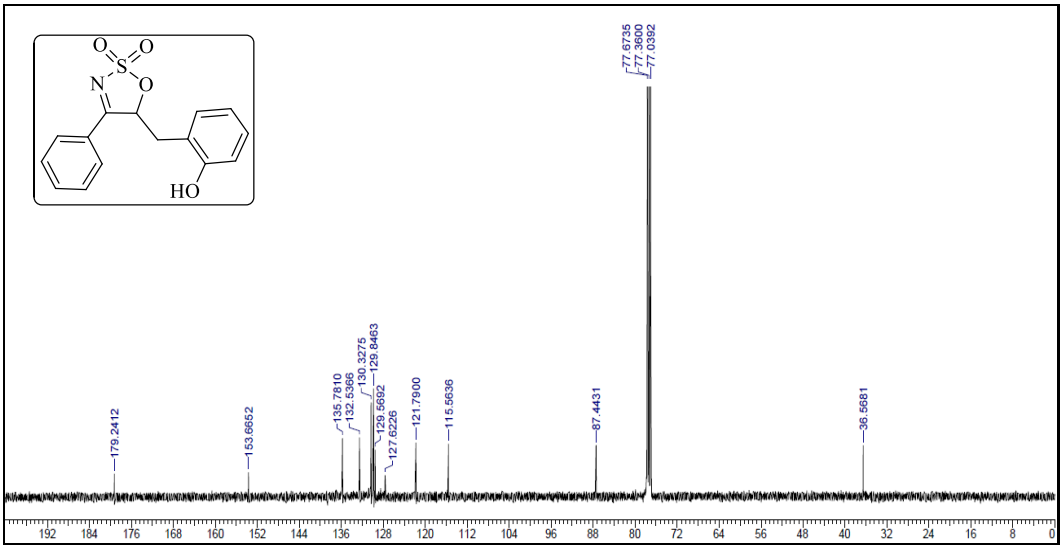


Figure 2.72 100 MHz ^{13}C NMR spectrum of **10** in $CDCl_3$

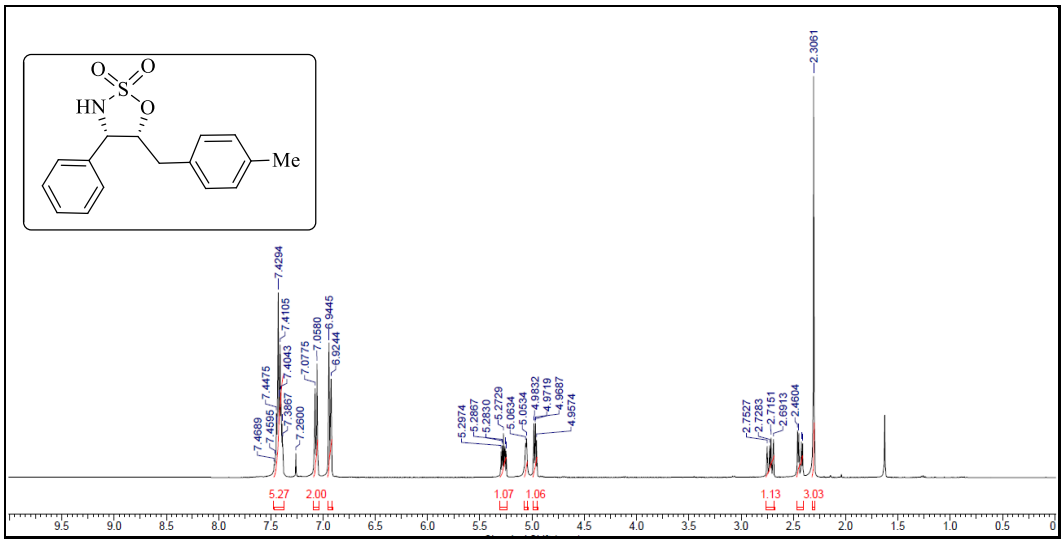


Figure 2.73 400 MHz ^{1}H NMR spectrum of **11** in $CDCl_3$

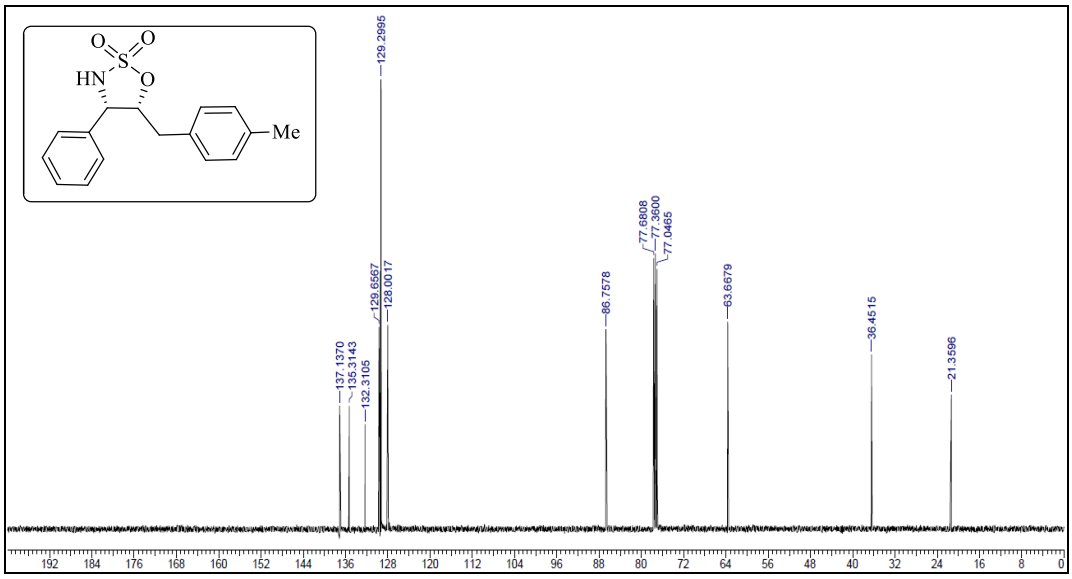


Figure 2.74 100 MHz ^{13}C NMR spectrum of **11** in $CDCl_3$

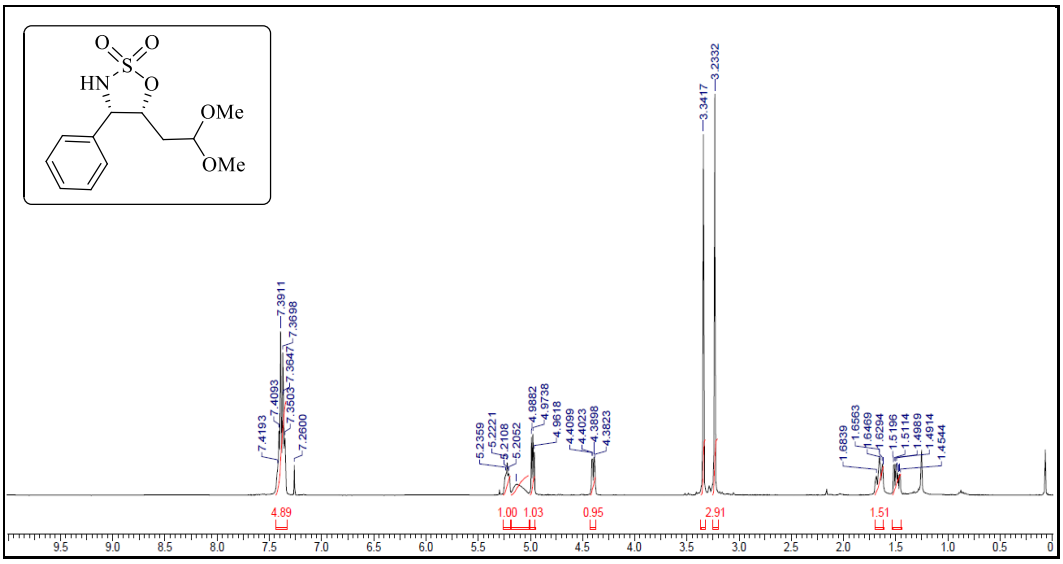


Figure 2.75 400 MHz ^{1}H NMR spectrum of **12** in $CDCl_3$

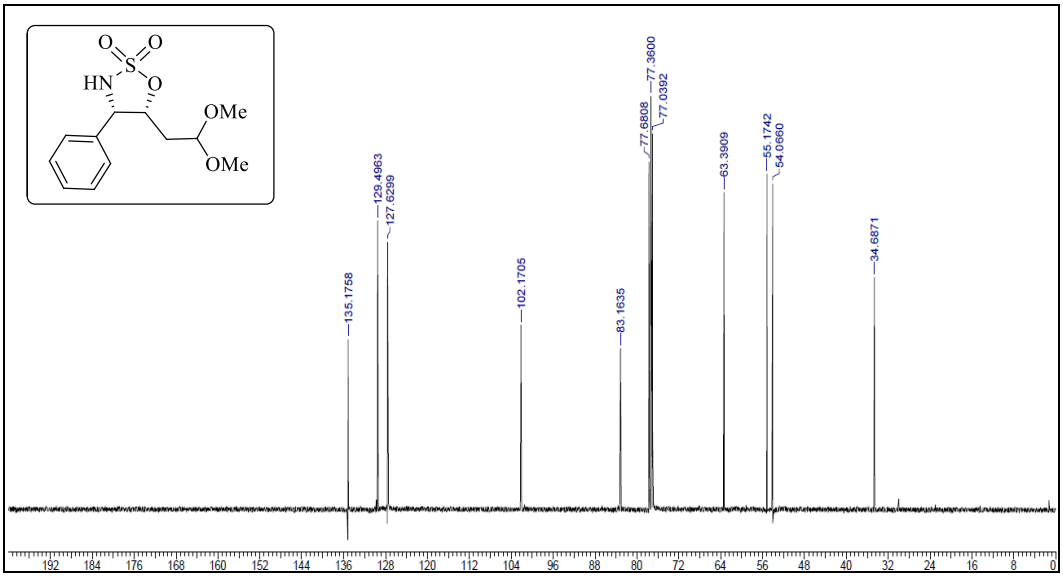


Figure 2.76 100 MHz ^{13}C NMR spectrum of **12** in $CDCl_3$

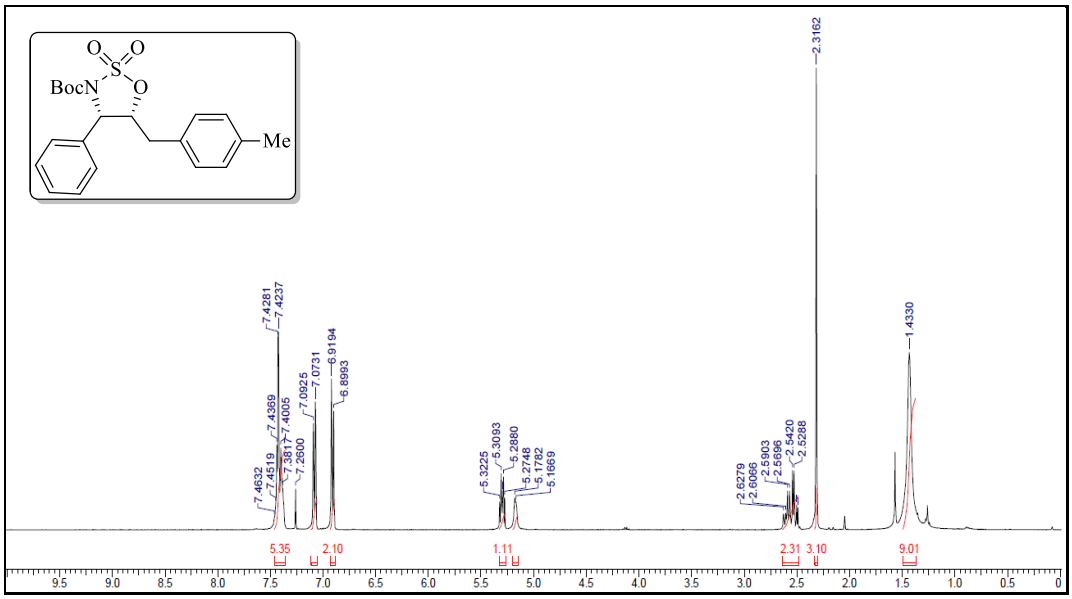


Figure 2.77 400 MHz ^{1}H NMR spectrum of **13** in $CDCl_3$

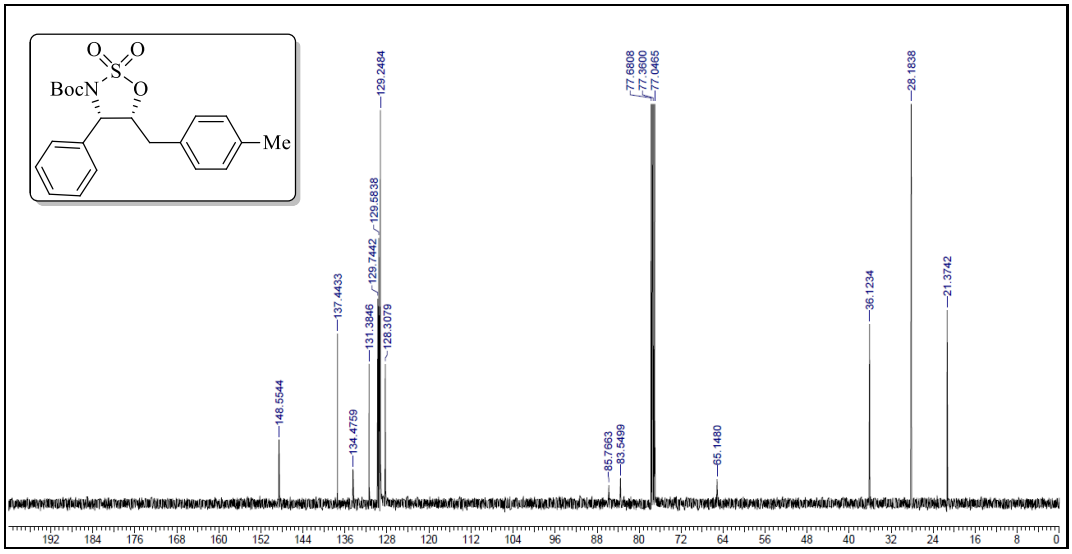


Figure 2.78 100 MHz ^{13}C NMR spectrum of **13** in $CDCl_3$

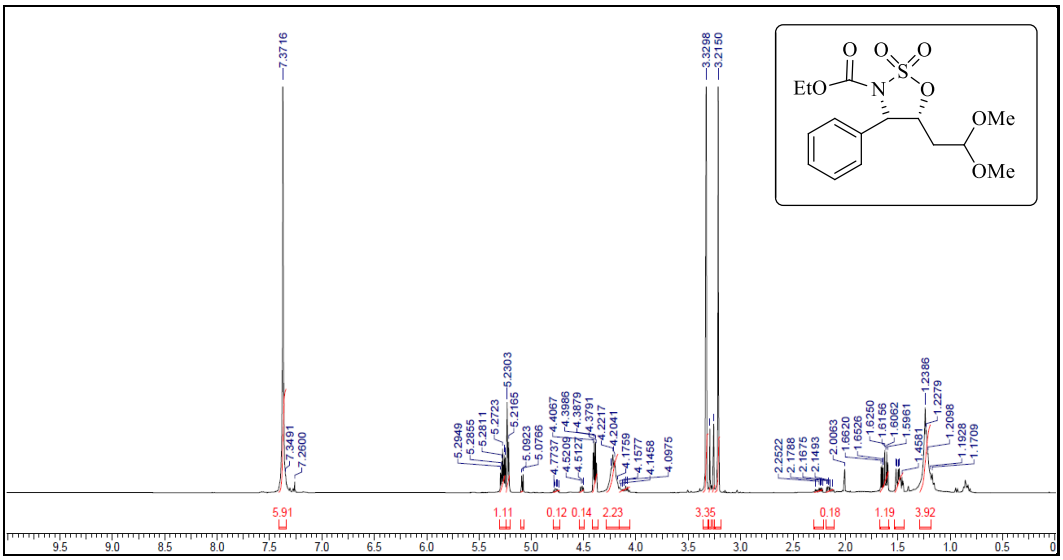


Figure 2.79 400 MHz ^{1}H NMR spectrum of **14** in $CDCl_3$

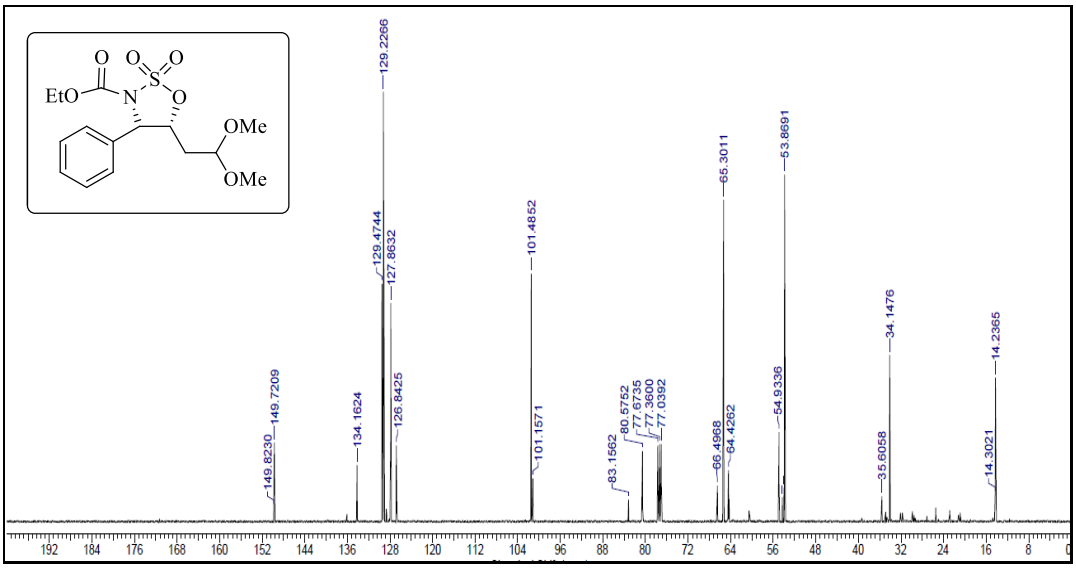


Figure 2.80 100 MHz ^{13}C NMR spectrum of **14** in $CDCl_3$

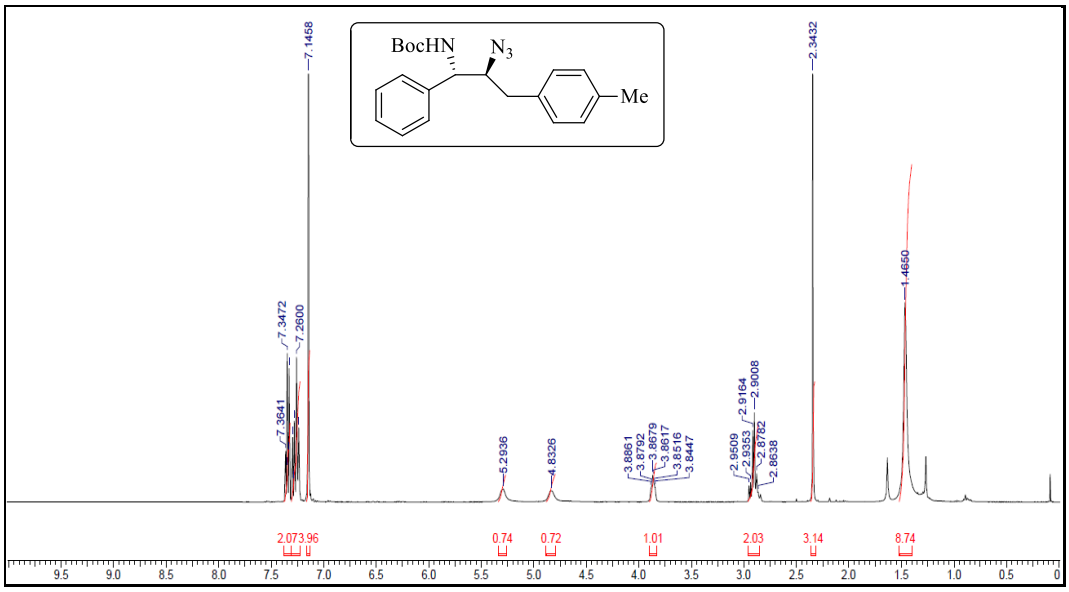


Figure 2.81 400 MHz ^{1}H NMR spectrum of **15** in $CDCl_3$

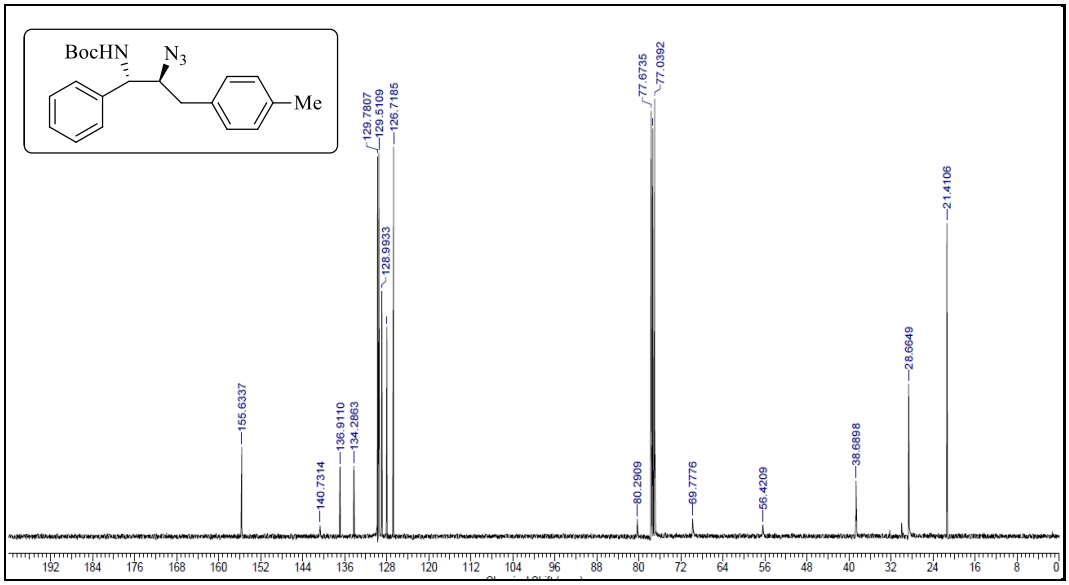


Figure 2.82 100 MHz ^{13}C NMR spectrum of **15** in $CDCl_3$

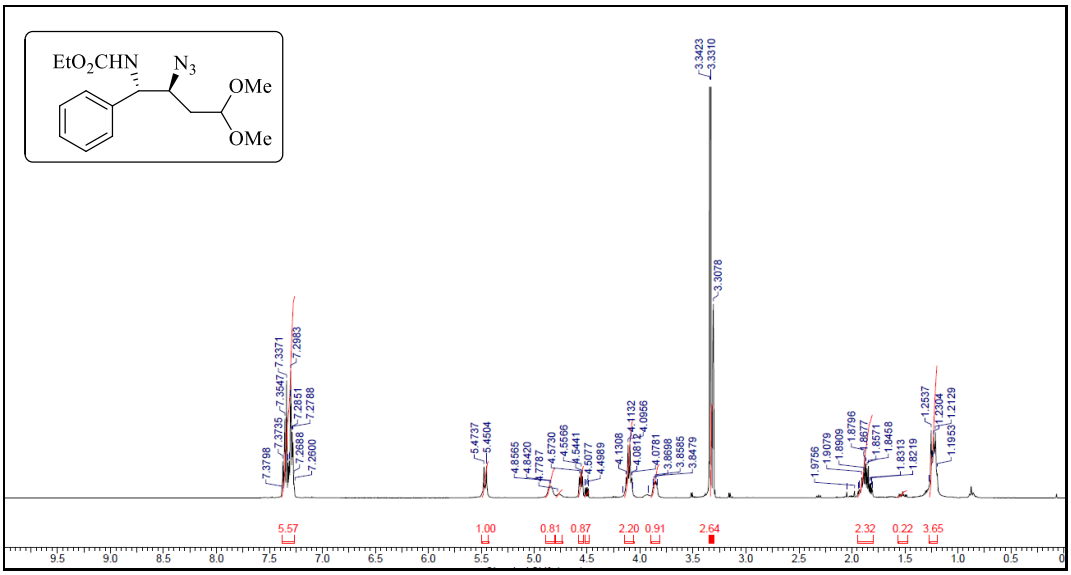


Figure 2.83 400 MHz ^{1}H NMR spectrum of **16** in $CDCl_3$

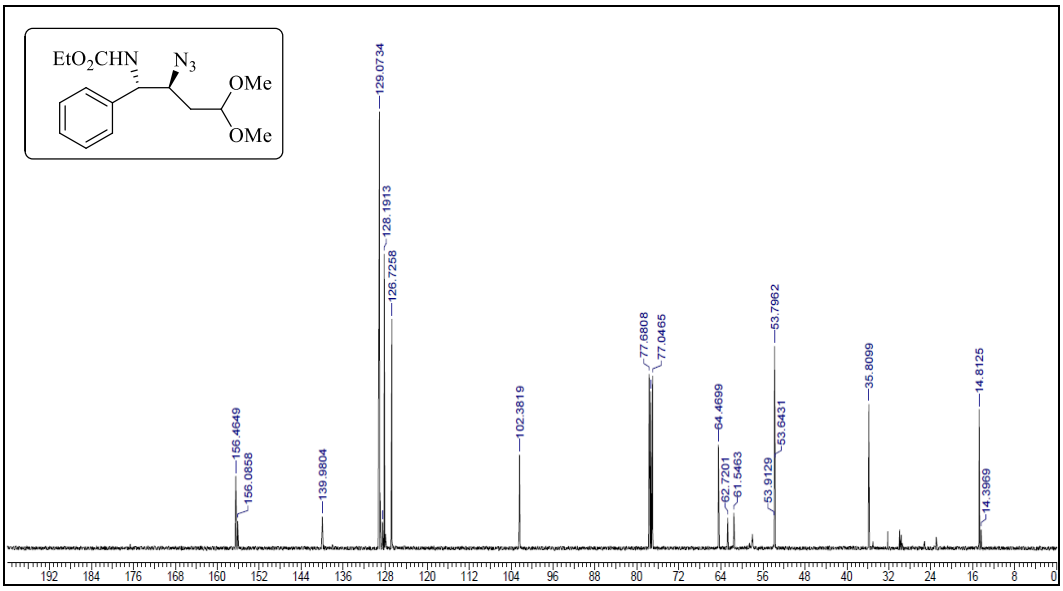


Figure 2.84 100 MHz ^{13}H NMR spectrum of **16** in $CDCl_3$

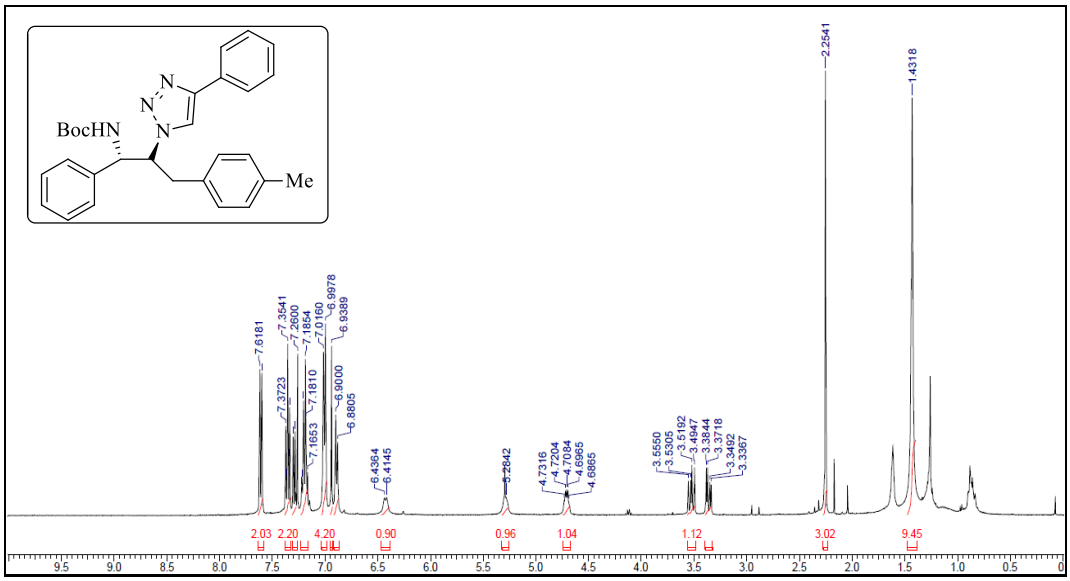


Figure 2.85 400 MHz ^{1}H NMR spectrum of **17** in $CDCl_3$

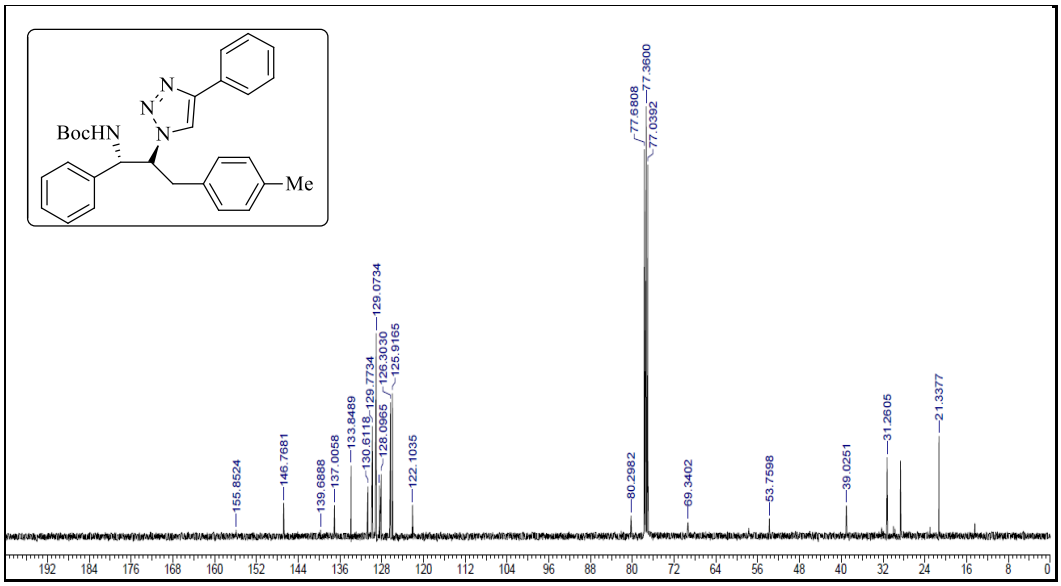


Figure 2.86 100 MHz ^{13}C NMR spectrum of **17** in $CDCl_3$

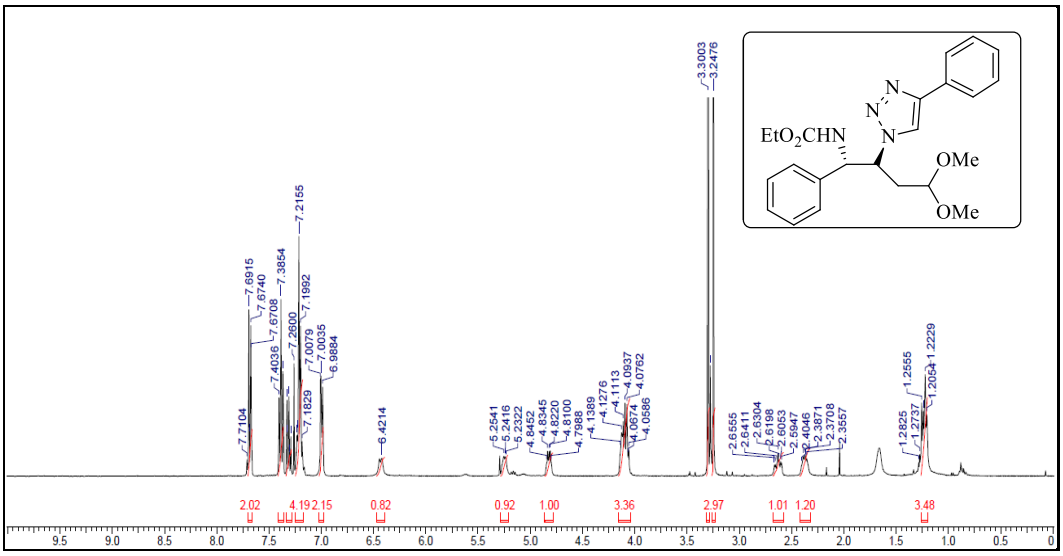


Figure 2.87 400 MHz ^{1}H NMR spectrum of **18** in $CDCl_3$

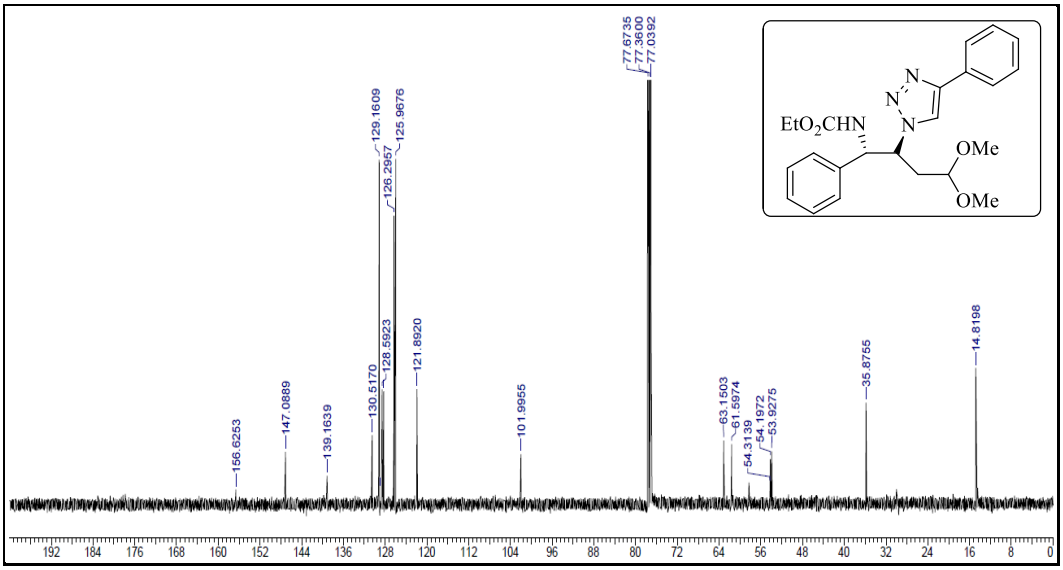


Figure 2.88 100 MHz ^{13}C NMR spectrum of **18** in $CDCl_3$

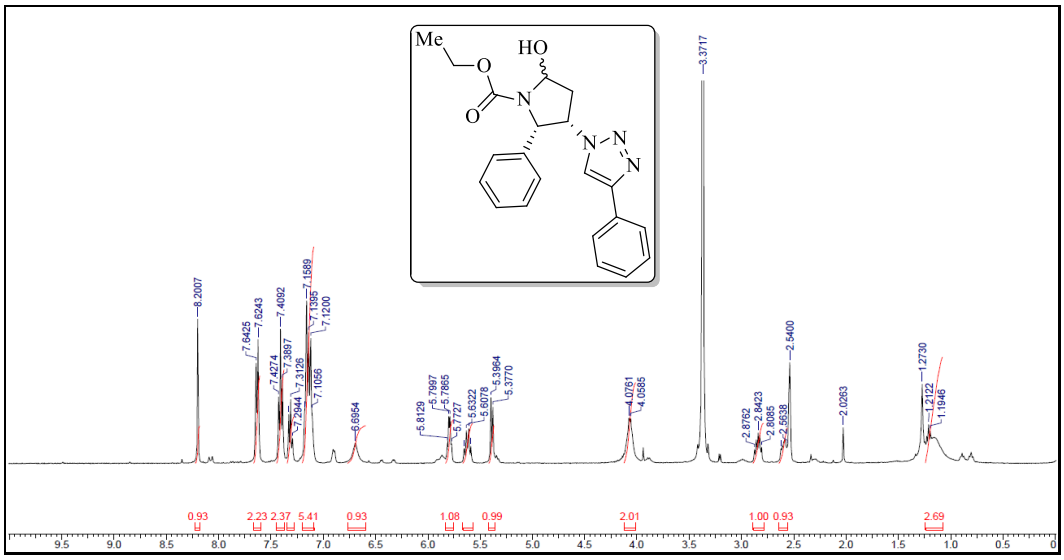


Figure 2.89 400 MHz ^{1}H NMR spectrum of **19** DMSO-d_6

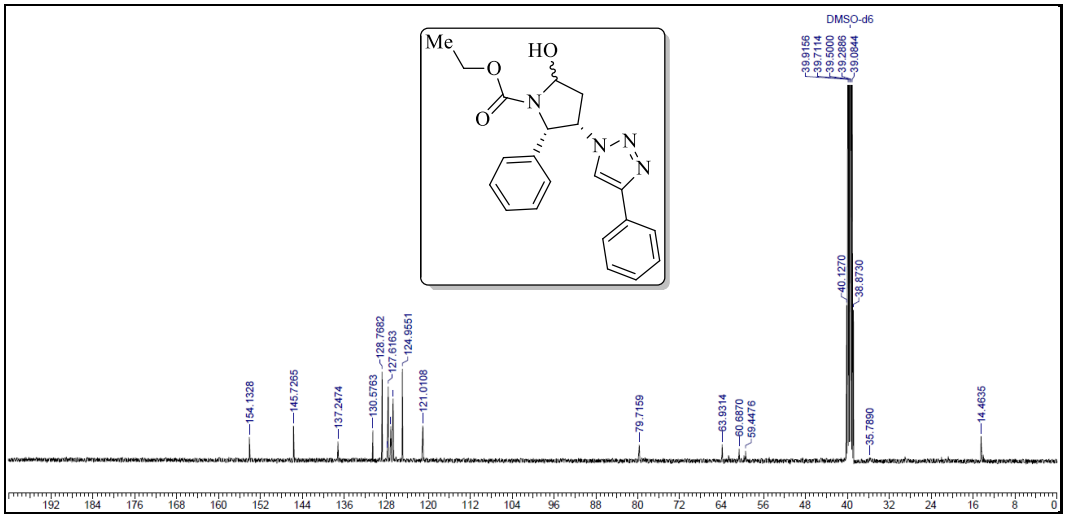


Figure 2.90 100 MHz ^{13}C NMR spectrum of **19** in DMSO-d_6

2.7 References

1. Wright J. B. (1965), The synthesis of 2,1,3-benzothiadiazine 2,2-dioxides and 1,2,3-benzoxathiazine 2,2-dioxides, *J. Org. Chem.*, 30, 3960-3962 (DOI: 10.1021/jo01022a521)
2. Kamal A., Sattur P. B., (1981), A Facile synthesis of 1,2,3-benzoxathiazine 2,2-dioxides, *Synthesis*, 4, 272-273 (DOI: 10.1055/s-1981-29410)
3. Okada M., Iwashita S., Koizumi N. (2000), Efficient general method for sulfamoylation of a hydroxyl group, *Tetrahedron Letters*, 41, 7047-7051 (DOI: 10.1016/S0040-4039(00)01130-8)
4. Kang S., Han J., Lee E.S., Choi E.B., Lee -K. H. (2010), Enantioselective synthesis of cyclic sulfamidates by using chiral rhodium-catalyzed asymmetric transfer hydrogenation, *Org. Lett.*, 12, 4184-4187 (DOI: 10.1021/ol1017905)
5. Lee S. A., Kwak S.H., Lee K. -I. (2011), Highly enantioselective synthesis of cyclic sulfamidates and sulfamides *via* rhodium-catalyzed transfer hydrogenation, *Chem. Commun.*, 47, 2372-2374 (DOI:10.1039/C0CC04166A)
6. Wang Y. -Q., Yu C. -B., Wang D. -W., Wang X. -B., Zhou Y. -G. (2008), Enantioselective synthesis of cyclic sulfamidates *via* Pd-catalyzed hydrogenation, *Org. Lett.*, 10, 2071-2074 (DOI: 10.1021/ol800591u)
7. Chang S., Lee E. E. (2010), Grignard additions to cyclic sulfamidate imines: synthesis of *N*-substituted quaternary sulfamidate building blocks, *Synthesis* 14, 2361-2366 (DOI: 10.1055/s-0029-1218778)
8. Nishimura T., Ebe Y., Fujimotoa H., Hayashi T. (2013), Asymmetric synthesis of gem-diaryl substituted cyclic sulfamidates and sulfamides by rhodium-catalyzed arylation of cyclic ketimines, *Chem. Commun.*, 49, 5504-5506 (DOI:10.1039/C3CC42071J)

9. Chen Y. -J., Chen Y. -H., Chen-Guo Feng C. -G., Lin G. -Q. (2014) Enantioselective rhodium-catalyzed arylation of cyclic N-sulfamidate alkylketimines: a new access to chiral β-alkyl-β-aryl amino alcohols, *Org. Lett.*, 16, 3400-3403 (DOI: 10.1021/ol501464e)
10. Jiang T., Wang Z., Xu M. -H. (2015) Rhodium-catalyzed asymmetric arylation of cyclic N-sulfonyl aryl alkyl ketimines: efficient access to highly enantioenriched α-tertiary amines, *Org. Lett.*, 17, 528-531 (DOI: 10.1021/ol503537w)
11. An Q., Shen J., Butt N., Liu D., Liu Y., Zhang W. (2014), Asymmetric domino reaction of cyclic *N*-sulfonylimines and simple aldehydes with *trans*-perhydroindolic acid as an organocatalyst, *Org. Lett*., 16, 4496-4499 (DOI: 10.1021/ol502033v)
12. Riaño I., Uria U., Carrillo L., Reyes E., Vicario J. L. (2015), 4-alkenyl-5*H*-1,2,3-oxathiazole 2,2-dioxides in catalytic and enantioselective [4 + 2] cycloaddition through iminium activation. Straightforward access to the trans-decaline framework and to densely functionalized cyclohexanes, *Org. Chem. Front.*, 2, 206-210 (DOI: 10.1039/C4QO00316K)
13. List B., Lerner R. A., Barbas III C. F. (2000), Proline-catalyzed direct asymmetric aldol reactions, *J. Am. Chem. Soc*., 122, 2395-2396 (DOI: 10.1021/ja994280y)
14. Hayashi Y., Yamaguchi J., Sumiya T., Shoji M. (2004), Direct proline-catalyzed asymmetric α-aminoxylation of ketones, *Angew. Chem. Int. Ed*., 43, 1112-1115 (DOI: 10.1002/anie.200353085)
15. Castañeda Á M., -Solla H. R., Concellón C., Amo V. D., (2012), Switching diastereoselectivity in proline-catalyzed aldol reactions, *J. Org. Chem*., 77, 10375-10381 (DOI: 10.1021/jo3020352)
16. Samanta S., Zhao C. -G, (2006), Organocatalytic enantioselective synthesis of α-hydroxy phosphonates, *J. Am. Chem. Soc*., 128, 7442-7443 (DOI: 10.1021/ja062091r)

17. Notz W., Tanaka F., Barbas III. C. F., (2004), Enamine-based organocatalysis with proline and diamines: The development of direct catalytic asymmetric aldol, Mannich, Michael, and Diels-Alder reactions, *Acc. Chem. Res*., 37, 580-591 (DOI: 10.1021/ar0300468)
18. Bertelsen S., Jørgensen K. A., (2009), Organocatalysis-after the gold rush, *Chem. Soc. Rev*., 38, 2178-2189 (DOI: 10.1039/b903816g)
19. Kellogg R. M., (2007), The crystallization behavior of proline and its role in asymmetric organocatalysis, *Angew. Chem. Int. Ed*., 46, 494-497 (DOI: 10.1002/anie.200603028)
20. Baig R. B. N., Varma R.S, (2012), Stereo- and regio-selective one-pot synthesis of triazole-based unnatural amino acids and b-amino triazoles, *Chem. Commun*., , 48, 5853-5855 (DOI: 10.1039/c2cc32392c)
21. Gajewski M., Seaver B. and EsslingerC. S. (2007), Design, synthesis, and biological activity of novel triazole amino acids used to probe binding interactions between ligand and neutral amino acid transport protein SN1, *Bioorg. Med. Chem. Lett*., 17, 4163-4166 (DOI: 10.1016/j.bmcl.2007.05.061)
22. Neu H. C., Fu K. P. (1979), Cefatrizine activity compared with that of other cephalosporins, *Antimicrob. Agents Chemother*. 15, 209-212 (DOI: 10.1128/AAC.15.2.209)
23. Alvarez R., Velázquez S., San-Félix A., Aquaro S., Clercq E. D., Perno C. -F., Karlsson A., Balzarini J., Camarasa M. J. (1994), 1,2,3-triazole-[2,5-bis-O-(tert-butyldimethylsilyl)-β-D-ribofuranosyl]-3'-spiro-5"-(4"-amino-1",2"-oxathiole2",2"-dioxide) (TSAO) analogs: synthesis and anti-HIV-1 activity, *J. Med. Chem*.,37, 4185-4194 (DOI: 10.1021/jm00050a015)
24. Shin J. -A., Lim Y. -G., and Lee K. -H. (2012), Copper-catalyzed azide-alkyne cycloaddition reaction in water using cyclodextrin as a phase transfer catalyst, *J. Org. Chem*., 77, 4117-4122 (DOI: 10.1021/jo3000095)
25. Rostovtsev V. V., Green L. G., Fokin V. V., Sharpless K. B. (2002), A stepwise Huisgen cycloaddition process: copper(I)-catalyzed

regioselective “ligation” of azides and terminal alkynes, *Angew. Chem. Int. Ed.*, 41, 2596-2599 (DOI: 10.1002/1521-3773(20020715)41:14<2596::AID-ANIE2596>3.0.CO;2-4)

26. Kallander L.S., Lu Q., Chen W., Tomaszek T., Yang G., Tew D., Meek T. D., Hofmann G. A., Schulz-Pritchard C.K., Smith W. W.,| Janson C.A., Ryan M. D., Zhang G.-F., Johanson K. O., Kirkpatrick R. B., Ho T. F., Fisher P W.., Mattern M. R., Johnson R. K., Hansbury M. J., Winkler J. D., Ward K. W., Veber D. F., Thompson S. K. (2005), 4-aryl-1,2,3-triazole: A novel template for a reversible methionine aminopeptidase 2 inhibitor, optimized to inhibit angiogenesis in vivo, *J. Med. Chem*., 48, 5644-5647 (DOI: 10.1021/jm050408c)
27. Oh S., Shin -S. W., Hamc J., Lee S. (2010), Acid-catalyzed synthesis of 10-substituted triazolyl artemisinins and their growth inhibitory activity against various cancer cells, *Bioorg. Med. Chem. Lett*. 20, 4112-4115 (DOI: 10.1016/j.bmcl.2010.05.074)
28. Agalave S.G., Maujan S. R., Pore V. S. (2011), Click chemistry: 1,2,3-triazoles as pharmacophores, *Chem. Asian J*., 6, 2696-2718 (DOI: 10.1002/asia.201100432)
29. Siddiquia N., Ahsan W., Alam S. M., Alia R., Jainb S., Akhtar J. (2011), Triazole : as potential bioactive agents, *Int J Pharm Sci Rev Res*, 18, 161 (Accession: 65069462)
30. Sheldrick G. M. (2008), A short history of SHELX, *Acta Cryst*., A64, 112-122 (DOI: 10.1107/S0108767307043930)

Chapter 3

Stereoselective synthesis of functionalized spiro-sulfamidate imine fused δ-lactone scaffold *via* a one-pot sequential three-component reaction

3.1 Introduction

Spiro-δ-lactone and their derivatives are commonly occurring building blocks found in various kinds of natural products and pharmaceuticals.[1-8] A range of biologically active compounds possessing these privileged scaffolds are well documented (**Figure 3.1**).[9-19]

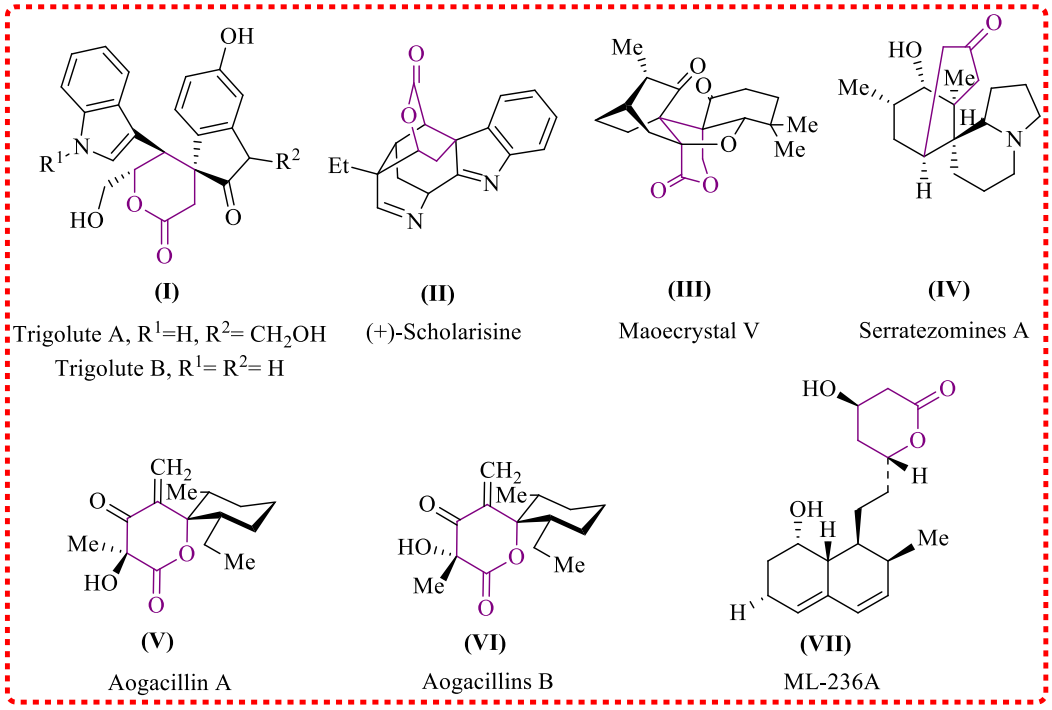
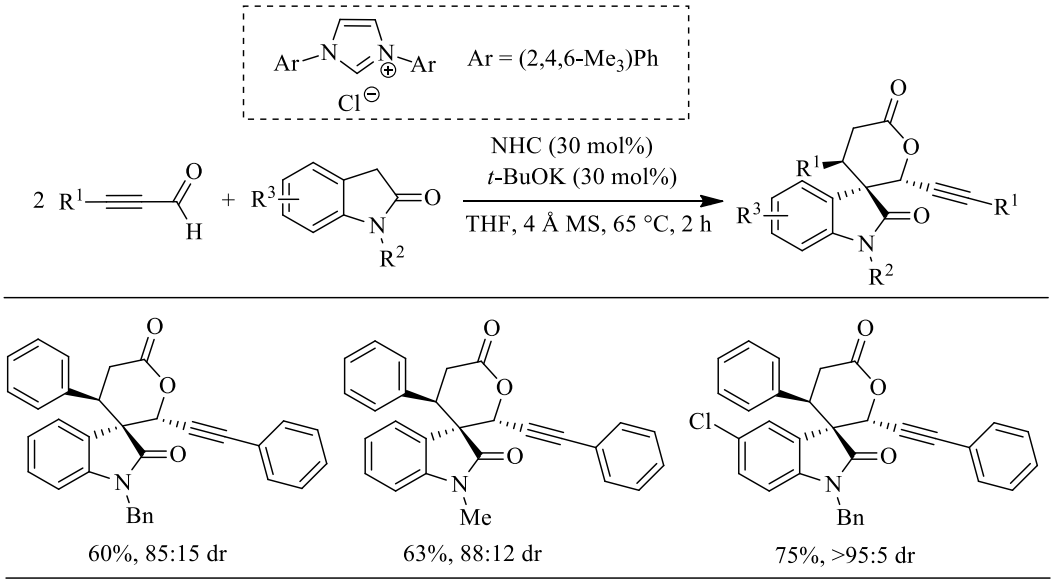


Figure 3.1 Respective examples containing spiro fused δ-lactone moieties

In view of the great applications, a few general and reliable protocols have been developed to construct this important scaffold.[20-28] Some of the important examples are summarized in **Section 3.2**.

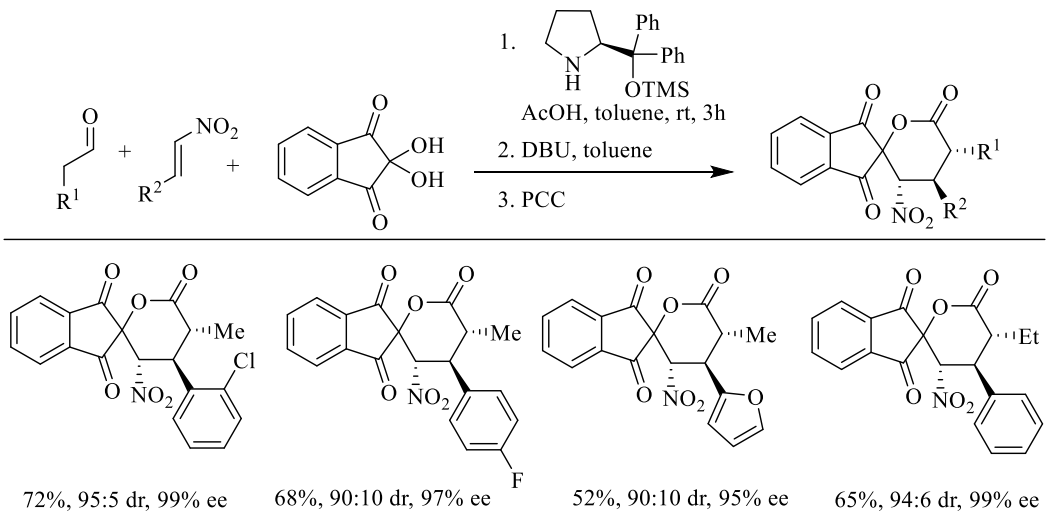
3.2 Review work

In 2012, Lu and his coworkers reported a NHC-catalyzed pseudo three-component highly stereoselective domino reaction between oxindole and alkynyl aldehydes in the presence of 30 mol% *t*-BuOK in THF at 65 ºC for 2 h to form spirooxindole 4*H*-pyran-2-one derivatives (major product) with three contiguous stereogenic centers in good yields with good to high diastereoselectivities.[20] Some of the promising results are summarized in **Scheme 3.1**.



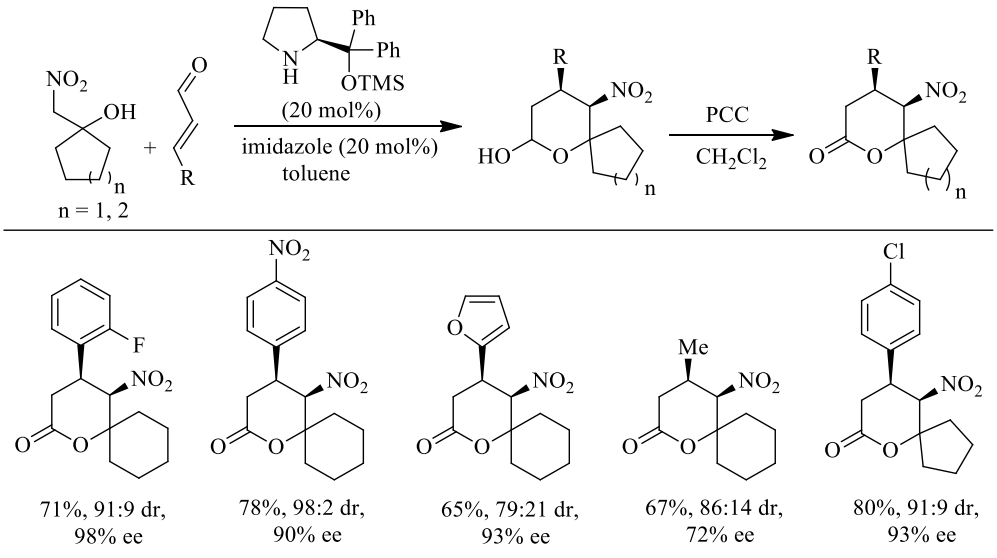
Scheme 3.1 Reaction between alkynyl aldehydes and oxindoles

A highly enantioselective preparation of oxa-spirocyclic indanone derivatives bearing four contiguous stereogenic centers and multiple functional groups in high yields and high stereoselectivities (up to 99% ee and 95:5 dr) *via* a cascade reaction of aldehydes, nitro-alkenes and ninhydrin in the presence of 10 mol% of (*S*)-2-(diphenyl((trimethylsilyl)oxy)methyl)pyrrolidine followed by DBU and oxidation by PCC in toluene is reported by Huang *et al.* in 2014.[21] Some of the examples are described in **Scheme 3.2**.



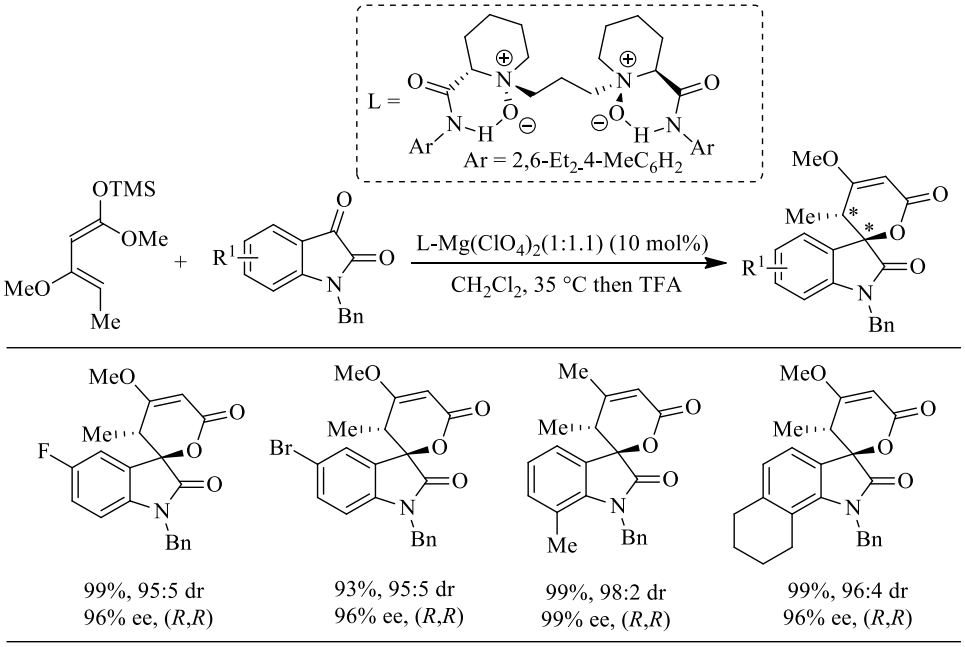
Scheme 3.2 Stereoselective synthesis of oxa-spirocyclic indanone derivatives

In 2013, Zhang *et al.* revealed an efficient asymmetric tandem Michael-hemiacetalization reaction between 1-nitromethylcycloalkanol and α,β-unsaturated aldehydes in the presence of 20 mol % of (*S*)-α,α-diphenylprolinol trimethylsilyl ether and 20 mol % of imidazole in toluene at 4 ºC to form spiro-δ-lactols which were *in situ* oxidized by using PCC.[23] This sequential method delivers spiro *cis*-δ-lactones with good overall yields as well as high to excellent enantioselectivities and diastereoselectivities as described in the **Scheme 3.3**.



Scheme 3.3 Synthesis of spiro-δ-lactone by Michael-hemiacetalization reaction

In 2013, Feng group reported a catalytic asymmetric hetero-Diels-Alder reaction of Brassard's diene with isatins under mild reaction conditions using 10 mol% of Mg(II)/*N*,*N*′-dioxide complex as catalyst at 35 ºC in CH_2Cl_2, followed by addition of TFA to the reaction mixture to afford the corresponding chiral spirolactones with excellent enantio- and diastereoselectivities (up to 99% ee and >99:1 dr) within 3 h as shown in **Scheme 3.4**.[24]



Scheme 3.4 HAD reaction of Brassard type diene with isatin derivatives

3.2.1 Conclusion

Summarizing all the review works, a few general and reliable methods are available for the efficient constructions of spiro-δ-lactones in a stereoselective manner. Despite these great efforts, there is no such method still available for the synthesis of spiro-δ-lactone fused cyclic sulfamidate imine moiety including the use of transition metal catalyst. In addition, example of direct alkylation at C-5 position of 5-membered cyclic sulfamidate imine is largely overlooked in spite of 5-memberd cyclic sulfamidate imines and their derivatives having huge applications in organic synthesis as reactive intermediates.[29-35] Apart from that, its several synthetic analogues show potential biological activities against

sulfatase, α-glucosidase and amyloglucosidase inhibitors.[36-37] Therefore, it would be highly interesting to develop a simple organocatalytic and efficient one-pot synthetic method for the stereoselective preparation of multi-functionalized spiro-δ-lactone fused cyclic sulfamidate imines using achiral starting materials.

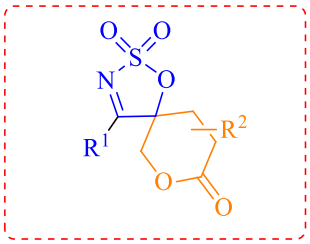


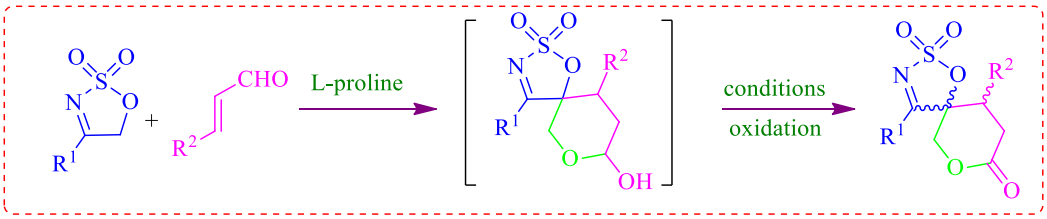
Figure 3.2 spiro-δ-lactone fused cyclic sulfamidate imine scaffold

3.3 Present work

The development of an organocatalytic efficient multi-component chemical transformation for the construction of structurally, stereochemically multifaceted architectures in a single synthetic operation using simple raw materials is one of the main focuses in synthetic organic chemistry as well as in modern drug discovery program[38-43]. This new synthetic technique is associated with several advantages as compared to a classical step-by-step processes because of potential structural modifications, reduction of the number of synthetic steps, avoidance of exhausting isolation and purification steps, belittlement of by-products. Moreover, it reduces the cost and environmental burden of the manufacturing process.[44-48]

In continuing our interest in the development of organocatalytic mediated one-pot protocol[49-54] for the synthesis of biologically important spiro-cyclic compounds[49-50] and 5-alkyl-substitituted cyclic sulfamidate imines,[53] herein, we describe a simple, mild, convenient and high-yielding one-pot three-component method for the stereoselective synthesis of functionalized spiro-sulfamidate imine fused δ-lactone derivatives *via* a Michael-condensation-hemiacetalization sequence process between 5-membered cyclic sulfamidate imine, *trans*-β-substituted acroleins and paraformaldehyde in the presence of

commercially available, cheap L-proline and DBU as the organocatalysts, followed by *in situ* oxidation of spiro-δ-lactol as shown in **Scheme 3.5**.



Scheme 3.5 Formation of spiro-sulfamidate imine fused δ-lactone derivatives

3.3.1 Results and discussion

3.3.1.1 Screening of solvents and catalysts

To optimize the reaction conditions, cyclic sulfamidate imine **1a** and *trans*-cinnamaldehyde **2a** were initially selected as model substrates in the presence of a catalytic amount of L-proline (20 mol %) in MeOH at room temperature under nitrogen atmosphere for 24 h, followed by the addition of formaldehyde and DABCO (30 mol %). Gratifyingly, after 30 h, a poor yield (37%) of desired spiro-sulfamidate imine fused δ-lactol (**4aa**) was isolated with a non-separable mixture of diastereomers. In order to simplify the isolation and characterization processes, finally, the crude spiro-δ-lactol (**4aa**) was converted into the corresponding more stable δ-lactone fused spiro-sulfamidate imines **5aa** (24%) and **6aa** (8%) with a moderate diastereoselectivity (**5aa/6aa** ratio of 7:3, entry 1, **Table 3.1**) using PCC in CH_2Cl_2 at 40 ºC for 8 h. To our delight, both the isomers **5aa** and **6aa** were fully separable by normal column chromatography technique. The desired spiro-δ-lactones **5aa** and **6aa** were fully characterized by their spectroscopic data (IR, ^1H, ^{13}C NMR and HRMS). The ^1H NMR data shows the appearance of characteristic double doublets of benzyl proton (δ 4.02) along with the disappearance of characteristic peak of starting material at δ 5.59. Total proton count at aliphatic region (5H) and aromatic region (10H) matches with our desired product. Further, ^{13}C NMR data shows appearance of 4 peaks (δ 95.0, 72.2, 45.4, 33.7 ppm) in the aliphatic regions and additional peaks in the aromatic region clears the formation of our desired spiro compound **5aa**. The quaternary carbon

assigned at δ 95.0 ppm. The HRMS spectrum shows the presence of molecular ion peak $[M+Na]^+$: 380.0556 which corresponds to the molecular weight of product of **5aa**. The relative configuration of major isomer **5aa** is cis-form, which was unequivocally assigned by its single crystal X-ray diffraction data (**Figure 3.3**). The poor yield of **4aa** (37%) was accounted due to the incomplete condensation-hemiacetalization reaction between paraformaldehyde and Michael adduct (**3aa**) in MeOH. Next, our efforts were focused on optimization of the step 2 by conducting the reactions in different organic solvents (instead of MeOH) such as THF, toluene and CH_2Cl_2 in the presence of DABCO (30 mol%) at room temperature for 16 h (**entries 2-4**). Surprisingly, in all these cases, the major spiro-δ-lactone (**5aa**) was isolated in good yields (59-65%, entries 2-4). Since, CH_2Cl_2 has a lower boiling point as well as is suitable media for PCC oxidation; it was chosen to be the best solvent for further investigations. In order to evaluate the effects of catalysts on this three step sequence process, we tested several readily available α-aminoacids (L-proline, glycine and L-phenyl alanine) and organic bases (DBU and Hünig base) as the catalysts. As shown in **Table 3.1**, glycine and L-phenyl alanine were inferior catalysts for this transformation which resulted in lower yields (entries 8 and 9). Collectively, the best results with respect to yield, time and diastereoselectivity were obtained by performing the reaction in CH_2Cl_2 with 20 mol% L-proline and 30 mol% DBU at room temperature. Under these optimal conditions, a very good yield (67%) of major isomer **5aa** and moderate diastereomeric ratio (3:1) were observed (entry 6).

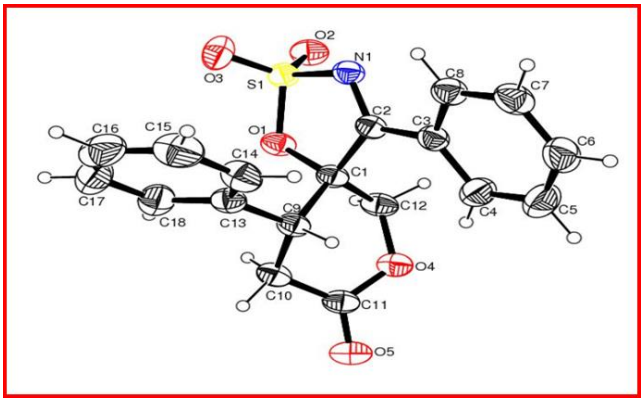
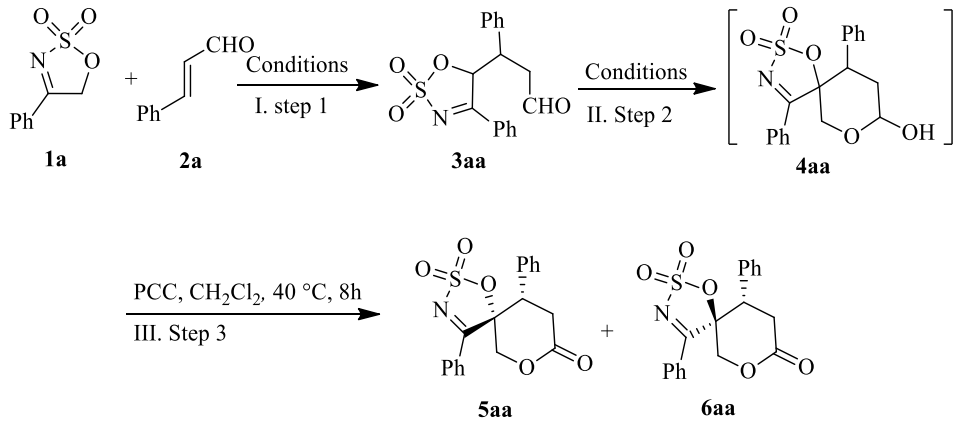


Figure 3.3 Crystal data and structure refinement for **5aa**

Table 3.1 Optimization of Michael-condensation-hemiacetalization sequence process

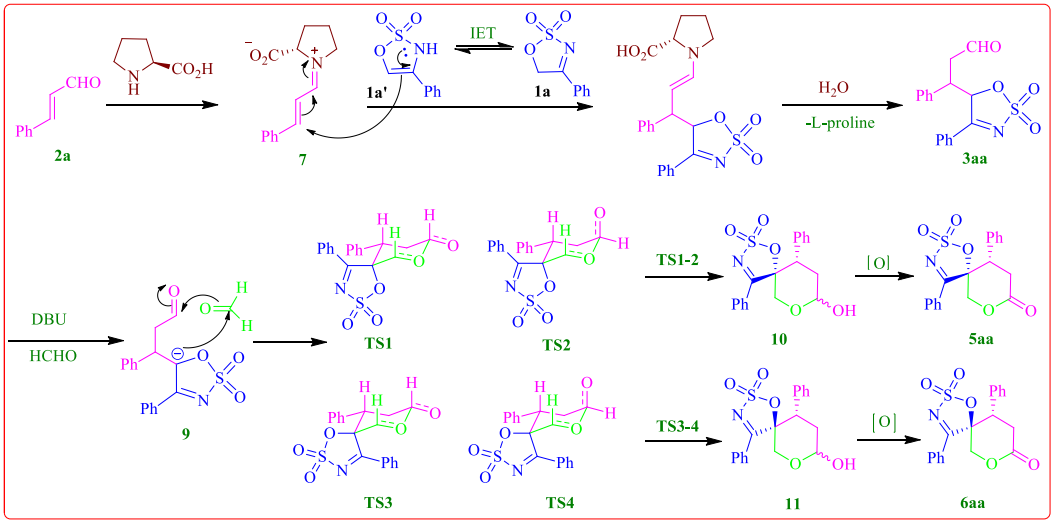


Entry	Conditions	dr[c] **5aa:6aa**	Yield[b] (%) **5aa:6aa**
1	I. L-proline, MeOH, rt, 24 h II. HCHO, DABCO, MeOH, 30 h	70:30	24:8
2	I. L-proline, MeOH, rt, 24 h II. HCHO, DABCO, THF, rt, 20 h	70:30	63:20
3	I. L-proline, MeOH, rt, 24 h II. HCHO, DABCO, CH_2Cl_2, rt, 16 h	75:25	65:19
4	I. L-proline, MeOH, rt, 24 h II. HCHO, DABCO, toluene, rt, 20 h	72:28	59:18
5	I. L-proline, CH_2Cl_2, rt, 24 h II. HCHO, DABCO, CH_2Cl_2, rt, 20 h	75:25	63:17
6.	I. L-proline, CH_2Cl_2, rt, 24 h II. HCHO, DBU, CH_2Cl_2, rt, 20 h	75:25	67:21
7	I. L-proline, CH_2Cl_2, rt, 24 h II. HCHO, (*i*-Pr)$_2$NEt, CH_2Cl_2, rt, 20 h	71:29	42:11
8.	I. Glycine, CH_2Cl_2, rt, 24 h II. HCHO, DBU, CH_2Cl_2, rt, 20 h	70:30	15:3
9.	I. L-phenyl-alanine, CH_2Cl_2, rt, 24 h II. HCHO, DBU, CH_2Cl_2, rt, 9 h	nd	>10

[a]Unless otherwise mentioned, all the reactions were performed with 5-memberd cyclic sulfamidate imines **1a-f** (0.2 mmol), **2a-j** (0.22 mmol) and L-proline (0.04 mmol) in dry CH_2Cl_2 (1.0 mL) at room temperature under nitrogen atmosphere for 24-30 h, after that HCHO (0.26 mmol) and DBU (0.06 mmol) were added for 7-9 h and followed by PCC (0.6 mmol) oxidation in CH_2Cl_2 (2.0 mL) at 40 ºC for 6-8 h. [b]Diastereomeric ratio was calculated by the corresponding peak of the ^1H NMR spectrum of the crude product. [c]Isolated yield after column chromatography. [d]Yield of mixture of diastereomers.

3.3.1.2 Plausible mechanism

A plausible mechanism for the formation of spiro-δ-lactones **5aa** and **6aa** has been depicted in **Scheme 3.6**. Presumably, in the first step, iminium species **7** is generated *via* a condensation reaction of *trans*-cinnamaldehyde **2a** with L-proline. Then the cyclic enamine **1a′** (tautomeric form of **1a**) attacks iminium species **7** to form intermediate **8** which undergoes hydrolysis to generate Michael adduct **3aa**. In the second step, a carbanion intermediate **9** is formed by removing an acidic proton from cyclic sulfamidate imine of **3aa** using a base which may attack formaldehyde and subsequently undergo intramolecular hemiacetalization through the chair-like six-membered **TS 1-4** leading to the spiro δ-lactols **10** and **11**. The resulting diastereoselectivity may be explained from the above transition states (**TS 1-4**). For instance, in general, the bulky phenyl group prefers to adopt an equatorial position rather than an axial one in a chair form of a six-membered ring as shown in **TS 1-TS 4**. Thus, the fate of diastereomeric ratio depends on the orientation of the C-O and C-C-Ph parts of cyclic sulfamidate imine in a chair-form. For example, in both the cases **TS 1** and **TS 2**, the smaller size C-O bond and larger size C-C-Ph substituents are adopted at an axial and an equatorial position respectively, which are energetically minima in comparison to the **TS3** and **TS4**. Finally, in the third step, spiro-δ-lactones **5aa** and **6aa** are obtained *via in situ* oxidation of corresponding **10** and **11** by pyridinium chlorochromate (PCC).



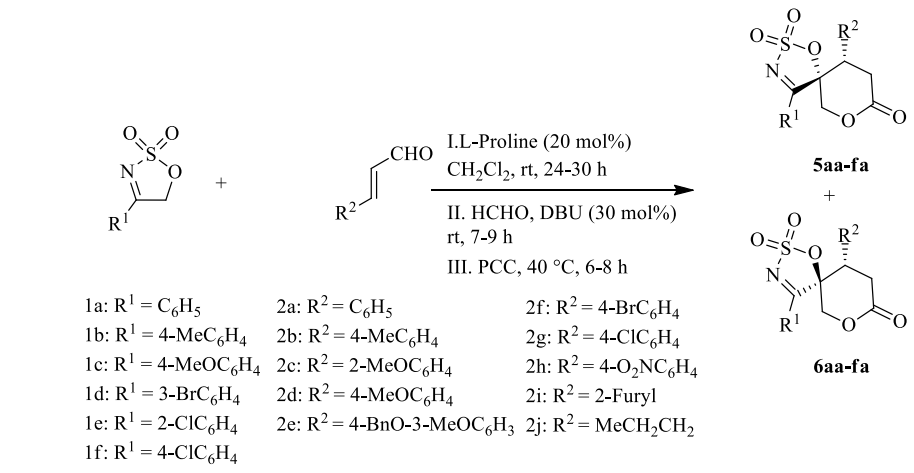
Scheme 3.6 Probable mechanism for the formation of spiro-δ-lactones

3.3.1.3 Generality and substrate scope

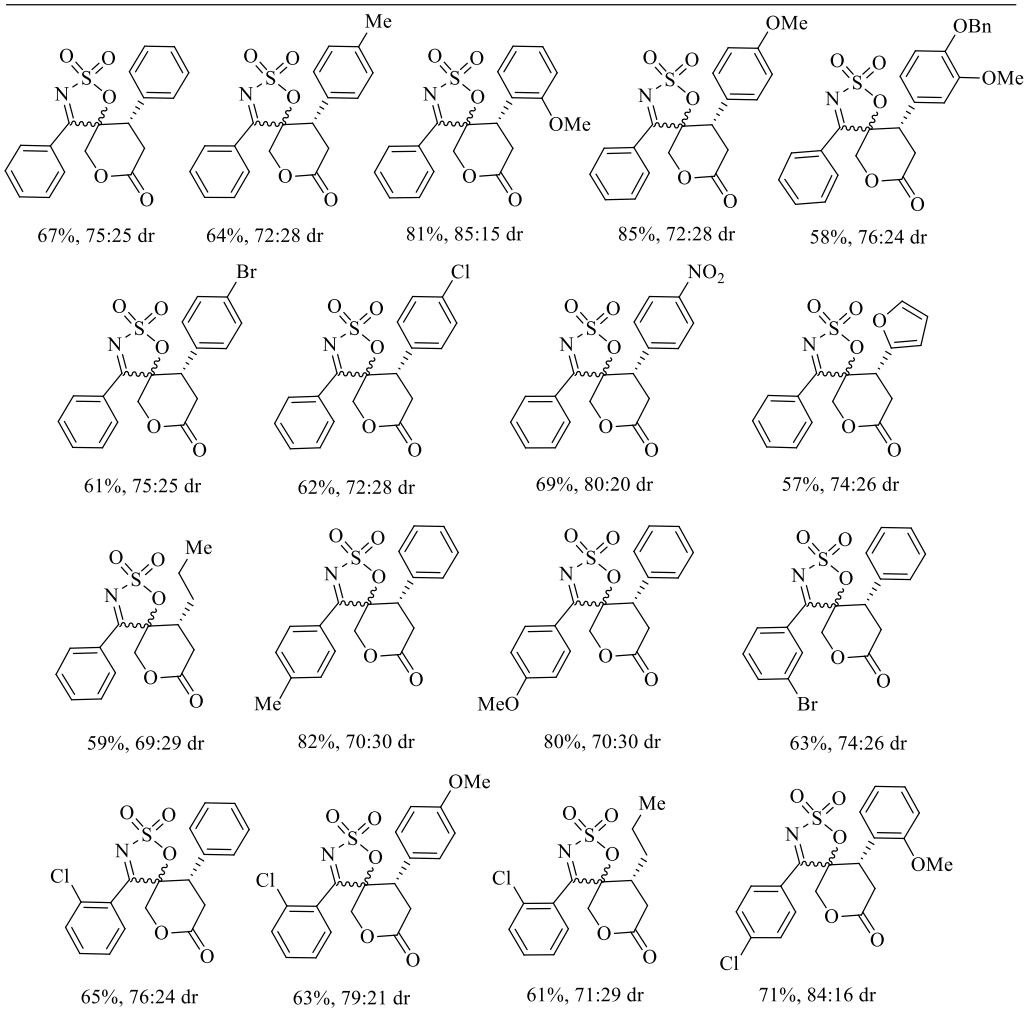
Next, we utilized these optimized reaction conditions to investigate the scope and generality of this sequential one-pot three component reaction by the various combinations of structurally varied diverse steric and stereoelectronic environments of β-aryl/alkyl-substituted acroleins (**1a-f**) with 4-aryl-substituted cyclic sulfamidate imines (**2a-j**) in the presence of a strong electrophilic paraformaldehyde. The resulting functionalized spiro-δ-lactols were further converted into the corresponding more stable spiro-δ-lactones through *in situ* oxidation by PCC. The results are summarized in **Table 3.2**. Neither electron donating (Me, OMe, OBn) nor electron withdrawing substituents (Br, Cl and NO_2) on the aromatic ring of *trans*-β-aryl-substituted acroleins had a noticeable effect on the outcome. All produced good to high overall yields (77-85%, entries 2-8) and moderate to good diastereomeric ratio values (72:28 to 85:15) of the spiro-δ-lactones **5ab-ah** and **6ab-ah**, when 4-phenyl-5*H*-1,2,3-oxathiazole-2,2-doxide (**1a**) was used as a nucleophile. Not only aryl but also a hetero-aryl-substituted β-acrolein **2i** (entry 9) afforded the good combined yield (75%) of spiro-δ-lactones **5ai** (57%) and **6ai** (18%) with a moderate dr (74:26). It is noteworthy that alkyl-substituted β-acroleins are well known to be poor Michael acceptors. Pleasantly, in our optimal conditions, alkyl-substituted β-acrolein **2j** (entry 10) reacted smoothly with a cyclic imine **1a**, leading to the desired spiro-δ-

lactones **5aj** and **6aj** in high combined yield 81% (59% of **5aj** and 22% of **6aj**). Similarly, incorporation of several functional groups such as electron donating (Me and OMe) and electron withdrawing (Cl and Br) groups on aryl rings of 4-aryl-substituted cyclic sulfamidate imines (**1b-f**, entries 11-17) did not pose any difficulty with β-aryl/alkyl-substituted acrolein derivatives by this sequential one-pot procedure and resulted in clean and complete Michael-condensation-hemiacetalization reactions, providing the corresponding anticipated products in high overall yields (80–83%) and a variable range of diastereomeric ratio values (70:30 to 84:16). Moreover, our current method excels in a variety of sensitive functional groups namely OMe, OBn, NO_2, Cl, Br, furyl etc.

Table 3.2 One-pot stereoselective synthesis of 4,10-disubstituted-1,7-dioxa-2-thia-3-azaspiro[4.5]dec-3-en-8-one-2,2-dioxides

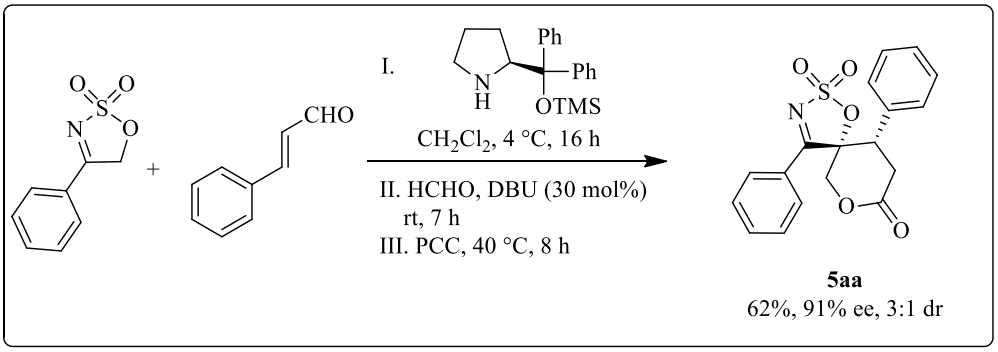


1a: $R^1 = C_6H_5$ 2a: $R^2 = C_6H_5$ 2f: $R^2 = 4\text{-}BrC_6H_4$
1b: $R^1 = 4\text{-}MeC_6H_4$ 2b: $R^2 = 4\text{-}MeC_6H_4$ 2g: $R^2 = 4\text{-}ClC_6H_4$
1c: $R^1 = 4\text{-}MeOC_6H_4$ 2c: $R^2 = 2\text{-}MeOC_6H_4$ 2h: $R^2 = 4\text{-}O_2NC_6H_4$
1d: $R^1 = 3\text{-}BrC_6H_4$ 2d: $R^2 = 4\text{-}MeOC_6H_4$ 2i: $R^2 = 2\text{-}Furyl$
1e: $R^1 = 2\text{-}ClC_6H_4$ 2e: $R^2 = 4\text{-}BnO\text{-}3\text{-}MeOC_6H_3$ 2j: $R^2 = MeCH_2CH_2$
1f: $R^1 = 4\text{-}ClC_6H_4$



3.3.1.4 Enantioselective synthesis of spirosulfamidate imine fused δ-lactone moiety

Moreover, after successfully developing an efficient, catalytic one-pot sequential process for the construction of functionalized spirosulfamidate imine fused δ-lactone moiety in a diastereoselective manner, next we turned our attention towards the enantioselective version of this reaction by using (*S*)-(-)-α,α-diphenyl-2-pyrrolidinemethanol trimethylsilyl ether as a catalyst which is well known to be a highly efficient catalyst for various organic transformations[55-58]. As shown in **Scheme 3.7**, the reaction between **1a** and *trans*-cinnamaldehyde (**2a**) proceeded smoothly in CH_2Cl_2 at room temperature by the use of 10 mol% loading of a catalyst, followed by the additions of formaldehyde and DBU and subsequent PCC oxidation of resulting spiro-δ-lactol, leading to the good yield (**5aa**, 62%) and enantioselectivity (70% ee) of major diastereomer **5aa**. Pleasantly, a significant improvement of enantioselectivity (91% ee) was obtained when the Michael reaction was conducted at 4 ºC. It should be noted that L-proline was given a very poor enantioselectivity (18% ee) in our present conditions.

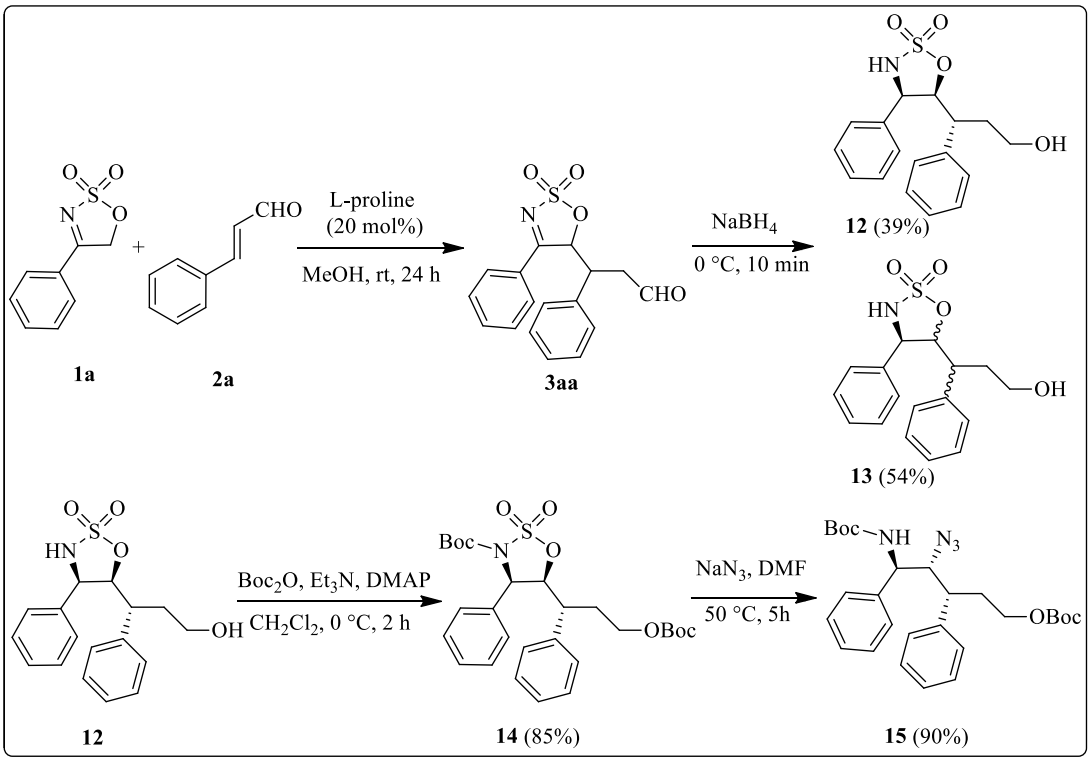


Scheme 3.7 One-pot enantioselective synthesis of spiro-δ-lactone

3.3.1.5 Synthesis of *trans*-*cis*-β-amino-α-azido derivative

Next, we have realized that the obtained Michael adduct **3aa** (57:43 dr) may be converted into the synthetically valuable intermediate β-amino-α-azido derivative. Towards this goal, the reductions of pro-chiral C=N bond and aldehyde group of Michael adduct **3aa** have been carried out *in situ* by $NaBH_4$ in MeOH at 0 ºC to furnish the cyclic sulfamidates **12** (37%) and **13** (54%) respectively. Afterwards,

the Boc protections of both NH and OH groups of compound **12** have been performed using Boc_2O in the presence of catalytic amount of DMAP in CH_2Cl_2, leading to compound **14** in excellent yield (85%). The relative configuration of the product **14** (*cis-trans*) was confirmed by ORTEP data (**Fig. 3.4**). Finally, *trans-cis*-β-amino-α-azido derivative **15** has been successfully achieved in 90% yield from **14** *via* a nucleophilic substitution reaction with NaN_3 in DMF at 50 ºC in a stereospecific manner (**Scheme 3.8**).



Scheme 3.8 Stereoselective synthesis of *trans-cis*-β-amino-α-azido compound

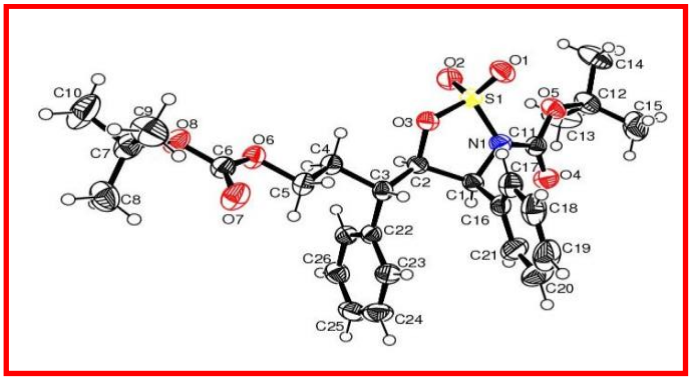


Figure 3.4 ORTEP diagram of compound **14**

3.4 Conclusion

A simple, organocatalytic (L-proline and DBU) and robust one-pot three-component reaction involving Michael-condensation-hemiacetalization sequence process for the stereoselective synthesis of previously unknown class of functionalized δ-lactone fused spiro-sulfamidate imine derivatives through *in situ* oxidation of spiro-δ-lactols by PCC as an oxidant has been developed. This three-step sequence process is coupled with several advantages such as being catalytic, mild reaction conditions (room temperature), excellent overall yield (≥88%), good diastereoselectivity (upto 5:1 dr) and broad substrate scope. In addition, diphenylprolinol silyl ether catalysed, highly efficient enantioselective version of this spiro-δ-lactone has been realized. Moreover, Michael adduct could be utilized for the transformation of synthetically valuable intermediate β-amino-α-azido compound.

3.5 Experimental Section

3.5.1 General Information

All reactions were carried out either under inert atmosphere or air and monitored by TLC using Merck 60 F_{254} pre coated silica gel plates (0.25 mm thickness) and the products were visualized by UV detection. Flash chromatography was carried out with silica gel (200-300 mesh). FT-IR spectra were recorded on a BrukerTensor-27 spectrometer. ^{1}H and ^{13}C NMR spectra were recorded on a Bruker Avance (III) 400 MHz spectrometer. Data for ^{1}H NMR are reported as a chemical shift (δ ppm), multiplicity (s = singlet, d = doublet, q = quartet, m = multiplet), coupling constant *J* (Hz), integration, and assignment, data for ^{13}C are reported as a chemical shift. High resolutions mass spectral analyses (HRMS) were carried out using ESI-TOF-MS. Single crystal X-ray structural studies were performed on a CCD Agilent Technologies (Oxford Diffraction) SUPER NOVA diffractometer. Data were collected at 293(2) K using graphite-monochromoated Mo Kα radiation (λ_{α} = 0.71073 Å). The strategy for the Data collection was evaluated by using the CrysAlisPro CCD software. The data were collected by the

standard 'phi-omega scan techniques, and were scaled and reduced using CrysAlisPro RED software. The structures were solved by direct methods using SHELXS-97 and refined by full matrix least-squares with SHELXL-97, refining on F^{21}.

The positions of all the atoms were obtained by direct methods. All non-hydrogen atoms were refined anisotropically. The remaining hydrogen atoms were placed in geometrically constrained positions and refined with isotropic temperature factors, generally $1.2U_{eq}$ of their parent atoms.

3.5.2 Materials

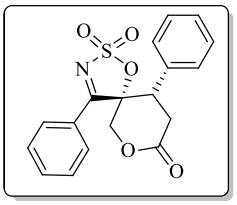
All these starting materials and catalysts were either purchased from commercial sources or synthesized by literature known procedures.[58] CH_2Cl_2 was dried over calcium hydride under argon atmosphere and distilled under reduced pressure before prior used.

General procedure for the synthesis of spiro-δ-lactone derivatives (Table 3 2):

To a stirred solution of 5-membered cyclic sulfamidate imine (**1a-f**, 0.2 mmol) and *trans*-β-aryl/alkyl-substituted acroleins (**2a-j**, 0.22 mmol) in CH_2Cl_2 in (1.0 mL) under nitrogen atmosphere was added L-proline (0.04 mmol) at room temperature. The progress of the reaction was monitored by TLC. After completion of the reaction, paraformaldehyde (0.26 mmol) and DBU (0.06 mmol) were added to the above reaction mixture. The stirring was continued for 7-9 h (monitored by TLC). After that PCC (0.6 mmol) in CH_2Cl_2 (2.0 mL) was added. The resulting mixture was refluxed at 40 ºC for 6-8 h. Then the reaction mixture was passed through celite-pad to remove the inorganic materials and washed with ethyl acetate. The combined organic phase was evaporated by rotary evaporator under reduced pressure to give the crude product. The crude product was purified by column chromatography over silica gel to furnish the pure spiro-δ-lactones. The products were characterized by their corresponding spectroscopic data (IR,

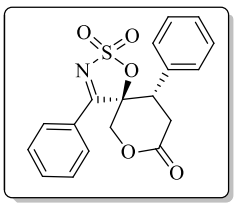
^{1}H and ^{13}C NMR, HRMS). All the products in **Table 3.2** have been synthesized by this procedure.

***Cis*-4,10-diphenyl-1,7-dioxa-2-thia-2,2-dioxide-3-azaspiro[4.5]dec-3-en-8-one**

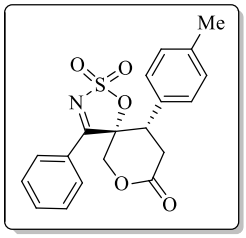


(5aa): white solid; **mp**: 138-140 °C; **IR** (KBr): *v* 2925, 1768, 1592, 1562, 1498, 1453, 1378, 1297, 1273, 1235, 1205 cm^{-1}; **^{1}H NMR** (400 MHz, $CDCl_3$): δ (major isomer) 8.05-8.07 (m, 2H), 7.77-7.82 (m, 1H), 7.61-7.66 (m, 2H), 7.28-7.30 (m, 1H), 7.21-7.25 (m, 2H), 6.88-6.90 (m, 2H), 5.16 (d, *J* = 13.6 Hz, 1H), 4.77 (d, *J* = 13.8 Hz, 1H), 4.02 (dd, *J* = 4.0, 13.5 Hz, 1H), 3.29-3.36 (m, 1H), 2.97-3.03 (m, 1H); **^{13}C NMR** (100 MHz, $CDCl_3$): δ (major isomer) 176.4, 168.7, 136.2, 132.2, 130.5, 130.4, 129.7, 129.6, 129.3, 128.8, 95.0, 72.2, 45.4, 33.7; **HRMS** (ESI) m/z calculated for $C_{18}H_{15}NO_5S$ $[M+Na]^+$: 380.0563, found 380.0566.

***Trans*-4,10-diphenyl-1,7-dioxa-2,2-dioxide-2-thia-3-azaspiro[4.5]dec-3-en-8-one (6aa):** white solid; **mp**: 130-132 °C; **IR** (KBr): *v* 3065, 2978, 2924, 2855, 1768, 1591, 1556, 1451, 1375, 1276, 1230 cm^{-1}; **^{1}H NMR** (400 MHz, $CDCl_3$): δ (minor isomer) 7.46-7.50 (m, 1H), 7.36-7.38 (m, 2H), 7.22-7.26 (m, 2H), 7.07-7.13 (m, 3H), 6.98-7.02 (m, 2H), 5.17 (d, *J* = 13.3 Hz, 1H), 4.72 (d, *J* = 13.3 Hz, 1H), 4.06-4.09 (m, 1H), 3.26-3.32 (m, 1H) 3.10-3.16 (m, 1H); **^{13}C NMR** (100 MHz, $CDCl_3$): δ (minor isomer) 178.04, 168.9, 134.8, 134.7, 130.2, 129.4, 129.2, 129.1, 128.3, 128.2, 96.9, 70.0, 46.9, 33.1; **HRMS** (ESI) m/z calculated for $C_{18}H_{15}NO_5S$ $[M+Na]^+$: 380.0563, found 380.0566.



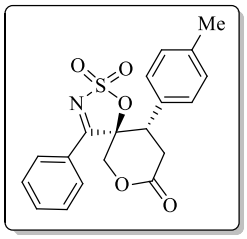
***Cis*-4-phenyl-10-(4-methylphenyl)-1,7-dioxa-2-thia-2,2-dioxide-3-azaspiro**



[4.5]dec-3-en-8-one (5ab): white solid; **mp**: 110-112 °C; **IR** (KBr): *v* 2956, 2924, 2857, 1754, 1632, 1595, 1561, 1517, 1449, 1377 cm^{-1}; **^{1}H NMR** (400 MHz, $CDCl_3$): δ (major isomer) 8.04-8.07 (m, 2H), 7.77-7.80 (m, 1H), 7.01-7.03 (m, 2H), 6.77-6.79 (m, 2H), 5.16 (d, *J* = 13.6 Hz, 1H), 4.75 (d, *J* = 13.5 Hz, 1H), 4.01 (dd, *J* = 4.3, 13.5 Hz, 1H), 3.25-3.33 (m, 1H), 2.94-2.99 (m, 1H); **^{13}C NMR** (100 MHz, $CDCl_3$): δ 176.4, 168.8, 139.5, 136.1,130.6, 130.3, 129.9,

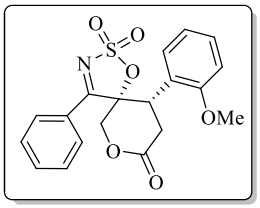
129.2, 128.7, 127.1, 95.1, 72.3, 45.0, 33.9, 21.4; **HRMS** (ESI) m/z calculated for $C_{19}H_{17}NO_5S$ $[M+Na]^+$: 394.0720, found 394.0726.

***Trans*-4-phenyl-10-(4-methylphenyl)-1,7-dioxa-2-thia-2,2-dioxide-3-azaspiro-**



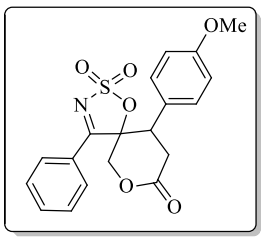
[4.5]dec-3-en-8-one (6ab): white solid; **mp**: 108-110 °C; **IR** (KBr): *ν* 2956, 1769, 1630, 1595, 1560, 1517, 1449, 1377, 1278, 1203 cm^{-1}; **^{1}H NMR** (400 MHz, $CDCl_3$): δ *(*minor isomer) 7.47-7.51(m, 1H), 7.35-7.37 (m, 2H), 7.21-7.25 (m, 2H), 6.85-6.90 (m, 4H), 5.16 (d, *J* = 13.3 Hz, 1H), 4.70 (d, *J* = 13.3 Hz, 1H), 4.01-4.05 (m, 1H), 3.24-3.30 (m, 1H), 3.06-3.12 (m. 1H), 2.19 (s, 3H); **HRMS** (ESI) m/z calculated for $C_{19}H_{17}NO_5S$ $[M+Na]^+$: 394.0720, found 394.0726.

***Cis*-4-phenyl-10-(2-methoxyphenyl)-1,7-dioxa-2-thia-2,2-dioxide-3-azaspiro**



[4.5]dec-3-en-8-one (5ac): white solid; **mp**: 146-148 °C; **IR** (KBr): ν 2961, 2933, 2842, 2359, 1768, 1594, 1561, 1495, 1462, 1374, 1330, 1298, 1253 cm^{-1}; **^{1}H NMR** (400 MHz, $CDCl_3$): δ *(*major isomer*)* 8.11-8.13 (m, 2H), 7.73-7.77 (m, 1H), 7.59-7.63 (m, 2H), 7.26-7.30 (m, 2H), 7.00-7,04 (m, 1H), 6.67-6.69 (m,1H), 5.03 (d, *J* = 13.6Hz, 1H), 4.70 (d, *J* =13.5Hz, 1H), 4.61 (dd, J_1 = 4.0 Hz, J_2 = 8.8 Hz, 1H), 3.26-3.33 (m, 1H), 3.14 (s, 3H), 2.92 (dd, J_1 = 4.0 Hz, J_2 = 10.2 Hz, 1H); **^{13}C NMR** (100 MHz, $CDCl_3$): δ (major isomer) 177.4, 170.0, 156.4, 135.5, 130.5, 130.3, 129.7, 129.7, 127.3, 121.4, 121.2, 110.3, 95.3, 71.9, 54.5, 37.7, 33.5; **HRMS** (ESI) m/z calculated for $C_{19}H_{17}NO_6S$ $[M+H]^+$: 388.0849, found 388.0916.

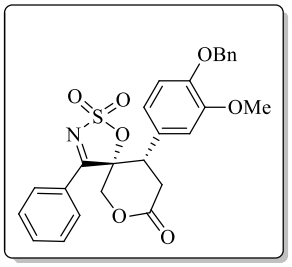
4-Phenyl-10-(4-methoxyphenyl)-1,7-dioxa-2-thia-2,2-dioxide-3-azaspiro



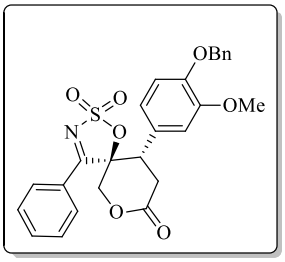
[4.5]dec-3-en-8-one (5ad & 6ad): white solid; **mp**: 110-112 °C; **IR** (KBr): *ν* 2960, 2935, 2842, 1752, 1611, 1593, 1561, 1515, 1448, 1374, 1305, 1256 cm^{-1}; **^{1}H NMR** (400 MHz, $CDCl_3$): δ (mixture of two diastereomers) 8.05-8.07 (m, 1.4H), 7.77-7.81(m, 0.7H), 7.62-7.65(m, 1.4H), 7.49-7.52(m, 0.3H), 7.39-7.43(m, 0.7H), 7.26-7.29(m, 0.9H), 6.88-6.90(m, 0.9H), 6.80-

6.83(m, 1H), 6.71-6.73(m, 1H), 6.59-6.61(m, 0.7H), 5.15-5.18(m, 1H), 4.68-4.76(m, 1H), 4.00-4.12(m, 1H), 3.73(s, 2.1H), 3.68(s, 0.9H), 3.22-3.30(m, 1H), 2.93-3.12(m, 1H); **^{13}C NMR** (100 MHz, $CDCl_3$): δ (major isomer) 176.5, 168.8, 160.3, 136.2, 130.3, 130.0, 129.4, 127.1, 124.3, 114.6, 95.4, 72.3, 55.5, 44.5, 34.1; **^{13}C NMR** (100 MHz, $CDCl_3$): δ (minor isomer) 178.3, 169.2, 160.0, 134.8, 130.6, 130.3, 129.2, 128.4, 126.4, 114.7, 97.3, 70.0, 55.6, 46.2, 33.3; **HRMS** (ESI) m/z calculated for $C_{19}H_{17}NO_6S$ $[M+Na]^+$: 410.0669 found 410.0664.

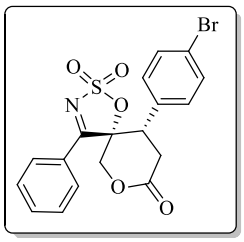
***Cis*-4-phenyl-10-(4-benzyloxy-3-methoxyphenyl)-1,7-dioxa-2-thia-2,2-dioxide-3-azaspiro[4.5]dec-3-en-8-one (5ae):** white solid; **mp**: 130-132 °C; **IR** (KBr): ν 2950, 2930, 2852, 1753, 1643, 1604, 1562, 1515, 1465, 1424, 1373, 1265 cm^{-1}; **^{1}H NMR** (400 MHz, $CDCl_3$): δ (major isomer) 8.00-8.02 (m, 2H), 7.74-7.78 (m,1H), 7.58-7.62 (m, 2H), 7.29-7.40 (m, 7H), 6.63-6.65 (m, 1H), 6.47-6.48 (m, 1H), 6.30-6.32 (m, 1H), 5.17 (d, *J* = 13.28 Hz, 1H), 5.05 (s, 2H), 4.74 (d, *J* = 13.5 Hz, 1H), 4.00 (dd, *J* = 4.8, 13.6Hz, 1H), 3.66 (s, 3H), 3.20-3.28 (m, 1H), 2.94-3.00 (m, 1H); **^{13}C NMR** (100 MHz, $CDCl_3$): δ (major isomer) 176.2, 168.3, 150.0, 149.0, 136.9, 136.0, 130.5, 130.2, 128.9, 128.3, 127.6, 125.2, 121.4, 115.6, 113.9, 112.0, 95.3, 72.4, 71.2, 56.1, 44.8, 34.2; **HRMS** (ESI) m/z calculated for $C_{26}H_{23}NO_7S[M+Na]^+$: 516.1087, found 516.1087.



***Trans*-4-phenyl-10-(4-benzyloxy-3-methoxyphenyl)-1,7-dioxa-2-thia-2,2-dioxide-3-azaspiro[4.5]dec-3-en-8-one (6ae):** white solid; **mp**: 130-132 °C; **IR** (KBr): ν 2957, 2924, 2853, 1771, 1632, 1594, 1560, 1516, 1456, 1376, 1269 cm^{-1}; **^{1}H NMR** (400 MHz, $CDCl_3$): δ (minor isomer) 7.26-7.47 (m, 10H), 7.19-7.23 (m, 2H), 6.52-6.56 (m, 2H), 6.38-6.41 (m, 1H), 5.10 (d, *J* = 13.56 Hz, 1H), 5.02-5.03 (m, 2H), 4.69 (d, *J* = 13.6 Hz, 1H), 4.01-4.04 (m, 1H), 3.69 (s, 3H), 3.20-3.26 (m, 1H), 3.05-3.12 (m, 1H); **HRMS** (ESI) m/z calculated for $C_{26}H_{23}NO_7S[M+Na]^+$: 516.1087, found 516.1087.

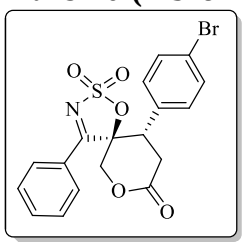


***Cis*-10-(4-bromophenyl)-4-phenyl-1,7-dioxa-2-thia-2,2-dioxide-3-azaspiro**



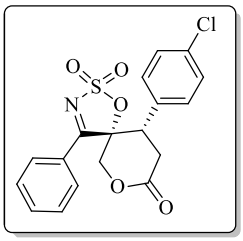
[4.5]dec-3-en-8-one (5af): white solid; **mp** 140-142 °C; **IR** (KBr): *ν* 2957, 2925, 2854, 1749, 1632, 1594, 1561, 1491, 1449, 1378, 1204 cm^{-1}; **^{1}H NMR** (400 MHz, $CDCl_3$): *δ* 8.04-8.06 (m, 2H), 7.78-7.82 (m, 1H), 7.62-7.66 (m, 2H), 7.35-7.37 (m, 2H), 6.76-6.78 (m, 2H), 5.17 (d, *J* = 13.6 Hz, 1H), 4.76 (d, *J* = 13.6 Hz, 1H), 4.00 (dd, *J* = 4.3, 13.6 Hz, 1H), 3.22-3.30 (m, 1H), 2.94-2.99 (m 1H); **^{13}C NMR** (100 MHz, $CDCl_3$): δ 176.1, 168.2, 136.4, 132.5, 131.3, 130.5, 130.4, 130.4, 126.9, 124.0, 94.5, 72.2, 44.9, 33.7.

***Trans*-10-(4-bromophenyl)-4-phenyl-1,7-dioxa-2-thia-3-azaspiro[4.5]dec-3-**



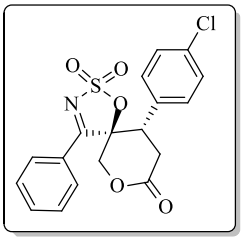
en-8-one 2,2-dioxide (6af): white solid; **mp**: 135-137 °C; **^{1}H NMR** (400 MHz, $CDCl_3$): δ (minor isomer) 7.54-7.58 (m, 1H), 7.40-7.43 (m, 2H), 7.28-7.34 (m, 2H), 7.18-7.23 (m, 2H), 6.82-6.84 (m, 2H), 5.14 (d, *J* = 13.3 Hz, 1H), 4.74 (d, *J* = 12.0Hz, 1H), 4.01-4.05 (m, 1H), 3.21-3.27 (m, 1H), 3.05-3.11 (m, 1H).

***Cis*-10-(4-chlorophenyl)-4-phenyl-1,7-dioxa-2-thia-2,2-dioxide-3-azaspiro**



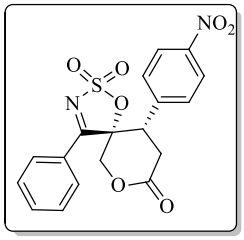
[4.5]dec-3-en-8-one 2,2-dioxide (5ag): white solid; **mp**: 128-130 °C; **IR** (KBr): ν 2959, 2924, 2854, 1750, 1636, 1594, 1561, 1493, 1450, 1378, 1204 cm^{-1}; **^{1}H NMR** (400 MHz, $CDCl_3$): δ (major isomer) 8.04-8.05 (m, 2H), 7.78-7.82 (m, 1H), 7.62-7.66 (m, 2H), 7.19-7.21 (m, 2H), 6.82-6.84 (m, 2H), 5.17 (d, *J* = 13.5 Hz, 1H), 4.76 (d, *J* = 13.6 Hz, 1H), 4.03 (dd, *J* = 4.3, 13.8 Hz, 1H), 3.22-3.30 (m, 1H), 2.94-2.99 (m, 1H); **^{13}C NMR** (100 MHz, $CDCl_3$): δ (major isomer) 176.1, 168.3, 136.4, 135.8, 130.8, 130.6, 130.4, 130.2, 129.6, 126.9, 94.7, 72.2, 44.8, 33.7; **HRMS** (ESI) m/z calculated for $C_{18}H_{14}ClNO_5S$ $[M+Na]^+$: 414.0170, found 414.0177.

***Trans*-10-(4-chlorophenyl)-4-phenyl-1,7-dioxa-2-thia-2,2-dioxide-3-azaspiro**



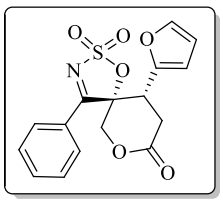
[4.5]dec-3-en-8-one (6ag): white solid; **mp**: 125-127 °C; **IR** (KBr): ν 2961, 2923, 2854, 1773, 1633, 1593, 1561, 1494, 1447, 1372, 1277, 1236 cm^{-1}; **^{1}H NMR** (400 MHz, $CDCl_3$): δ (minor isomer) 7.53-7.57 (m, 1H), 7.41-7.44 (m, 2H), 7.29-7.33 (m, 2H), 7.03-7.07 (m, 2H), 6.88-6.91 (m, 2H), 5.15 (d, *J* = 13.6 Hz, 1H), 4.74 (d, *J* = 13.6 Hz, 1H), 4.03-4.07 (m, 1H), 3.20-3.26 (m, 1H), 3.06-3.12 (m, 1H); **HRMS** (ESI) m/z calculated for $C_{18}H_{14}ClNO_5S[M+Na]^+$: 414.0170, found 414.0177.

***Cis*-10-(4-Nitrophenyl)-4-phenyl-1,7-dioxa-2-thia-2,2-dioxide-3-azaspiro**



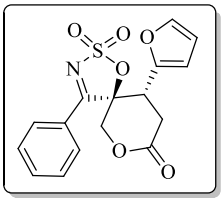
[4.5]dec-3-en-8-one (5ah): white solid; **mp**: 138-140 °C; **IR** (KBr): ν 2924, 2853, 1737, 1596, 1561, 1522, 1448, 1373, 1348, 1202 cm^{-1}; **^{1}H NMR** (400 MHz, $CDCl_3$): δ (major isomer) 8.06-8.12 (m, 4H), 7.82-7.86 (m, 1H), 7.66-7.70 (m, 2H), 7.07-7.10 (m, 2H), 5.19 (d, *J* = 13.6 Hz, 1H), 4.80 (d, *J* = 13.6 Hz, 1H), 4.11-4.16 (m, 1H), 3.30-3.38 (m, 1H), 3.00-3.05 (m, 1H); **^{13}C NMR** (100 MHz, $CDCl_3$): δ (major isomer) 175.8, 167.8, 148.7, 139.1, 136.7, 130.7, 130.5, 130.0, 126.6, 124.5, 94.1, 72.1, 45.2, 33.3; **HRMS** (ESI) m/z calculated for $C_{18}H_{14}N_2O_7S$ $[M+Na]^+$: 425.0414 , found: 424.0418.

***Cis*-4-phenyl-10-(2-furyl)-1,7-dioxa-2-thia-2,2-dioxide-3-azaspiro[4.5]dec-3-**



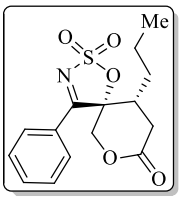
en-8-one (5ai): white solid; **mp**: 108-110 °C; **IR** (KBr): ν 2992, 2961, 2925, 1754, 1589, 1557, 1451, 1411, 1371, 1243 cm^{-1}; **^{1}H NMR** (400 MHz, $CDCl_3$): δ (major isomer) 8.08-8.11 (m, 2H), 7.75-7.80 (m, 1H), 7.62-7.66 (m, 2H), 7.26-7.27 (m, 1H), 6.29-6.31 (m, 1H), 6.15-6.16 (m, 1H), 5.04 (d, *J* = 13.6 Hz, 1H), 4.67 (d, *J* = 13.6 Hz, 1H), 4.27 (dd, *J* = 4.5, 13.3 Hz, 1H), 3.21-3.29 (m, 1H), 3.08-3.13 (m, 1H) ; **^{13}C NMR** (100 MHz, $CDCl_3$): δ (major isomer) 176.4, 167.5, 146.6, 143.8, 136.0, 130.5, 130.3, 128.6, 111.1, 110.1, 93.6, 72.1, 39.8, 31.5; **HRMS** (ESI) m/z calculated for $C_{16}H_{13}NO_6S$ $[M+Na]^+$: 370.0356, found 370.0354.

Trans-4-phenyl-10-(2-furyl)-1,7-dioxa-2-thia-2,2-dioxide-3-azaspiro[4.5]dec-



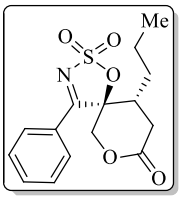
3-en-8-one (6ai): white solid; **mp**: 111-113 °C; **IR** (KBr): ν 2977, 2937, 1781, 1591, 1557, 1449, 1381, 1280, 1247, 1205 cm^{-1}; **^{1}H NMR** (400 MHz, $CDCl_3$): δ (minor isomer) 7.52-7.59 (m, 3H), 7.32-7.36 (m, 2H), 7.04-7.05 (m, 1H), 6.10-6.11 (m, 1H), 6.03-6.05 (m, 1H), 5.19 (d, *J* = 13.3 Hz, 1H), 4.67 (d, *J* = 13.3 Hz, 1H), 4.11-4.14 (m, 1H), 3.27-3.33 (m, 1H), 3.03.-3.09 (m, 1H); **HRMS** (ESI) m/z calculated for $C_{16}H_{13}NO_6S$ $[M+Na]^+$: 370.0356, found 370.0354.

***Cis*-4-phenyl-10-propyl-1,7-dioxa-2-thia-2,2-dioxide-3-azaspiro[4.5]dec-3-en-**



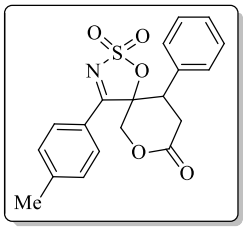
8-one (5aj): gummy compound; **IR** (KBr): ν 2963, 2930, 2872, 1761, 1592, 1558, 1452, 1372, 1291, 1203 cm^{-1}; **^{1}H NMR** (400 MHz, $CDCl_3$): δ (major isomer) 8.07-8.09 (m, 2H), 7.75-7.79 (m, 1H), 7.59-7.64 (m, 2H), 4.98 (d, *J* = 13.2 Hz, 1H), 4.59 (d, *J* = 13.5 Hz, 1H), 2.88-2.94 (m, 1H), 2.81-2.86 (m, 1H), 2.55-2.62 (m, 1H), 1.55 (s, 3H), 1.25 (s, 1H), 0.76 (t, *J* = 7.3 Hz, 3H); **^{13}C NMR** (100 MHz, $CDCl_3$): δ (major isomer) 177.1, 168.6, 136.3, 130.4, 130.3, 126.7, 96.0, 72.3, 39.4, 32.6, 30.6, 19.3, 13.8; **HRMS** (ESI) m/z calculated for $C_{15}H_{17}NO_5S[M+Na]^+$: 346.0720, found 346.0768.

***Trans*-4-phenyl-10-propyl-1,7-dioxa-2-thia-3-azaspiro[4.5]dec-3-en-8-one 2,2-**



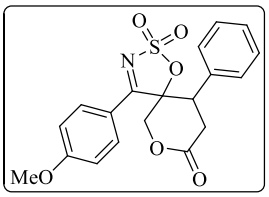
dioxide (6aj): gummy compound; **IR** (KBr): ν 2959, 2924, 2854, 1742, 1638, 1462, 1405, 1378, 1261, 1203, 1102 cm^{-1}; **^{1}H NMR** (400 MHz, $CDCl_3$): δ (minor isomer) 7.94-7.96 (m, 2H), 7.71-7.75 (m, 1H), 7.75-7.61 (m, 2H), 4.95 (d, *J* = 13.6 Hz, 1H), 4.63 (d, *J* = 13.2 Hz, 1H), 4.20-4.29 (m, 1H), 2.90-2.96 (m, 1H), 2.70-2.77 (m, 1H), 2.44-2.50 (m, 1H), 1.25-1.26 (m, 1H), 1.16-1.18 (m, 1H), 0.78 (t, *J* = 7.0 Hz, 3H); **HRMS** (ESI) m/z calculated for $C_{15}H_{17}NO_5S[M+Na]^+$: 346.0720, found 346.0768.

10-Phenyl-4-(4-methylphenyl)-1,7-dioxa-2-thia-2,2-dioxide-3-azaspiro



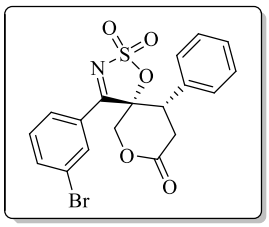
[4.5]dec-3-en-8-one (5ba & 6ba): white solid; **mp**: 120-122 °C; **IR** (KBr): ν 2958, 2925, 2869, 2360, 2338, 1760, 1609, 1585, 1550, 1498, 1454, 1375, 1297, 1204 cm^{-1}; **^{1}H NMR** (400 MHz, $CDCl_3$): δ (mixture of diastereomer) 7.96-7.98 (m 1.3H), 7.41-7.43 (m, 1.3H), 7.26-7.29 (m, 1.05H), 7.20-7.24 (m, 1.4H), 7.10-7.14 (m, 1.3H), 7.00-7.04 (m, 1.3H), 6.90-6.93 (m, 1.3H), 5.11-5.16 (m, 1H), 4.73 (d, *J* = 13.5 Hz, 0.65H), 4.66 (d, *J* = 13.6 Hz, 0.35 H), 4.05-4.09 (m, 1H), 3.25-3.35 (m, 1H), 3.12-3.18 (m, 0.35H), 2.95-3.01 (m, 0.65H), 2.52 (s, 1.95H), 2.34 (s, 1.05H); **^{13}C NMR** (100 MHz, $CDCl_3$): δ (major isomer) 176.1, 168.9, 148.1, 132.4, 131.1, 129.9, 129.4, 129.2, 128.9, 124.2, 94.9, 72.4, 45.3, 33.7, 22.4; **^{13}C NMR** (100 MHz, $CDCl_3$): δ (minor isomer) 177.6, 169.1, 146.7, 134.8, 130.7, 130.6, 129.5, 129.1, 128.3, 125.4, 96.9, 70.2, 46.9, 33.1, 22.1; **HRMS** (ESI) m/z calculated for $C_{19}H_{17}NO_5S[M+Na]^+$: 394.0720, found 394.0726.

4-(4-methoxyphenyl)-10-phenyl-1,7-dioxa-2-thia-2,2-dioxide-3-azaspiro



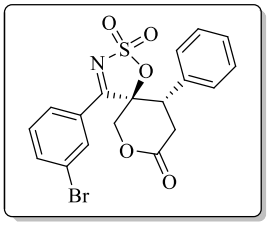
[4.5]dec-3-en-8-one (5ca & 6ca): white solid; **mp**: 152-154 °C; **IR** (KBr): ν 3010, 2932, 2849, 2361, 2339, 1751, 1606, 1582, 1543, 1513, 1457, 1428, 1406, 1368, 1314, 1267, 1203, 1175, 1129, 1073, 1053, 1020 cm^{-1}; **^{1}H NMR** (400 MHz, $CDCl_3$): δ 8.05-8.07 (m, 1.5H), 7.35-7.37 (m, 0.75H), 7.26-7.30 (m, 0.75H), 7.21-7.25 (m, 1.75H), 7.14-7.16 (m, 0.75H), 7.08-7.10 (m, 1.5H), 6.93-6.95 (m, 1.5H), 6.66-6.69 (m, 0.5H), 5.07-5.13 (m, 1H), 4.73 (d, *J* = 13.5 Hz, 0.75H), 4.64 (d, *J* = 13.3 Hz, 0.25H), 4.03-4.09 (m, 1H), 3.97 (s, 2.25H), 3.82 (s, 0.75H), 3.27-3.36 (m, 1H), 3.13-3.19 (m. 0.25H), 2.95-3.01 (m, 0.75H); **^{13}C NMR** (100 MHz, $CDCl_3$): δ (major isomer) 175.2, 168.9, 166.1, 133.4, 133.3, 129.5, 129.2, 128.9, 119.0, 115.8, 94.7, 72.6, 56.3, 45.5, 33.7; **^{13}C NMR** (100 MHz, $CDCl_3$): δ (minor isomer) 176.5, 169.1, 165.3,135.2, 132.5, 129.5, 129.1, 128.4, 120.0, 114.6, 96.6, 70.3, 56.1, 47.1, 33.2; **HRMS** (ESI) m/z calculated for $C_{19}H_{17}NO_6S$ $[M+Na]^+$: 410.0669, found 410.0686.

***Cis*-4-(3-bromophenyl)-10-phenyl-1,7-dioxa-2-thia-2,2-dioxide-3-azaspiro**



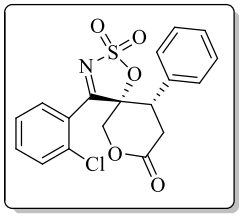
[4.5]dec-3-en-8-one (5da): white solid; **mp** 128-130 °C; **IR** (KBr): ν 2958, 2924, 2855, 1751, 1589, 1555, 1456, 1381, 1204, 1053 cm^{-1}; **^{1}H NMR** (400 MHz, $CDCl_3$): δ (major isomer) 8.19-8.20 (m, 1H), 7.90-7.96 (m, 2H), 7.50-7.54 (m, 1H), 7.26-7.31 (m, 3H), 6.89-6.91 (m, 2H), 5.09 (d, *J* = 13.6 Hz, 1H), 4.75 (d, *J* = 13.5 Hz, 1H), 3.95 (dd, *J* = 4, 13.6 Hz, 1H), 3.28-3.36 (m, 1H), 2.99-3.04 (m, 1H); **^{13}C NMR** (100 MHz, $CDCl_3$): δ (major isomer) 175.4, 168.5, 138.9, 133.4, 132.1, 131.6, 129.8, 129.4, 128.9, 128.8, 128.6, 124.6, 95.0, 71.9, 45.2, 33.7.

***Trans*-4-(3-bromophenyl)-10-phenyl-1,7-dioxa-2-thia-2,2-dioxide-3-azaspiro**



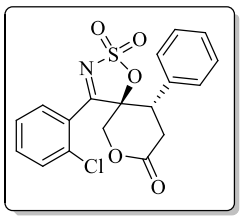
[4.5]dec-3-en-8-one (6da): white solid; **mp**: 122-124 °C; **IR** (KBr): ν 2959, 2924, 2854, 1736, 1590, 1554, 1456, 1376, 1201, 1080 cm^{-1}; **^{1}H NMR** (400 MHz, $CDCl_3$): δ (minor isomer) 7.57-7.60 (m, 1H), 7.33-7.34 (m, 2H), 7.10-7.21 (m, 4H), 6.99-7.01 (m, 2H), 5.12 (d, *J* = 13.3 Hz, 1H), 4.70 (d, 13.6 Hz, 1H), 4.05-4.09 (m, 1H), 3.28-3.35 (m, 1H), 3.07-3.13 (m, 1H).

***Cis*-4-(2-chlorophenyl)-10-phenyl-1,7-dioxa-2-thia-2,2-dioxide-3-azaspiro**



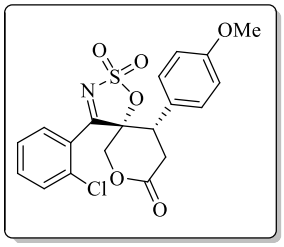
[4.5]dec-3-en-8-one (5ea): white solid; **mp**: 130-132°C; **IR** (KBr): ν 2959, 2926, 2857, 2362, 2338, 1753, 1621, 1457, 1385, 1206, 1156, 1123, 1085, 1053 cm^{-1}; **^{1}H NMR** (400 MHz, $CDCl_3$): δ (major isomer) 7.52-7.58 (m, 2H), 7.33-7.42 (m, 4H), 7.19-7.21 (m, 2H), 7.00-7.02 (m, 1H), 4.90 (d, *J* = 13.08 Hz, 1H), 4.79 (d, *J* = 13.08 Hz, 1H), 3.62 (dd, *J* = 5.24, 13.04 Hz, 1H), 3.06-3.14 (m, 1H), 2.91-2.97 (m, 1H); **^{13}C NMR** (100 MHz, $CDCl_3$): δ (major isomer) 177.0, 167.1, 134.3, 133.9, 133.8, 132.0, 129.9, 129.8, 129.4, 128.6, 128.6, 127.5, 96.0, 72.2, 43.9, 35.7; **HRMS** (ESI) m/z calculated for $C_{18}H_{14}ClNO_5S[M+Na]^+$: 414.0173, found 414.0177.

***Trans*-4-(2-chlorophenyl)-10-phenyl-1,7-dioxa-2-thia-3-azaspiro[4.5]dec-3-**



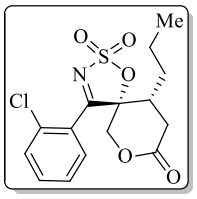
en-8-one 2,2-dioxide (6ea): white solid; **mp** 125-127°C; **IR** (KBr): ν 2960, 2923, 2853, 1769, 1637, 1593, 1561, 1492, 1448, 1377, 1277 cm^{-1}; **^{1}H NMR** (400 MHz, $CDCl_3$): δ (minor isomer) 7.34-7.37 (m, 1H), 7.26-7.30 (m, 1H), 7.13-7.18 (m, 3H), 7.07-7.10 (m, 2H), 7.00-7.04 (m, 1H), 6.57-6.59 (m, 1H), 5.24 (d, *J* = 13.04 Hz, 1H), 4.84 (dd, *J* = 1.48, 12.8 Hz, 1H), 3.87-3.90 (m, 1H), 3.27-3.33 (m, 1H), 2.77-2.83 (m, 1H); **HRMS** (ESI) m/z calculated for $C_{18}H_{14}ClNO_5S$ $[M+Na]^+$: 414.0173, found 414.0177.

***Cis*-4-(2-chlorophenyl)-10-(4-methoxyphenyl)-1,7-dioxa-2-thia-3-azaspiro**



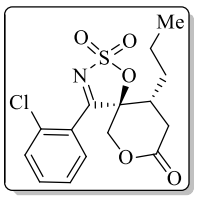
[4.5]dec-3-en-8-one 2,2-dioxide (5ed): white solid; **mp**: 126-128 °C; **IR** (KBr): ν 2960, 2924, 1753, 1610, 1563, 1514, 1468, 1378, 1304, 1255 cm^{-1}; **^{1}H NMR** (400 MHz, $CDCl_3$): δ 7.37-7.39 (m, 1H), 7.29-7.33 (m, 1H), 7.04-7.09 (m, 1H), 6.97-7.00 (m, 2H), 6.63-6.66 (m, 3H), 5.21 (d, *J* = 13.0 Hz, 1H), 4.81 (d, *J* = 13.0 Hz, 1H), 3.80-3.84 (m, 1H), 3.72 (s, 3H), 3.23-3.29 (m, 1H), 2.73-2.79 (m, 1H); **^{13}C NMR** (100 MHz, $CDCl_3$): δ 177.0, 167.3, 160.2, 133.3, 133.0, 131.5, 129.3, 128.4, 126.9, 114.9, 96.8, 69.5, 55.7, 45.6, 34.5; **HRMS** (ESI) m/z calculated for $C_{19}H_{16}ClNO_6S[M+Na]^+$: 444.0279, found 444.0546.

***Cis*-4-(2-chlorophenyl)-10-propyl-1,7-dioxa-2-thia-2,2-dioxide-3-azaspiro**



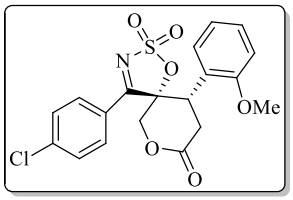
[4.5]dec-3-en-8-one (5ej): white solid; **mp**: 80-82 °C; **IR** (KBr): ν 2963, 2934, 2875, 2361, 2338, 1755, 1624, 1468, 1433, 1385, 1289, 1206 cm^{-1}; **^{1}H NMR** (400 MHz, $CDCl_3$): δ (major isomer) 7.55-7.63 (m, 2H), 7.46-7.50 (1H), 7.32-7.34 (m, 1H), 4.53-4.63 (m, 2H), 2.83-2.92 (m, 1H), 2.44-2.53 (m, 2H), 1.48-1.58 (m, 3H), 1.25-1.31 (m, 1H), 0.97 (t, *J* = 6.8 Hz, 3H); **^{13}C NMR** (100 MHz, $CDCl_3$): δ 177.5, 167.6, 133.8, 133.3, 132.0, 127.9, 127.8, 127.0, 96.8, 70.7, 36.9, 32.1, 31.9, 19.5, 14.1; **HRMS** (ESI) m/z calculated for $C_{15}H_{16}ClNO_5S[M+Na]^+$: 380.0330, found 380.0316.

Trans-**4-(2-chlorophenyl)-10-propyl-1,7-dioxa-2-thia-2,2-dioxide-3-azaspiro**



[4.5]dec-3-en-8-one (6ej): white solid; **mp**: 80-82 °C; **IR** (KBr): ν 2962, 2928, 2873, 1744, 1622, 1466, 1383, 1207 cm^{-1}; **^{1}H NMR** (400 MHz, $CDCl_3$): δ (minor isomer) 7.54-7.62 (m, 2H), 7.44-7.48 (m, 1H), 7.33-7.36 (m, 1H), 4.90 (d, *J* = 12.6 Hz, 1H), 4.64-4.68 (m, 1H), 2.94-3.00 (m, 1H), 2.55-2.61 (m, 1H), 2.30-2.36 (m, 1H), 1.57 (s, 1H), 1.25 (s, 3H), 0.84 (t, *J* = 7.04 Hz, 3H); **HRMS** (ESI) m/z calculated for $C_{15}H_{16}ClNO_5S[M+Na]^+$: 380.0330, found 380.0316.

***Cis*-4-(4-chlorophenyl)-10-(2-methoxyphenyl)-1,7-dioxa-2-thia-3-azaspiro**



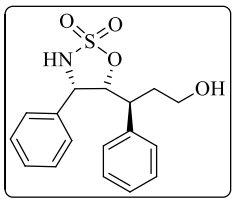
[4.5]dec-3-en-8-one 2,2-dioxide (5fc): white solid; **mp**: 142-144 °C; **IR** (KBr): ν 2967, 2938, 1772, 1587, 1553, 1494, 1463, 1367, 1251 cm^{-1}; **^{1}H NMR** (400 MHz, $CDCl_3$): δ (major isomer) 8.07 (d, *J* = 8.4 Hz, 2H), 7.59 (d, *J* = 8.4 Hz, 2H), 7.26-7.31 (m, 2H), 7.01-7.04 (m, 1H), 6.69-6.72 (m, 1H), 4.98 (d, *J* = 13.6 Hz, 1H), 4.68 (d, *J* = 13.6 Hz, 1H), 4.53-4.57 (m, 1H), 3.27-3.33 (m, 1H), 3.21 (s, 3H), 2.89-2.94 (m, 1H); **^{13}C NMR** (100 MHz, $CDCl_3$): δ (major isomer) 176.5, 169.9, 156.3, 142.3, 131.7, 130.5, 130.2, 129.8, 125.8, 121.6, 120.9, 110.4, 95.0, 71.7, 54.6, 37.9, 33.5; **HRMS** (ESI) m/z calculated for $C_{19}H_{16}ClNO_6S[M+Na]^+$: 444.0279, found 444.0546.

One-pot enantioselective synthesis of 4,10-diphenyl-1,7-dioxa-2-thia-2,2-dioxide-3-azaspiro[4.5]dec-3-en-8-one (Scheme 3.9):

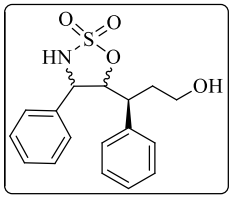
To a stirred solution of 4-phenyl-*5H*-1,2,3-oxathiazole-2,2-dioxides (**1a**, 39.4 mg, 0.2 mmol) and *trans*-cinnamaldehyde (**2a**, 29.1 mg, 0.22 mmol) in CH_2Cl_2 (1.0 mL) under nitrogen atmosphere was added (*S*)-(-)-α,α-diphenyl-2-pyrrolidinemethanol trimethylsilyl ether (6.5 mg, 0.02 mmol) at 4 °C. The progress of the reaction was monitored by TLC. After completion of the reaction, paraformaldehyde (7.8 mg, 0.26 mmol) and DBU (9.12 mg, 0.06 mmol) were added to the above reaction mixture. The stirring was continued for 7 h (monitored by TLC) at ambient temperature. After that PCC (129.3 mg, 0.6

mmol) in CH_2Cl_2 (2.0 mL) was added and the resulting mixture was refluxed at 40 ºC for 8 h. Then the reaction mixture was passed through celite-pad to remove the inorganic materials and washed with ethyl acetate. The combined organic phase was evaporated by rotary evaporator under reduced pressure to give the crude product. The crude product was purified by column chromatography over silica-gel to furnish the pure spiro-δ-lactone **5aa** (44.2 mg). The product was characterized by its corresponding spectroscopic data (IR, ^{1}H and ^{13}C NMR, HRMS). Enantiomers of major isomer **5aa** were separated by HPLC using a Chiralpak AD-H column (20:80 *i*-PrOH/hexane, UV 220 nm, flow rate 1 mL/min) $T_{R(minor)}$ = 11.89 min, $T_{R(major)}$ = 28.11 min. Major isomer was obtained in 91% ee.

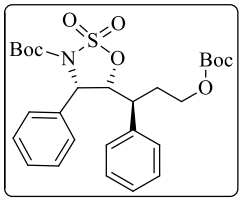
***cis-trans*-3-Hydroxy-1-phenylpropyl-4-phenyl-1,2,3-oxathiazolidine-2,2-dioxide (12): (**39%); **^{1}H NMR** (400 MHz, $CDCl_3$): δ 7.24-7.27 (m, 1H), 7.11-7.19 (m, 5H), 6.89-6.91 (m, 2H), 6.61-6.63 (m, 2H), 5.43 (s, 1H), 5.36 (dd, J_1 = 5.3 Hz, J_2 = 10.8 Hz, 1H), 4.40 (d, J = 4.5 Hz, 1H), 3.26-3.32 (m, 1H), 3.08-3.15 (m, 1H), 2.66-2.71 (m, 1H), 2.05-2.13 (m, 1H), 1.66-1.75 (m, 1H) ; **^{13}C NMR** (100 MHz, $CDCl_3$): δ 137.1, 135.6, 129.3, 129.0, 128.9, 128.8, 128.7, 127.9, 87.9, 63.8, 59.7, 42.7, 37.2; **HRMS** (ESI) m/z calculated for $C_{17}H_{19}NO_4S$ $[M+Na]^+$: 356.0927, found 356.0927.



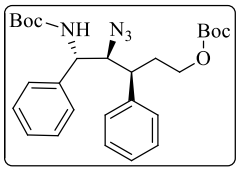
3-Hydroxy-1-phenylpropyl-4-phenyl-1,2,3-oxathiazolidine-2,2-dioxide (13): (54%) ; **^{1}H NMR** (400 MHz, $CDCl_3$): δ 7.41-7.44 (m, 5H), 7.23-7.28 (m, 3H), 7.02-7.04 (m, 2H), 5.36 (dd, J_1 = 5.8 Hz, J_2 = 8.9 Hz, 1H), 5.02-5.04 (m, 1H), 4.70 (d, J = 4.52Hz, 1H), 3.31-3.37 (m, 1H), 3.04-3.11 (m,1H), 2.76-2.82 (m, 1H), 1.73-1.78 (m, 2H); **HRMS** (ESI) m/z calculated for $C_{17}H_{19}NO_4S$ $[M+Na]^+$: 356.0927, found 356.0927.



***tert*-Butyl-5-((tert-butoxycarbonyl)oxy)-1-phenylpropyl)4-phenyl-1,2,3-oxathiazolidine-2,2-dioxide-3-carboxylate (14)**: (85%); **^{1}H NMR** (400 MHz, $CDCl_3$): δ 7.33-7.37 (m, 1H), 7.21-7.29 (m, 5H), 6.98-7.00 (m, 2H), 6.69-6.71 (m, 1H), 5.34 (dd, J_1 =



5.28Hz, J_2 = 11.04 Hz, 1H), 4.81 (s, 1H), 3.74-3.80 (m, 1H), 3.67-3.71 (m, 1H), 2.62-2.68 (m, 1H), 2.30-2.38 (m, 1H), 1.84-1.93 (m, 1H), 1.42 (s, 18H); **^{13}C NMR** (100 MHz, $CDCl_3$): δ 153.5, 148.4, 135.8, 133.8, 129.5, 129.3, 129.0, 128.7, 128.6, 85.8, 85.0, 64.6, 63.9, 42.6, 33.1, 28.2, 28.1; **HRMS** (ESI) m/z calculated for $C_{27}H_{35}NO_8S$ $[M+Na]^+$: 556.1981, found 556.2094.

***tert*-Butyl-(2-azido-5-((tert-butoxycarbonyl)oxy)-1,3-diphenylpentyl) carbamate (15):** 

(90%) ; **^{1}H NMR** (400 MHz, $CDCl_3$): δ 7.30-7.36 (m, 4H), 7.25-7.28 (m, 4H), 7.20-7.22 (m, 2H), 5.16 (brs, 1H), 5.04 (m, 1H), 3.88-3.94 (m, 2H), 3.77-3.83 (m, 1H), 2.91-2.97 (m, 1H), 2.26-2.32 (m, 1H), 2.08-2.17 (m, 1H), 1.46 (s, 9H), 1.43 (s, 9H); **^{13}C NMR** (100 MHz, $CDCl_3$): δ 155.0, 153.3, 140.5, 139.3, 128.8, 128.7, 128.6, 127.7, 127.4, 126.4, 81.8, 79.9, 72.4, 64.5, 55.0, 45.2, 31.5, 28.3, 27.7; **HRMS** (ESI) m/z calculated for $C_{27}H_{36}N_4O_5$ $[M+Na]^+$: 519.2574, found 519.2625.

Table 3.3 Crystal data for compound **5aa**

Compound	**Compound 5aa**
Empirical formula	$C_{18}H_{15}NO_5S$
Molecular weight	357.37
Temperature	150(2) K
Wavelength (Å)	1.5418
Crystal system, space group	monoclinic, P 21/c
a (Å)	13.0861(5)
b (Å)	10.1079(4)
c (Å)	12.7818(4)
α (^{o})	90
β (^{o})	93.908(4)
γ (^{o})	90
Volume (Å^3)	1686.76(11)
Z, Calculated density (mg/m^3)	4,1.407
Absorption coefficient (mm^{-1})	1.966
F(000)	744
Crystal size (mm)	0.33 x 0.26 x 0.21 mm
θ range (deg)	3.39 to 71.97
Limiting indices	-16<=h<=16, -12<=k<=12, -11<=l<=15
Reflections collected / unique	11142 / 3279 [R(int) = 0.0306]
Completeness to θ = 71.97	98.8
Max. and min. transmission	0.6829 and 0.5631
Data / restraints / parameters	0.6829 and 0.5631
Goodness-of-fit on F^2	1.015
Final R indices [I>2sigma(I)]	R1 = 0.0473, wR2 = 0.1328
R indices (all data)	R1 = 0.0619, wR2 = 0.1511
Largest diff. peak and hole (e.A^{-3})	0.375 and -0.412
CCDC	**992922**

Table 3.4 Crystal data for compound **14**

Compound	**Compound 14**
Empirical formula	$C_{27}H_{35}NO_8S$
Molecular weight	533.6337
Temperature	150(2) K
Wavelength (Å)	1.54184 A
Crystal system, space group	Orthorhombic, P n a 21
a (Å)	10.8218(2)
b (Å)	13.6430(2)
c (Å)	19.3609(4)
α (^{o})	90
β (^{o})	90
γ (^{o})	90
Volume (Å^3)	2858.48(9)
Z, Calculated density (mg/m^3)	4,1.240
Absorption coefficient (mm^{-1})	1.403
F(000)	1136
Crystal size (mm)	0.26 x 0.21
θ range (deg)	3.96 to 72.25
Limiting indices	-6<=h<=13, -15<=k<=16, -23<=l<=23
Reflections collected / unique	20258 / 5534 [R(int) = 0.0311]
Completeness to θ = 72.25	
Max. and min. transmission	0.7571 and 0.6546
Data / restraints / parameters	5534 / 1 / 340
Goodness-of-fit on F^2	1.050
Final R indices [I>2sigma(I)]	R1 = 0.0419, wR2 = 0.1110
R indices (all data)	R1 = 0.0434, wR2 = 0.1130
Largest diff. peak and hole (e.A^{-3})	-0.026(15)
CCDC	**C1005799**

3.6 Copies of ^{1}H, ^{13}C NMR spectra and HPLC data of some important compounds described in Chapter 3

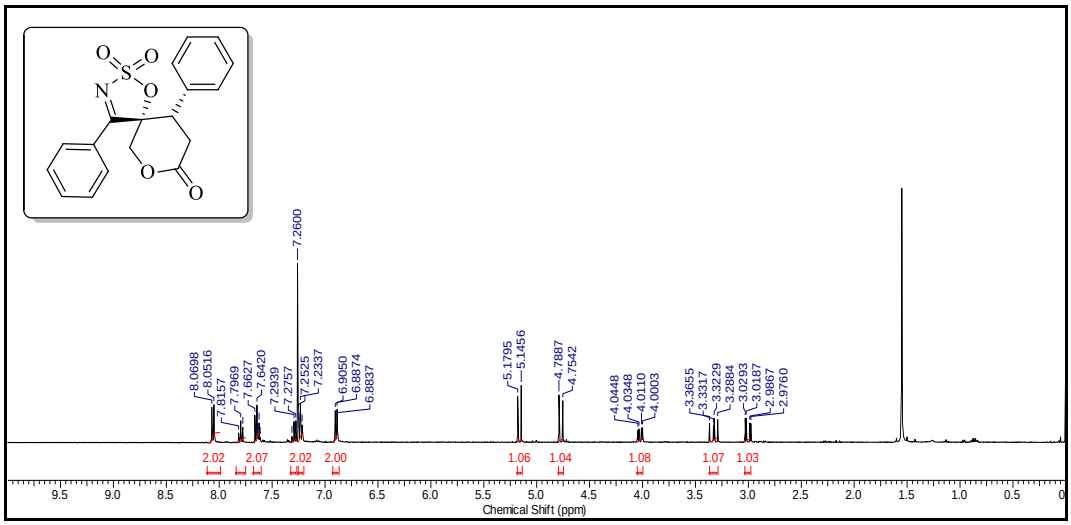


Figure 3.5 400 MHz ^{1}H NMR spectrum of **5aa** in $CDCl_3$

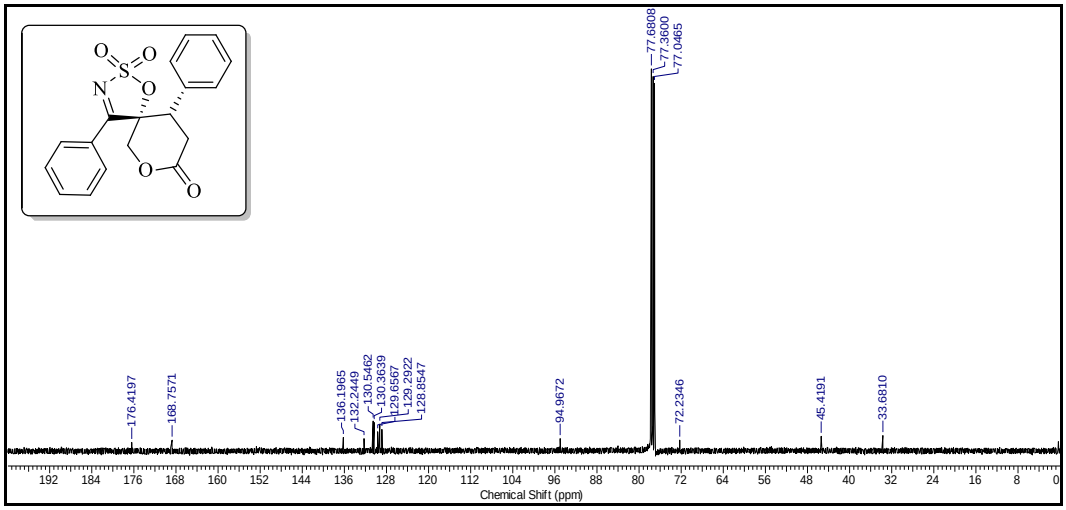


Figure 3.6 100 MHz ^{13}C NMR spectrum of **5aa** in $CDCl_3$

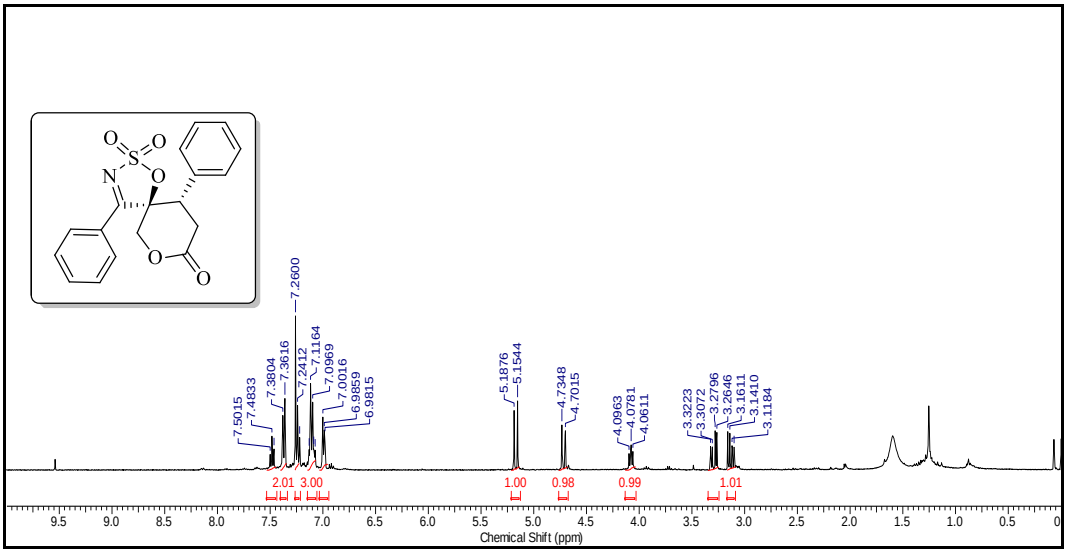


Figure 3.7 400 MHz ^{1}H NMR spectrum of **6aa** in $CDCl_3$

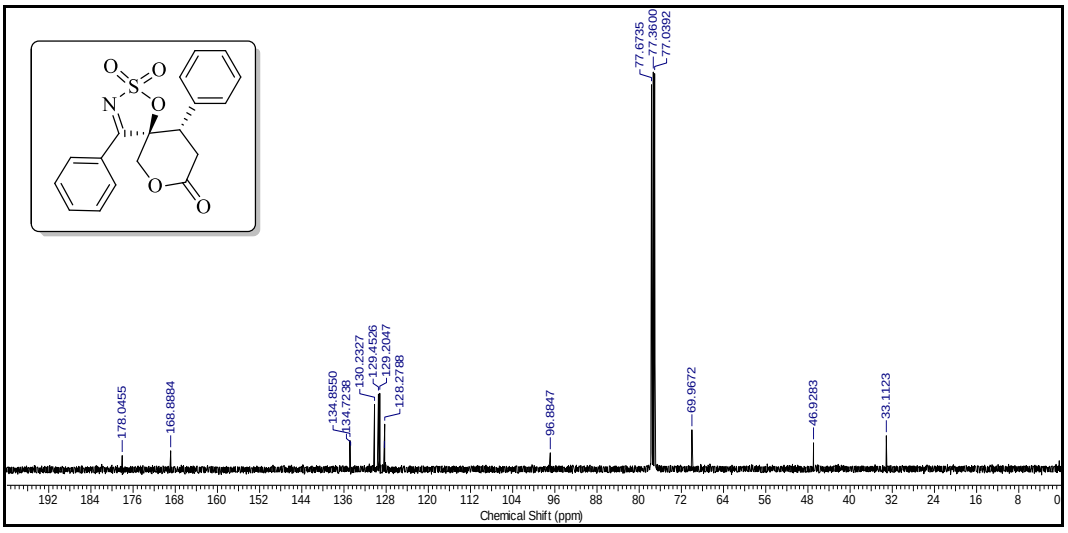


Figure 3.8 100 MHz ^{13}C NMR spectrum of **6aa** in $CDCl_3$

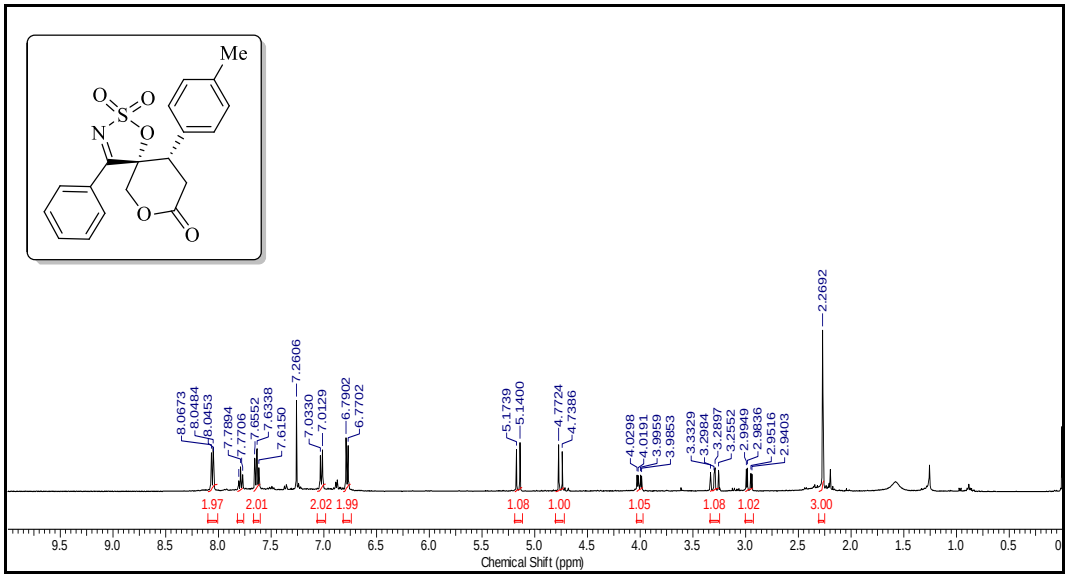


Figure 3.9 400 MHz ^{1}H NMR spectrum of **5ab** in $CDCl_3$

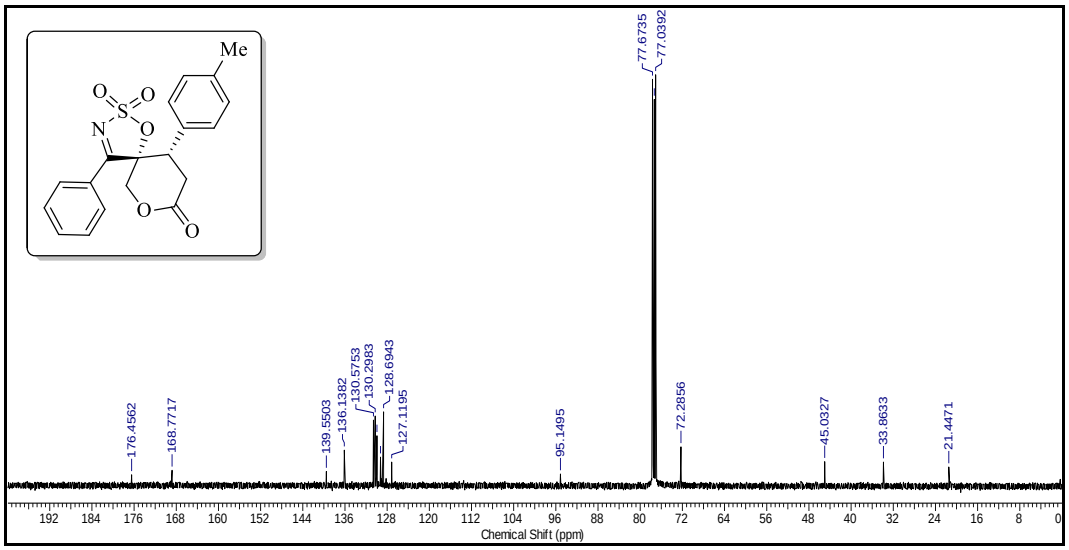


Figure 3.10 100 MHz ^{13}C NMR spectrum of **5ab** in $CDCl_3$

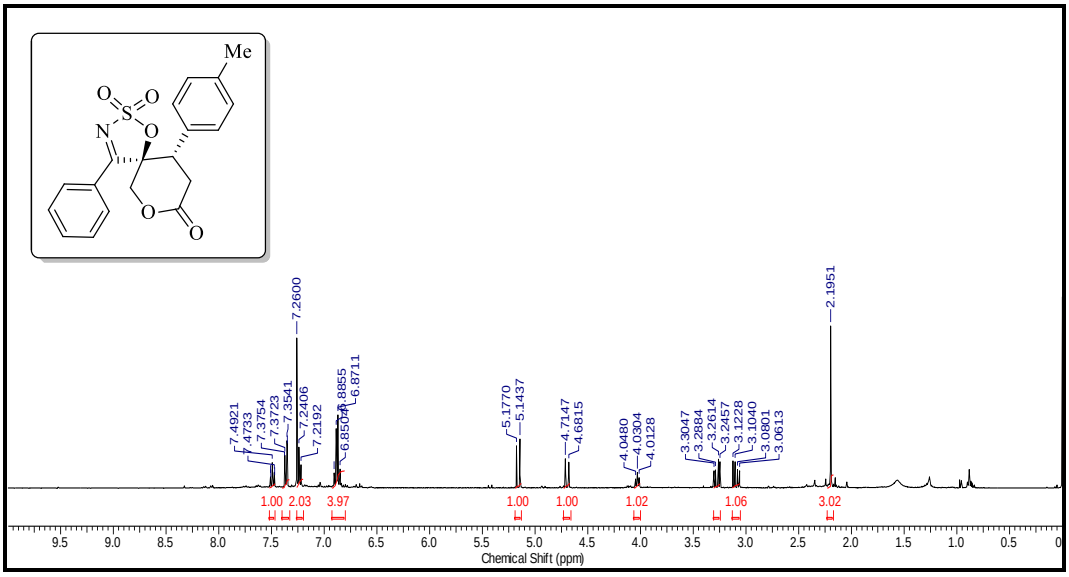


Figure 3.11 400 MHz ^{1}H NMR spectrum of **6ab** in $CDCl_3$

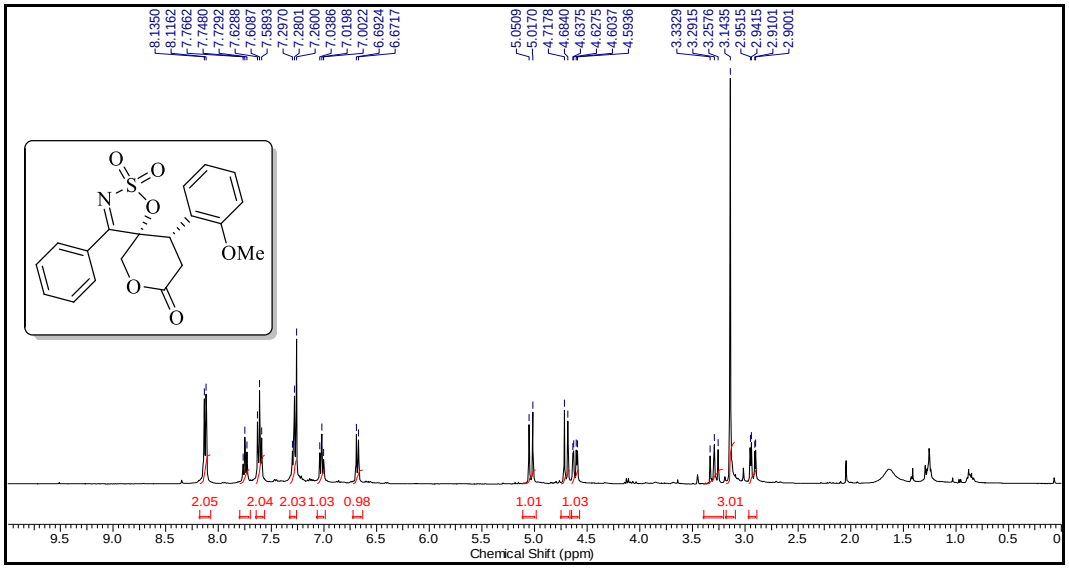


Figure 3.12 400 MHz ^{1}H NMR spectrum of **5ac** in $CDCl_3$

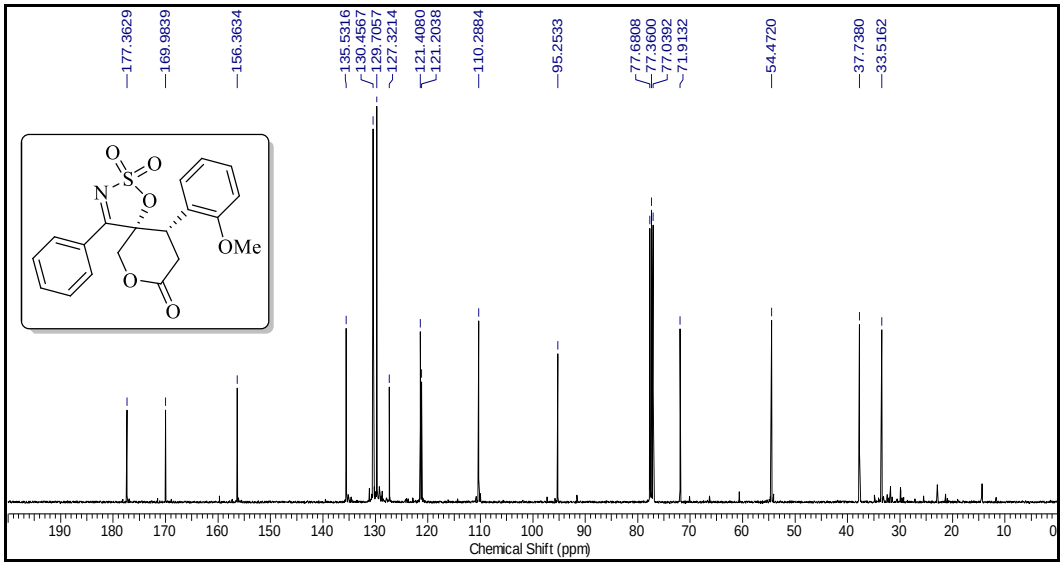


Figure 3.13 100 MHz ^{13}C NMR spectrum of **5ac** in $CDCl_3$

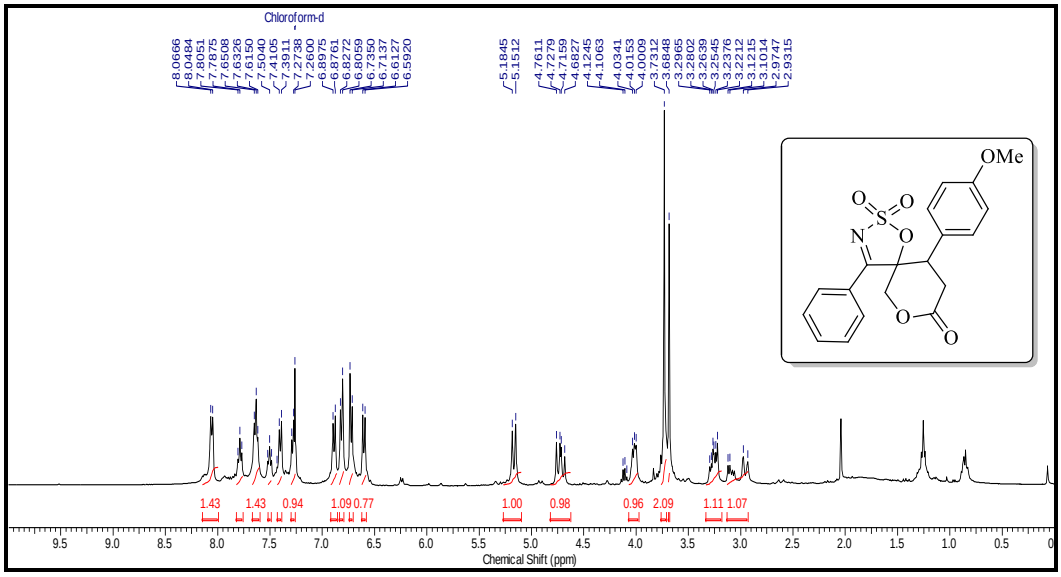


Figure 3.14 400 MHz ^{1}H NMR spectrum of **5ad & 6ad** in $CDCl_3$

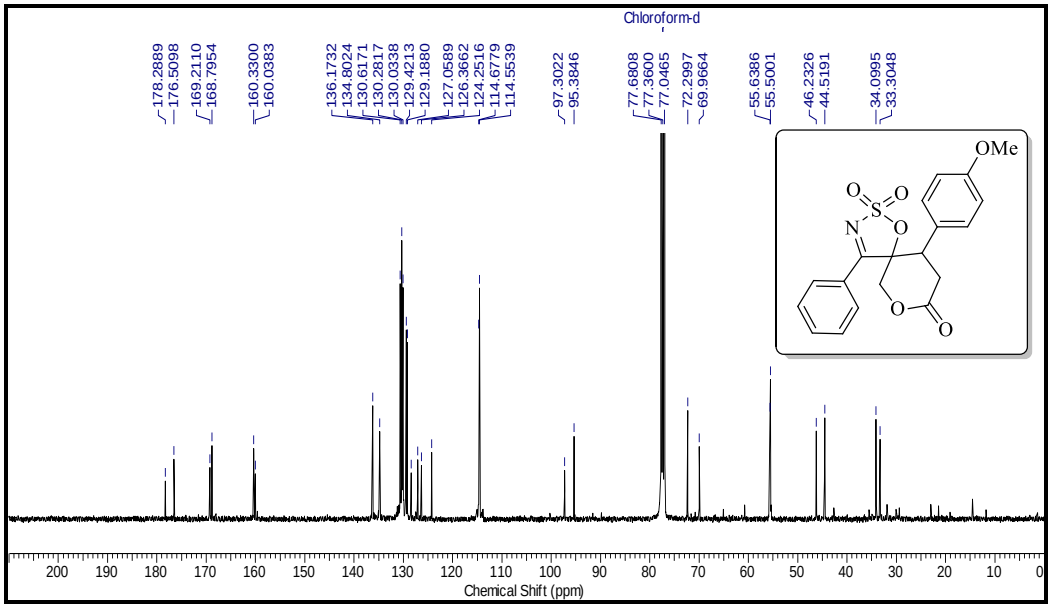


Figure 3.15 100 MHz ^{13}C NMR spectrum of **5ad & 6ad** in $CDCl_3$

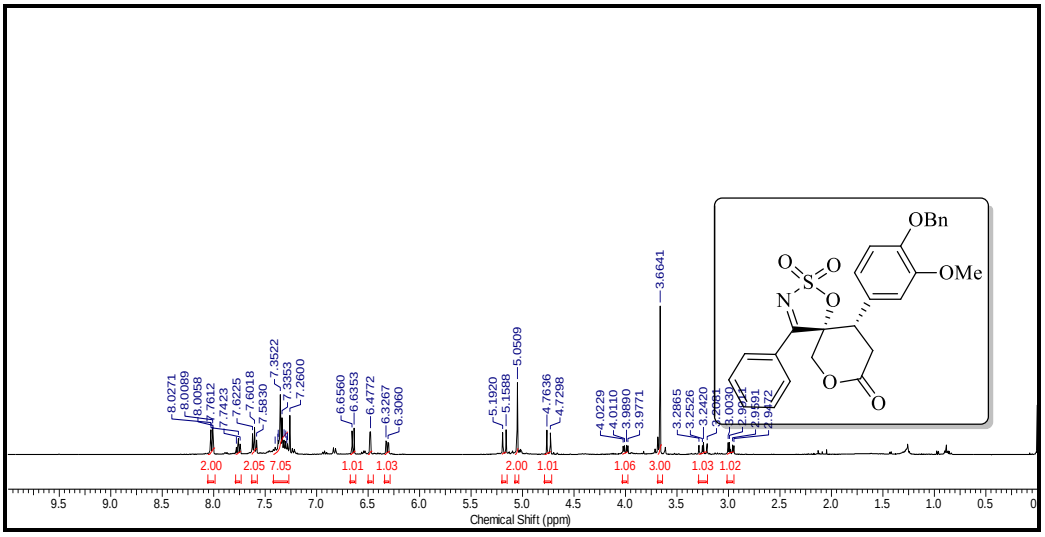


Figure 3.16 400 MHz ^{1}H NMR spectrum of **5ae** in $CDCl_3$

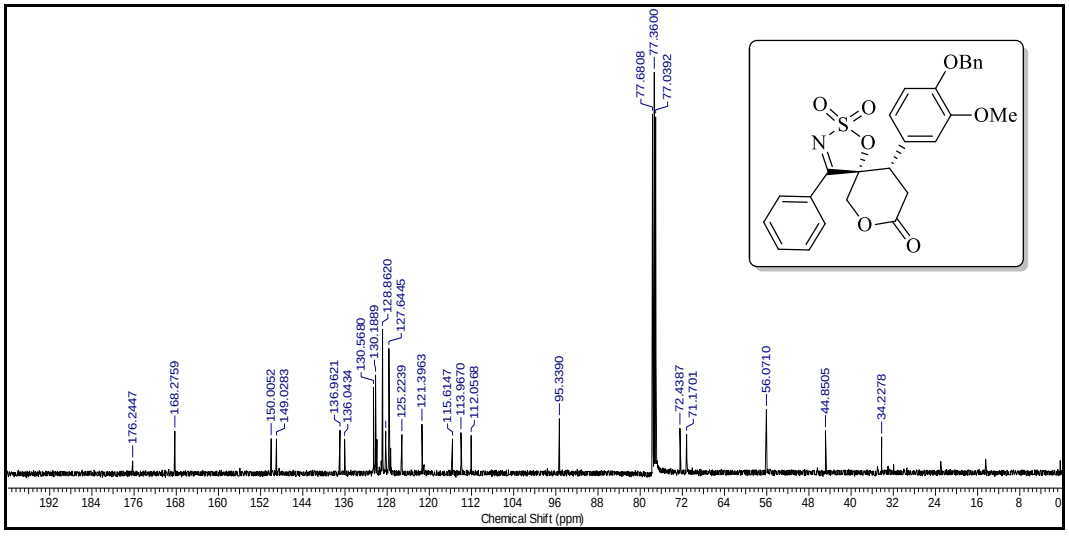


Figure 3.17 100 MHz ^{13}C NMR spectrum of **5ae** in $CDCl_3$

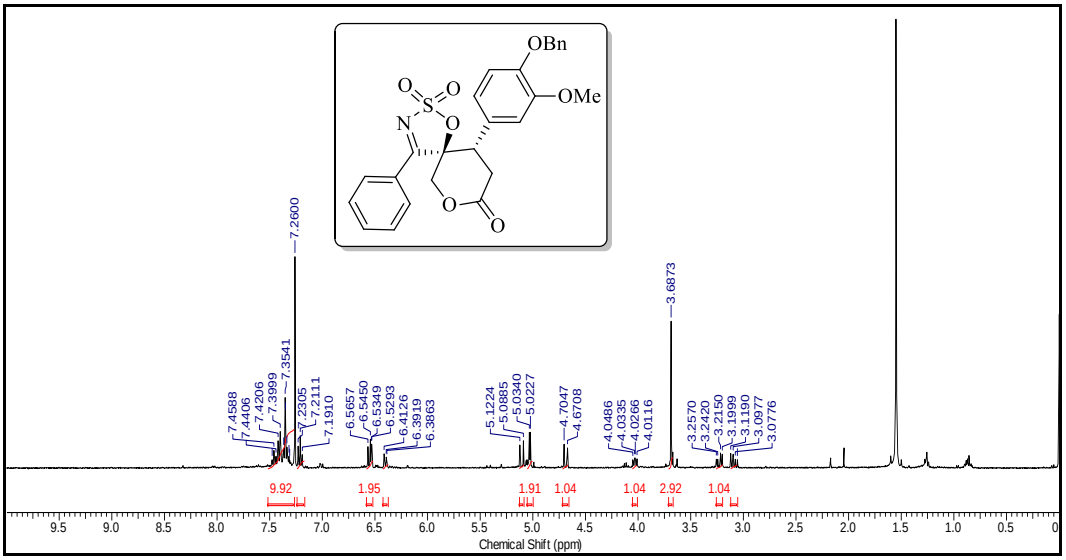


Figure 3.18 400 MHz ^{1}H NMR spectrum of **6ae** in $CDCl_3$

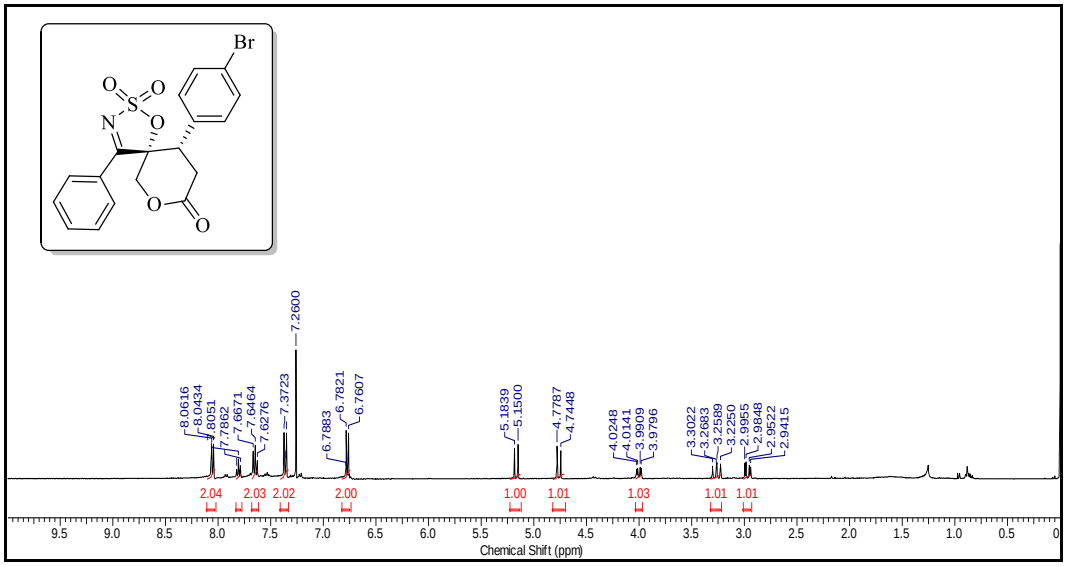


Figure 3.19 400 MHz ^{1}H NMR spectrum of **5af** in $CDCl_3$

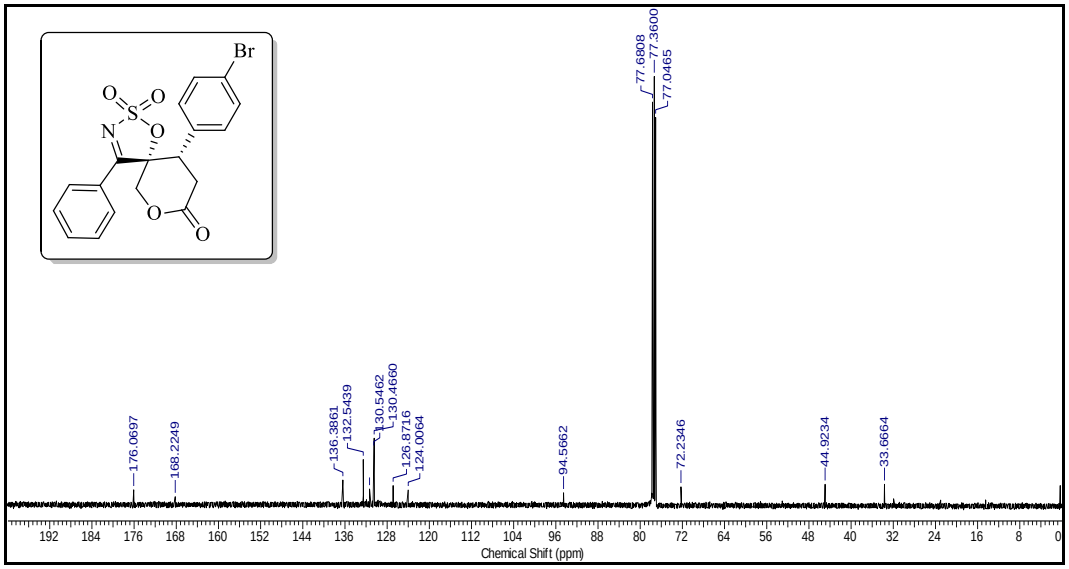


Figure 3.20 100 MHz ^{13}C NMR spectrum of **5af** in $CDCl_3$

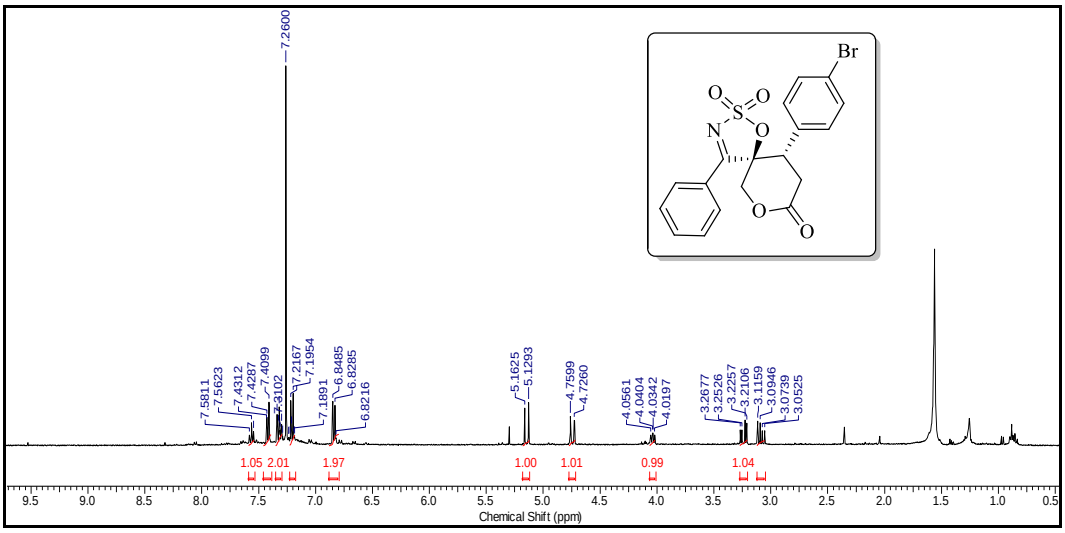


Figure 3.21 400 MHz ^{1}H NMR spectrum of **6af** in $CDCl_3$

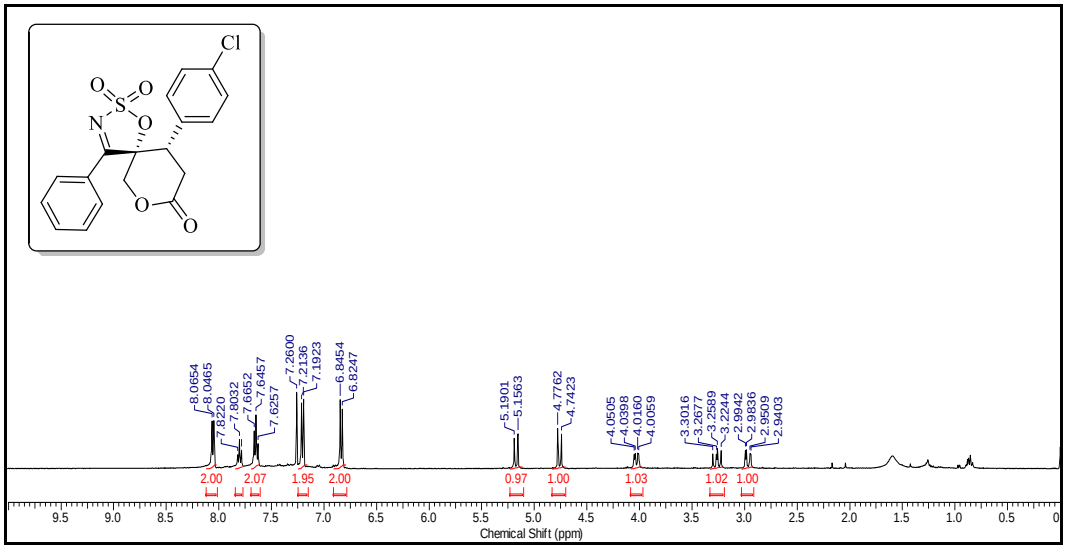


Figure 3.22 400 MHz ^{1}H NMR spectrum of **5ag** in $CDCl_3$

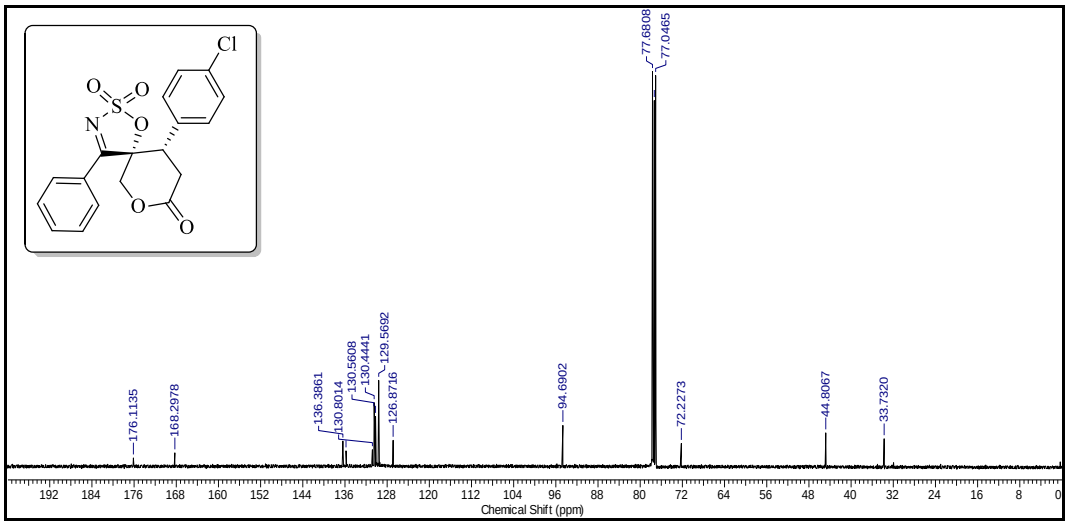


Figure 3.23 100 MHz ^{13}C NMR spectrum of **5ag** in $CDCl_3$

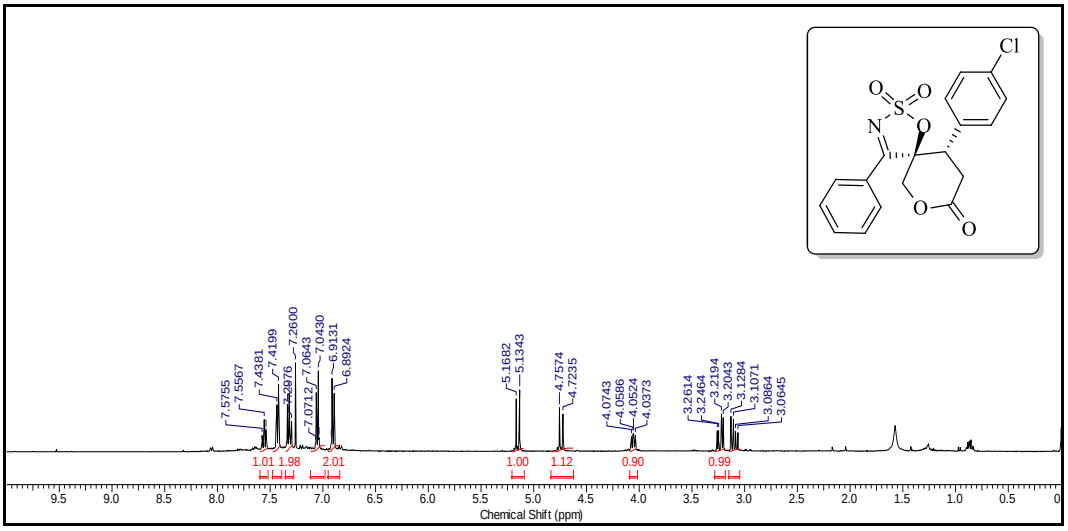


Figure 3.24 400 MHz ^{1}H NMR spectrum of **6ag** in $CDCl_3$

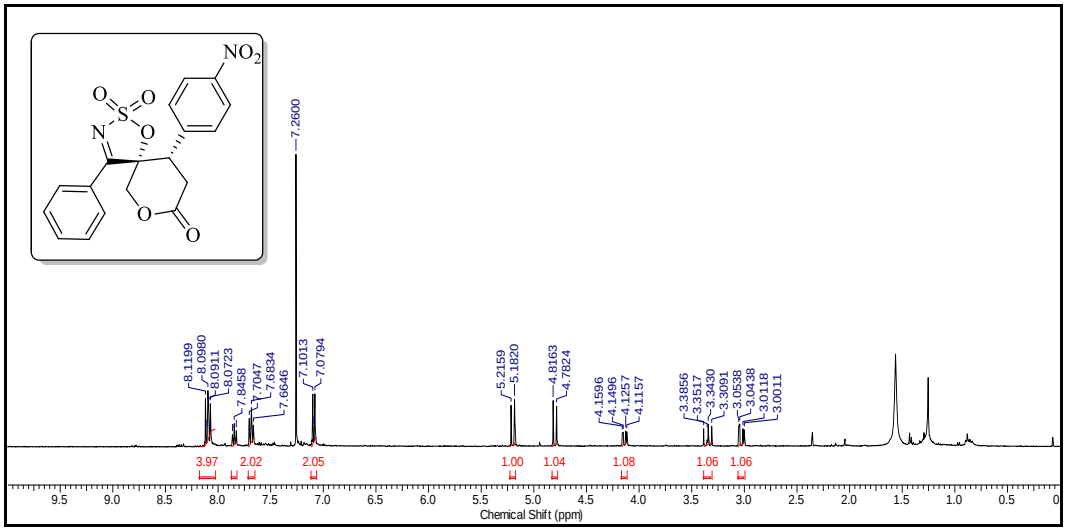


Figure 3.25 400 MHz ^{1}H NMR spectrum of **5ah** in $CDCl_3$

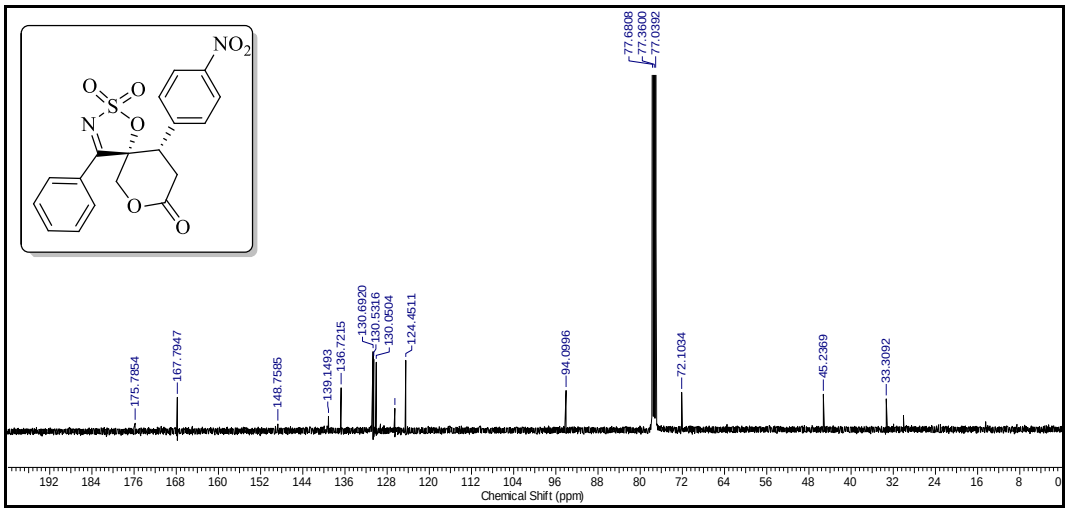


Figure 3.26 100 MHz ^{13}C NMR spectrum of **5ah** in $CDCl_3$

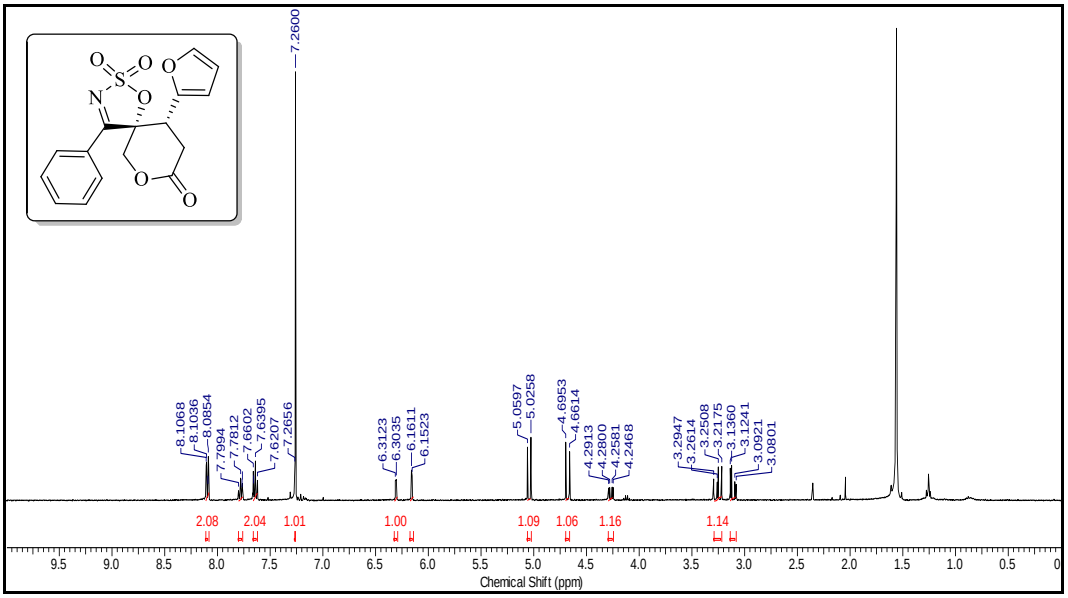


Figure 3.27 400 MHz ^{1}H NMR spectrum of **5ai** in $CDCl_3$

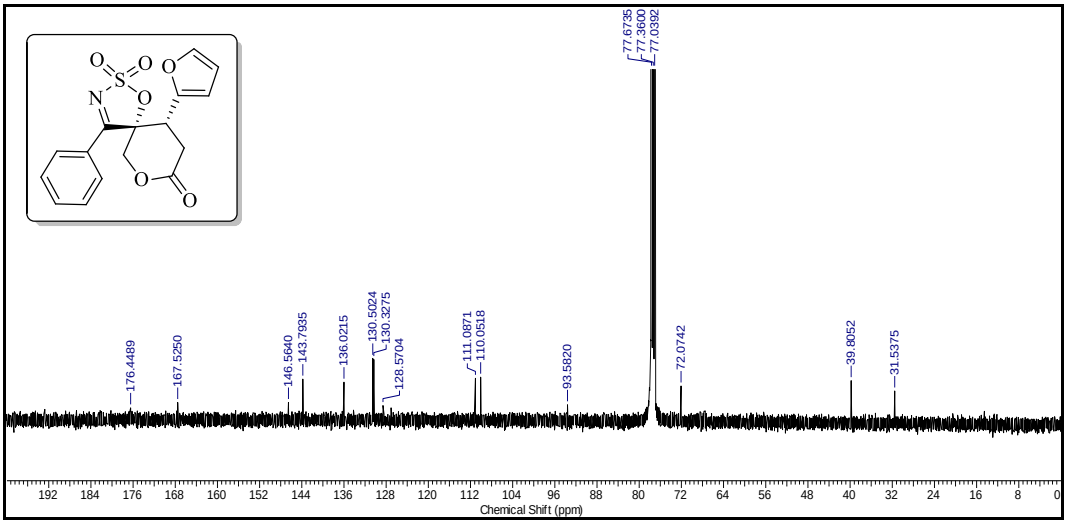


Figure 3.28 100 MHz ^{13}C NMR spectrum of **5ai** in $CDCl_3$

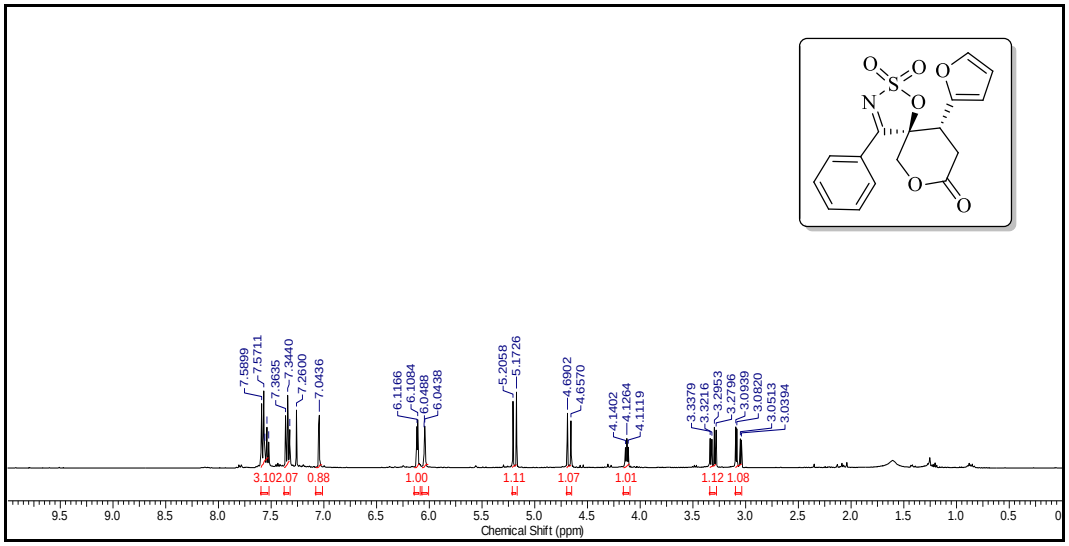


Figure 3.29 400 MHz ^{1}H NMR spectrum of **6ai** in $CDCl_3$

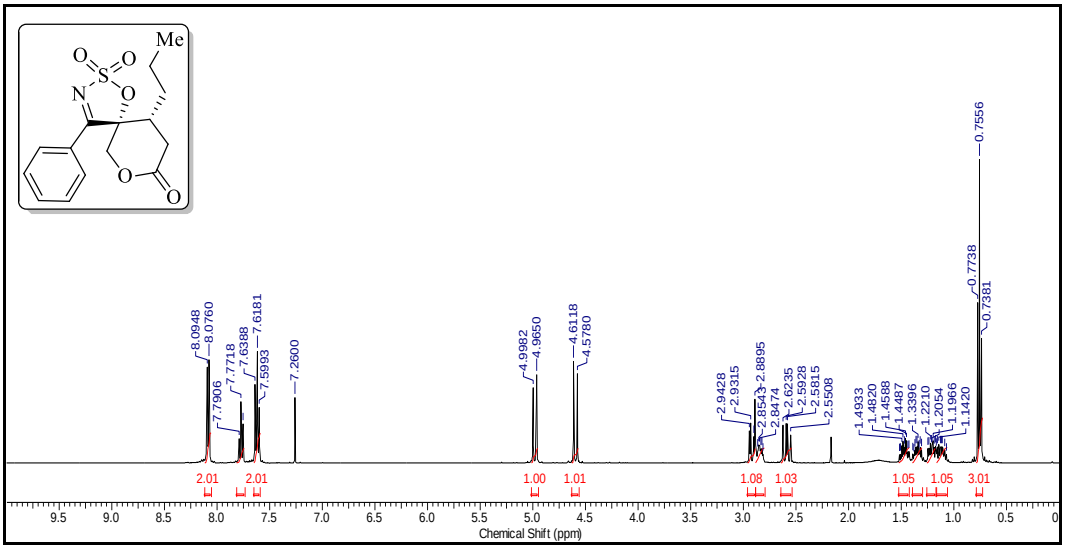


Figure 3.30 400 MHz ^{1}H NMR spectrum of **5aj** in $CDCl_3$

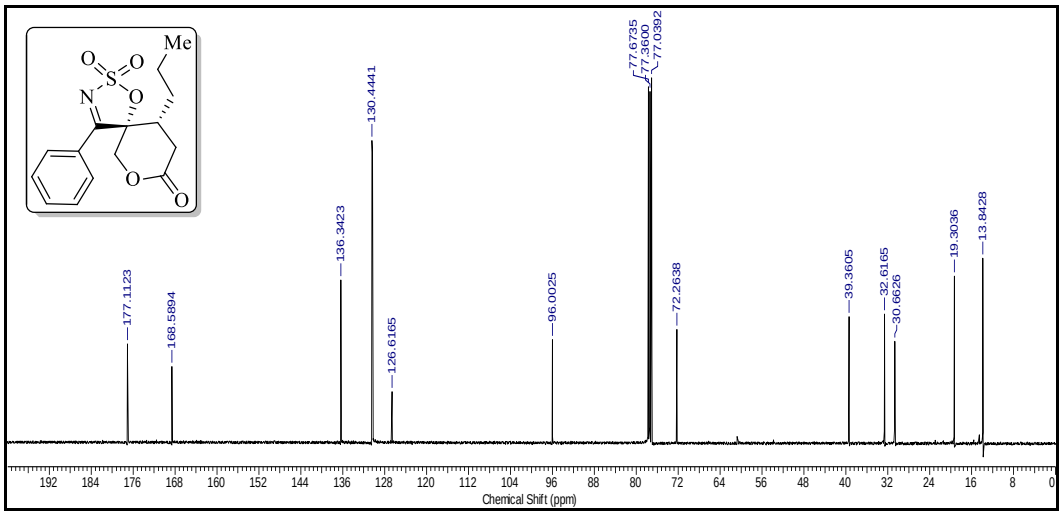


Figure 3.31 100 MHz ^{13}C NMR spectrum of **5aj** in $CDCl_3$

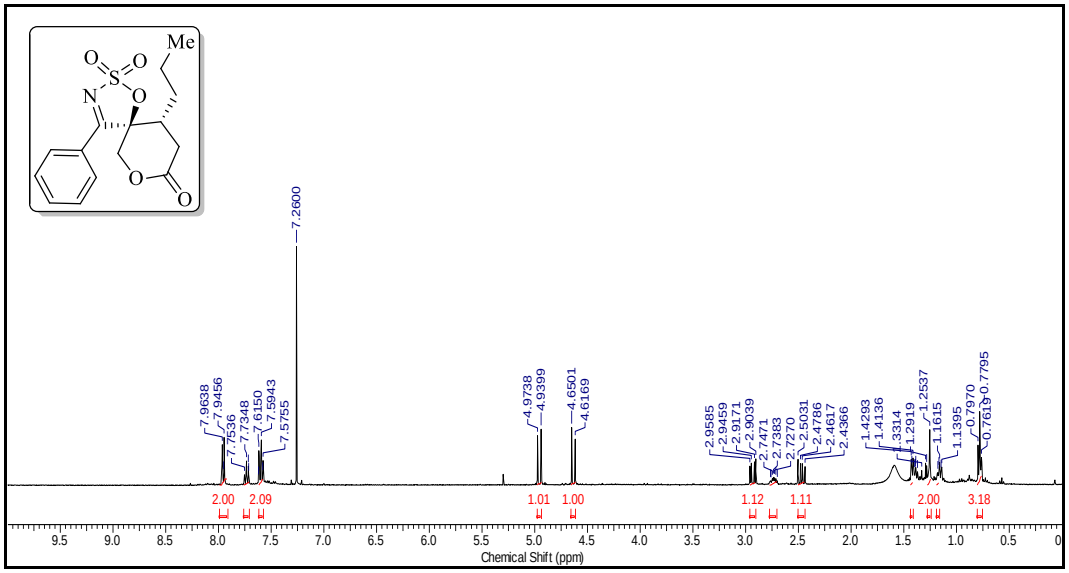


Figure 3.32 400 MHz ^{1}H NMR spectrum of **6aj** in $CDCl_3$

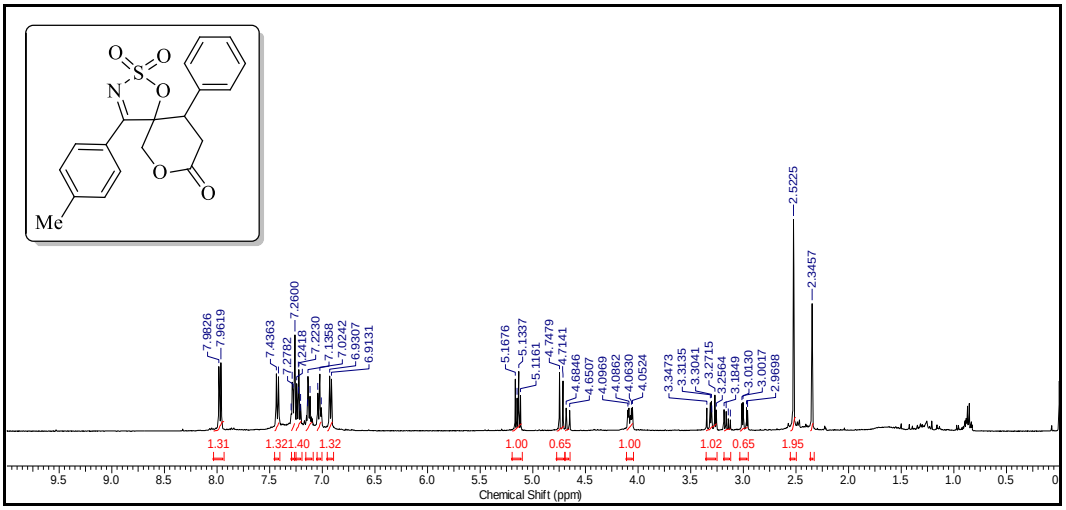


Figure 3.33 400 MHz ^{1}H NMR spectrum of **5ba & 6ba** in $CDCl_3$

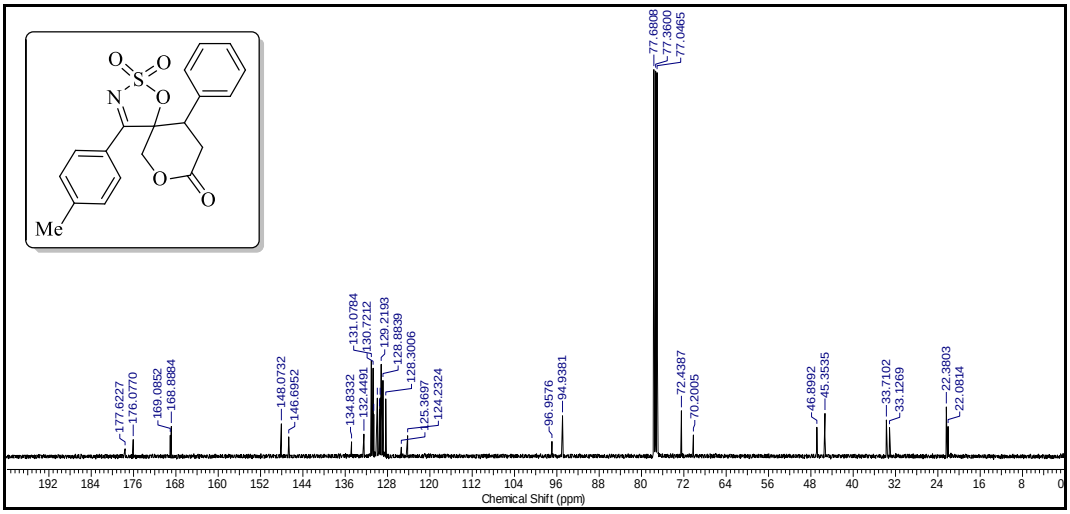


Figure 3.34 100 MHz ^{13}C NMR spectrum of **5ba & 6ba** in $CDCl_3$

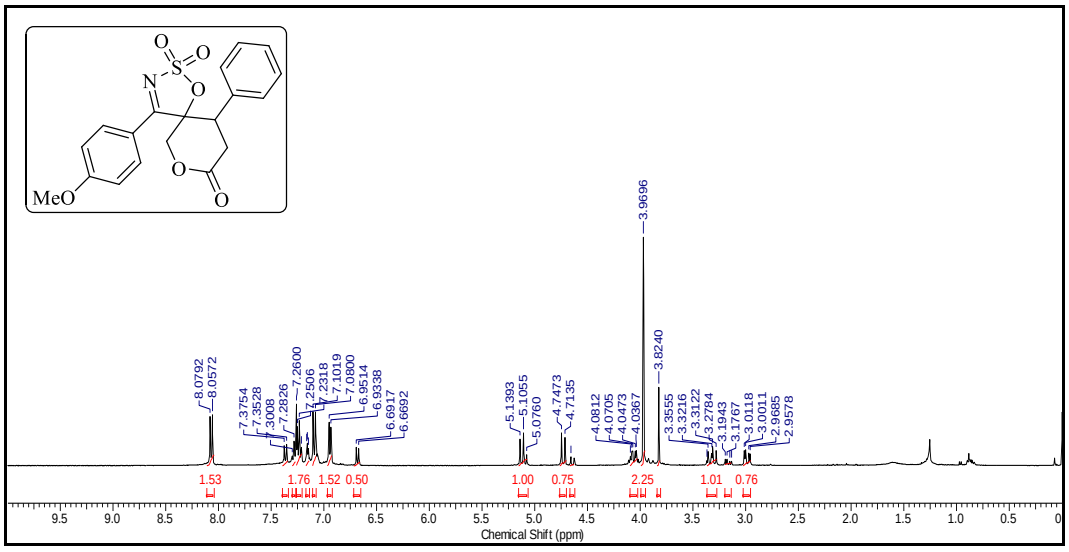


Figure 3.35 400 MHz ^{1}H NMR spectrum of **5ca & 6ca** in $CDCl_3$

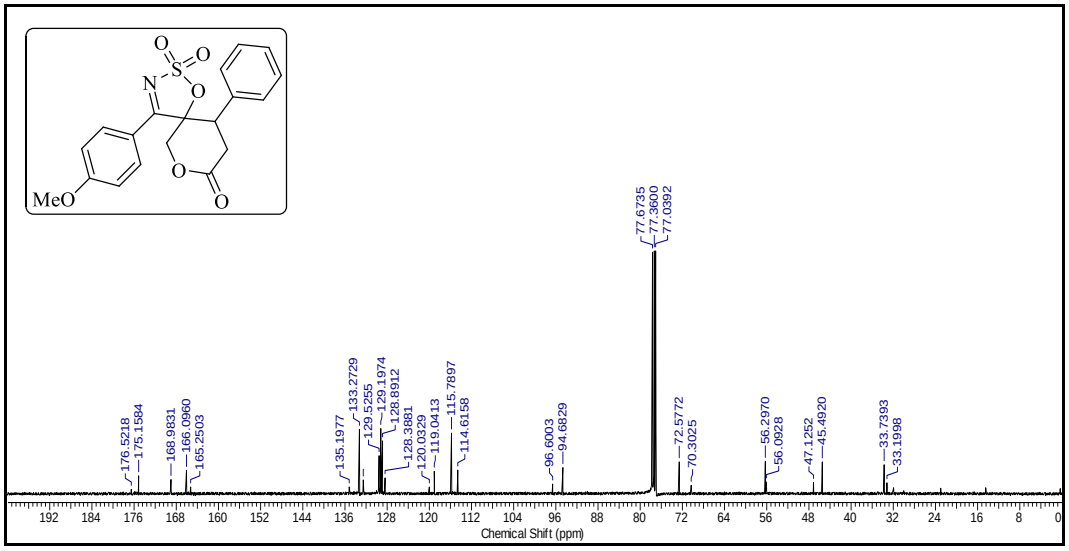


Figure 3.36 100 MHz ^{13}C NMR spectrum of **5ca & 6ca** in $CDCl_3$

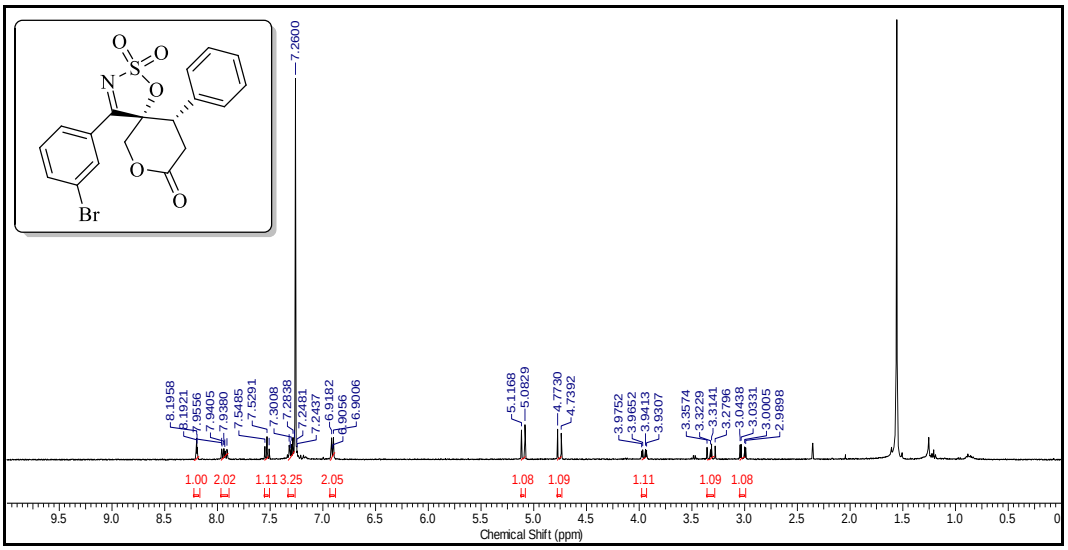


Figure 3.37 400 MHz ^{1}H NMR spectrum of **5da** in $CDCl_3$

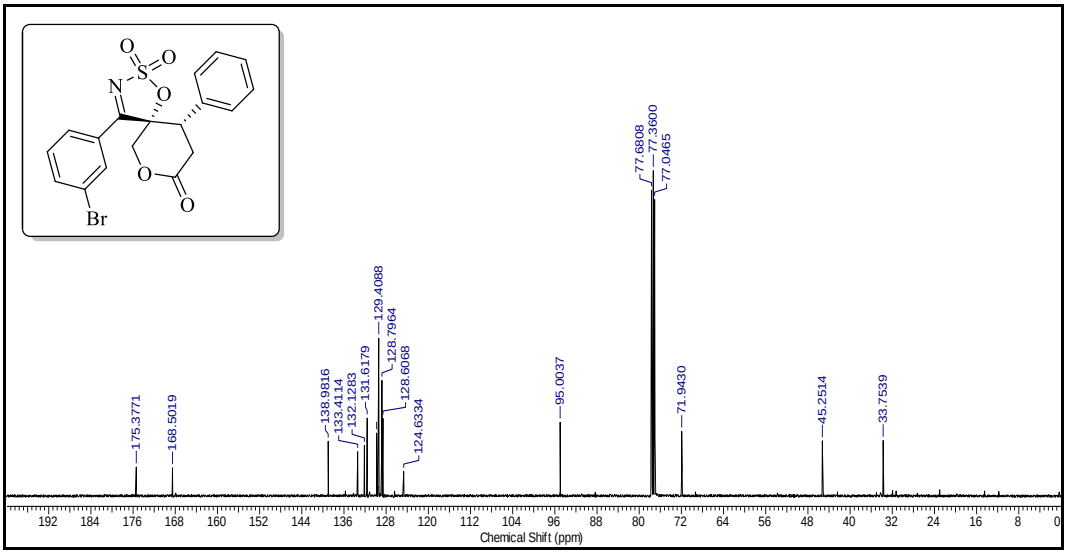


Figure 3.38 100 MHz ^{13}C NMR spectrum of **5da** in $CDCl_3$

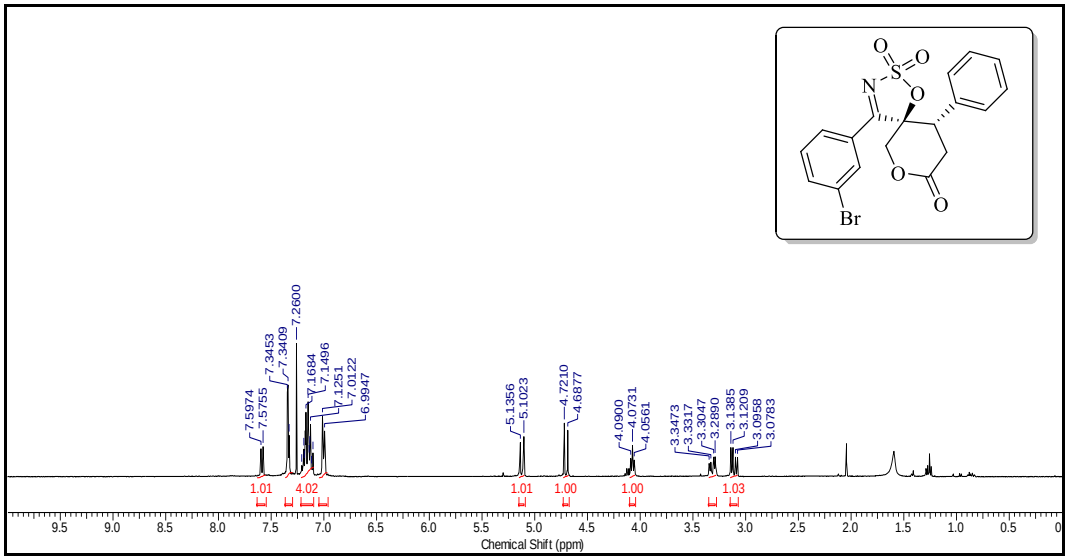


Figure 3.39 400 MHz ^{1}H NMR spectrum of **6da** in $CDCl_3$

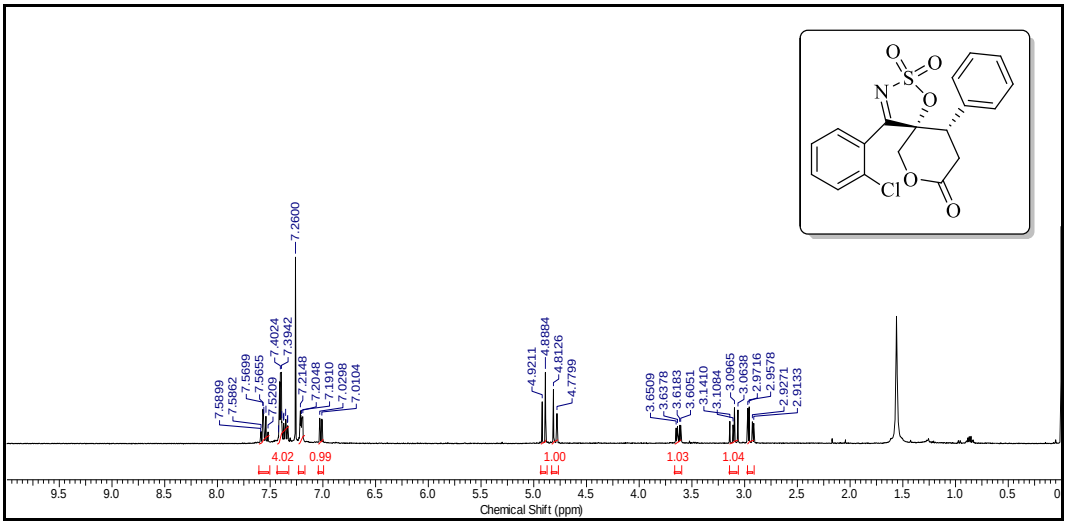


Figure 3.40 400 MHz ^{1}H NMR spectrum of **5ea** in $CDCl_3$

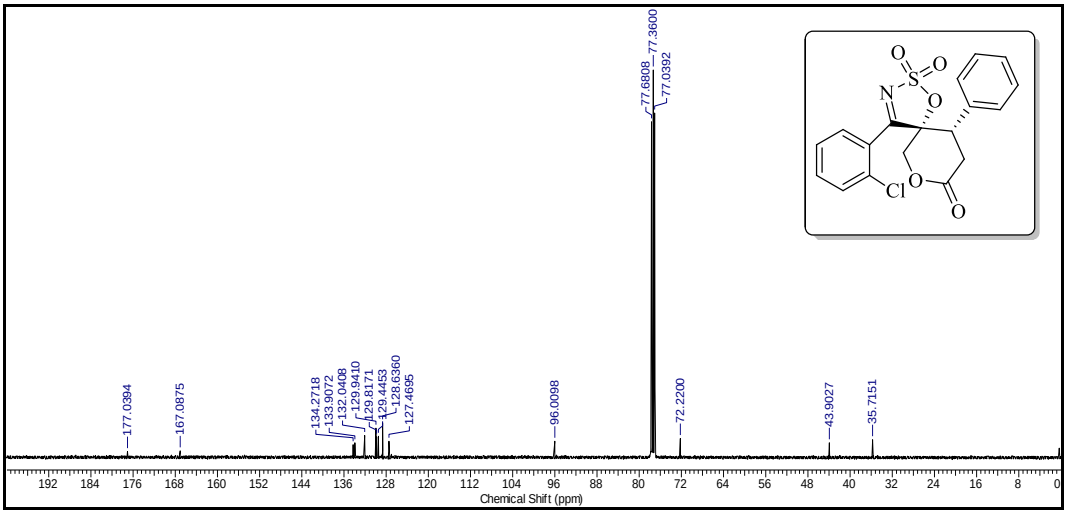


Figure 3.41 100 MHz ^{13}C NMR spectrum of **5ea** in $CDCl_3$

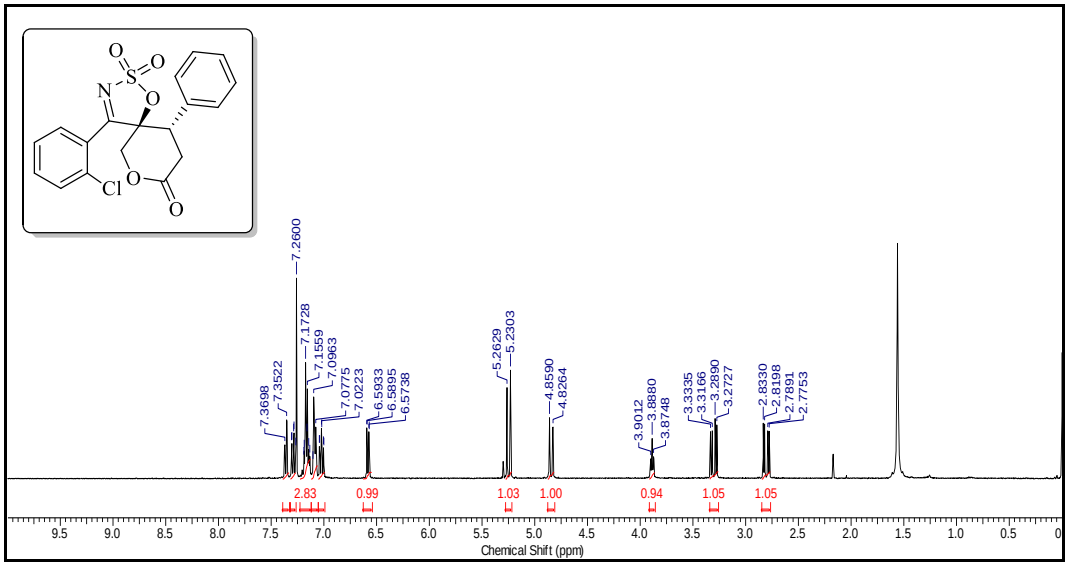


Figure 3.42 400 MHz ^{1}H NMR spectrum of **6ea** in $CDCl_3$

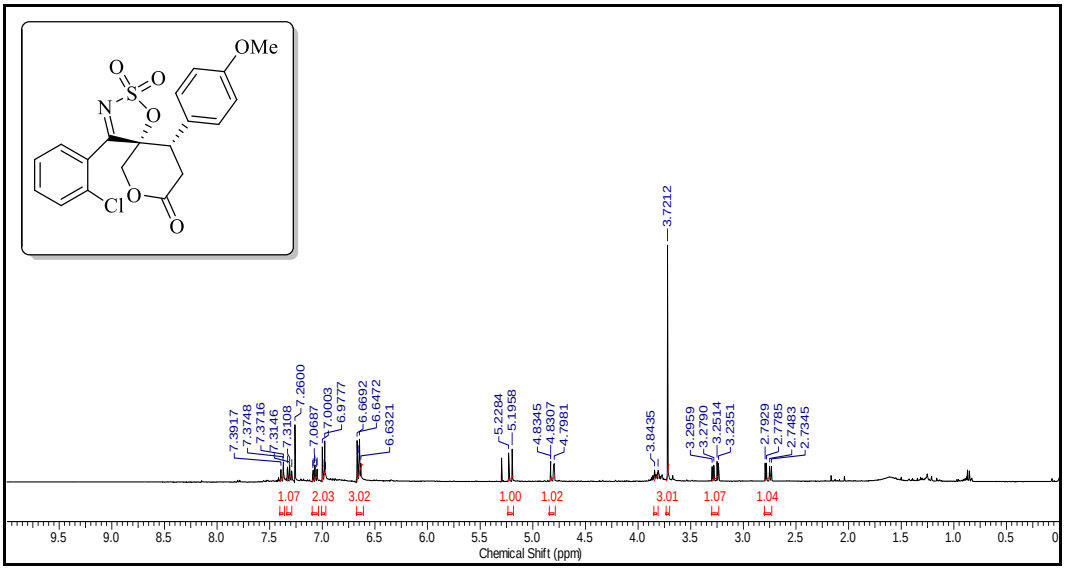


Figure 3.43 400 MHz ^{1}H NMR spectrum of **5ed** in $CDCl_3$

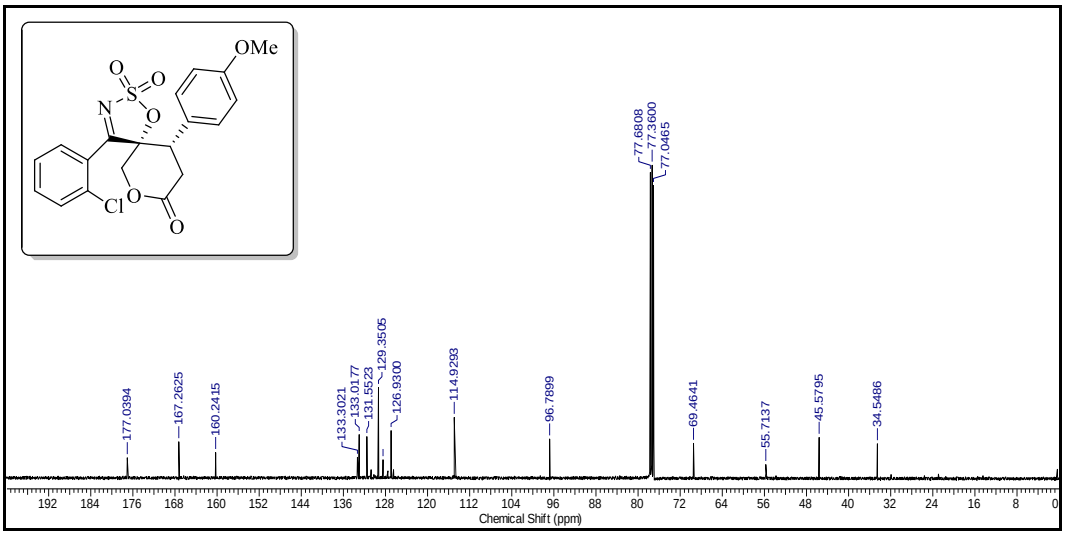


Figure 3.44 100 MHz ^{13}C NMR spectrum of **5ed** in $CDCl_3$

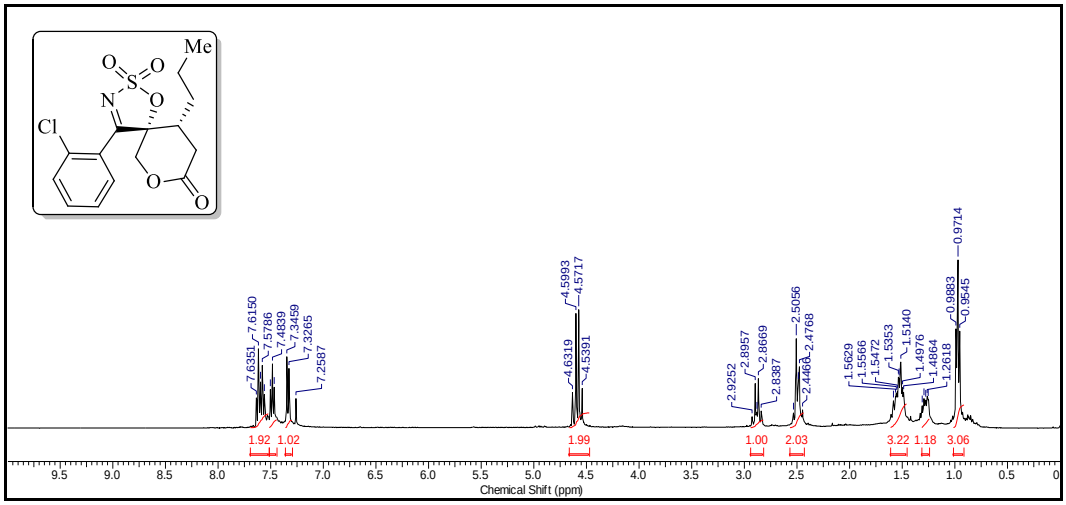


Figure 3.45 400 MHz ^{1}H NMR spectrum of **5ej** in $CDCl_3$

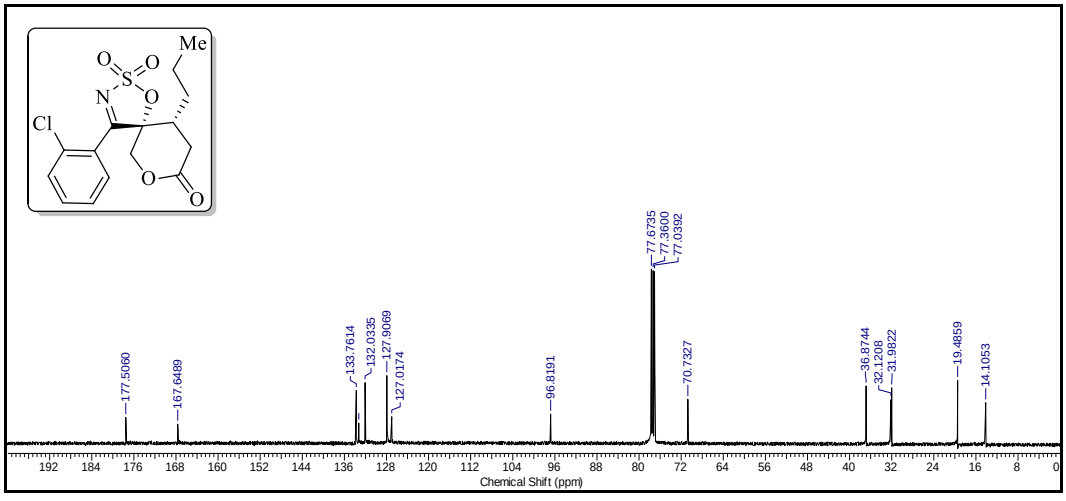


Figure 3.46 100 MHz ^{13}C NMR spectrum of **5ej** in $CDCl_3$

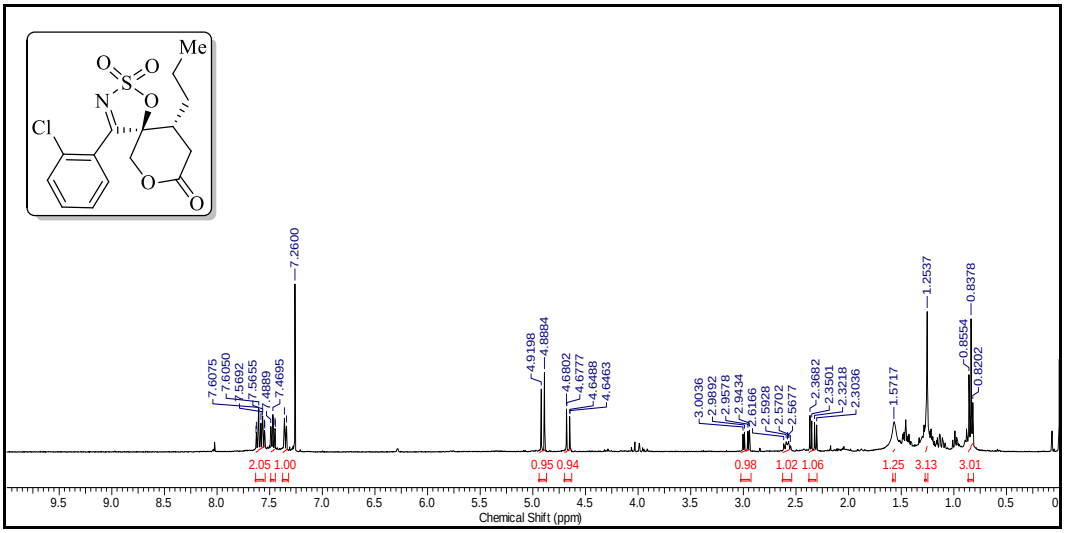


Figure 3.47 400 MHz ^{1}H NMR spectrum of **6ej** in $CDCl_3$

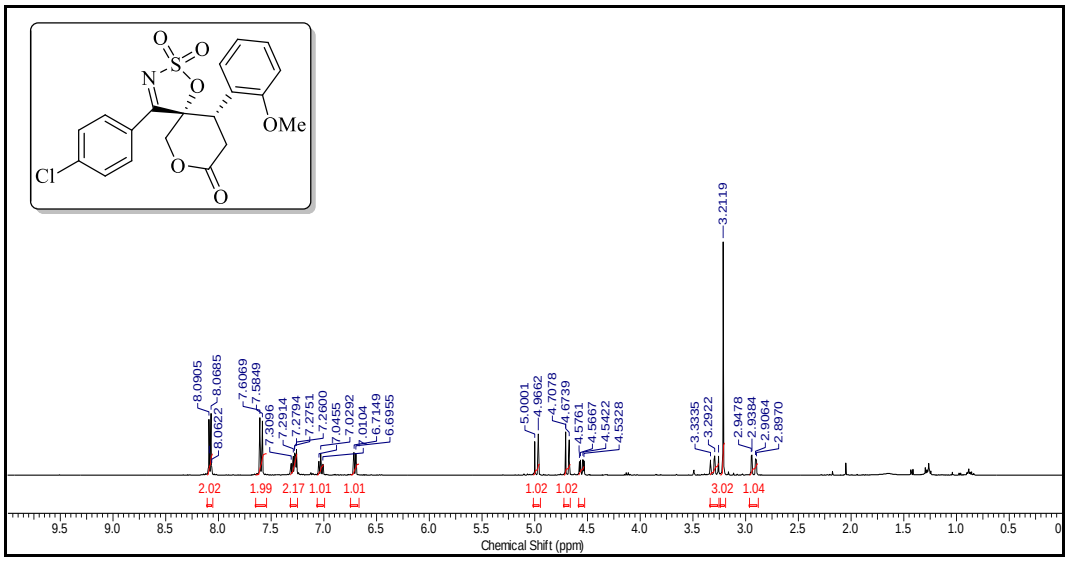


Figure 3.48 400 MHz ^{1}H NMR spectrum of **5fc** in $CDCl_3$

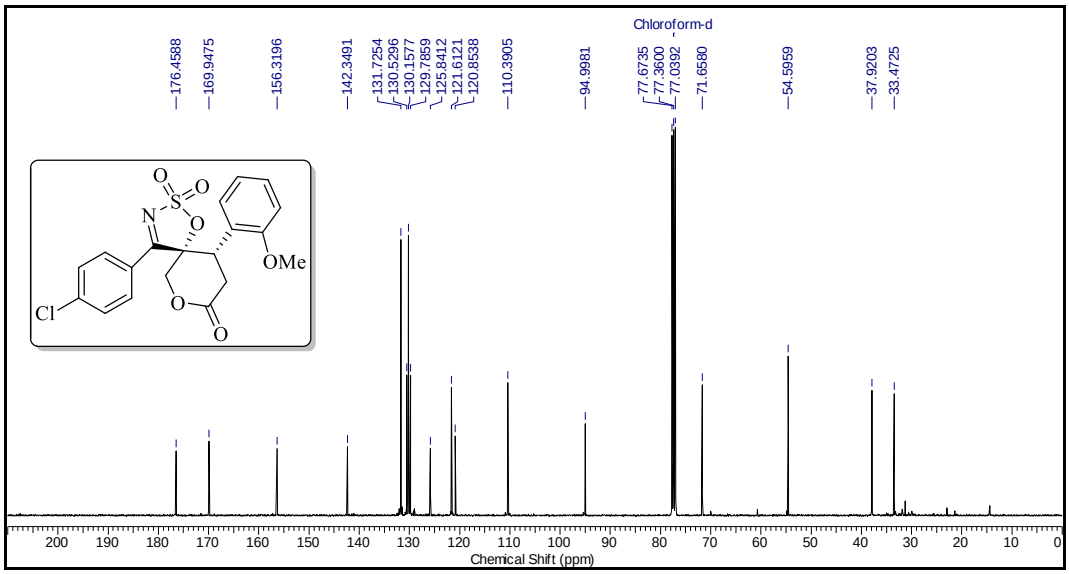


Figure 3.49 100 MHz ^{13}C NMR spectrum of **5fc** in $CDCl_3$

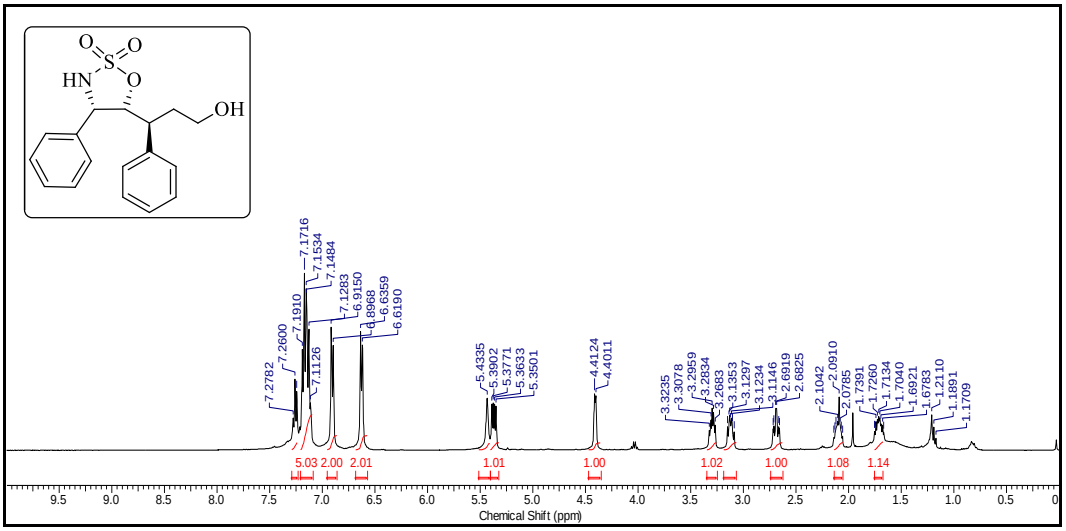


Figure 3.50 400 MHz ^{1}H NMR spectrum of **12** in $CDCl_3$

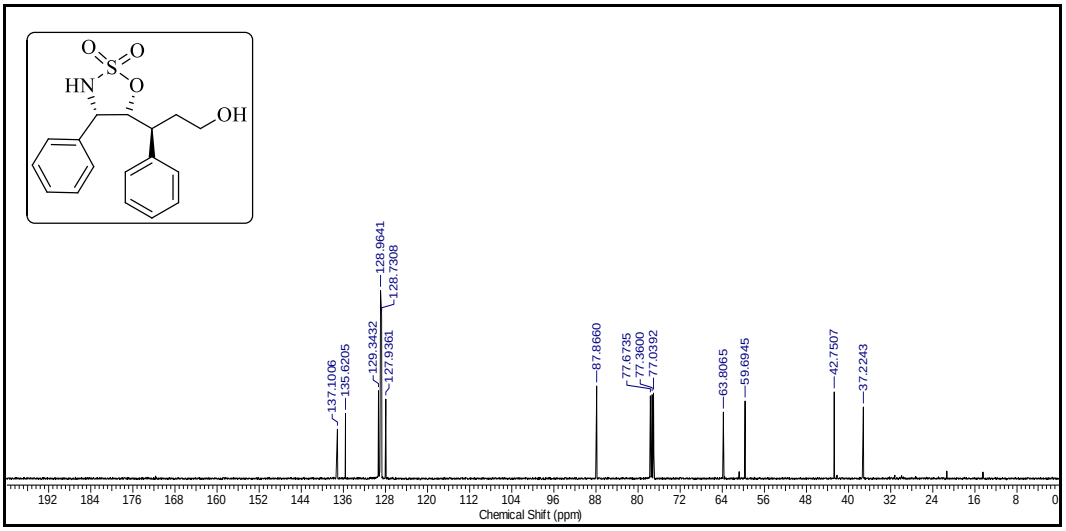


Figure 3.51 100 MHz ^{13}C NMR spectrum of **12** in $CDCl_3$

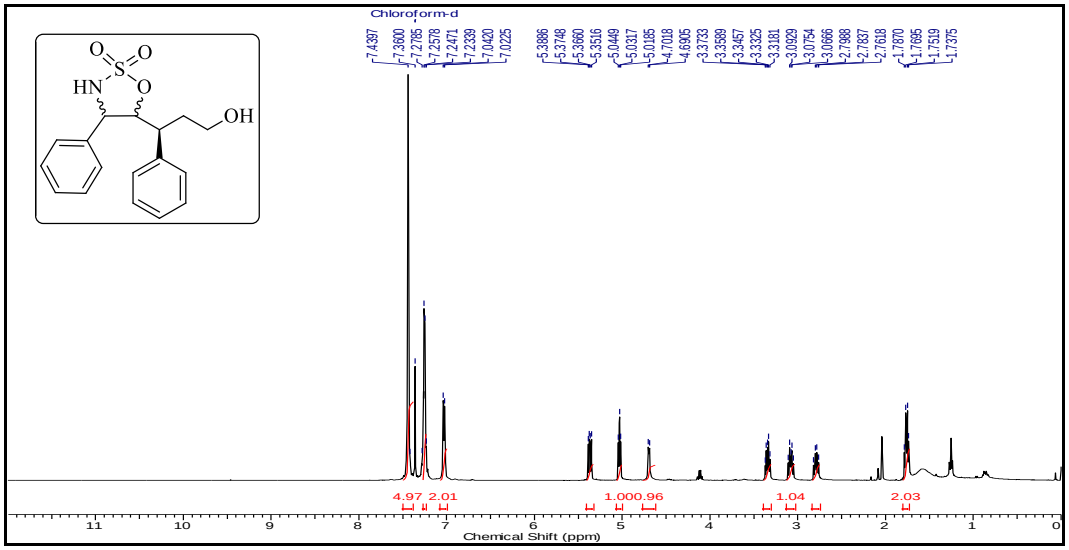


Figure 3.52 400 MHz ^{1}H NMR spectrum of **13** in $CDCl_3$

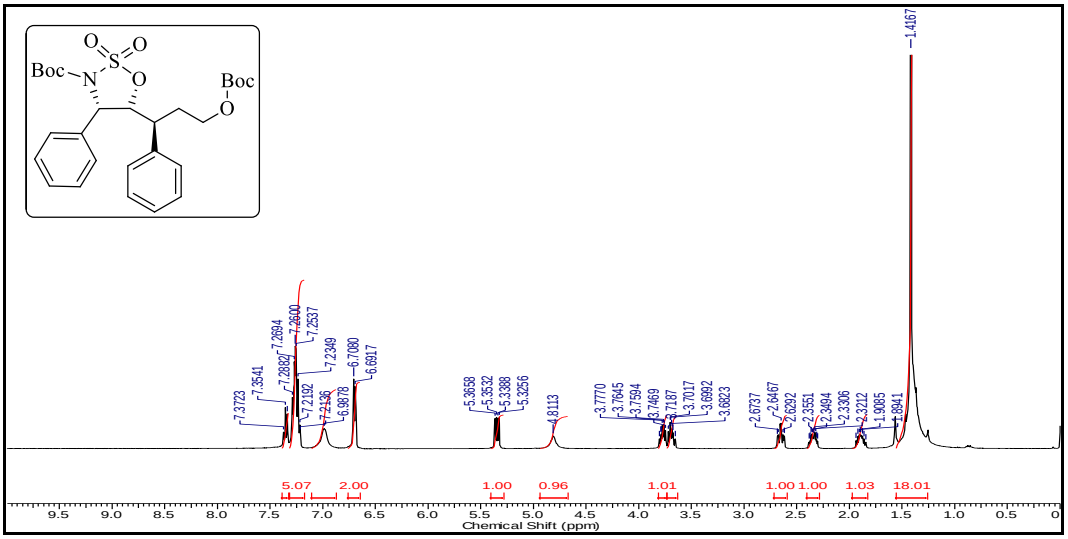


Figure 3.53 400 MHz ^{1}H NMR spectrum of **14** in $CDCl_3$

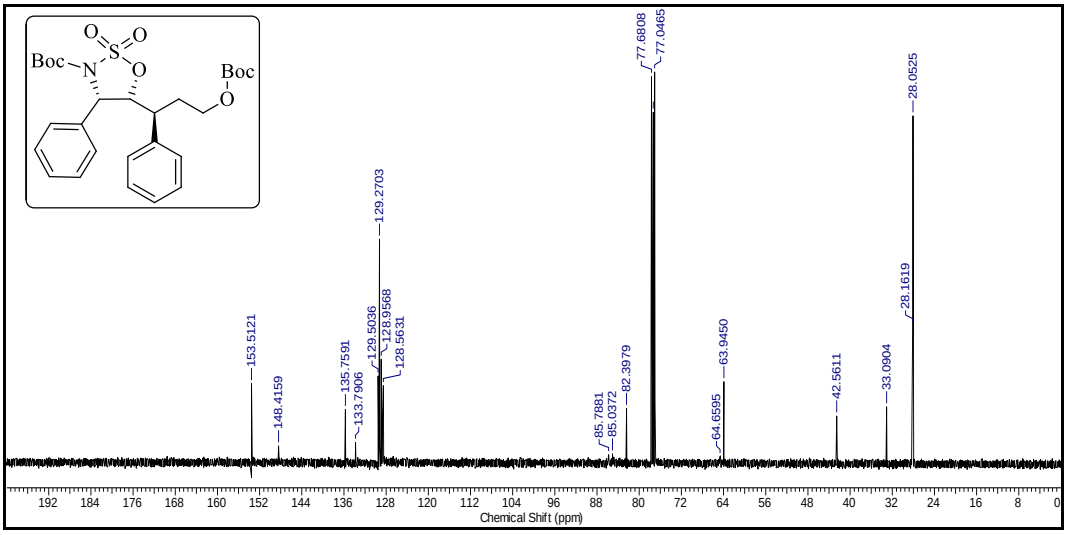


Figure 3.54 100 MHz ^{13}C NMR spectrum of **14** in $CDCl_3$

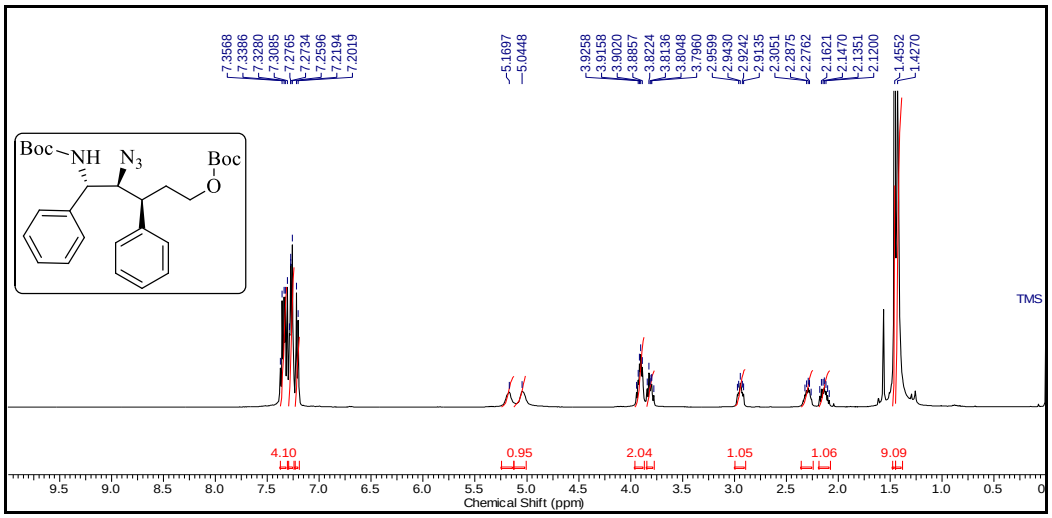


Figure 3.55 400 MHz ^{1}H NMR spectrum of **15** in $CDCl_3$

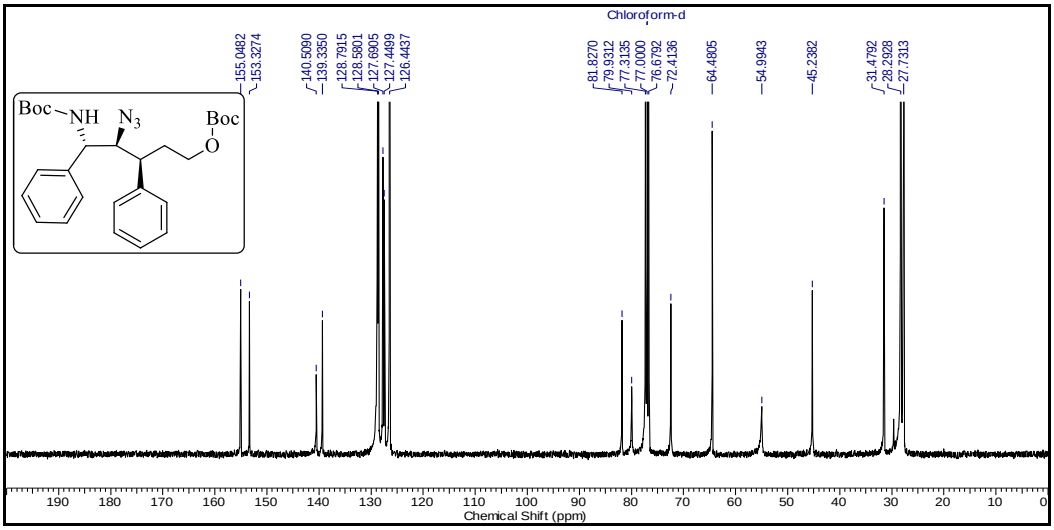
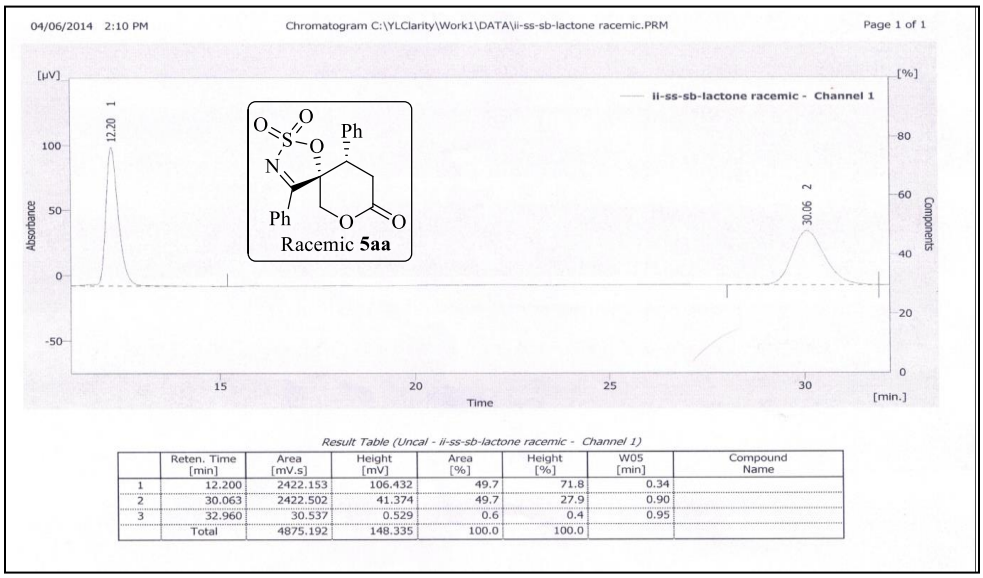


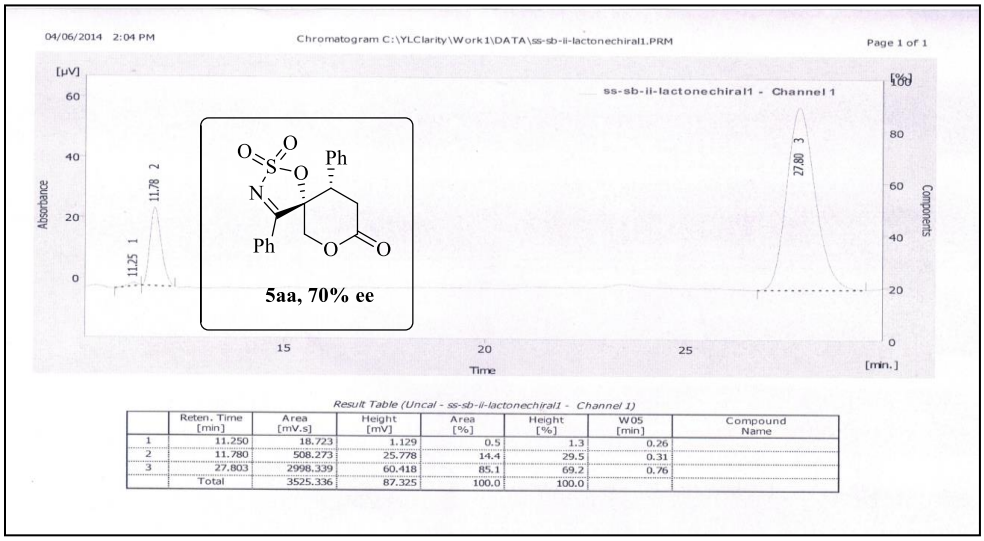
Figure 3.56 100 MHz ^{13}C NMR spectrum of **15** in $CDCl_3$



Result Table (Uncal - ii-ss-sb-lactone racemic - Channel 1)

	Reten. Time [min]	Area [mV.s]	Height [mV]	Area [%]	Height [%]	W05 [min]	Compound Name
1	12.200	2422.153	106.432	49.7	71.8	0.34	
2	30.063	2422.502	41.374	49.7	27.9	0.90	
3	32.960	30.537	0.529	0.6	0.4	0.95	
	Total	4875.192	148.335	100.0	100.0		

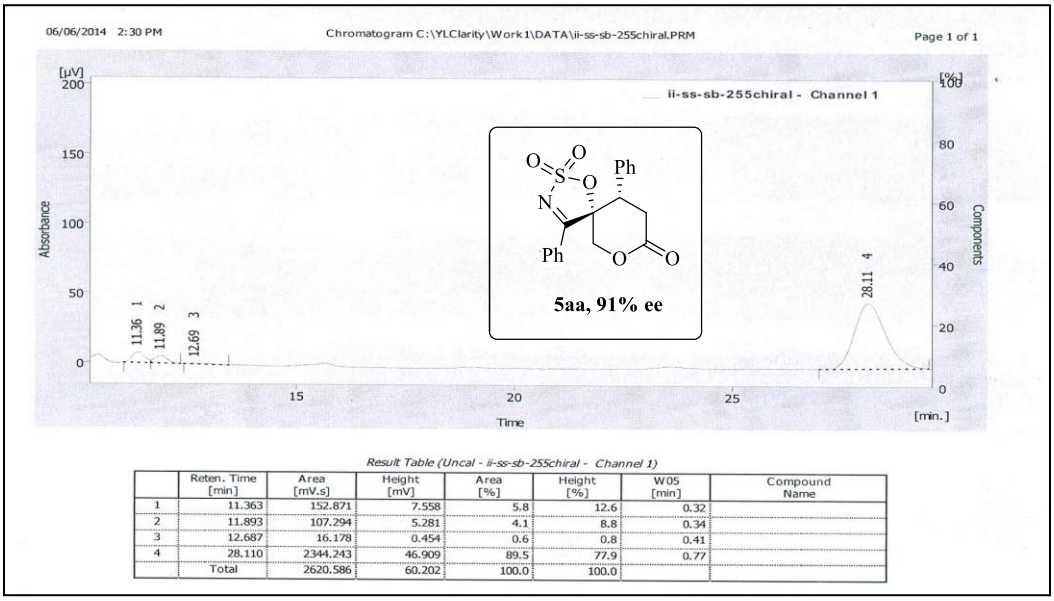
Fig 3.57 HPLC data of racemic **5aa**



Result Table (Uncal - ss-sb-ii-lactonechiral1 - Channel 1)

	Reten. Time [min]	Area [mV.s]	Height [mV]	Area [%]	Height [%]	W05 [min]	Compound Name
1	11.250	18.723	1.129	0.5	1.3	0.26	
2	11.780	508.273	25.778	14.4	29.5	0.31	
3	27.803	2998.339	60.418	85.1	69.2	0.76	
	Total	3525.336	87.325	100.0	100.0		

Fig 3.58 HPLC data of **5aa**



	Reten. Time [min]	Area [mV.s]	Height [mV]	Area [%]	Height [%]	W05 [min]	Compound Name
1	11.363	152.871	7.558	5.8	12.6	0.32	
2	11.893	107.294	5.281	4.1	8.8	0.34	
3	12.687	16.178	0.454	0.6	0.8	0.41	
4	28.110	2344.243	46.909	89.5	77.9	0.77	
	Total	2620.586	60.202	100.0	100.0		

Fig 3.59 HPLC data of **5aa**

3.7 References

1. Ma S.-S., Mei A.-L., Guo Z.-K., Liu S.-B., Zhao Y.-X., Yang D.-L., Zheng Y.-B., Jiang B., Dai H.-F. (2013), Two new types of bisindole alkaloid from trigonostemon lutescens, *Org. Lett.*, 15, 1492-1495 (DOI: 10.1021/ol4002619)
2. Cai X.-H., Tan Q.-G., Liu Y.-P., Feng T., Du Z.-Z., Li W.-Q., Luo X.-D. (2008), A Cage-monoterpene indole alkaloid from alstonia scholaris, *Org. Lett.*, 10, 577-580 (DOI: 10.1021/ol702682h)
3. Takata K., Iwatsuki M., Yamamoto T., Shirahata T., Nonaka K., Masuma R., Hayakawa Y., Hanaki H., Kobayashi Y., Petersson G.A., Omura S., Shiomi K. (2013), Aogacillins A and B produced by *Simplicillium* sp.

FKI-5985: new circumventors of arbekacin resistance in MRSA, *Org. Lett.*, 15, 4678-4681 (DOI: 10.1021/ol401975z)

4. Adams G. L., Carroll P. J., Smith A. B. III., (2013), Access to the Akuammiline family of alkaloids: total synthesis of (+)-Scholarisine A, *J. Am. Chem. Soc.*, 135, 519-528 (DOI: 10.1021/ja3111626)
5. Smith M. W., Snyder S. A., (2013), A concise total synthesis of (+)-Scholarisine A empowered by a unique C-H arylation, *J. Am. Chem. Soc.*, 135, 12964-12967 (DOI: 10.1021/ja406546k)
6. Kitano M., Yamada T., Amagata T., Minoura K., Tanaka R., Numata A. (2012), Novel pyridino-α-pyrone sesquiterpene type pileotin produced by a sea urchin-derived Aspergillus sp., *Tetrahedron Lett.*, 53, 4192-4194 (DOI: 10.1016/j.tetlet.2012.05.144)
7. Lu P., Gu Z., Zakarian A. (2013), Total synthesis of Maoecrystal V: early-stage C-H functionalization and lactone assembly by radical cyclization, *J. Am. Chem. Soc.*, 135, 14552-14555 (DOI: 10.1021/ja408231t)
8. Morita H., Arisaka M., Yoshida N., Kobayashi J. (2000), Serratezomines A-C, new alkaloids from lycopodium serratum var. serratum, *J. Org. Chem.*, 65, 6241-6245 (DOI: 10.1021/jo000661e)
9. Djigoué G. B., Ngatcha B. T., Roy J., Poirier D. (2013), Synthesis of 5α-Androstane-17-spiro-δ-lactones with a 3-keto, 3-hydroxy, 3-spirocarbamate or 3-spiromorpholinone as inhibitors of 17β-hydroxysteroid dehydrogenases, *Molecules,* 18, 914-933 (DOI: 10.3390/molecules18010914)
10. Bydal P., Luu-The V., Labrie F., Poirier D. (2009), Steroidal lactones as inhibitors of 17β-hydroxysteroid dehydrogenase type 5: chemical synthesis, enzyme inhibitory activity, and assessment of estrogenic and androgenic activities, *Eur. J. Med. Chem.*, 44, 632-644 (DOI: 10.1016/j.ejmech.2008.03.020)
11. Kitano M., Yamada T., Amagata T., Minoura K., Tanaka R., Numata A. (2012), Novel pyridino-α-pyrone sesquiterpene type pileotin produced by

a sea urchin-derived *Aspergillus* sp., *Tetrahedron Lett.*, 53, 4192-4194 (DOI: 10.1016/j.tetlet.2012.05.144)

12. Oberdorf C., Schepmann D., Vela J. M., Buschmann H., Holenz J., Wünsch B. (2012), Thiophene bioisosteres of spirocyclic σ receptor ligands: relationships between substitution pattern and σ receptor affinity, *J. Med. Chem*., 55, 5350-5360 (DOI: 10.1021/jm300302p)
13. Meyer C., Neue B., Schepmann D., Yanagisawa S., Yamaguchi J., Würthwein E.-U., Itami K., Wünsch B. (2013), Improvement of σ_1 receptor affinity by late-stage C–H-bond arylation of spirocyclic lactones, *Bioorg. Med. Chem.*, 21, 1844-1856 (DOI: 10.1016/j.bmc.2013.01.038)
14. Rouillard F., Roy J., Poirier D. (2008), Chemical synthesis of (S)-spiro(estradiol-17,2-[1,4]oxazinan)-6-one derivatives bearing two levels of molecular diversity, *Eur. J. Org. Chem.*, 2446-2453 (DOI: 10.1002/ejoc.200701077)
15. Bautista E., Toscano A., Calzada F.; Díaz, E.; Yépez-Mulia, L.; Ortega, A. (2013), Hydroxyclerodanes from *Salvia shannoni*, *J. Nat. Prod.*, 76, 1970-1975 (DOI: 10.1021/np400606g)
16. Igarashi Y., Zhou T., Sata S., Matsumoto T., Yu L., Oku N. (2013), Akaeolide, a carbocyclic polyketide from marine-derived Streptomyces, *Org. Lett.*, 15, 5678-5681 (DOI: 10.1021/ol402661r)
17. Miller L. H., Su X.-Z. (2011), Artemisinin: discovery from the chinese herbal garden, *Cell*, 146, 855-858 (DOI: 10.1016/j.cell.2011.08.024)
18. Istvan E. S., Deisenhofer J. (2001), Structural mechanism for statin inhibition of HMG-CoA reductase, *Science*, 292, 1160-1164 (DOI: 10.1126/science.1059344)
19. Endo A. (1985), Compactin (ML-236B) and related compounds as potential cholesterol-lowering agents that inhibit HMG-CoA reductase. *J. Med. Chem.*, 28, 401-405 (DOI: 10.1021/jm00382a001)
20. Du D., Hu Z., Jin J., Lu Y., Tang W., Wang B., Lu T. (2012), N-heterocyclic carbene-catalyzed three-component domino reaction of

alkynyl aldehydes with oxindoles, *Org. Lett.*, 14, 1274-1277 (DOI: 10.1021/ol300148f)

21. Xie X., Peng C., Leng H.-J., Wang B., Tang Z.-W., Huang W. (2014), Asymmetric synthesis of oxa-spirocyclic indanones with structural complexity *via* an organocatalytic Michael-Henry-acetalization cascade, *Synlett*., 25, 143-147 (DOI: 10.1055/s-0033-1340077)
22. Li X., Yang L., Peng C., Xie X., Leng H.-J., Wang B., Tang Z.-W., He G., Ouyang, L., Huang, W., Han, B. (2013), Organocatalytic tandem Morita-Baylis-Hillman-Michael reaction for asymmetric synthesis of a drug-like oxa-spirocyclic indanone scaffold, *Chem. Commun*., 49, 8692-8694 (DOI: 10.1039/c3cc44004d)
23. Wei M.-H., Zhou Y.-R., Gu L.-H., Luo F., Zhang F.-L. (2013), Asymmetric organocatalytic Michael-hemiacetalization reaction: access to chiral spiro cis-δ-lactones by *in situ* oxidation of spiro δ-lactols, *Tetrahedron Lett.*, 54, 2546-2548 (DOI: 10.1016/j.tetlet.2013.03.039)
24. Zheng J., Lin L., Kuang Y., Zhao J., Liu X., Feng X. (2014), Magnesium(II)-catalyzed asymmetric hetero-Diels-Alder reaction of Brassard's dienes with isatins, *Chem.Commun.*, 50, 994-996 (DOI: 10.1039/c3cc47800a)
25. Hempel C., Weckenmann N. M., Maichle- Moessmer C., Nachtsheim B. (2012), A hypervalent iodine-mediated spirocyclization of 2-(4-hydroxybenzamido)-acrylates-unexpected formation of δ-spirolactones, *J. Org. Biomol. Chem.*, 10, 9325-9329 (DOI: 10.1039/c2ob26815a)
26. Fujioka H., Komatsu H., Nakamura T., Miyoshi A., Hata K., Ganesh J., Muraia K., Kita Y. (2010), Organic synthesis using a hypervalent iodine reagent: unexpected and novel domino reaction leading to spiro cyclohexadienone lactones, *Chem. Commun.* 2010, 46, 4133-4135 (DOI: 10.1039/b925687c)
27. Helm M. D., Silva M. D., Sucunza D., Helliwell M., Procter, D. J. (2009), SmI2-mediated dialdehyde 'radical then aldol' cyclization cascades: a

feasibility study, *Tetrahedron*, 65, 10816-10829 (DOI: 10.1016/j.tet.2009.09.035)

28. Zhao S., Lin, J.-B., Zhao, Y.-Y., Liang, Y.-M., Xu, P.-F. (2014), Hydrogen-bond-directed formal [5 + 1] annulations of oxindoles with ester-linked bisenones: facile access to chiral spirooxindole δ‑lactones, *Org. Lett.*, 16, 1802-1805 (DOI: 10.1021/ol500547e)
29. Meléndez R. E., Lubell W. D. (2003), Synthesis and reactivity of cyclic sulfamidites and sulfamidates, *Tetrahedron*, 59, 2581-2616 (DOI: 10.1016/S0040-4020(03)00284-9)
30. Nicolaou K. C., Snyder S. A., Longbottom D. A., Nalbandian A. Z., Huang X. (2004), New uses for the burgess reagent in chemical synthesis: methods for the facile and stereoselective formation of sulfamidates, glycosylamines, and sulfamides, *Chem. Eur. J.*, 10, 5581-5606 (DOI: 10.1002/chem.200400503)
31. Bower J. F., Szeto P., Gallagher T. (2007), Enantiopure 1,4-benzoxazines *via* 1,2-cyclic sulfamidates. synthesis of Levofloxacin, *Org. Lett.*, 9, 3283-3286 (DOI: 10.1021/ol0712475)
32. Lee H.-K., Kang S., Choi B. E. (2012), Stereoselective synthesis of norephedrine and norpseudoephedrine by using asymmetric transfer hydrogenation accompanied by dynamic kinetic resolution, *J. Org. Chem.*, 77, 5454-5460 (DOI: 10.1021/jo300867y)
33. Han J., Kang S., Lee H.-K. (2011), Dynamic kinetic resolution in the stereoselective synthesis of 4,5-diaryl cyclic sulfamidates by using chiral rhodium-catalyzed asymmetric transfer hydrogenation, *Chem. Commun.*, 47, 4004-4006 (DOI: 10.1039/c0cc05289b)
34. Lee S. A., Kwak S. H., Lee K.-I. (2011), Highly enantioselective synthesis of cyclic sulfamidates and sulfamides *via* rhodium-catalyzed transfer hydrogenation, *Chem. Commun.*, 47, 2372-2374 (DOI: 10.1039/c0cc04166a)

35. Kang S., Han J., Lee E. S., Choi E. B., Lee H.-K. (2010), Sulfamidates by using chiral rhodium-catalyzed asymmetric transfer hydrogenation, *Org. Lett.*, 12, 4184-4187 (DOI: 10.1021/ol1017905)
36. Woo L. W. L., Leblond B., Purohit A., Potter B. V. L. (2012), Synthesis and evaluation of analogues of estrone-3-o-sulfamate as potent steroid sulfatase inhibitors, *Bioorg. Med. Chem.*, 20, 2506-2519 (DOI: 10.1016/j.bmc.2012.03.007)
37. Benltifa M., Kiss M. D., Garcia- Moreno M. I., Mellet C. O., Gueyrard D., Wadouachi A.(2009), Regioselective synthesis and biological evaluation of spiro-sulfamidate glycosides from exo-glycals, *Tetrahedron: Asymmetry*, 20, 1817-1823 (DOI: 10.1016/j.tetasy.2009.07.012)
38. Zhou J. (2010), Recent advances in multicatalyst promoted asymmetric tandem reactions, *Chem. Asian J.*, 5, 422-434 (DOI: 10.1002/asia.200900458)
39. Ambrosini L. M., Lambert T. H. (2010), Multicatalysis: advancing synthetic efficiency and inspiring discovery, *Chem Cat Chem*, 2, 1373-1380 (DOI: 10.1002/cctc.200900323)
40. Patil N. T., Shinde V. S., Gajula B. (2012), A one-pot catalysis: the strategic classification with some recent examples, *Org. Biomol. Chem.*, 10, 211-224 (DOI: 10.1039/c1ob06432k)
41. Alba A.-N., Companyo X., Viciano M., Rios R. (2009), Organocatalytic Domino Reactions, *Curr. Org. Chem.*, 13, 1432-1474 (DOI: 10.2174/138527209789055054)
42. Grondal C., Jeanty M., Enders D. (2010), Organocatalytic cascade reactions as a new tool in total synthesis, *Nat. Chem.*, 2, 167-178 (DOI: 10.1038/nchem.539)
43. Vaxelaire C., Winter P., Christmann M. (2011), One-pot reactions accelerate the synthesis of active pharmaceutical ingredients, *Angew. Chem. Int. Ed.*, 50, 3605-3607 (DOI: 10.1002/anie.201100059)
44. Tietze L. F. (1996), Domino reactions in organic synthesis, *Chem. Rev.*, 96, 115-136 (DOI: 10.1021/cr950027e)

45. Schreiber S. L. (2000).,Target-oriented and diversity-oriented organic synthesis in drug discovery, *Science*, 287, 1964-1969 (DOI: 10.1126/science.287.5460.1964)
46. Zhu J.-P., Bienayme H. (2005). Multicomponent reactions, Wiley-VCH: Weinheim, (ISBN: 978-3-527-30806-4)
47. Trost B. M. (1995), Atom economy - a challenge for organic synthesis: homogeneous catalysis leads the way, *Angew. Chem., Int. Ed.* 34, 259-281 (DOI: 10.1002/anie.199502591)
48. Torssell S., Keinle M., Somfai P. (2005), 1,3-dipolar cycloadditions of carbonyl ylides to aldimines: a three-component approach to syn-α-hydroxy-β-amino esters, *Angew. Chem., Int. Ed.* , 44, 3096-3099 (DOI: 10.1002/anie.200500296)
49. Srivastava A., Mobin S. M., Samanta S. (2014), (±)-CSA catalyzed one-pot synthesis of 6,7-dihydrospiro[indole-3,1′-isoindoline]-2,3′,4(1*H*,5*H*)-trione derivatives: easy access of spirooxindoles and ibophyllidine-like alkaloids, *Tetrahedron Lett.*, 55, 1863-1867 (DOI: 10.1016/j.tetlet.2014.01.154)
50. Srivastava A., Singh S., Samanta S. (2013), (±)-CSA catalyzed Friedel-crafts alkylation of indoles with 3-ethoxycarbonyl-3-hydoxyisoindolin-1-one: an easy access of 3-ethoxycarbonyl-3-indolylisoindolin-1-ones bearing a quaternary a-amino acid moiety, *Tetrahedron Lett.*, 54, 1444-1448; (DOI: 10.1016/j.tetlet.2013.01.010)
51. Singh S., Srivastava A., Samanta S. (2012), Rapid access of 2,3,4-trisubstituted-2,3,4,9-tetrahydrothiopyrano[2,3-*b*]indole derivatives *via* one-pot three component reaction using organocatalysis, *Tetrahedron Lett.* 2012, 53, 6087-6090 (DOI: 10.1016/j.tetlet.2012.08.125)
52. Majee D., Srivastava, A., Mobin S. M., Samanta S. (2013), L-Proline catalyzed highly efficient synthesis of Z-5- alkylidene cyclic sulfamidate imines: an easy access to 5-alkyl-substituted cyclic sulfamidate imines, *RSC. Adv.*, 3, 11502-11506 (DOI: 10.1039/c3ra40299a)

53. Biswas S., Jaiswal P. K., Singh S., Mobin M. S., Samanta, S. (2013), L-Proline catalyzed stereoselective synthesis of (E)-methyl-α-indol-2-yl-β-aryl/alkyl acrylates: easy access to substituted carbazoles, γ-carbolines and prenostodione, *Org. Biomol. Chem.*, 11, 7084-7087 (DOI: 10.1039/c3ob41573b)
54. Palomo C., Mielgo A. (2006), Diarylprolinol ethers: expanding the potential of enamine/iminium-ion catalysis, *Angew. Chem., Int. Ed.*, 45, 7876-7880 (DOI: 10.1002/anie.200602943)
55. Mielgo A., Palomo C. (2008), α,α-diarylprolinol ethers: new tools for functionalization of carbonyl compounds, *Chem. Asian J.*, 3, 922-948 (DOI: 10.1002/asia.200700417)
56. Hayashi Y., Gotoh H., Hayashi T., Shoji M. (2005), Diphenylprolinol silyl ethers as efficient organocatalysts for the asymmetric Michael Reaction of aldehydes and nitroalkenes, *Angew. Chem., Int. Ed.*, 44, 4212-4215 (DOI: 10.1002/anie.200500599)
57. Marigo M., Wabnitz T. C., Fielenbach D., Jørgensen K. A. (2005), Enantioselective organocatalyzed α sulfenylation of aldehydes. *Angew. Chem., Int. Ed.*, 44,794-797 (DOI: 10.1002/anie.200462101)
58. Wang Y. -Q., Yu C. -B., Wang D. -W., Wang X. -B., Zhou Y. -G. (2008), Enantioselective synthesis of cyclic sulfamidates via Pd-catalyzed hydrogenation, *Org. Lett.*, 10, 2071-2074 (DOI: 10.1021/ol800591u)

Chapter 4

Unprecedented synthesis of 4,6-diarylpicolinates *via* a domino reaction of cyclic sulfamidate imines with Morita-Baylis-Hillman acetates of nitroolefins /nitrodienes

4.1 Introduction

Design and development of an innovative approach towards the rapid access to important class of functionalized pyridines, mainly picolinates through one-pot operations is one of the active research areas in synthetic as well as in medicinal chemistry because this popular heterocyclic core has been largely found in a variety of biologically active natural molecules(**Figure 4.1**).[1-5]

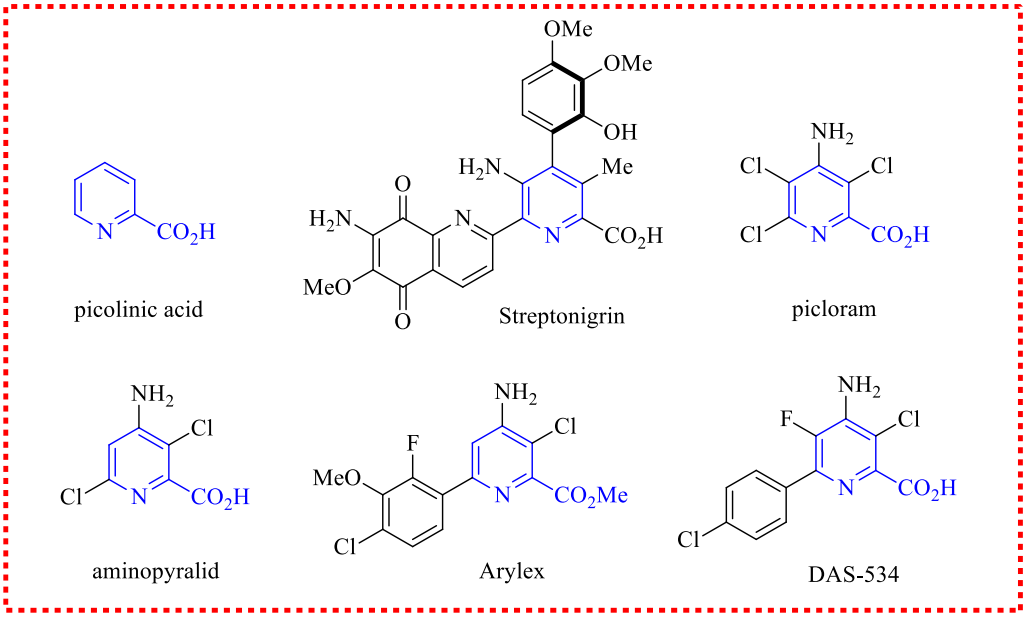
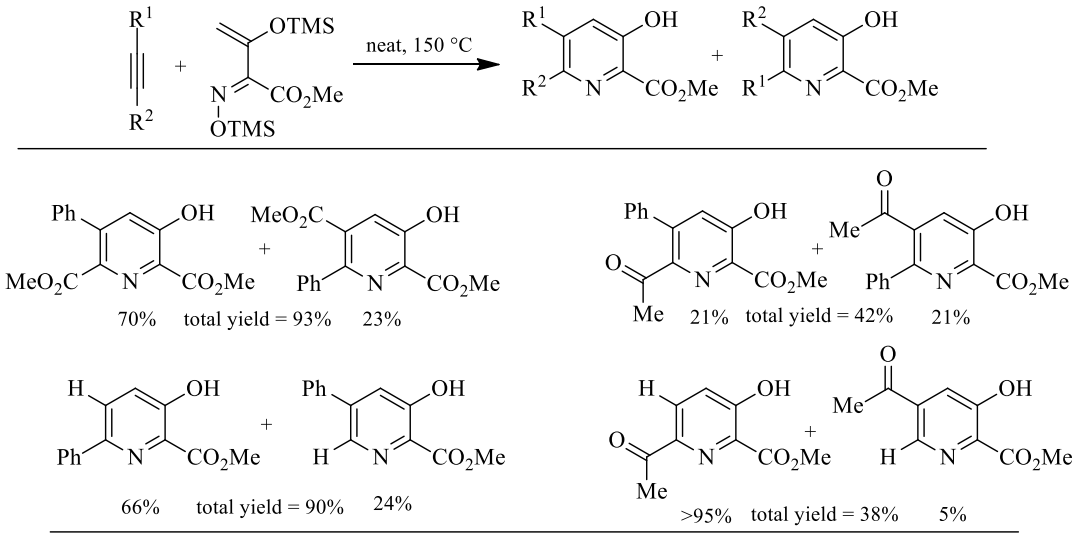


Figure 4.1 Some natural product and biologically active compounds containing picoline moiety

Moreover, substituted picolinates have shown their applications in versatile fields like pharmaceutical research,[6-7] functional materials,[8-9] agrochemicals,[10-11] polymer,[12] catalysis[13-14] and in co-ordination chemistry.[15-16] Owing to their broad spectrum of applications, huge efforts have been devoted towards the synthesis of picolinate scaffolds by adopting several classical and modern techniques such as condensation reactions of ketones with amines, multicomponent reactions, cycloaddition reactions, transition-metal salt catalyzed C-H bond functionalization, etc.[17-25] Some of the important literature reports have been described in **Section 4.2**.

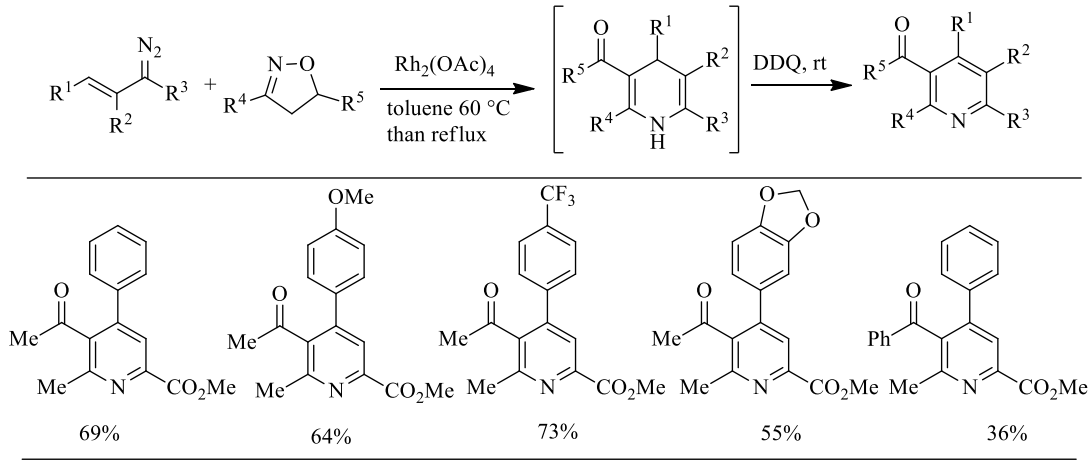
4.2 Review of Literature

A hetero-Diels-Alder reaction of silylated enol oximes with unsymmetrical alkynes at 150 ºC was carried out under neat conditions to provide the 3,5,6-trisubstituted picolinates in a regioselective manner as reported by Arndt and co-workers in 2007.[26] The current protocol provides good yields of title compounds and allows with several functionalities as discussed in **Scheme 4.1**.



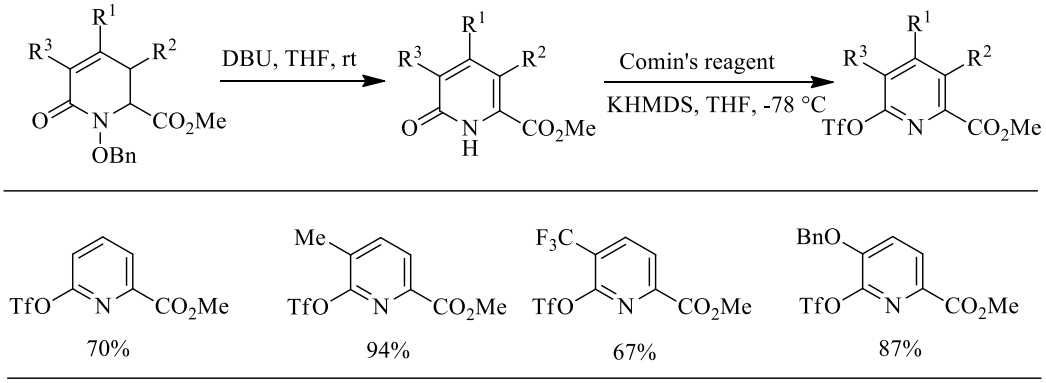
Scheme 4.1 Synthesis of 3-hydroxy picolinates from unsymmetrical alkynes

In 2008, Davies group introduced a one-pot synthesis of highly functionalized picolinates *via* a rhodium carbenoid induced ring expansion of isoxazoles followed by a rearrangement/tautomerization/oxidation sequence. [27] A wide variety of picolinates in moderate to good yield could be obtained by utilizing this current methodology as described in **Scheme 4.2**.



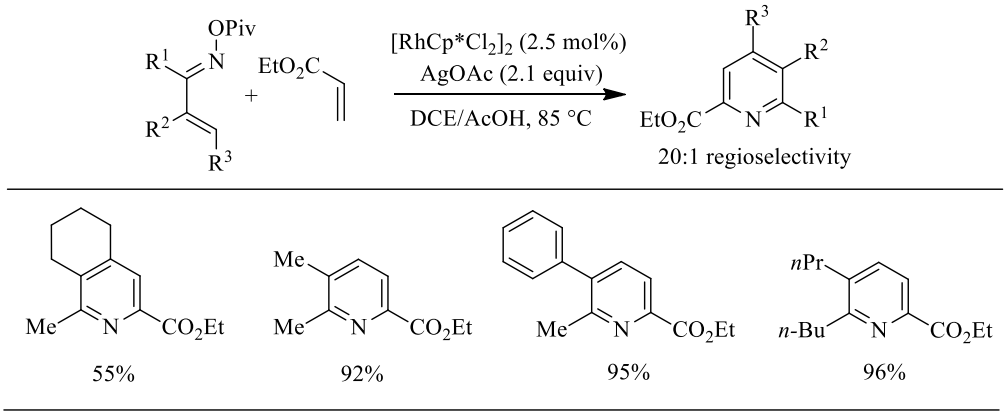
Scheme 4.2 One-pot synthesis of highly functionalized picolinates

In 2009, Donohoe *et al.* revealed a breakthrough result by a multistep synthesis of di- and trisubstituted picolinates with alkyl, aryl and alkoxy substituents.[28] DBU promoted deprotection of benzyl protected lactam followed by aromatization with Comin's reagent under basic conditions to afford pyridine triflates in good to excellent yields (67-94%) as shown in the **Scheme 4.3**.



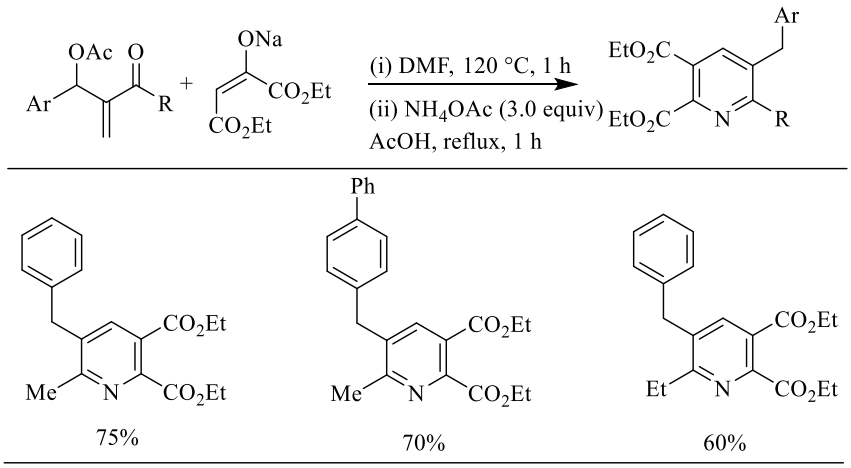
Scheme 4.3 DBU promoted synthesis of substituted picolinates

Rovis *et al*. has developed an interesting method for the regioselective synthesis of an important class of picolinate derivatives in good to excellent yields through a regioselective coupling reaction between α,β-unsaturated O-pivaloyl oxime and ethyl acrylate at 85 °C using Rh-salt/AgOAc as the combined catalytic system (**Scheme 4.4**). [29]



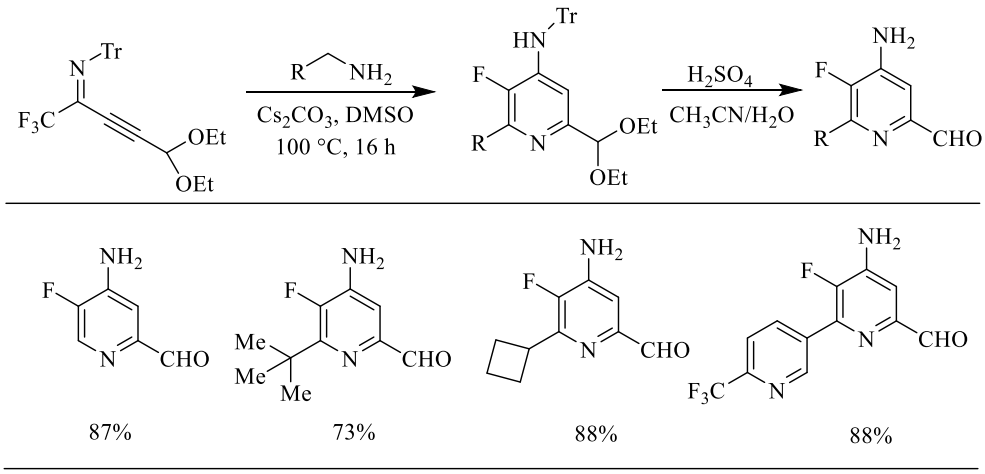
Scheme 4.4 Formation of substituted picolinates by using different α,β-unsaturated *O*-pivaloyl oximes

In 2013, Kim *et al.* revealed a completely different approach for the synthesis of poly-substituted pyridines by using MBH adducts of methyl vinyl ketone and sodium diethyl oxaloacetate in presence of NH_4OAc as nitrogen source.[30] Some of the important examples are described in **Scheme 4.5**.



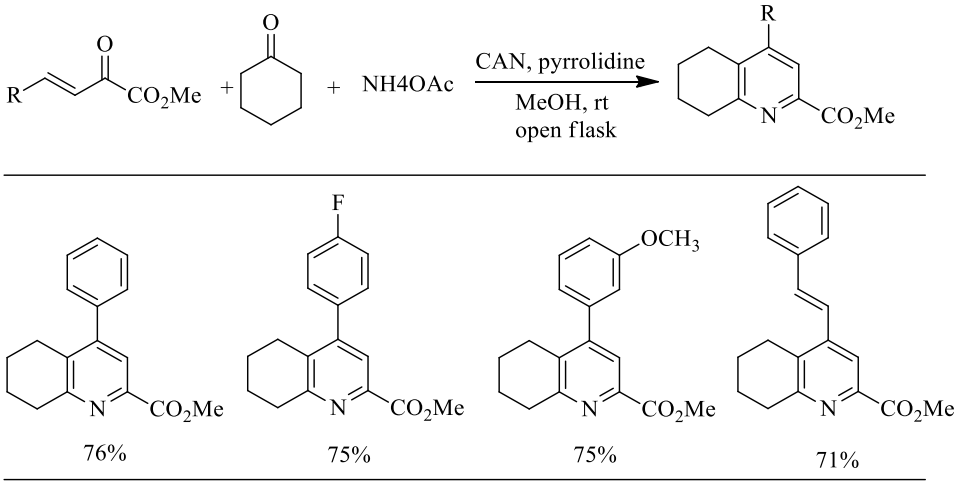
Scheme 4.5 Synthesis of poly-substituted picolinates

In 2015, Whiteker and his co-workers reported a two-step sequential method for the preparation of synthesis of fluoropicolinates derivative by a cascade cyclization of fluoroalkyl alkynylimines and amine using Cs_2CO_3 in DMSO.[31] Some of the promising results are summarized in **Scheme 4.6**.



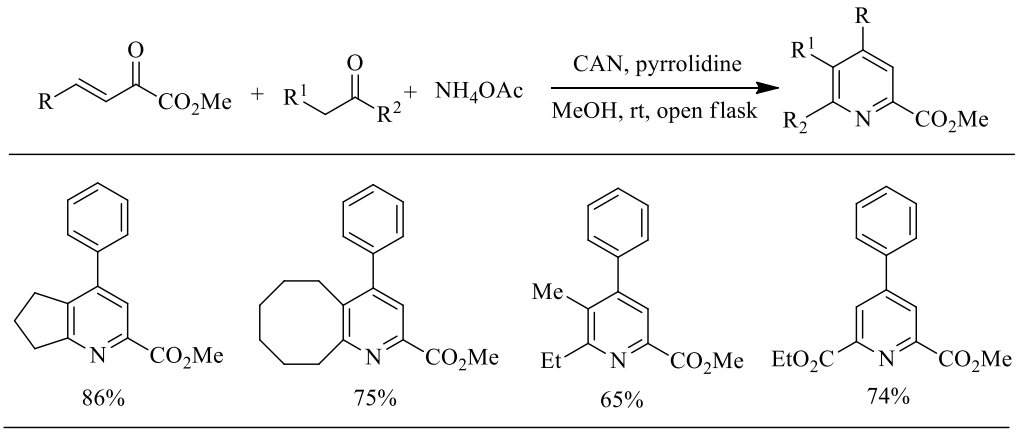
Scheme 4.6 Synthesis of substituted 4-amino-5-fluoro-6- alkylpicolinaldehydes by cascade cyclization

CAN/pyrrolidine mediated tandem three-component annulation reaction for the access to functionalized picolinates involving β,γ-unsaturated α-ketoester, ketones and ammonium acetate has been nicely described by Zhu and co-workers in 2015 (**Scheme 4.7**).[32]



Scheme 4.7 Cyclization reaction between β,γ-unsaturated α-ketoesters, and cyclohexanone

Further they used varieties of carbonyl compounds to achieve various substituted picolinate moiety **(Scheme 4.8)**.



Scheme 4.8 Cyclization reaction between β,γ-unsaturated α-ketoesters, and and ketones

4.2.1 Conclusion

From all of the above literature survey, we can conclude that there are substantial numbers of simple and easy procedure to synthesize pyridine in good to excellent yield. Despite such huge effort for pyridine synthesis, access to functionalized picolinic acid **(Figure 4.2)** derivatives (carboxylic acid at C-2 position on pyridine ring) has received very less attention. Few literatures reported for the synthesis of picolinic acid derivatives. However, they suffer from one or more practical difficulties, such as use of expensive metal salts, limited substrate scope, poor chemical yields with multiple side products, harsh reaction conditions, etc. Therefore, it is a great challenge in synthetic organic chemistry to establish a simple, metal-free, efficient new synthetic procedure for the rapid construction of multifunctionalzed picolinate frameworks under metal-free conditions.

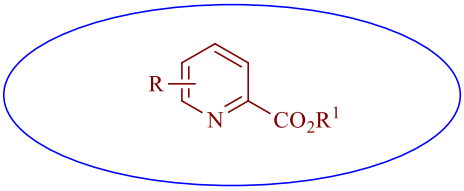
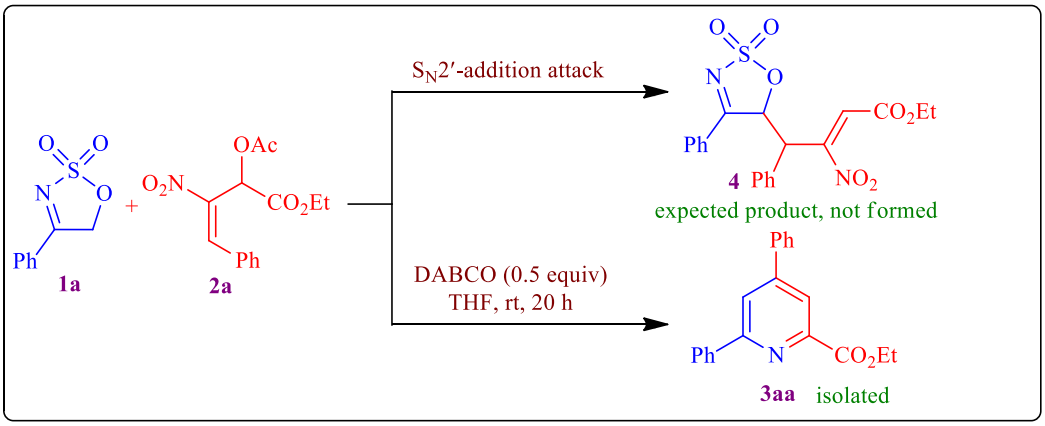


Figure 4.2 Picolinic acid derivative

4.3 Present Work

The efficient and environmentally sustainable synthesis of functionalized picolinic acids has taken a huge attention to synthetic organic chemist because of their biological and pharmaceutical importance. Substituted picolinic acid systems are important privileged structures of many biologically and pharmaceutically important compounds as described in introduction **Section 4.1**. In this line, we have found that 5-membered cyclic sulfamidate imines could act as potential nucleophiles[33-34] as discussed in **Section 2.3** while reacting with several aryl aldehydes/α,β-unsaturated aldehydes. On the other hand, MBH-acetates[35-38] of nitroolefins have been used as suitable 1,3-binucleophiles in the S_N2' addition-elimination sequence reaction with several nucleophiles to construct various 5/6-membered heterocycles. With this understanding, we thought that cyclic sulfamidate imines may also attack MBH acetates of nitroolefins in an S_N2' addition manner in the presence of a base (**Scheme 4.9**).



Scheme 4.9 DABCO mediated domino reaction between 4-phenyl- 5*H*-1,2,3-oxathiazole-2,2-dioxide and MBH acetate of *trans*-β-nitrostrene

To verify our idea, we chose a model reaction between 4-phenyl-5*H*-1,2,3-oxathiazole-2,2-dioxide **(1a,** 1.0 equiv**)** and MBH acetate **(2a,** 1.1 equiv**)** using 50 mol % of 1,4-diazabicyclo[2.2.2]octane (DABCO) as an organobase in THF at room temperature. Greatly, after 20 h we isolated ethyl 4,6-diphenylpicolinate **(3aa)** with 32% yield instead of addition adduct **4**. The product **3aa** was fully

characterized by its spectroscopic data (IR ^{1}H, ^{13}C and HRMS). ^{1}H NMR data shows the disappearance of 5.60 singlet peak which indicates the total consuming of **1a.** Additional ^{1}H NMR peak in the region δ 7.43-8.28 ppm corresponding aromatic protons of pyridine moiety. Moreover, 4.52 (q, *J* = 7.0Hz) and 1.48 (t, *J* = 7.0 Hz) correspond to the CO_2Et group. In addition, ^{13}C NMR spectrum contains 16 peaks (14 of aromatic region and 2 of CO_2Et group) clears the formation of our desired picolinate derivative **3aa.** The HRMS spectrum shows the presence of molecular ion peak $[M+H]^+$: 304.1334, which corresponds to the molecular weight of product of **3aa**.

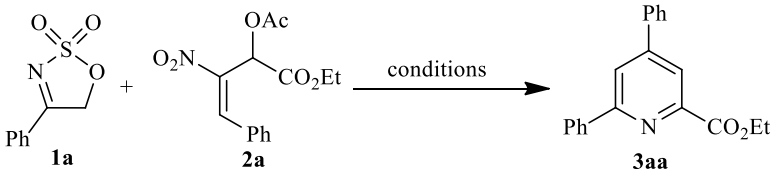
This inspiring result gave us an opportunity to develop a new synthetic method for the synthesis of functionalized picolinates under a metal free condition.[39-42]

4.3.1 Results and discussions

4.3.1.1 Screening of solvents and bases

In view of the above interesting results, we further examined this domino reaction in order to improve the chemical yield of **3aa**. Thus, on increasing the amount of DABCO from 0.5 to 1.5 equivalents, the yield of **3aa** was dramatically improved from 32% to 84% (entries 2 and 3, **Table 4.1**) after 10-12 h. Interestingly, excellent yields (87-92%, entries 4 and 5) of **3aa** were obtained within short time spans (3-6 h) when the reaction was performed under heating conditions (45-55 °C). For this catalyst, screening of organic solvents revealed that nonpolar solvents like toluene, CH_2Cl_2, MeCN, and EtOAc produced better yields (79-86%, entries 6-9) as compared to polar ones (DMSO, DMF, and EtOH, 40−58% yields, entries 10-12) under identical conditions. Considering the yield of **3aa** (92%, entry 5), THF was chosen as the best solvent for this reaction. Next, we investigated the influence of several common organic bases, namely DBU, DMAP, DIPEA, pyridine, triethylamine, and quinine, on this domino reaction at 55 °C for 6 h. Surprisingly, all of these bases produced inferior results (11-50% yields of **3aa**, entries 13-18) as compared to DABCO (92%, 3 h, entry 5).

Table 4.1 Optimization of the domino reaction[a]

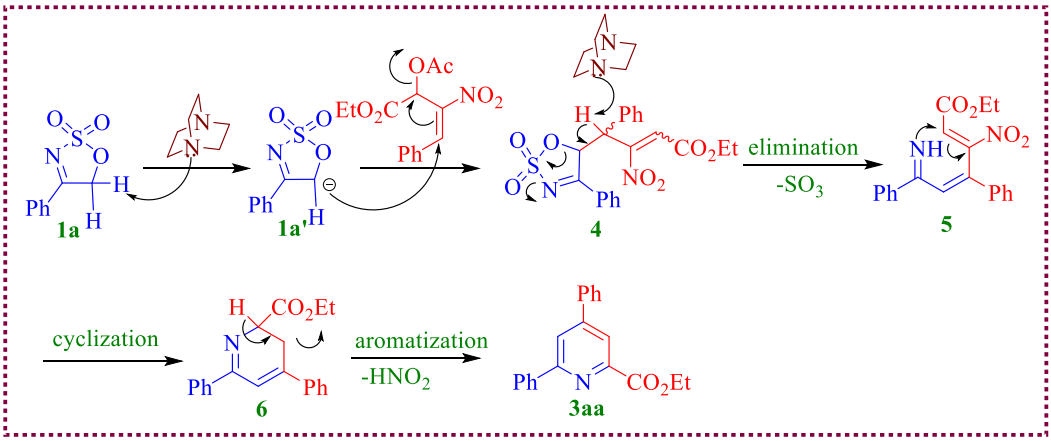


entry	base	solvent	temp (°C)	time (h)	yield (%)[b]
1[c]	DABCO	THF	rt	20	32
2[d]	DABCO	THF	rt	14	62
3	DABCO	THF	rt	10	84
4	DABCO	THF	45	6	87
5	DABCO	THF	55	3	92
6	DABCO	toluene	55	3	86
7	DABCO	CH_2Cl_2	55	3	80
8	DABCO	MeCN	55	3	79
9	DABCO	EtOAc	55	3	84
10	DABCO	DMSO	55	5	48
11	DABCO	DMF	55	5	40
12	DABCO	EtOH	55	5	58
13	DBU	THF	55	6	12
14	DMAP	THF	55	6	18
15	C_6H_5N	THF	55	6	30
16	DIPEA	THF	55	6	11
17	Et_3N	THF	55	6	42
18	Quinine	THF	55	6	50

[a]Unless otherwise noted, all the reactions were performed with compound **1a** (0.2 mmol), MBH acetate **2a** (0.22 mmol) and DABCO (0.3 mmol, 1.5 equiv) in specified solvent (0.5 ml) and temperature. [b]Isolated yield after column chromatography. [c]0.5 equivalent of DABCO. [d]1.0 equivalent of DABCO

4.3.1.2 Plausible mechanism

From the above reaction, we propose a plausible mechanism for the formation of **3aa** as shown in **Scheme 4.10**. At first, carbanion ion **1a′** is generated from **1a** *via* abstraction of an active methylene proton by a base which undergoes S_N2' reaction with MBH adduct **2a** to generate intermediate **4**. Later, it may convert into triene intermediate **5** through elimination of SO_3 in the influence of base, which is subsequently cyclized to form cyclic intermediate **6**.[43] Finally, the product **3aa** forms from intermediate **6** through elimination of HNO_2.



Scheme 4.10 Plausible mechanism for this domino reaction

4.3.1.3 Generality and substrate scope

After successfully establishing the reaction parameters for the synthesis of 4,6-diphenylpicolinate, the scope and limitation of this reaction were examined by performing the reaction using a series of 4-aryl-substituted cyclic sulfamidate imines **1a-g** with MBH acetates derived from nitroolefins **2a-l** under the present conditions as shown in **Table 4.1**. The results showed that electron-donating (Me, OMe, OBn) substituents on aryl rings of MBH acetates **2b-e** are slightly less reactive (3-5 h vs 2.5-3 h) toward **1a** as compared to electron-withdrawing ones (F, Cl, CN and NO_2). However, all of the reactions led to high to excellent yields (84−93%) of 4,6-diarylpicolinates **3ab-ai**. Moreover, heteroaryl-substituted MBH acetates **2j,k** ran smoothly with **1a** *via* this procedure, delivering high yields of

85% and 86% of the desired products **3aj** and **3ak**, respectively. Furthermore, incorporation of several substituents (Me, MeO, F, Cl, and Br) on the aryl rings of cyclic sulfamidate imines **1b-g** did not show any difficulty for the annulations with several MBH acetates **2a-l** under standard conditions. Consequently, high to excellent yields (82-91%) of the corresponding picolinate derivatives **3ba-gk**) were isolated within short timespans (3-6 h). The structure of **3bd** was confirmed by its single crystal X-ray data as shown in **Figure 4.3**. This metal-free domino procedure is mild enough to sustain several functionalities such as Me, OMe, OBn, F, Cl, NO_2, CN, CO_2Et, furan, thiophene etc. Therefore, this method provides further opportunity for the synthesis of important therapeutic targets through necessary synthetic modifications of these functional groups.

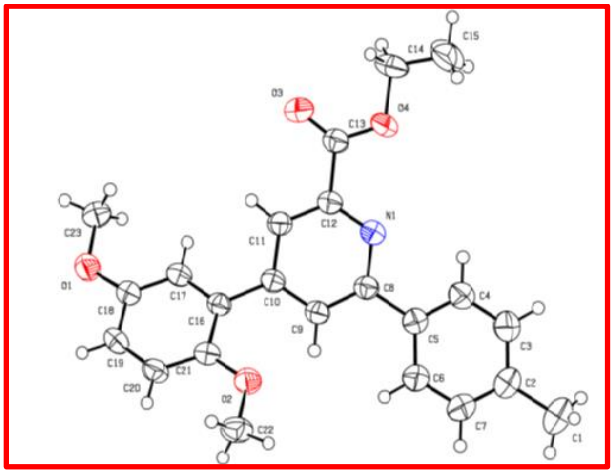
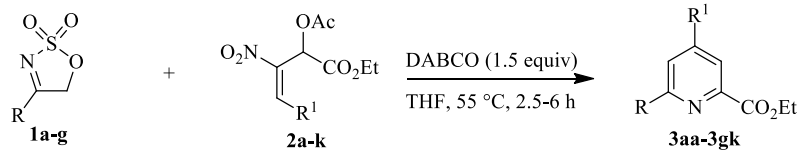


Figure 4.3 ORTEP diagram of compound **3bd (CCDC)**

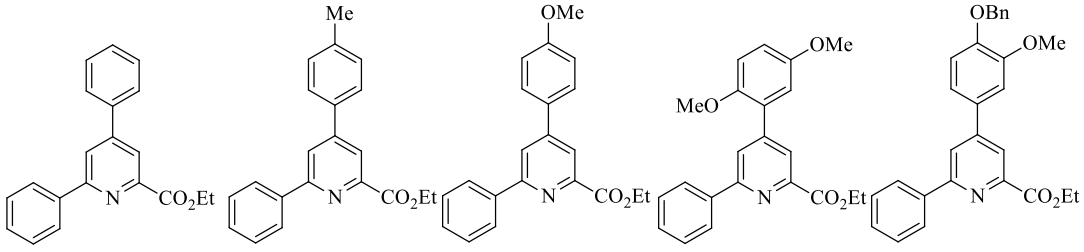
Table 4.2 Substrate Scope of 4,6-diarylpicolinate synthesis.



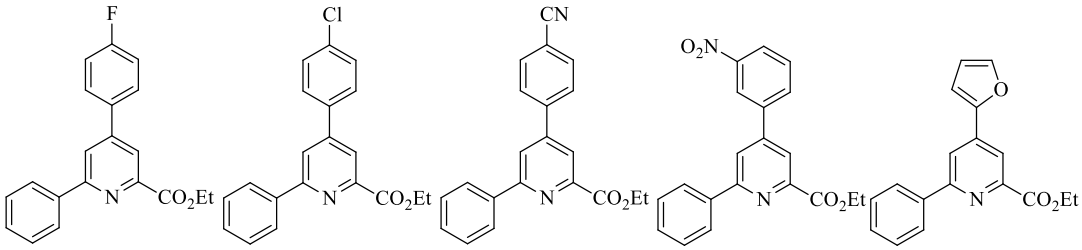
1a-g + **2a-k** → **3aa-3gk**

1a: R = Ph, **1b**: R = 4-MeC_6H_4
1c: R = 4-$MeOC_6H_4$, **1d**: R = 4-FC_6H_4
1e: R = 4-ClC_6H_4, **1f**: R^1 = 2-ClC_6H_4
1g: R = 4-BrC_6H_4,

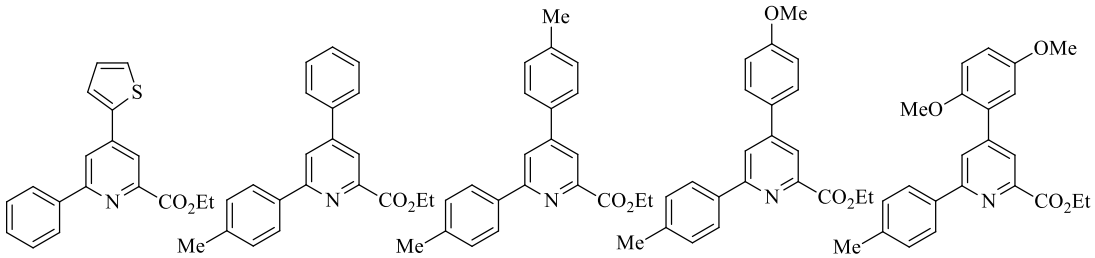
2a: R^1 = Ph, **2b**: R^1 = 4-MeC_6H_4
2c: R^1 = 4-$MeOC_6H_4$, **2d**: R^1 = 2,5-$(MeO)_2C_6H_3$
2e: R^1 = 3-MeO-4-$BnOC_6H_3$, **2f**: R^1 = 4-FC_6H_4
2g: R^1 = 4-ClC_6H_4, **2h**: R^1 = 4-CNC_6H_4
2i: R^1 = 3-$O_2NC_6H_4$, **2j**: R^1 = 2-furyl
2k: R^1 = 2-thiophenyl, **2l**: R^1 = 4-$CF_3C_6H_4$



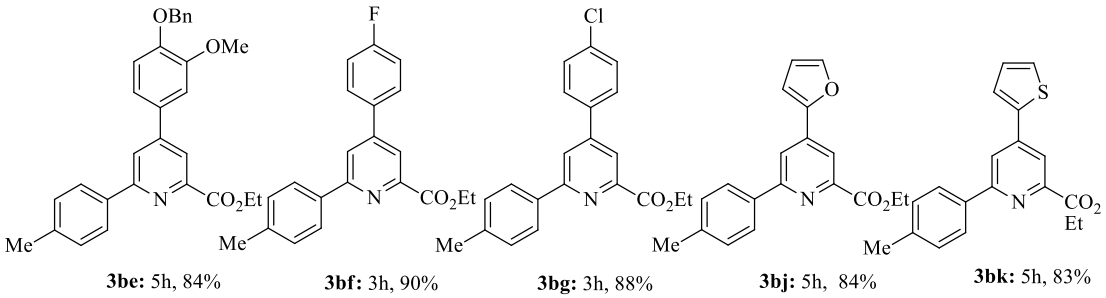
3aa: 3 h, 92% **3ab:** 3 h, 90% **3ac:** 4 h, 89% **3ad:** 5 h, 86% **3ae:** 5 h,84%



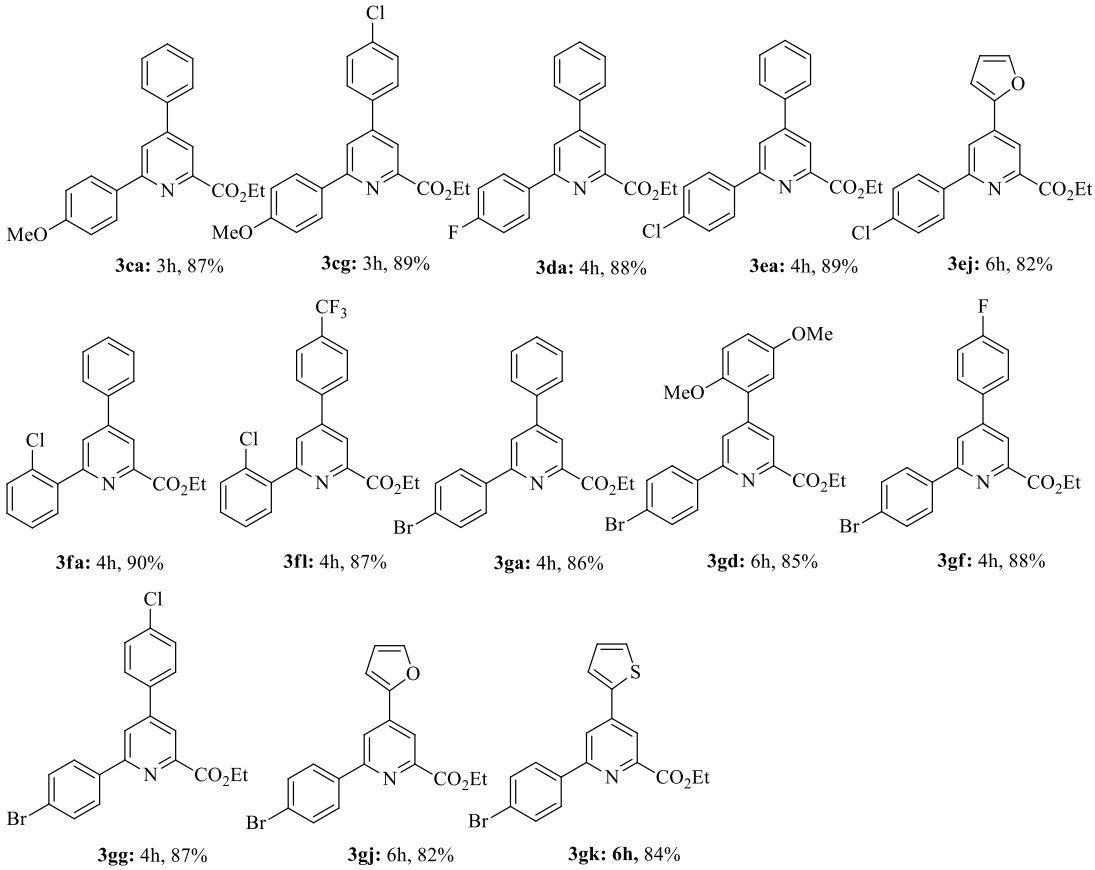
3af: 2.5h, 93% **3ag:** 2.5h, 91% **3ah:** 2.5h, 90% **3ai:** 3h, 87% **3aj:** 5h, 85%



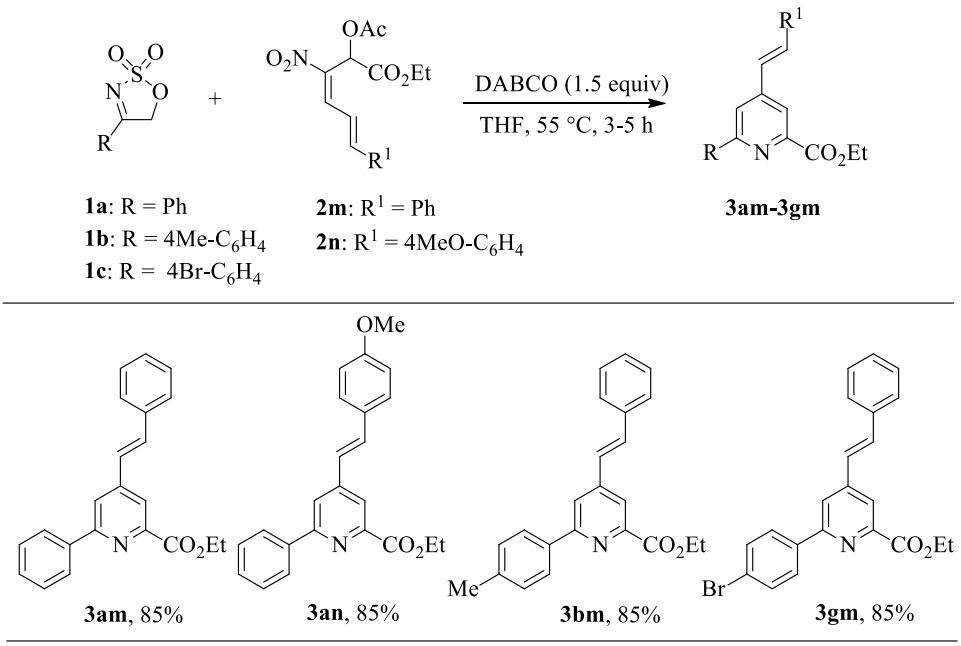
3ak: 5h, 86% **3ba:** 3h, 91% **3bb:** 3h, 90% **3bc:** 4h, 87% **3bd:** 5h, 85%



3be: 5h, 84% **3bf:** 3h, 90% **3bg:** 3h, 88% **3bj:** 5h, 84% **3bk:** 5h, 83%



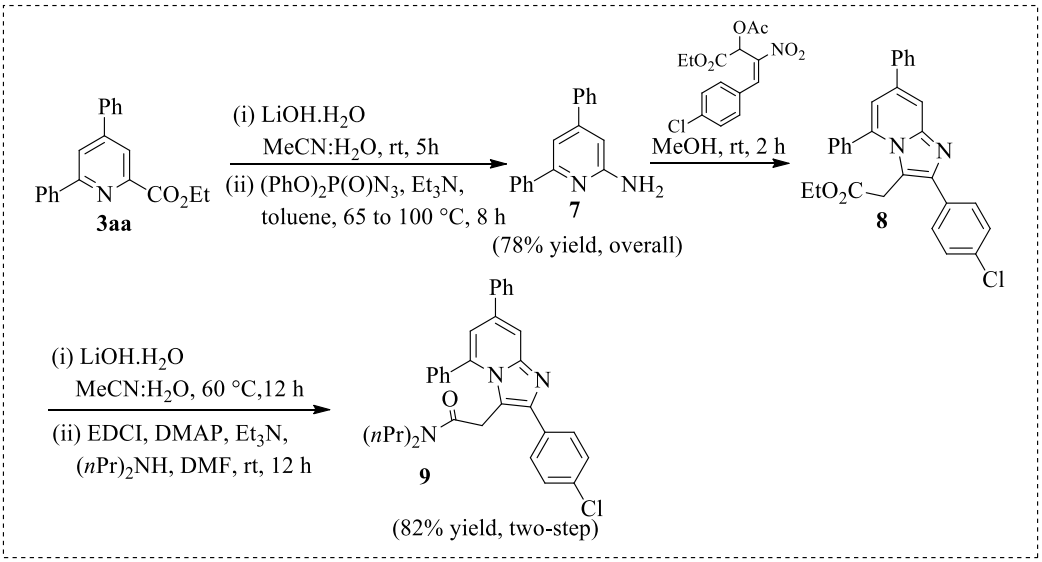
To explore the further possible substrate scope, we employed more chemically challenging MBH acetates of nitrodienes **2m-n** as acceptors in the domino reaction with a variety of 4-aryl-substituted cyclic sulfamidate imines **1a-g** under the present conditions. Interestingly, the cyclic imines **1a, 1b** and **1g** attacked nitrodienes **2m** and **2 n** exclusively at the β-position by this current procedure. As a consequence, high yields (79-85%) of the corresponding 6-aryl-(*E*)-4-styryl-substituted picolinates **3am-gm** were obtained as shown in **Scheme 4.11**. To our best knowledge this is the first successful synthetic protocol for access to (*E*)-4-styrylpicolinates in a one-pot manner including transition-metal salt mediated reactions.



Scheme 4.11 One pot synthesis of (*E*)-6 aryl-4-styryl-substituted picolinates

4.3.1.4 Synthesis of 2-(2-(4-Chlorophenyl)-5,7-diphenylimidazo [1,2-*a*]pyridin-3-yl)-*N*,*N*-dipropylacetamide

To show the potential utility of our current methodology, the synthesized picolinates **3aa** was further transformed into a synthetically as well as pharmaceutically useful 2-aminopyridine **7** in 78% combined yield (two steps) *via* a hydrolysis of ester group of **3aa** by using LiOH in MeCN/H_2O at room temperature, followed by *in-situ* azidonation/Curtius rearrangement/ hydrolysis of resultant picolinic acid in the presence of $(PhO)_2P(O)N_3/Et_3N$ in toluene under heating conditions. Furthermore, the resultant 2-amino-4,6-diphenylpyridine **(7)** was subjected to the reaction with MBH acetate **2g** in MeOH, providing a biologically attractive imidazo[1,2-*a*]pyridine derivative **8**[44-45] in 81% yield. Finally, anxiolytic drug alpidem derivative **9**[46] was synthesized in high yield (82%, two-step) *via* a hydrolysis of ester group of **8**, followed by amidation reaction of the resultant acid with dipropylamine using EDCI/DMAP as an efficient amide bond coupling reagent which is depicted in **Scheme 4.12**.



Scheme 4.12 Synthesis of 2-amino-4,6-diphenylpyridine (**7**) and Alpidem derivative (**9**)

4.4 Conclusion

In this work, we have developed a first, simple, convenient, metal-free, and general new domino synthetic technique for the rapid access to an important class of 4,6-diarylpicolinates from several 4-aryl-5*H*-1,2,3-oxathiazole-2,2-dioxides and MBH acetates of nitroalkenes/nitrodienes in the presence of DABCO as a cheap organobase under heating conditions. Moreover, this metal-free domino technique delivers high to excellent yields of above title compounds and excels for a wide range of sensitive functional groups. Furthermore, high yield of anxiolytic drug alpidem derivative has been successfully obtained through our synthetic methodology. Therefore, we believe this new domino method will gain great importance in synthetic organic and medicinal chemistry as a powerful tactic for the access to functionalized picolinates.

4.5 Experimental Section

4.5.1 General Information

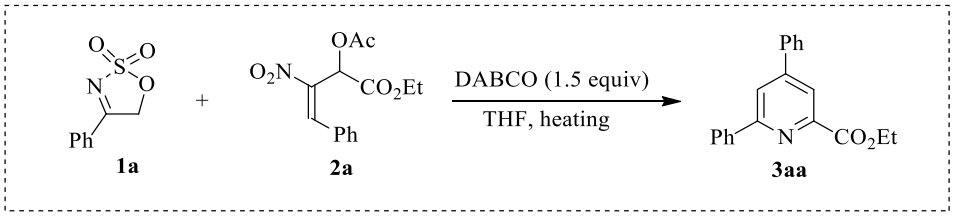
All of the 4-aryl-5*H*-1,2,3-oxathiazole-2,2-doxides **1a-g**[47] and MBH acetates of nitroolefins/nitrodienes **2a-l**[48] were synthesized by known literature procedures. All of the catalysts were purchased from commercial sources. All reactions were carried out either under inert atmosphere or air and monitored by TLC using Merck 60 F_{254} pre coated silica gel plates (0.25 mm thickness) and the products were visualized by UV detection. Flash chromatography was carried out with silica gel (200-300 mesh). FT-IR spectra were recorded on a BrukerTensor-27 spectrometer. ^{1}H and ^{13}C NMR spectra were recorded on a Bruker Avance (III) 400 MHz spectrometer. Data for ^{1}H NMR are reported as a chemical shift (δ ppm), multiplicity (s = singlet, d = doublet, t = triplet, q = quartet, m = multiplet), coupling constant *J* (Hz), integration, and assignment, data for ^{13}C are reported as a chemical shift. High resolutions mass spectral analyses (HRMS) were carried out using ESI-TOF-MS. Single crystal X-ray structural studies were performed on a CCD Agilent Technologies (Oxford Diffraction) SUPER NOVA diffractometer. Data were collected at 293(2) K using graphite-monochromoated Mo Kα radiation (λα = 0.71073 Å). The strategy for the data collection was evaluated by using the CrysAlisPro CCD software. The data were collected by the standard 'phi-omega scan techniques, and were scaled and reduced using CrysAlisPro RED software. The structures were solved by direct methods using SHELXS-97 and refined by full matrix least-squares with SHELXL-97, refining on F^2.[49]

4.5.2 Materials

All these starting materials and catalysts were either purchased from commercial sources or synthesized by literature known procedures[50]. All the solvents dried and distilled under reduced pressure before prior used.

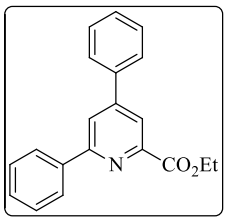
Representative procedure for the synthesis of ethyl 4,6-diphenylpicolinate (3aa):

To a solution of compound **1a** (39.4 mg, 0.2 mmol), **2a** (67.39 mg, 0.22 mmol) and DABCO (33.6 mg, 0.3 mmol) in THF (0.5 mL) was added at room temperature. Then the reaction mixture was heated at 55 °C for 3 h (monitored by TLC). Upon completion of the reaction, the reaction mixture was extracted with ethyl acetate (3 × 10 mL), washed with water and brine respectively, dried with Na_2SO_4 to afford the crude product. Finally it was obtained in a pure form (55.7 mg, 92%) through column chromatography over silica-gel using EtOAc/hexane (1:4, v/v) as the eluent. The product was fully characterized by its spectroscopic data (IR, ^{1}HNMR, ^{13}C NMR and HRMS).



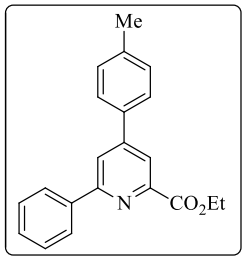
All the synthesized products in **Table 4.2** and **Scheme 4.11** were followed the above procedure. All the products were characterized by their corresponding spectroscopic data (^{1}H, ^{13}C NMR and HRMS).

Ethyl-4,6-diphenylpicolinate (3aa): white solid (55.7 mg, 92%); **mp**: 65-67 °C;

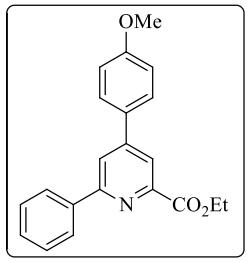


R_f = 0.76 (EtOAc:hexane=1:4); **IR** (KBr): ν 2984, 2932, 2902, 1714, 1600, 1546, 1425, 1372, 1345 cm^{-1}; **^{1}H NMR** (400 MHz, $CDCl_3$): δ 8.28 (s,1H), 8.09-8.13 (m, 3H), 7.73-7.75 (m, 2H), 7.43-7.55 (m, 6H), 4.52 (q, *J* = 7.0 Hz, 2H), 1.48 (t, *J* = 7.0 Hz, 3H); **^{13}C NMR** (100 MHz, $CDCl_3$): δ 165.9, 158.6, 150.7, 149.3, 139.0, 138.1, 129.8, 129.6, 129.1, 127.6, 127.4, 121.8, 121.8 (2C), 62.2, 14.6; **HRMS** (ESI) m/z calculated for $C_{20}H_{17}NO_2[M+H]^+$: 304.1332, found 304.1334.

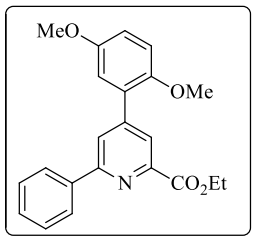
Ethyl-6-phenyl-4-(4-methylphenyl)picolinate (3ab): white solid (57.1 mg, 90%); **mp**: 66-68 °C; $\mathbf{R_f}$ = 0.76 (EtOAc:hexane = 1:4); **IR** (KBr): ν 2994, 2952, 2925, 2901, 2854, 1715, 1601, 1544, 1516, 1451, 1430, 1370, 1345, 1279 cm^{-1}; **^{1}H NMR** (400 MHz, $CDCl_3$): δ 8.27 (s, 1H), 8.11-8.13 (m, 2H), 8.07 (s, 1H), 7.64-7.65 (m, 2H), 7.48-7.52 (m, 2H), 7.42-7.46 (m, 1H), 7.32-7.34 (m, 2H), 4.52 (q, *J* = 7.0 Hz, 2H), 2.43 (s, 3H), 1.49 (t, *J* = 7.0 Hz, 3H); **^{13}C NMR** (100 MHz, $CDCl_3$): δ 165.9, 158.5, 150.5, 149.2, 139.9, 139.0, 135.0, 130.2, 129.6, 129.0, 127.6, 127.2, 121.5, 121.4, 62.1, 21.5, 14.6; **HRMS** (ESI) m/z calculated for $C_{21}H_{19}NO_2[M+H]^+$: 318.1489, found: 318.1492.



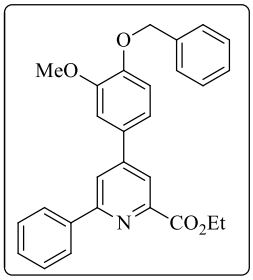
Ethyl-4-(4-methoxyphenyl)-6-phenylpicolinate (3ac): orange solid (59.3 mg, 89%); **mp**: 79-81 °C; $\mathbf{R_f}$ = 0.50 (EtOAc:Hexane = 1:4); **IR** (KBr): ν 2963, 2926, 2853, 1715, 1606, 1544, 1516, 1458, 1433, 1371, 1349, 1255 cm^{-1}. **^{1}H NMR** (400 MHz, $CDCl_3$): δ 8.21 (s, 1H), 8.06-8.08 (m, 2H), 8.00 (s, 1H), 7.65-7.67 (m, 2H), 7.38-7.48 (m, 3H), 6.98-7.00 (m, 2H), 4.48 (q, *J* = 7.0 Hz, 2H), 3.83 (s, 3H), 1.45 (t, *J* = 7.0 Hz, 3H); **^{13}C NMR** (100 MHz, $CDCl_3$): δ 168.0, 161.1, 158.5, 150.0, 149.1, 139.1, 130.1, 129.6, 129.0, 128.6, 127.5, 121.1, 121.0, 114.9, 62.1, 55.8, 14.6; **HRMS** (ESI) m/z calculated for $C_{21}H_{19}NO_3$ $[M+H]^+$: 334.1438, found 334.1439.



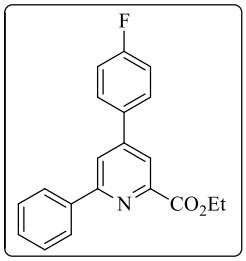
Ethyl-4-(2,5-dimethoxyphenyl)-6-phenylpicolinate (3ad): yellow solid (62.4 mg, 86%); **mp**: 80-82 °C; $\mathbf{R_f}$ = 0.50 (EtOAc:hexane = 1:4); **IR** (KBr): ν 2961, 2928, 2837, 2483, 1719, 1596, 1543, 1503, 1466, 1427, 1368, 1303 cm^{-1}; **^{1}H NMR** (400 MHz, $CDCl_3$): δ 8.21 (s, 1H), 8.07-8.09 (m, 3H), 7.42-7.51 (m, 3H), 6.97-6.98 (m, 3H), 4.50 (q, *J* = 7.0 Hz, 2H), 3.83 (s, 3H), 3.80 (s, 3H), 1.47 (t, *J* = 7.0 Hz, 3H); **^{13}C NMR** (100 MHz, $CDCl_3$): δ 166.0, 157.9, 154.2, 151.1, 148.5, 148.4, 139.2, 129.5, 129.0, 128.4, 127.7, 124.6, 124.3, 116.5, 115.3, 113.2, 62.1, 56.6, 56.2, 14.6; **HRMS** (ESI) m/z calculated for $C_{22}H_{21}NO_4$ $[M+H]^+$: 364.1543, found 364.1548.



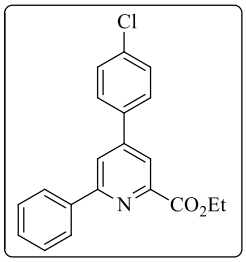
Ethyl-4-(4-(benzyloxy)-3-methoxyphenyl)-6-phenylpicolinate (3ae): light greenish solid (73.7 mg, 84%); **mp**: 83-85 °C; $\mathbf{R_f}$ = 0.43 (EtOAc:hexane = 1:4); **IR** (KBr): ν 2982, 2936, 2871, 2581, 1715, 1593, 1453, 1516, 1468, 1453, 1430, 1384, 1368, 1348, 1264 cm^{-1}; **^{1}H NMR** (400 MHz, $CDCl_3$): δ 8.24 (s, 1H), 8.10-8.12 (m, 2H), 8.03 (s, 1H), 7.47-7.51 (m, 5H), 7.38-7.41 (m, 2H), 7.33-7.35 (m,1H), 7.26 (s, 2H), 7.01-7.03 (m, 2H), 5.24 (s, 2H), 4.53 (q, *J* = 6.8 Hz, 2H), 4.01 (s, 3H), 1.49 (t, *J* = 6.8 Hz, 3H); **^{13}C NMR** (100 MHz, $CDCl_3$): δ 168.0, 158.5, 150.5, 150.4, 149.8, 149.2, 139.2, 137.0, 131.1, 129.7, 129.1, 128.9, 128.3, 127.8, 127.5, 121.4, 121.3, 120.1, 114.4, 110.9, 71.3, 62.2, 56.6, 14.8; **HRMS** (ESI) m/z calculated for $C_{28}H_{25}NO_4$ $[M+H]^+$: 440.1856, found 440.1857.



Ethyl-4-(4-fluorophenyl)-6-phenylpicolinate (3af): white solid (59.9 mg, 93%); **mp**: 90-92 °C; $\mathbf{R_f}$ = 0.80 (EtOAc:hexane = 1:4); **IR** (KBr): ν 2994, 2952, 2902, 1714, 1605, 1550, 1512, 1435, 1371, 1345, 1283, 1238 cm^{-1}; **^{1}H NMR** (400 MHz, $CDCl_3$): δ 8.22 (d, *J* = 1.5 Hz, 1H), 8.09-8.12 (m, 2H), 8.02 (d, *J* = 1.5 Hz, 1H), 7.70-7.73 (m, 2H), 7.45-7.52 (m, 3H), 7.19-7.23 (m, 2H), 4.51 (q, *J* = 7.2 Hz, 2H), 1.48 (t, *J* = 7.2 Hz, 3H); **^{13}C NMR** (100 MHz, $CDCl_3$): δ 165.8, 164.0 (J_{C-F} = 248.0 Hz), 158.7, 149.6, 149.3, 138.8, 134.1, 134.1, 129.8, 129.3, 129.2, 129.1, 127.6, 121.6, 121.5, 116.7, 116.5, 62.3, 14.6; **HRMS** (ESI) m/z calculated for $C_{20}H_{16}FNO_2[M+H]^+$: 322.1238, found 322.1241.

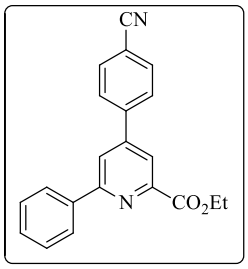


Ethyl-4-(4-chlorophenyl)-6-phenylpicolinate (3ag): light greenish solid; (61.4 mg, 91%); **mp**: 91-93 °C; $\mathbf{R_f}$ = 0.76 (EtOAc:hexane = 1:4); **IR** (KBr): ν 2994, 2950, 2898, 1713, 1602, 1543, 1491, 1432, 1372, 1345 cm^{-1}; **^{1}H NMR** (400 MHz, $CDCl_3$): δ 8.22 (s, 1H), 8.09-8.11 (m, 2H), 8.02 (s, 1H), 7.66-7.67 (m, 2H), 7.44-7.51 (m, 5H), 4.51 (q, *J* = 7.2 Hz, 2H), 1.48 (t, *J* = 7.2 Hz, 3H); **^{13}C NMR** (100 MHz, $CDCl_3$): δ 166.7, 158.7, 149.4 (2C), 138.7, 136.4,

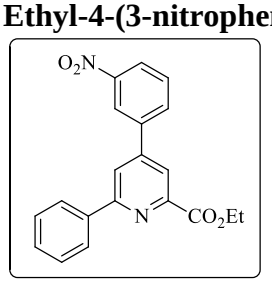


136.0, 129.8, 129.7, 129.1, 128.7, 127.6, 121.5, 121.4, 62.3, 14.6; **HRMS** (ESI) m/z calculated for $C_{20}H_{16}ClNO_2[M+H]^+$: 338.0942, found 338.0938.

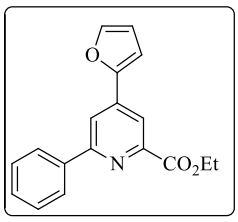
Ethyl-4-(4-cyanophenyl)-6-phenylpicolinate (3ah): white solid (59.1 mg, 90%); **mp**: 105-107 °C; $\mathbf{R_f}$ = 0.46 (EtOAc:hexane = 1:4); **IR** (KBr): ν 2993, 2951, 2900. 2354, 2323, 2225, 1716, 1599, 1543, 1506, 1433 cm^{-1}; **^{1}H NMR** (400 MHz, $CDCl_3$): δ 8.24 (s, 1H), 8.10-8.12 (m, 2H), 8.05 (s, 1H), 7.83 (s, 4H), 7.46-7.52 (m, 3H), 4.52 (q, *J* = 7.2 Hz, 2H), 1.48 (t, *J* = 7.2 Hz, 3H); **^{13}C NMR** (100 MHz, $CDCl_3$): δ 165.5, 159.0, 149.6, 148.7, 142.5, 138.4, 133.3, 130.1, 129.2, 128.2, 127.6, 121.6 (2C), 118.5, 113.5, 62.4, 14.6; **HRMS** (ESI) m/z calculated for $C_{21}H_{16}N_2O_2[M+Na]^+$: 351.1104, found 3351.1106.



Ethyl-4-(3-nitrophenyl)-6-phenylpicolinate (3ai): white solid (60.6 mg, 87%) ; **mp** 110-112 °C; $\mathbf{R_f}$ = 0.43 (EtOAc:hexane = 1:4); **IR** (KBr): ν 2984, 2929, 2871, 1723, 1599, 1531, 1443, 1423, 1350 cm^{-1}; **^{1}H NMR** (400 MHz, $CDCl_3$): δ 8.60 (s, 1H), 8.34-8.37 (m, 1H), 8.29 (s, 1H), 8.11-8.15 (m, 3H), 8.06-8.08 (m, 1H), 7.72-7.76 (m, 1H), 7.46-7.55 (m, 3H), 4.54 (q, *J* = 7.2 Hz, 2H), 1.50 (t, *J* = 7.2 Hz, 3H); **^{13}C NMR** (100 MHz, $CDCl_3$): δ 165.5, 159.2, 149.8, 149.3, 148.2, 139.9, 138.5, 133.4, 130.7, 130.2, 129.3, 127.7, 124.4, 122.5, 121.6 (2C), 62.5, 14.7; **HRMS** (ESI) m/z calculated for $C_{20}H_{16}N_2O_4[M+Na]^+$: 371.1002, found 371.1027.

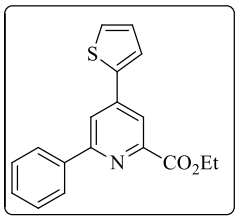


Ethyl-4-(2-furyl)-6-phenylpicolinate (3aj): white solid; (49.8 mg, 85%); **mp**: 69-71 °C; $\mathbf{R_f}$ = 0.66 (EtOAc:hexane = 1:4); **IR** (KBr): ν 2973, 2926, 2905, 2858, 1735, 1612, 1568, 1551, 1489, 1451, 1428, 1368, 1341, 1247 cm^{-1}; **^{1}H NMR** (400 MHz, $CDCl_3$): δ 8.23-8.24 (m, 1H), 8.09-8.11 (m, 3H), 7.57-7.58 (m, 1H), 7.42-7.51 (m, 3H), 7.00 (d, *J* = 3.5 Hz, 1H), 6.55-6.56 (m, 1H), 4.50 (q, *J* = 7.0 Hz, 2H), 1.48 (t, *J* = 7.0 Hz, 3H); **^{13}C NMR** (100 MHz, $CDCl_3$): δ 165.7, 158.6, 151.1, 149.2, 144.4, 139.5, 138.8, 129.7, 129.0, 127.5, 117.9, 117.4, 112.6, 109.8,

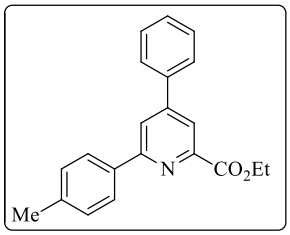


62.2, 14.6; **HRMS** (ESI) m/z calculated for $C_{18}H_{15}NO_3$ $[M+H]^+$: 294.1125, found 294.1128.

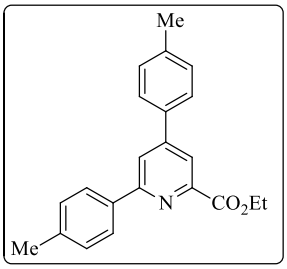
Ethyl-6-phenyl-4-(2-thiophenyl)picolinate (3ak): yellow powder (53.2 mg, 86%); **mp**: 75-77 °C; $\mathbf{R_f}$ = 0.66 (EtOAc:hexane = 1:4); IR (KBr): ν 2975, 2924, 2901, 1737, 1597, 1552, 1477, 1432, 1367, 1321, 1235, 1212 cm^{-1}; **^{1}H NMR** (400 MHz, $CDCl_3$): δ 8.23-8.24 (m, 1H), 8.08-8.10 (m, 2H), 8.02-8.03 (m, 1H), 7.63-7.64 (m, 1H), 7.45-7.52 (m, 4H), 7.16-7.18 (m, 1H), 4.51 (q, *J* = 7.0 Hz, 2H), 1.48 (t, *J* = 7.0 Hz, 3H); **^{13}C NMR** (100 MHz, $CDCl_3$): δ 165.7, 158.8, 149.4, 143.6, 140.9, 138.7, 129.8, 129.1, 128.8, 128.0, 127.5, 126.3, 119.9, 119.7, 62.3, 14.6; **HRMS** (ESI) m/z calculated for $C_{18}H_{15}NO_2S[M+H]^+$: 310.0896, found 310.0904.



Ethyl-4-phenyl-6-(4-methylphenyl)picolinate (3ba): light yellowish solid (57.7 mg, 91%); **mp**: 63-65 °C; $\mathbf{R_f}$ = 0.76 (EtOAc:hexane = 1:4); **IR** (KBr): ν 2976, 2923, 2855, 1732, 1600, 1543, 1367, 1238 cm^{-1}; **^{1}H NMR** (400 MHz, $CDCl_3$): δ 8.11 (s, 1H), 7.89-7.92 (m, 3H), 7.58-7.60 (m, 2H), 7.33-7.40 (m, 3H), 7.16-7.18 (m, 2H), 4.39 (q, *J* = 7.0 Hz, 2H), 2.28 (s, 3H), 1.35 (t, *J* = 7 Hz, 3H); **^{13}C NMR** (100 MHz, $CDCl_3$): δ 165.9, 158.5, 150.5, 149.1, 139.7, 138.0, 136.1, 129.8, 129.6, 129.4, 127.4 (2C),121.4, 121.3, 62.1, 21.6, 14.6; **HRMS** (ESI) m/z calculated for $C_{21}H_{19}NO_2[M+H]^+$: 318.1489, found 318.1492.

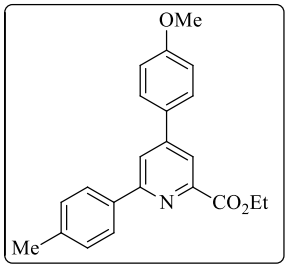


Ethyl-4,6-bis-(4-methylphenyl)picolinate (3bb): pale yellow solid; (59.6 mg, 90%); **mp**: 65-67 °C; $\mathbf{R_f}$ = 0.73 (EtOAc:Hexane = 1:4); IR (KBr): ν 1713, 1600, 1544, 1514, 1435, 1368, 1344, 1257, 1239 cm^{-1}; **^{1}H NMR** (400 MHz, $CDCl_3$): δ 8.24 (d, *J* = 1.7 Hz, 1H), 8.03-8.04 (m, 2H), 8.01 (s, 1H), 7.63-7.65 (m, 2H), 7.29-7.33 (m, 4H), 4.52 (q, *J* = 7.0 Hz, 2H), 2.42 (s, 3H), 2.42 (s, 3H), 1.49 (t, *J* = 7.0 Hz, 3H); **^{13}C NMR** (100 MHz, $CDCl_3$): δ 166.0, 158.5, 150.3, 149.0, 139.8, 139.7, 136.2, 135.1, 130.1, 129.7, 127.4, 127.2,



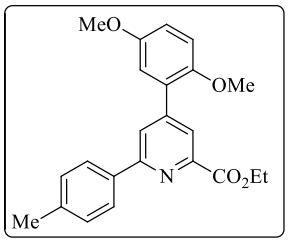
121.2, 121.1, 62.1, 21.5, 21.5, 14.6; **HRMS** (ESI) m/z calculated for $C_{22}H_{21}NO_2[M+H]^+$: 332.1651, found 332.1655.

Ethyl-4-(4-methoxyphenyl)-6-(4-methylphenyl)picolinate (3bc): light



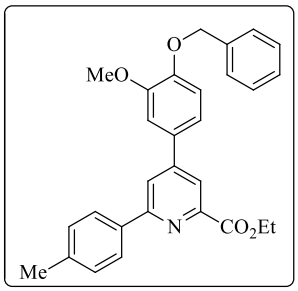
yellowish solid (60.4 mg, 87%); **mp**: 78-80 °C; $\mathbf{R_f}$ = 0.50 (EtOAc:hexane = 1:4); **IR** (KBr): ν 2980, 2903, 1716, 1602, 1543, 1512, 1462, 1434, 1402, 1372, 1348, 1290 cm^{-1}; **^{1}H NMR** (400 MHz, $CDCl_3$): δ 8.21 (s, 1H), 8.02 (s, 3H), 7.68-7.70 (m, 2H), 7.29-7.30 (m, 2H), 7.02-7.04 (m, 2H), 4.51 (q, *J* = 6.8 Hz, 2H), 3.87 (s, 3H), 2.41 (s, 3H), 1.48 (t, *J* = 6.8 Hz, 3H); **^{13}C NMR** (100 MHz, $CDCl_3$): δ 165.1, 160.1, 157.5, 148.9, 148.1, 138.7, 135.3, 129.3, 128.8, 127.6, 126.4, 119.9, 119.7, 113.9, 61.1, 54.7, 20.6, 13.6; **HRMS** (ESI) m/z calculated for $C_{22}H_{21}NO_3[M+H]^+$: 348.1594, found 348.1595.

Ethyl-4-(2,5-dimethoxyphenyl)-6-(4-methylphenyl)picolinate (3bd): light



yellowish solid (64.1 mg, 85%); **mp**: 80-82 °C; $\mathbf{R_f}$ = 0.50 (EtOAc:hexane = 1:4); **IR** (KBr): ν 2987, 2961, 2940, 2906, 2836, 1717, 1638, 1596, 1541, 1468, 1426, 1302, 1256 cm^{-1}; **^{1}H NMR** (400 MHz, $CDCl_3$): δ 8.18 (s, 1H), 8.04 (s, 1H), 7.98-8.00 (m, 2H), 7.28-7.30 (m, 2H), 6.95-6.98 (m, 3H), 4.49 (q, *J* = 6.5 Hz, 2H), 3.82 (s, 3H), 3.79 (s, 3H), 2.41 (s, 3H), 1.46 (t, *J* = 6.5 Hz, 3H); **^{13}C NMR** (100 MHz, $CDCl_3$): δ 166.1, 157.8, 154.2, 151.1, 148.4, 148.2, 139.6, 136.4, 129.7, 128.4, 127.5, 124.2, 124.0, 116.5, 115.2, 113.1, 62.0, 56.6, 56.2, 21.6, 14.6; **HRMS** (ESI) m/z calculated for $C_{23}H_{23}NO_4[M+H]^+$: 378.1700, found 378.1697.

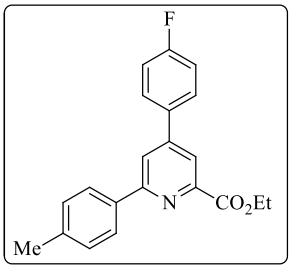
Ethyl-4-(4-benzyloxy-3-methoxyphenyl)-6-(4-methylphenyl)picolinate (3be):



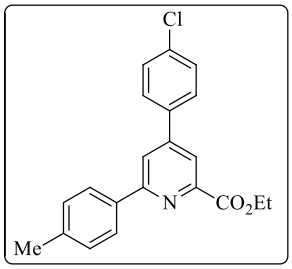
light yellowish solid (76.1 mg, 84%); **mp**: 96-98 °C; $\mathbf{R_f}$ = 0.50 (EtOAc:hexane = 1:4); **IR** (KBr): ν 2855, 1715, 1593, 1540, 1516, 1463, 1433, 1409, 1380, 1348, 1263 cm^{-1}; **^{1}H NMR** (400 MHz, $CDCl_3$): δ 8.11 (s, 1H), 7.94 (s, 1H), 7.91 (s, 2H), 7.38-7.39 (m, 2H), 7.29-7.32 (m,

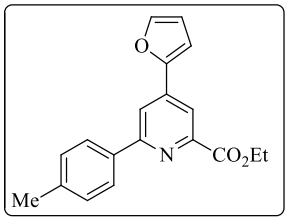
2H), 7.21-7.23 (m, 3H), 7.16-7.17 (m, 2H), 6.91-6.93 (m, 1H), 5.14 (s, 2H), 4.43 (q, J = 7.0 Hz, 2H), 3.91 (s, 3H), 2.33 (s, 3H), 1.40 (t, J = 7.0 Hz, 3H); **^{13}C NMR** (100 MHz, $CDCl_3$): δ 166.0, 158.5, 150.4, 150.2, 149.7, 149.0, 139.7, 136.9, 136.2, 131.1, 129.7, 128.9, 128.2, 127.5, 127.4, 121.1, 121.0, 120.1, 114.4, 110.8, 71.2, 62.1, 56.5, 21.6, 14.6; **HRMS** (ESI) m/z calculated for $C_{29}H_{27}NO_4[M+H]^+$: 454.2013, found 454.2020.

Ethyl-4-(4-fluorophenyl)-6-(4-methylphenyl)picolinate (3bf): white solid (60.5 mg, 90%); **mp**: 88-90 °C; **R_f** = 0.80 (EtOAc:hexane = 1:4); **IR** (KBr): ν 2989, 2923, 2860, 1712, 1603, 1548, 1510, 1437, 1372, 1345, 1241 cm^{-1}; **^{1}H NMR** (400 MHz, $CDCl_3$): δ 8.17 (s, 1H), 7.99-8.01 (m, 3H), 7.67-7.70 (m, 2H), 7.27-7.29 (m, 2H), 7.17-7.21 (m, 2H), 4.50 (q, J = 7.0 Hz, 2H), 2.40 (s, 3H), 1.47 (t, J = 7.0 Hz, 3H); **^{13}C NMR** (100 MHz, $CDCl_3$): δ 165.8, 163.9 (J_{C-F} = 248.0 Hz) 158.6, 149.4, 149.2, 139.9, 135.9, 134.2, 134.1, 129.8, 129.2 (2C), 127.4, 121.2, 121.0, 116.6, 116.4, 62.2, 21.5, 14.6; **HRMS** (ESI) m/z calculated for $C_{21}H_{18}FNO_2[M+H]^+$: 336.1394, found 336.1392.

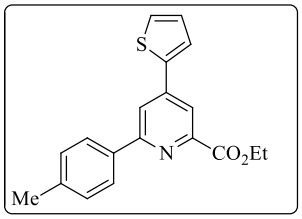


Ethyl-4-(4-chlorophenyl)-6-(4-methylphenyl)picolinate (3bg): light yellowish solid (61.9 mg, 88%); **mp**: 90-92 °C; **R_f** = 0.76 (EtOAc: hexane = 1:4); **IR** (KBr): ν 2976, 2925, 2858, 1724, 1600, 1542, 1491, 1441, 1366, 1242, 1165, 1089, 1021 cm^{-1}; **^{1}H NMR** (400 MHz, $CDCl_3$): δ 8.18 (s, 1H), 8.01 (s, 1H), 7.99 (s, 2H), 7.64-7.66 (m, 2H), 7.47-7.49 (m, 2H), 7.28-7.30 (m, 2H), 4.51 (q, J = 7.0 Hz, 2H), 2.41 (s, 3H), 1.47 (t, J = 7.0 Hz, 3H); **^{13}C NMR** (100 MHz, $CDCl_3$): δ 165.8, 158.7, 149.2 (2C), 139.9, 136.5, 135.9, 135.9, 129.8, 129.7, 128.6, 127.4, 121.1, 121.0, 62.2, 21.6, 14.6; **HRMS** (ESI) m/z calculated for $C_{21}H_{18}ClNO_2[M+H]^+$: 352.1099, found 352.1100.

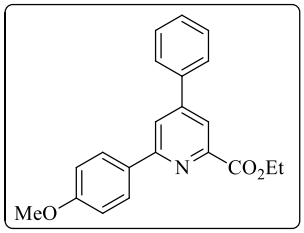


Ethyl-4-(2-furyl)-6-(4-methylphenyl)picolinate (3bj): gummy liquid (51.6 mg, 84%); 

R_f = 0.66 (EtOAc:hexane = 1:4); **IR** (KBr): ν 2922, 2853, 1719, 1609, 1548, 1486, 1431, 1371 cm^{-1}; **^{1}H NMR** (400 MHz, $CDCl_3$): δ 8.21 (d, *J* = 1.5 Hz, 1H), 8.09 (d, *J* = 1.3 Hz, 1H), 8.00-8.02 (m, 2H), 7.57-7.58 (m, 1H), 7.28-7.30 (m, 2H), 7.00-7.01 (m, 1H), 6.55-6.57 (m 1H), 4.50 (q, *J* = 7.2 Hz, 2H), 2.41 (s, 3H), 1.48 (t, *J* = 7.2 Hz, 3H); **^{13}C NMR** (100 MHz, $CDCl_3$): δ 165.8, 158.6, 151.3, 149.1, 144.4, 139.9, 139.5, 136.0, 129.8, 127.4, 117.7, 117.1, 112.6, 109.8, 62.2, 21.6, 14.6; **HRMS** (ESI) m/z calculated for $C_{19}H_{17}NO_3[M+H]^+$: 308.1281, found 308.1286.

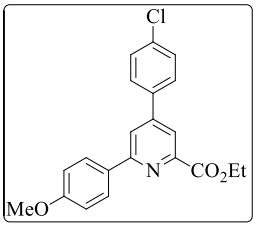
Ethyl-4-(2-thiophenyl)-6-(4-methylphenyl)picolinate (3bk): yellow powder (53.6 mg, 83%); 

mp: 80-82 °C; **R_f** = 0.76 (EtOAc:hexane = 1:4); **IR** (KBr): ν 2923, 2855, 1736, 1593, 1548, 1420, 1366, 1320, 1237 cm^{-1}; **^{1}H NMR** (400 MHz, $CDCl_3$): δ 8.20 (d, *J* = 1.2 Hz, 1H), 7.98-8.00 (m, 3H), 7.62 (d, *J* = 3.8 Hz, 1H), 7.44 (d, *J* = 5.2 Hz, 1H), 7.28-7.31 (m, 2H), 7.14-7.16 (m, 1H), 4.51 (q, *J* = 7.0 Hz, 2H), 2.41 (s, 3H), 1.48 (t, *J* = 7.0 Hz, 3H); **^{13}C NMR** (100 MHz, $CDCl_3$): δ 165.8, 158.7, 149.2, 143.5, 141.0, 139.9, 135.9, 129.8, 128.8, 127.8, 127.4, 126.2, 119.6, 119.4, 62.2, 21.6, 14.6; **HRMS** (ESI) m/z calculated for $C_{19}H_{17}NO_2S[M+H]^+$: 324.1053, found 324.1057.

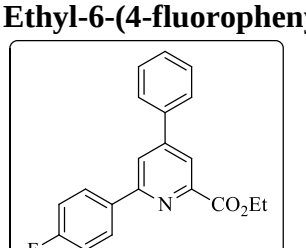
Ethyl-6-(4-methoxyphenyl)-4-phenylpicolinate (3ca): yellow powder (53.3 mg, 87%); 

mp: 77-79 °C; **R_f** = 0.50 (EtOAc:hexane = 1:4); **IR** (KBr): ν 2970, 2926, 2852, 1734, 1601, 1543, 1515, 1451, 1415, 1366, 1345, 1234 cm^{-1}; **^{1}H NMR** (400 MHz, $CDCl_3$): δ 8.18 (s, 1H), 8.06 (d, *J* = 8.2 Hz, 2H), 7.99 (s, 1H), 7.68-7.70 (m, 2H), 7.44-7.50 (m, 3H), 6.98 (d, *J* = 8.7 Hz, 2H), 4.48 (q, *J* = 7.0 Hz, 2H), 3.83 (s, 3H), 1.45 (t, *J* = 7.0 Hz, 3H); **^{13}C NMR** (100 MHz, $CDCl_3$): δ 165.9, 161.1, 158.2, 150.5, 149.0, 138.1, 131.5, 129.6, 129.4, 128.9, 127.4, 121.1, 120.9, 114.4, 62.1, 55.6, 14.6; **HRMS** (ESI) m/z calculated for $C_{21}H_{19}NO_3[M+H]^+$: 334.1438, found 334.1444.

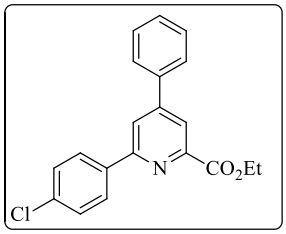
Ethyl-4-(4-chlorophenyl)-6-(4-methoxyphenyl)picolinate (3cg): yellowish solid (65.5 mg, 89%); **mp**: 92-94 °C; $\mathbf{R_f}$ = 0.50 (EtOAc: hexane = 1:4); **IR** (KBr): ν 2988, 2960, 2936, 2901, 1730, 1601, 1543, 1516, 1487, 1462, 1421, 1366, 1347, 1311 cm^{-1} ; **^{1}H NMR** (400 MHz, $CDCl_3$): δ 8.15 (s, 1H), 8.06-8.08 (m, 2H), 7.96 (s, 1H), 7.64-7.66 (m, 2H), 7.47-7.49 (m, 2H), 7.00-7.02 (m, 2H), 4.50 (q, *J* = 7.0 Hz, 2H), 3.86 (s, 3H), 1.47 (t, *J* = 7.0 Hz, 3H); **^{13}C NMR** (100 MHz, $CDCl_3$): δ 165.8, 161.2, 158.3, 149.2 (2C), 136.6, 135.9, 131.3, 129.7, 128.9, 128.7, 120.8, 120.6, 114.5, 62.2, 55.6, 14.6; **HRMS** (ESI) m/z calculated for $C_{21}H_{18}ClNO_3[M+Na]^+$: 390.0867, found 390.0882.



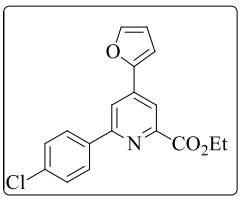
Ethyl-6-(4-fluorophenyl)-4-phenylpicolinate (3da): orange solid; (56.5 mg,88%); **mp**: 91-93 °C; $\mathbf{R_f}$ = 0.76 (EtOAc:hexane = 1:4); **IR** (KBr): ν 2989, 2920, 2856, 1711, 1602, 1547, 1510, 1447, 1419, 1372, 1344, 1259 cm^{-1}; **^{1}H NMR** (400 MHz, $CDCl_3$): δ 8.27 (s, 1H), 8.10-8.13 (m, 2H), 8.03 (s, 1H), 7.72-7.74 (m, 2H), 7.47-7.55 (m, 3H), 7.16-7.20 (M, 2H), 4.51 (q, *J* = 7.0 Hz, 2H), 1.48 (t, *J* = 7.0 Hz, 3H); **^{13}C NMR** (100 MHz, $CDCl_3$): δ 165.8, 164.2 (J_{C-F} = 248.0 Hz) 157.6, 150.9, 149.3, 137.9, 135.2, 129.8, 129.6, 129.5, 127.4, 121.8, 121.4, 116.2, 116.0, 62.3, 14.7; **HRMS** (ESI) m/z calculated for $C_{20}H_{16}FO_2[M+H]^+$: 322.1238, found 322.1233.



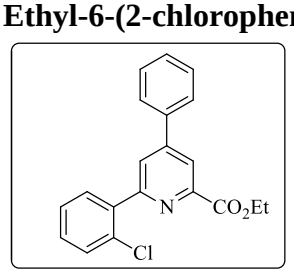
Ethyl-6-(4-chlorophenyl)-4-phenylpicolinate (3ea): pale yellow solid; (60.1 mg, 89%); **mp**: 85-87 °C; $\mathbf{R_f}$ = 0.83 (EtOAc:Hexane = 1:4); **IR** (KBr): ν 2983, 2959, 2855, 1725, 1598, 1546, 1490, 1444, 1406, 1369, 1345, 1242 cm^{-1}; **^{1}H NMR** (400 MHz, $CDCl_3$): δ 8.27 (s, 1H), 8.06-8.08 (m, 3H), 7.71-7.73 (m, 2H), 7.45-7.54 (m, 5H), 4.51 (q, *J* = 7.0 Hz, 2H), 1.48 (t, *J* = 7.0 Hz, 3H); **^{13}C NMR** (100 MHz, $CDCl_3$): δ 165.7, 157.3, 150.9, 149.3, 137.8, 137.3, 135.9, 129.8, 129.5, 129.3, 128.8, 127.4, 122.0, 121.4, 62.2, 14.6; **HRMS** (ESI) m/z calculated for $C_{20}H_{16}ClNO_2[M+H]^+$: 338.0942, found 338.0945.



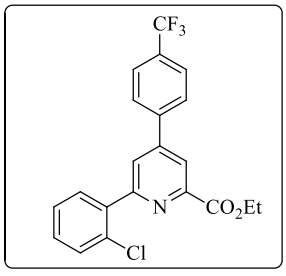
Ethyl-6-(4-chlorophenyl)-4-(2-furyl)picolinate (3ej): pale yellow solid; (53.7 mg, 82%); **mp**: 89-91 °C; $\mathbf{R_f}$ = 0.83 (EtOAc:Hexane = 1:4); **IR** (KBr): ν 2980, 2960, 2925, 2853, 1721, 1610, 1547, 1491, 1368, 1342, 1244 cm^{-1}; **^{1}H NMR** (400 MHz, $CDCl_3$): δ 8.22 (s, 1H), 8.03-8.06 (m, 3H), 7.58-7.59 (m, 1H), 7.44-7.46 (m, 2H), 7.01-7.02 (m, 1H), 6.56-6.57 (m, 1H), 4.50 (q, *J* = 7.0 Hz, 2H), 1.47 (t, *J* = 7.0 Hz, 3H); **^{13}C NMR** (100 MHz, $CDCl_3$): δ 165.8, 157.3, 151.0, 149.2, 144.6, 139.7, 137.2, 136.0, 129.2, 128.8, 118.2, 117.1, 112.7, 110.1, 62.3, 14.6; **HRMS** (ESI) m/z calculated for $C_{18}H_{14}ClNO_3[M+H]^+$: 328.0735, found 328.0751.



Ethyl-6-(2-chlorophenyl)-4-phenylpicolinate (3fa): white solid; (60.8 mg, 90%); **mp**: 90-92 °C; $\mathbf{R_f}$ = 0.66 (EtOAc:Hexane = 1:4); **IR** (KBr): ν 2991, 2960, 2942, 2901, 1718, 1640, 1601, 1548, 1499, 1479, 1447, 1425, 1386, 1368, 1343, 1288, 1237 cm^{-1}; **^{1}H NMR** (400 MHz, $CDCl_3$): δ 8.35 (s, 1H), 8.05 (s, 1H), 7.71-7.74 (m, 3H), 7.48-7.54 (s, 4H), 7.34-7.41 (m, 2H), 4.52 (q, *J* = 6.5 Hz, 2H), 1.48 (t, *J* = 6.5 Hz, 3H); **^{13}C NMR** (100 MHz, $CDCl_3$): δ 165.7, 157.9, 149.6, 149.3, 138.9, 137.7, 132.6, 132.3, 130.4, 130.3, 129.8, 129.5, 127.5, 127.5, 126.2, 122.1, 62.3, 14.7; **HRMS** (ESI) m/z calculated for $C_{20}H_{16}ClNO_2[M+H]^+$: 338.0942, found 338.0943.

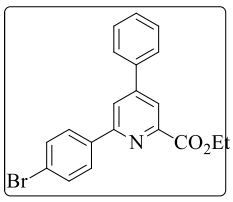


Ethyl-6-(2-chlorophenyl)-4-(4-trifluoromethylphenyl)picolinate (3fl): pale yellow solid; (70.6 mg, 87%); **mp**: 99-101 °C; $\mathbf{R_f}$ = 0.56 (EtOAc:Hexane = 1:4); **IR** (KBr): ν 2989, 2924, 2854, 1715, 1605, 1546, 1378, 1327, 1256 cm^{-1}; **^{1}H NMR** (400 MHz, $CDCl_3$): δ 8.34 (d, *J* = 1.4 Hz, 1H), 8.06 (d, *J* = 1.4 Hz, 1H), 7.77-7.85 (m, 4H), 7.71-7.74 (m, 1H), 7.48-7.50 (m, 1H), 7.35-7.42 (m, 2H), 4.52 (q, *J* = 7.0 Hz, 2H), 1.46 (t, *J* = 7.0 Hz, 3H); **^{13}C NMR** (100 MHz, $CDCl_3$): δ 165.4, 158.1, 149.5, 148.2, 141.2, 141.2, 138.5, 132.5, 132.3,131.6, 130.5, 130.4, 128.0, 127.6, 126.6, 126.5, 126.5, 126.5, 126.5,

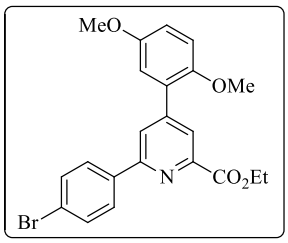


125.5, 122.8, 122.1, 62.5, 14.6; **HRMS** (ESI) m/z calculated for $C_{21}H_{15}ClF_3NO_2[M+H]^+$: 406.0816, found 406.0819.

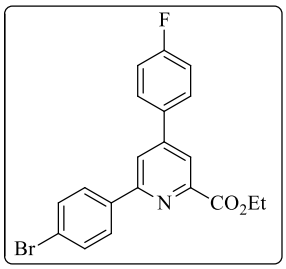
Ethyl-6-(4-bromophenyl)-4-phenylpicolinate (3ga): light green solid; (65.7 mg, 86%); **mp**: 93-95 °C; $\mathbf{R_f}$ = 0.83 (EtOAc:Hexane = 1:4); **IR** (KBr): ν 2982, 2926, 2901, 2854, 1727, 1596, 1548, 1488, 1442, 1405, 1369, 1345 cm^{-1}; **^{1}H NMR** (400 MHz, $CDCl_3$): δ 8.28 (s, 1H), 8.04 (s, 1H), 7.99-8.01 (m, 2H), 7.72-7.73 (m, 2H), 7.61-7.63 (m, 2H), 7.47-7.55 (m, 3H), 4.51 (q, *J* = 7.0 Hz, 2H), 1.48 (t, *J* = 7.0 Hz, 3H); **^{13}C NMR** (100 MHz, $CDCl_3$): δ 165.7, 157.3, 150.9, 149.3, 137.8, 137.8, 132.2, 129.9, 129.5, 129.1, 127.4, 124.3, 122.1, 121.4, 62.3, 14.6; **HRMS** (ESI) m/z calculated for $C_{20}H_{16}{}^{79}BrNO_2[M+H]^+$: 382.0437, found 382.0457; **HRMS** (ESI) m/z calculated for $C_{20}H_{16}{}^{81}BrNO_2[M+H]^+$: 384.0418, found 384.0434.



Ethyl-6-(4-bromophenyl)-4-(2,5-dimethoxyphenyl)picolinate (3gd): orange solid; (75.2 mg, 85%) ; **mp**: 99-101 °C; $\mathbf{R_f}$ = 0.50 (EtOAc:hexane = 1:4); **IR** (KBr): ν 2960, 2933, 2834, 1734, 1639, 1598, 1545, 1495, 1462, 1421, 1400, 1371, 1339, 1301, 1278, 1249 cm^{-1}; **^{1}H NMR** (400 MHz, $CDCl_3$): δ 8.21 (s, 1H), 8.03 (s, 1H), 7.96-7.98 (m, 2H), 7.59-7.62 (m, 2H), 6.96-6.97 (m, 3H), 4.49 (q, *J* = 7.2 Hz, 2H), 3.82 (s, 3H), 3.79 (s, 3H), 1.46 (t, *J* = 7.0 Hz, 3H); **^{13}C NMR** (100 MHz, $CDCl_3$): δ 165.8, 156.6, 154.2, 151.0, 148.6, 148.6, 138.0, 132.2, 129.2, 128.1, 124.6, 124.3, 124.1, 116.5, 115.4, 113.1, 62.1, 56.6, 56.2, 14.6; **HRMS** (ESI) m/z calculated for $C_{22}H_{20}{}^{79}BrNO_4[M+H]^+$: 442.0648, found 442.0656; **HRMS** (ESI) m/z calculated for $C_{22}H_{20}{}^{81}BrNO_4[M+H]^+$: 444.0629, found 444.0644.

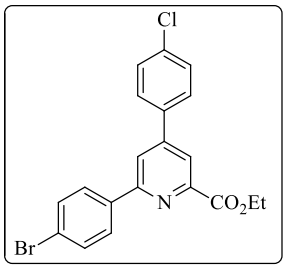


Ethyl-6-(4-bromophenyl)-4-(4-fluorophenyl)picolinate (3gf): pale yellow solid;



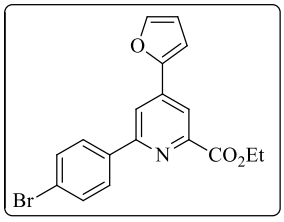
(70.4 mg, 88%); **mp**: 100-102 °C; $\mathbf{R_f}$ = 0.83 (EtOAc:Hexane = 1:4); **IR** (KBr): ν 2987, 2925, 2905, 1717, 1640, 1603, 1549, 1512, 1490, 1439, 1397, 1369, 1345, 1281 cm^{-1}; **^{1}H NMR** (400 MHz, $CDCl_3$): δ 8.22 (s, 1H), 7.98-8.00 (m 3H), 7.69-7.72 (m, 2H), 7.60-7.62 (m, 2H), 7.19-7.23 (m, 2H), 4.51 (q, *J* = 7.0 Hz, 2H), 1.47 (*t*, *J* = 7.0 Hz, 3H); **^{13}C NMR** (100 MHz, $CDCl_3$): δ 165.6, 164.0 (J_{C-F} = 248.0 Hz), 157.4, 149.8, 149.4, 137.7, 133.9, 132.3, 129.3, 129.1, 124.4, 121.8, 121.1, 116.7, 116.5, 62.3, 14.6; **HRMS** (ESI) m/z calculated for $C_{20}H_{15}{}^{79}BrFNO_2[M+H]^+$: 400.0343, found 400.0352; **HRMS** (ESI) m/z calculated for $C_{20}H_{15}{}^{81}BrFNO_2[M+H]^+$: 402.0323, found 402.0337.

Ethyl-6-(4-bromophenyl)-4-(4-chlorophenyl)picolinate (3gg): pale yellow



solid; (72.5 mg, 87%); **mp**: 105-107 °C; $\mathbf{R_f}$ = 0.83 (EtOAc:Hexane = 1:4); **IR** (KBr): ν 2980, 2924, 2855, 1725, 1602, 1543, 1494, 1442, 1368, 1241 cm^{-1}; **^{1}H NMR** (400 MHz, $CDCl_3$): δ 8.22-8.23 (m, 1H), 7.98-8.00 (m, 2H), 7.97 (s, 1H), 7.61-7.67 (m, 4H), 7.49-7.51 (m, 2H), 4.51 (q, *J* = 7.0 Hz, 2H), 1.47 (t, *J* = 7.0 Hz, 3H); **^{13}C NMR** (100 MHz, $CDCl_3$): δ 165.6, 157.5, 149.6, 149.5, 137.6, 136.2, 136.2, 132.3, 129.8, 129.1, 128.7, 124.5, 121.8, 121.1, 62.4, 14.6; **HRMS** (ESI) m/z calculated for $C_{20}H_{15}{}^{79}BrClNO_2[M+H]^+$: 416.0047, found 416.0058; **HRMS** (ESI) m/z calculated for $C_{20}H_{15}{}^{81}BrClNO_2[M+H]^+$: 418.0027, found 418.0037.

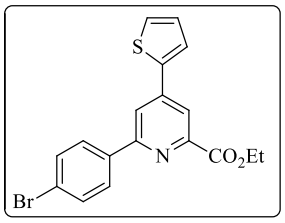
Ethyl-6-(4-bromophenyl)-4-(2-furyl)picolinate (3gi): brown solid; (61.0 mg,



82%); **mp**: 100-102 °C; $\mathbf{R_f}$ = 0.50 (EtOAc:hexane = 1:4); **IR** (KBr): ν 2974, 2925, 2855, 1730, 1609, 1546, 1486, 1418, 1367, 1339, 1241 cm^{-1}; **^{1}H NMR** (400 MHz, $CDCl_3$): δ 8.23 (s, 1H), 8.05 (s, 1H), 7.96-7.98 (m, 2H), 7.59-7.61 (m, 3 H), 7.00-7.01 (m, 1H), 6.56 (s, 1H), 4.50 (q, *J* = 7.2 Hz, 2H), 1.47 (t, *J* = 7.04 Hz, 3H); **^{13}C NMR** (100 MHz, $CDCl_3$): δ 164.5, 156.3, 149.9, 148.2,

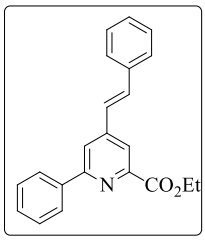
143.5, 138.7, 136.6, 131.1, 128.0, 123.3, 117.1, 116.0, 111.6, 109.1, 61.2, 13.6; **HRMS** (ESI) m/z calculated for $C_{18}H_{14}{}^{79}BrNO_3[M+H]^+$: 372.0230, found 372.0245; **HRMS** (ESI) m/z calculated for $C_{18}H_{14}{}^{81}BrNO_3[M+H]^+$: 374.0210, found 374.0225.

Ethyl-6-(4-bromophenyl)-4-(2-thiophenyl)picolinate (3gk): yellowish solid ;



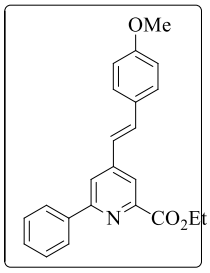
(65.2 mg, 84%); **mp**: 101-103 °C; $\mathbf{R_f}$ = 0.73 (EtOAc:hexane = 1:4); **IR** (KBr): ν 2979, 2925, 2901, 2856, 2360, 2338, 1731, 1598, 1549, 1485, 1443, 1422, 1368, 1323, 1239, 1211 cm^{-1}.**^{1}H NMR** (400 MHz, $CDCl_3$): δ 8.23-8.24 (m, 1H), 7.98-7.99 (m, 2H), 7.96 (s, 1H), 7.63-7.64 (m, 2H), 7.61 (s, 1H), 7.47-7.48 (m, 1H), 7.16-7.19 (m, 1H), 4.51 (q, *J* = 7.0 Hz, 1H), 1.48 (t, *J* = 7.0 Hz, 3H); **^{13}C NMR** (100 MHz, $CDCl_3$): δ 165.6, 157.3, 151.0, 149.3, 144.6, 139.7, 137.6, 132.2, 129.0, 124.3, 118.2, 117.0, 112.7, 110.1, 62.3, 14.6; **HRMS** (ESI) m/z calculated for $C_{18}H_{14}{}^{79}BrNO_2S[M+H]^+$: 388.0001, found 388.0009; **HRMS** (ESI) m/z calculated for $C_{18}H_{14}{}^{81}BrNO_2S[M+H]^+$: 389.9981, found 389.9988.

(*E*)-Ethyl-6-phenyl-4-styrylpicolinate (3am): light yellow liquid; (56.0 mg,

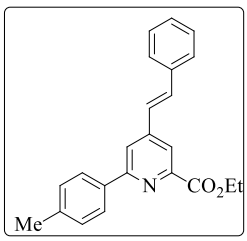


85%); $\mathbf{R_f}$ = 0.80 (EtOAc:Hexane = 1:4); **IR** (KBr): ν 3059, 2980, 1738, 1595, 1546, 1432, 1370, 1252, 1193, 1084, 1025 cm^{-1}; **^{1}H NMR** (400 MHz, $CDCl_3$): δ 8.17 (s, 1H), 8.09 (d, *J* = 7.6 Hz, 2H), 7.91 (s, 1H), 7.58 (d, *J* = 7.6 Hz, 2H), 7.39-7.52 (m, 7H), 7.12-7.18 (m, 1H), 4.52 (q, *J* = 7.2 Hz, 2H), 1.49 (t, *J* = 7.2 Hz, 3H); **^{13}C NMR** (100 MHz, $CDCl_3$): δ 165.7, 158.3, 148.8, 146.6, 138.7, 135.9, 134.1, 129.4, 129.0, 128.9, 128.8, 127.3, 127.1, 125.5, 120.9, 120.3, 61.9, 14.3; **HRMS** (ESI) m/z calculated for $C_{22}H_{19}NO_2[M+H]^+$: 330.1489, found 330.1478.

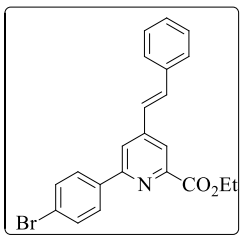
(*E*)-Ethyl-4-(4-methoxystyryl)-6-phenylpicolinate (3an): light yellow gummy liquid; (58.9 mg, 82%); $\mathbf{R_f}$ = 0.65 (EtOAc:hexane = 1:4); **IR** (neat): ν 1738, 1714, 1591, 1579, 1545, 1510, 1435, 1249 cm^{-1}; **^{1}H NMR** (400 MHz, $CDCl_3$): δ 8.07 (s, 1H), 8.01 (d, *J* = 7.6 Hz, 2H), 7.81 (s, 1H), 7.31-7.46 (m, 6H), 6.85-6.95 (m, 2H), 4.43 (q, *J* = 7.2 Hz, 2H), 3.77 (s, 3H), 1.41 (t, *J* = 7.2 Hz, 3H); **^{13}C NMR** (100 MHz, $CDCl_3$): δ 166.1, 160.7, 158.5, 149.0, 147.3, 139.1, 134.0, 129.6, 129.0, 129.0, 128.9, 127.5, 123.5, 120.9, 120.4, 114.7, 62.2, 55.7, 14.7; **HRMS** (ESI) m/z calculated for $C_{23}H_{21}NO_3$ $[M+H]^+$: 360.1594, found 360.1595.



(*E*)-Ethyl-4-styryl-6-(4-methylphenyl)picolinate (3bm): light yellow liquid; (54.9 mg, 80%); $\mathbf{R_f}$ = 0.76 (EtOAc:Hexane = 1:4); **IR** (KBr): ν 3029, 2979, 2855, 1738, 1714, 1636,1596, 1546,1447, 1424, 1253 cm^{-1}; **^{1}H NMR** (400 MHz, $CDCl_3$): δ 8.06 (s, 1H), 7.92 (d, *J* = 7.8 Hz, 2H), 7.81 (s, 1H), 7.49 (d, *J* = 7.8 Hz, 2H), 7.17-7.38 (m, 6H), 7.03-7.07 (m, 1H), 4.43 (q, *J* = 7.0 Hz, 2H), 2.34 (s, 3H), 1.40 (t, *J* = 7.0 Hz, 3H); **^{13}C NMR** (100 MHz, $CDCl_3$): δ 165.8, 158.3, 148.8, 146.5, 139.5, 136.0, 135.9, 134.0, 129.5, 129.0, 128.9, 127.2, 127.1, 125.6, 120.6, 120.0, 61.9, 21.3, 14.4; **HRMS** (ESI) m/z calculated for $C_{23}H_{21}NO_2[M+H]^+$: 344.1645, found 344.1635.

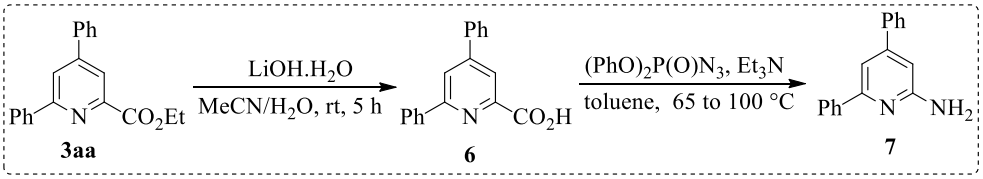


(*E*)-Ethyl-6-(4-bromophenyl)-4-styrylpicolinate (3gm): light yellow gummy liquid; (67.7 mg, 79%); $\mathbf{R_f}$ = 0.73 (EtOAc:hexane = 1:4); **IR** (KBr): ν 3058, 2979, 2923, 1737, 1716, 1635, 1597, 1545, 1491, 1446, 1251 cm^{-1}; **^{1}H NMR** (400 MHz, $CDCl_3$): δ 8.18 (s, 1H), 7.98 (d, *J* = 8.0 Hz, 2H), 7.88 (s, 1H), 7.57-7.63 (m, 4H), 7.35-7.47 (m, 4H), 7.11-7.16 (m, 1H), 4.51 (q, *J* = 7.2 Hz, 2H), 1.48 (t, *J* = 7.2 Hz, 3H); **^{13}C NMR** (100 MHz, $CDCl_3$): δ 165.5, 157.0, 148.9, 146.8, 137.5, 135.8, 134.4, 131.9, 129.1, 128.9, 128.8, 127.2, 125.2, 124.0, 120.5, 62.0, 14.3; **HRMS** (ESI) m/z calculated for $C_{22}H_{18}{}^{79}BrNO_2[M+H]^+$



: 408.0594, found 408.0614; calculated for $C_{22}H_{18}{}^{81}BrNO_2[M+H]^+$: 410.0574, found 410.0607.

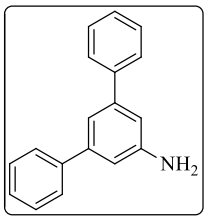
Synthesis of 2-amino-4,6-diphenylpyridine from **3aa** (**7**):



The ethyl 4,6-diphenylpicolinate (**3aa**, 303.3 mg, 1.0 mmol) and $LiOH.H_2O$ (210 mg, 5.0 mmol) in $MeCN/H_2O$ (5.0 ml, 4:1) was taken in a round bottom flask. Then the reaction mixture was allowed to stir for 5 h (monitored by TLC). After completion of the reaction, organic solvent was removed by rotary evaporator and acidified by 1M acetic acid. Then water layer was extracted with ethyl acetate (5 × 10 ml), washed with brine solution and dried with Na_2SO_4. Evaporation of the solvent left the crude 4,6-diphenylpicolinic acid (**6**) which was reasonable pure and directly used for the next step without further purification.

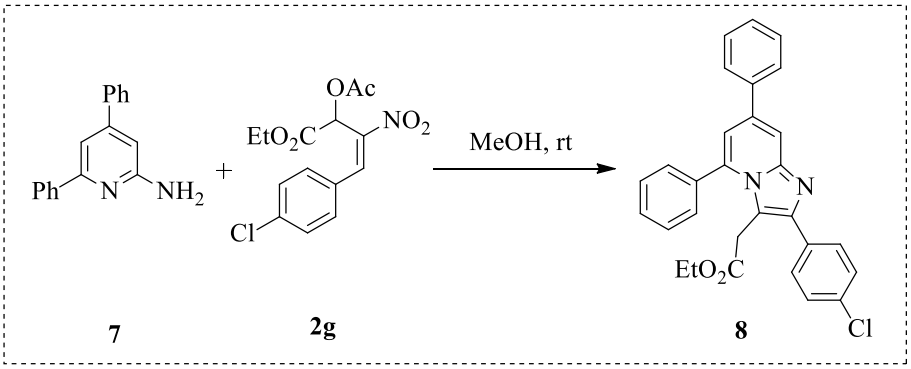
A mixture of above 4,6-diphenylpicolinic acid (**6**), DPPA (385.0 mg, 1.4 mmol), and triethylamine (405.0 mg, 4.0 mmol) in toluene (2.0 ml) was heated at 65 °C for 2 h and then 100 °C for 6 h. After completion of the reaction (monitored by TLC), the reaction mixture was extracted with ethyl acetate (3 × 10 ml) before being quenched with water. The combined organic layer was washed with brine solution and dried over sodium sulphate. Afterwards, the organic phase was concentrated under reduced pressure to furnish the crude product. It was purified by flash chromatography over silica gel using EtOAc/hexane (2:3 v/v) as the eluent to give 4,6-diphenylpyridin-2-amine (**7**) in 78% yield (191.9 mg, overall) as a white solid.

2-Amino-4,6-diphenylpyridine (7):[51] pale yellow solid; $\mathbf{R_f}$ = 0.50 (EtOAc:Hexane = 2:3); **^{1}H NMR** (400 MHz, $CDCl_3$): δ 7.97 (d, *J* = 7.6Hz, 2H), 7.64 (d, *J* = 7.4Hz, 2H), 7.39-7.49 (m, 6H), 7.31 (s, 1H), 6.67 (s, 1H), 4.66 (br s, 2H); **^{13}C NMR** (100 MHz, $CDCl_3$): δ 158.8, 156.5, 151.2, 139.5, 139.0, 128.8, 128.7, 128.7, 128.5, 126.9 (2C), 110.0, 105.1; **HRMS** (ESI) m/z calculated For $C_{17}H_{14}N_2[M+H]^+$: 247.1230; Found 247.1228.

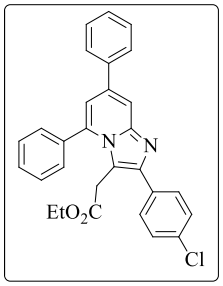


Typical Procedure for the Synthesis of Ethyl 2-(2-(4-Chlorophenyl)-5,7-diphenylimidazo[1,2-*a*]pyridin-3-yl)acetate(8):

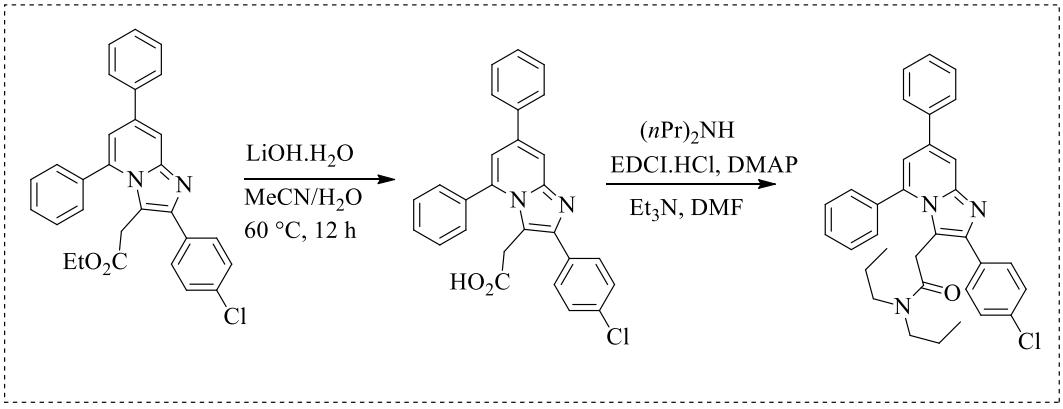
2-Amino-4,6-diphenylpyridine (123.0 mg, 0.5 mmol) and MBH acetate (**2g**, 180.23 mg, 0.55 mmol) were stirred in MeOH (4.0 ml) for 2 h (monitored by TLC). Upon completion of the reaction, the reaction mixture was extracted by ethyl acetate (3 × 10 ml) before being removed MeOH. The combined organic layer was washed with brine solution, dried over sodium sulphate. The organic phase was removed by rotary evaporator to furnish the crude product which was purified by flash chromatography over silica gel (EtOAc/hexane = 2:3 as an eluent) to give ethyl 2-(2-(4-chlorophenyl)-5,7-diphenylimidazo[1,2-*a*]pyridin-3-yl)acetate (**8**, 81%) as yellow solid product.



Ethyl-2-(2-(4-chlorophenyl)-5,7-diphenylimidazo[1,2-*a*]pyridin-3-yl)acetate



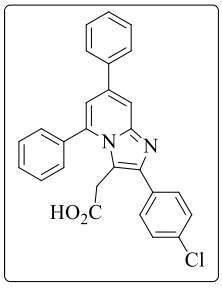
(8): yellow solid; $\mathbf{R_f}$ = 0.45 (EtOAc:hexane = 2:3); (189.0 mg, 81%); **IR** (neat) ν 1731, 1597, 1545, 1487, 1473, 1367, 1254, 1186 cm^{-1}; **^{1}H NMR** (400 MHz, $CDCl_3$): δ 7.92 (s, 1H), 7.69 (d, *J* = 7.6 Hz, 2H), 7.58 (d, *J* = 8.4 Hz, 2H), 7.39-7.54 (m, 10H), 6.96 (s, 1H), 3.89 (q, 7.2 Hz, 2H), 3.54 (s, 2H), 1.10 (t, *J* = 7.2Hz, 3H); **^{13}C NMR** (100 MHz, $CDCl_3$): δ 169.7, 146.9, 146.2, 138.6, 138.3, 137.1, 134.4, 134.0, 132.9, 130.1, 129.9, 129.5, 129.0, 128.7, 128.3, 128.2, 126.7, 115.2, 114.8, 113.5, 61.0, 32.3, 13.9; **HRMS** (ESI) m/z calculated for $C_{29}H_{23}ClN_2O_2$ $[M+H]^+$: 467.1521, found 467.1509.



Lithium hydroxide (126.0 mg, 3.0 mmol) was added to a stirred solution of ethyl 2-(2-(4-chlorophenyl)-5,7-diphenylimidazo[1,2-*a*]pyridin-3-yl)acetate (140.0 mg, 0.3 mmol) in MeCN/H_2O (4.0 mL, 3:1). Afterwards, the reaction mixture was heated at 60 °C for 12 h. After completion of the reaction (monitored by TLC), solvent was removed by rotary evaporator to provide the crude mass which was acidified with 1M acetic acid solution. Then water layer was extracted with ethyl acetate (5 × 10 ml). The combined organic layer was washed with brine, dried over Na_2SO_4. Next the organic phase was evaporated under reduced pressure to obtain the crude product as white solid which was sufficiently pure to carry out next step.

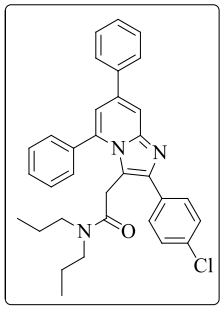
A mixture of imidazopyridine carboxylic acid, EDCI.HCl (0.4 mmol), Et_3N (0.6 mmol), DMAP (0.06 mmol) and N,N-dipropyl amine (0.3 mmol) in DMF (1.0 mL) was stirred at room tem.p.erature under argon atmosphere for 12h (monitored by TLC). After that, the reaction mixture was extracted with ethyl acetate (3 × 10 mL) before being quenched with saturated NH_4Cl solution. Combined rganic layer was washed with brine, dried with Na_2SO_4. Next evaporation of organic slovent left the crude materials which was by column chromatography over silica gel (EtOAc/hexane 1:4 as a mixture of solvent) to furnish the pure product (128.4 mg, 82% yield, two-step) as white solid.

2-(2-(4-Chlorophenyl)-5,7-diphenylimidazo[1,2-a]pyridin-3-yl)acetic acid:



white solid; $\mathbf{R_f}$ = 0.20 (EtOAc:hexane = 3:2); **^{1}H NMR** (400 MHz, DMSO-d_6): δ 7.91 (s, 1H), 7.84 (d, *J* = 7.6 Hz, 2H), 7.76 (d, *J* = 8.4 Hz, 2H), 7.55-7.77 (m, 2H), 7.36-7.57 (m, 8H), 6.90 (s, 1H), 3.04 (s, 2H); **HRMS** (ESI) m/z calculated for $C_{27}H_{19}ClN_2O_2$ $[M+H]^+$: 439.1208, found 439.1226.

2-(2-(4-Chlorophenyl)-5,7-diphenylimidazo[1,2-*a*]pyridin-3-yl)-N,N-



dipropylacetamide (9): yellow solid; $\mathbf{R_f}$ = 0.40 (EtOAc:Hexane = 2:3); **^{1}H NMR** (400 MHz, $CDCl_3$): δ 7.89 (s, 1H), 7.67 (d, *J* = 7.2 Hz, 2H), 7.36-7.58 (m, 12H), 6.89 (s, 1H), 3.49 (s, 2H), 3.09 (t, *J* = 7.2 Hz, 2H), 2.65 (t, *J* = 8.0 Hz, 2H), 1.45-1.51 (m, 2H), 1.19-1.24 (m, 2H), 0.87 (t, *J* = 7.2 Hz, 3H), 0.73 (t, *J* = 7.2 Hz, 3H); **^{13}C NMR** (100 MHz, $CDCl_3$): δ 168.2, 146.9, 145.6, 138.5, 138.4, 136.7, 135.2, 133.6, 133.4, 130.1, 130.0, 129.1, 129.0, 128.5, 128.1, 128.0, 126.7, 116.6, 115.1, 113.6, 49.6, 48.4, 31.5, 21.8, 20.9, 11.5, 11.2; **HRMS** (ESI) m/z calculated for $C_{33}H_{32}ClN_3O$ $[M+H]^+$: 522.2307, found 522.2313.

Table 4.3 Crystal data for compound **3bd**

Compound	**3bd**
Empirical formula	$C_{23}H_{23}NO_4$
Formula weight	377.42
Temperatute	293(2) K
Wave length (Å)	0.71073
Crystal system, space group	MONOCLINIC, P21/c
a (Å)	20.1569(13)
b (Å)	7.4950(6)
c (Å)	13.1446(5)
α (°)	90
β (°)	95.770(7)
γ (°)	90
Volume ($Å^3$)	1975.8(2)
Z, Calculated density (mg/m^3)	4, 1.269
Absorption coefficient (mm^{-1})	0.087
F(000)	800
Crystal size (mm)	0.50 x 0.40 x 0.20
Θ range (deg)	2.90 to 25.00
Limiting indices	-20<=h<=23, -8<=k<=8, -15<=l<=15
Reflections collected / unique	16437 / 3466 [R(int) = 0.0369]
Com.p.leteness to Θ = 25	99.9%
Max. and min. transmission	0.9829 and 0.9579
Absorption correction	Semi-empirical from equivalents
Data / restrains / parameters	3466 / 0 / 257
Goodness-of-fit on F^2	0.773
Final R indices [I>2sigma(I)]	R1 = 0.0586, wR2 = 0.2271
R indices (all data)	R1 = 0.0674, wR2 = 0.2411
Largest diff. peak and hole ($e.A^{-3}$)	0.207 and -0.162
CCDC	**1456731**

4.6 Copies of ^{1}H and ^{13}C NMR spectra of some important compounds described in Chapter 4

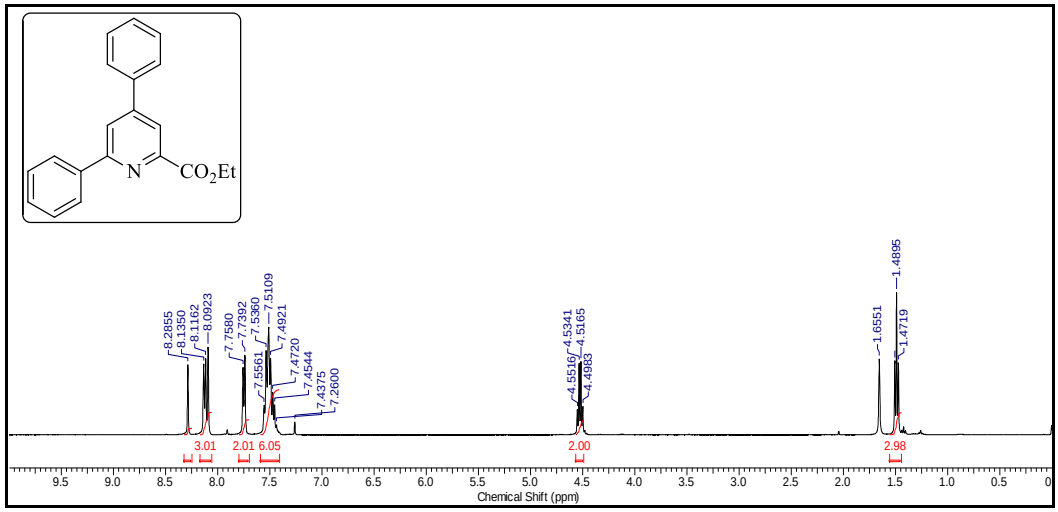


Figure 4.4 400 MHz ^{1}H NMR spectrum of **3aa** in $CDCl_3$

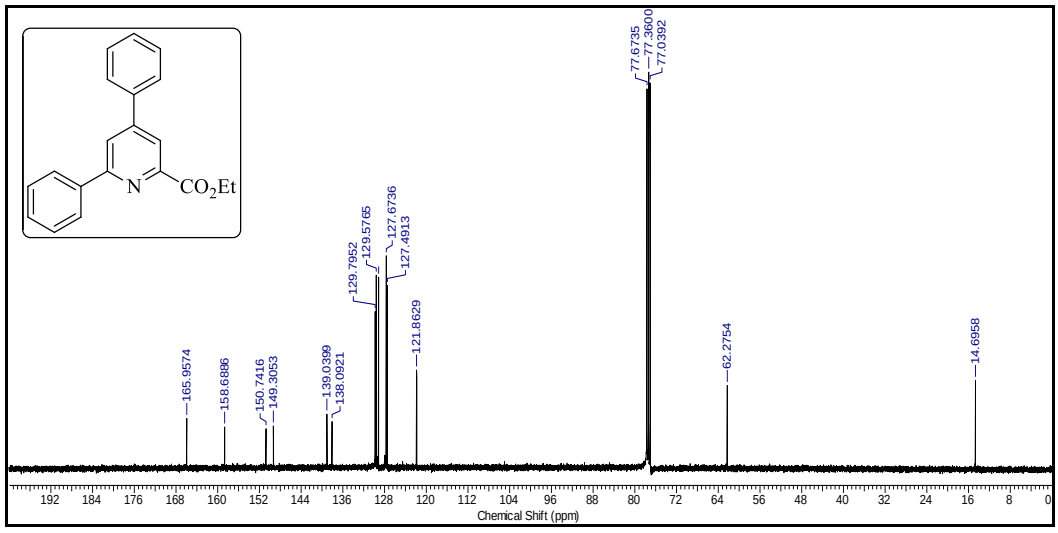


Figure 4.5 100 MHz ^{13}C NMR spectrum of **3aa** in $CDCl_3$

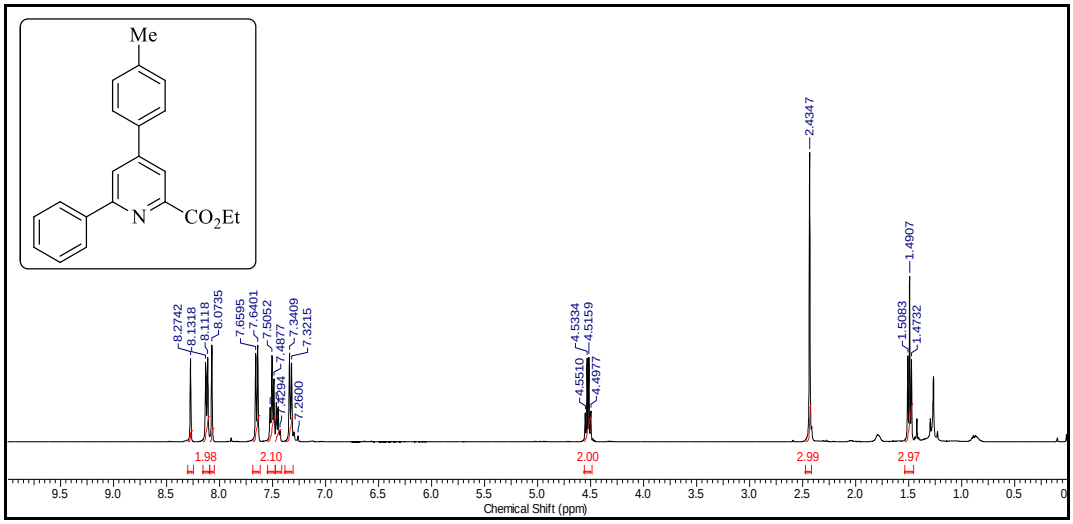


Figure 4.6 400 MHz ^{1}H NMR spectrum of **3ab** in $CDCl_3$

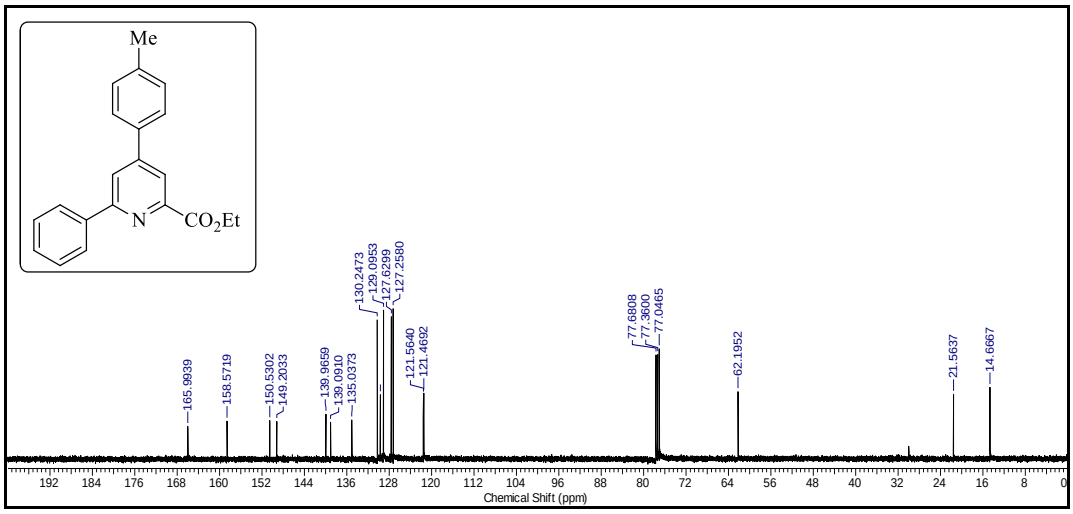


Figure 4.7 100 MHz ^{13}C NMR spectrum of **3ab** in $CDCl_3$

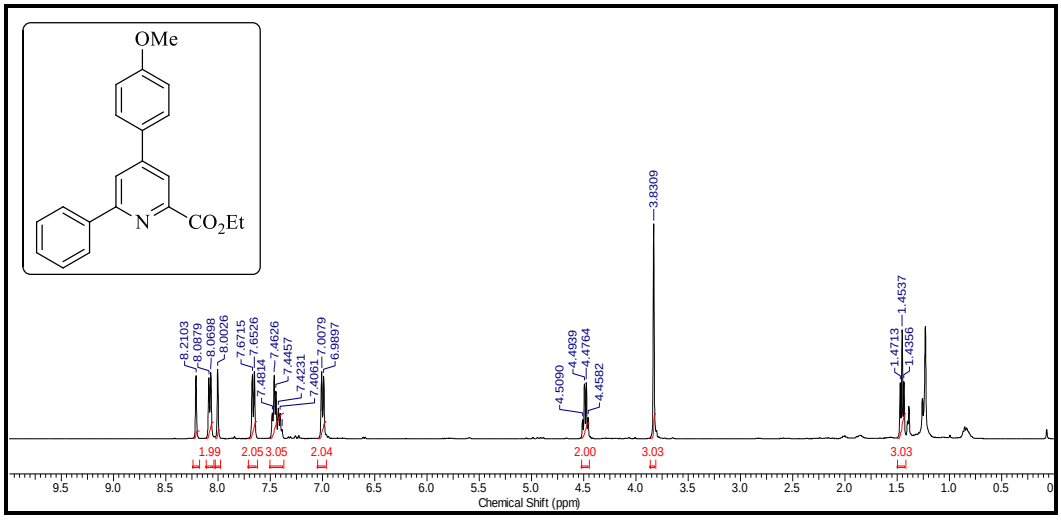


Figure 4.8 400 MHz ^{1}H NMR spectrum of **3ac** in $CDCl_3$

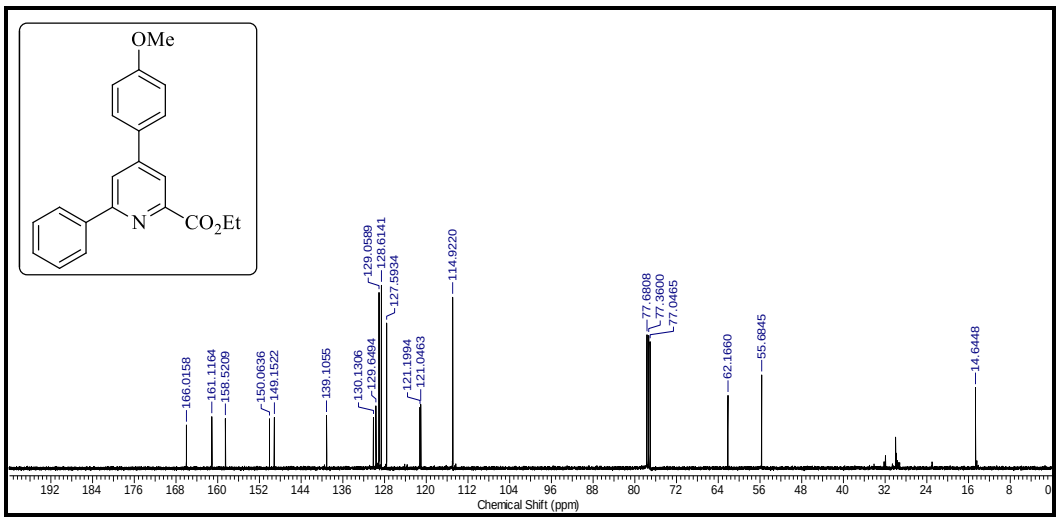


Figure 4.9 100 MHz ^{13}C NMR spectrum of **3ac** in $CDCl_3$

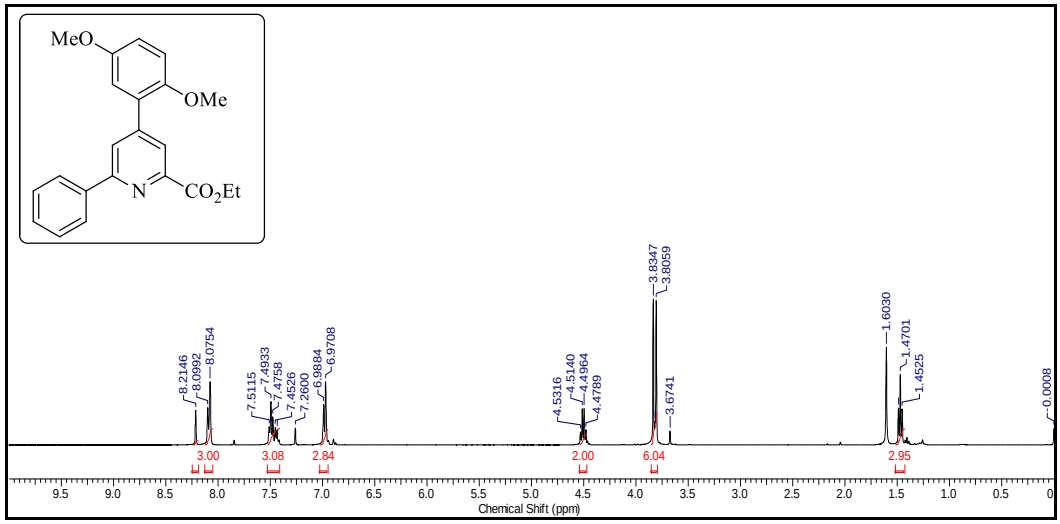


Figure 4.10 400 MHz ^{1}H NMR spectrum of **3ad** in $CDCl_3$

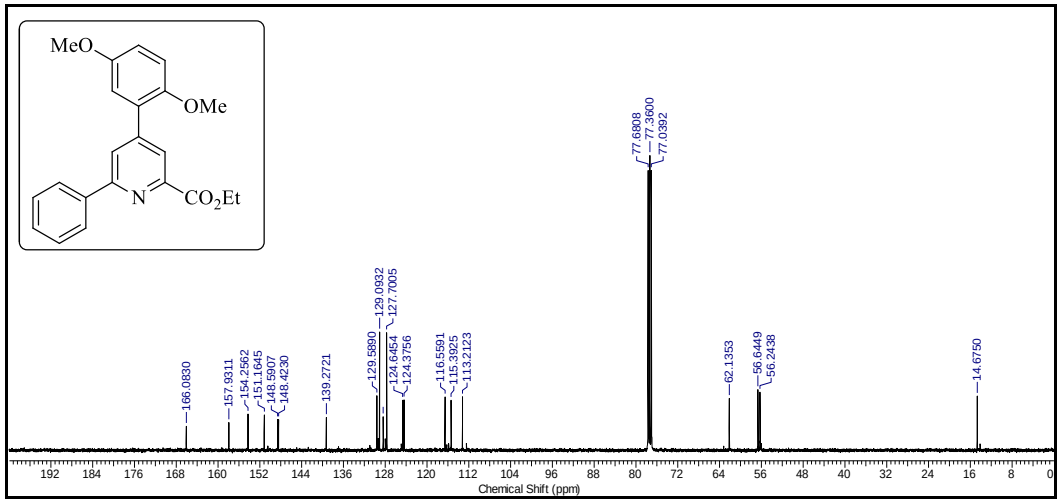


Figure 4.11 100 MHz ^{13}C NMR spectrum of **3ad** in $CDCl_3$

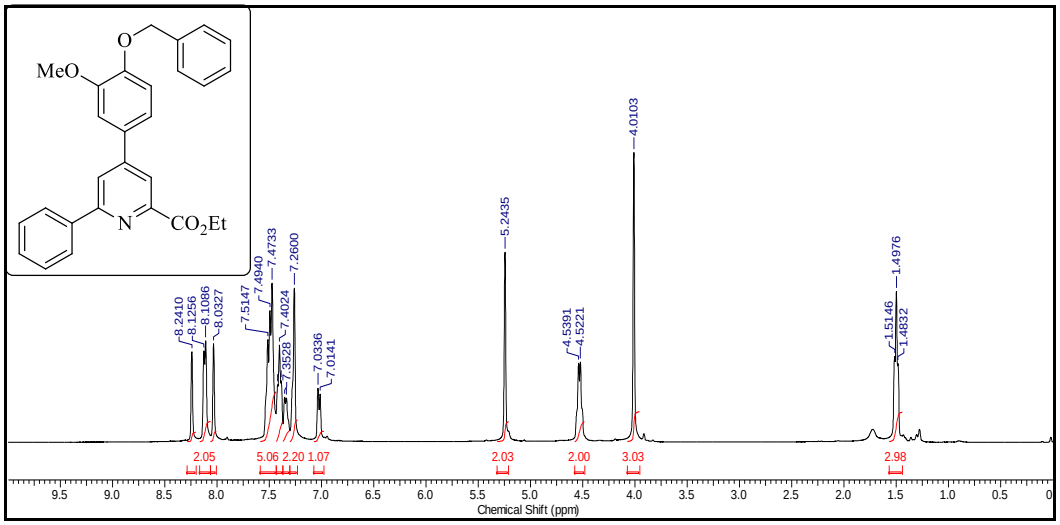


Figure 4.12 400 MHz ^{1}H NMR spectrum of **3ae** in $CDCl_3$

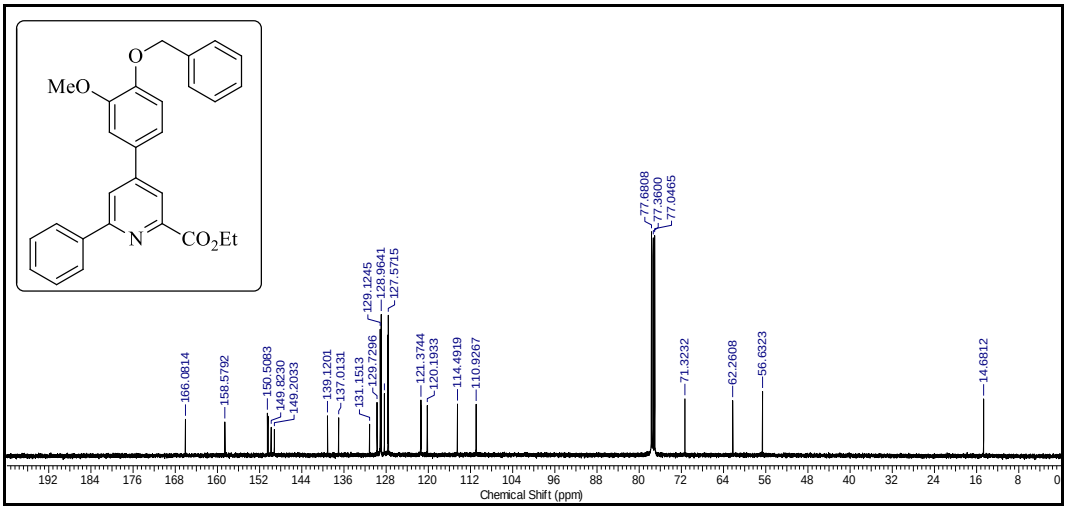


Figure 4.13 100 MHz ^{13}C NMR spectrum of **3ae** in $CDCl_3$

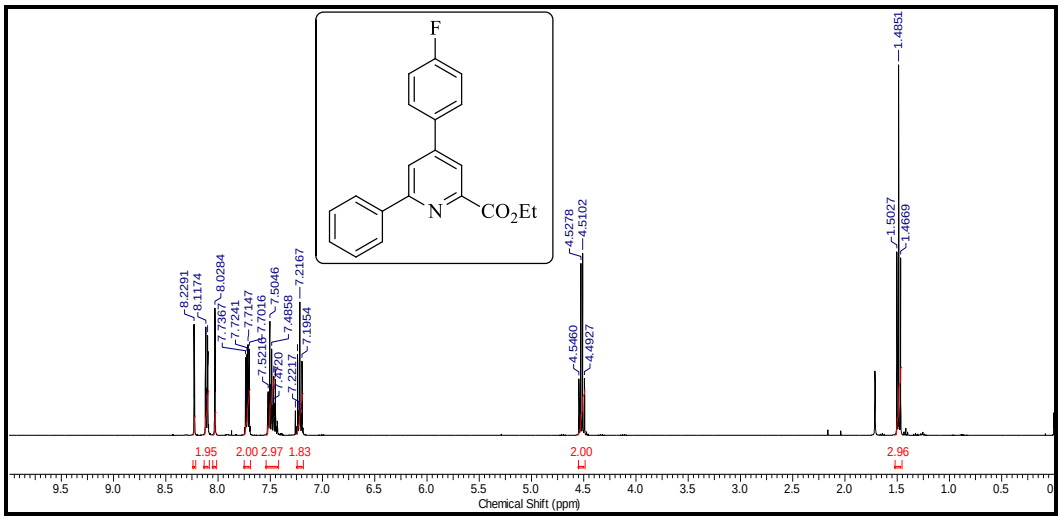


Figure 4.14 400 MHz ^{1}H NMR spectrum of **3af** in $CDCl_3$

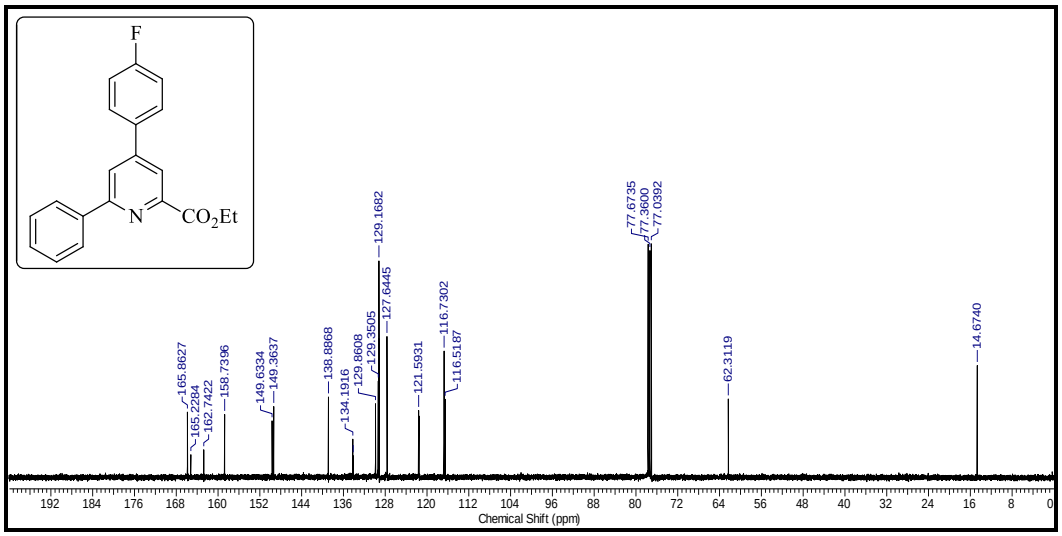


Figure 4.15 100 MHz ^{13}C NMR spectrum of **3af** in $CDCl_3$

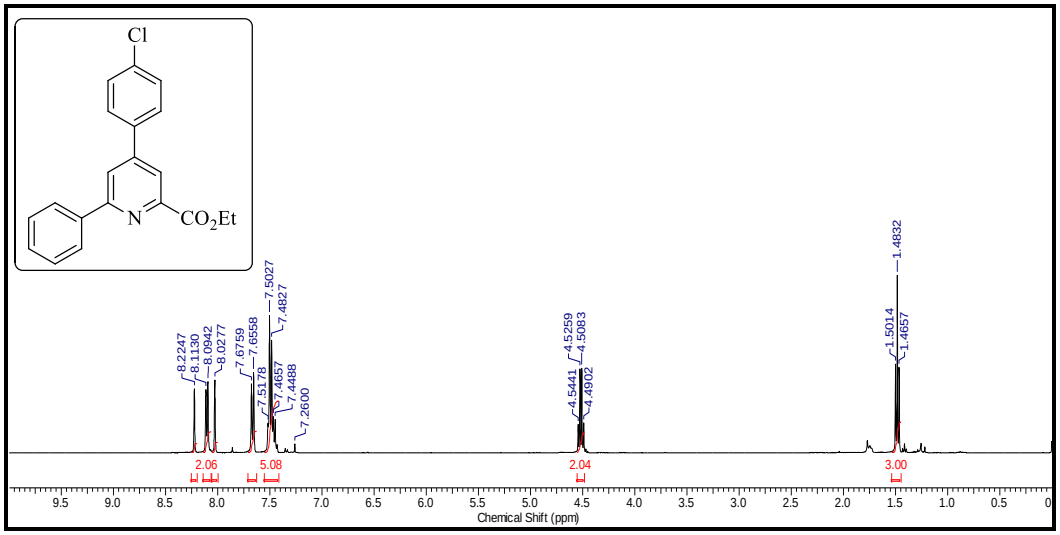


Figure 4.16 400 MHz ^{1}H NMR spectrum of **3ag** in $CDCl_3$

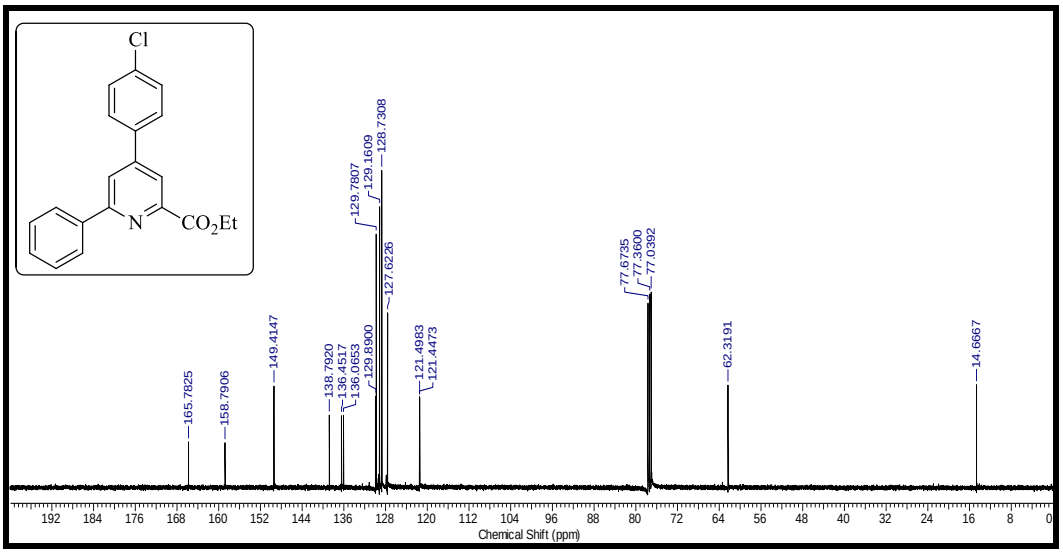


Figure 4.17 100 MHz ^{13}C NMR spectrum of **3ag** in $CDCl_3$

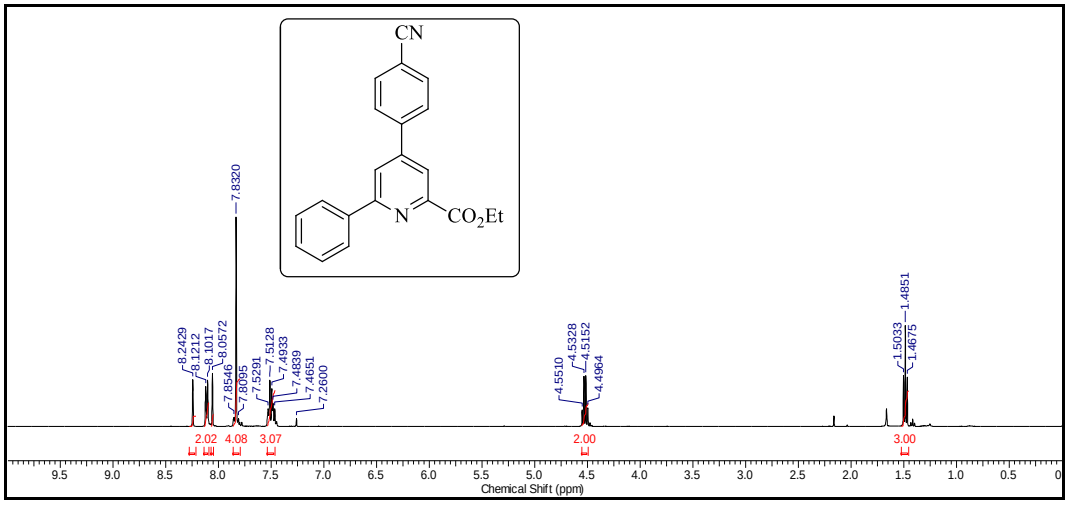


Figure 4.18 400 MHz ^{1}H NMR spectrum of **3ah** in $CDCl_3$

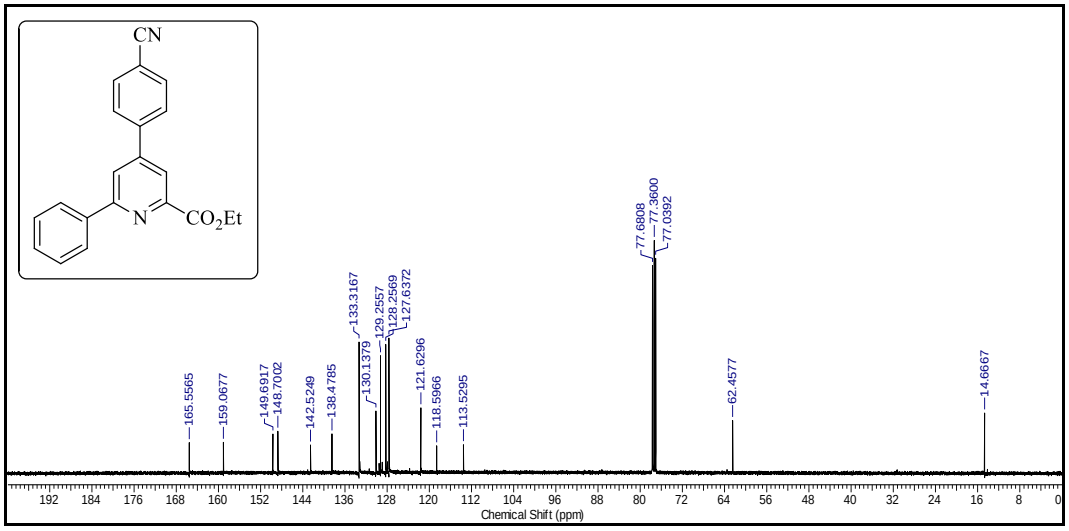


Figure 4.19 100 MHz ^{13}C NMR spectrum of **3ah** in $CDCl_3$

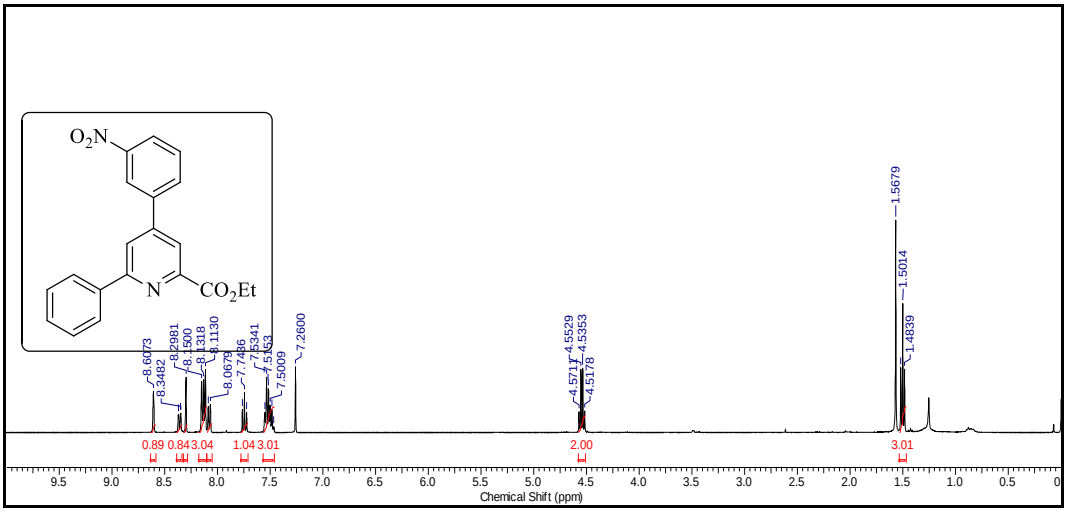


Figure 4.20 400 MHz ^{1}H NMR spectrum of **3ai** in $CDCl_3$

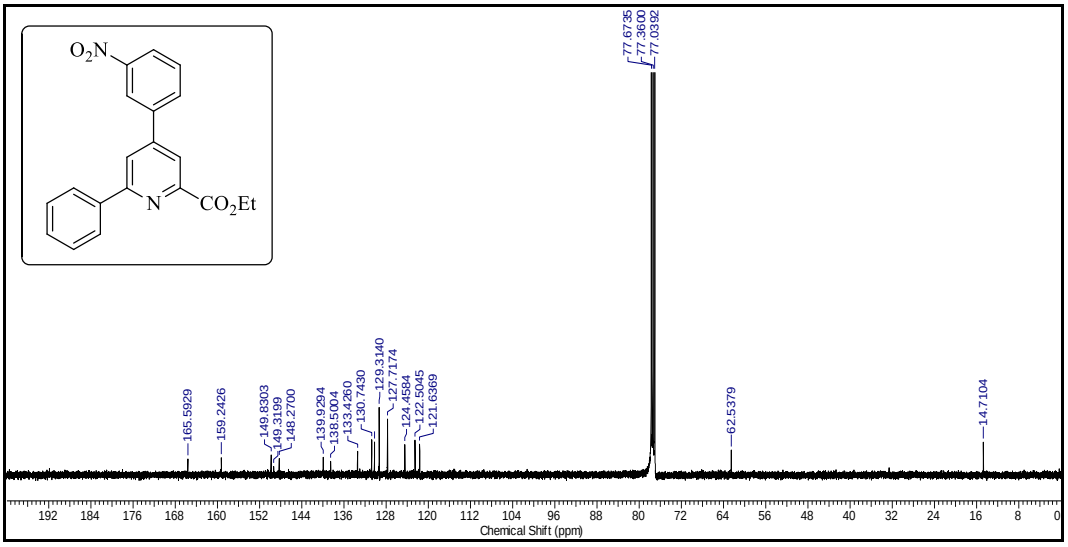


Figure 4.21 100 MHz ^{13}C NMR spectrum of **3ai** in $CDCl_3$

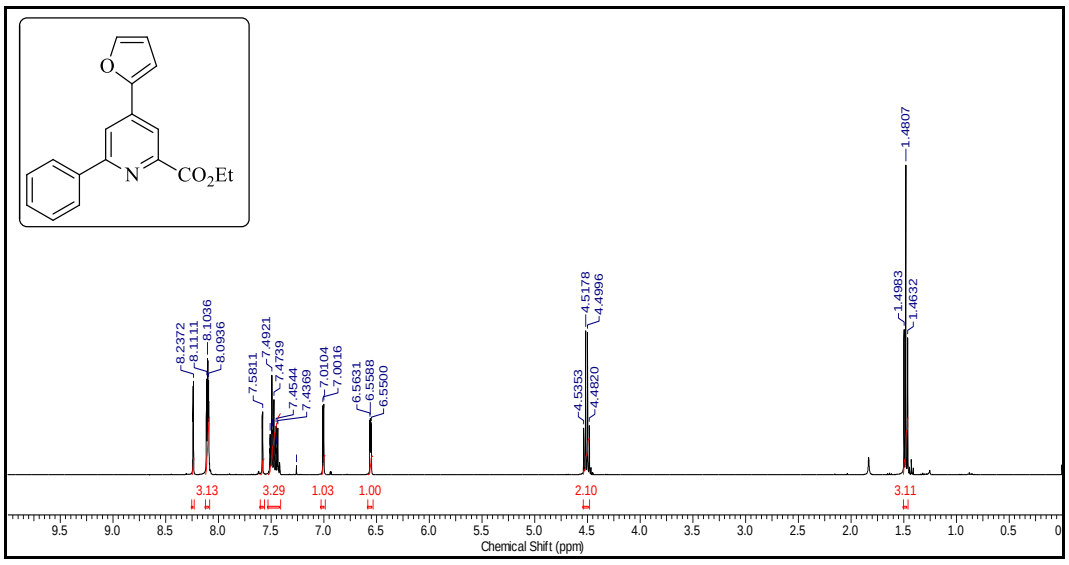


Figure 4.22 400 MHz ^{1}H NMR spectrum of **3aj** in $CDCl_3$

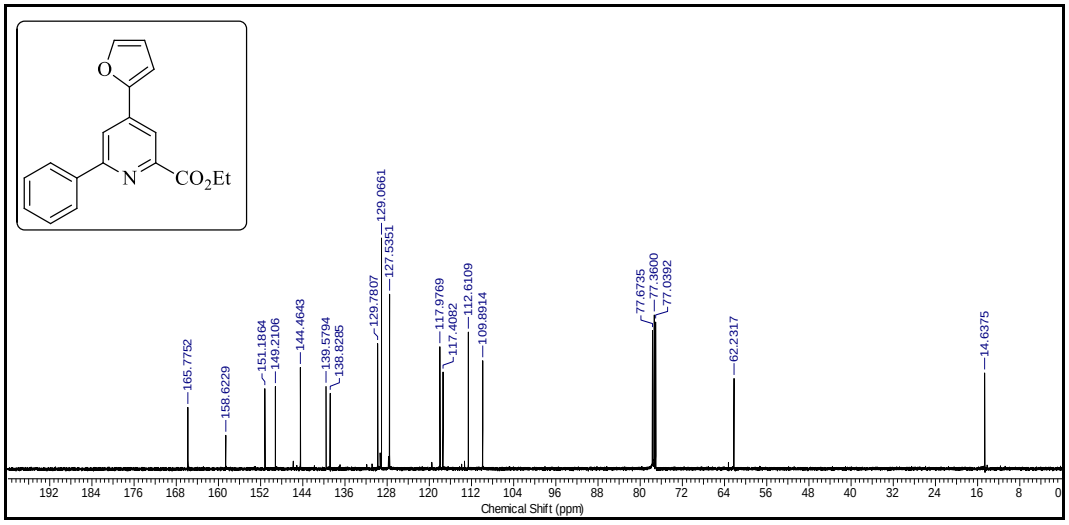


Figure 4.23 100 MHz ^{13}C NMR spectrum of **3aj** in $CDCl_3$

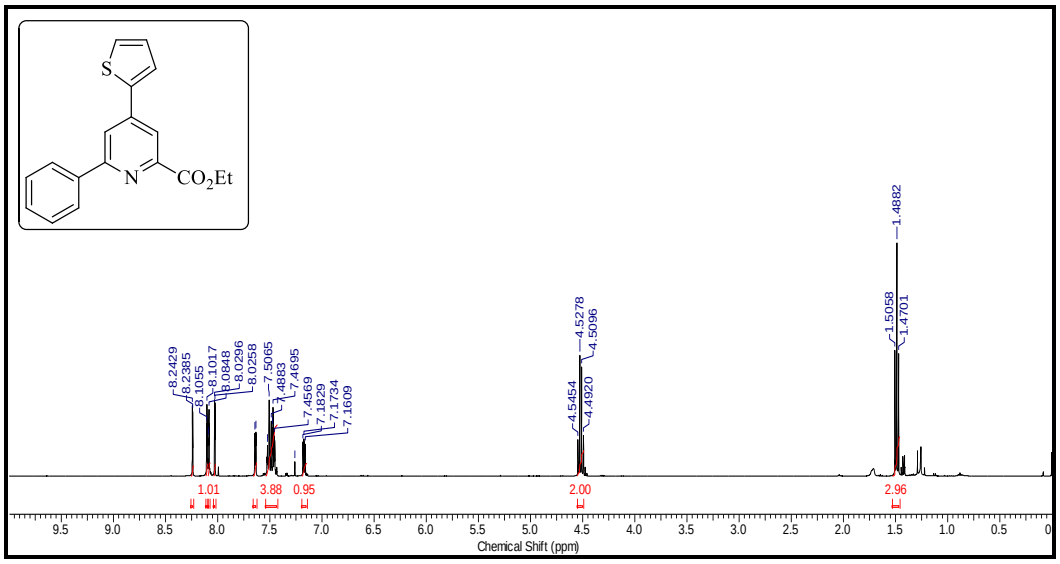


Figure 4.24 400 MHz ^{1}H NMR spectrum of **3ak** in $CDCl_3$

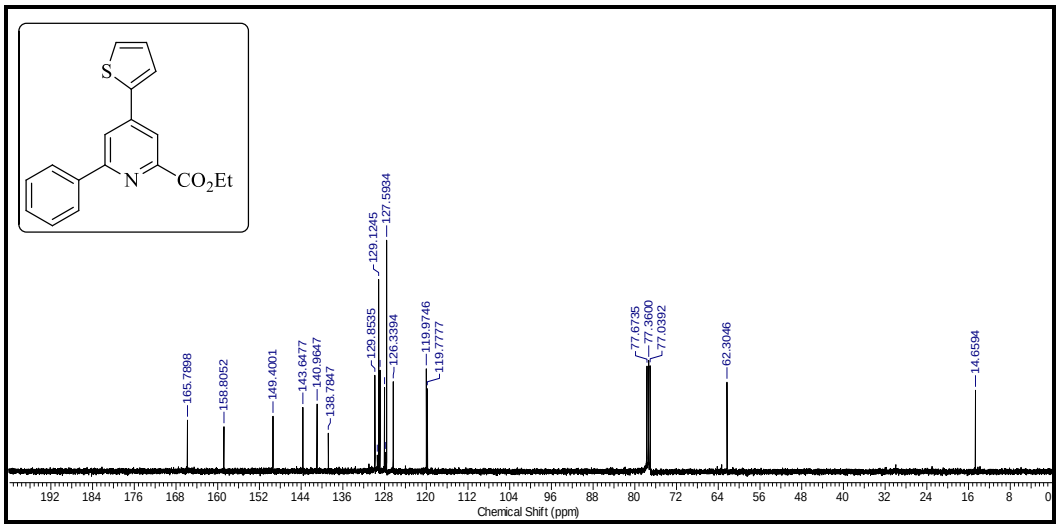


Figure 4.25 100 MHz ^{13}C spectrum of **3ak** in $CDCl_3$

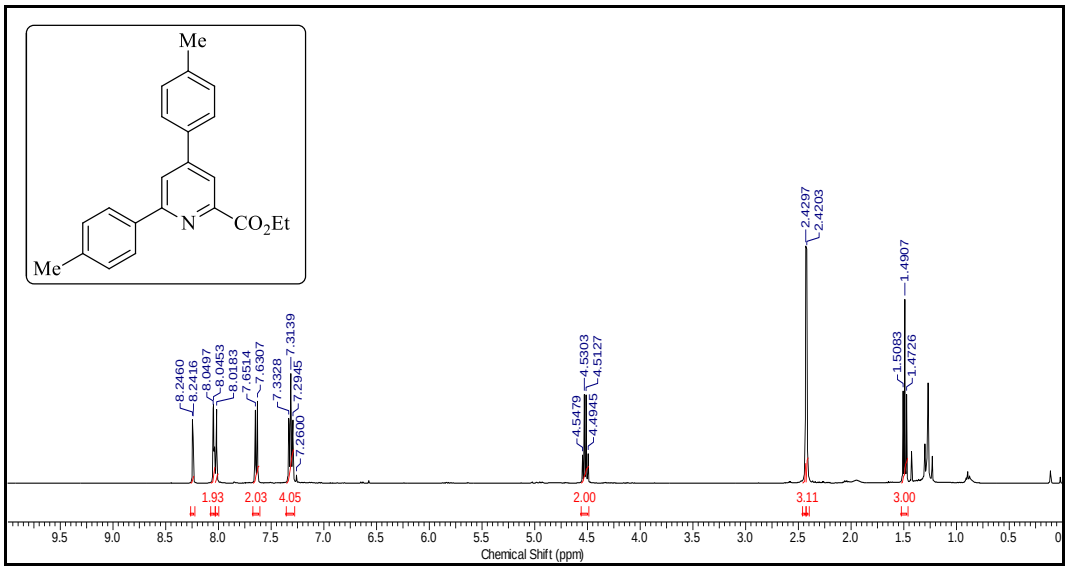


Figure 4.26 400 MHz ^{1}H NMR spectrum of **3bb** in $CDCl_3$

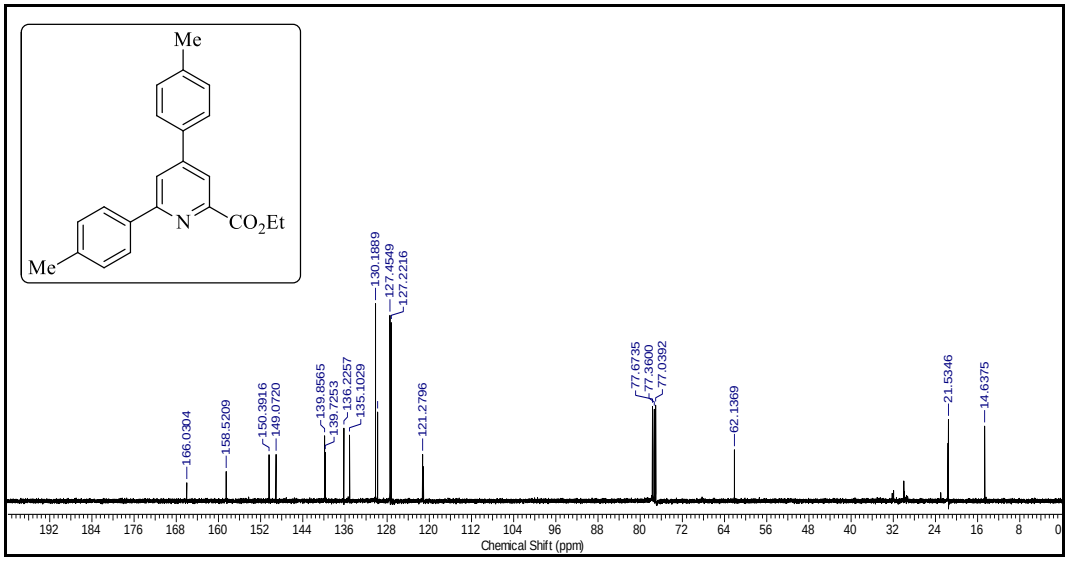


Figure 4.27 100 MHz ^{13}C NMR spectrum of **3bb** in $CDCl_3$

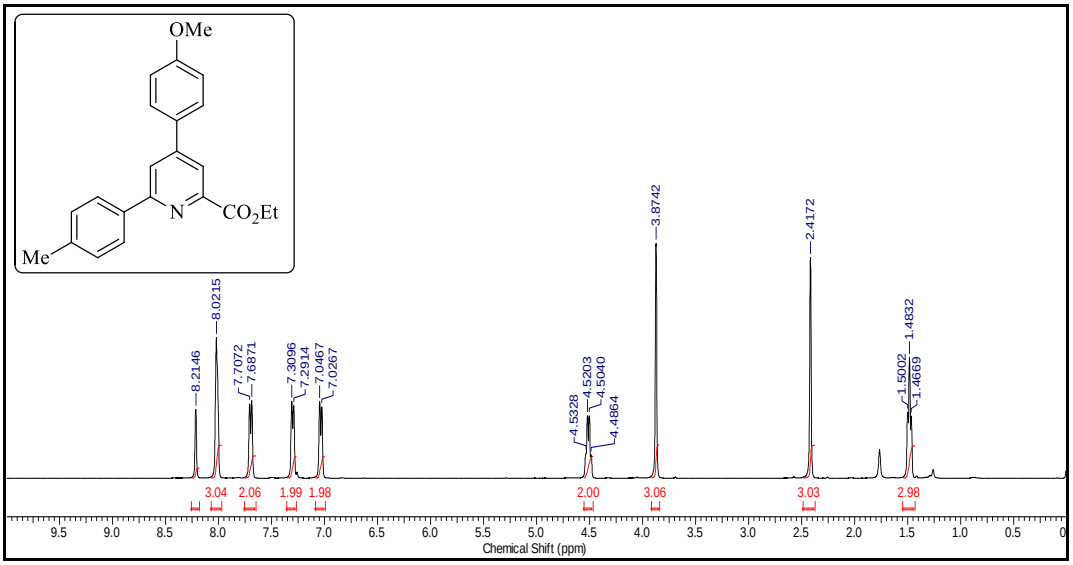


Figure 4.28 400 MHz ^{1}H NMR spectrum of **3bc** in $CDCl_3$

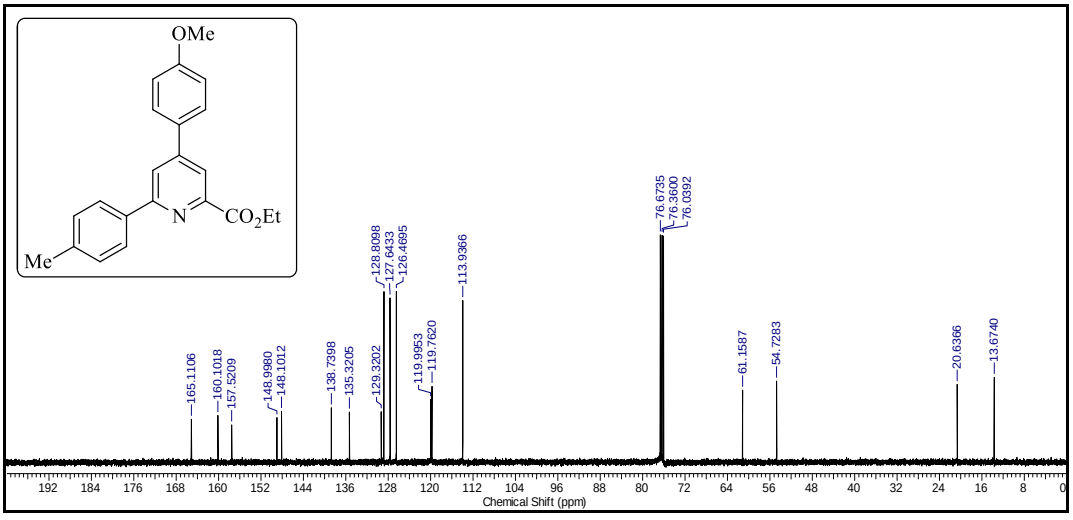


Figure 4.29 100 MHz ^{13}C NMR spectrum of **3bc** in $CDCl_3$

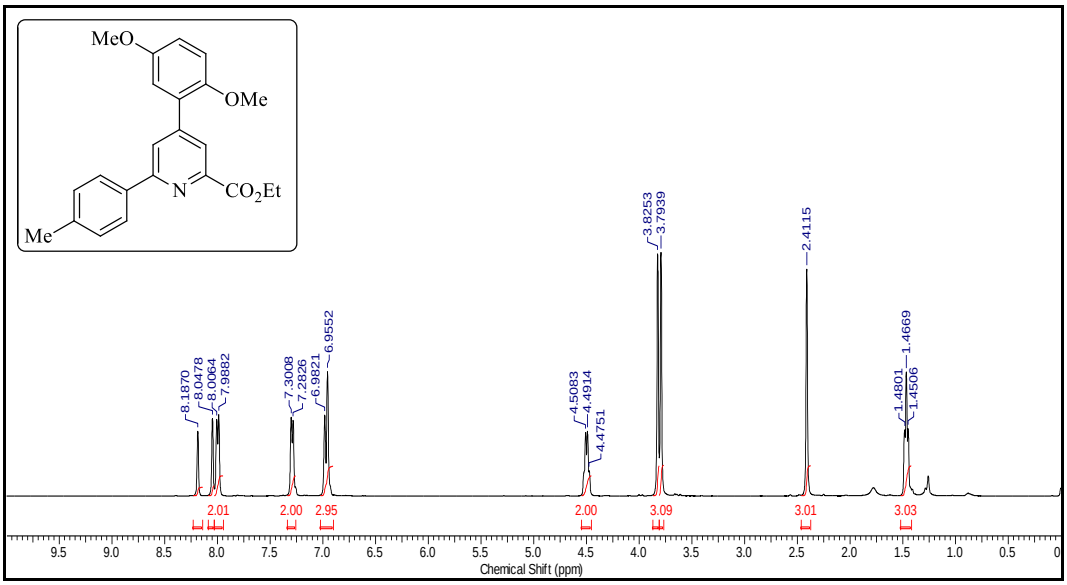


Figure 4.30 400 MHz ^{1}H NMR spectrum of **3bd** in $CDCl_3$

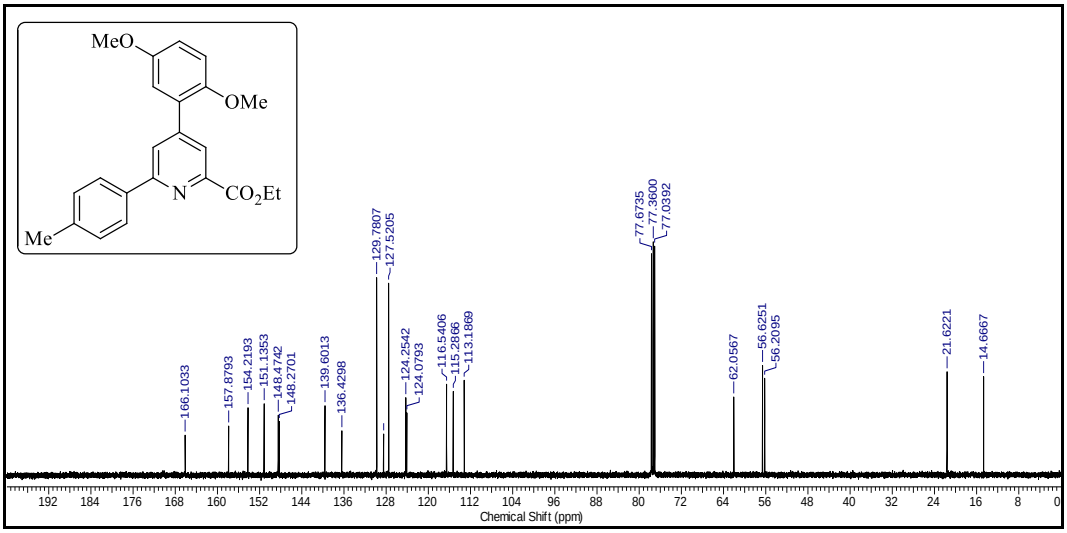


Figure 4.31 100 MHz ^{13}C NMR spectrum of **3bd** in $CDCl_3$

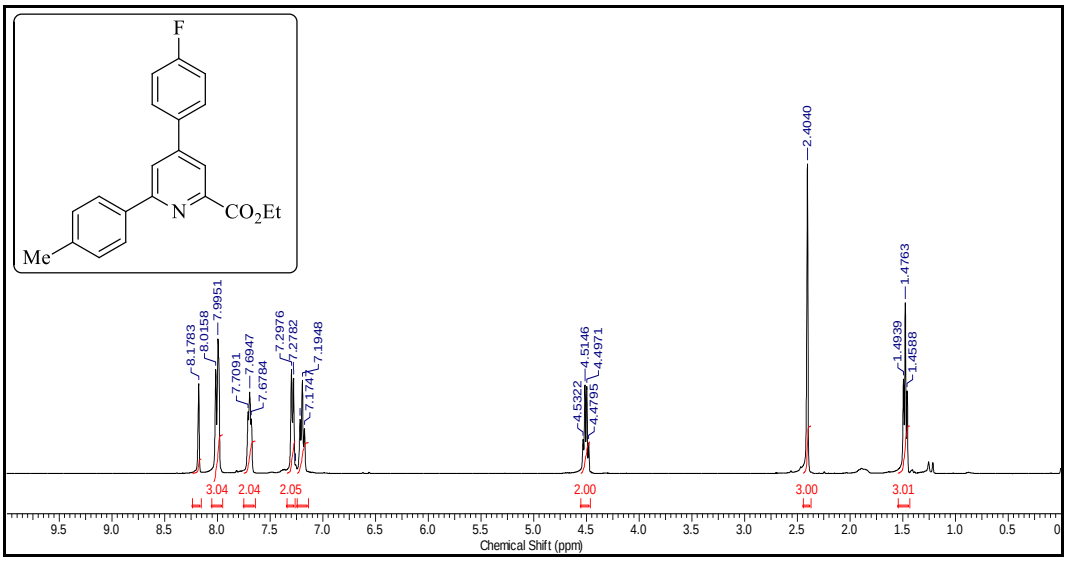


Figure 4.32 400 MHz ^{1}H NMR spectrum of **3bf** in $CDCl_3$

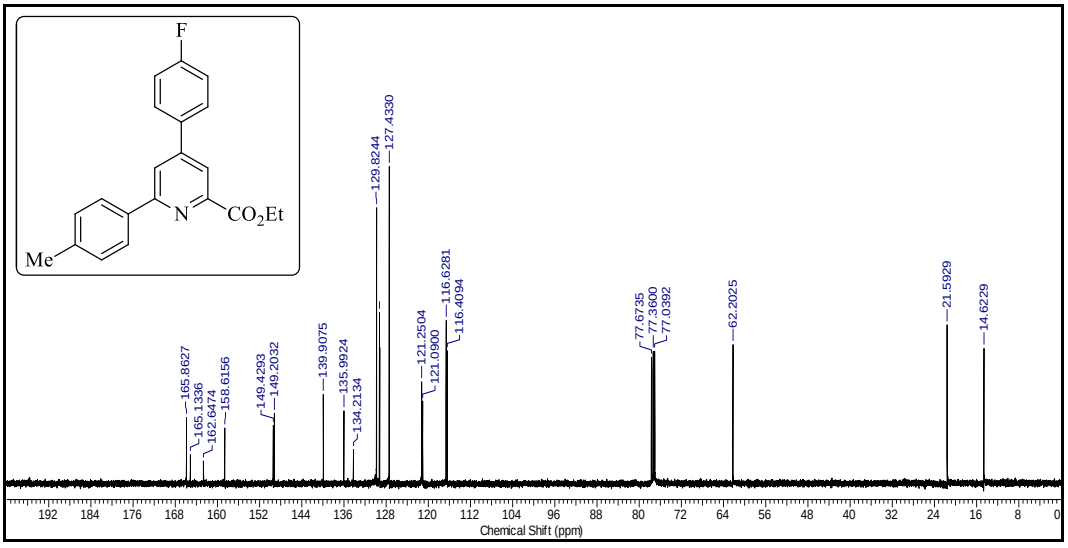


Figure 4.33 100 MHz ^{13}C NMR spectrum of **3bf** in $CDCl_3$

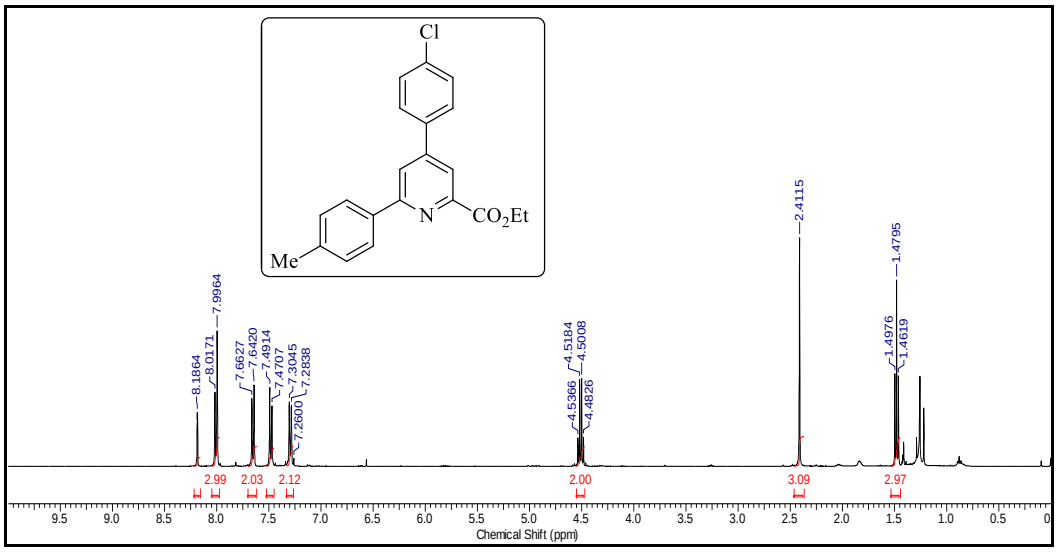


Figure 4.34 400 MHz ^{1}H NMR spectrum of **3bg** in $CDCl_3$

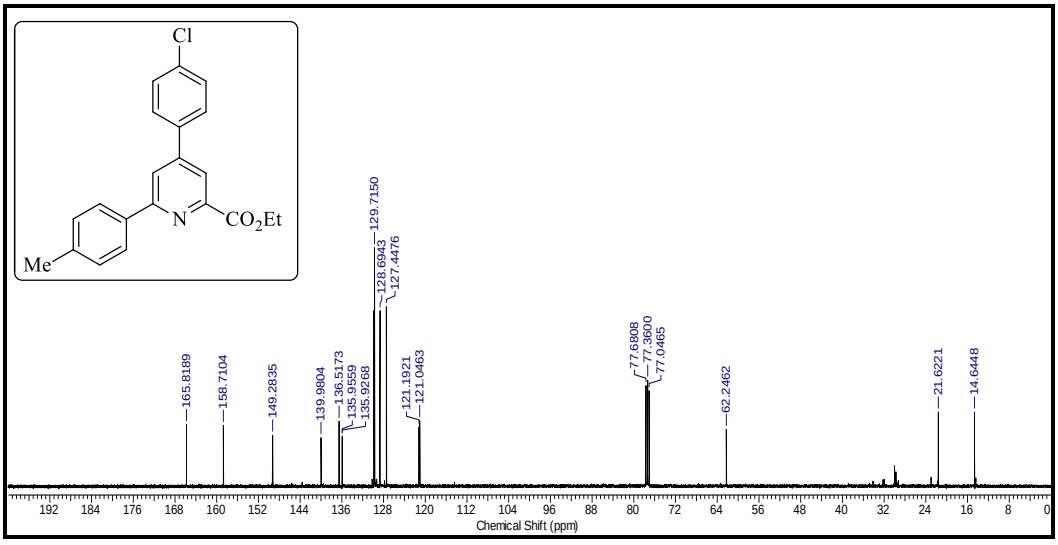


Figure 4.35 100 MHz ^{13}C NMR spectrum of **3bg** in $CDCl_3$

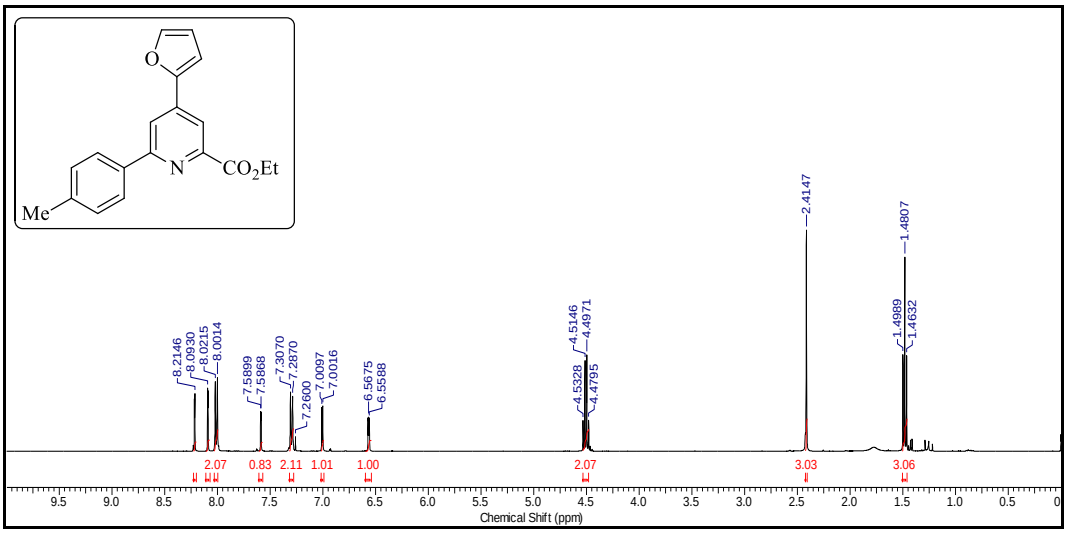


Figure 4.36 400 MHz ^{1}H NMR spectrum of **3bj** in $CDCl_3$

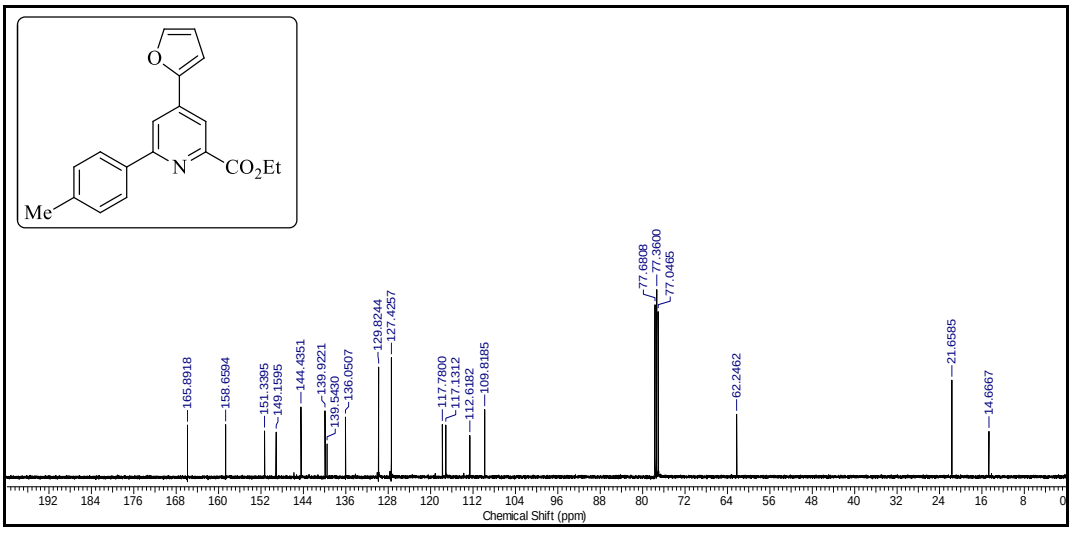


Figure 4.37 100 MHz ^{13}C NMR spectrum of **3bj** in $CDCl_3$

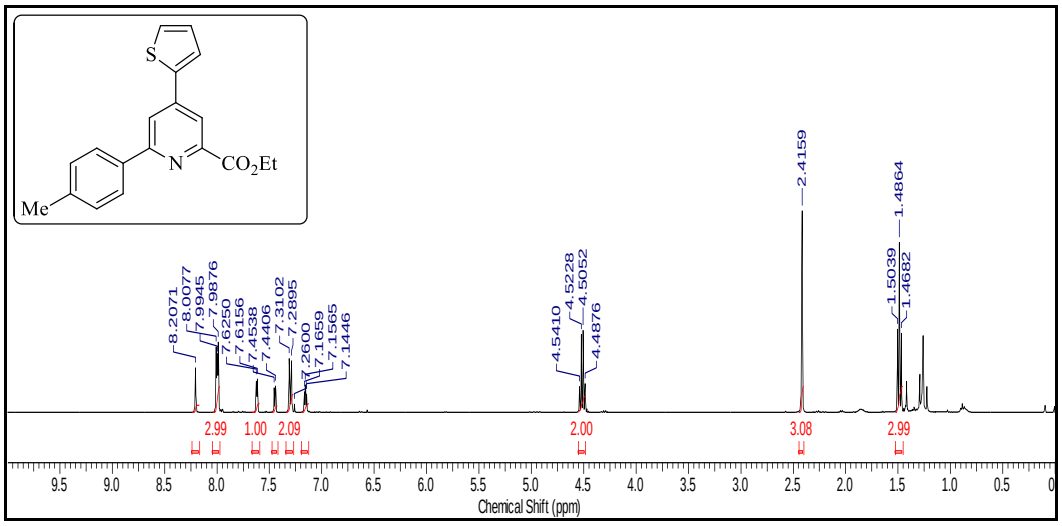


Figure 4.38 400 MHz ^{1}H NMR spectrum of **3bk** in $CDCl_3$

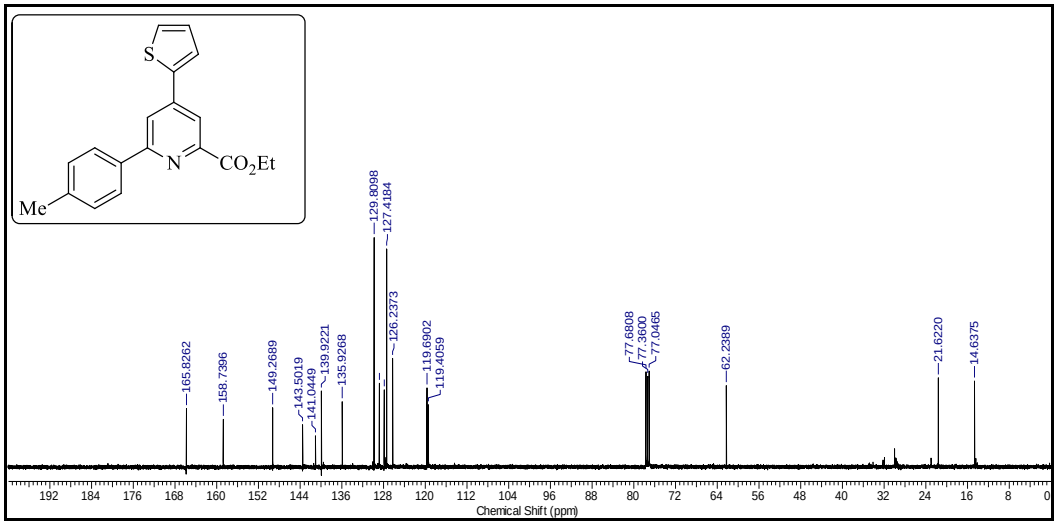


Figure 4.39 100 MHz ^{13}C NMR spectrum of **3bk** in $CDCl_3$

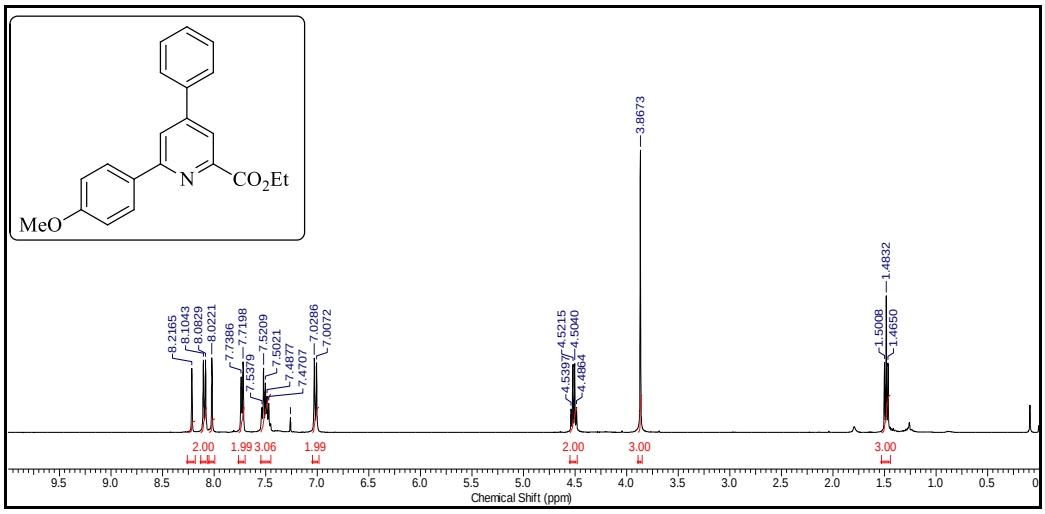


Figure 4.40 400 MHz ^{1}H NMR spectrum of **3ca** in $CDCl_3$

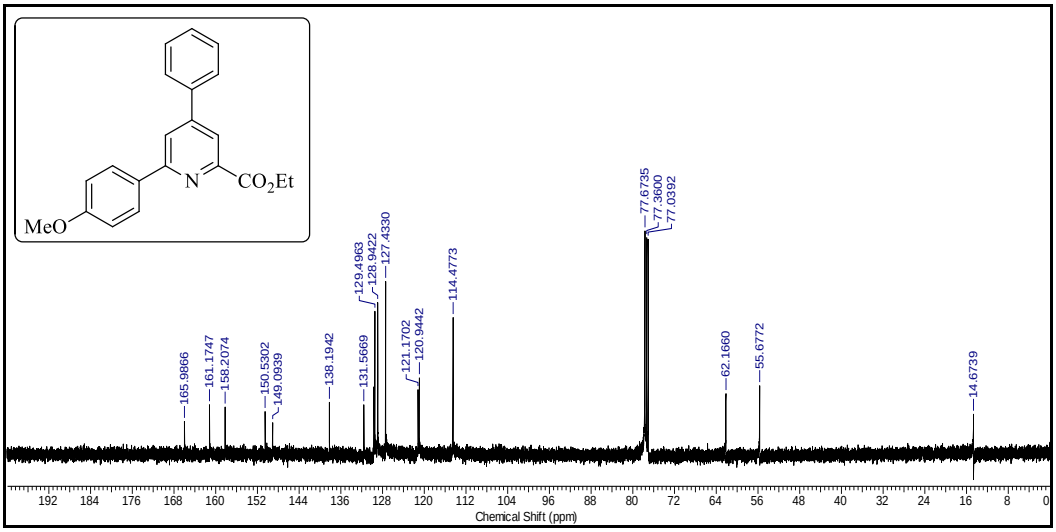


Figure 4.41 100 MHz ^{13}C NMR spectrum of **3ca** in $CDCl_3$

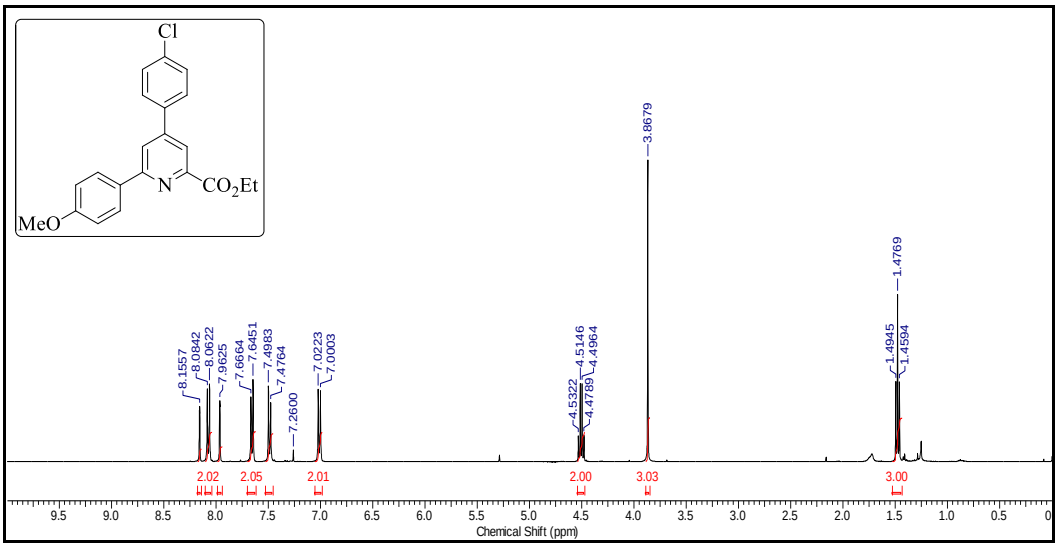


Figure 4.42 400 MHz ^{1}H NMR spectrum of **3cg** in $CDCl_3$

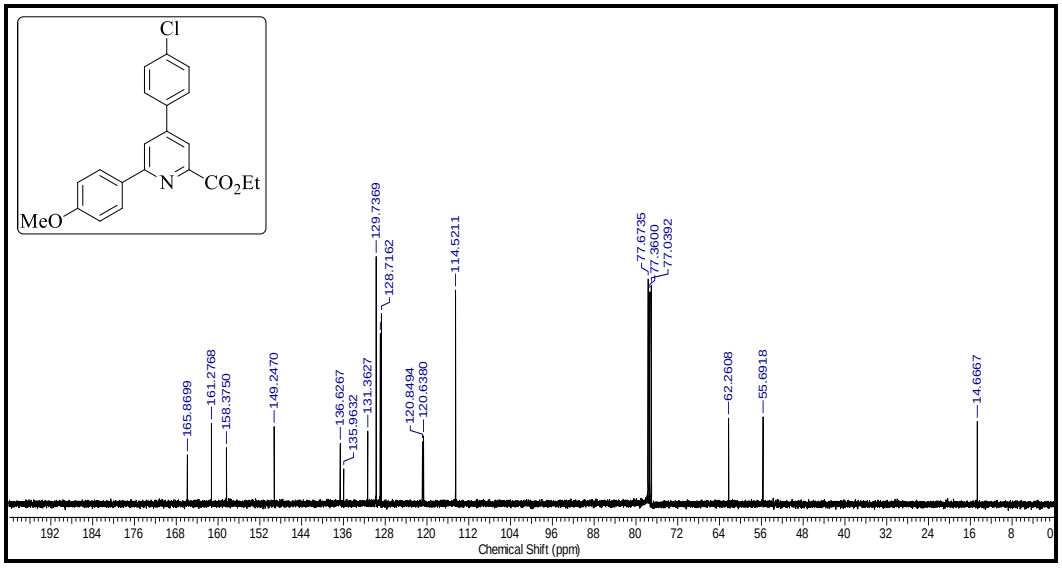


Figure 4.43 100 MHz ^{13}C NMR spectrum of **3cg** in $CDCl_3$

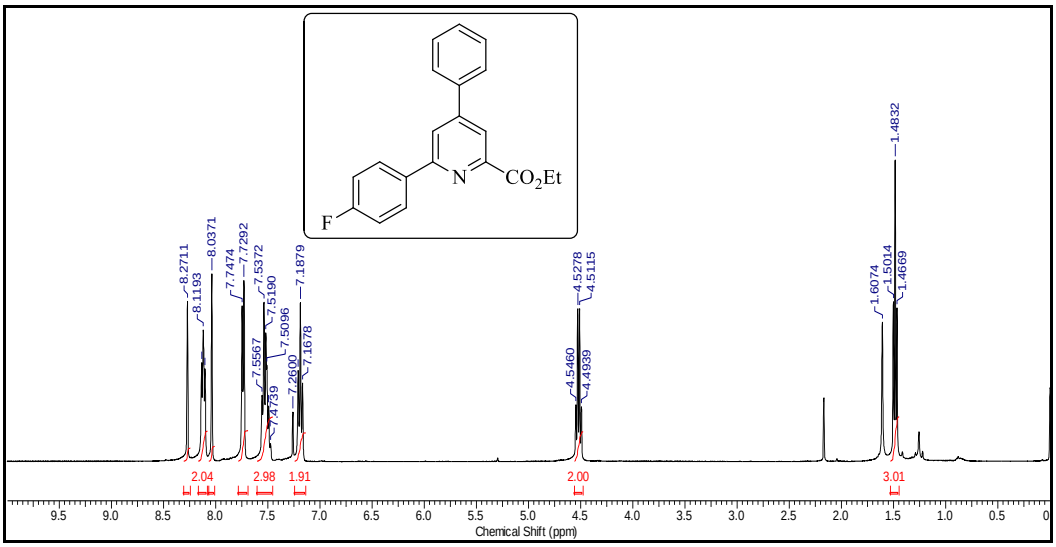


Figure 4.44 400 MHz ^{1}H NMR spectrum of **3da** in $CDCl_3$

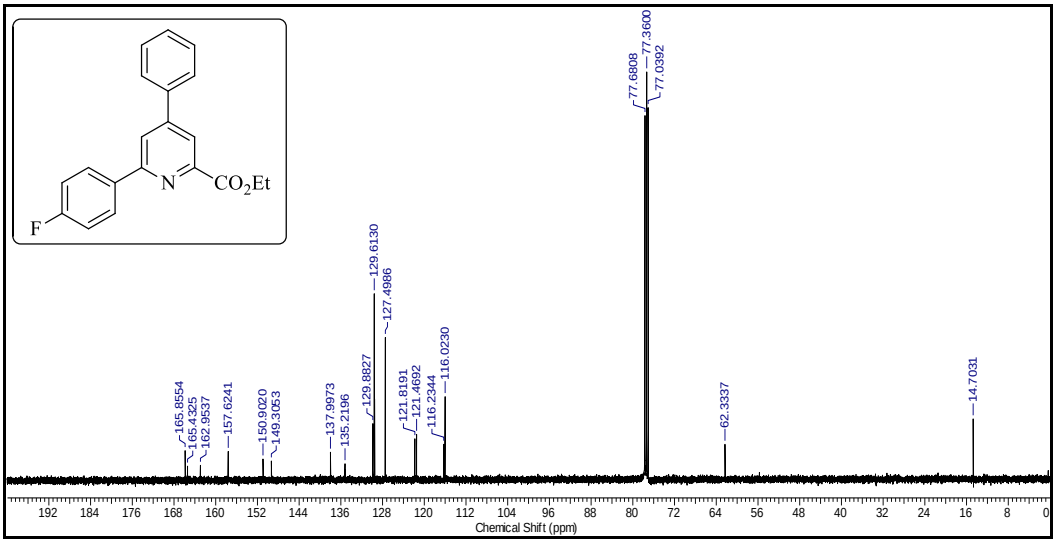


Figure 4.45 100 MHz ^{13}C NMR spectrum of **3da** in $CDCl_3$

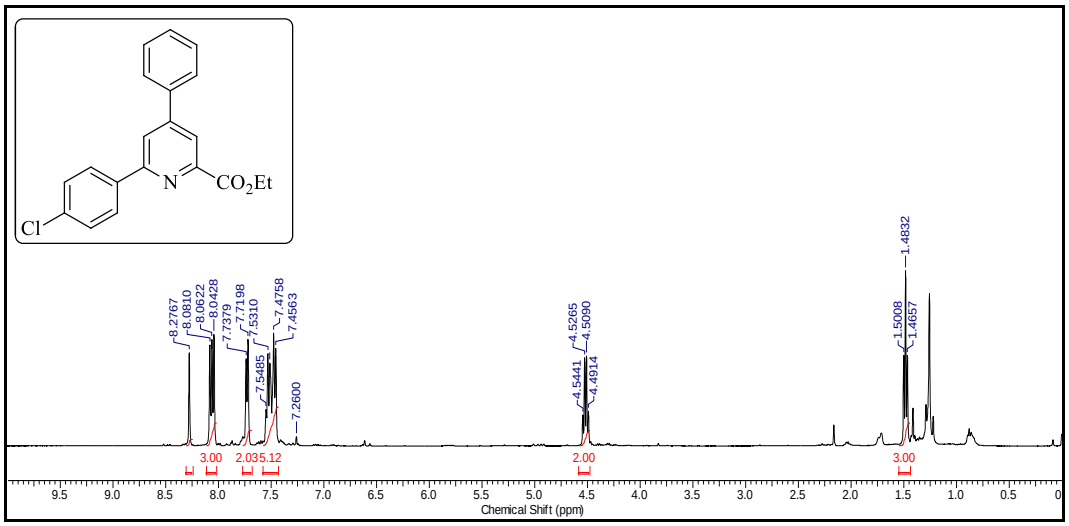


Figure 4.46 400 MHz ^{1}H NMR spectrum of **3ea** in $CDCl_3$

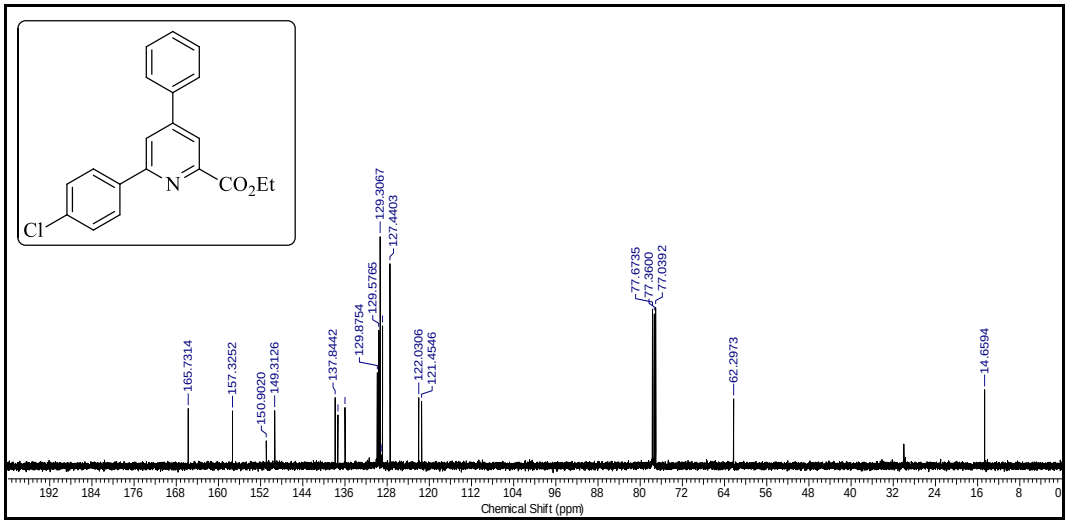


Figure 4.47 100 MHz ^{1}H NMR spectrum of **3ea** in $CDCl_3$

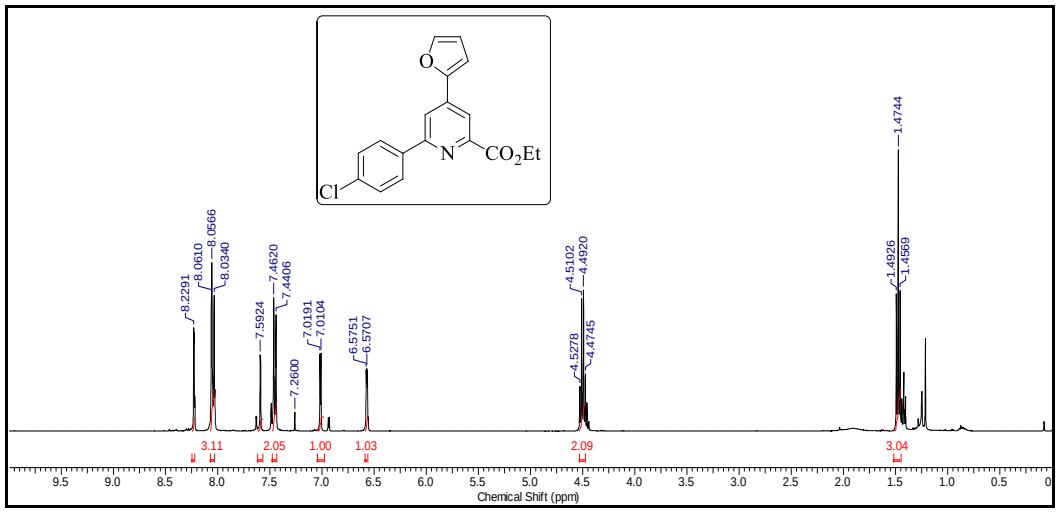


Figure 4.48 400 MHz ^{1}H NMR spectrum of **3ej** in $CDCl_3$

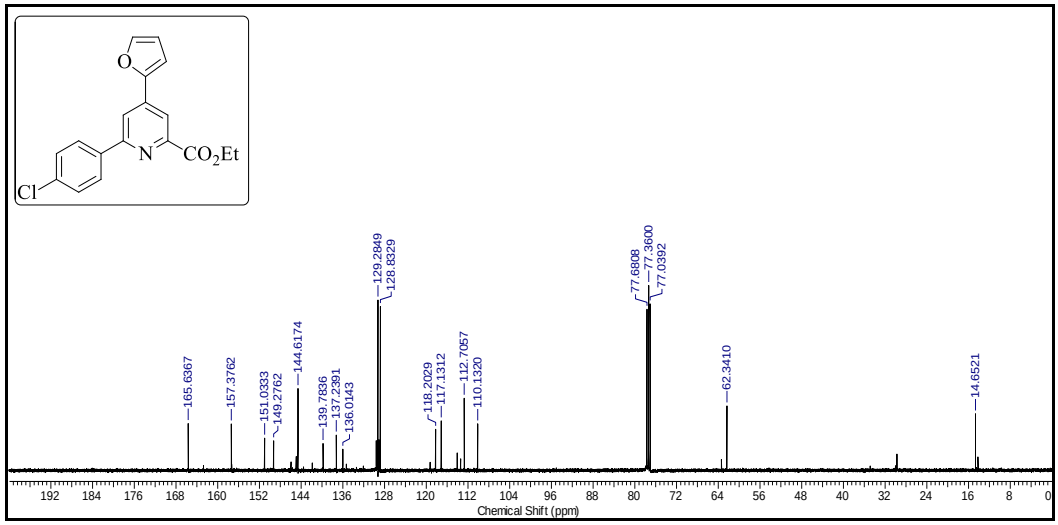


Figure 4.49 100 MHz ^{13}C NMR spectrum of **3ej** in $CDCl_3$

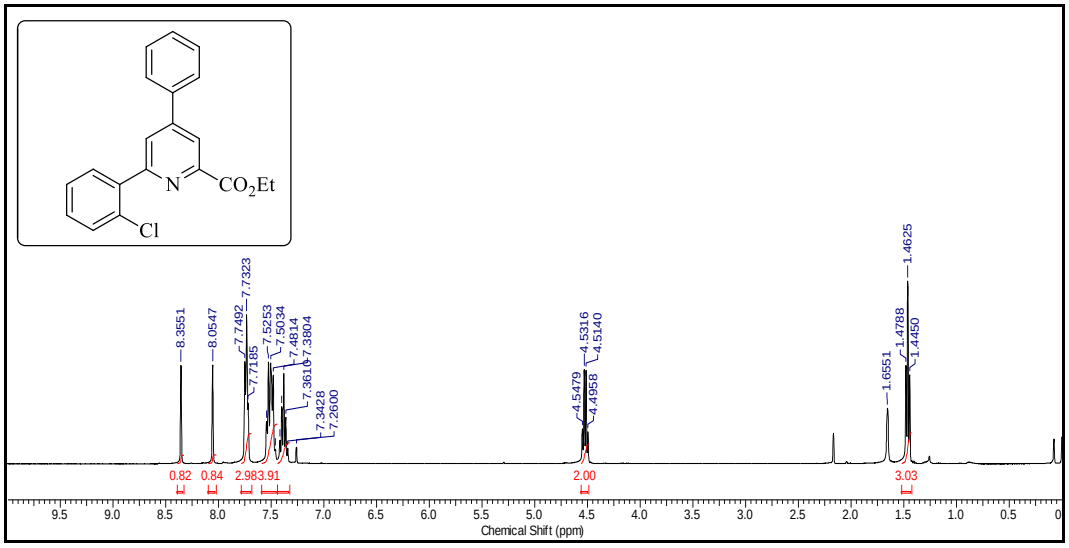


Figure 4.50 400 MHz ^{1}H NMR spectrum of **3fa** in $CDCl_3$

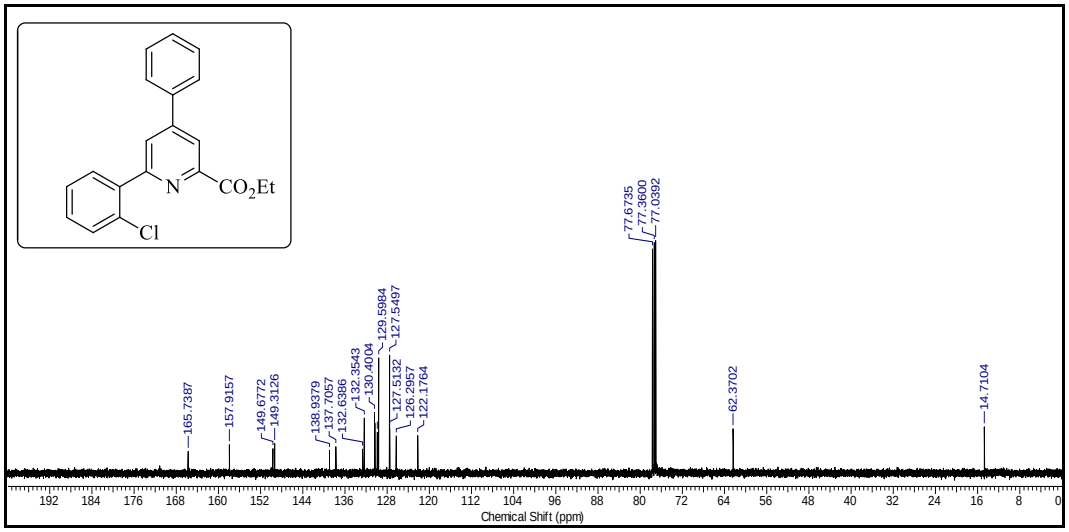


Figure 4.51 100 MHz ^{13}C NMR spectrum of **3fa** in $CDCl_3$

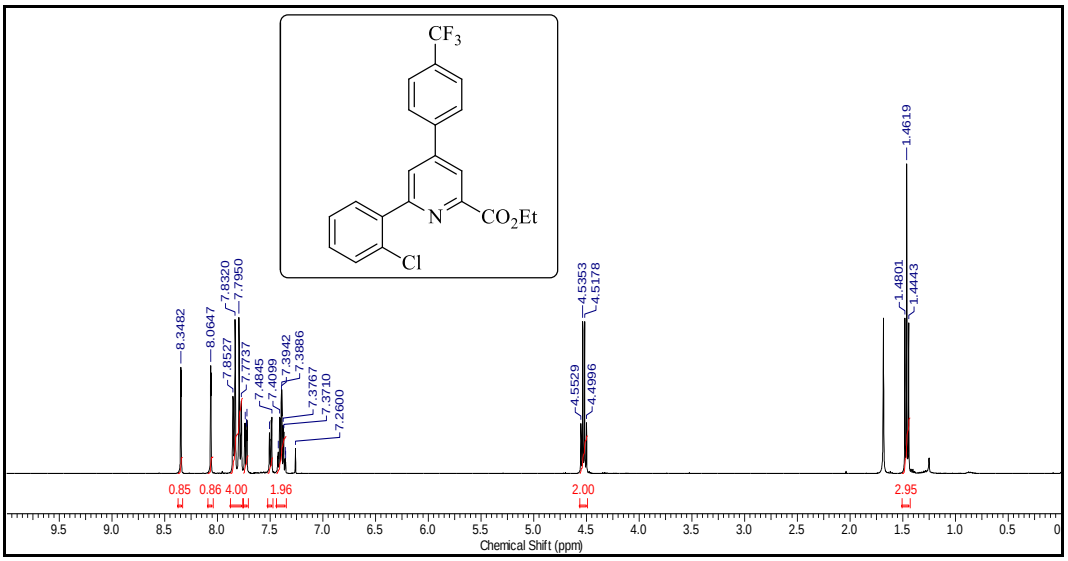


Figure 4.52 400 MHz ^{1}H NMR spectrum of **3fl** in $CDCl_3$

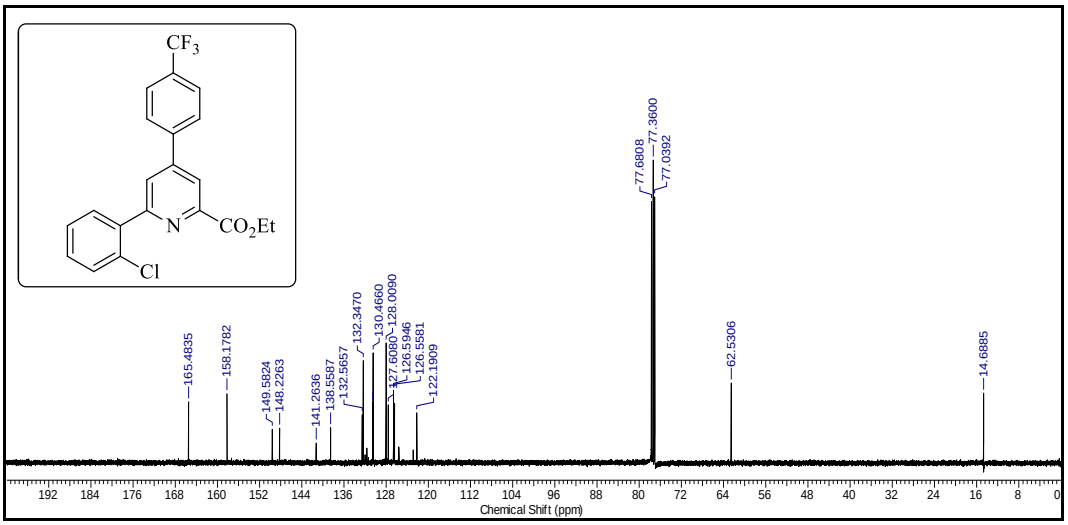


Figure 4.53 100 MHz ^{13}C NMR spectrum of **3fl** in $CDCl_3$

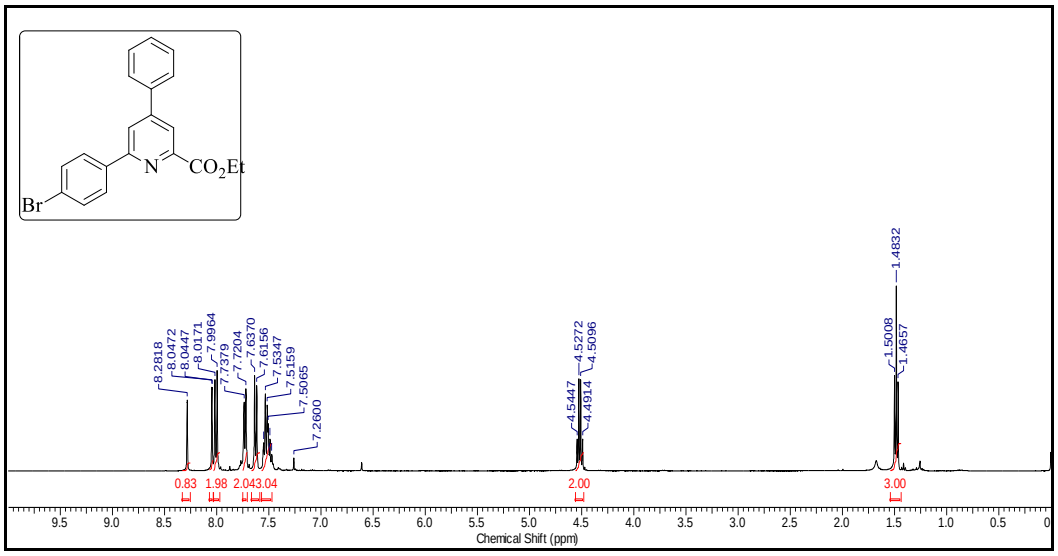


Figure 4.54 400 MHz ^{1}H NMR spectrum of **3ga** in $CDCl_3$

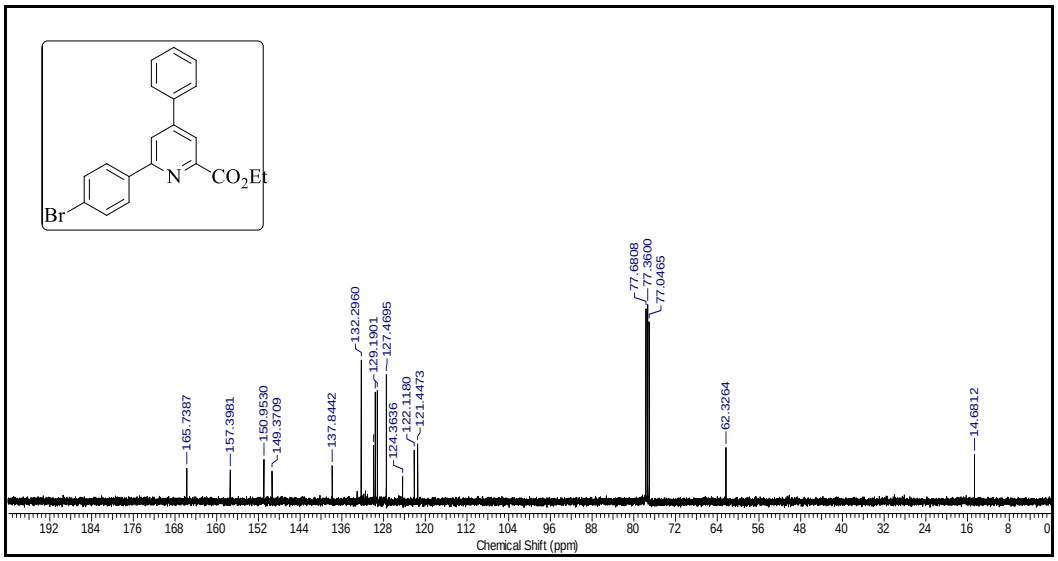


Figure 4.55 100 MHz ^{13}C NMR spectrum of **3ga** in $CDCl_3$

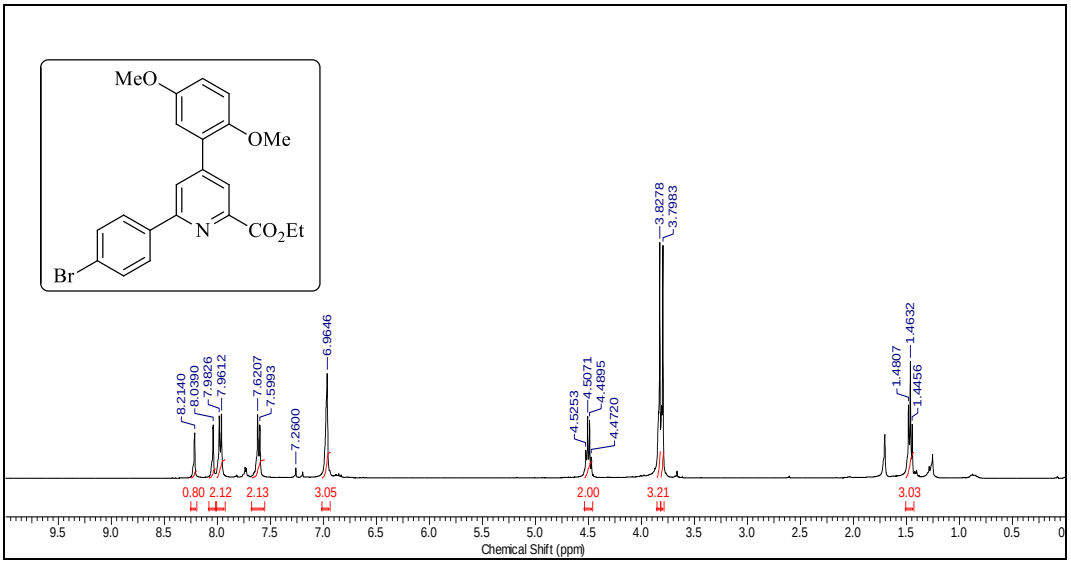


Figure 4.56 400 MHz ^{1}H NMR spectrum of **3gd** in $CDCl_3$

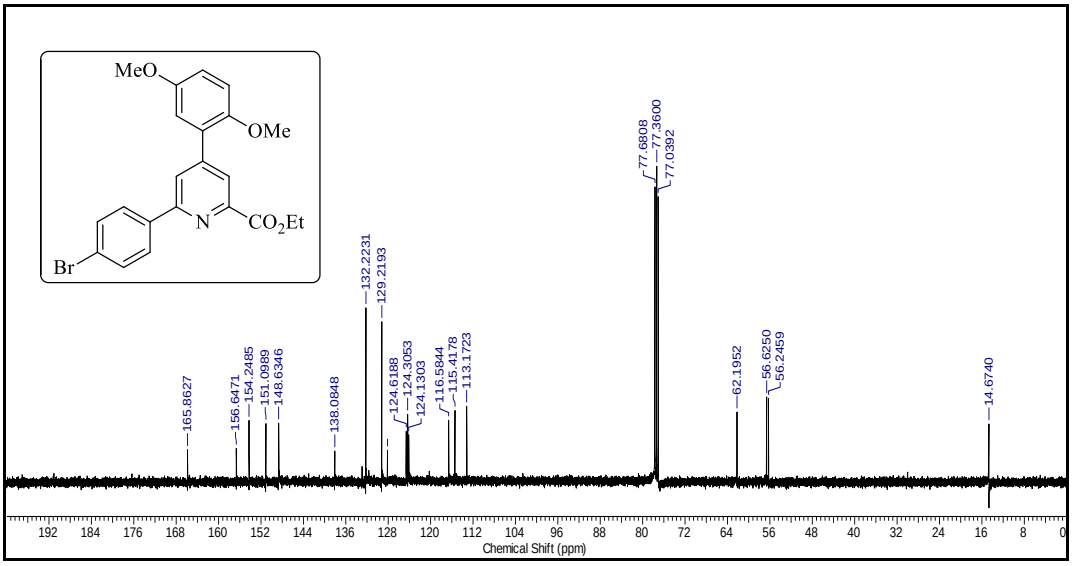


Figure 4.57 100 MHz ^{13}C NMR spectrum of **3gd** in $CDCl_3$

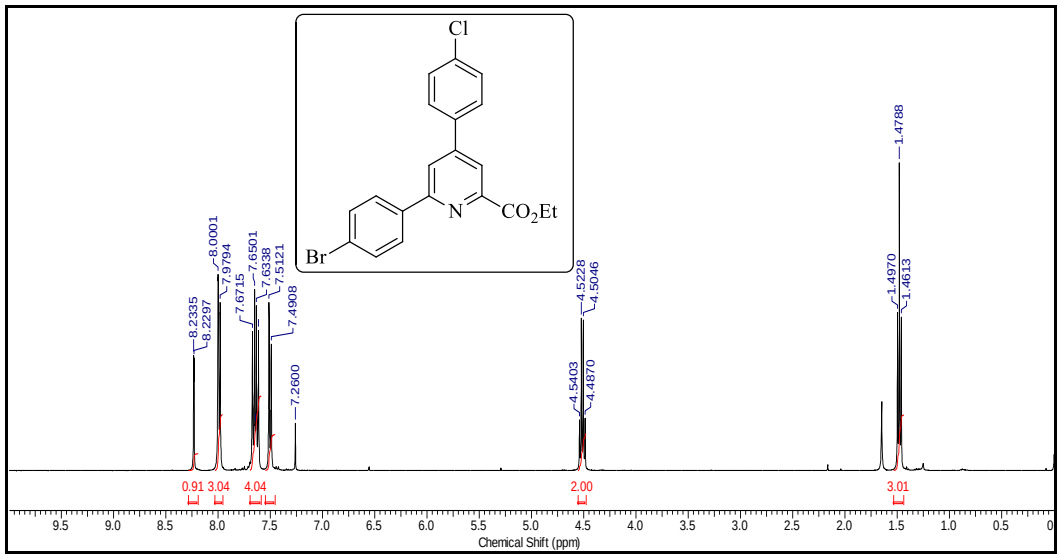


Figure 4.58 400 MHz ^{1}H NMR spectrum of **3gg** in $CDCl_3$

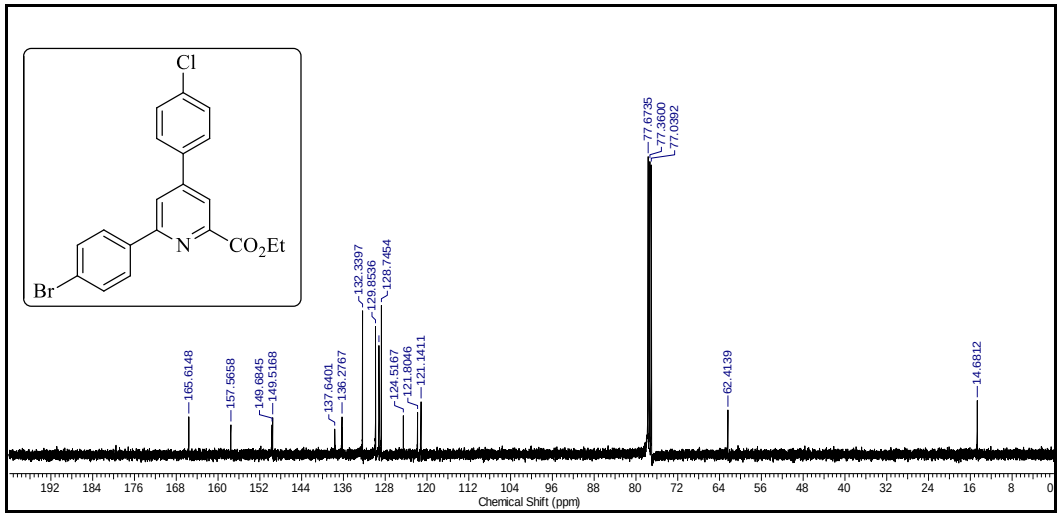


Figure 4.59 100 MHz ^{13}C NMR spectrum of **3gg** in $CDCl_3$

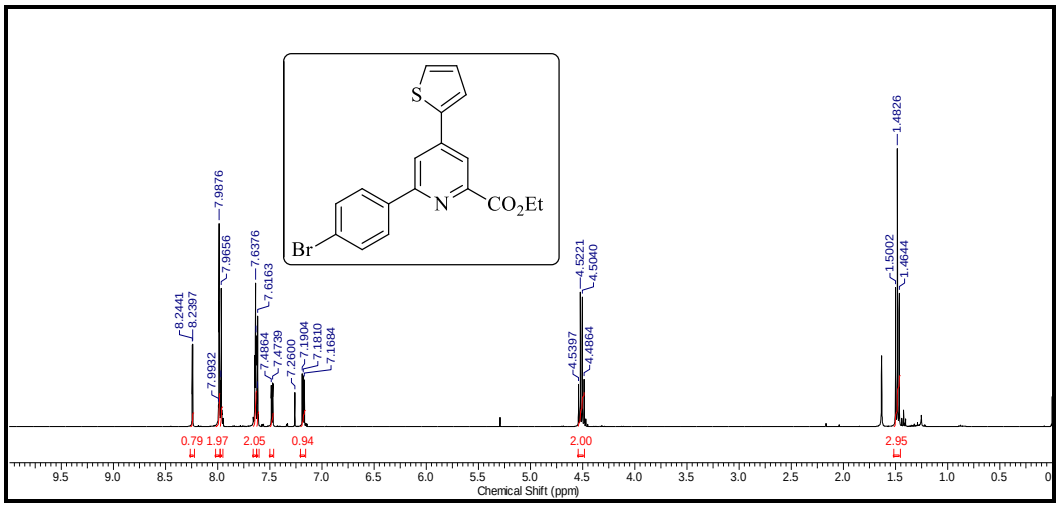


Figure 4.60 400 MHz ^{1}H NMR spectrum of **3gk** in $CDCl_3$

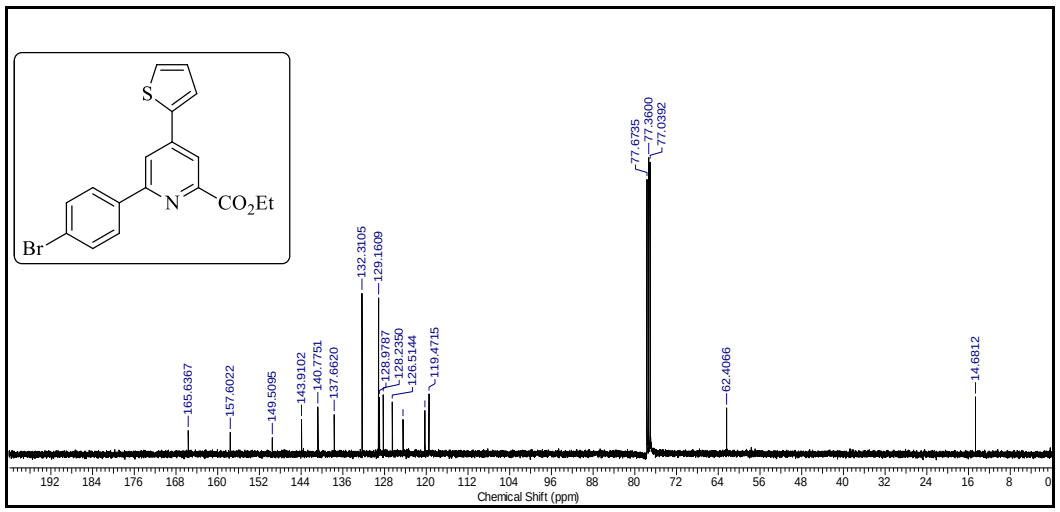


Figure 4.61 100 MHz ^{13}C NMR spectrum of **3gk** in $CDCl_3$

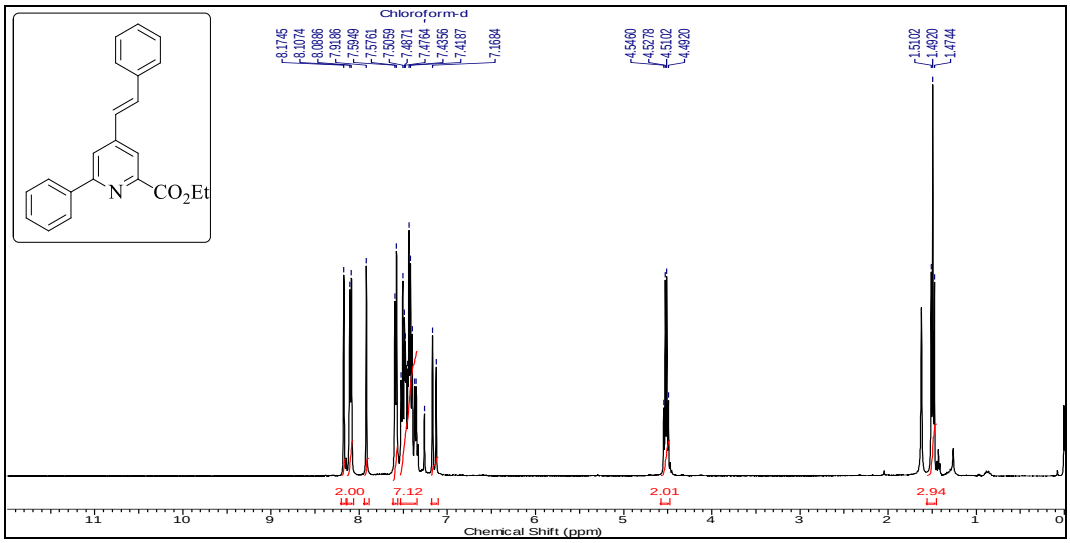


Figure 4.62 400 MHz ^{1}H NMR spectrum of **3am** in $CDCl_3$

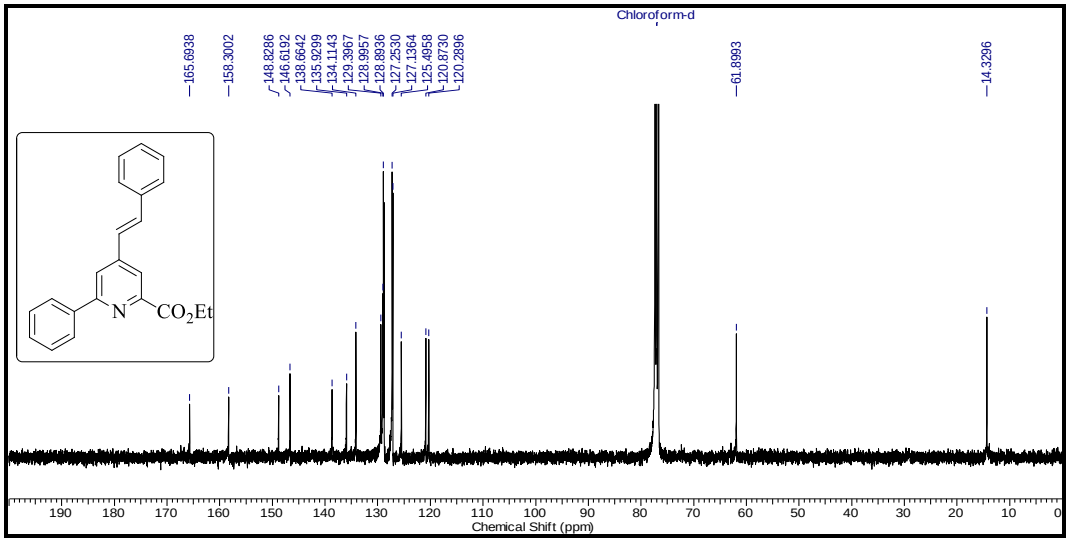


Figure 4.63 100 MHz ^{13}C NMR spectrum of **3am** in $CDCl_3$

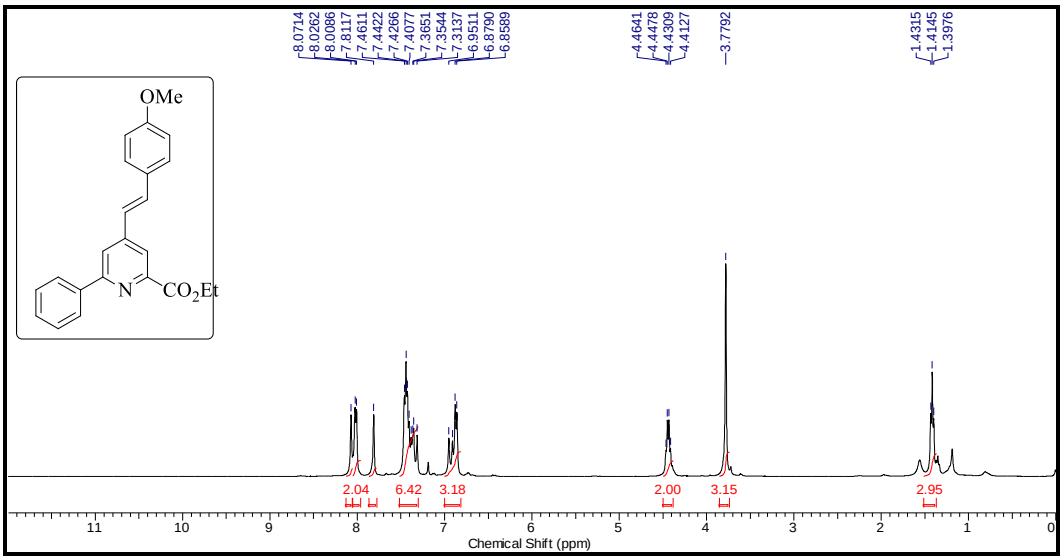


Figure 4.64 400 MHz ^{1}H NMR spectrum of **3an** in $CDCl_3$

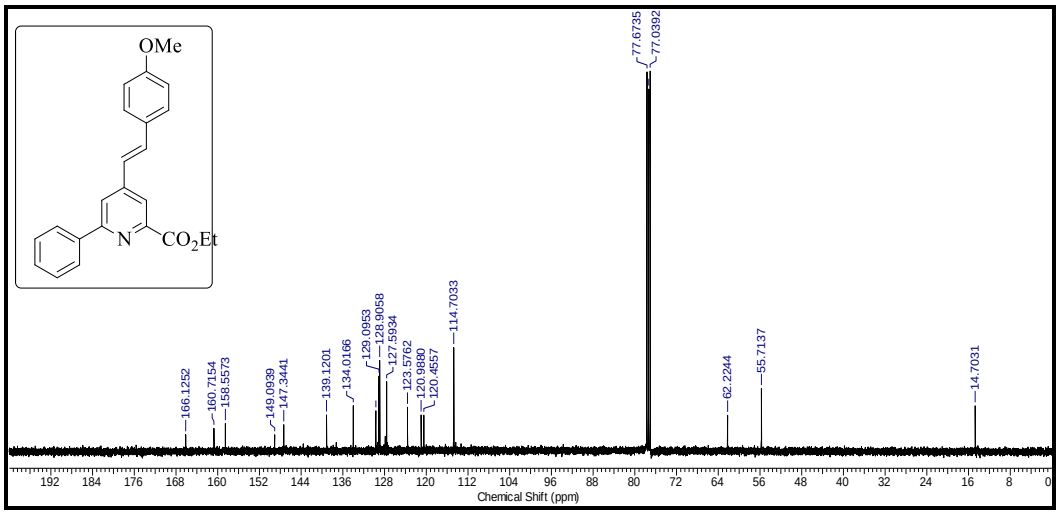


Figure 4.65 100 MHz ^{13}C NMR spectrum of **3an** in $CDCl_3$

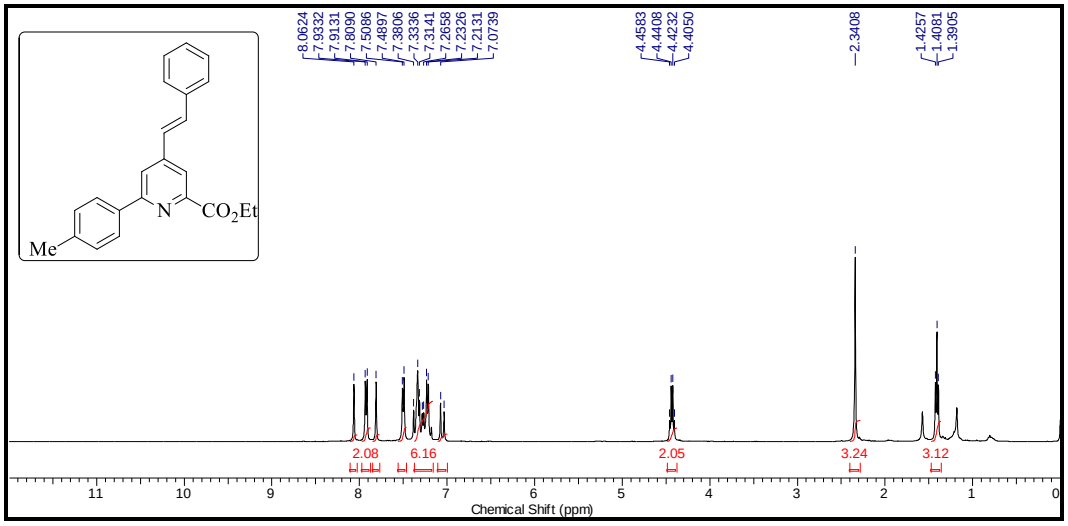


Figure 4.66 400 MHz ^{1}H NMR spectrum of **3bm** in $CDCl_3$

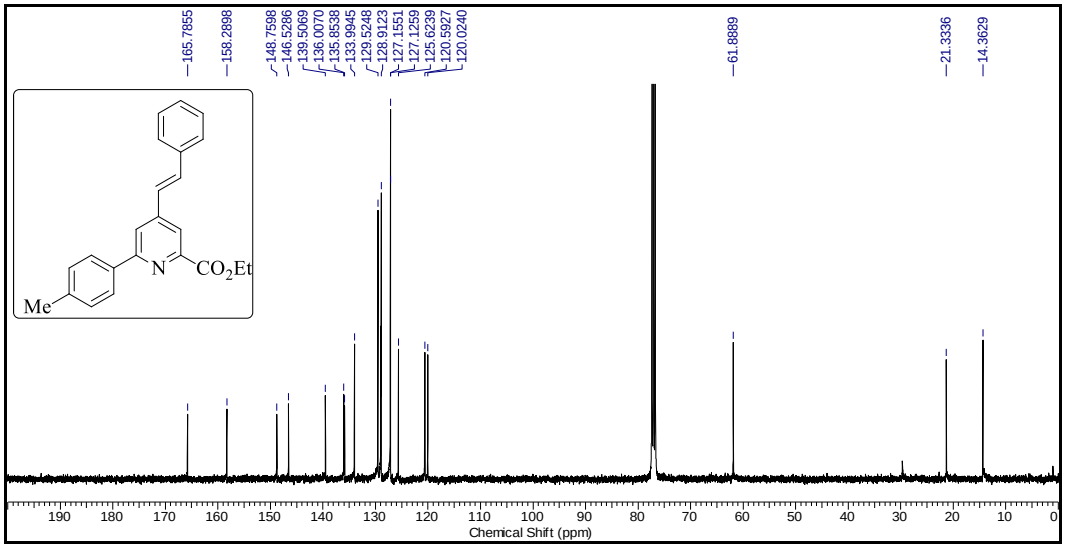


Figure 4.67 100 MHz ^{13}C NMR spectrum of **3bm** in $CDCl_3$

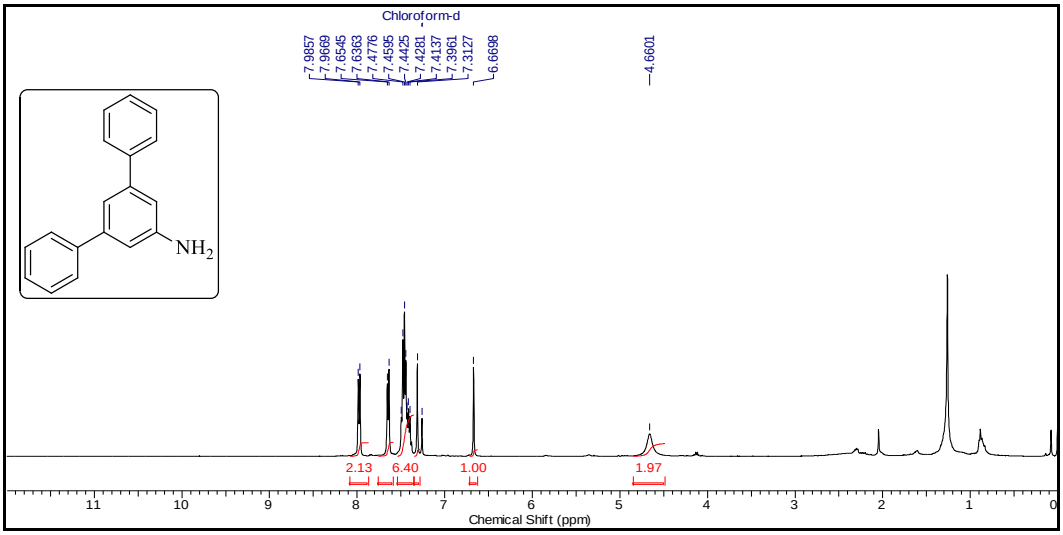


Figure 4.68 400 MHz ^{1}H NMR spectrum of **7** in $CDCl_3$

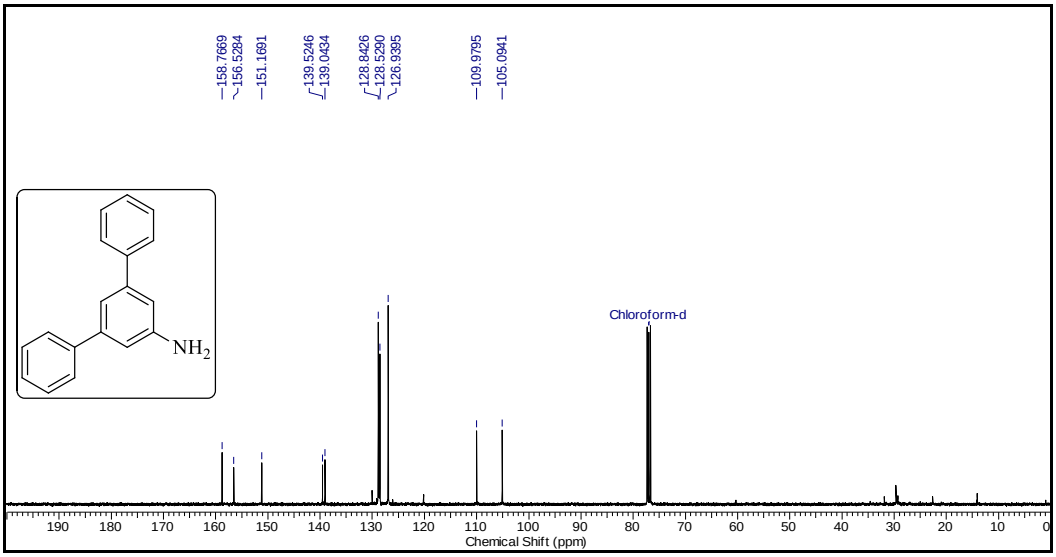


Figure 4.69 100 MHz ^{13}C NMR spectrum of **7** in $CDCl_3$

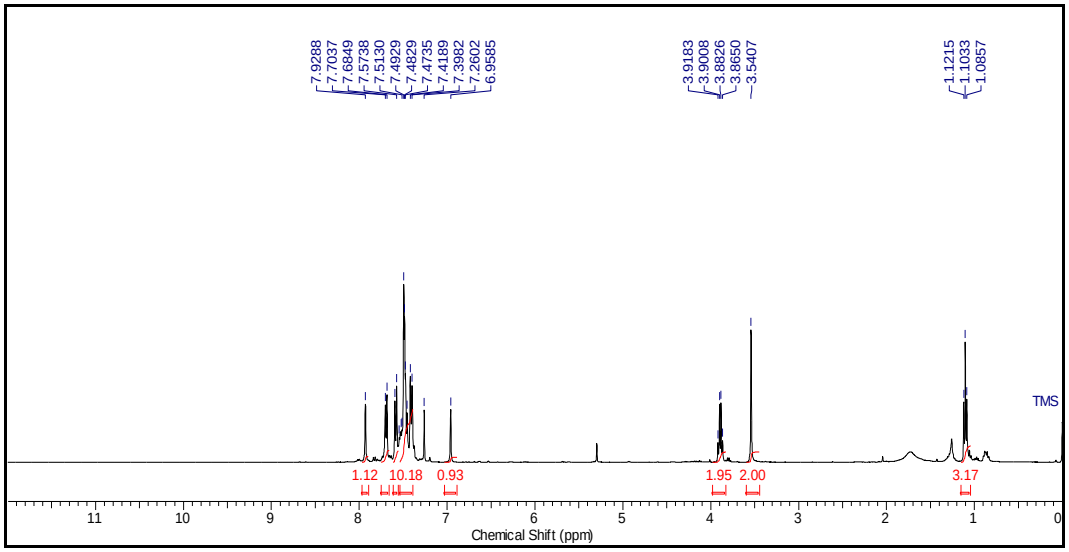


Figure 4.70 400 MHz ^{1}H NMR spectrum of **8** in $CDCl_3$

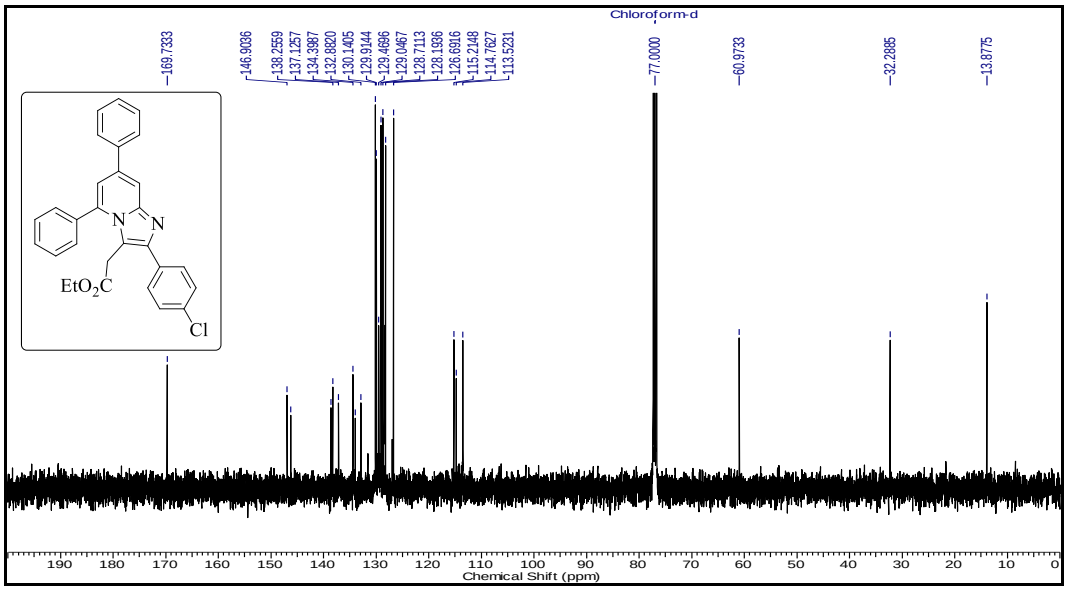


Figure 4.71 100 MHz ^{13}C NMR spectrum of **8** in $CDCl_3$

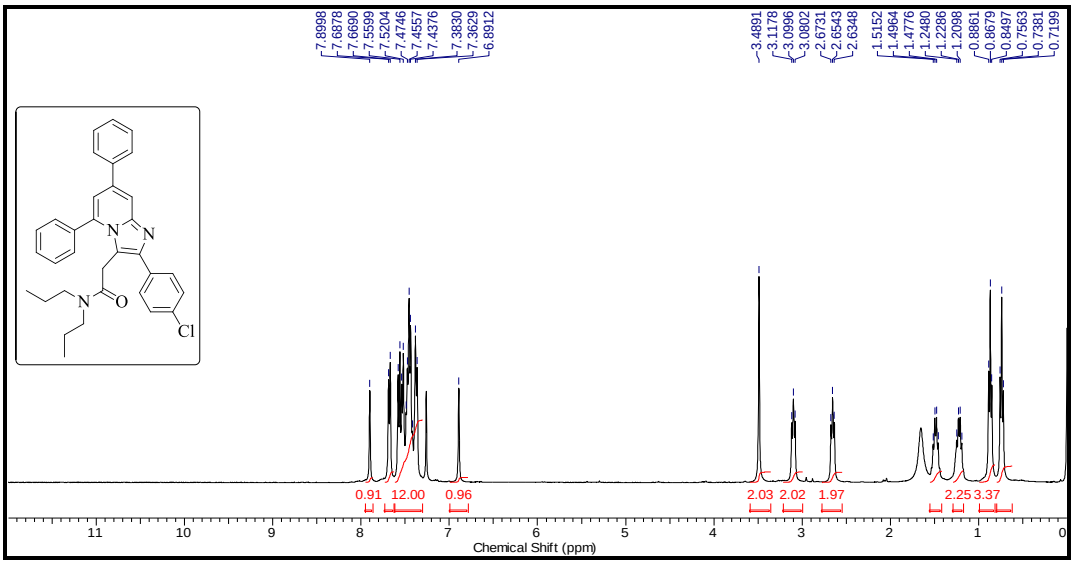


Figure 4.72 400 MHz ^{1}H NMR spectrum of **9** in $CDCl_3$

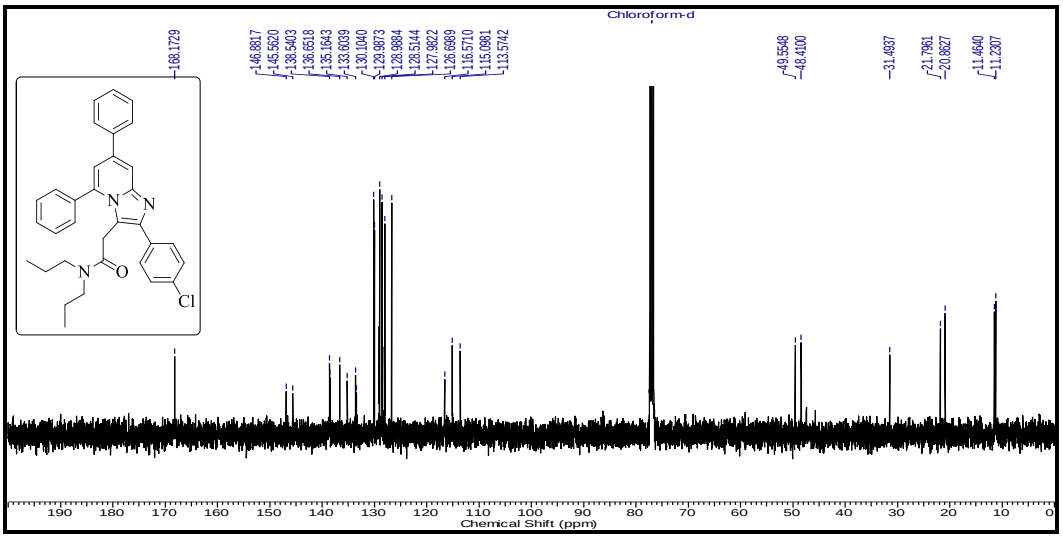


Figure 4.73 100 MHz ^{13}C NMR spectrum of **9** in $CDCl_3$

4.7 References

1. Gribble, G. W., Joule, J. A. (2015), Progress in heterocyclic chemistry, *Elsevier: Amsterdam*, 19, 314-352 (ISBN: 9780081000243)
2. Hopper D. W., Kuterer K. M. K., Crombie A. L., Clemens, J. J. (2009), In progress in heterocyclic chemistry, Eds. *Elsevier: Amsterdam*, 20, 289-332
3. Hill M. D. (2010), Recent strategies for the synthesis of pyridine derivatives, *Chem. Eur. J.* 2010, 16, 12052-12062 (DOI: 10.1002/chem.201001100)
4. Fu P., Wang S. X., Hong K., Li, X., Liu P. P., Wang Y., Zhu, W. (2011), Cytotoxic bipyridines from the marine-derived actinomycete *actinoalloteichus cyanogriseus* WH1-2216-6, *J. Nat. Prod.*, 74, 1751-1756 (DOI: 10.1021/np200258h)
5. Donohoe T. J., Jones C. R., Kornahrens A. F., Barbosa L. C. A., Walport L. J., Tatton M. R., O'Hagan M., Rathi A. H., Baker D. B. (2013), Total synthesis of the antitumor antibiotic (±)-Streptonigrin: firstand second-generation routes for de novo pyridine formation using ring-closing metathesis, *J. Org. Chem.*, 78, 12338-12350 (DOI: 10.1021/jo402388f)
6. Roth H. J., Kleemann A. (1988) Drug Synthesis in Pharmaceutical Chemistry, John Wiley and Sons, New York, Vol. 1.
7. Chen Y.L., Braselton J., Forman J., Gallaschun R. J., Mansbach R., Schmidt A. W., Seeger T. F., Sprouse J. S., Tingley, F. D. III, Winston E., Schulz D. W. (2008), *J. Med. Chem.*, 51, 1377-1384 (DOI: 10.1021/jm070578k)
8. Müller T. J. J., Bunz, U. H. F. (2007), Functional organic materials, Eds.; *Wiley-VCH: Weinheim*, (ISBN: 978-3-527-31302-0)
9. Sasabe H., Kido J. (2011), Multifunctional materials in high-performance OLEDs: challenges for solid-state lighting, *Chem. Mater.*, 23, 621-630 (DOI:10.1021/cm1024052)

10. Masters R. A., Lo W. C., Gast R. E. (2012), Aminopyralid. in modern crop protection compounds, 2nd ed., Kraemer, W., Ed.; *Wiley-VCH: Weinheim*, p 287
11. Henry G. D. (2004), De novo synthesis of substituted pyridines, *Tetrahedron*, 60, 6043-6061 (DOI: 10.1016/j.tet.2004.04.043)
12. Kang N.-G., Changez M., Lee J.-S. (2007), Living anionic polymerization of the amphiphilic monomer 2-(4-vinylphenyl)pyridine, *Macromolecules*, 40, 8553-8559 (DOI: 10.1021/ma071349a)
13. Murugan R., Scriven, E. F. V. (2003), *Aldrichimica acta*, 36, 21
14. De Rycke N., Couty F., David O. R. P. (2011), Increasing the reactivity of nitrogen catalysts, *Chem. Eur. J.*, 17, 12852-12871 (DOI: 10.1002/chem.201101755)
15. Bora D., Deb B., Fuller, A. L., Slawin A. M. Z., Derek Woollins J., Dutta D. K. (2010), Dicarbonyliridium(I) complexes of pyridine ester ligands and their reactivity towards various electrophiles, *Inorg. Chim. Acta*, 363, 1539-1546 (DOI: 10.1016/j.ica.2010.01.015)
16. Chan Y.-T., Moorefield C. N., Soler M., Newkome G. R. (2010), Unexpected isolation of a pentameric metallomacrocycle from the Fe^{II}-mediated complexation of 120º juxtaposed 2,2′:6′,2′′-terpyridine ligands, *Chem. Eur. J.*, 16, 1768-1711 (DOI: 10.1002/chem.200902988)
17. Eliel E. L., McBride R. T., Kaufmann S. (1953), Abnormal chichibabin reactions. The condensation of phenylacetaldehyde and homoveratric aldehyde with ammonia, *J. Am. Chem. Soc.*, 75, 4291-4296 (DOI: 10.1021/ja01113a043)
18. Allais C., Grassot J.-M., Rodriguez J., Constantieux T. (2014), Metal-free multicomponent syntheses of pyridines. *Chem. Rev.*, 114, 10829-10868 (DOI: 10.1021/cr500099b)
19. Simon C., Constantieux T., Rodriguez J. (2004), Utilisation of 1,3-dicarbonyl derivatives in multicomponent reactions, *Eur. J. Org. Chem.*, 4957-4980 (DOI: 10.1002/ejoc.200400511)

20. Neely J. M., Rovis T. (2014), Pyridine synthesis by [4 + 2] cycloadditions of 1-azadienes: hetero-Diels Alder and transition metal-catalysed approaches, *Org. Chem. Front.* 2014, 1, 1010-1015 (DOI: 10.1039/c4qo00187g)
21. Wang Y.-F., Toh K. K., Ng E. P. J., Chiba S. (2011), Mn(III)-mediated formal [3+3]-annulation of vinyl azides and cyclopropanols: a divergent synthesis of azaheterocycles, *J. Am. Chem. Soc.*, 133, 6411-6421 (DOI: 10.1021/ja200879w)
22. Parthasarathy K., Jeganmohan M., Cheng C.-H. (2008), Rhodium-catalyzed one-pot synthesis of substituted pyridine derivatives from α,β-unsaturated ketoximes and alkynes, *Org. Lett.* 2008, 10, 325-328 (DOI: 10.1021/ol7028367)
23. Martin R. M., Bergman R. G., Ellman J. A. (2012), Synthesis of pyridines from ketoximes and terminal alkynes *via* C-H bond functionalization, *J. Org. Chem.*, 77, 2501-2507 (DOI: 10.1021/jo202280e)
24. Wei Y., Yoshikai N. (2013), Modular pyridine synthesis from oximes and enals through synergistic copper/iminium catalysis, *J. Am. Chem. Soc.*, 135, 3756-3759 (DOI: 10.1021/ja312346s)
25. Jiang Y., Park C.-M. (2014), A catalyst-controlled selective synthesis of pyridines and pyrroles, *Chem. Sci.*, 5, 2347-2351 (DOI: 10.1039/c4sc00125g)
26. Lu J.-Y., Arndt H.-D. (2007), Hetero Diels-Alder synthesis of 3-hydroxypyridines: access to the Nosiheptide core, *J. Org. Chem.*, 72, 4205-4212 (DOI: 10.1021/jo0703505)
27. Manning J. R., Davies H. M. L. (2008), One-pot synthesis of highly functionalized pyridines *via* a rhodium carbenoid induced ring expansion of isoxazoles, *J. Am. Chem. Soc.*, 130, 8602-8603 (DOI: 10.1021/ja803139k)
28. Donohoe T. J., Bower J. F., Basutto J. A., Fishlock L. P., Procopiou P. A., Callens C. K. A. (2009), Ring-closing metathesis for the synthesis of

heteroaromatics: evaluating routes to pyridines and pyridazines, *Tetrahedron*, 65, 8969-8980 (DOI: 10.1016/j.tet.2009.07.076)

29. Neely J. M., Rovis T. (2013), Rh(III)-catalyzed regioselective synthesis of pyridines from alkenes and α,β-unsaturated oxime esters, *J. Am. Chem. Soc.*, 135, 66-69 (DOI: 10.1021/ja3104389)
30. Yu J., Kim K. H., Lee H. J., Kim J. N. (2013), An efficient synthesis of poly-substituted phenols and pyridines from Morita-Baylis-Hillman acetates and diethyl oxaloacetate, *Bull. Korean Chem. Soc.*, 34, 3027-3032 (DOI: 10.5012/bkcs.2013.34.10.3027)
31. Johnson P. L., Renga J. M., Galliford C. V., Whiteker, G. T., Giampietro N. C. (2015), Synthesis of novel fluoropicolinate herbicides by cascade cyclization of fluoroalkyl alkynylimines, *Org. Lett.*, 17, 2905-2907 (DOI: 10.1021/acs.orglett.5b01176)
32. Zhu C., Bi B., Ding Y., Zhang T., Chen Q.-Y. (2015), A mild and facile synthesis of polyfunctionalized pyridines: merging three-component cyclization and aerobic oxidation by amine/metal catalysts, *Org. Biomol. Chem.*, 13, 6278-6285 (DOI: 10.1039/c5ob00630a)
33. Majee D., Srivastava A., Mobin S. M., Samanta S. (2013), L-Proline catalyzed highly efficient synthesis of Z-5- alkylidene cyclic sulfamidate imines: an easy access to 5-alkyl-substituted cyclic sulfamidate imines, *RSC Adv.*, 3, 11502-11506 (DOI: 10.1039/c3ra40299a)
34. Majee D., Biswas S., Mobin S. M., Samanta S. (2014), An expedient one-pot sequential three-component reaction for the stereoselective synthesis of functionalized spiro-sulfamidate imine fused δ-lactone scaffold, *Tetrahedron Lett.*, 55, 4553-4558 (DOI: 10.1016/j.tetlet.2014.06.088)
35. Nair D. K., Mobin S. M., Namboothiri I. N. N. (2012), Synthesis of imidazopyridines from the MoritaBaylisHillman acetates of nitroalkenes and convenient access to Alpidem and Zolpidem. *Org. Lett.*, 14, 4580-4583 (DOI: 10.1021/ol3020418)
36. Gopi E., Kumar T., Menna-Barreto R. F. S., Valença W. O., da Silva E. N., Jr., Namboothiri I. N. N. (2015), Imidazoles from nitroallylic acetates

and α-bromonitroalkenes with amidines: synthesis and trypanocidal activity studies, *Org. Biomol. Chem.*, 13, 9862-9871 (DOI: 10.1039/c5ob01444a)

37. Huang W.-Y., Chen Y.-C., Chen K. (2012), Efficient synthesis of tetrasubstituted furans from nitroallylic acetates and 1,3-dicarbonyl/a-activating ketones by Feist-Bénary addition-elimination, *Chem. Asian J.*, 7, 688-691 (DOI: 10.1002/asia.201100988)
38. Magar D. R., Ke Y.-J., Chen K. (2013), Three-component synthesis of functionalized *N*-protected tetrasubstituted pyrroles by an addition-elimination-aromatization process, *Asian J. Org. Chem.*, 2, 330 (DOI: 10.1002/ajoc.201200193)
39. Dagar A., Biswas S., Samanta S. (2015), A catalyst-free, efficient green MCR protocol for access to functionalized γ-carbolines in water, *RSC Adv.*, 5, 52497-52507 (DOI: 10.1039/c5ra08422a)
40. Biswas S., Jaiswal P. K., Singh S., Mobin S. M., Samanta S. (2013), L-Proline catalyzed stereoselective synthesis of (*E*)-methyl-α-indol-2-yl-β-aryl/alkyl acrylates: easy access to substituted carbazoles, γ-carbolines and prenostodione, *Org. Biomol. Chem.*, 11, 7084-7087 (DOI: 10.1039/c3ob41573b)
41. Jaiswal P. K., Biswas S., Singh S., Samanta S. (2013), An organocatalytic highly efficient approach to the direct synthesis of substituted carbazoles in water, *Org. Biomol. Chem.*, 11, 8410-8418 (DOI: 10.1039/c3ob42034e)
42. Biswas S., Dagar A., Srivastava A., Samanta S. (2015), Access to substituted carbazoles in water by a one-pot sequential reaction of α,β-substituted nitro olefins with 2-(3-formyl-1*H*-indol-2-yl)acetates, *Eur. J. Org. Chem.*, 4493-4503 (DOI: 10.1002/ejoc.201500470)
43. Jiang Y., Park C.-M., Loh T.-P. (2014), Transition-metal-free synthesis of substituted pyridines *via* ring expansion of 2-allyl-2*H*-azirines, *Org. Lett.*, 16, 3432-3435 (DOI: 10.1021/ol501010k)

44. Enguehard-Gueiffier C., Gueiffier A. (2007), Recent progress in the pharmacology of imidazo[1,2,*a*] pyridines, *Mini-Rev. Med. Chem.*, 7, 888-899 (PMID: 17897079)
45. Bagdi A. K., Santra S., Monir K., Hajra A. (2015), Synthesis of imidazo[1,2-a]pyridines: a decade update *Chem. Commun*., 51, 1555-1575 (DOI: 10.1039/c4cc08495k)
46. Chernyak N., Gevorgyan V. (2010), General and efficient copper-catalyzed three-component coupling reaction towards imidazoheterocycles: one-pot synthesis of Alpidem and Zolpidem, *Angew. Chem., Int. Ed.*, 49, 2743-2746 (DOI: 10.1002/anie.200907291)
47. Wang Y.-Q., Yu C.-B., Wang D.-W., Wang X.-B., Zhou Y.-G. (2008), Enantioselective synthesis of cyclic sulfamidates *via* Pd-catalyzed hydrogenation, *Org. Lett.*, 10, 2071-2074 (DOI: 10.1021/ol800591u)
48. Reddy R. J., Chen, K. (2011), Highly efficient organocatalytic kinetic resolution of activated nitroallylic acetates with aldehydes *via* conjugate addition-elimination, *Org. Lett.*, 13, 1458-1461 (DOI: 10.1021/ol200133y)
49. Sheldrick G. M., *Acta Crystallogr., Sect. A,* 2008, **A64**, 112-122. *Program for Crystal Structure Solution and Refinement;* University of Goettingen: Goettingen, Germany, 1997.
50. Wu P., Cai X.-M., Yan C.-G. (2006), Microwave irradiation induced synthesis of 2-amino-4,6-diarylpyridines, *Chin. J. Org. Chem.*, 12, 1673-1676

Chapter 5

DABCO promoted domino reaction of cyclic sulfamidate imines with Morita-Baylis-Hillman acetates: a metal-free approach to functionalized nicotinic acid derivatives.

5.1 Introduction

A metal-free based domino approach for the construction of poly-functionalized pyridine containing an ester, nitrile or acetyl group at C-3 position (as surrogate of nicotinic acid or niacin or vitamin B_3) is a key research topic in chemical science[1-5] because this evergreen aza-heterocycle as well as its nicotinic acid

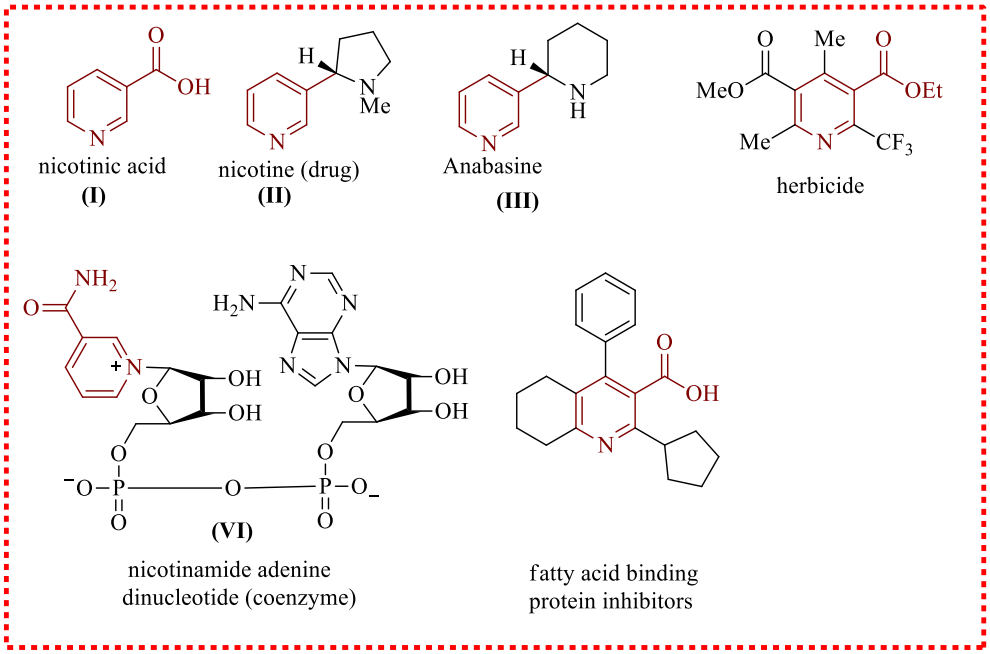


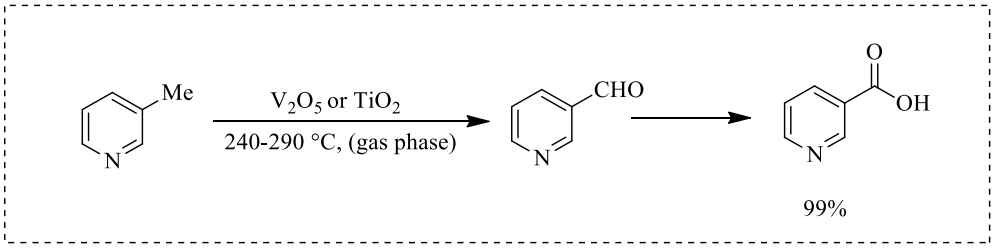
Figure 5.1 Several biologically active natural products having a nicotinic scaffold

frameworks constitute several marketable drugs,[2.5] biologically active natural products,[3-5] pharmaceuticals,[6,7] agrochemicals,[8,9] functional materials,[10,11] and ligands for catalysis[12] (**Figure 5.1**). Owing to their vast applications

including the treatment of human health, several chemists have been devoted towards the efficient synthesis of nicotinic acid derivatives by adopting several modern techniques.[13-35] A few recent reports on the synthesis of nicotinic acid derivatives have been discussed in the review **Section 5.2**.

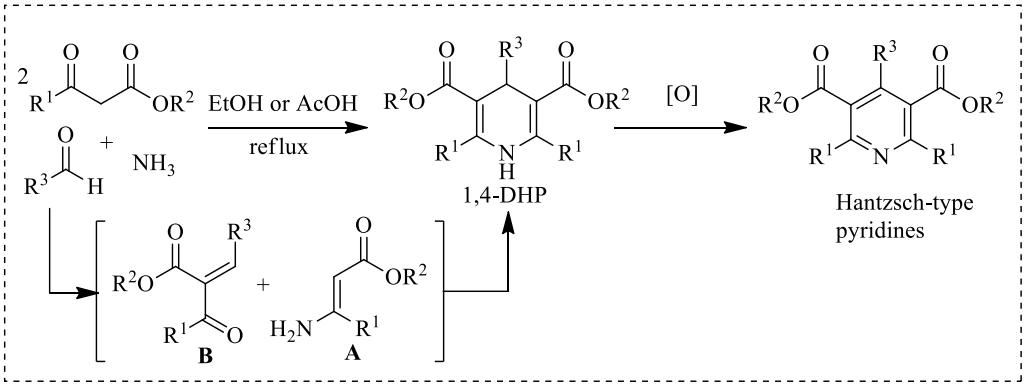
5.2 Review of literature

In 1994, Krishnan *et al*. has developed a synthetic route for the synthesis of unsubstituted nicotinic acid from 3-picoline *via* oxidation reaction in gaseous phase by using vanadium pentoxide on the high surface titanium dioxide (5-50 wt % vanadium) as discussed in **Scheme 5.1**.[36]



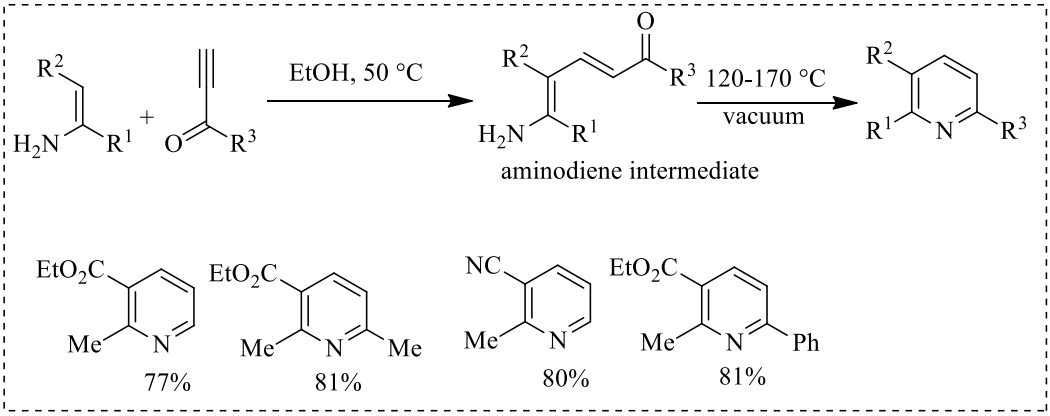
Scheme 5.1 Synthesis of nitotinic acid

Meyers and co-workers explored a two-step protocol for the synthesis of pyridine derivatives by Hantzsch-type pseudo four component reaction of 2 equivalent of a 1,3-dicarbonyl derivative, an aldehyde and ammonia to provide 1,4-dihydropyridines (DHPs).[37] The latter on subsequent oxidation gives symmetrical pyridines (**Scheme 5.2**).



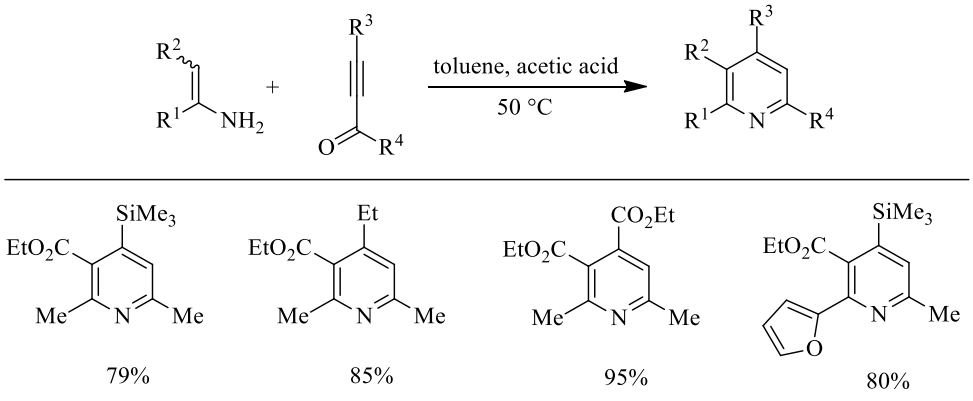
Scheme 5.2 Synthesis of nicotinate derivative *via* Hantzsch's type synthesis

In 1957, Bohlmann and Rahtz reported for the first time a regioselective two-step synthetic procedure for the synthesis of nicotinate/nictinonitrile derivatives by performing the reaction between enamines and ethynyl ketones in ethanol at 50 °C, followed by isomerization-cyclization of isolated intermediate at high temperatures 120-170 °C in vacuum condition (**Scheme 5.3**).[13,14]



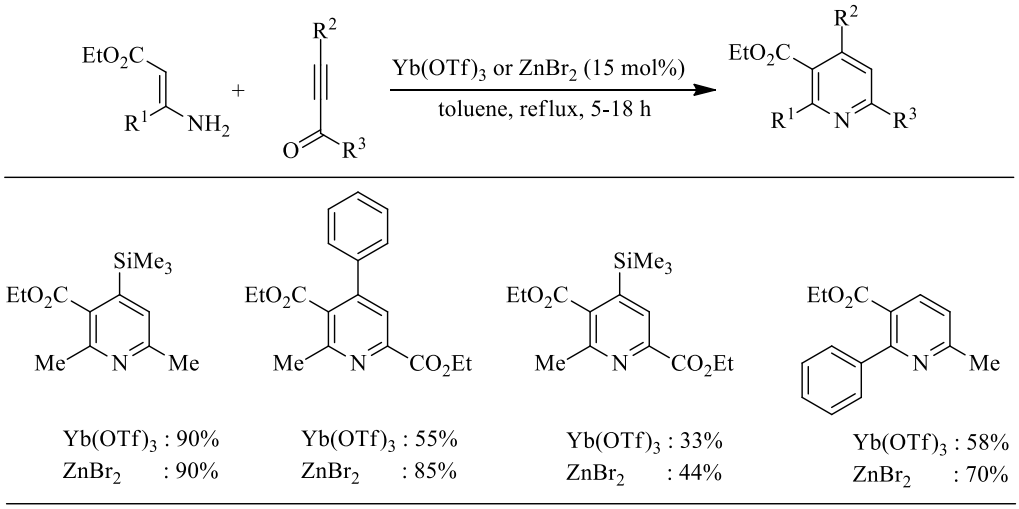
Scheme 5.3 The original Bohlmann-Rahtz pyridine synthesis (1957)

The above two-step synthetic method further improved into a one-pot manner by performing the reaction in the presence of several Lewis acids/Brønsted acids. In this direction, in 2001, Bagley *et al.* developed a one-pot protocol for the access to functionalized nicotinate in high to excellent yield by the reaction of several enaminoesters and ethynyl ketones at 50 ºC in toluene promoted by acetic acid.[38] Few examples are included in **Scheme 5.4**.



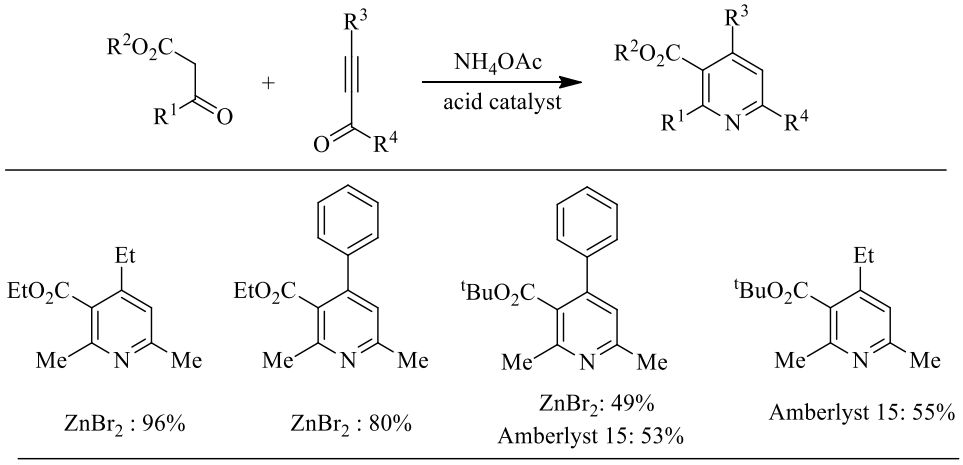
Scheme 5.4 Brønsted acid promoted synthesis of functionalized nicotinates

Interestingly, Bagley *et al.* has further developed that Bohlmann-Rahtz heteroannulation reaction could be efficiently performed in the presence of a catalytic amount of transition metal-salt ($Yb(OTf)_3$, $ZnBr_2$) under refluxing conditions (**Scheme 5.5**).[39] However, the current method is associated with a limited substrate scope due to the practical difficulty of the synthesis and isolation of enamine substrates which renders the practical applicability of current method.



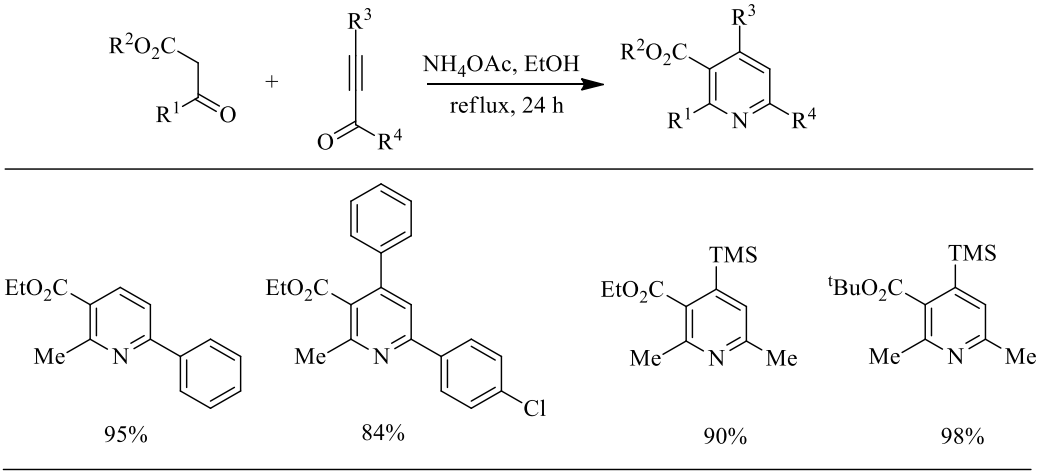
Scheme 5.5 Lewis acid promoted synthesis of functionalized nicotinates

In order to bypass the above problems, the combinations of several β-ketoesters and ammonium acetate (*in situ* generated enaminoester) have been employed in the one-pot three component reaction with a number of alkynones catalyzed by several Brønsted or Lewis acids or Amberlyst 15 ion exchange resin, resulting in good to excellent yields of polysubstituted nicotinate derivatives.[40] Few examples are given in **Scheme 5.6**.



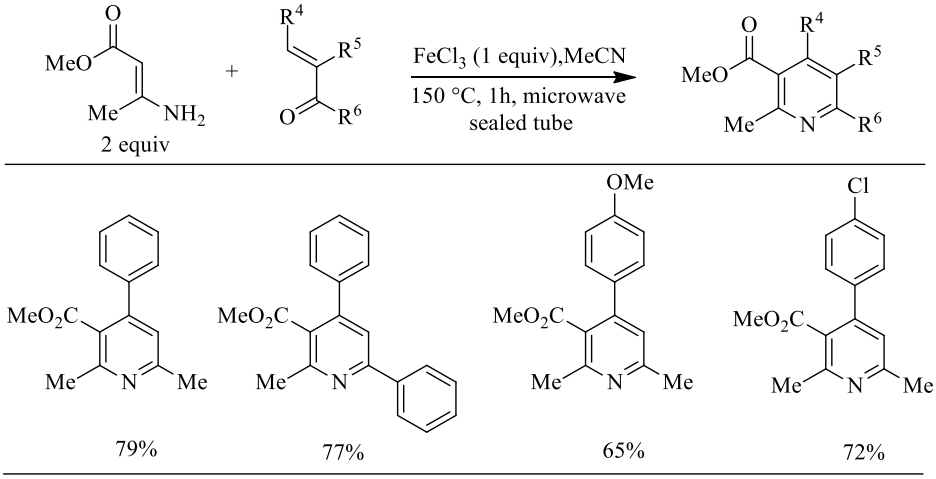
Scheme 5.6 Multicomponent synthesis of polyfunctionalized nicotinate derivatives.

It should be noted that the above reaction could be performed in ethanol under catalyst-free conditions. However, the completion of reaction required for longer time (24 h) as reported by Bagley and his co-workers (**Scheme 5.7**).[41]



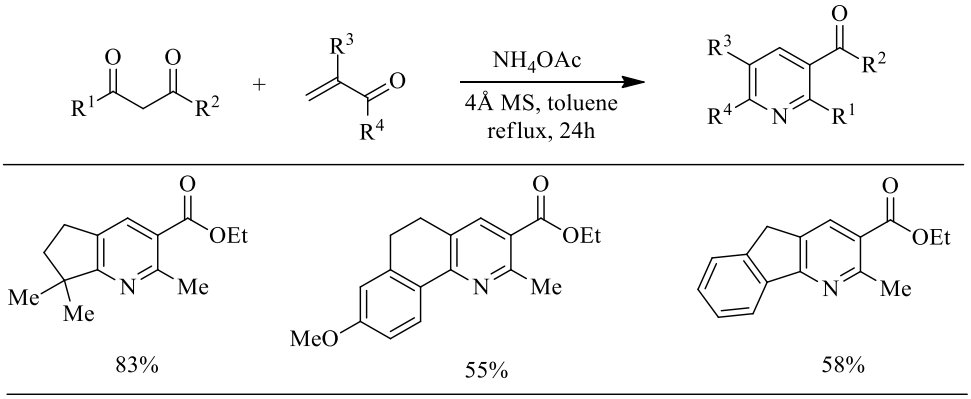
Scheme 5.7 Three component reaction for the synthesis of polysubstituted nicotinate

In 2017, Nishiwaki and his group has documented a novel [3+3] cyclization reaction for the synthesis of highly substituted nicotinates from enaminoesters and α, β-unsaturated ketones in MeCN at 150ºC under microwave irradiation for 1h promoted by stoichiometric amount of $FeCl_3$ (**Scheme 5.8**).[42]



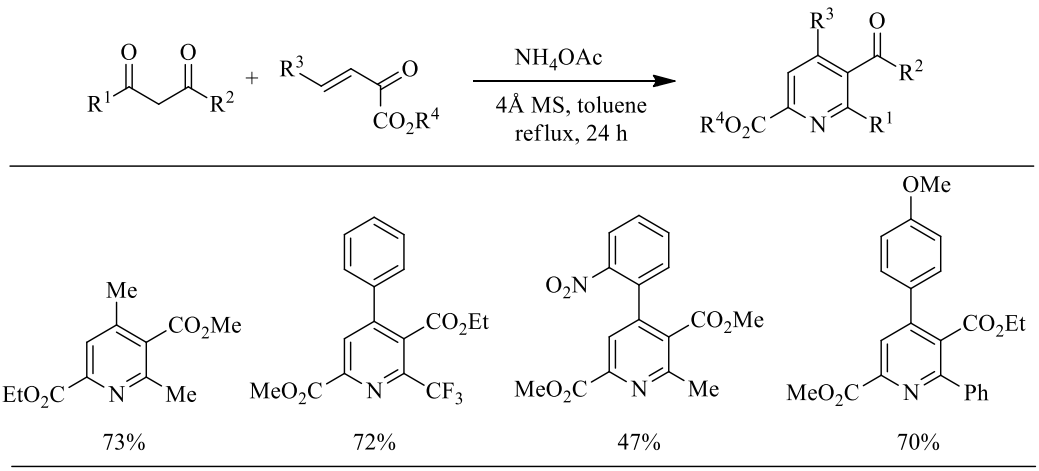
Scheme 5.8 Formation of highly substituted nicotinates from α, β-unsaturated ketones

In 2008, an interesting three-component domino reaction was carried out by involving the direct condensation of 1,3-dicarbonyls, acroleins as Michael acceptors and NH_4OAc in the presence of 4Å molecular sieves (MS) to provide a series of nicotinates in a satisfactory level of yields as developed by Rodriguez and co-workers.[19] A few examples are given in **Scheme 5.9**.



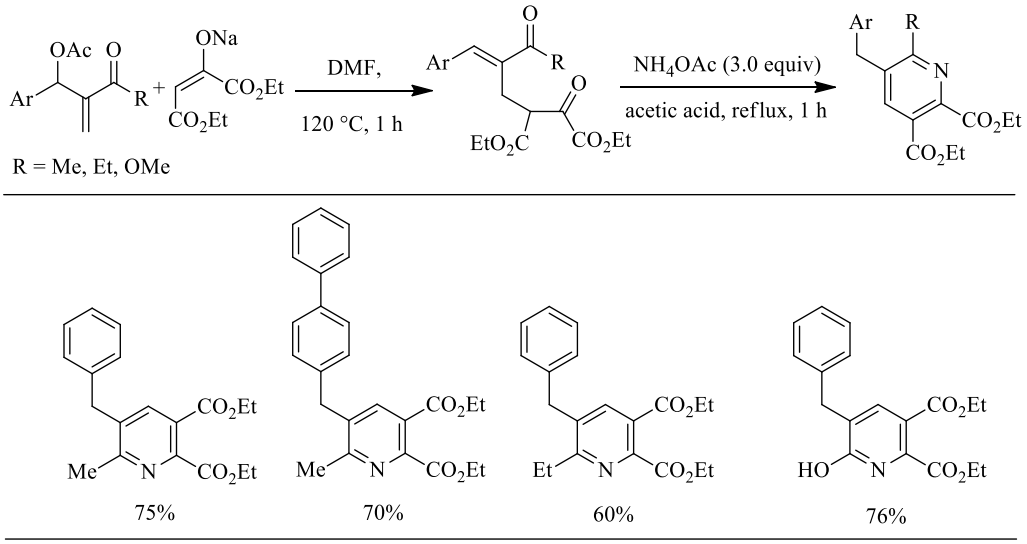
Scheme 5.9 Synthesis of substituted nicotinate from 1,3-dicarbonyls

In 2009, the same group also developed an alternative procedure for the preparation of interesting functionalized nicotinate derivatives by using β,γ-unsaturated α-ketoesters as acceptors in the place of acroleins promoted by acetic acid.[18] This three component reaction offers desired pyridine derivatives in medium to excellent yields with completely regioselective manner (**Scheme 5.10**).



Scheme 5.10 Multi-component approach towards the synthesis of trisubstituted nicotinates.

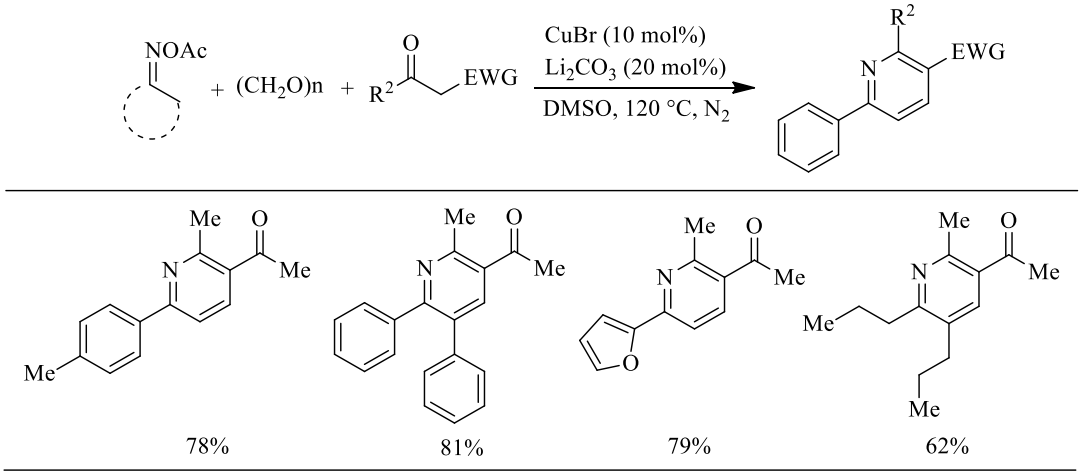
Several Morita-Baylis-Hillman acetates of methyl vinyl ketone have been utilized as bis-electrophiles in the S_N2' reaction with sodium diethyl oxalacetate in DMF at 120 °C to provide MBH adducts which were further converted into nicotinate derivatives by *in situ* iminocyclization using NH_4OAc as N-source in AcOH for 1 h under refluxing conditions as reported by Kim *et al*. in 2013 (**Scheme 5.11**).[32]



Scheme 5.11 Synthesis of poly-substituted nicotinates using MBH acetates of MVK

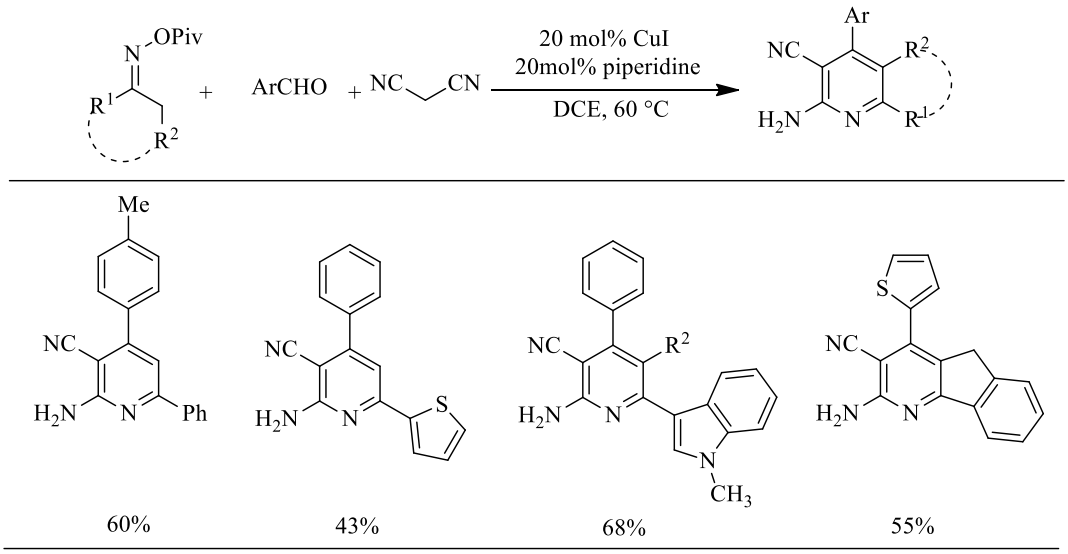
Synthesis of 3-acetyl pyridine and nicotinonitrile derivatives (Surrogate of nicotinate)

In 2015, Jiang and co-workers revealed a Cu-catalyzed three component cascade annulation reaction taking various oxime acetates, activated methylene compounds, and a wide range of aldehydes bearing aryl, heteroaryl, vinyl, and trifluoromethyl groups to provide the tri- or tetrasubstituted nicotinate.[43] This one-pot procedure is mild enough to prepare a vide verities of substituted nicotinate derivatives. (**Scheme 5.12**)



Scheme 5.12 Synthesis of substituted nicotinate with various oxime acetates and active methylene compounds

An excellent procedure for the synthesis of 2-aminonicotinonitriles by copper-catalyzed cyclization of oxime ester, aldehyde and malonitrile at 60ºC in DCE was described by Cui group in 2014.[44] Some of the examples are described in **Scheme 5.13.**



Scheme 5.13 Multicomponent fashion for the synthesis of 2-aminonicotinonitriles

5.2.1 Conclusion

The review work suggested that several efficient and practical synthetic methods have been reported for the synthesis of functionalized nicotinate derivatives in good to excellent yields. However, the use of metal-salts and strong acids, lack of generality, poor chemical yields with multiple by-products, harsh reaction conditions, multi-steps *etc.* are major drawbacks of all the above literature procedures. To solve the above difficulties, the development of a simple, efficient, metal-free based new synthetic technique for the construction of an important class of functionalized nicotinic acid derivatives from simple raw materials remains a difficult task for synthetic organic chemist.

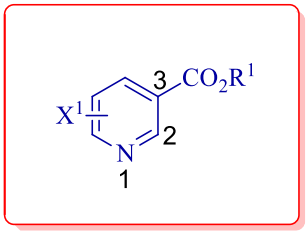
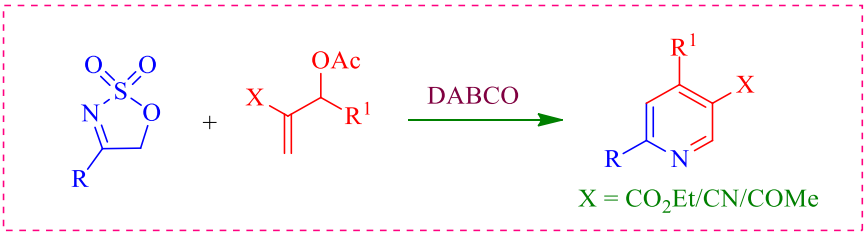


Figure 5.2 Functionalized nicotinate

5.3 Present work

A facile and metal-free pot-economy synthesis of diverse substituted nicotinate derivative is still demanding in synthetic as well as medicinal chemistry. Recently we have reported a novel DABCO promoted one-pot protocol for the synthesis of 4,6-diarylpicolinates *via* a domino S_N2' addition-elimination sequence reaction of 5-membered cyclic sulfamidate imines as nucleophiles with Morita-Baylis-Hillman acetates derived from nitroolefins (**Scheme 4.3**).[45] With this understanding, we assumed that a similar kind of pyridine derivative may be obtained by employing β-unsubstituted MBH acetate of acrylate[46,47] as well-known nucleophilic acceptor instead of taking β-substituted MBH acetate of nitroolefin in the domino reaction with cyclic sulfamidate imines which may proceed in the S_N2 manner, leading to nicotinic acid derivatives. Here in, we report an interesting domino reaction of several cyclic sulfamidate imines with different types of aryl-substituted MBH acetates bearing ester/nitrile/acetyl groups in 2-MeTHF as an eco-friendly solvent promoted by DABCO to afford a novel series of 4,6-diarylnicotinates/nicotinonitriles/3-acetylpyridines as shown in **Scheme 5.14**).



Scheme 5.14 DABCO mediated domino reaction of MBH acetates with cylic sulfamidate imines.

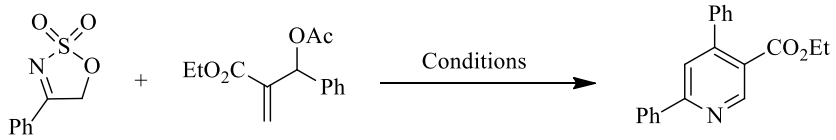
5.3.1 Results and discussion

5.3.1.1 Screening of solvents and bases

Taking the test substrate 4-phenyl-5*H*-1,2,3-oxathiazole-2,2-dioxide (**1a**) and MBH acetate of acrylate (**2a**), the reaction was carried out in 2-MeTHF as a green solvent at room temperature in the presence 1.5 equivalent of 1,4-diazabicyclo[2.2.2]octane (DABCO) as an organobase under O_2 atmosphere. Interestingly after 60h we were able to isolate our desired product 4,6-diarylnicotinate (**3aa**) in 10% yield (entry **1**, **Table 5.1**). The product **3aa** was fully characterized by its spectroscopic data (IR ^{1}H, ^{13}C and HRMS). The absence of singlet at 5.60 in ^{1}H NMR data indicates full consuming of **1a.** ^{1}H NMR spectrum shows that 7.37-9.13 ppm peaks indicate the corresponding aromatic protons of pyridine moiety. Furthermore, 4.17 (q, J = 7.2Hz) and 1.07 (t, J = 7.2 Hz) correspond to the CO_2Et group. In addition, ^{13}C NMR spectrum contains 17 peaks (15 of aromatic region and 2 of CO_2Et group) clears the formation of our desired nicotinate derivative **3aa.** The HRMS spectrum shows the presence of molecular ion peak $[M+H]^+$: 304.1362 which corresponds to the molecular weight of product of **3aa**. Gratifyingly, on increasing the reaction temperature from 45 °C to 70 °C, significant yield of **3aa** was enhanced from 52% to 82% after 48h (entries **2-3**). This interesting result promoted us to investigate the above unprecedented domino reaction in various common organic solvents and all the results were summarized in **Table 5.1.** Results indicated that polar solvents namely DMSO, DMF and EtOH reaction gave poor yields (21-33% , entries **9-11**) of **3aa** as compared to the non-polar ones (59-79%, entries **6-8**). Considering the yield (82%, entry **3**) and environment benign nature of 2-MeTHF, it was chosen as the best solvent for this conversion. Next, we tested this domino reaction in the presence several common organic bases namely DBU, DMAP, DIPEA, Et_3N and quinine at 70 °C for 60 h. Surprisingly, all these bases led to unsatisfactory results (5-52% yields of **3aa**, entries **12-16**) as compared to DABCO (82%, 48h, entry **3**). In summary, the optimum reaction condition was using 4-phenyl-5*H*-1,2,3-oxathiazole-2,2-dioxide (**1a,** 1.0 equiv) and 1.1 equivalent of MBH acetate of

acrylate (**2a**) in presence of 1.5 equivalent DABCO in 2-MeTHF at 70 ºC to get the 4-6-diarylnicotinates (**3aa**) with 83% yield. It should be noted that a mediocre yield (56%, entry 5) of **3aa** was obtained when the same reaction was carried out under open atmosphere instead of O_2 balloon.

Table 5.1 Optimization of the reaction conditions[a]

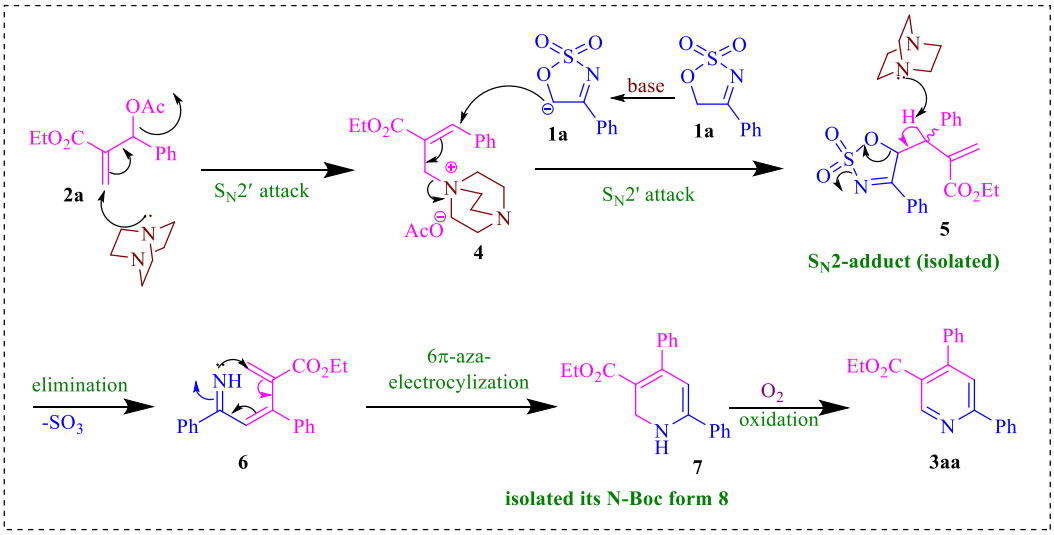


entry	base	solvent	temp(ºC)	time (h)	yield[b](%)
1	DABCO	2-MeTHF	rt	60	10
2	DABCO	2-MeTHF	45	60	52
3	DABCO	2-MeTHF	70	48	82
4[c]	DABCO	2-MeTHF	70	48	83
5[d]	DABCO	2-MeTHF	70	48	56
6	DABCO	THF	70	48	79
7	DABCO	toluene	70	48	74
8	DABCO	EtOAc	70	48	59
9	DABCO	DMSO	70	48	33
10	DABCO	DMF	70	48	27
11	DABCO	EtOH	70	48	21
12	DBU	2-MeTHF	70	60	5
13	DIPEA	2-MeTHF	70	60	<8
14	DMAP	2-MeTHF	70	60	41
15	Et_3N	2-MeTHF	70	60	32
16	Quinine	2-MeTHF	70	60	53

[a]Reaction conditions: 1a (0.2 mmol), 2a (0.22 mmol) and base (0.3 mmol) in solvent (1.0 mL) were heated at specified temperature under O_2 atmosphere. [b]Isolated yield. [c]DABCO (2.5 equiv.). [d]Open air.

5.3.1.2 Plausible mechanism

A reasonable mechanism for this domino reaction had been proposed as per the above conducting reaction results and depicted in **Scheme 5.15**. At first, DABCO may attack at the β-position of MBH acetate **2a** in a S_N2' fashion to form a reactive allylammonium salt **4**.[46,47] Next step a carbanion intermediate **1a′** is generated from **1a** *via* abstraction of an active methylene proton by a base which nucleophilically attack intermediate **4** to form a give an isolable S_N2 adduct **5** in a non-separable mixture of diastereomer (dr = 3:1). After that, in presence of base intermediate **5** eliminates SO_3 to form azatriene intermediate **6** which subsequently cyclize *via* 6π-aza-electrocyclization process.[27-30] to form dihyropyridine **7** and it is isolated in its *N*-Boc form **8**. Finally aromatization of dihyropyridine **7** occurs in the presence of O_2 to form our desired compound **3aa**.



Scheme 5.15 Possible mechanism of this domino reaction

5.3.1.3 Generality and substrate scope

Getting optimal conditions in hand we took several 4-aryl/heteroaryl-substituted cyclic sulfamidate imines (**1a-i**) as nucleophiles in the one-pot reaction with a diverse range of aryl substituted MBH acetates of acrylate (**2a-j**) to evaluate the scope and generality of the reaction. As shown in **Table 5.2** MBH acetates with

electron donating (Me, OMe, OBn) groups on the aryl rings (**2b-c**) reacts slower towards **1a** (48-72 h) as compared to MBH acetates with electron withdrawing ones such as F, Cl, Br, CF_3, CN and NO_2 (**2d- j**) (36-40 h). However in all the cases reaction occurred smoothly to form 4,6-diarylnicoytinates (**3ab-3aj**) with high yields (77-87%). The structure of compound **3ai** was established by its Single Crystal X-ray Diffraction data as shown **Figure 5.3**. Moreover, a range of cyclic sulfamidate imines (**1b-h**) possessing both electron rich (Me, OMe) and electron poor (F, Cl, Br) functionalities on the aryl nuclei used in this procedure which attacked MBH acetates (**2a-j**) in a S_N2 manner, resulting in good to high yields (74-86%) of the corresponding nicotinates (**3ba-3hg**). It is noticeable that electron withdrawing functionalities (e.g. F, Cl, Br) on the aryl ring of cyclic sulfamidate imines reduce their nucleophilicities, as a consequence slowing the rates of the reactions (48-60h). Moreover cyclic imines having heteroaryl-substituents such as thiophene (**1i**)/ furan (**1g**) also proceeded very well with a variety of MBH acetates under the present conditions leading to satisfactory chemical yields (70-77%) of 6-heteroaryl-substituted nicotinates (**3ia-3jg**). From the sustainable point of view several synthetically useful functionalities such as Me, OMe, OBn, F, Cl, Br, CF_3, NO_2, CN, CO_2Et, CO_2Me, hiophene, furan etc. remain unaltered in the present mild conditions. Furthermore, this protocols offers an easy route to synthesize unsymmetrical substituted nicotinates which cannot achieve by traditional Hantzsch pyridine synthesis which affords substituted symmetrical pyridines.[48]

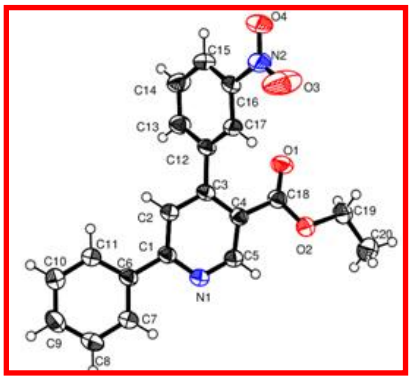
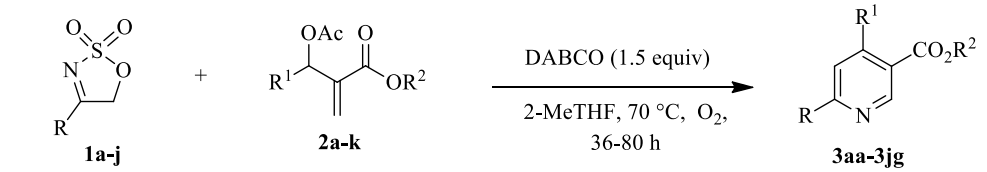


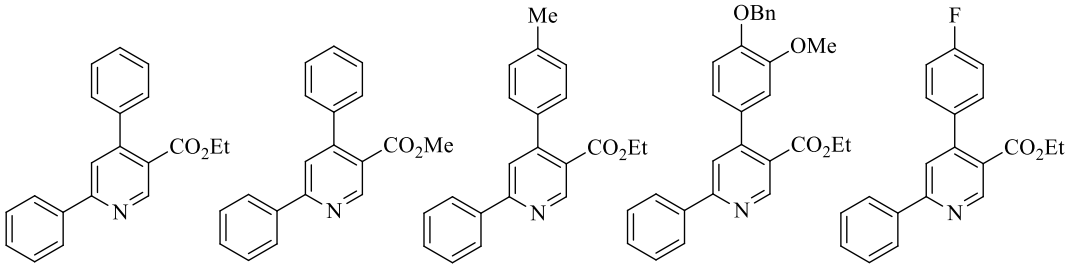
Figure 5.3 ORTEP diagram of compound **3ai (CCDC** 1522097**)**

Table 5.2 Substrate scope of 4,6-diarylnicotinate synthesis

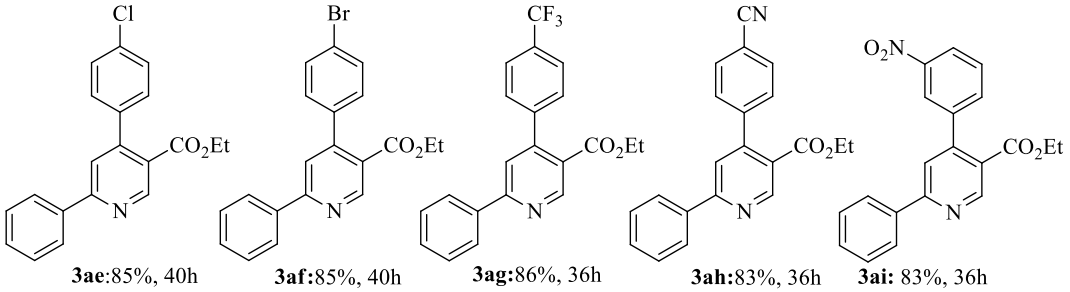


1a-j + **2a-k** → **3aa-3jg**

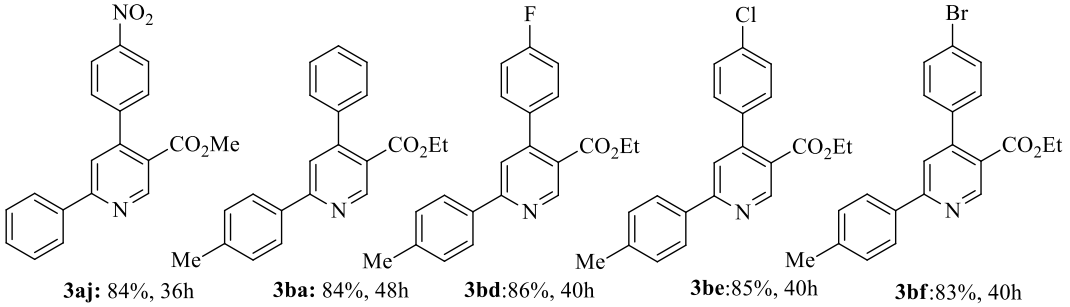
1a: R = C_6H_5, **2a**: R^1 = C_6H_5, **2a′**: R^2 = Me,
1b: R = 4-MeC_6H_4, **2b**: R^1 = 4-MeC_6H_4,
1c: R = 4-$MeOC_6H_4$, **2c:** R^1 = 3-MeO-4-OBn-C_6H_3,
1d: R = 2,5-$(MeO)_2C_6H_3$, **2d**: R^1 = 4-FC_6H_4,
1e: R = 4-FC_6H_4, **2e**: R^1 = 4-ClC_6H_4,
1f: R = 4-ClC_6H_4, **2f**: R^1 = 4-BrC_6H_4,
1g: R = 2-ClC_6H_4, **2g**: R^1 = 4-$CF_3C_6H_4$,
1h: R = 4-BrC_6H_4, **2h**: R^1 = 4-CNC_6H_4,
1i: R = C_4H_3S, **2i**: R^1 = 3-$NO_2C_6H_4$,
1j: R = C_4H_3O, **2j**: R^1 = 4-$NO_2C_6H_4$,



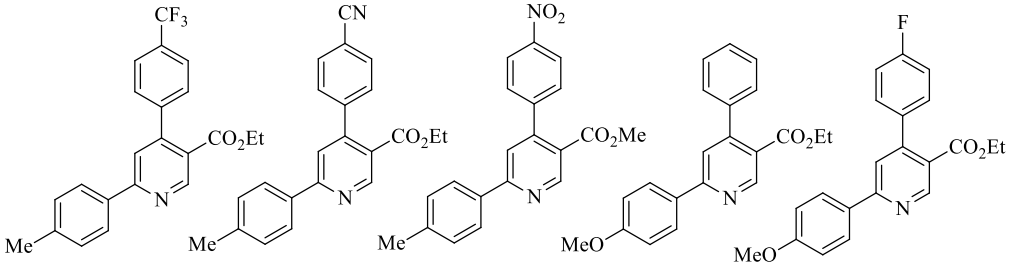
3aa: 82%, 48h **3aa':**80%, 48h **3ab:** 81%, 48h **3ac:** 77%, 72h **3ad**:87%, 40h



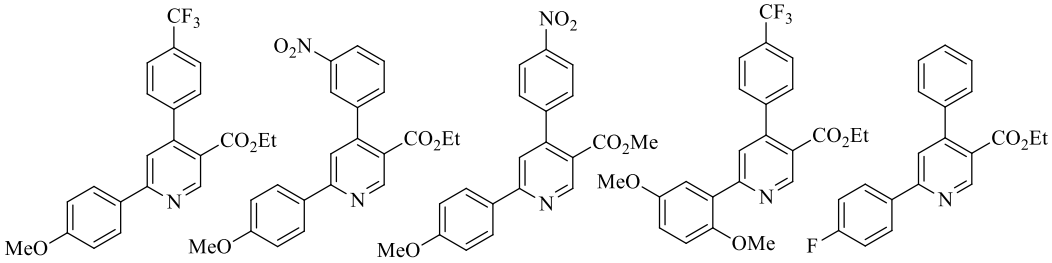
3ae:85%, 40h **3af:**85%, 40h **3ag:**86%, 36h **3ah:**83%, 36h **3ai:** 83%, 36h



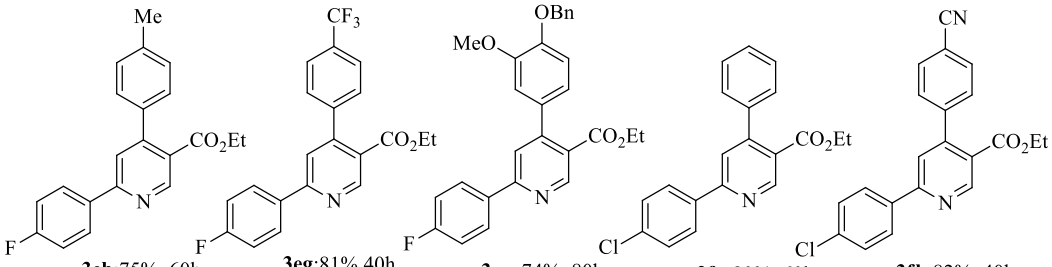
3aj: 84%, 36h **3ba:** 84%, 48h **3bd**:86%, 40h **3be**:85%, 40h **3bf**:83%, 40h



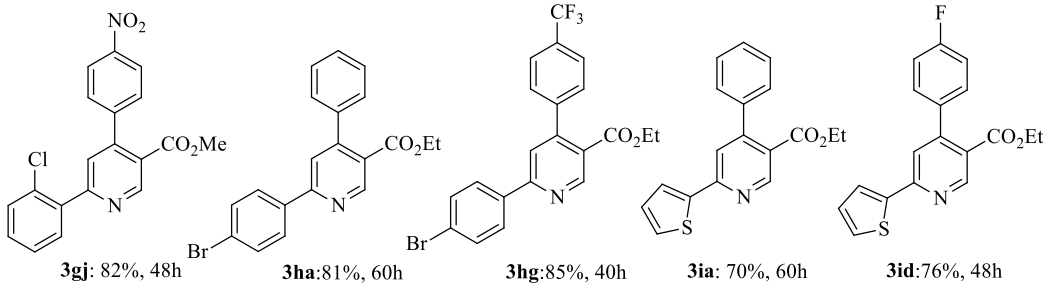
3bg:85%, 36h **3bh:**83%, 36h **3bj:** 84%, 36h **3ca:** 83%, 48h **3cd**:85%, 40h



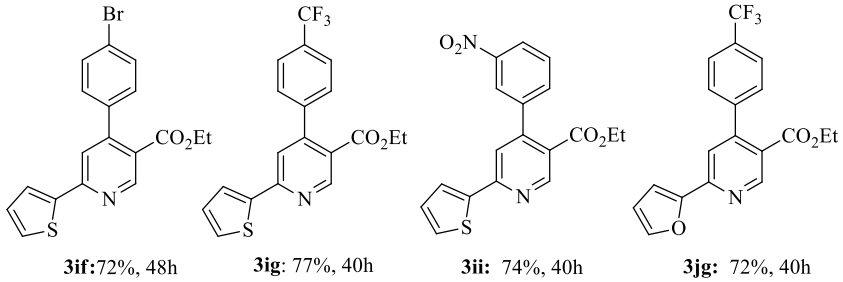
3cg:84%, 36h **3ci**: 82%, 36h **3cj**: 84%, 36h **3dg**: 77%, 36h **3ea**:77%, 60h



3eb:75%, 60h **3eg**:81%,40h **3ec**: 74%, 80h **3fa**:80%, 60h **3fh**:82%, 40h



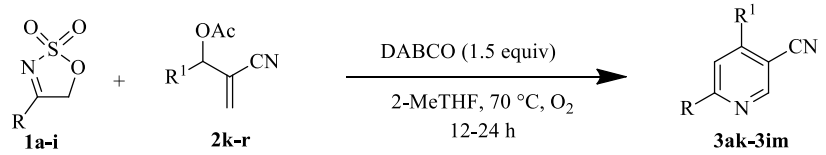
3gj: 82%, 48h **3ha**:81%, 60h **3hg**:85%, 40h **3ia**: 70%, 60h **3id**:76%, 48h



3if:72%, 48h **3ig**: 77%, 40h **3ii:** 74%, 40h **3jg:** 72%, 40h

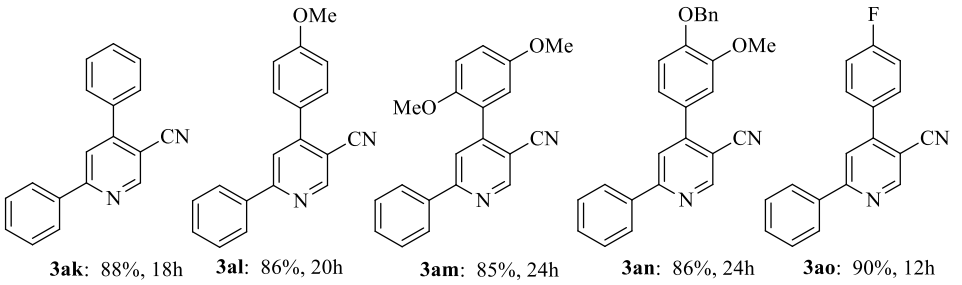
After successfully developing this simple metal-free one-pot synthesis of 4,6-diarylnicotinates, we then applied the same procedure for the preparation of synthetically more challenging[49-52] 4,6- diarylnicotinonitriles by involving the aryl-substituted MBH acetates derived from an acrylonitrile as reactive electrophiles. The obtained results in **Table 5.3** shows that the nature of substituents such as electron rich (Me, OMe, OBn) or electron deficient (F, Cl, Br, CF_3) and their positions on the aryl-rings of MBH adducts (**2k-r**) did not affect the reactions with a diverse range of aryl substituted cyclic imines (**1a-h**) under established conditions. All these reactions performed smoothly and providing consistently high to excellent yields (80-90%) of the corresponding 4,6-diarylnicotinonitriles (**3ak-3hr**, surrogates of nicotinic acid) after 12-24 h. Not only aryl substituted cyclic imine, but heteroaryl-substituted cyclic imine (**3i**) also obtained good yields (75-80%) of 6-thiophenyl-2-arylnicotinonitriles (**3ik-3im**) after 24 h when a 4-thiophenyl cyclic sulfamidate imine (**1i**) was used.

Table 5.3 Substrate scope of 4,6-diarylnicotinonitriles

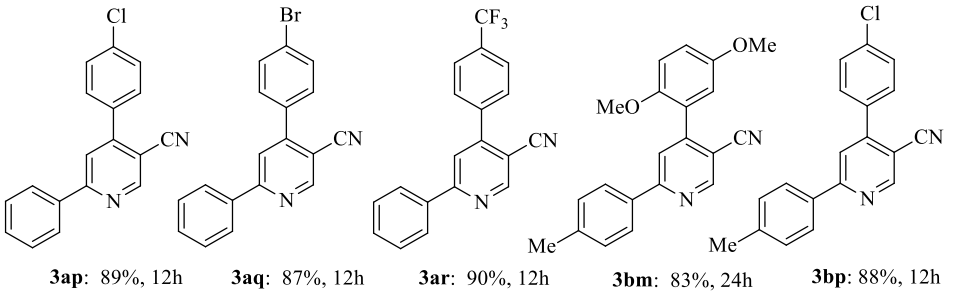


1a-i **2k-r** **3ak-3im**

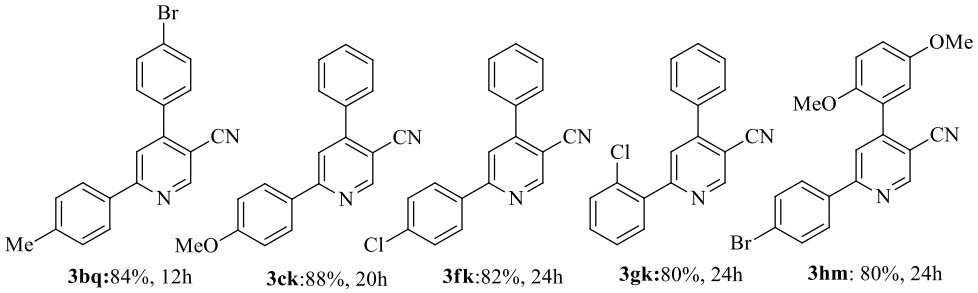
2k: $R^1 = C_6H_5$,
2l: $R^1 = 4\text{-}MeOC_6H_4$,
2m: $R^1 = 2,5\text{-}MeOC_6H_3$,
2n: $R^1 = 3\text{-}MeO\text{-}4\text{-}OBn\text{-}C_6H_3$,
2o: $R^1 = 4\text{-}FC_6H_4$,
2p: $R^1 = 4\text{-}ClC_6H_4$,
2q: $R^1 = 4\text{-}BrC_6H_4$,
2r: $R^1 = 4\text{-}CF_3C_6H_4$,



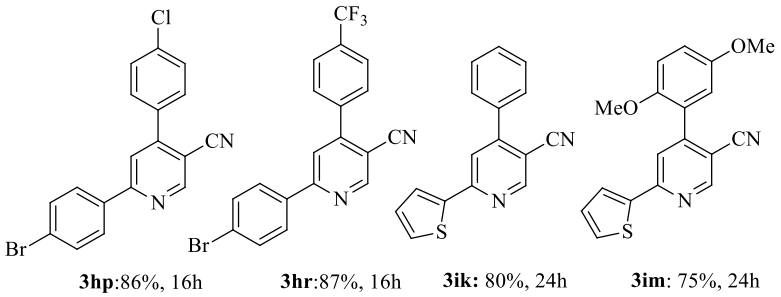
3ak: 88%, 18h **3al**: 86%, 20h **3am**: 85%, 24h **3an**: 86%, 24h **3ao**: 90%, 12h



3ap: 89%, 12h **3aq**: 87%, 12h **3ar**: 90%, 12h **3bm**: 83%, 24h **3bp**: 88%, 12h



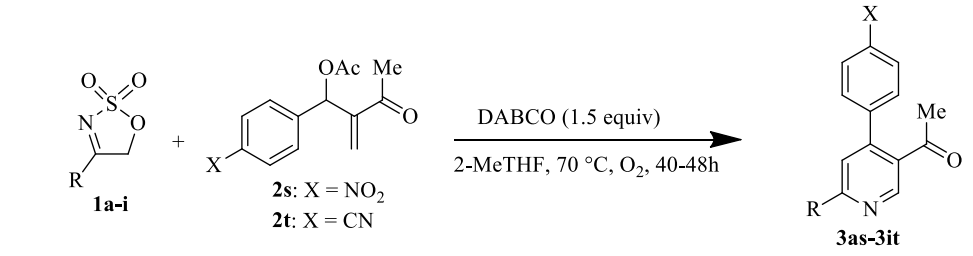
3bq:84%, 12h **3ck**:88%, 20h **3fk**:82%, 24h **3gk:**80%, 24h **3hm**: 80%, 24h

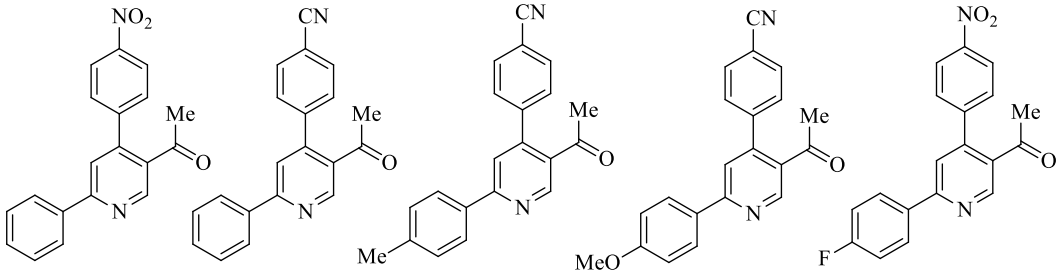


3hp:86%, 16h **3hr**:87%, 16h **3ik:** 80%, 24h **3im**: 75%, 24h

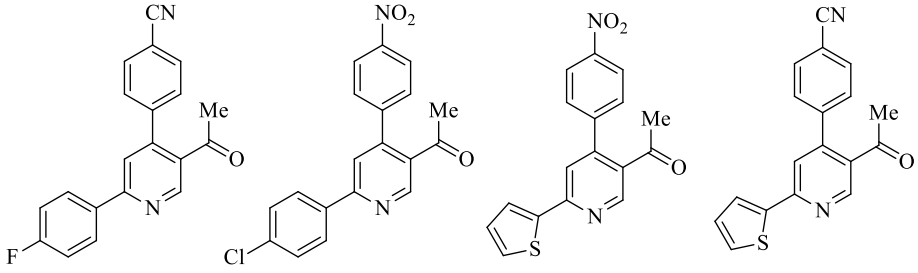
For further enrichment of the substrate scope, we were inspired to use chemically more challenging aryl substituted MBH acetates of MVK (**2s-2t**) for this domino reaction. After performed the reactions using various cyclic imines (**1a-i**) we were very pleased to say that all the reactions were very clean and furnished 74-83% yield of 3-acetylpyridines (**3as-3it**) after 40-48 h (**Table 5.4**). It should be notable that these types of acetyl pyridines are very difficult to prepare through conventional procedure. *[43, 44, 53-55]*

Table 5.4 Substrate scope of 3-acetyl-4,6-diarylpyridines





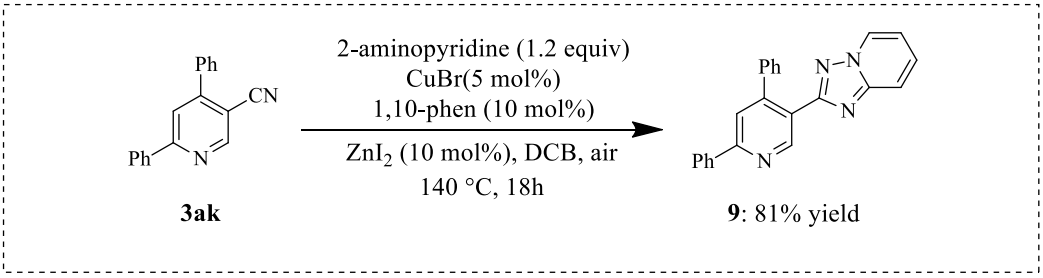
3as: 82% **3at**:80% **3bt**: 82% **3ct:** 83% **3es**:74%



3et:73% **3fs**:75% **3is**:76% **3it**:74%

5.3.1.4 Synthesis of triazolopyridine derivative

To check the potential utility of the prepared compounds we have started with the final nitrile compound **3ak**. Nitrile compound was reacted with 2 amino pyridine in the presence of 5 mol % CuBr and 10 mol% 1,10-phenanthroline (1,10-Phen) in 1,2-dichlorobenzene (DCB) at 130 °C under an air atmosphere.[56] After 18 h we got triazolopyridine derivative **9** with 81% yield which has structural similarity with the potential PDE10A inhibitor (**Scheme 5.16**).[57]



Scheme 5.16 Synthesis of trizolopyridine derivative **9**

5.4 Conclusion

In that part, we have established a general, expedient, metal-free based novel domino reaction of several aryl/heteroaryl-substituted cyclic sulfamidate imines as suitable nucleophiles with a broad range of MBH acetates bearing ester/cyano/acetyl groups in the presence of DABCO as a base under O_2 atmosphere at 70 °C. This unprecedented tactic delivers a series of pharmacologically valuable 3-carboxylate/cyano/acetyl-4,6-diarylpyridine derivatives in high to excellent yields. Moreover, this smart pot-economy approach eliminates the use of highly expensive and toxic metal-salts, strong acids, large excess of external oxidants, multistep etc. In addition, the operational simplicity, broad substrate generality, compatibility with a variety of functional groups on the aryl rings and high to excellent yields make this procedure more powerful alternative to the established methods

5.5 Experimental section

5.5.1 General information

All the 4-aryl/heteroaryl-*5H*-1,2,3-oxathiazole-2,2-dioxides (**1a-j**)[58] and Morita-Baylis-Hillman acetates (**2a-2l**)[59,60] were synthesized by literature known procedures. All the bases were purchased from commercial sources (Sigma-Aldrich). All the reactions were carried out under O_2 atmosphere and monitored by TLC using Merck 60 F_{254} pre coated silica gel plates (0.25 mm thickness) and the products were visualized by UV detection. Flash chromatography was carried out with silica gel (200-300 mesh). FT-IR spectra were recorded on a BrukerTensor-27 spectrometer. ^{1}H and ^{13}C NMR spectra were recorded on a Bruker Avance (III) 400 MHz spectrometer. Data for ^{1}H NMR are reported as a chemical shift (δ ppm), multiplicity (s = singlet, d = doublet, t = triplet, q = quartet, m = multiplet), coupling constant *J* (Hz), integration, and assignment, data for ^{13}C are reported as a chemical shift. High resolutions mass spectral analyses (HRMS) were carried out using ESI-TOF-MS.

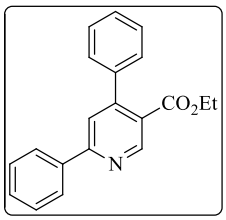
Representative one-pot procedure for the synthesis of ethyl 4,6-diphenylnicotinate (3aa):

To a stirred solution of compound **1a** (39.4 mg, 0.2 mmol) and **2a** (54.6 mg, 0.22 mmol) in 2-MeTHF (1.0 mL) was added DABCO (33.6 mg, 0.3 mmol) at room temperature. Then the reaction mixture was heated at 70 °C for 48h under O_2 atmosphere (monitored by TLC). Upon completion of the reaction, the reaction mixture was extracted with ethyl acetate (3 × 10 mL), washed with water and brine respectively, dried over Na_2SO_4. The combined organic phases were evaporated under reduced pressure to afford the crude product. Finally it was obtained in a pure form (49.7 mg, 82%) through column chromatography over silica-gel using a mixture of EtOAc/hexane (1:4, v/v) as the eluent. The product

was fully characterized by its spectroscopic data (IR, ^{1}HNMR, ^{13}C NMR and HRMS).

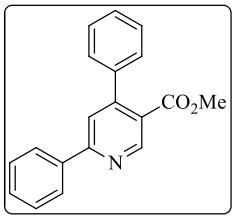
All the products (**3ab-3jg**) in Table **5.1**, **3al-3in** in Table **5.2** and **3at-3iu** in Table **5.3** were synthesized following the above procedure. All the products were characterized by their corresponding spectroscopic data (IR, ^{1}H, ^{13}C NMR and HRMS).

Ethyl 4,6-diphenylnicotinate (3aa):[27] white solid; (49.7 mg, 82%); **mp**: 110-



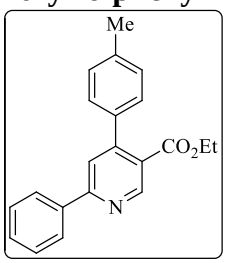
112 °C; $\mathbf{R_f}$ = 0.85 (EtOAc:hexane = 1:4); **IR** (KBr): ν 1700, 1585, 1534, 1493, 1467, 1443, 1363, 1299 cm^{-1}; **^{1}H NMR** (400 MHz, $CDCl_3$): δ 9.13 (s, 1H), 8.07 (d, *J* = 6.8 Hz, 2H), 7.72 (s, 1H), 7.44-7.51 (m, 6H), 7.37-7.39 (s, 2H), 4.17 (q, *J* = 7.2 Hz, 2H), 1.07 (t, *J* = 7.2 Hz, 3H); **^{13}C NMR** (100 MHz, $CDCl_3$): δ 167.1, 159.8, 151.5, 151.4, 139.5, 138.6, 130.1, 129.2, 128.6, 128.5, 128.3, 127.6, 125.1, 122.0, 61.5, 14.0; **HRMS** (ESI) m/z calculated for $C_{20}H_{18}NO_2$ $[M+H]^+$: 304.1332, found 304.1362.

Methyl 4,6-diphenylnicotinate (3aa´):[35] white solid; (46.3 mg, 80%); **mp**:



108-110 °C; $\mathbf{R_f}$ = 0.85 (EtOAc:hexane = 1:4); **IR** (KBr): ν 1704, 1588, 1535, 1494, 1468, 1432, 1371, 1297, 1228, cm^{-1}; **^{1}H NMR** (400 MHz, $CDCl_3$): δ 9.13 (s, 1H), 8.06 (d, *J* = 6.8 Hz, 2H), 7.72 (s, 1H), 7.45-7.51 (m, 6H), 7.37-7.39 (m, 2H), 3.73 (s, 3H); **^{13}C NMR** (100 MHz, $CDCl_3$): δ 167.4, 160.0, 151.6, 151.5, 139.3, 138.5, 130.2, 129.2, 128.8, 128.6, 128.3, 127.6, 124.6, 122.1, 52.5; **HRMS** (ESI) m/z calculated for $C_{19}H_{15}NO_2Na$ $[M+Na]^+$: 312.0995, found 312.0981.

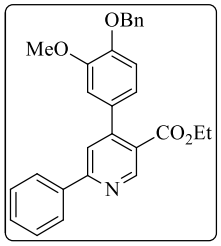
Ethyl 6-phenyl-4-(4-methylphenyl)nicotinate (3ab):[27] white solid; (51.4 mg,



81%); **mp**: 114-116 °C; $\mathbf{R_f}$ = 0.85 (EtOAc:hexane = 1:4); **IR** (KBr): ν 1696, 1594, 1573, 1534, 1468, 1444, 1373, 1299, 1231 cm^{-1}; **^{1}H NMR** (400 MHz, $CDCl_3$): δ 9.09 (s, 1H), 8.04 (d, *J* = 6.7 Hz, 2H), 7.69 (s, 1H), 7.43-7.49 (m, 3H), 7.23-7.28 (m, 4H), 4.19 (q, *J* = 7.0 Hz, 2H), 2.41 (s, 3H), 1.11 (t, *J* = 7.0 Hz, 3H); **^{13}C NMR** (100 MHz, $CDCl_3$): δ 167.2, 159.7, 151.4, 151.3, 138.6,

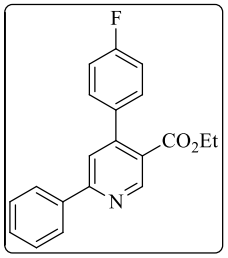
138.6, 136.4, 130.0, 129.3, 129.1, 128.3, 127.5, 125.1, 122.0, 61.5, 21.5, 14.1; **HRMS** (ESI) m/z calculated for $C_{21}H_{19}NO_2Na[M+Na]^+$: 340.1308, found 340.1312.

Ethyl 4-(4-benzyloxy-3-methoxyphenyl)-6-phenylnicotinate (3ac): white solid;



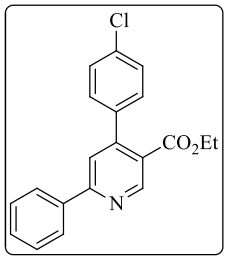
(67.7 mg, 77%); **mp**: 125-127 °C; $\mathbf{R_f}$ = 0.62 (EtOAc:hexane = 1:4); **IR** (KBr): ν 1704, 1591, 1533, 1510, 1467, 1414, 1373, 1303, 1240, 1205 cm^{-1}; **^{1}H NMR** (400 MHz, $CDCl_3$): δ 9.07 (s, 1H), 8.06 (d, *J* = 6.7 Hz, 2H), 7.71 (s, 1H), 7.44-7.50 (m, 5H), 7.36-7.40 (m, 2H), 7.31-7.33 (m, 1H), 6.93-6.97 (m, 2H), 6.88-6.90 (m, 1H), 5.21 (s, 2H), 4.19 (q, *J* = 7.2 Hz, 2H), 3.91 (s, 3H), 1.10 (t, *J* = 7.2 Hz, 3H); **^{13}C NMR** (100 MHz, $CDCl_3$): δ 167.4, 159.6, 151.1, 150.8, 149.6, 148.8, 138.5, 137.1, 132.3(2C), 130.0, 129.1, 128.8, 128.2, 127.5, 125.3, 121.7, 120.9, 113.8, 112.2, 71.2, 61.5, 56.3, 14.1; **HRMS** (ESI) m/z calculated for $C_{28}H_{25}NO_4Na[M+Na]^+$: 462.1676, found 462.1664.

Ethyl 4-(4-fluorophenyl)-6-phenylnicotinate (3ad): white solid; (55.9 mg,



87%); **mp**: 118-120 °C; $\mathbf{R_f}$ = 0.84 (EtOAc:hexane = 1:4); **IR** (KBr): ν 1697, 1594, 1536, 1507, 1469, 1401, 1370, 1301, 1226 cm^{-1}; **^{1}H NMR** (400 MHz, $CDCl_3$): δ 9.14 (s, 1H), 8.05 (d, *J* = 6.5 Hz, 2H), 7.67 (s, 1H), 7.46-7.52 (m, 3H), 7.33-7.36 (m, 2H), 7.14 (t, *J* = 8.7 Hz, 2H), 4.20 (q, *J* = 7.2 Hz, 2H), 1.13 (t, *J* = 7.2 Hz, 3H); **^{13}C NMR** (100 MHz, $CDCl_3$): δ 166.8, 163.2 (d, J_{C-F}= 246 Hz) 160.0, 151.6, 150.5, 138.4, 135.5 (d, J_{C-F}= 3.6 Hz), 130.2 (d, J_{C-F}= 8.0 Hz), 129.2, 127.6, 124.9, 122.0, 115.6 (d, J_{C-F}= 21.8 Hz), 61.6, 14.1; **HRMS** (ESI) m/z calculated for $C_{20}H_{16}FNO_2Na[M+Na]^+$:344.1057, found 344.1044.

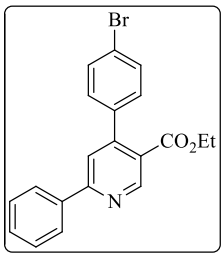
Ethyl 4-(4-chlorophenyl)-6-phenylnicotinate (3ae):[27] white solid; (57.3 mg,



85%); **mp**: 122-124 °C; $\mathbf{R_f}$ = 0.80 (EtOAc:hexane = 1:4); **IR** (KBr): ν 1696, 1596, 1573, 1532, 1490, 1468, 1399, 1371, 1296, 1230cm^{-1}; **^{1}H NMR** (400 MHz, $CDCl_3$): δ 9.15 (s, 1H), 8.06 (d, *J* = 6.8 Hz, 2H), 7.66 (s, 1H), 7.46-4.51 (m, 3H),

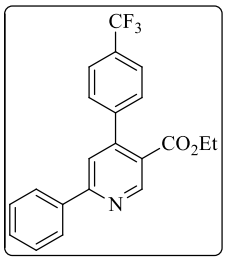
7.42-7.44 (m, 2H), 7.30-7.32 (m, 2H), 4.21 (q, *J* = 7.2 Hz, 2H), 1.14 (t, *J* = 7.2 Hz, 3H) ; **^{13}C NMR** (100 MHz, $CDCl_3$) δ 166.7, 160.1, 151.7, 150.4, 138.4, 137.9, 134.9, 130.3, 129.8, 129.2, 128.8, 127.6, 124.6, 121.8, 61.6, 14.1; **HRMS** (ESI) m/z calculated for $C_{20}H_{16}ClNO_2Na[M+Na]^+$: 360.0762, found 360.0791.

Ethyl 4-(4-bromophenyl)-6-phenylnicotinate (3af): light yellow solid; (64.8



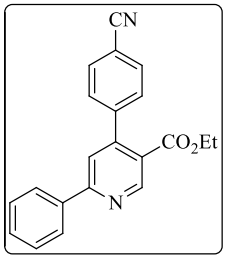
mg, 85%); **mp**: 130-132 °C; $\mathbf{R_f}$ = 0.85 (EtOAc:hexane = 1:4); **IR** (KBr): ν 1697, 1597, 1573, 1531, 1489, 1469, 1446, 1394, 1376, 1361, 1298, 1233 cm^{-1}; **^{1}H NMR** (400 MHz, $CDCl_3$): δ 9.15 (s, 1H), 8.04-8.06 (m, 2H), 7.65 (s, 1H), 7.56-7.60 (m, 2H), 7.45-7.51 (m, 3H), 7.22-7.25 (m, 2H), 4.20 (q, *J* = 7.2 Hz, 2H), 1.14 (t, *J* = 7.2 Hz, 3H); **^{13}C NMR** (100 MHz, $CDCl_3$): δ 166.6, 160.1, 151.8, 150..4, 138.4, 138.3, 131.7, 130.3, 130.0, 129.2, 127.6, 124.5, 123.0, 121.8, 61.6, 14.1; **HRMS** (ESI) m/z calculated for $C_{20}H_{16}{}^{79}BrNO_2Na[M+Na]^+$: 404.0257, found 404.0202; calculated for $C_{20}H_{16}{}^{81}BrNO_2Na[M+Na]^+$: 406.0237, found 406.0186.

Ethyl 6-phenyl-4-(4-trifluoromethylphenyl)nicotinate (3ag): white solid; (63.8

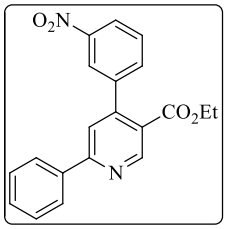


mg, 86%); **mp**: 127-129 °C; $\mathbf{R_f}$ = 0.75 (EtOAc:hexane = 1:4); **IR** (KBr): ν 1699, 1592, 1574, 1537, 1471, 1362, 1328, 1302, 1234 cm^{-1}; **^{1}H NMR** (400 MHz, $CDCl_3$): δ 9.22 (s, 1H), 8.06-8.08 (m, 2H), 7.72 (d, *J* = 8.0 Hz, 2H), 7.68 (s, 1H), 7.48-7.53 (m, 5H), 4.19 (q, *J* = 7.2 Hz, 2H), 1.10 (t, *J* = 7.2 Hz, 3H); **^{13}C NMR** (100 MHz, $CDCl_3$): δ 166.2, 160.1, 151.8, 150.4, 143.3, 138.0, 131.3, 131.0, 130.6, 130.5, 130.3, 129.3, 128.8, 127.7, 125.7, 125.5, 125.5, 125.4, 125.4, 124.4, 123.0, 121.8, 61.7, 14.0; **HRMS** (ESI) m/z calculated for $C_{21}H_{16}F_3NO_2Na[M+Na]^+$: 394.1025, found 394.1025.

Ethyl 4-(4-cyanophenyl)-6-phenylnicotinate (3ah): light yellow solid; (54.5 mg, 83%); **mp**: 130-132 °C; $\mathbf{R_f}$ = 0.45 (EtOAc:hexane = 1:4); **IR** (KBr): ν 2225, 1697, 1591, 1572, 1535, 1502, 1468, 1444, 1403, 1374, 1362, 1318, 1300, 1231 cm^{-1}; **^{1}H NMR** (400 MHz, $CDCl_3$): δ 9.15 (s, 1H), 7.98-8.00 (m, 2H), 7.67 (d, *J* = 8.0 Hz, 2H), 7.56 (s, 1H), 7.38-7.42 (m, 5H), 4.12 (q, *J* = 7.2 Hz, 2H), 1.06 (t, *J* = 7.2 Hz, 3H); **^{13}C NMR** (100 MHz, $CDCl_3$): δ 165.6, 160.0, 151.8, 149.6, 144.0, 137.7, 131.9, 130.2, 128.9 (2C), 127.3, 123.6, 121.1, 118.5, 112.1, 61.4, 13.8; **HRMS** (ESI) m/z calculated for $C_{21}H_{17}N_2O_2[M+H]^+$: 329.1285, found 329.1283.



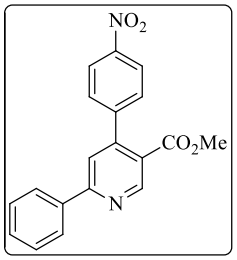
Ethyl 4-(3-nitrophenyl)-6-phenylnicotinate (3ai): light yellow solid; (57.8 mg, 83%); **mp**: 135-137 °C; $\mathbf{R_f}$ = 0.45 (EtOAc:hexane = 1:4); **IR** (KBr): ν 1720, 1593, 1579, 1528, 1481, 1470, 1443, 1362, 1348, 1286, 1245, 1230 cm^{-1}; **^{1}H NMR** (400 MHz, $CDCl_3$): δ 9.26 (s, 1H), 8.31 (d, *J* = 8.0 Hz, 1H), 8.26 (s, 1H), 8.07-8.09 (m, 2H), 7.62-7.70 (m, 3H), 7.48-7.53 (m, 3H), 4.22 (q, *J* = 6.8 Hz, 2H), 1.16 (t, *J* = 3H); **^{13}C NMR** (100 MHz, $CDCl_3$): δ 165.6, 160.2, 151.9, 149.0, 148.0, 140.9, 137.6, 134.2, 130.2, 129.1, 129.0, 127.3, 123.6, 123.2, 123.1, 121.5, 61.5, 13.8; **HRMS** (ESI) m/z calculated for $C_{20}H_{17}N_2O_4[M+H]^+$: 349.1183, found 349.1189.



Crystallographic data: Single crystal X-ray structural of **3ai** was collected at 150(2) K using graphite monochromated Mo Kα radiation (λα = 0.71073 Å) (**Figure 5.3**). The strategy for the Data collection was evaluated by using the CrysAlisPro CCD software. The data were collected by the standard 'phi-omega scan techniques, and were scaled and reduced using CrysAlisPro RED software. The structure was solved by direct methods using SHELXS-97, and refined by full matrix least-squares with SHELXL-97, refining on *F2*. The positions of all the atoms were obtained by direct methods. All non-hydrogen atoms were refined anisotropically. The remaining hydrogen atoms were placed in geometrically constrained positions, and refined with isotropic temperature factors, generally

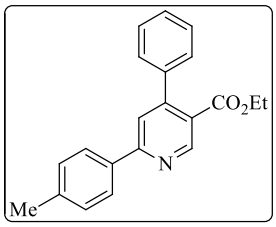
1.2*Ueq* of their parent atoms. The crystal data are summarized in Table 1. The CCDC number of **3ai** (**1522097)** can be obtained free of charge *via* www.ccdc.cam.ac.uk (or from the Cambridge Crystallographic Data Centre,12 union Road, Cambridge CB21 EZ, UK; Fax: (+44) 1223-336-033; or deposit@ccdc.cam.ac.uk).

Methyl 4-(4-nitrophenyl)-6-phenylnicotinate (3aj): light yellow solid; (56.1



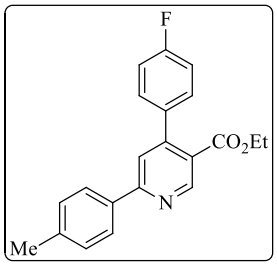
mg, 84%); **mp**: 136-138 °C; $\mathbf{R_f}$ = 0.45 (EtOAc:hexane = 1:4); **IR** (KBr): ν 1721, 1589, 1579, 1538, 1508, 1474, 1445, 1433, 1355, 1348, 1322, 1295, 1247, 1231 cm^{-1}; **^{1}H NMR** (400 MHz, $CDCl_3$): δ 9.26 (s, 1H), 8.33 (d, *J* = 8.8 Hz, 2H), 8.06-8.09 (m, 2H), 7.67 (s, 1H), 7.49-7.54 (m, 5H), 3.77 (s, 3H); **^{13}C NMR** (100 MHz, $CDCl_3$): δ 165.9, 160.2, 151.8, 149.5, 147.7, 145.8, 137.6, 130.3, 129.1, 129.0, 127.3, 123.4, 123.1, 121.3, 52.3; **HRMS** (ESI) m/z calculated for $C_{19}H_{15}N_2O_4[M+H]^+$: 335.1026, found 335.1026.

Ethyl 4-phenyl-6-(4-methylphenyl)nicotinate (3ba): white solid; (55.2 mg,



84%); **mp**: 114-116 °C; $\mathbf{R_f}$ = 0.85 (EtOAc:hexane = 1:4); **IR** (KBr): ν 1698, 1588, 1532, 1469, 1443, 1363, 1310, 1232 cm^{-1}; **^{1}H NMR** (400 MHz, $CDCl_3$): δ 9.12 (s, 1H), 7.97 (d, *J* = 8.2 Hz, 2H), 7.69 (s, 1H), 7.44-7.45 (m, 3H), 7.36-7.38 (m, 2H), 7.29 (d, *J* = 8.0 Hz, 2H), 4.17 (q, *J* = 7.2 Hz, 2H), 2.41 (s, 3H), 1.07 (t, *J* = 7.2 Hz, 3H); **^{13}C NMR** (100 MHz, $CDCl_3$): δ 167.1, 159.8, 151.4, 151.4, 140.3, 139.6, 135.7, 129.9, 128.6, 128.5, 128.3, 127.5, 124.7, 121.6, 61.4, 21.6, 14.0; **HRMS** (ESI) m/z calculated for $C_{21}H_{20}NO_2[M+H]^+$: 318.1489, found 318.1491.

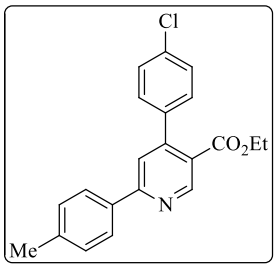
Ethyl 4-(4-fluorophenyl)-6-(4-methylphenyl)nicotinate (3bd): white solid;



(57.7 mg, 86%); **mp**: 125-127 °C; $\mathbf{R_f}$ =0.84 (EtOAc:hexane = 1:4); **IR** (KBr): ν 1696, 1594, 1533, 1507, 1469, 1448, 1369, 1298, 1227 cm^{-1}; **^{1}H NMR** (400 MHz, $CDCl_3$): δ 9.12 (s, 1H), 7.96 (d, *J* = 8.0 Hz, 2H),

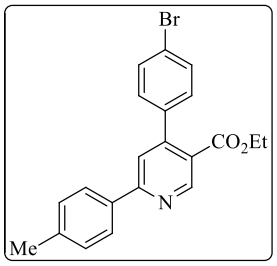
7.64 (s, 1H), 7.29-7.36 (m, 4H), 7.14 (t, *J* = 8.5 Hz, 2H), 4.19 (q, *J* = 7.2 Hz, 2H), 2.41 (s, 3H), 1.13 (t, *J* = 7.2 Hz, 3H); **^{13}C NMR** (100 MHz, $CDCl_3$): δ 166.9, 163.2(d, J_{C-F}= 246.0 Hz),160.0, 151.6, 150.4, 140.5, 135.6 (d, J_{C-F}= 3.6 Hz), 130.2, 129.9, 127.5, 124.5, 121.6, 115.7, 115.4, 61.5, 21.6, 14.1; **HRMS** (ESI) m/z calculated for $C_{21}H_{19}FNO_2[M+H]^+$ 336.1394, found 336.1386.

Ethyl 4-(4-chlorophenyl)-6-(4-methylphenyl)nicotinate (3be): white solid;



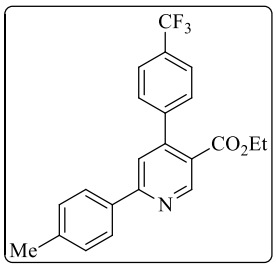
(59.7 mg, 85%); **mp**: 127-129 °C; **R_f** = 0.80 (EtOAc:hexane = 1:4); **IR** (KBr): ν 1694, 1593, 1570, 1530, 1491, 1468, 1397, 1362, 1293, 1231, 1183 cm^{-1}; **^{1}H NMR** (400 MHz, $CDCl_3$) δ 9.14 (s, 1H), 7.96 (d, *J* = 8.0 Hz, 2H), 7.63 (s, 1H), 7.41-7.43 (m, 2H), 7.29-7.31 (m, 4H), 4.20 (q, *J* = 7.0 Hz, 2H), 2.41 (s, 3H), 1.14 (t, *J* = 7.0Hz, 3H); **^{13}C NMR** (100 MHz, $CDCl_3$): δ 166.7, 160.0, 151.7, 150.3, 140.5, 138.1, 135.5, 134.8, 129.9, 129.8, 128.7, 127.5, 124.3, 121.5, 61.6, 21.6, 14.1; **HRMS** (ESI) m/z calculated for $C_{21}H_{18}ClNO_2Na[M+Na]^+$: 374.0918, found 374.0908.

Ethyl 4-(4-bromophenyl)-6-(4-methylphenyl)nicotinate (3bf): white solid;

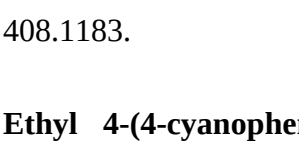


(65.7 mg, 83%); **mp**: 135-137 °C; **R_f** = 0.84 (EtOAc:hexane = 1:4); **IR** (KBr): ν 1694, 1594, 1570, 1530, 1488, 1467, 1393, 1361, 1294, 1232cm^{-1}; **^{1}H NMR** (400 MHz, $CDCl_3$) *δ* 9.11 (s, 1H), 7.93 (d, *J* = 6.7 Hz, 2H), 7.60 (s, 1H), 7.55 (d, *J* = 6.7 Hz, 2H), 7.26 (d, *J* = 7.2 Hz, 2H), 7.20-7.22 (m, 2H), 4.17 (q, *J* = 7.0 Hz, 2H), 2.38 (s, 3H), 1.12 (t, *J* = 7.0 Hz, 3H); **^{13}C NMR** (100 MHz, $CDCl_3$): δ 166.6, 160.0, 151.7, 150.3, 140.5, 138.5, 135.5, 131.6, 130.0, 129.9, 127.5, 124.2, 122.9, 121.4, 61.6, 21.6, 14.1; **HRMS** (ESI) m/z calculated for $C_{21}H_{19}{}^{79}BrNO_2[M+H]^+$: 396.0594, found 396.0589; calculated for $C_{21}H_{19}{}^{81}BrNO_2[M+H]^+$: 398.0574, found 398.0574.

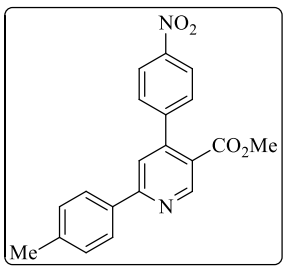
Ethyl 6-(4-methylphenyl)-4-(4-trifluoromethylphenyl)nicotinate (3bg): white solid; (65.5 mg, 85%); **mp**: 134-136 °C; $\mathbf{R_f}$ = 0.75 (EtOAc:hexane = 1:4); **IR** (KBr): ν 1698, 1592, 1571, 1536, 1470, 1363, 1327, 1296, 1233 cm^{-1}; **^{1}H NMR** (400 MHz, $CDCl_3$): δ 9.20 (s, 1H), 7.97 (d, *J* = 8.2 Hz, 2H), 7.71 (d, *J* = 8.0 Hz, 2H), 7.64 (s, 1H), 7.48 (d, *J* = 8.0 Hz, 2H), 7.30 (d, *J* = 8.0 Hz, 2H), 4.18 (q, *J* = 7.2 Hz, 2H), 2.42 (s, 3H), 1.10 (t, *J* = 7.2 Hz, 3H); **^{13}C NMR** (100 MHz, $CDCl_3$): δ 166.3, 160.2, 151.9, 150.2, 143.5, 140.7, 135.4, 131.2, 130.9, 130.5, 130.2, 130.0, 128.8, 127.5, 125.7, 125.5, 125.4, 125.4, 125.3, 124.0, 123.0, 121.4, 61.6, 21.6, 14.0; **HRMS** (ESI) m/z calculated for $C_{22}H_{18}F_3NO_2Na[M+Na]^+$: 408.1182, found 408.1183.



Ethyl 4-(4-cyanophenyl)-6-(4-methylphenyl)nicotinate (3bh): white solid; (56.8 mg, 83%); **mp**: 134-136 °C; $\mathbf{R_f}$ = 0.45 (EtOAc:hexane = 1:4); **IR** (KBr) ν 2227, 1696, 1592, 1532, 1503, 1469, 1363, 1322, 1296, 1232 cm^{-1}; **^{1}H NMR** (400 MHz, $CDCl_3$): δ 9.13 (s, 1H), 7.89 (d, *J* = 8.0 Hz, 2H), 7.66 (d, *J* = 8.4 Hz, 2H), 7.53 (s, 1H), 7.38 (d, *J* = 8.0 Hz, 2H), 7.22 (d, *J* = 8.4 Hz, 2H), 4.11 (q, *J* = 7.2 Hz, 2H), 2.34 (s, 3H), 1.06 (t, *J* = 7.2Hz, 3H; **^{13}C NMR** (100 MHz, $CDCl_3$): δ 165.7, 160.0, 151.8, 149.5, 144.2, 140.5, 134.9, 131.9, 129.7, 128.9, 127.2, 123.2, 120.8, 118.5, 112.1, 61.3, 21.3, 13.8; **HRMS** (ESI) m/z calculated for $C_{22}H_{19}N_2O_2[M+H]^+$: 343.1441, found 343.1449.

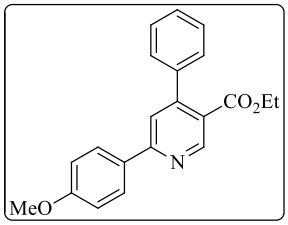


ethyl 4-(4-nitrophenyl)-6-(4-methylphenyl)nicotinate (3bj): white solid; (58.5 mg, 84%); **mp**: 140-142 °C; $\mathbf{R_f}$ = 0.45 (EtOAc:hexane = 1:4); **IR** (KBr): ν 1712, 1587, 1538, 1513, 1432, 1346, 1318, 1291, 1228 cm^{-1}; **^{1}H NMR** (400 MHz, $CDCl_3$): δ 9.23 (s,1H), 8.32 (d, *J* = 8.0, 2H), 7.97 (d, *J* = 8.0 Hz, 2H), 7.63 (s, 1H), 7.52 (d, *J* = 8.4 Hz, 2H), 7.31 (d, *J* = 8.0 Hz, 2H), 3.76 (s, 3H), 2.42 (s, 3H); **^{13}C NMR** (100 MHz, $CDCl_3$): δ 166.0,

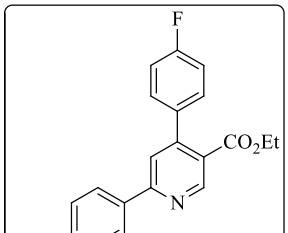


160.2, 151.9, 149.5, 147.7, 146.0, 140.7, 134.8, 129.7, 129.1, 127.2, 123.4, 122.7, 120.9, 52.3, 21.4; **HRMS** (ESI) m/z calculated for $C_{20}H_{17}N_2O_4[M+H]^+$: 349.1183, found 349.1184.

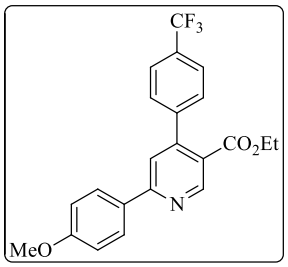
Ethyl 6-(4-methoxyphenyl)-4-phenylnicotinate (3ca):[27] white solid; (57.3 mg, 83%); **mp**: 120-122 °C; $\mathbf{R_f}$ = 0.80 (EtOAc:hexane = 1:4); **IR** (KBr): ν 1713, 1591, 1530, 1514, 1472, 1443, 1420, 1363, 1320, 1300, 1252, 1231 cm^{-1}; **^{1}H NMR** (400 MHz, $CDCl_3$): δ 9.10 (s, 1H), 8.04 (d, *J* = 8.8 Hz, 2H), 7.64 (s, 1H), 7.43-7.44 (m, 3H), 7.36-7.37 (m, 2H), 7.00 (d, 8.5 Hz, 2H), 4.16 (q, *J* = 7.2 Hz, 2H), 3.86 (s, 3H), 1.07 (t, *J* = 7.2 Hz, 3H); **^{13}C NMR** (100 MHz, $CDCl_3$): δ 167.1, 161.5, 159.4, 151.5, 151.4, 139.7, 131.1, 129.0, 128.5, 128.5, 128.3, 124.2, 121.1, 114.5, 61.4, 55.7, 14.0; **HRMS** (ESI) m/z calculated for $C_{21}H_{20}NO_3[M+H]^+$ 334.1438, found 334.1452.



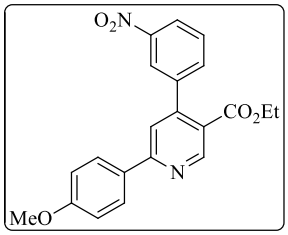
Ethyl 4-(4-fluorophenyl)-6-(4-methoxyphenyl)nicotinate (3cd): white solid; (59.7 mg, 85%); **mp**: 131-133 °C; $\mathbf{R_f}$ = 0.80 (EtOAc:hexane = 1:4); **IR** (KBr) ν 1693, 1601, 1533, 1509, 1469, 1366, 1299, 1251, 1224 cm^{-1}; **^{1}H NMR** (400 MHz, $CDCl_3$): δ 9.10 (s, 1H), 8.03 (d, *J* = 8.8 Hz, 2H), 7.59 (s, 1H), 7.32-7.35 (m, 2H), 7.13 (t, *J* = 8.5 Hz, 2H), 7.00 (d, *J* = 8.5 Hz, 2H), 4.18 (q, *J* = 7.2 Hz, 2H), 3.86 (s, 3H), 1.13 (t, *J* = 7.2 Hz, 3H); **^{13}C NMR** (100 MHz, $CDCl_3$): δ 166.8, 163.1(d, J_{C-F}= 246 Hz), 161.6, 159.6, 151.7, 150.4, 135.7 (d, J_{C-F}= 3.6 Hz), 130.9, 130.2 (d, J_{C-F}= 8.0 Hz), 129.0, 124.0, 121.1, 115.6 (d, J_{C-F}= 21.9 Hz), 114.6, 61.5, 55.7, 14.1; **HRMS** (ESI) m/z calculated for $C_{21}H_{18}FNO_3Na[M+Na]^+$: 374.1163, found 374.1161.



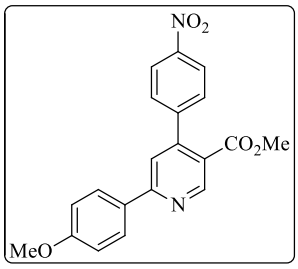
Ethyl 6-(4-methoxyphenyl)-4-(4-trifluoromethylphenyl)nicotinate (3cg): white solid; (67.4 mg. 84%); **mp**: 140-142 °C; $\mathbf{R_f}$ = 0.67 (EtOAc:hexane = 1:4); **IR** (KBr): ν 1700, 1606, 1595, 1574, 1536, 1521, 1470, 1363, 1325, 1300, 1251, 1232 cm^{-1}; **^{1}H NMR** (400 MHz, $CDCl_3$): δ 9.17 (s, 1H), 8.04



(d, *J* = 8.7 Hz, 2H), 7.70 (d, *J* = 8.0 Hz, 2H), 7.59 (s, 1H), 7.47 (d, *J* = 7.7 Hz, 2H), 7.00 (d, *J* = 8.8 Hz, 2H), 4.17 (q, *J* = 7.0 Hz, 2H), 3.86 (s, 3H), 1.09 (t, *J* = 7.0 Hz, 3H); **^{13}C NMR** (100 MHz, $CDCl_3$): δ 166.3, 161.7, 159.8, 151.9, 150.2, 143.5, 131.1, 130.8, 130.7, 130.4, 130.1, 129.0, 128.8, 128.4, 125.7, 125.4, 125.4, 125.3, 125.3, 123.4, 123.0, 120.8, 120.3, 114.6, 61.5, 55.6, 14.0; **HRMS** (ESI) m/z calculated for $C_{22}H_{18}F_3NO_3Na[M+Na]^+$: 424.1131, found 424.1127.

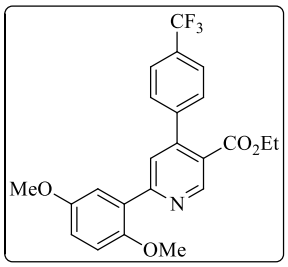
Ethyl 6-(4-methoxyphenyl)-4-(3-nitrophenyl)nicotinate (3ci): white solid; 

(65.6 mg, 82%); **mp**: 142-144 °C; **R_f** = 0.40 (EtOAc:hexane = 1:4); **IR** (KBr): ν 1704, 1586, 1535, 1466, 1442, 1347, 1297, 1255, 1223 cm^{-1}; **^{1}H NMR** (400 MHz, $CDCl_3$): δ 9.22 (s, 1H), 8.30 (d, *J* = 8.0 Hz, 1H), 8.25 (s, 1H), 8.05 (d, *J* = 8.8 Hz, 2H), 7.61-7.69 (m, 3H), 7.01 (d, *J* = 8.8 Hz, 2H), 4.20 (q, *J* = 6.8Hz, 2H), 3.87 (s, 3H), 1.51 (t, *J* = 6.8 Hz, 3H); **^{13}C NMR** (100 MHz, $CDCl_3$): δ 165.6, 161.5, 159.8, 151.9, 148.9, 147.9, 141.1, 134.3, 130.1, 129.0, 128.8, 123.2, 123.0, 122.7, 120.5, 114.3, 61.3, 55.4, 13.8; **HRMS** (ESI) m/z calculated for $C_{21}H_{17}N_2O_5Na[M+Na]^+$: 401.1108, found 401.1121.

Methyl 6-(4-methoxyphenyl)-4-(4-nitrophenyl)nicotinate (3cj): light yellow 

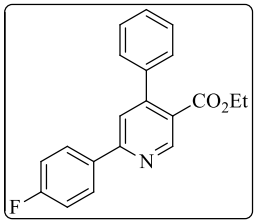
solid; (61.2 mg, 84%); **mp**: 144-146 °C; **R_f** = 0.35 (EtOAc:hexane = 1:4); **IR** (KBr): ν 1724, 1590, 1542, 1514, 1476, 1435, 1353, 1292, 1242 cm^{-1}; **^{1}H NMR** (400 MHz, $CDCl_3$): δ 9.21 (s, 1H), 8.31 (d, *J* = 8.4 Hz, 2H), 8.04 (d, *J* = 8.8 Hz, 2H), 7.59 (s, 1H), 7.51 (d, *J* = 8.8 Hz, 2H), 7.01 (d, *J* = 8.8 Hz, 2H), 3.88 (s, 3H), 3.76 (s, 3H); **^{13}C NMR** (100 MHz, $CDCl_3$): δ 165.9, 161.5, 159.8, 151.8, 149.4, 147.6, 146.1, 130.0, 129.0, 128.8, 123.3, 122.2, 120.3, 114.3, 55.4, 52.2; **HRMS** (ESI) m/z calculated for $C_{20}H_{17}N_2O_5[M+H]^+$: 365.1132, found 365.1137.

Ethyl 6-(2,5-dimethoxyphenyl)-4-(4-trifluoromethyl phenyl)nicotinate (3dg):

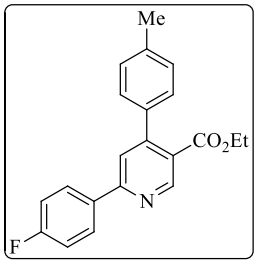


white solid; (66.4 mg, 77%); **mp**: 146-148 °C; $\mathbf{R_f}$ =0.63(EtOAc:hexane = 1:4); **IR** (KBr): ν 1720, 1587, 1541, 1502, 1466, 1424, 1370, 1326, 1285, 1229, 1205 cm^{-1}; **^{1}H NMR** (400 MHz, $CDCl_3$): δ 9.19 (s, 1H), 7.89 (s, 1H), 7.70 (d, *J* = 8.0 Hz, 2H), 7.47-7.51 (m, 3H), 6.93-6.99 (m, 2H), 4.18 (q, *J* = 7.2 Hz, 2H), 3.84 (s, 3H), 3.80 (s, 3H), 1.09 (t, *J* = 7.2 Hz, 3H); **^{13}C NMR** (100 MHz, $CDCl_3$)*δ*165.5, 157.7, 153.3, 150.9, 150.3, 148.0, 142.5, 130.1, 129.7, 129.4, 129.1, 129.0, 127.9, 127.4, 125.3, 124.7, 124.4, 124.4, 124.4, 124.3, 123.0, 122.0, 116.2, 115.1, 112.4, 60.6, 55.6, 55.2, 13.0; **HRMS** (ESI) m/z calculated for $C_{23}H_{21}F_3NO_4[M+H]^+$: 432.1417, found 432.1401.

Ethyl 6-(4-fluorophenyl)-4-phenylnicotinate (3ea): white solid; (49.5 mg, 77%); **mp**: 119-121 °C; $\mathbf{R_f}$ = 0.83 (EtOAc:hexane = 1:4); **IR** (KBr) ν 1697, 1584, 1534, 1514, 1468, 1366, 1297, 1230 cm^{-1}; **^{1}H NMR** (400 MHz, $CDCl_3$): δ 9.10 (s, 1H), 8.05-8.08 (m, 2H), 7.66 (s, 1H), 7.44-7.45 (m, 3H), 7.36-7.37 (m, 2H), 7.17 (t, *J* = 8.8 Hz, 2H), 4.17 (q, *J* = 7.0 Hz, 2H), 1.07 (t, *J* = 7.0 Hz, 3H); **^{13}C NMR** (100 MHz, $CDCl_3$): δ 167.04, 164.3(d, J_{C-F}= 248 Hz), 158.7, 151.6, 151.5, 139.4, 134.7 (d, J_{C-F} = 3.6 Hz), 129.5 (d, J_{C-F} = 8.7 Hz) 128.7, 128.6, 128.3, 125.0, 121.6, 116.2 (d, J_{C-F}= 21.0 Hz), 61.5, 14.0; **HRMS** (ESI) m/z calculated for $C_{20}H_{17}FNO_2[M+H]^+$: 322.1238, found 322.1224.

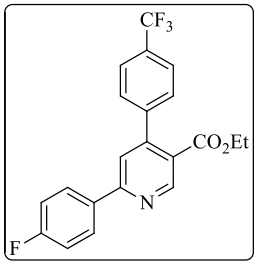


Ethyl 6-(4-fluorophenyl)-4-(4-methylphenyl)nicotinate (3eb): white solid; (50.3 mg, 75%); **mp**: 126-128 °C; $\mathbf{R_f}$ = 0.83 (EtOAc:hexane = 1:4); **IR** (KBr): ν 1692, 1598, 1535, 1510, 1468, 1363, 1323, 1300, 1231 cm^{-1}; **^{1}H NMR** (400 MHz, $CDCl_3$): δ 9.07 (s, 1H), 8.03-8.06 (m, 2H), 7.64 (s, 1H), 7.26 (s, 4H), 7.15 (t, *J* = 8.5 Hz, 2H), 4.19 (q, *J* = 7.0 Hz, 2H), 2.41 (s, 3H), 1.12(t, *J* = 7.0Hz, 3H); **^{13}C NMR** (100 MHz, $CDCl_3$): δ 167.1, 164.3(d, J_{C-F}= 248 Hz), 158.6, 151.5, 151.4, 138.7, 136.3, 134.8 (d, J_{C-F}= 3.6.0



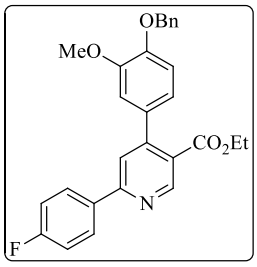
Hz), 129.5 (d, J_{C-F}= 8.0 Hz), 129.3, 128.2, 125.0, 121.6, 116.2(d, J_{C-F}= 21.0 Hz), 61.5, 21.5, 14.1; **HRMS** (ESI) m/z calculated for $C_{21}H_{18}FNO_2Na[M+Na]^+$: 358.1214, found 358.1207.

Ethyl 6-(4-fluorophenyl)-4-(4-trifluoromethylphenyl)nicotinate (3eg): white



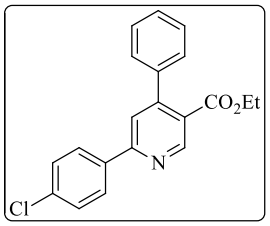
solid; (66.6 mg, 81%); **mp**: 145-147 °C; $\mathbf{R_f}$ = 0.72 (EtOAc:hexane = 1:4); **IR** (KBr): ν 1694, 1595, 1534, 1514, 1469, 1407, 1365, 1325, 1299, 1233 cm^{-1}; **^{1}H NMR** (400 MHz, $CDCl_3$): δ 9.19 (s, 1H), 8.05-8.09 (m, 2H), 7.72 (d, *J* = 8.0 Hz, 2H), 7.62 (s, 1H), 7.48 (d, *J* = 8.0 Hz, 2H), 7.18 (t, *J* = 8.8 Hz, 2H), 4.18 (q, *J* = 7.2 Hz, 2H), 1.09 (t, 3H); **^{13}C NMR** (100 MHz, $CDCl_3$): δ 166.2, 164.5 (d, J_{C-F}= 249 Hz), 159.1, 152.0, 150.4, 143.2, 134.4 (d, J_{C-F} = 3.6 Hz), 131.4, 131.0, 130.7, 130.4, 129.6 (d, J_{C-F} = 8.0 Hz), 128.8, 125.7, 125.5, 125.5, 125.5, 125.4, 124.3, 123.0, 121.4, 116.4 (d, J_{C-F}= 21.8 Hz), 61.7, 14.0; **HRMS** (ESI) m/z calculated for $C_{21}H_{15}F_4NO_2Na[M+Na]^+$: 412.0931, found 412.0935.

Ethyl 4-(4-benzyloxy-3-methoxyphenyl)-6-(4-fluorophenyl)nicotinate (3ec):

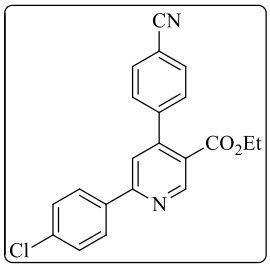


white solid; (67.7mg, 74%); **mp**: 135-137 °C; $\mathbf{R_f}$ = 0.60 (EtOAc:hexane = 1:4); **IR** (KBr) ν 1728, 1601, 1584, 1537, 1509, 1471, 1454, 1411, 1366, 1318, 1261, 1231, 1205, cm^{-1}; **^{1}H NMR** (400 MHz, $CDCl_3$): δ 9.03 (s, 1H), 8.03-8.07 (m, 2H), 7.65 (s, 1H), 7.45-7.47 (m, 2H), 7.38 (t, *J* = 7.0 Hz, 2H), 7.31-7.33 (m, 1H), 7.16 (t, *J* = 8.2 Hz, 2H), 6.86-6.97 (m, 3H), 5.2 (s, 2H), 4.18 (q, *J* = 7.2 Hz, 2H), 3.91 (s, 3H), 1.09 (t, *J* =7.2 Hz, 3H); **^{13}C NMR** (100 MHz, $CDCl_3$): δ 167.4, 164.2(d, J_{C-F} = 248.0 Hz), 158.6, 151.2, 150.9, 149.7, 148.8, 137.1, 134.8 (d, J_{C-F}= 3.6 Hz), 132.3, 129.5 (d, J_{C-F}= 8.7 Hz), 128.9, 128.2, 127.5, 125.3, 121.4, 120.9, 116.2 (d, J_{C-F}= 21.1 Hz), 113.9, 112.2, 71.2, 61.5, 56.4, 14.1; **HRMS** (ESI) m/z calculated for $C_{28}H_{24}FNO_4Na[M+Na]^+$: 480.1582, found 480.1564.

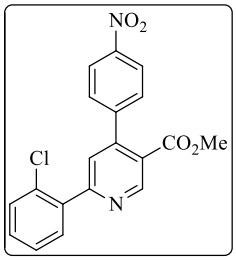
Ethyl 6-(4-chlorophenyl)-4-phenylnicotinate (3fa):[27] white solid; (53.9 mg, 80%); **mp**: 124-126 °C; $\mathbf{R_f}$ = 0.85 (EtOAc:hexane = 1:4); **IR** (KBr): ν 1702, 1590, 15321, 1494, 1467, 1363, 1308, 1290, 1232, cm^{-1}; **^{1}HNMR** (400 MHz, $CDCl_3$): δ 9.11 (s, 1H), 8.01 (d, *J* = 8.5 Hz, 2H), 7.68 (s, 1H), 7.44-7.47 (m, 5H), 7.35-7.37 (m, 2H), 4.17 (q, *J* = 7.2 Hz, 2H), 1.07 (t, *J* = 7.2 Hz, 3H); **^{13}C NMR** (100 MHz, $CDCl_3$): δ 167.0, 158.5, 151.6, 151.5, 139.3, 137.0, 136.4, 129.4, 128.9, 128.8, 128.6, 128.3, 125.3, 121.7, 61.6, 14.0; **HRMS** (ESI) m/z calculated for $C_{20}H_{16}ClNO_2Na[M+Na]^+$: 360.0762, found 360.0785.



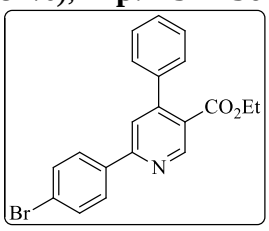
Ethyl 6-(4-chlorophenyl)-4-(4-cyanophenyl)nicotinate (3fh): white solid; (59.4 mg, 82%); **mp**: 138-140 °C; $\mathbf{R_f}$ = 0.44 (EtOAc:hexane = 1:4); **IR** (KBr): ν 2224, 1717, 1589, 1536, 1501, 1470, 1404, 1363, 1281, 1225, cm^{-1}; **^{1}H NMR** (400 MHz, $CDCl_3$): δ 9.21 (s, 1H), 8.01 (d, *J* = 8.8 Hz, 2H), 7.75 (d, *J* = 8.0 Hz, 2H), 7.61 (s, 1H), 7.45-7.48 (m, 4H), 4.20 (q, *J* = 7.2 Hz, 2H), 1.14 (t, *J* = 7.2 Hz, 3H); **^{13}C NMR** (100 MHz, $CDCl_3$): δ 165.5, 158.7, 151.8, 149.7, 143.9, 136.5, 136.1, 131.9, 129.2, 128.9, 128.6, 123.8, 120.9, 118.4, 112.3, 61.5, 13.8; **HRMS** (ESI) m/z calculated for $C_{21}H_{16}ClNO_2[M+H]^+$: 363.0895, found 363.0916.



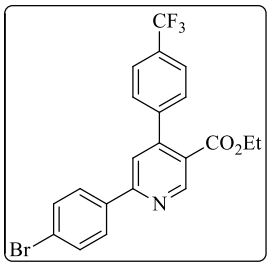
Methyl 6-(2-chlorophenyl)-4-(4-nitrophenyl)nicotinate (3gj): White solid; (60.4 mg, 82%); **mp**: 150-152 °C; $\mathbf{R_f}$ = 0.45 (EtOAc:hexane = 1:4); **IR** (KBr) ν 1714, 1584, 1539, 1508, 1438, 1427, 1354, 1317, 1293, 1246, 1230 cm^{-1}; **^{1}H NMR** (400 MHz, $CDCl_3$): δ 9.26 (s, 1H), 8.31 (d, *J* = 8.4 Hz, 2H), 7.68-7.70 (m, 2H), 7.49-7.55 (m, 3H), 7.39-7.51 (m, 2H), 3.79 (s, 3H); **^{13}C NMR** (100 MHz, $CDCl_3$) δ 165.9, 159.7, 151.5, 148.3, 147.8, 145.3, 137.6, 132.1, 131.6, 130.5, 130.4, 129.2, 127.3, 125.9, 123.7, 123.5, 52.5; **HRMS** (ESI) m/z calculated for $C_{19}H_{14}ClN_2O_4[M+H]^+$: 369.0637, found 369.0640.



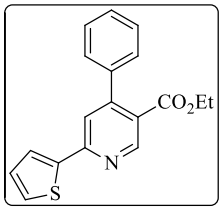
Ethyl 6-(4-bromophenyl)-4-phenylnicotinate (3ha): white solid; (61.7mg, 81%); **mp**: 134-136 °C; $\mathbf{R_f}$ = 0.85 (EtOAc:hexane = 1:4); **IR** (KBr): ν 1702, 1589, 1532, 1492, 1466, 1443, 1367, 1307, 1232 cm^{-1}; **^{1}H NMR** (400 MHz, $CDCl_3$) δ 9.10 (s, 1H), 7.95 (d, *J* = 8.2 Hz, 2H), 7.68 (s, 1H), 7.62 (d, *J* = 8.5 Hz, 2H), 7.44-7.45 (m, 3H), 7.35-7.37 (m, 2H), 4.17 (q, *J* = 7.2 Hz, 2H), 1.07 (t, *J* = 7.2 Hz, 3H); **^{13}C NMR** (100 MHz, $CDCl_3$): δ 167.0, 158.6, 151.6, 151.5, 139.3, 137.4, 132.3, 129.1, 128.8, 128.6, 128.3, 125.4, 124.8, 121.7, 61.6, 14.0; **HRMS** (ESI) m/z calculated for $C_{20}H_{16}{}^{79}BrNO_2Na[M+Na]^+$: 404.0257, found 404.0246. calculated for $C_{20}H_{16}{}^{81}BrNO_2Na[M+Na]^+$: 406.0237, found 406.0234.



Ethyl 6-(4-bromophenyl)-4-(4-trifluoromethylphenyl)nicotinate (3hg): white solid; (76.4 mg, 85%); **mp**: 150-152 °C; $\mathbf{R_f}$ = 0.74 (EtOAc:hexane = 1:4); **IR** (KBr): ν 1700, 1590, 1539, 1471, 1367, 1327, 1299, 1228 cm^{-1}; **^{1}H NMR** (400 MHz, $CDCl_3$): δ 9.19 (s, 1H), 7.95 (d, *J* = 8.5 Hz, 2H), 7.72 (d, *J* = 8.2 Hz, 2H), 7.62-7.64 (m, 3H), 7.47 (d, *J* = 8.0 Hz, 2H), 4.18 (q, *J* = 7.2 Hz, 2H), 1.09 (t, *J* = 7.2 Hz, 3H); **^{13}C NMR** (100 MHz, $CDCl_3$): δ 166.2, 159.0, 152.0, 150.5, 143.1, 137.1, 132.4, 131.0, 130.7, 129.1, 128.8, 125.6, 125.5, 125.5, 125.4, 125.1, 124.7, 123.0, 121.5, 61.7, 14.0; **HRMS** (ESI) m/z calculated for $C_{21}H_{15}{}^{79}BrF_3NO_2Na[M+Na]^+$: 472.0130, found 472.0111. calculated for $C_{21}H_{15}{}^{81}BrF_3NO_2Na[M+Na]^+$: 474.0111, found 474.0110.

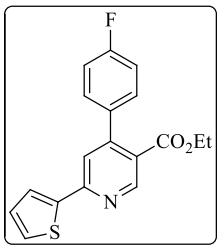


Ethyl 4-phenyl-6-(thiophen-2-yl)nicotinate (3ia): white solid; (43.3 mg, 70%); **mp**: 110-112 °C; $\mathbf{R_f}$ = 0.82 (EtOAc:hexane = 1:4); **IR** (KBr): ν 1693, 1585, 1525, 1468, 1378, 1364, 1303, 1236, 1207, cm^{-1}; **^{1}H NMR** (400 MHz, $CDCl_3$): δ 9.02 (s, 1H), 7.66 (d, *J* = 3.5 Hz, 1H), 7.60 (s, 1H), 7.44-7.47 (m, 4H), 7.34-7.36 (m, 2H), 7.13 (t, *J* = 4.0 Hz, 1H), 4.15 (q, *J* = 7.2 Hz, 2H), 1.06 (t, *J* = 7.2 Hz, 3H); **^{13}C NMR** (100 MHz, $CDCl_3$): δ 166.7, 154.8, 151.6, 151.5, 144.0, 139.3, 129.4,

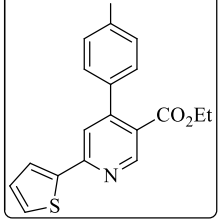


128.7, 128.6, 128.5, 128.2, 126.4, 124.6, 120.1, 61.4, 14.0; **HRMS** (ESI) m/z calculated for $C_{18}H_{15}NO_2SNa[M+Na]^+$: 332.0716, found 332.0726.

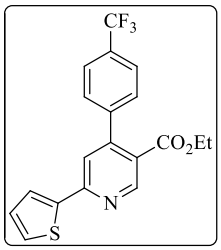
Ethyl 4-(4-fluorophenyl)-6-(thiophen-2-yl)nicotinate (3id): white solid; (49.7 mg, 76%); **mp**: 1120-122 °C; $\mathbf{R_f}$ = 0.83 (EtOAc:hexane = 1:4); **IR** (KBr): ν 1707, 1587, 1527, 1508, 1471, 1374, 1299, 1226, cm^{-1}; **^{1}H NMR** (400 MHz, $CDCl_3$): δ 9.02 (s, 1H),7.66 (d, *J* = 3.4 Hz, 1H), 7.55 (s, 1H), 7.47 (d, *J* = 4.7 Hz, 1H), 7.31-7.34 (m, 2H), 7.12-7.16 (m, 3H), 4.17 (q, *J* = 7.2 Hz, 2H), 1.12 (t, *J* = 7.2 Hz, 3H); **^{13}C NMR** (100 MHz, $CDCl_3$): δ 166.5, 163.2 (d, J_{C-F}= 247 Hz),154.9, 151.8, 150.6, 143.8, 135.3 (d, J_{C-F}= 2.9 Hz), 130.1(d, J_{C-F}= 8.0 Hz), 129.6, 128.6, 126.5, 124.3, 120.1, 115.6 (d, J_{C-F}= 21.8 Hz) 61.5, 14.1; **HRMS** (ESI) m/z calculated for $C_{18}H_{14}FNO_2S[M+Na]^+$: 350.0621, found 350.0628.



Ethyl 4-(4-bromophenyl)-6-(thiophen-2-yl)nicotinate (3if): white solid; (55.7 mg, 72%); **mp**:127-129 °C; $\mathbf{R_f}$ = 0.84 (EtOAc:hexane = 1:4); **IR** (KBr): ν 1693, 1588, 1524, 1487, 1467, 1425, 1395, 1371, 1303, 1235, 1207, cm^{-1}; **^{1}H NMR** (400 MHz, $CDCl_3$): δ 9.04 (s, 1H), 7.67 (d, *J* = 2.6 Hz, 1H), 7.58 (d, *J* = 8.2 Hz, 2H), 7.54 (s, 1H), 7.48 (d, *J* = 4.5 Hz, 1H), 7.22 (d, *J* = 8.2 Hz, 2H), 7.13-7.15 (m, 1H), 4.18 (q, *J* = 7.2 Hz, 2H), 1.13 (t, *J* = 7.2 Hz, 3H); **^{13}C NMR** (100 MHz, $CDCl_3$): δ 166.3, 155.1, 152.0, 150.5, 143.8, 138.3, 131.7, 130.0, 129.7, 128.7, 126.6, 124.1, 123.1, 119.9, 61.6, 14.1; **HRMS** (ESI) m/z calculated for $C_{18}H_{14}{}^{79}BrNO_2SNa[M+Na]^+$: 409.9821, found 409.9821. calcdfor $C_{18}H_{14}{}^{81}BrNO_2SNa[M+Na]^+$: 411.9801, found 411.9800.

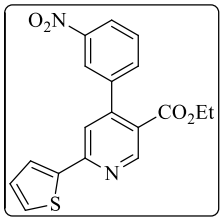


Ethyl 6-(thiophen-2-yl)-4-(4-trifluoromethylphenyl)nicotinate (3ig): white solid; (58.1 mg, 77%); **mp**: 130-132°C; $\mathbf{R_f}$ = 0.72 (EtOAc:hexane = 1:4); **IR** (KBr): ν 1707, 1588, 1530, 1473, 1366, 1330, 1231 cm^{-1}; **^{1}H NMR** (400 MHz, $CDCl_3$): δ 9.10 (s, 1H), 7.71 (d, *J* = 8.2 Hz, 2H), 7.67 (d, *J* = 3 Hz, 1H), 7.55 (s, 1H), 7.45-7.50 (m, 3H), 7.14 (t, *J* = 4 Hz, 1H), 4.16 (q, *J* =

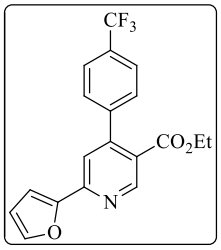


7.2 Hz, 2H), 1.08 (t, *J* = 7.2 Hz, 3H); **^{13}C NMR** (100 MHz, $CDCl_3$): δ 166.0, 155.2, 152.1, 150.4, 143.7, 143.1, 131.3, 130.9, 130.6, 130.3, 129.9, 128.7, 128.4, 126.7, 125.7, 125.5, 125.4, 125.4, 125.4, 123.8, 123.0, 119.9, 61.6, 14.0; **HRMS** (ESI) m/z calculated for $C_{19}H_{14}F_3NO_2SNa[M+Na]^+$: 400.0590, found 400.0588.

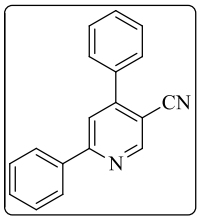
Ethyl 4-(3-nitrophenyl)-6-(thiophen-2-yl)nicotinate (3ii): white solid; (52.4mg, 74%); **mp**: 140-142 °C; **R_f** = 0.40 (EtOAc:hexane = 1:4); **IR** (KBr): ν 1700, 1588, 1530, 1471, 1428, 1347, 1304, 1240, 1211 cm^{-1}; **^{1}H NMR** (400 MHz, $CDCl_3$): δ 9.15 (s, 1H), 8.31 (d, *J* = 7.6 Hz, 1H), 8.24 (s, 1H), 7.61-7.70 (m, 3H), 7.56 (s, 1H), 7.52 (d, *J* = 4.8 Hz, 1H), 7.14-7.16 (m, 1H), 4.20 (q, *J* = 7.2 Hz, 2H), 1.15 (t, *J* = 7.2 Hz, 3H); **^{13}C NMR** (100 MHz, $CDCl_3$)*δ* 165.3, 155.2, 152.1, 149.1, 148.0, 143.2, 140.7, 134.2, 129.8, 129.1, 128.5, 126.7, 123.1(2C), 123.0, 119.6, 61.4, 13.8; **HRMS** (ESI) m/z calculated for $C_{18}H_{15}N_2O_4S[M+H]^+$: 355.0747, found 355.0768.



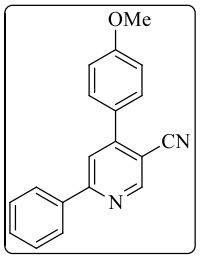
Ethyl 6-(furan-2-yl)-4-(4-(trifluoromethylphenyl)nicotinate (3jg): white solid; (51.9mg, 72%); **mp**: 117-119°C; **R_f** = 0.70 (EtOAc:hexane = 1:4); **IR** (KBr): ν 1719, 1603, 1572, 1539, 1490, 1469, 1332, 1281, 1236 cm^{-1}; **^{1}H NMR** (400 MHz, $CDCl_3$): δ 9.11 (s, 1H), 7.70 (d, *J* = 7.8 Hz, 2H), 7.62 (s, 1H), 7.57 (s, 1H), 7.46 (d, *J* = 8.0Hz, 2H), 7.23 (d, *J* = 3.2 Hz, 1H), 6.58-6.59 (m, 1H), 4.17 (q, *J* = 7.2 Hz, 2H), 1.08 (t, *J* = 7.2 Hz, 3H); **^{13}C NMR** (100 MHz, $CDCl_3$): δ 166.1, 152.9, 152.1, 151.7, 150.4, 144.9, 143.2, 131.3, 130.9, 130.6, 130.3, 128.7, 128.4, 125.7, 125.5, 125.4, 125.4, 125.4, 123.8, 123.0, 119.6, 112.9, 111.7, 61.6, 14.0; **HRMS** (ESI) m/z calculated for $C_{19}H_{15}F_3NO_3[M+H]^+$: 362.0999, found 362.0994.



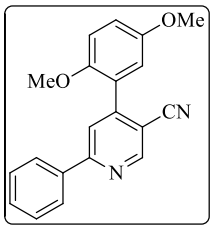
4,6-Diphenylnicotinonitrile (3ak):[7] white solid; (45.1 mg, 88%); **mp**:115-117 °C; $\mathbf{R_f}$ = 0.80 (EtOAc:hexane = 1:4); **IR** (KBr): ν 3054, 2925, 2853,2225, 1585, 1532, 1470, 1442, 1369, 1072, 1019, 879, 774, 739, 688, 636cm^{-1}; **^{1}H NMR** (400 MHz, $CDCl_3$): δ 9.00 (s, 1H), 8.07-8.10 (m, 2H), 7.88 (s, 1H), 7.66-7.68 (m, 2H), 7.51-7.59 (m, 6H); **^{13}C NMR** (100 MHz, $CDCl_3$): δ 160.8, 154.3, 153.3, 137.8, 136.2, 130.9, 130.5, 129.5, 129.3, 128.7, 127.7, 120.6, 117.4, 106.8; **HRMS** (ESI) m/z calcd for $C_{18}H_{12}N_2$ $[M+Na]^+$: 279.0893, found 279.0893.



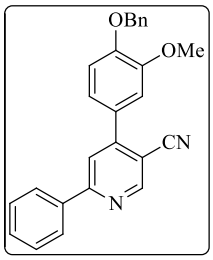
4-(4-Methoxyphenyl)-6-phenylnicotinonitrile (3al): white solid; (49.2 mg, 86%); **mp**: 118-120°C; $\mathbf{R_f}$ = 0.67 (EtOAc:hexane = 1:4); **IR** (KBr): ν 2217, 1608, 1581, 1510, 1467, 1373, 1298, 1251 cm^{-1}; **^{1}H NMR** (400 MHz, $CDCl_3$): δ 8.96 (s, 1H), 8.07 (d, *J* = 7.5 Hz, 2H), 7.84 (s, 1H), 7.65 (d, *J* = 8.5 Hz, 2H), 7.50-7.52 (m, 3H), 7.08 (d, *J* = 8.2 Hz, 2H), 3.89 (s, 3H); **^{13}C NMR** (100 MHz, $CDCl_3$): δ 161.6, 160.7, 154.4, 152.9, 137.9, 130.8, 130.2, 129.3, 128.4, 127.7, 120.3, 117.8, 115.0, 106.5, 55.8; **HRMS** (ESI) m/z calculated for $C_{19}H_{14}N_2ONa[M+Na]^+$: 309.0998, found 309.0999.



4-(2,5-Dimethoxyphenyl)-6-phenylnicotinonitrile (3am): white solid; (53.7 mg, 85%); **mp**: 129-131°C; $\mathbf{R_f}$ = 0.57 (EtOAc:hexane = 1:4); **IR** (KBr): ν 2223, 1587, 1532, 1502, 1475, 1450, 1409, 1372, 1311, 1264, 1226, cm^{-1}; **^{1}H NMR** (400 MHz, $CDCl_3$): δ 8.96 (s, 1H), 8.06 (d, *J* = 7.8 Hz, 2H), 7.83 (s, 1H), 7.49-7.51 (m, 3H), 6.98-7.03 (m, 2H), 6.89 (s, 1H), 3.83 (s, 3H), 3.82 (s, 3H); **^{13}C NMR** (100 MHz, $CDCl_3$): δ 160.5, 154.0, 153.2, 150.8, 150.7, 138.0, 130.6, 129.3, 127.7, 125.9, 121.8, 117.3, 116.6, 116.3, 113.0, 109.1, 56.3, 56.2; **HRMS** (ESI) m/z calculated for $C_{20}H_{16}N_2O_2Na[M+Na]^+$: 339.1104, found 339.1118.

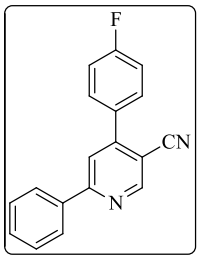


4-(4-Benzyloxy-3-methoxyphenyl)-6-phenylnicotinonitrile (3an): white solid; (67.4 mg, 86%); **mp**: 132-134 °C; $\mathbf{R_f}$ = 0.35 (EtOAc:hexane = 1:4); **IR** (KBr): ν



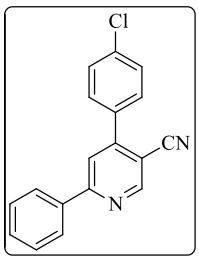
2217, 1591, 1515, 1474, 1331, 1269, 1223,cm^{-1}; **^{1}H NMR** (400 MHz, $CDCl_3$): ***δ*** 8.96 (s, 1H), 8.06-8.08 (m, 2H), 7.85 (s, 1H), 7.46-7.54 (m, 5H), 7.40 (t, *J* = 7.0 Hz, 2H), 7.31-7.35 (m, 1H), 7.25-7.26 (m, 1H), 7.18-7.21 (m, 1H), 7.04 (d, *J* = 8.2Hz, 1H), 5.24 (s, 2H), 3.99 (s, 3H); **^{13}C NMR** (100 MHz, $CDCl_3$): δ 160.7, 154.4, 152.9, 150.3, 150.2, 137.9, 136.8, 130.8, 129.3, 129.0, 128.4, 127.7, 127.5, 121.6, 120.2, 117.8, 114.2, 112.2, 106.5, 71.3, 56.6; **HRMS** (ESI) m/z calculated for $C_{26}H_{20}N_2O_2Na$ $[M+Na]^+$: 415.1417, found 415.1422.

4-(4-Fluorophenyl)-6-phenylnicotinonitrile (3ao): white solid; (49.3 mg, 90%);



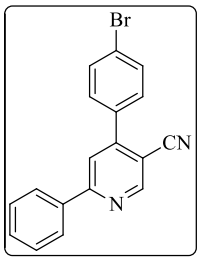
mp: 124-126°C; $\mathbf{R_f}$ = 0.75 (EtOAc:hexane = 1:4); **IR** (KBr): ν 2223, 1598, 1580, 1537, 1509, 1473, 1442, 1371, 1226, 1216, cm^{-1}; **^{1}H NMR** (400 MHz, $CDCl_3$): δ 8.99 (s, 1H), 8.07-8.09 (m, 2H), 7.84 (s, 1H), 7.65-7.68 (m, 2H), 7.51-7.52 (m, 3H), 7.26 (t, *J* = 8.2 Hz, 2H); **^{13}C NMR** (100 MHz, $CDCl_3$): δ 164.2(d, $J_{C\text{-}F}$= 250 Hz), 160.9, 154.3, 152.2, 137.6, 132.3 (d, $J_{C\text{-}F}$= 3.6 Hz), 131.0, 130.8 (d, $J_{C\text{-}F}$= 8.0 Hz), 129.4, 127.7, 120.4, 117.3, 116.8(d, $J_{C\text{-}F}$= 21.8 Hz), 106.7; **HRMS** (ESI) m/z calculated for $C_{18}H_{11}FN_2Na$ $[M+Na]^+$: 297.0798, found 297.0796.

4-(4-Chlorophenyl)-6-phenylnicotinonitrile (3ap): white solid; (51.6 mg, 89%);



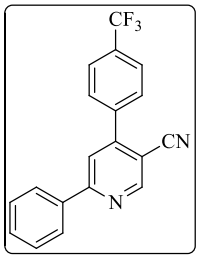
mp: 132-134 °C; $\mathbf{R_f}$ = 0.78 (EtOAc:hexane = 1:4); **IR** (KBr): ν 2222, 1534, 1493, 1470, 1441, 1369, 1243, cm^{-1}; **^{1}H NMR** (400 MHz, $CDCl_3$): δ 8.99 (s, 1H), 8.06-8.09 (m, 2H), 7.83 (s, 1H), 7.60-7.62 (m, 2H), 7.51-7.55 (m, 5H); **^{13}C NMR** (100 MHz, $CDCl_3$): δ 161.0, 154.3, 152.0, 137.6, 136.9, 134.6, 131.0, 130.0, 129.8, 129.4, 127.7, 120.3, 117.2, 106.6 ; **HRMS** (ESI) m/z calculated for $C_{18}H_{11}ClN_2Na$ $[M+Na]^+$: 313.0503, found 313.0507.

4-(4-Bromophenyl)-6-phenylnicotinonitrile (3aq): white solid; (58.1 mg, 87%);



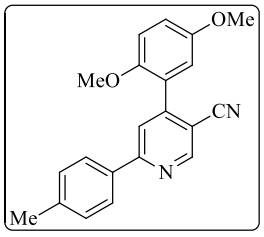
mp:141-143 °C; $\mathbf{R_f}$ = 0.77 (EtOAc:hexane = 1:4); **IR** (KBr): ν 2222, 1588, 1531, 1489, 1469, 1441, 1366, 1282, 1242 cm^{-1}; **^{1}H NMR** (400 MHz, $CDCl_3$): δ 9.00 (s, 1H), 8.07-8.08 (m, 2H), 7.84 (s, 1H), 7.70 (d, *J* = 8.5Hz, 2H), 7.52-7.55 (m, 5H); **^{13}C NMR** (100 MHz, $CDCl_3$): δ 161.0, 154.3, 152.1, 137.6, 135.0, 132.8, 131.0, 130.2, 129.4, 127.7, 125.2, 120.3, 117.2, 106.6; **HRMS** (ESI) m/z calculated for $C_{18}H_{11}{}^{79}BrN_2Na$ $[M+Na]^+$: 356.9998, found 356.9997. calculated for $C_{18}H_{11}{}^{81}BrN_2Na$ $[M+Na]^+$: 358.9878, found 358.9982.

6-Phenyl-4-(4-trifluoromethylphenyl)nicotinonitrile (3ar): white solid; (58.3



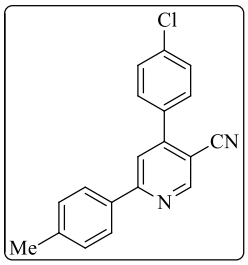
mg, 90%); **mp**: 138-140°C; $\mathbf{R_f}$ = 0.73 (EtOAc:hexane = 1:4); **IR** (KBr): ν 2226, 1586, 1537, 1474, 1443, 1369, 1324cm^{-1}; **^{1}H NMR** (400 MHz, $CDCl_3$): δ 9.04 (s, 1H), 8.08-8.10 (m, 2H), 7.87 (s, 1H), 7.77-7.86 (m, 4H), 7.53-7.54 (m, 3H); **^{13}C NMR** (100 MHz, $CDCl_3$): δ 161.1, 154.3, 151.8, 139.7, 137.5, 133.0, 132.6, 132.3, 132.0, 131.2, 129.5, 129.2, 127.8, 126.6, 126.5, 126.5, 126.5, 125.4, 122.7, 120.5, 116.9, 106.8; **HRMS** (ESI) m/z calculated for $C_{19}H_{11}F_3N_2Na$ $[M+Na]^+$: 347.0767, found 347.0779.

4-(2,5-Dimethoxyphenyl)-6-(4-methylphenyl)nicotinonitrile (3bm): white

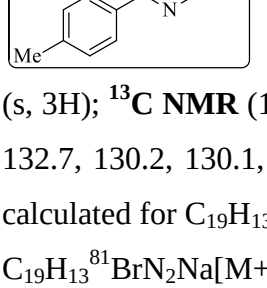


solid: (54.8 mg, 83%); **mp**: 122-124 °C; $\mathbf{R_f}$ = 0.57(EtOAc:hexane = 1:4); **IR** (KBr): ν 2227, 1587, 1537, 1507, 1465, 1409, 1369, 1266, 1227 cm^{-1}; **^{1}H NMR** (400 MHz, $CDCl_3$): δ 8.93 (s, 1H), 7.96 (d, *J* = 8.0 Hz, 2H), 7.80 (s, 1H), 7.31 (d, *J* = 8.0 Hz, 2H), 6.98-7.02 (m, 2H), 6.89 (s, 1H), 3.83 (s, 3H), 3.82 (s, 3H), 2.42 (s, 3H); **^{13}C NMR** (100 MHz, $CDCl_3$): δ 160.5, 154.0, 153.2, 150.7, 150.6, 141.0, 135.2, 130.0, 127.6, 126.0, 121.4, 117.5, 116.5, 116.4, 113.0, 108.8, 56.3, 56.2, 21.7; **HRMS** (ESI) m/z calculated for $C_{21}H_{18}N_2O_2Na$ $[M+Na]^+$: 353.1260, found 353.1251.

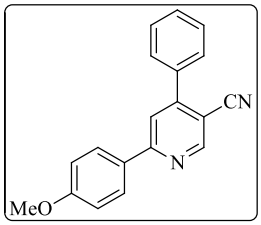
4-(4-Chlorophenyl)-6-(4-methylphenyl)nicotinonitrile (3bp): white solid; (53.5 mg, 88%); **mp**: 136-138 °C; $\mathbf{R_f}$ = 0.80 (EtOAc:hexane = 1:4); **IR** (KBr): ν 2222, 1591, 1531, 1469, 1372, cm^{-1}; **^{1}H NMR** (400 MHz, $CDCl_3$): δ 8.97 (s, 1H), 7.98 (d, *J* = 8.0 Hz, 2H), 7.80 (s, 1H), 7.59-7.61 (m, 2H), 7.52-7.54 (m, 2H), 7.32 (d, *J* = 8.0 Hz, 2H), 2.43 (s, 3H); **^{13}C NMR** (100 MHz, $CDCl_3$): δ 161.0, 154.3, 151.9, 141.5, 136.9, 134.8, 134.7, 130.1, 130.0, 129.8, 127.6, 119.9, 117.3, 106.3, 21.7; **HRMS** (ESI) m/z calculated for $C_{19}H_{13}ClN_2Na$ $[M+Na]^+$: 327.0659, found 327.0659.



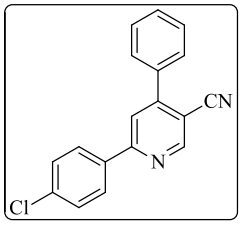
4-(4-Bromophenyl)-6-(4-methylphenyl)nicotinonitrile (3bq): white solid; (58.5 mg, 84%); **mp**: 148-150 °C; $\mathbf{R_f}$ = 0.77 (EtOAc:hexane = 1:4); **IR** (KBr): ν 2220, 1589, 1527, 1488, 1466, 1368, 1280, 1252 cm^{-1}; **^{1}H NMR** (400 MHz, $CDCl_3$): δ 8.97 (s, 1H), 7.97 (d, *J* = 7.8 Hz, 2H), 7.80 (s, 1H), 7.70 (d, *J* = 8.2 Hz, 2H), 7.53 (d, *J* = 8.0 Hz, 2H), 7.32 (d, *J* = 8.0 Hz, 2H), 2.43 (s, 3H); **^{13}C NMR** (100 MHz, $CDCl_3$): ***δ*** 161.0, 154.3, 151.9, 141.5, 135.2, 134.8, 132.7, 130.2, 130.1, 127.6, 125.21, 119.8, 117.3, 106.2, 21.7; **HRMS** (ESI) m/z calculated for $C_{19}H_{13}{}^{79}BrN_2Na[M+Na]^+$: 371.0154, found 371.0151. calculated for $C_{19}H_{13}{}^{81}BrN_2Na[M+Na]^+$: 371.0154, found 371.0151.



6-(4-Methoxyphenyl)-4-phenylnicotinonitrile (3ck): white solid: (50.4 mg, 88%); **mp**: 122-124 °C; $\mathbf{R_f}$ = 0.67 (EtOAc:hexane = 1:4); **IR** (KBr): ν 2220, 1585, 1530, 1469, 1418, 1370, 1319, 1283, 1244 cm^{-1}; **^{1}H NMR** (400 MHz, $CDCl_3$): δ 8.93 (s, 1H), 8.05 (d, *J* = 8.8 Hz, 2H), 7.79 (s, 1H), 7.64-7.66 (m, 2H), 7.54-7.55 (m, 3H), 7.01 (d, *J* = 8.7 Hz, 2H), 3.87 (s, 3H); **^{13}C NMR** (100 MHz, $CDCl_3$): δ 162.0, 160.3, 154.2, 153.0, 136.3, 130.3, 130.2, 129.4, 129.2, 128.6, 119.5, 117.6, 114.7, 105.9, 55.7; **HRMS** (ESI) m/z calculated for $C_{19}H_{14}N_2ONa$ $[M+Na]^+$: 309.0998, found 309.0998.

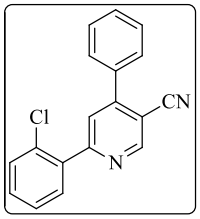


6-(4-Chlorophenyl)-4-phenylnicotinonitrile (3fk): white solid; (47.6 mg, 82%);



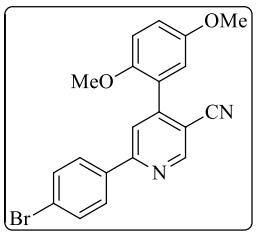
mp: 133-135 °C; $\mathbf{R_f}$ = 0.77 (EtOAc:hexane = 1:4); **IR** (KBr): ν 2220, 1591, 1528, 1468, 1405, 1369, cm^{-1}; **^{1}H NMR** (400 MHz, $CDCl_3$): δ 8.98 (s, 1H), 8.04 (d, *J* = 8.5 Hz, 2H), 7.84 (s, 1H), 7.65-7.67 (m, 2H), 7.56-7.57 (m, 3H), 7.49 (d, *J* = 8.5 Hz, 2H); **^{13}C NMR** (100 MHz, $CDCl_3$): δ 159.5, 154.3, 153.5, 137.2, 136.1, 136.1, 130.6, 129.6, 129.5, 129.0, 128.6, 120.3, 117.3, 107.1; **HRMS** (ESI) m/z calculated for $C_{18}H_{11}ClN_2Na$ $[M+Na]^+$: 313.0503, found 313.0511.

6-(2-Chlorophenyl)-4-phenylnicotinonitrile (3gk): white solid; (46.4 mg, 80%);



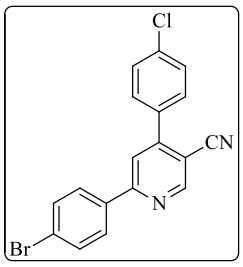
mp: 132-134 °C; $\mathbf{R_f}$ = 0.78 (EtOAc:hexane = 1:4); **IR** (KBr): ν 3068, 2923, 2221, 1590, 1525, 1463, 1434, 1368, 1257, 1079, 1032, 900, 744, 694cm^{-1}; **^{1}H NMR** (400 MHz, $CDCl_3$): δ 9.04 (s, 1H), 7.89 (s, 1H), 7.67-7.69 (m, 3H), 7.51-7.57 (m, 4H), 7.40-7.43 (m, 2H); **^{13}C NMR** (100 MHz, $CDCl_3$): δ 160.3, 154.1, 152.4, 137.8, 135.8, 132.4, 131.9, 131.1, 130.8, 130.6, 129.5, 128.8, 127.6, 125.3, 117.2, 107.3; **HRMS** (ESI) m/z calculated for $C_{18}H_{11}ClN_2Na$ $[M+Na]^+$: 313.0503, found 313.0498.

6-(4-Bromophenyl)-4-(2,5-dimethoxyphenyl)nicotinonitrile (3hm): white

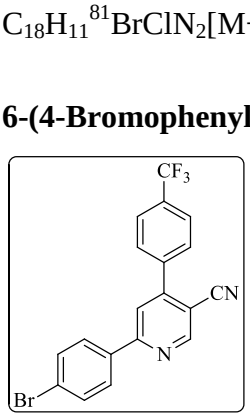


solid; (63.1 mg, 80%); **mp**: 130-132°C; $\mathbf{R_f}$ = 0.63 (EtOAc:hexane = 1:4); **IR** (KBr): ν 2218, 1587, 1533, 1499, 1472, 1444, 1357, 1310, 1228 cm^{-1}; **^{1}H NMR** (400 MHz, $CDCl_3$): δ 8.94 (s, 1H), 7.94 (d, *J* = 8.5 Hz, 2H), 7.80 (s, 1H), 7.63 (d, *J* = 8.5 Hz, 2H), 7.00-7.01 (m, 2H), 6.87-6.88 (m, 1H), 3.83 (s, 3H), 3.82 (s, 3H); **^{13}C NMR** (100 MHz, $CDCl_3$): δ 159.3, 154.0, 153.3, 151.0,150.7, 136.8, 132.5, 129.2, 125.7, 125.4, 121.5, 117.2, 116.7, 116.4, 113.0, 109.5, 56.3, 56.2; **HRMS** (ESI) m/z calculated for $C_{20}H_{15}BrN_2O_2Na$ $[M+Na]^+$: 417.0209, found 417.0200.

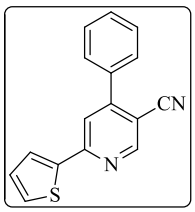
6-(4-Bromophenyl)-4-(4-chlorophenyl)nicotinonitrile (3hp): white solid; (63.3 mg, 86%); **mp**: 159-161°C; $\mathbf{R_f}$ = 0.77 (EtOAc:hexane = 1:4); **IR** (KBr): ν 2220, 1588, 1530, 1492, 1466, 1400, 1366cm^{-1}; **^{1}H NMR** (400 MHz, $CDCl_3$): δ 8.99 (s, 1H), 7.96 (d, *J* = 8.5 Hz, 2H), 7.81 (s, 1H), 7.65 (d, *J* = 8.2 Hz, 2H), 7.59-7.61 (m, 2H), 7.53-7.56 (m, 2H); **^{13}C NMR** (100 MHz, $CDCl_3$): *δ*159.8, 154.4, 152.3, 137.1, 136.4, 134.4, 132.6, 130.0, 129.9, 129.2, 125.8, 120.0, 117.0, 107.0; **HRMS** (ESI) m/z calculated for $C_{18}H_{11}{}^{79}BrClN_2[M+H]^+$: 368.9789, found 368.9794; calculated for $C_{18}H_{11}{}^{81}BrClN_2[M+H]^+$ 370.9768, found 370.9773.



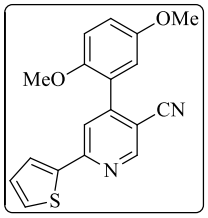
6-(4-Bromophenyl)-4-(4-trifluoromethylphenyl)nicotinonitrile (3hr): white solid; (69.9 mg, 87%); **mp**: 165-167 °C; $\mathbf{R_f}$ = 0.80 (EtOAc:hexane = 1:4); **IR** (KBr): ν 2221, 1587, 1536, 1476, 1368, 1331 cm^{-1}; **^{1}H NMR** (400 MHz, $CDCl_3$): δ 9.03 (s, 1H), 7.97 (d, *J* = 8.2 Hz, 2H), 7.83-7.84 (m, 3H), 7.76-7.78 (m, 2H), 7.66 (d, *J* = 8.2 Hz, 2H); **^{13}C NMR** (100 MHz, $CDCl_3$): δ 159.9, 154.3, 152.0, 139.5, 136.3, 132.8, 132.7, 132.4, 129.2, 129.2, 126.6, 126.6, 126.5, 126.5, 126.0, 125.3, 122.6, 120.2, 116.8, 107.1; **HRMS** (ESI) m/z calculated for $C_{19}H_{11}{}^{79}BrF_3N_2[M+H]^+$: 403.0052, found 403.0052; calculated for $C_{19}H_{11}{}^{81}BrF_3N_2[M+H]^+$: 405.0032, found 405.0036.



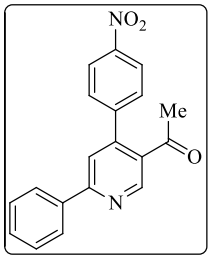
4-Phenyl-6-(thiophen-2-yl)nicotinonitrile (3ik): pale yellow solid; (41.9 mg, 80%); **mp**:116-118 °C; $\mathbf{R_f}$ = 0.75 (EtOAc:hexane = 1:4); **IR** (KBr): ν 2221, 1586, 1522, 1468, 1424, 1375, 1260, 1236 cm^{-1}; **^{1}H NMR** (400 MHz, $CDCl_3$): *δ*8.85 (s, 1H), 7.73-7.74 (m, 2H), 7.64-7.66 (m, 2H), 7.53-7.57 (m, 4H), 7.16 (t, *J* = 4.2 Hz, 1H); **^{13}C NMR** (100 MHz, $CDCl_3$): *δ*155.7, 154.3, 153.1, 143.3, 136.0, 130.7, 130.5, 129.5, 128.9, 128.6, 127.5, 118.7, 117.4, 106.2; **HRMS** (ESI) m/z calculated for $C_{16}H_{10}N_2ONa$ $[M+Na]^+$: 285.0457, found 285.0451.



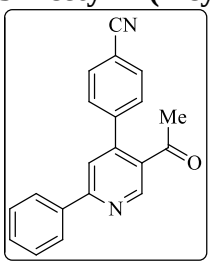
4-(2,5-Dimethoxyphenyl)-6-(thiophen-2-yl)nicotinonitrile (3im): pale yellow solid; (48.3 mg, 75%); **mp**: 134-136°C; $\mathbf{R_f}$ = 0.55 (EtOAc:hexane = 1:4); **IR** (KBr): ν 2216, 1586, 1527, 1502, 1472, 1432, 1413, 1365, 1308, 1230 cm^{-1}; **^{1}H NMR** (400 MHz, $CDCl_3$): δ 8.81 (s, 1H), 7.70 (s, 1H), 7.68 (d, *J* = 3.4 Hz, 1H), 7.51 (d, *J* = 4.7 Hz, 1H), 7.14 (t, *J* = 4.2 Hz, 1H), 6.99-7.03 (m, 2H), 6.87 (d, *J* = 2.4Hz, 1H), 3.82 (s, 6H); **^{13}C NMR** (100 MHz, $CDCl_3$): δ 155.5, 154.0, 153.2, 150.7, 150.7, 143.5, 130.4, 128.8, 127.3, 125.7, 119.9, 117.3, 116.6, 116.3, 113.0, 108.6, 56.3, 56.2; **HRMS** (ESI) m/z calculated for $C_{18}H_{14}N_2O_2SNa$ $[M+Na]^+$: 345.0668, found 345.0650.



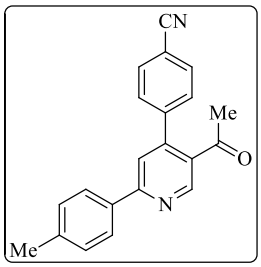
3-Acetyl-4-(4-nitrophenyl)-6-phenylpyridine (3as): light yellow solid: (52.2 mg, 82%); **mp**: 137-139 °C; $\mathbf{R_f}$ = 0.40 (EtOAc:hexane = 1:4); **IR** (KBr): ν 1682, 1590, 1526, 1507, 1479, 1444, 1350, 1271, 1234 cm^{-1}; **^{1}H NMR** (400 MHz, $CDCl_3$): δ 9.06 (s, 1H), 8.34 (d, *J* = 7.6 Hz, 2Hz), 8.06-8.09 (m, 2H), 7.68 (s, 1H), 7.50-7.54 (m, 5H), 2.40 (s, 3H); **^{13}C NMR** (100 MHz, $CDCl_3$): δ 199.2, 159.9, 150.2, 147.9, 147.7, 145.7, 137.6, 131.8, 130.3, 129.2, 129.0, 127.3, 123.9, 121.4, 29.8; **HRMS** (ESI) m/z calculated for $C_{19}H_{15}N_2O_3[M+H]^+$: 319.1077, found 319.1079.



3-Acetyl-4-(4-cyanophenyl)-6-phenylpyridine (3at): white solid; (47.7 mg, 80%); **mp**: 132-134 °C; $\mathbf{R_f}$ = 0.38 (EtOAc:hexane = 1:4); **IR** (KBr): ν 2226, 1681, 1587, 1525, 1480, 1441, 1414, 1361, 1328, 1276, 1235 cm^{-1}; **^{1}H NMR** (400 MHz, $CDCl_3$): δ 9.02 (s, 1H), 8.05-8.07 (m, 2H), 7.76-7.78 (m, 2H), 7.66 (s, 1H), 7.48-7.51 (m, 4H), 7.46 (s, 1H), 2.35 (s, 3H); **^{13}C NMR** (100 MHz, $CDCl_3$): δ 199.8, 160.1, 150.4, 148.2, 143.9, 138.0, 132.7, 132.3, 130.5, 129.3, 129.3, 127.6, 121.6, 118.6, 112.9, 30.2; **HRMS** (ESI) m/z calculated for $C_{20}H_{14}N_2ONa$ $[M+Na]^+$: 321.0998, found 321.1008.

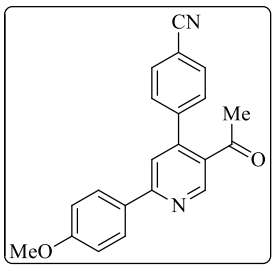


3-Acetyl-4-(4-cyanophenyl)-6-(4-methylphenyl)pyridine (3bt): white solid;



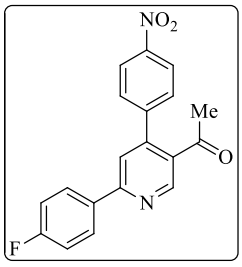
(51.2 mg, 82%); **mp**:136-138 °C; $\mathbf{R_f}$ = 0.39 (EtOAc:hexane = 1:4); **IR** (KBr): ν 2221, 1684, 1590, 1527, 1482, 1413, 1360, 1276, 1239, cm^{-1}; **^{1}H NMR** (400 MHz, $CDCl_3$): δ 9.00 (s, 1H), 7.96 (d, *J* = 8.2 Hz, 2H), 7.75-7.77 (m, 2H), 7.63 (s, 1H), 7.45-7.48 (m, 2H), 7.31 (d, *J* = 7.8 Hz, 2H), 2.42 (s, 3H), 2.35 (s, 3H); **^{13}C NMR** (100 MHz, $CDCl_3$): δ 199.7, 160.2, 150.4, 148.2, 144.1, 140.9, 135.2, 132.7, 132.0, 130.1, 129.3, 127.5, 121.3, 118.6, 112.9, 30.2, 21.7; **HRMS** (ESI) m/z calculated for $C_{21}H_{16}N_2ONa$ $[M+Na]^+$: 335.1155, found 335.1154.

3-**Acetyl-4-(4-cyanophenyl)-6-(4-methoxyphenyl)pyridine (3ct):** white solid;



(54.5 mg, 83%); **mp**138-140 °C; $\mathbf{R_f}$ = 0.35 (EtOAc:hexane = 1:4); **IR** (KBr) ν 2224, 1735, 1673, 1607, 1588, 1524, 1469, 1440, 1371, 1277, 1251cm^{-1}; **^{1}H NMR** (400 MHz, $CDCl_3$): δ 8.99 (s, 1H), 8.03-8.05 (m, 2H), 7.76 (d, *J* = 8.3 Hz, 2H), 7.58 (s, 1H), 7.45-7.47 (m, 2H), 7.02 (d, *J* = 9.0 Hz, 2H), 3.88 (s, 3H), 2.35 (s, 3H); **^{13}C NMR** (100 MHz, $CDCl_3$): δ 199.6, 161.8, 159.8, 150.5, 148.2, 144.3, 132.7, 131.5, 130.5, 129.3, 129.1, 120.8, 118.7, 114.7, 112.8, 55.7, 30.1; **HRMS** (ESI) m/z calculated for $C_{21}H_{16}N_2O_2Na[M+Na]^+$: 351.1104, found 351.1101.

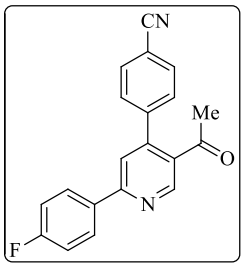
3-Acetyl-4-(4-nitrophenyl)-6-(4-fluorophenyl)pyridine (3es): light yellow



solid; (49.8 mg, 74%); **mp**: 147-149 °C; $\mathbf{R_f}$ = 0.35 (EtOAc:hexane = 1:4); **IR** (KBr): ν 1682, 1591, 1533, 1508, 1480, 1412, 1347, 1278, 1229 cm^{-1}; **^{1}H NMR** (400 MHz, $CDCl_3$): δ 9.03 (s, 1H), 8.33 (d, *J* = 8.5 Hz, 2H), 8.06-8.09 (m, 2H), 7.63 (s, 1H), 7.52 (d, *J* = 8.7 Hz, 2H), 7.19 (t, *J* = 8.5 Hz, 2H), 2.39 (s, 3H); **^{13}C NMR** (100 MHz, $CDCl_3$): δ 199.4, 164.6(d, J_{C-F} = 249 Hz), 159.1, 150.5,148.2, 148.1, 145.9, 134.1 (d, J_{C-F} = 3.6.0 Hz), 132.1, 129.6(d, J_{C-F} = 8.7 Hz) , 129.5, 124.2, 121.3, 116.4 (d , J_{C-F} = 21.8 Hz), 30.1;

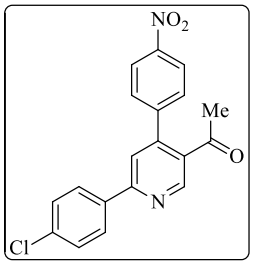
HRMS (ESI) m/z calculated for $C_{19}H_{13}FN_2O_3Na[M+Na]^+$: 359.0802, found 359.0802.

3-Acetyl-4-(4-cyanophenyl)-6-(4-fluorophenyl)pyridine (3et): white solid;



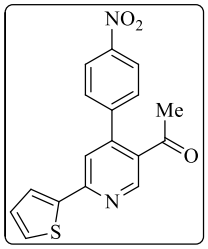
(46.8 mg, 74%); **mp**: 142-144 °C; $\mathbf{R_f}$ = 0.45 (EtOAc:hexane = 1:4); **IR** (KBr): ν 2219, 1683, 1593, 1528, 1481, 1412, 1362, 1277, 1228 cm^{-1}; **^{1}H NMR** (400 MHz, $CDCl_3$): δ 8.99 (s, 1H), 8.05-8.08 (m, 2H), 7.77 (d, *J* = 8.0 Hz, 2H), 7.61 (s, 1H), 7.47 d, *J* = 8.0 Hz, 2H), 7.19 (t, *J* = 8.5 Hz, 2H), 2.35 (s, 3H); **^{13}C NMR** (100 MHz, $CDCl_3$): δ 199.7, 164.5(d, J_{C-F}= 249.0 Hz), 159.0, 150.4, 148.3, 143.9, 134.2, 134.1 132.8, 132.3, 129.6, 129.5, 129.3, 128.5, 128.4, 128.0, 127.9, 127.3, 125.9, 121.3, 118.6, 116.5, 116.2, 113.0, 30.2; **HRMS** (ESI) m/z calculated for $C_{20}H_{14}FN_2O$ $[M+H]^+$: 317.1085, found 317.1079.

3-Acetyl-4-(4-nitrophenyl)-6-(4-chlorophenyl)pyridine (3fs): light yellow



solid; (54.2 mg, 77%); **mp**:151-153 °C; $\mathbf{R_f}$ = 0.45 (EtOAc:hexane = 1:4); **IR** (KBr): ν 1682, 1589, 1530, 1510, 1475, 1404, 1347, 1279, 1238cm^{-1}; **^{1}H NMR** (400 MHz, $CDCl_3$): δ 9.04 (s, 1H), 8.34 (d, *J* = 8.2 Hz, 2H), 8.03 (d, *J* = 8.5 Hz, 2H), 7.65 (s, 1H), 7.47-7.53 (m, 4H), 2.39 (s, 3H); **^{13}C NMR** (100 MHz, $CDCl_3$): δ 199.4, 158.9, 150.5, 148.3, 148.1, 145.8, 137.0, 136.3, 132.4, 129.6, 129.5, 128.9, 124.2, 121.4, 30.2; **HRMS** (ESI) m/z calculated for $C_{19}H_{14}ClN_2O_3[M+H]^+$: 353.0687, found 353.0673.

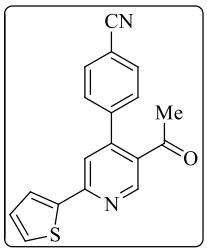
3-Acetyl-4-(4-nitrophenyl)-6-(thiophen-2-yl)pyridine (3is): light yellow solid;



(49.3 mg, 76%); **mp**: 136-138 °C; $\mathbf{R_f}$ = 0.40 (EtOAc:hexane = 1:4); **IR** (KBr) ν 1681, 1588, 1529, 1506, 1425, 1347, 1278, 1239 cm^{-1}; **^{1}H NMR** (400 MHz, $CDCl_3$): δ 8.95 (s, 1H), 8.33 (d, *J* = 8.4 H, 2H), 7.69 (d, *J* = 3.2 H, 1H), 7.49-7.55 (m, 4H), 7.15-7.17 (m, 1H), 2.39 (s, 3H); **^{13}C NMR** (100 MHz, $CDCl_3$):

δ 198.4, 155.0, 150.5, 147.9, 145.6, 143.1, 131.2, 130.0, 129.1, 128.5, 126.7, 123.8, 119.6, 29.6; **HRMS** (ESI) m/z calculated for $C_{17}H_{13}N_2O_3S[M+H]^+$: 325.0642, found 325.0653.

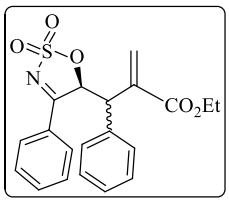
3-Acetyl-4-(4-cyanophenyl)-6-(thiophen-2-yl)pyridine (3it): light yellow solid;



(45.0 mg, 74%); **mp**: 132-134 °C; $\mathbf{R_f}$ = 0.35 (EtOAc:hexane = 1:4); **IR** (KBr): ν 2219, 1682, 1587, 1521, 1480, 1426, 1357, 1305, 1278, 1235 cm^{-1}; **^{1}H NMR** (400 MHz, $CDCl_3$): δ 8.91 (s, 1H), 7.77 (d, *J* = 8.0 Hz, 2H), 7.69 (d, *J* = 3.2 Hz, 1H), 7.51-7.54 (m, 2H), 7.45 (d, *J* = 8.0 Hz, 2H), 7.14-7.17 (m, 1H), 2.34 (s, 3H); **^{13}C NMR** (100 MHz, $CDCl_3$): δ 198.8, 154.9, 150.4, 148.1, 143.6, 143.2, 132.4, 131.5, 129.9, 128.9, 128.5, 126.6, 119.5, 118.3, 112.7, 29.7; **HRMS** (ESI) m/z calculated for $C_{18}H_{13}N_2OS[M+H]^+$: 305.0743, found 305.0764.

The synthesis of intermediate 5: To a stirred solution of compound **1a** (39.4 mg, 0.2 mmol) and **2a** (54.6 mg, 0.22 mmol) in 2-MeTHF (1.0 mL) was added DABCO (33.6 mg, 0.3 mmol) at room temperature. Then the reaction mixture was heated at 70 °C for 30 min O_2 atmosphere (monitored by TLC). After that, the reaction mixture was extracted with ethyl acetate (3 × 10 mL), washed with water and brine respectively, dried over Na_2SO_4. The combined organic phases were evaporated under reduced pressure to afford the crude product which was purified through column chromatography through column chromatography over silica-gel using a mixture of EtOAc/hexane (1:2, v/v) as the eluent. The intermediate **5** was fully characterized by its spectroscopic data (IR, ^{1}HNMR, ^{13}C NMR and HRMS).

Intermediate 5: (90% combined yield of a mixture of diastereomer); **IR** (KBr): ν

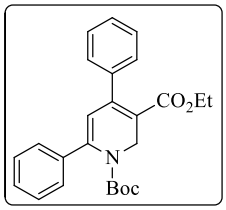


1710, 1601, 1570, 1495, 1451, 1374, 1302, 1273, 1200, cm^{-1}; **^{1}H NMR** (400 MHz, $CDCl_3$): δ *(*mixture of diastereomer *dr* = 3:1*) δ* 7.84 (d, *J* = 7.7 Hz, 1.5H), 7.80 (d, *J* = 7.7 Hz, 0.5H), 7.73 (t, *J* = 7.2 Hz, 0.75H), 7.67 (t, *J* = 7.2 Hz, 0.25H), 7.59 (t, *J* = 7.6 Hz, 1.5H), 7.51 (t, *J* = 7.5 Hz, 0.5H), 7.33-7.40 (m, 1.25H), 7.19-7.29

(m, 2.25H), 6.93 (d, *J* = 7.2 Hz, 1.5H), 6.59 (s, 0.75H), 6.56-6.57 (m, 1H), 6.35 (d, *J* = 3.2 Hz, 0.25H), 6.01 (s, 0.75H), 5.71 (s, 0.25H), 4.80 (s, 0.25H), 4.72 (s, 0.75H), 4.19-4.30 (m, 1.5H), 4.00-4.15 (m, 0.5H), 1.31 (t, *J* = 7.2Hz, 2.25H), 1.19 (t, *J* = 7.2Hz, 0.75H); **^{13}C NMR** (100 MHz, $CDCl_3$): δ (major diastereomer) 178.4, 166.7, 138.2, 135.2, 132.5, 132.2, 130.1, 129.8, 129.5, 129.1, 128.5, 128.3, 89.0, 61.9, 49.4, 14.4; **HRMS** (ESI) m/z calculated for $C_{20}H_{19}NSO_5Na$ $[M+Na]^+$: 408.0876, found 408.0897.

One-pot synthesis of ethyl N-Boc-4,6-diphenyl-1,2-dihydropyridine-3-carboxylate (8):

A mixture of compound **1a** (39.4 mg, 0.2 mmol), **2a** (54.6 mg, 0.22 mmol), Boc_2O (0.3 mmol) and DABCO (33.6 mg, 0.3 mmol) in 2-MeTHF (1.0 mL) was heated at 70 °C for 48h under inert atmosphere (monitored by TLC). Upon completion of the reaction, the reaction mixture was extracted with ethyl acetate (3 × 10 mL), washed with water and brine respectively, dried over Na_2SO_4. The combined organic phases were evaporated under reduced pressure to afford the crude product. Finally it was obtained in a pure form **8** through column chromatography over silica-gel using a mixture of EtOAc/hexane (1:4, v/v) as an eluent.

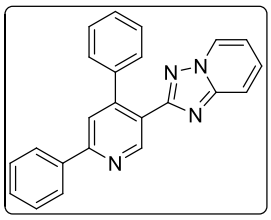
Ethyl 1-tert-butoxycarbonyl-4,6-diphenyl-1,2-dihydropyridine-3-carboxylate (8): 

(51.0 mg, 62%); **^{1}H NMR** (400 MHz, $CDCl_3$): δ 7.40-7.42 (m, 2H), 7.33-7.37 (m, 6H), 7.27-7.29 (m, 2H), 6.00 (s, 1H), 4.79 (s, 2H), 4.03 (q, *J* = 7.2 Hz, 2H), 1.12 (s, 9H), 1.03 (t, *J* = 7.2 Hz, 3H); **^{13}C NMR** (100 MHz, $CDCl_3$): δ 165.8, 153.0, 146.0, 144.5, 139.6, 138.1, 128.9, 128.5, 128.2, 128.1, 128.0, 127.1, 117.5, 117.5, 81.9, 60.6, 45.5, 27.9, 14.0; **HRMS** (ESI) m/z calculated for $C_{25}H_{27}NO_4Na[M+Na]^+$: 428.1832, found 428.183.

Synthesis of 2-(4,6-diphenylpyridin-3-yl)-[1,2,4]triazolo[1,5-*a*]pyridine (9): A mixture of compound **3al** (0.2 mmol, 52.0 mg), 2-aminopyridine (0.24 mmol, 24

mg), CuBr (0.01 mmol, 1.5 mg), 1,10-phenanthroline (0.01 mmol, 1.8 mg) and ZnI_2 (0.02 mmol 6.4 mg) 1,2-dichlorobenzene (0.4 ml) was stirred at 130 ° C for 18 h. After cooling to room temperature, the reaction was diluted with EtOAc and filtered through celite. The filtrate was concentrated and purified by column chromatography (eluent: EtOAc:hexane = 1:3) on silica gel to afford compound **9**.

2-(4,6-Diphenylpyridin-3-yl)-[1,2,4]triazolo[1,5-*a*]pyridine (9): White solid;



(56.3 mg, 81%); **mp**: 173-175 °C; $\mathbf{R_f}$ = 0.20 (EtOAc:hexane = 1:4); **IR** (KBr): ν 1632, 1589, 1576, 1556, 1500, 1456, 1425, 1386, 1356, 1327, 1305, 1259, 1211; **^{1}H NMR** (400 MHz, $CDCl_3$): δ 9.21 (s, 1H), 8.49 (d, J = 6.4 Hz, 1H), 8.11 (d, J = 7.6 Hz, 2H), 7.82 (s, 1H), 7.68-7.71 (m, 1H), 7.43-7.52 (m, 4H), 7.30-7.38 (m, 5H), 6.97-7.00 (m, 1H); **^{13}C NMR** (100 MHz, $CDCl_3$): δ 162.5, 158.1, 151.7, 151.1, 150.0, 139.1, 138.8, 129.4, 129.3, 128.8 (2C), 128.3, 128.2, 128.1, 127.2, 124.3, 121.8, 116.6, 113.7; **HRMS** (ESI) m/z calculated for $C_{23}H_{17}N_4[M+H]^+$: 349.1448, found 349.1475.

Table 5.5 Crystal data for compound **3ai**

Compound	**3ai**
Empirical formula	$C_{20}H_{16}N_2O_4$
Formula weight	348.35
Temperatute	293(2) K
Wave length (Å)	0.71073
Crystal system, space group	Triclinic, P-1
a (Å)	8.1889(3)
b (Å)	10.3419(5)
c (Å)	10.9166(4)
α (°)	105.058(4)
β (°)	98.466(3)
γ (°)	99.563(3)
Volume ($Å^3$)	862.59(6)
Z, Calculated density (mg/m^3)	2, 1.341
Absorption coefficient (mm^{-1})	0.095
F(000)	364
Crystal size (mm)	0.230 x 0.180 x 0.130
Θ range (deg)	2.947 to 32.231 deg.
Limiting indices	-12<=h<=12, -15<=k<=15, -15<=l<=16
Reflections collected / unique	10763 / 5548 [R(int) = 0.0262]
Completeness to Θ = 25.242	99.8 %
Max. and min. transmission	1.00000 and 0.77304
Absorption correction	Semi-empirical from equivalents
Refined method	Full-matrix least-squares on F^2
Data / restrains / parameters	5548 / 0 / 236
Goodness-of-fit on F^2	1.070
Final R indices [I>2sigma(I)]	R1 = 0.0624, wR2 = 0.1619
R indices (all data)	R1 = 0.0967, wR2 = 0.1867
Largest diff. peak and hole ($e.A^{-3}$)	0.260 and -0.234
CCDC	**1522097**

5.6 Copies of ^{1}H and ^{13}C NMR spectra of some important compounds described in Chapter 6

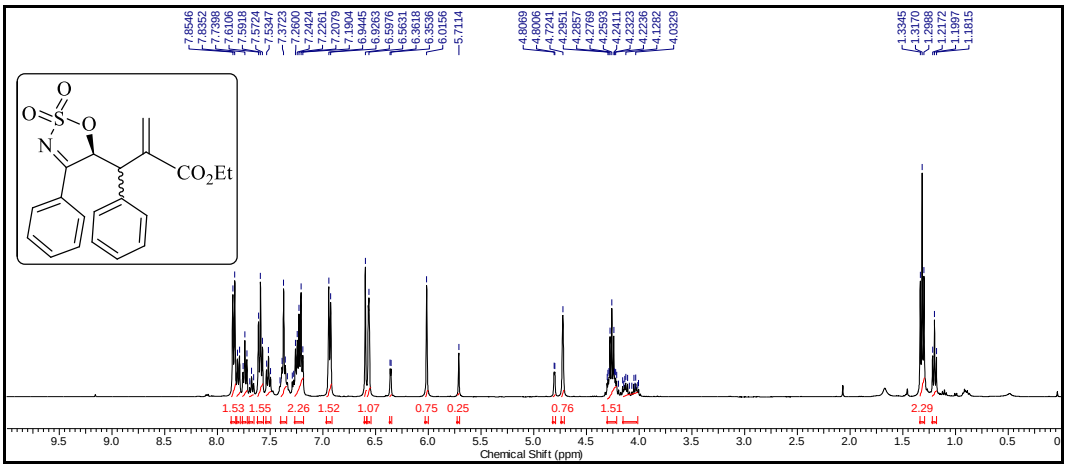


Figure 5.4 400 MHz ^{1}H NMR spectrum of **5** in $CDCl_3$

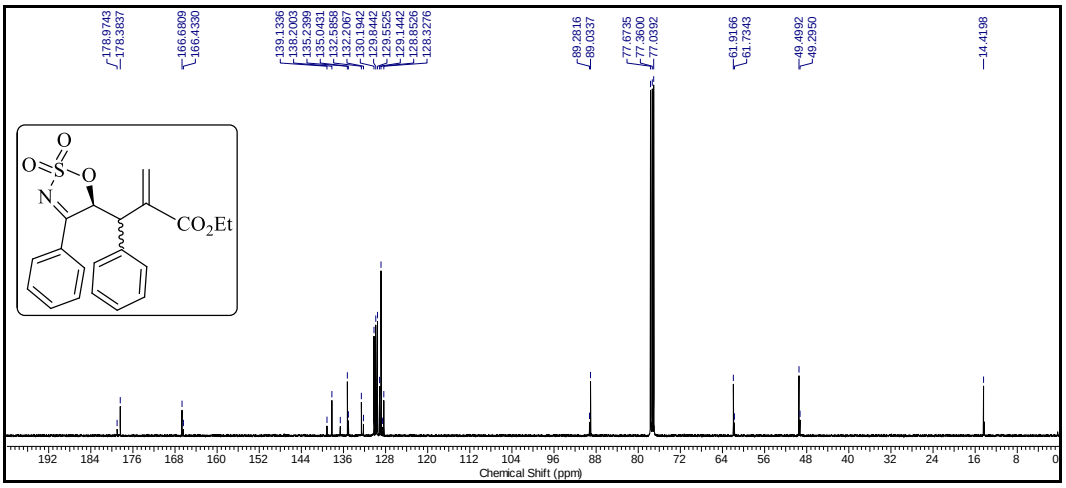


Figure 5.5 100 MHz ^{13}C NMR spectrum of **5** in $CDCl_3$

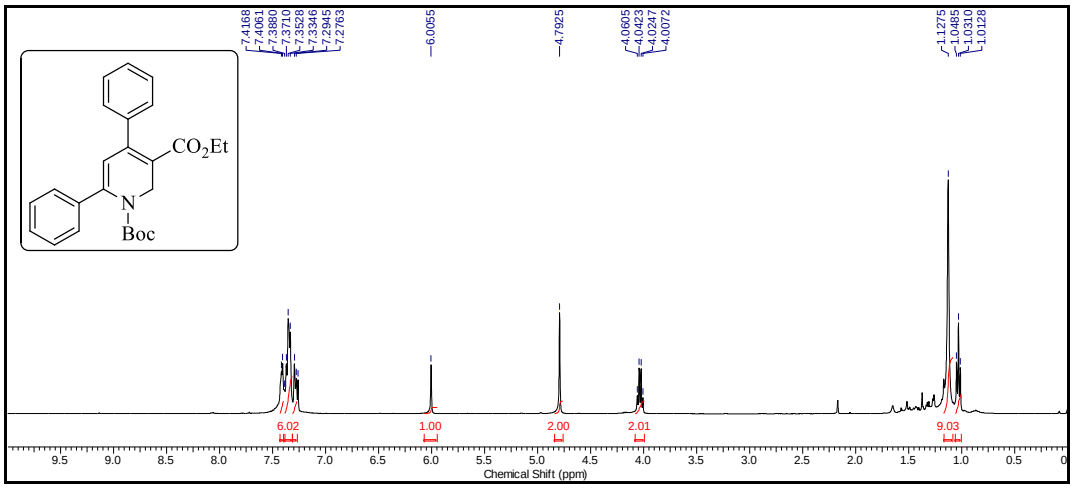


Figure 5.6 400 MHz ^{1}H NMR spectrum of **8** in $CDCl_3$

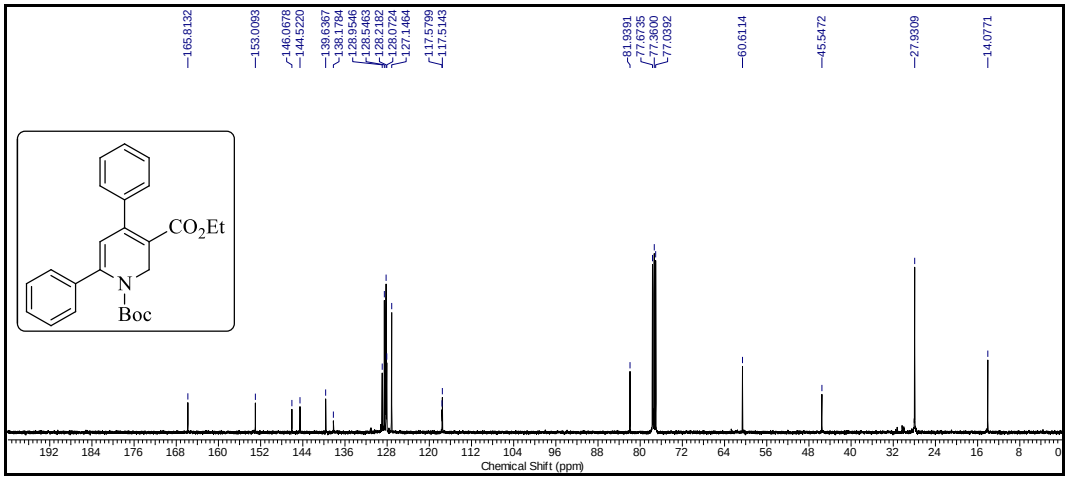


Figure 5.7 100 MHz ^{13}C NMR spectrum of **8** in $CDCl_3$

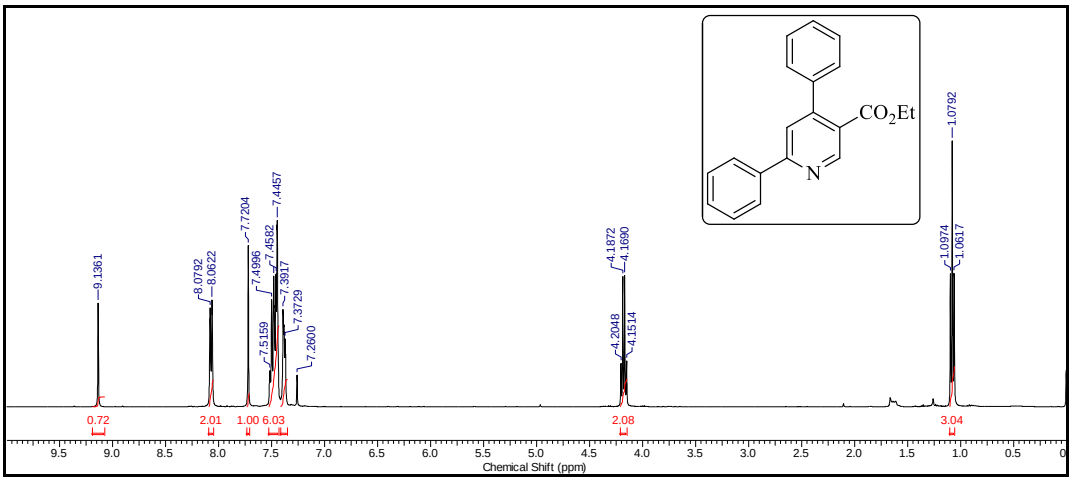


Figure 5.8 400 MHz ^{1}H NMR spectrum of **3aa** in $CDCl_3$

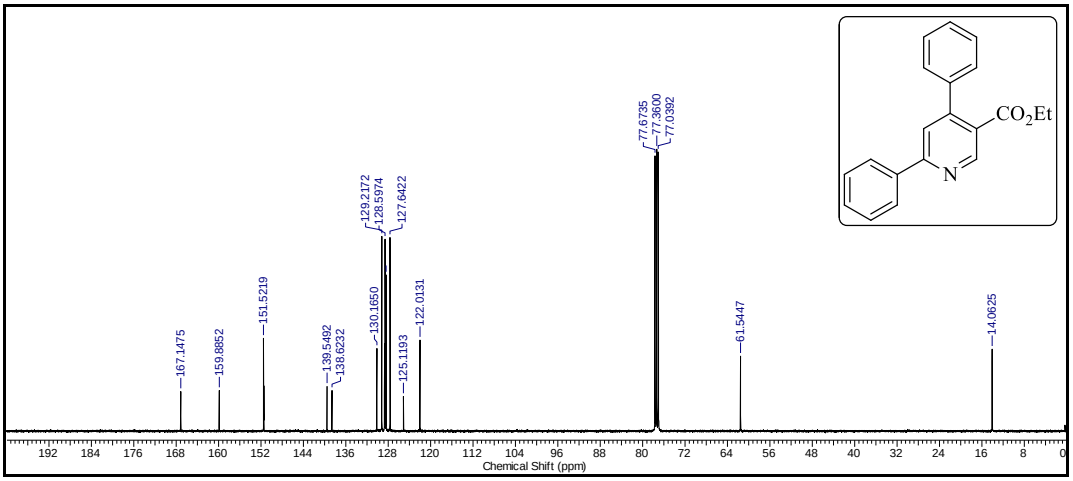


Figure 5.9 100 MHz ^{13}C NMR spectrum of **3aa** in $CDCl_3$

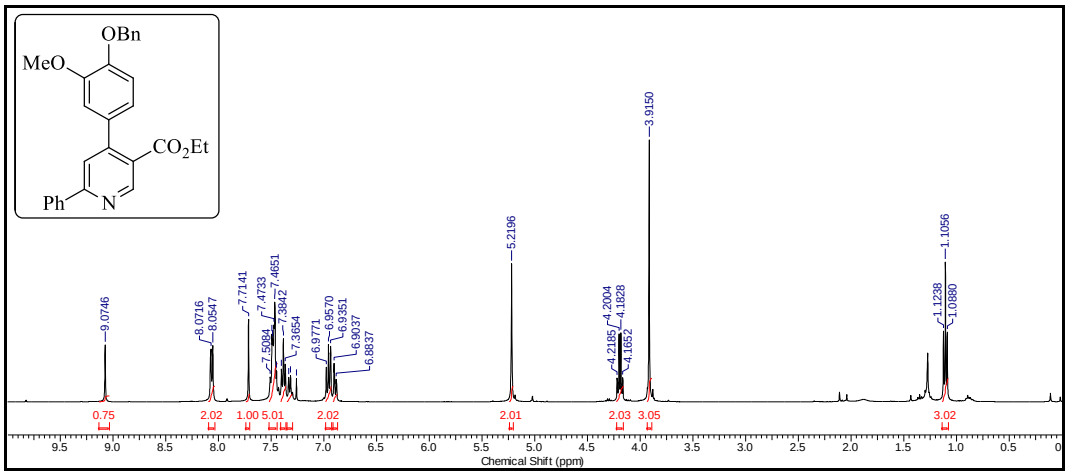


Figure 5.10 400 MHz ^{1}H NMR spectrum of **3ac** in $CDCl_3$

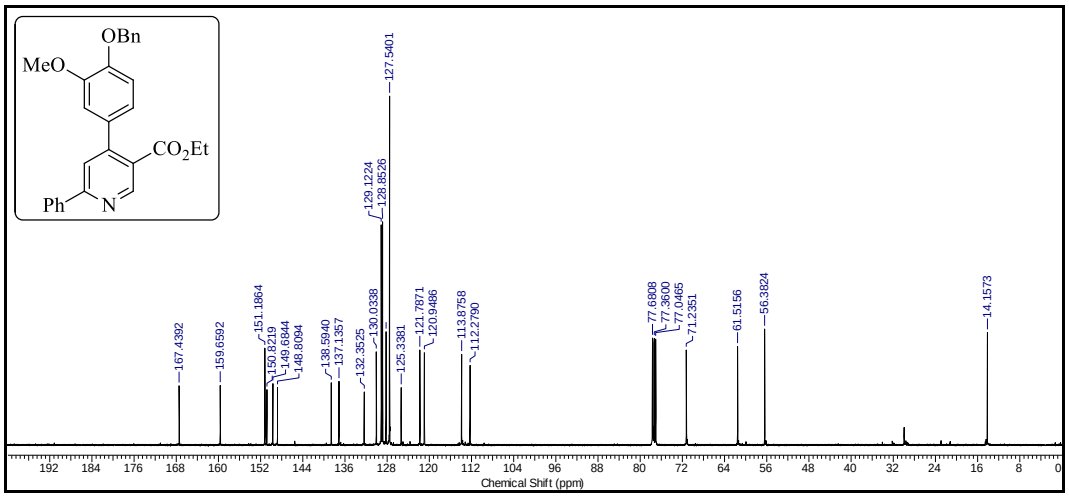


Figure 5.11 100 MHz ^{13}C NMR spectrum of **3ac** in $CDCl_3$

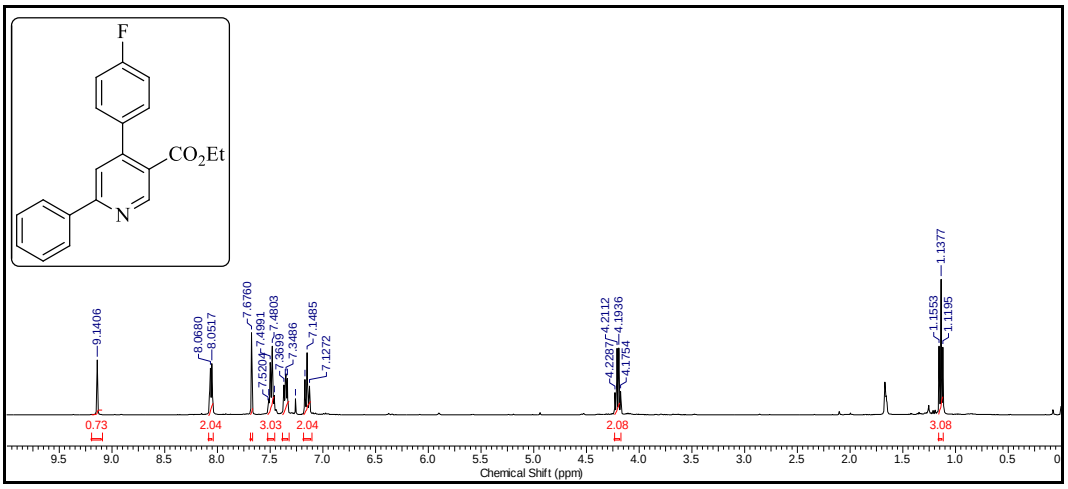


Figure 5.12 400 MHz ^{1}H NMR spectrum of **3ad** in $CDCl_3$

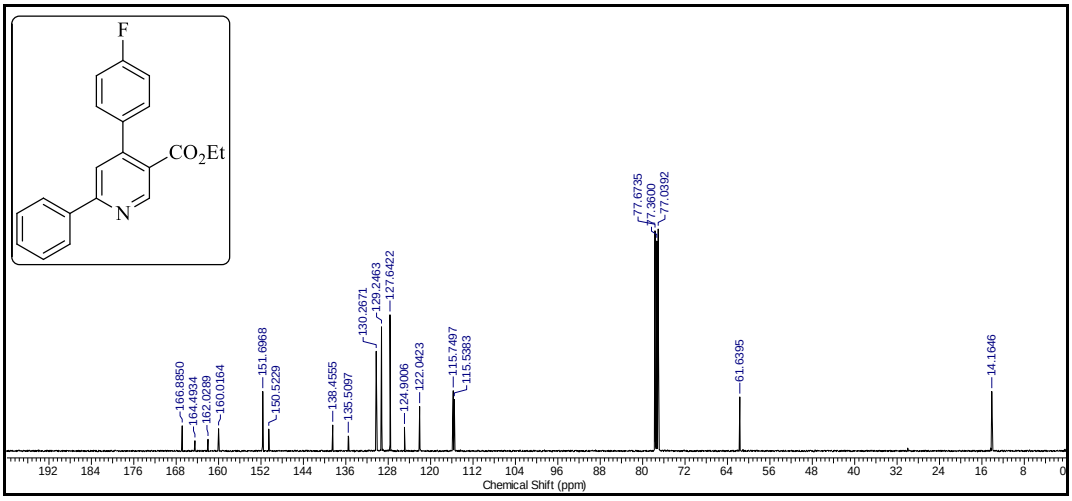


Figure 5.13 100 MHz ^{13}C NMR spectrum of **3ad** in $CDCl_3$

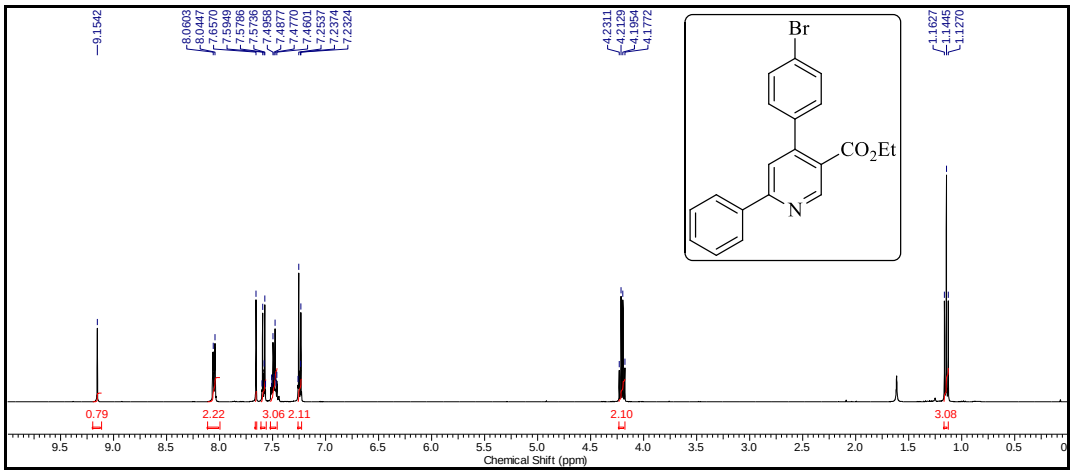


Figure 5.14 400 MHz ^{1}H NMR spectrum of **3af** in $CDCl_3$

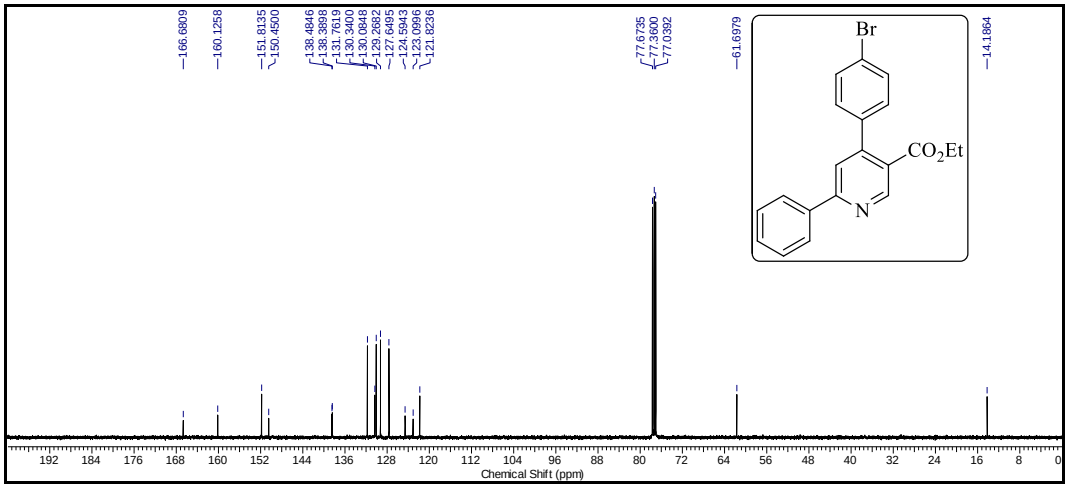


Figure 5.15 100 MHz ^{13}C NMR spectrum of **3af** in $CDCl_3$

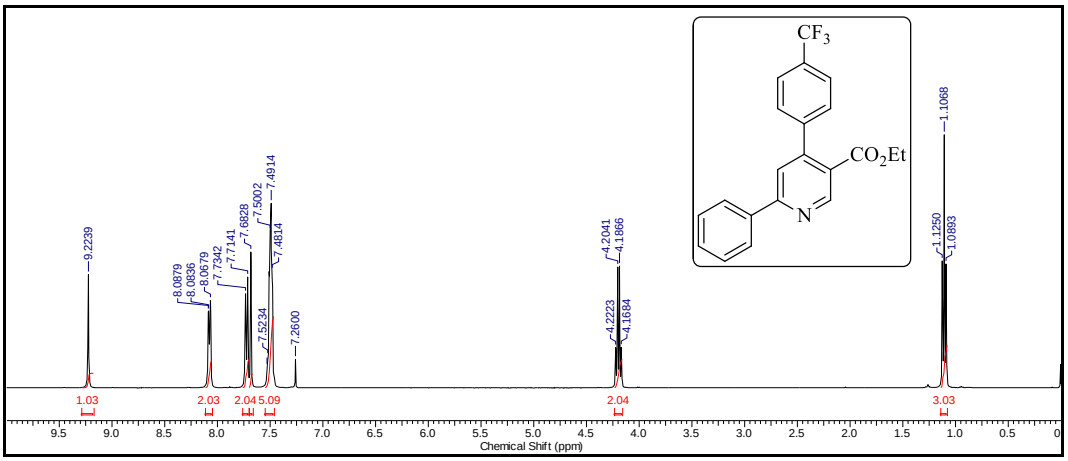


Figure 5.16 400 MHz ^{1}H NMR spectrum of **3ag** in $CDCl_3$

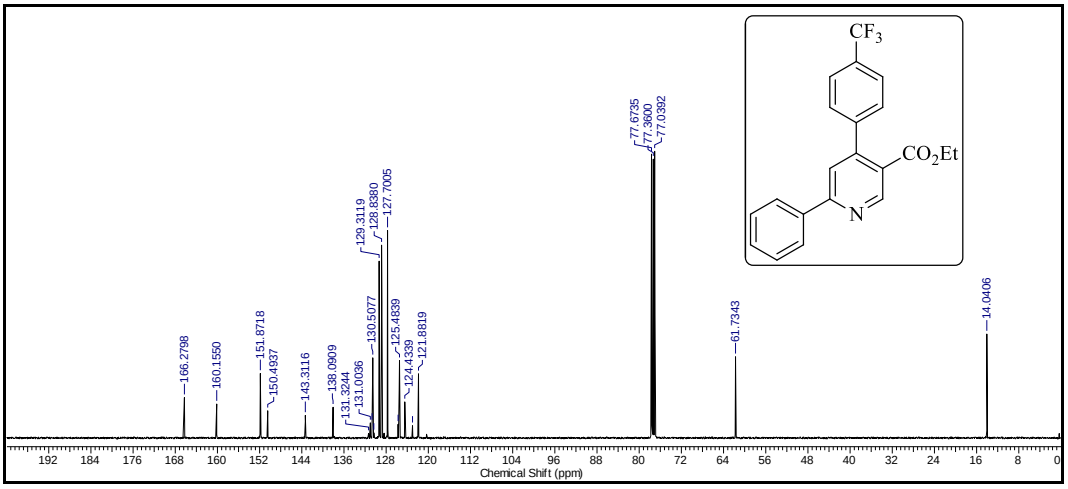


Figure 5.17 100 MHz ^{13}C NMR spectrum of **3ag** in $CDCl_3$

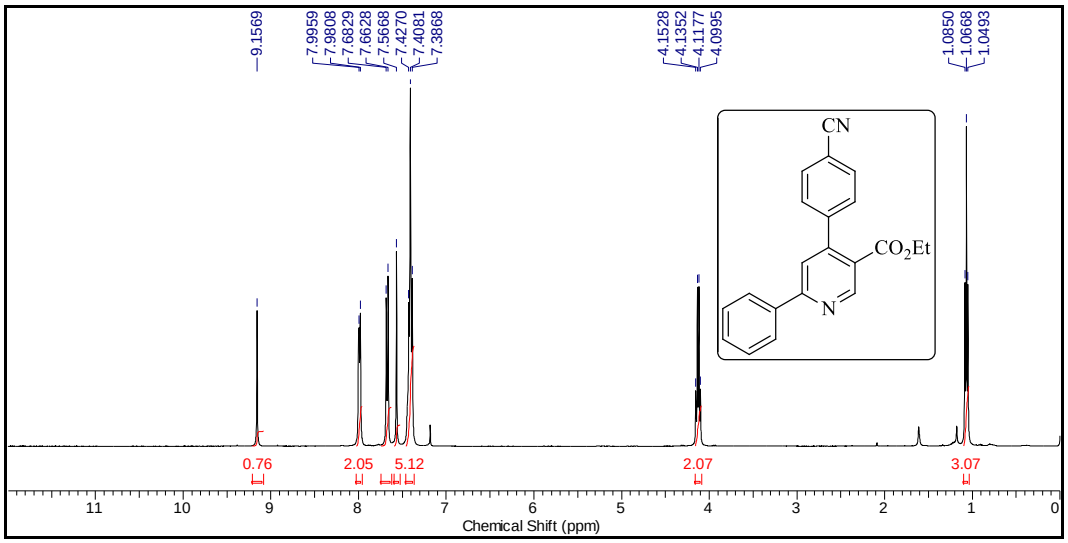


Figure 5.18 400 MHz ^{1}H NMR spectrum of **3ah** in $CDCl_3$

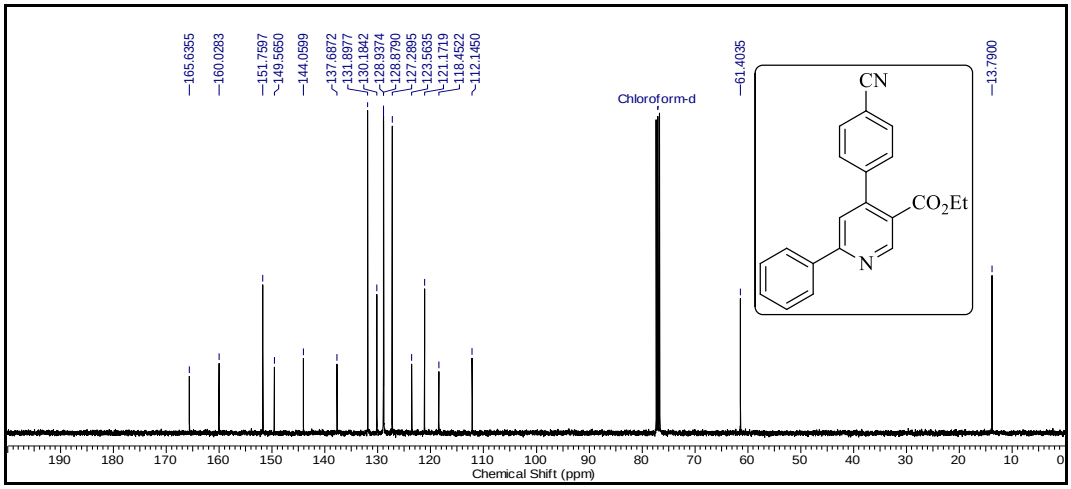


Figure 5.19 100 MHz ^{13}C NMR spectrum of **3ah** in $CDCl_3$

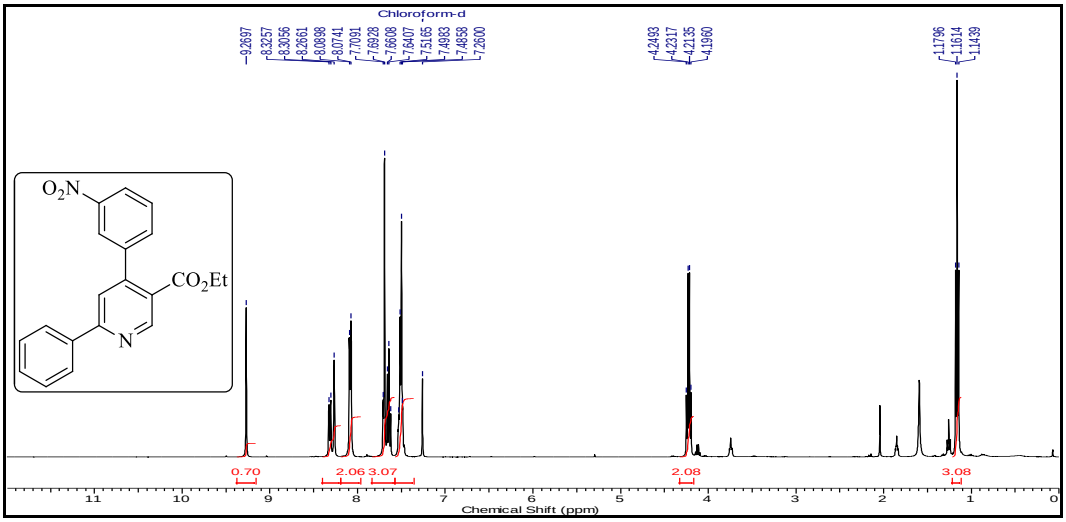


Figure 5.20 400 MHz ^{1}H NMR spectrum of **3ai** in $CDCl_3$

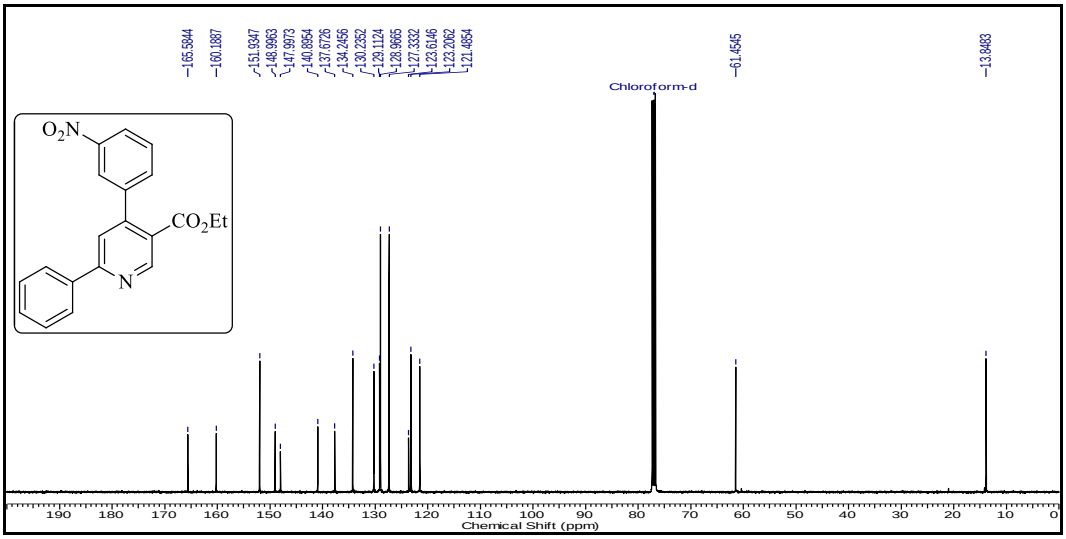


Figure 5.21 100 MHz ^{13}C NMR spectrum of **3ai** in $CDCl_3$

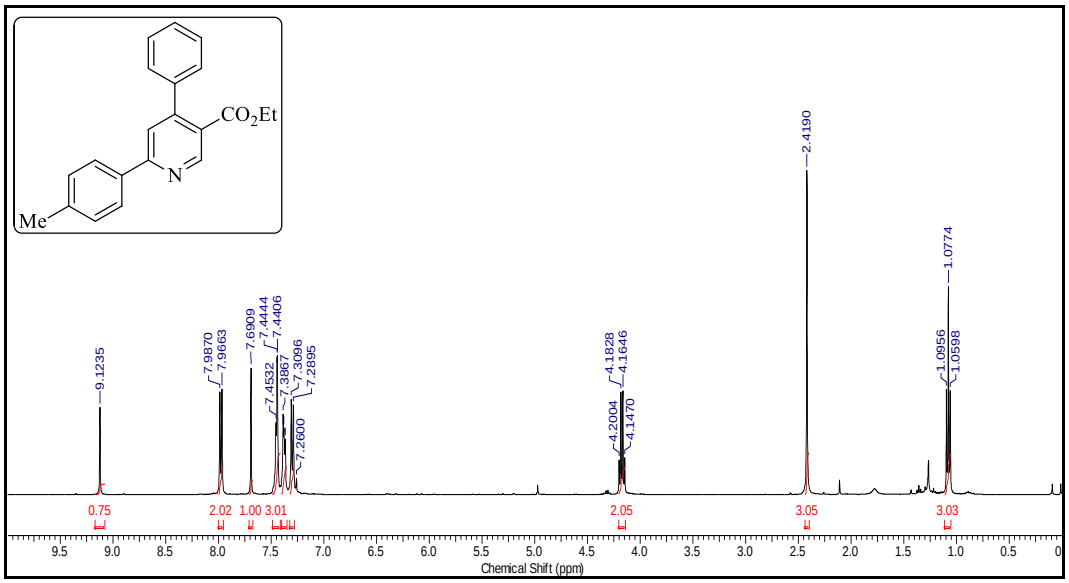


Figure 5.22 400 MHz ^{1}H NMR spectrum of **3ba** in $CDCl_3$

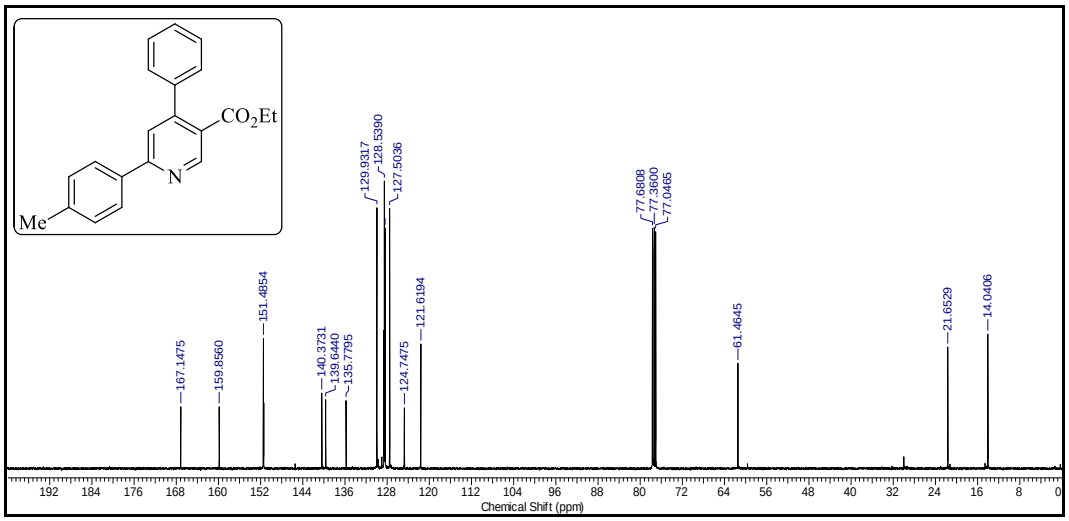


Figure 5.23 100 MHz ^{13}C NMR spectrum of **3ba** in $CDCl_3$

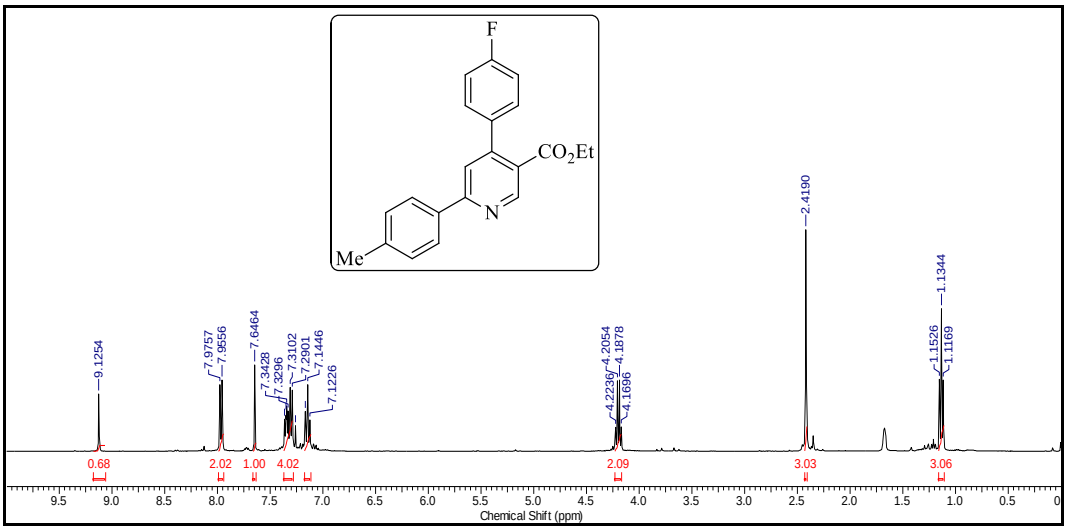


Figure 5.24 400 MHz ^{1}H NMR spectrum of **3bd** in $CDCl_3$

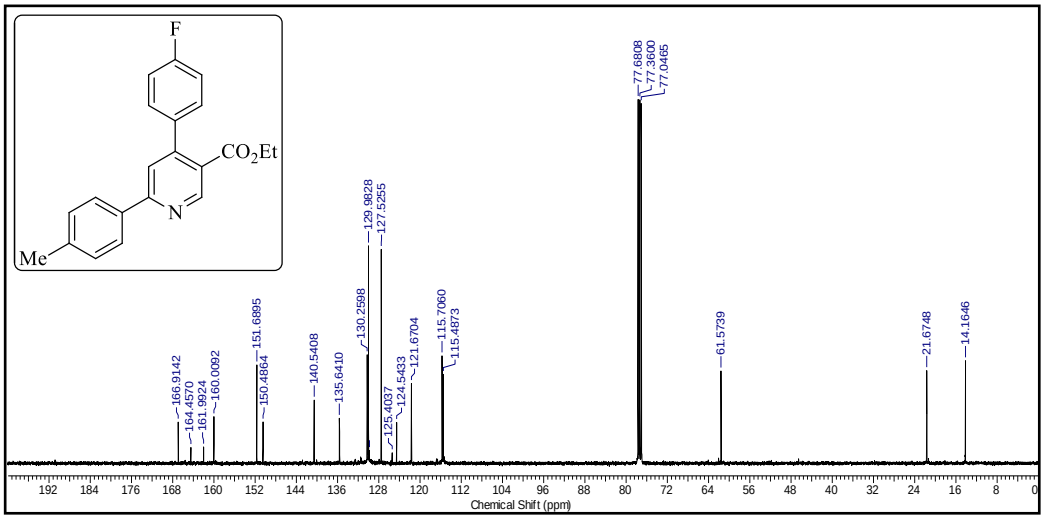


Figure 5.25 100 MHz ^{13}C NMR spectrum of **3bd** in $CDCl_3$

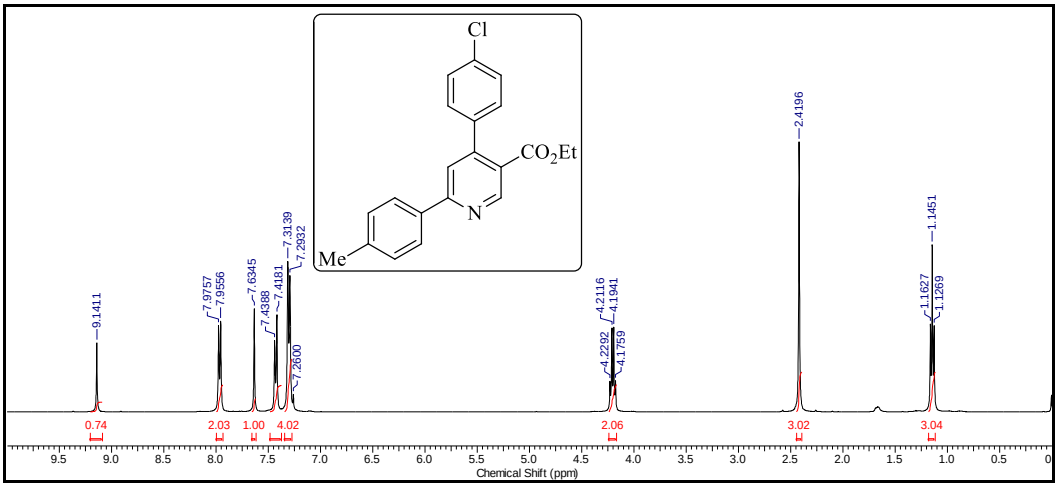


Figure 5.26 400 MHz ^{1}H NMR spectrum of **3be** in $CDCl_3$

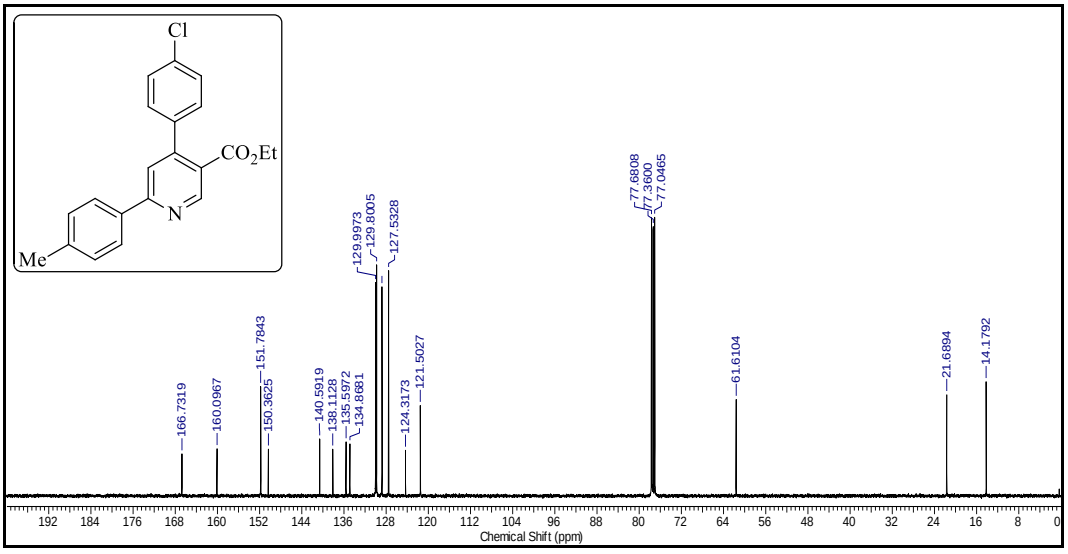


Figure 5.27 100 MHz ^{13}C NMR spectrum of **3be** in $CDCl_3$

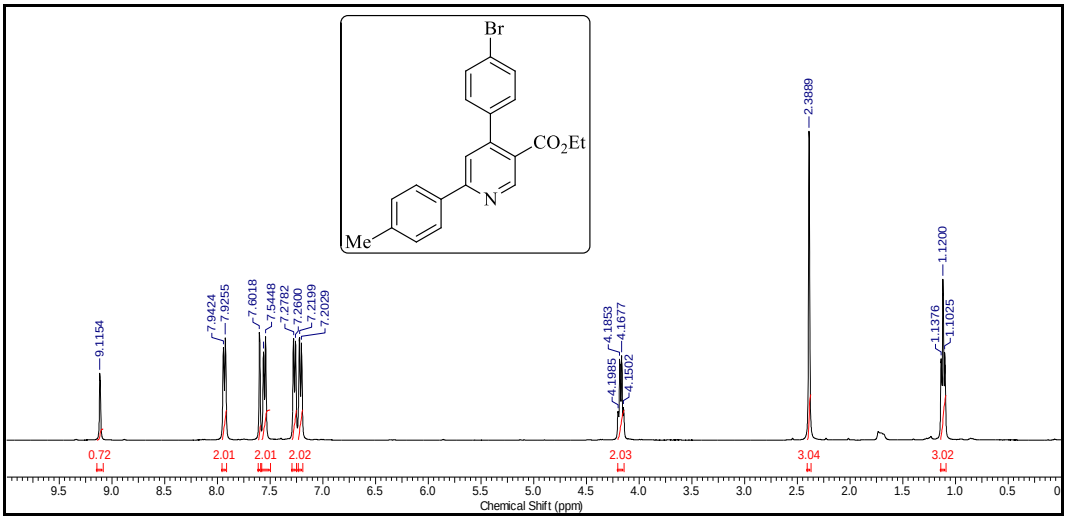


Figure 5.28 400 MHz ^{1}H NMR spectrum of **3bf** in $CDCl_3$

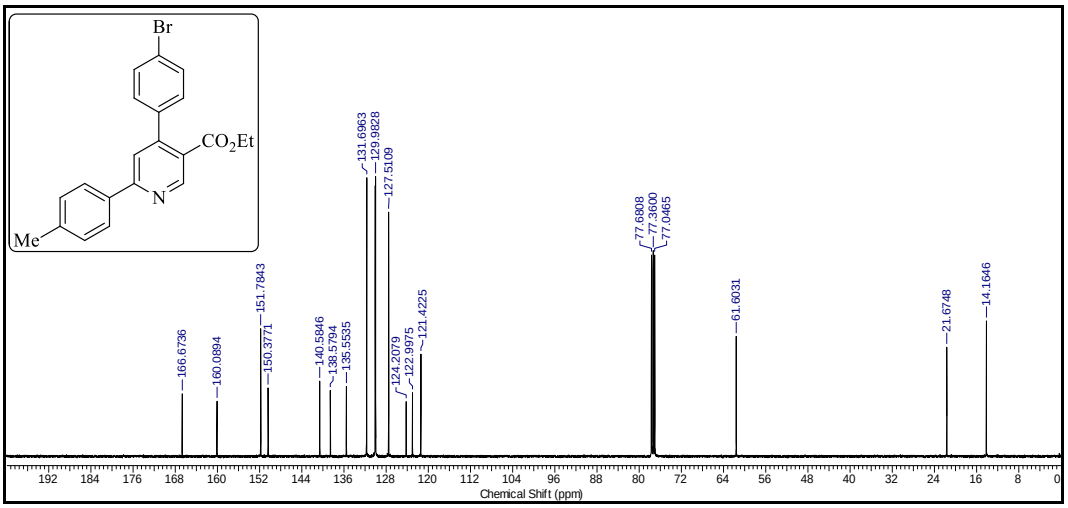


Figure 5.29 100 MHz ^{13}C NMR spectrum of **3bf** in $CDCl_3$

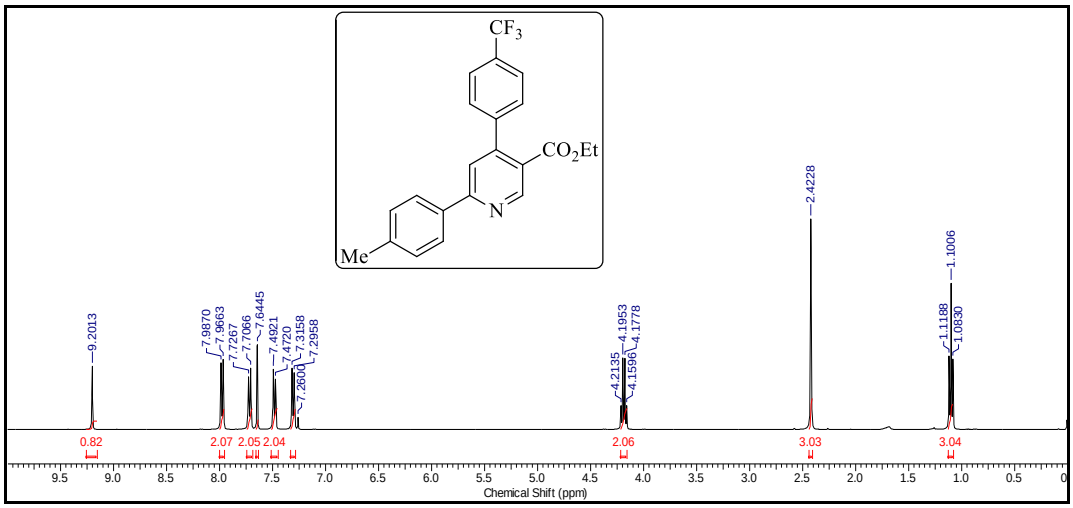


Figure 5.30 400 MHz ^{1}H NMR spectrum of **3bg** in $CDCl_3$

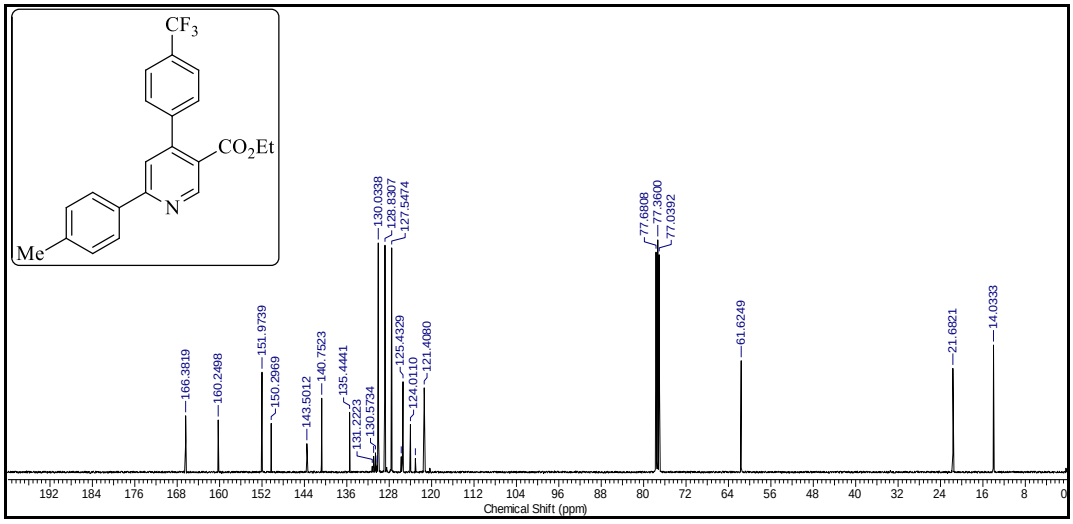


Figure 5.31 100 MHz ^{13}C NMR spectrum of **3bg** in $CDCl_3$

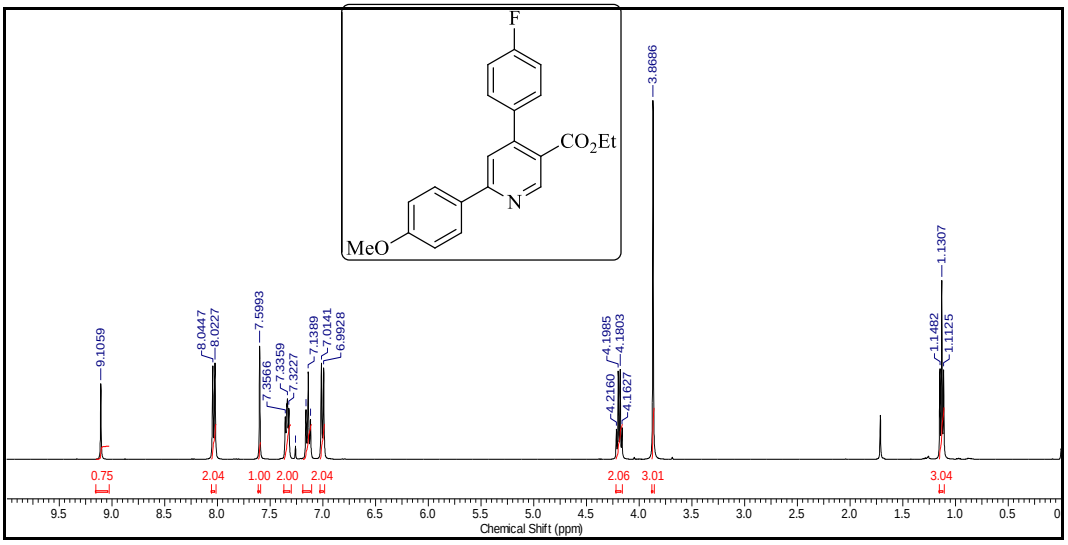


Figure 5.32 400 MHz ^{1}H NMR spectrum of **3cd** in $CDCl_3$

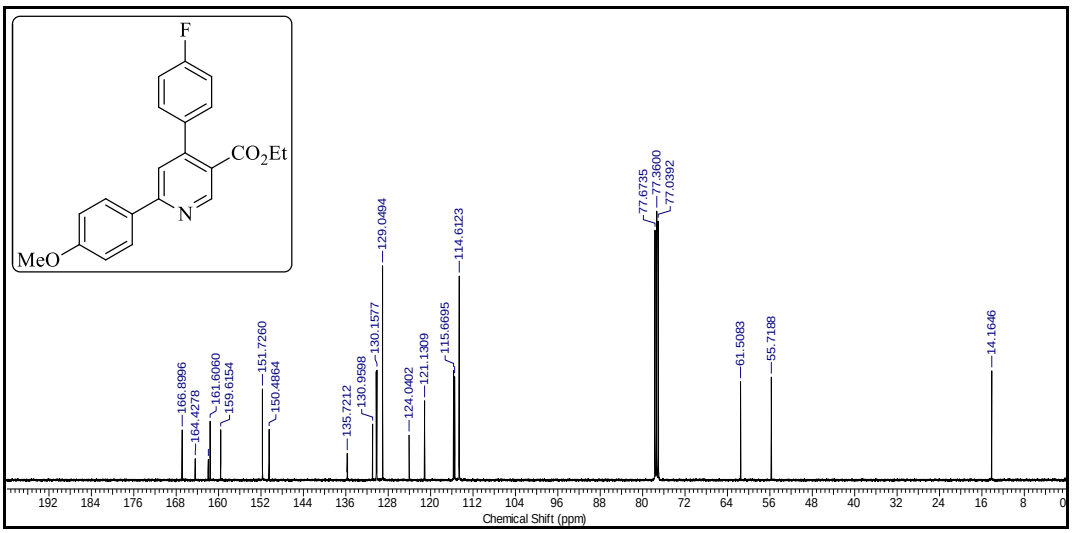


Figure 5.33 100 MHz ^{13}C NMR spectrum of **3cd** in $CDCl_3$

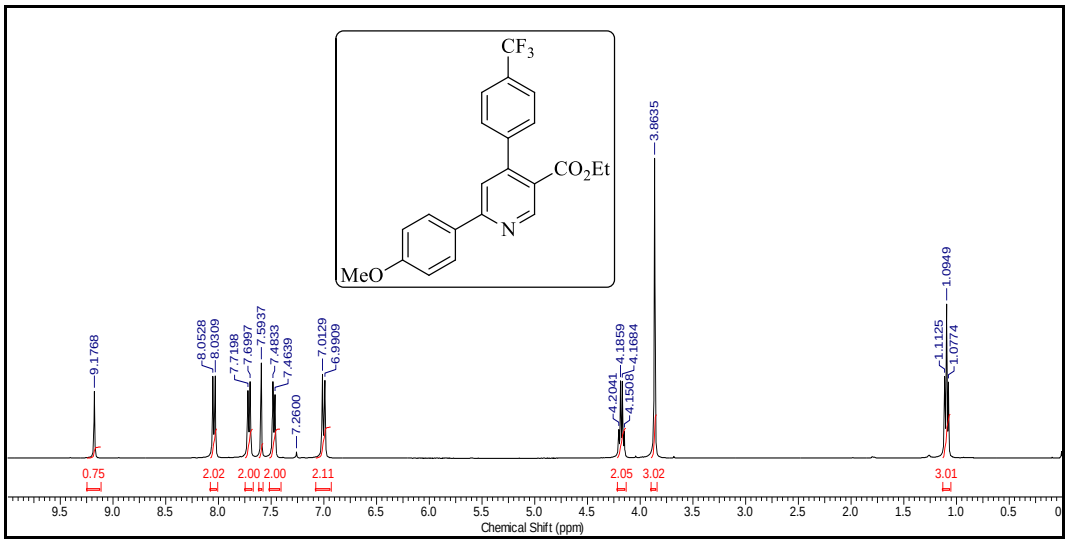


Figure 5.34 400 MHz ^{1}H NMR spectrum of **3cg** in $CDCl_3$

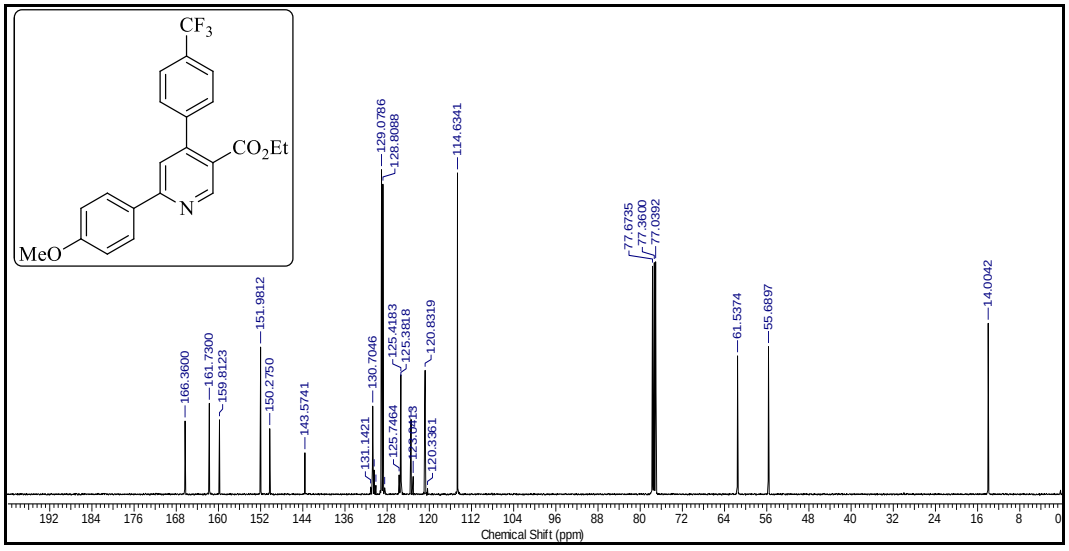


Figure 5.35 100 MHz ^{13}C NMR spectrum of **3cg** in $CDCl_3$

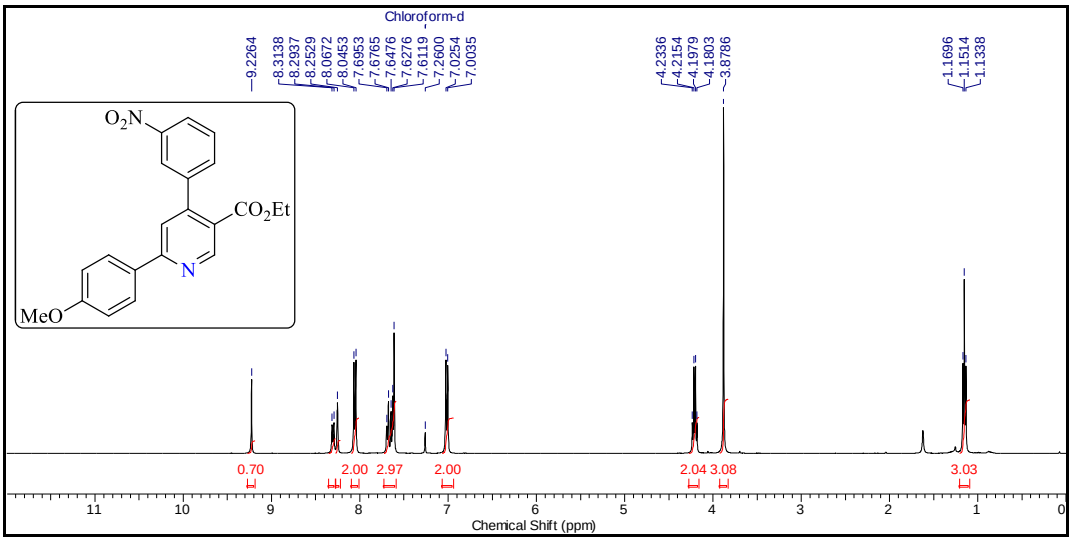


Figure 5.36 400 MHz ^{1}H NMR spectrum of **3ci** in $CDCl_3$

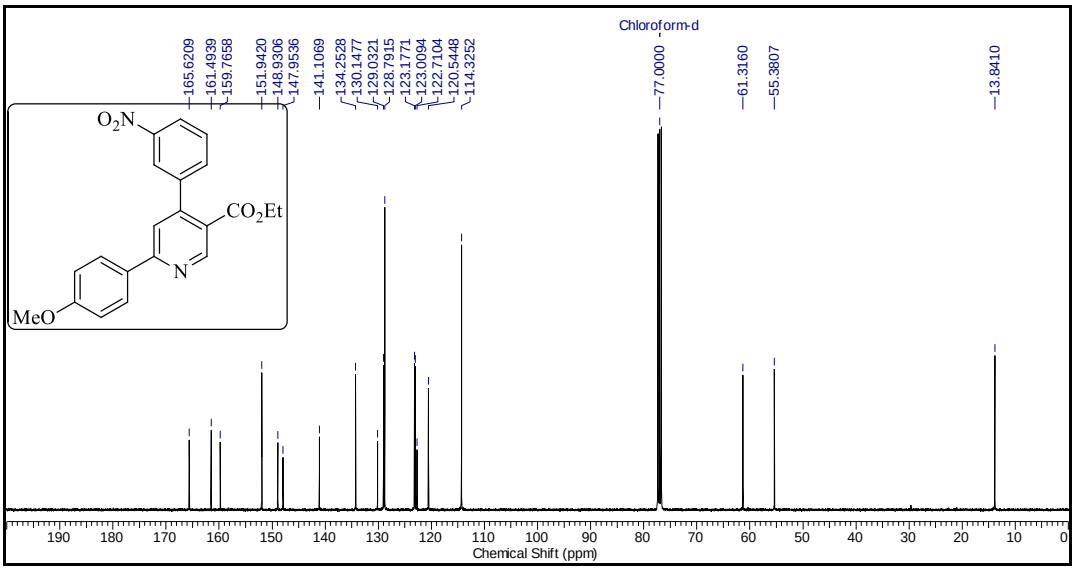


Figure 5.37 100 MHz ^{13}C NMR spectrum of **3ci** in $CDCl_3$

\

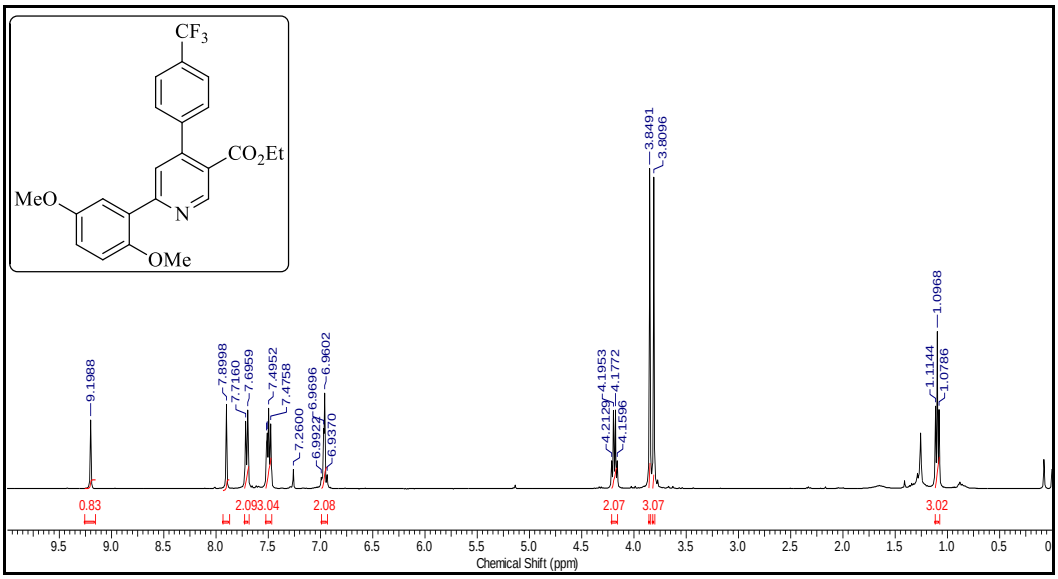


Figure 5.38 400 MHz ^{1}H NMR spectrum of **3dg** in $CDCl_3$

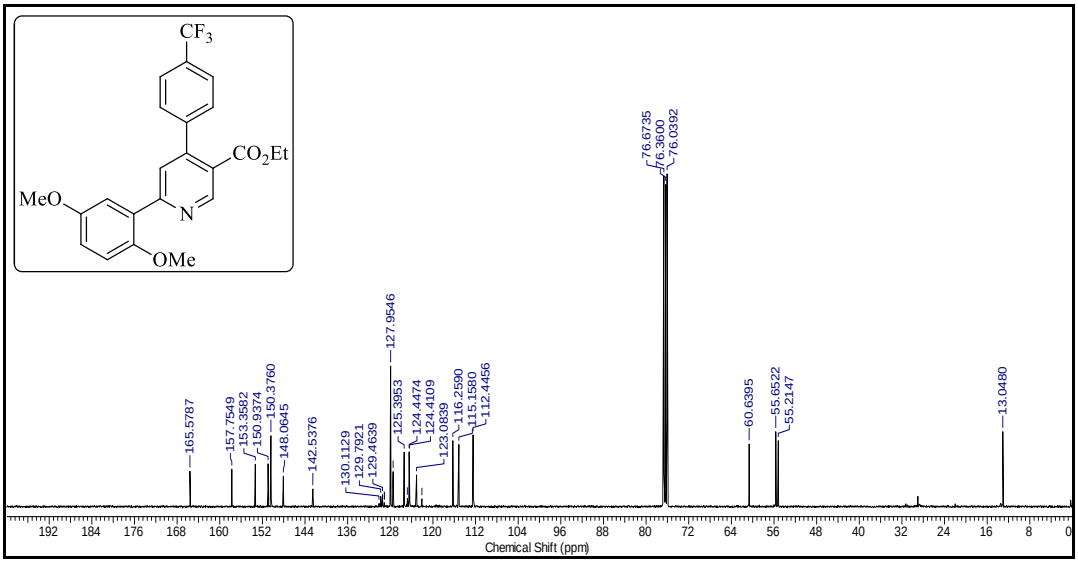


Figure 5.39 100 MHz ^{13}C NMR spectrum of **3dg** in $CDCl_3$

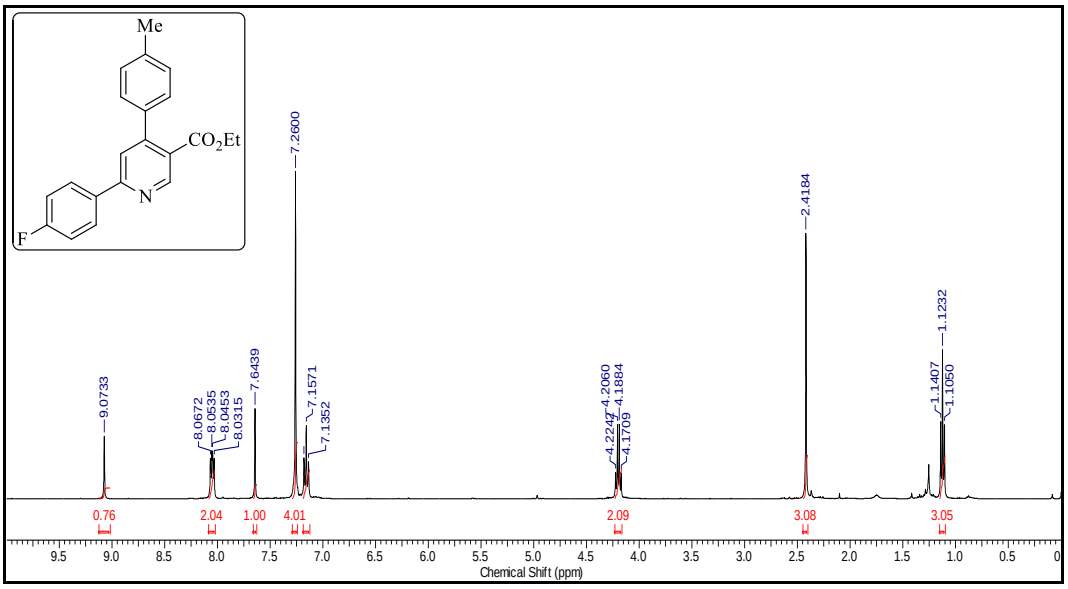


Figure 5.40 400 MHz ^{1}H NMR spectrum of **3eb** in $CDCl_3$

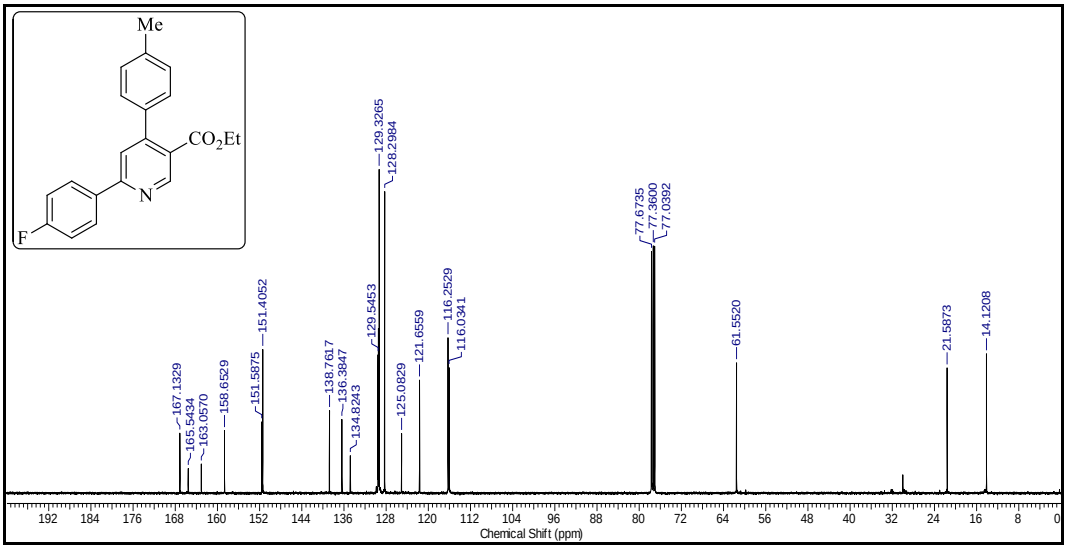


Figure 5.41 100 MHz ^{13}C NMR spectrum of **3eb** in $CDCl_3$

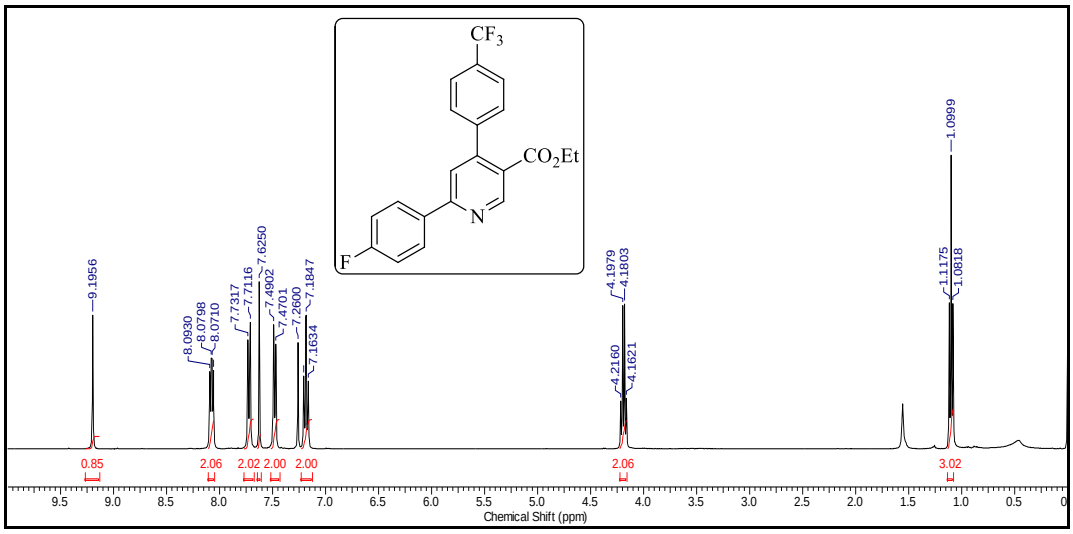


Figure 5.42 400 MHz ^{1}H NMR spectrum of **3eg** in $CDCl_3$

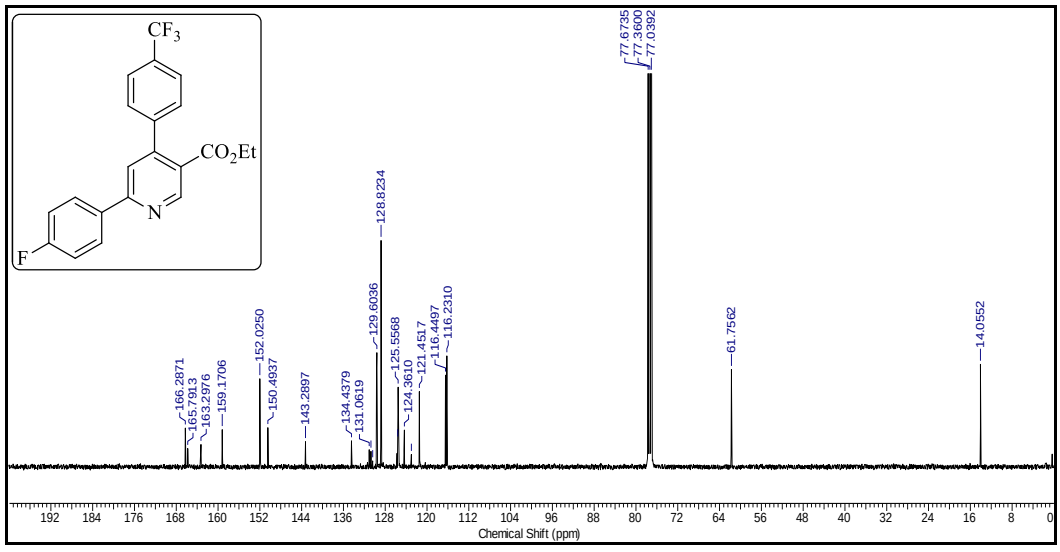


Figure 5.43 100 MHz ^{13}C NMR spectrum of **3eg** in $CDCl_3$

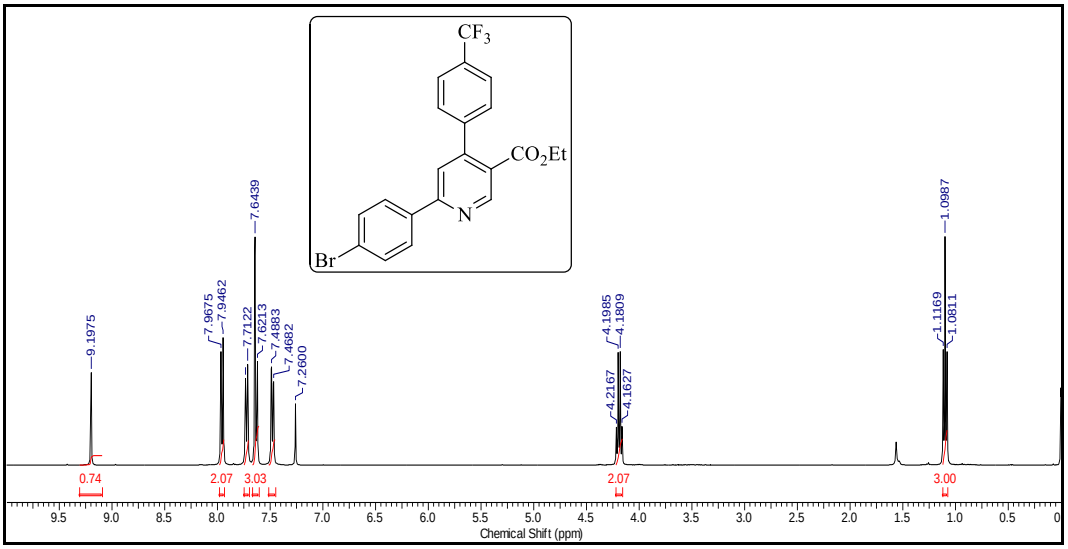


Figure 5.44 400 MHz ^{1}H NMR spectrum of **3hg** in $CDCl_3$

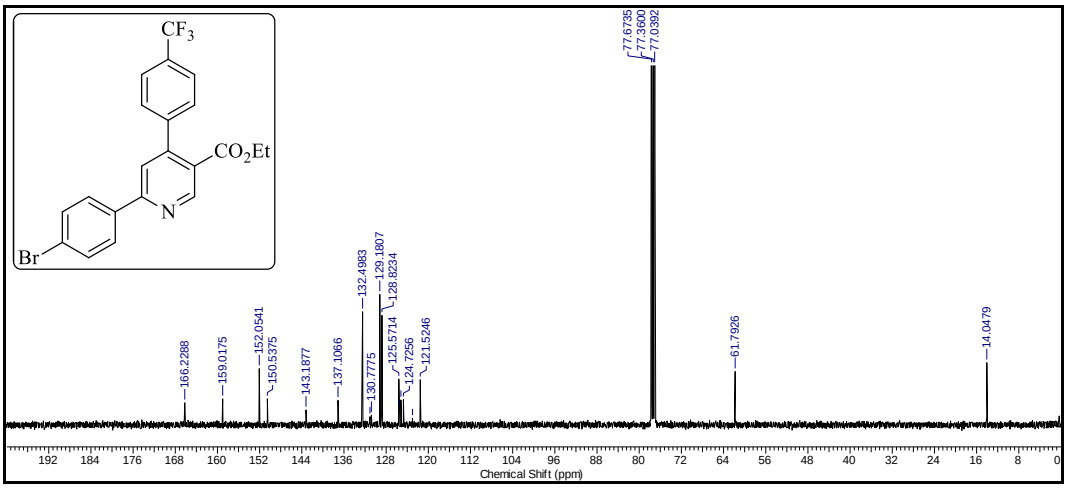


Figure 5.45 100 MHz ^{13}C NMR spectrum of **3hg** in $CDCl_3$

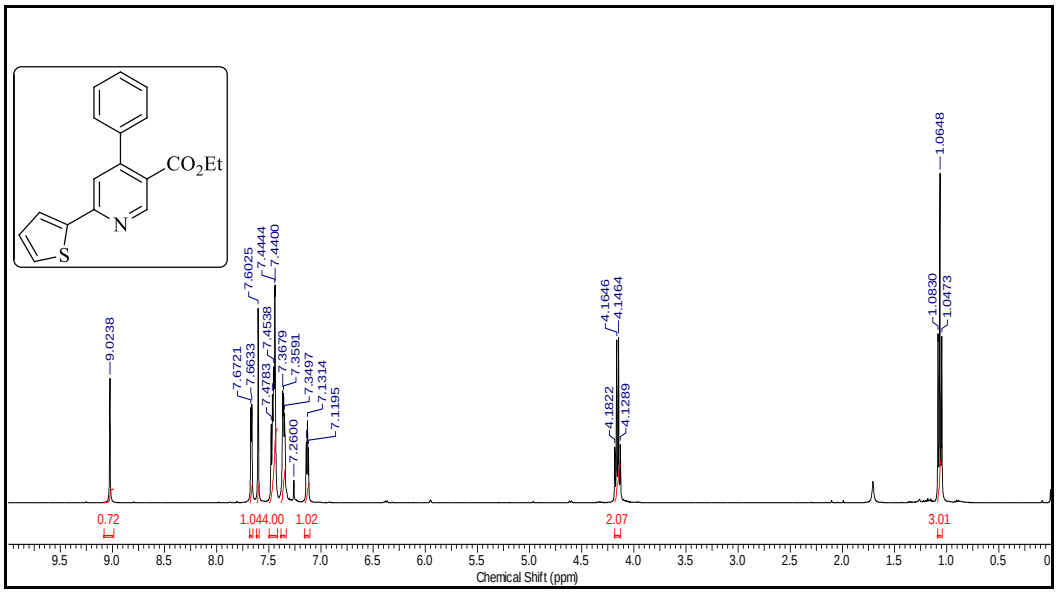


Figure 5.46 400 MHz ^{1}H NMR spectrum of **3ia** in $CDCl_3$

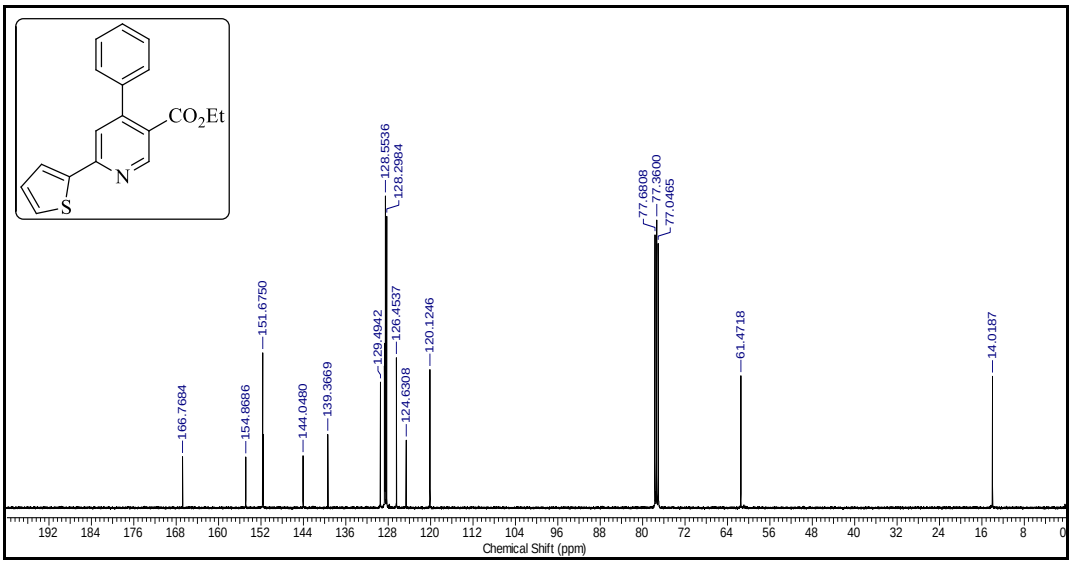


Figure 5.47 100 MHz ^{13}C NMR spectrum of **3ia** in $CDCl_3$

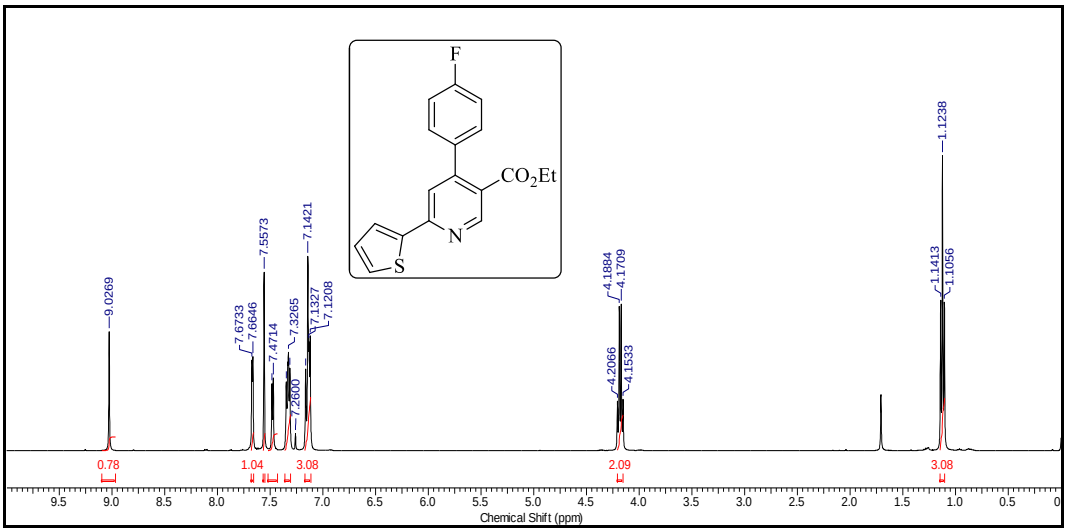


Figure 5.48 400 MHz ^{1}H NMR spectrum of **3id** in $CDCl_3$

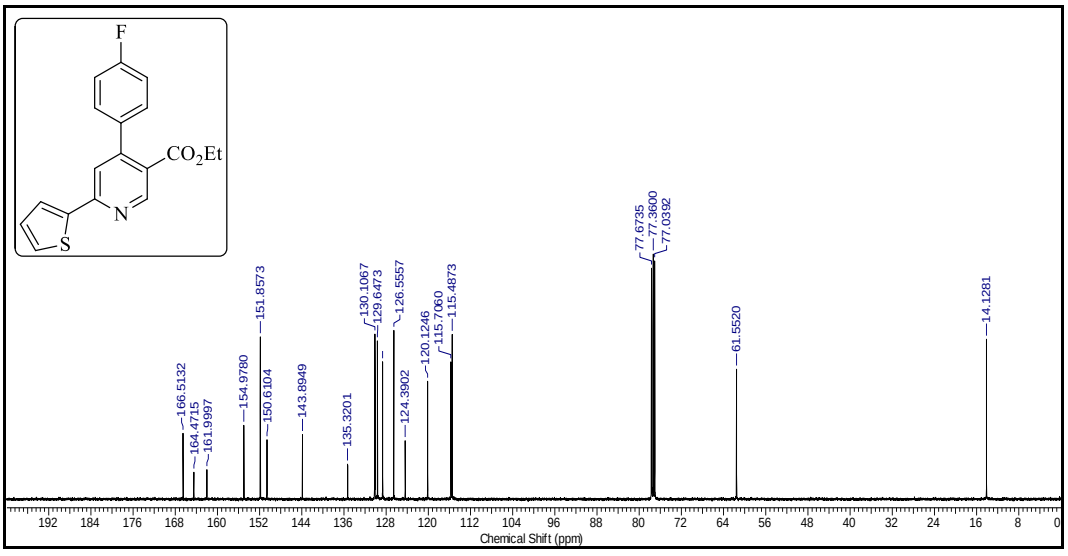


Figure 5.49 100 MHz ^{13}C NMR spectrum of **3id** in $CDCl_3$

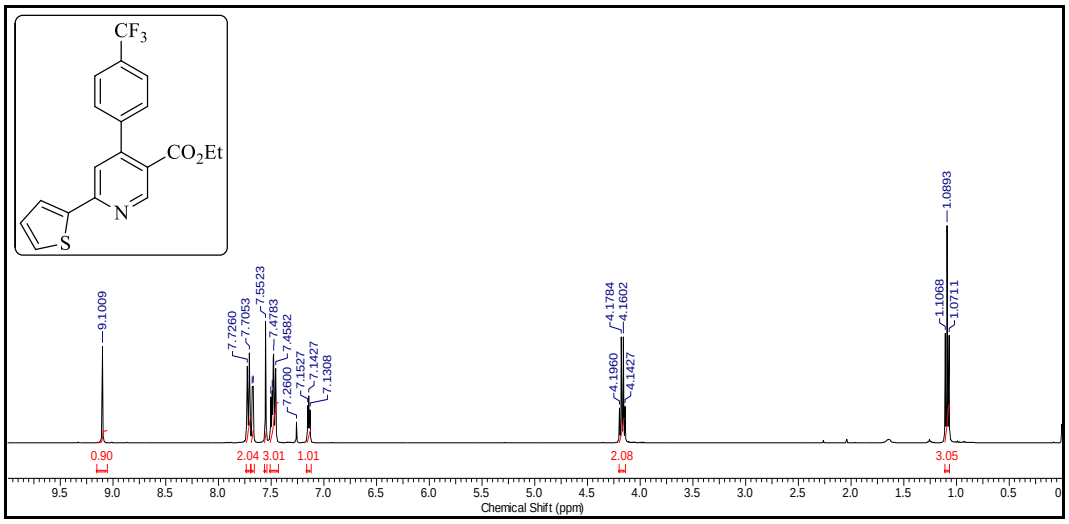


Figure 5.50 400 MHz ^{1}H NMR spectrum of **3ig** in $CDCl_3$

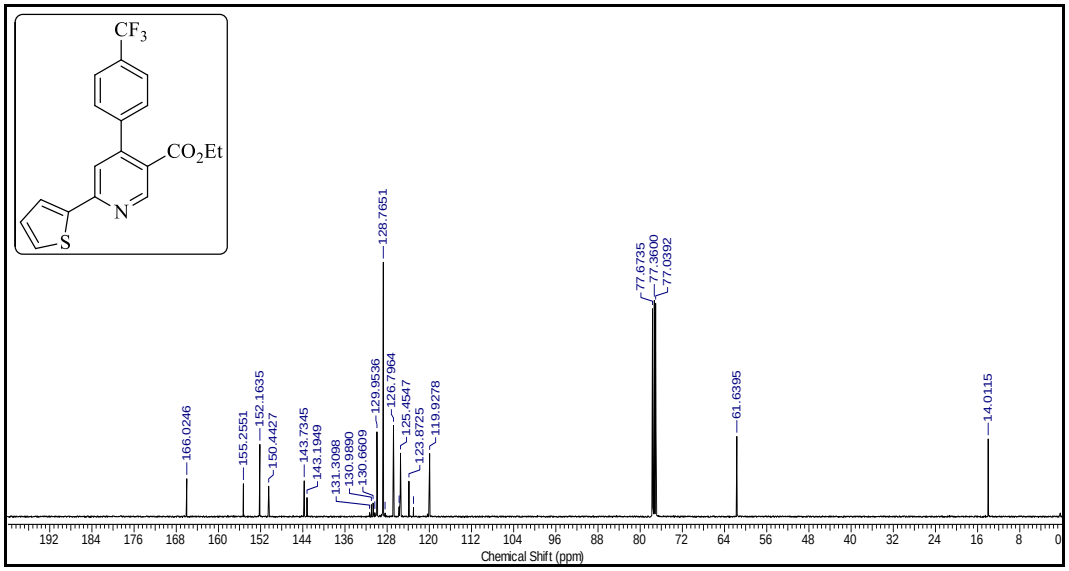


Figure 5.51 100 MHz ^{13}C NMR spectrum of **3ig** in $CDCl_3$

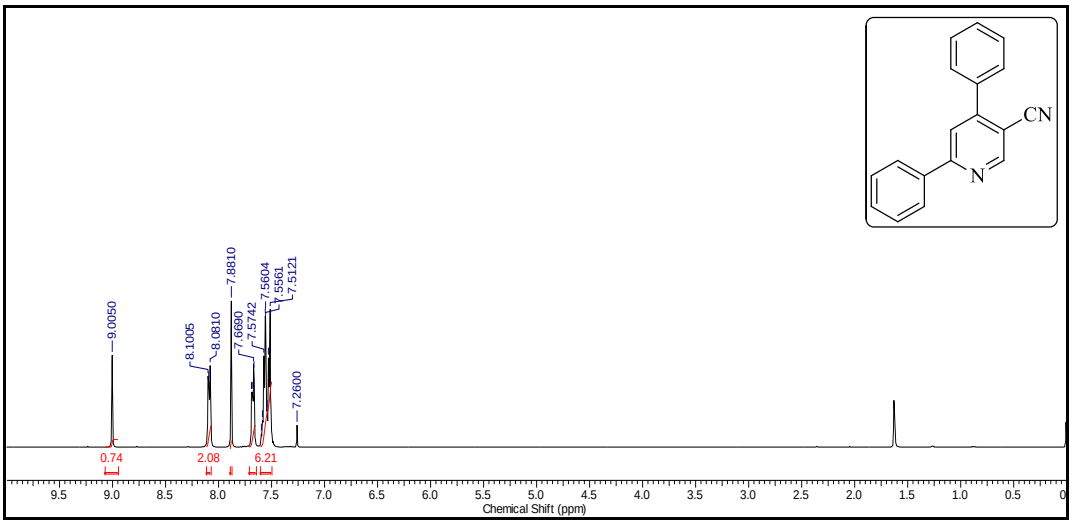


Figure 5.52 400 MHz ^{1}H NMR spectrum of **3ak** in $CDCl_3$

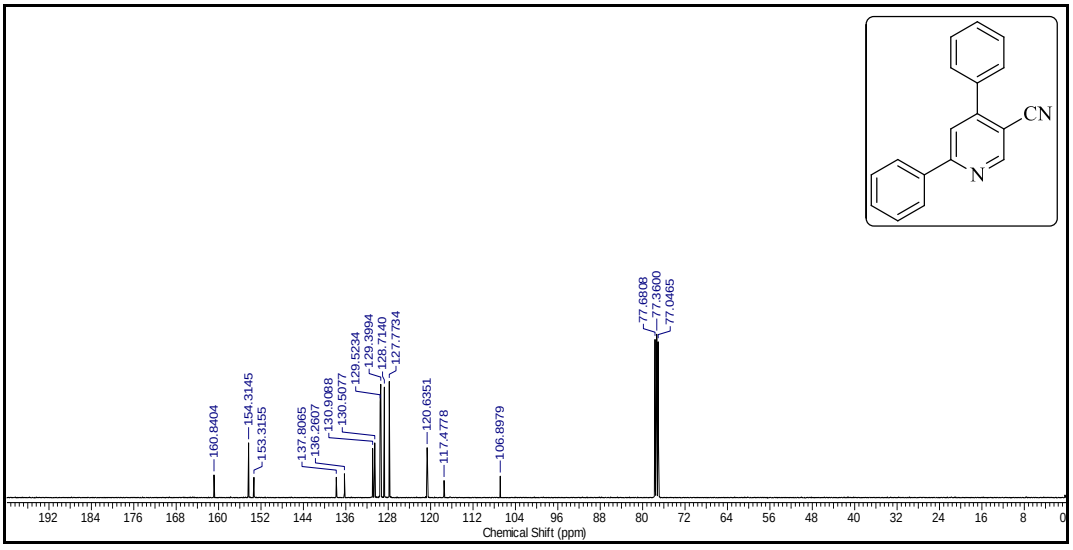


Figure 5.53 100 MHz ^{13}C NMR spectrum of **3ak** in $CDCl_3$

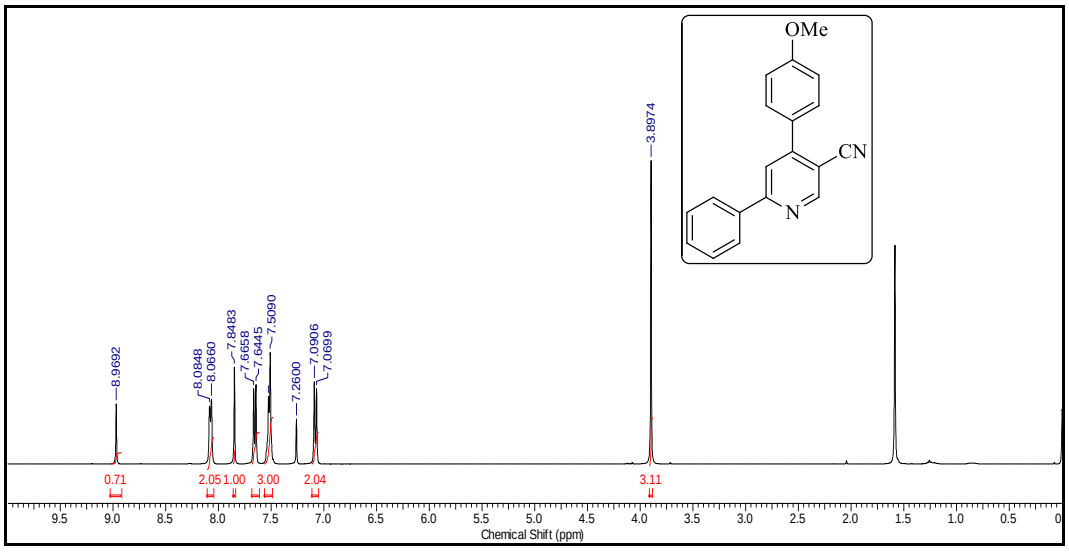


Figure 5.54 400 MHz ^{1}H NMR spectrum of **3al** in $CDCl_3$

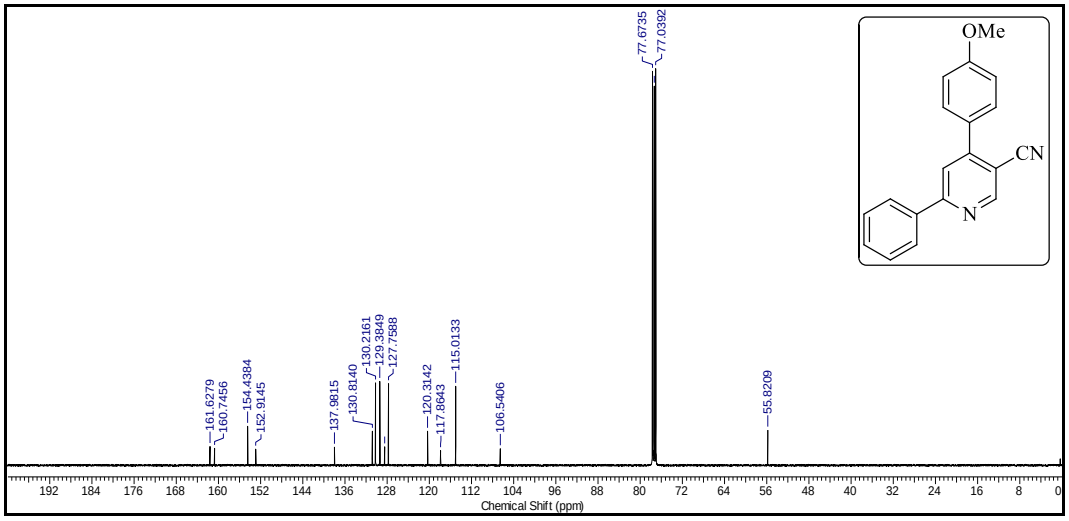


Figure 5.55 100 MHz ^{13}C NMR spectrum of **3al** in $CDCl_3$

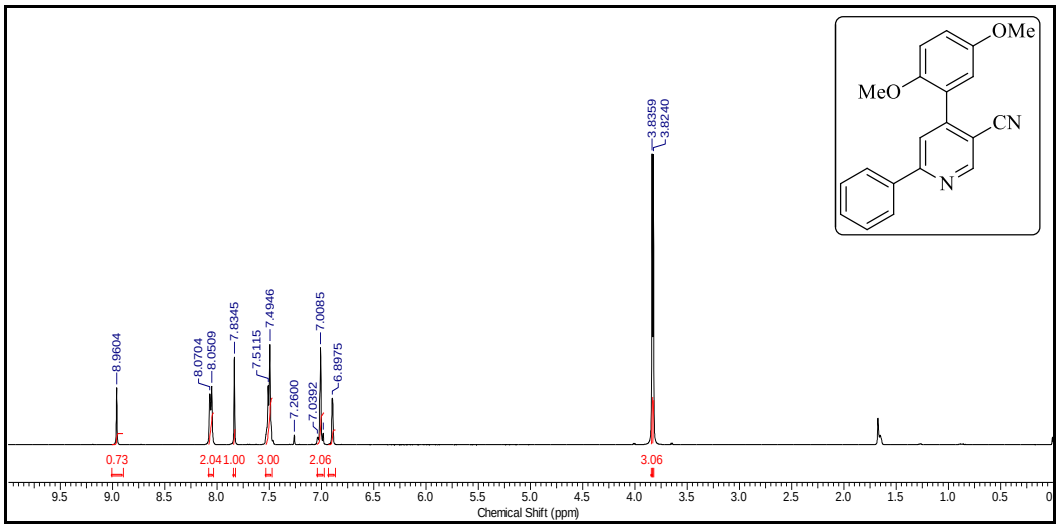


Figure 5.56 400 MHz ^{1}H NMR spectrum of **3am** in $CDCl_3$

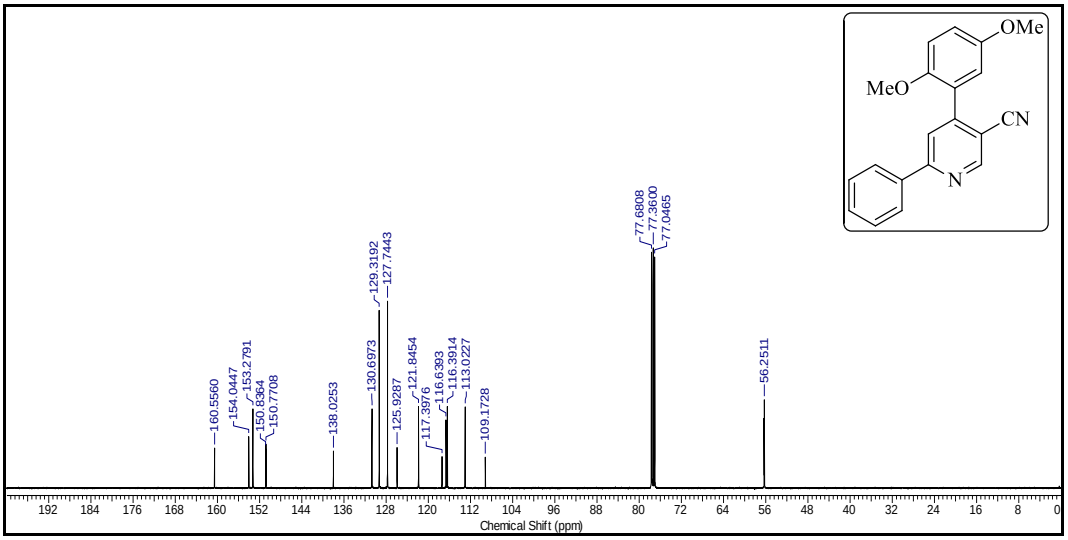


Figure 5.57 100 MHz ^{13}C NMR spectrum of **3am** in $CDCl_3$

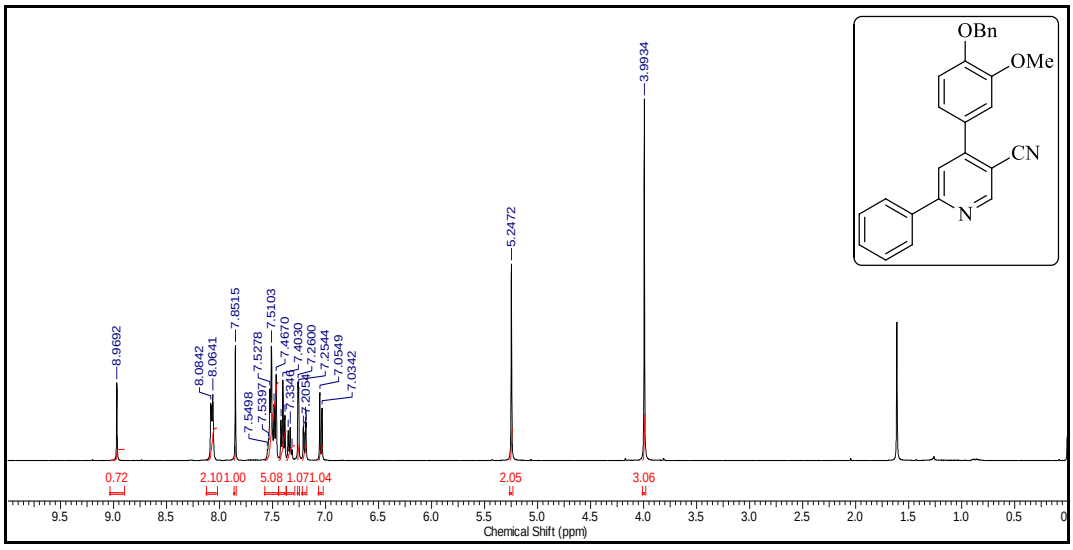


Figure 5.58 400 MHz ^{1}H NMR spectrum of **3an** in $CDCl_3$

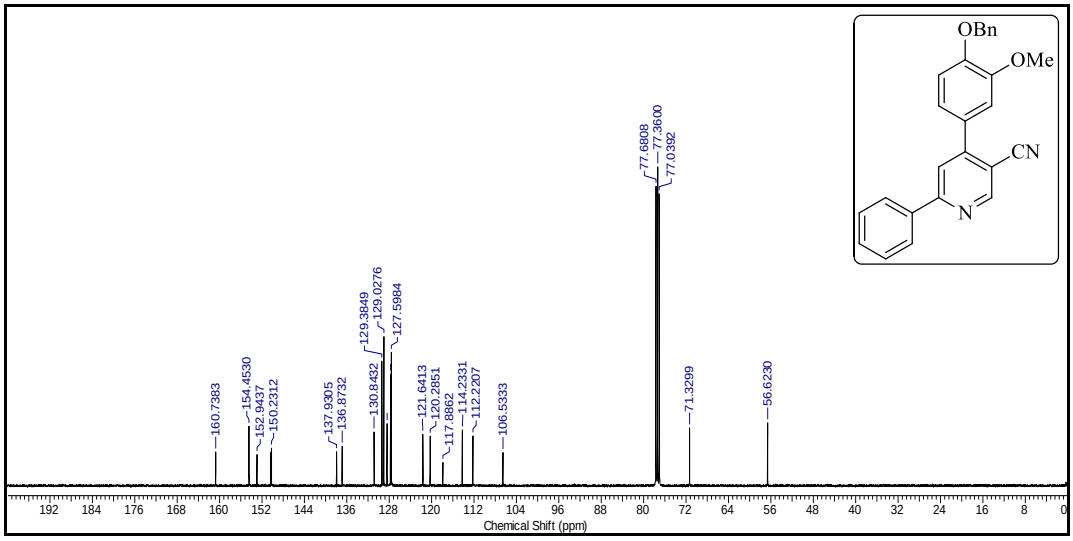


Figure 5.59 100 MHz ^{13}C NMR spectrum of **3an** in $CDCl_3$

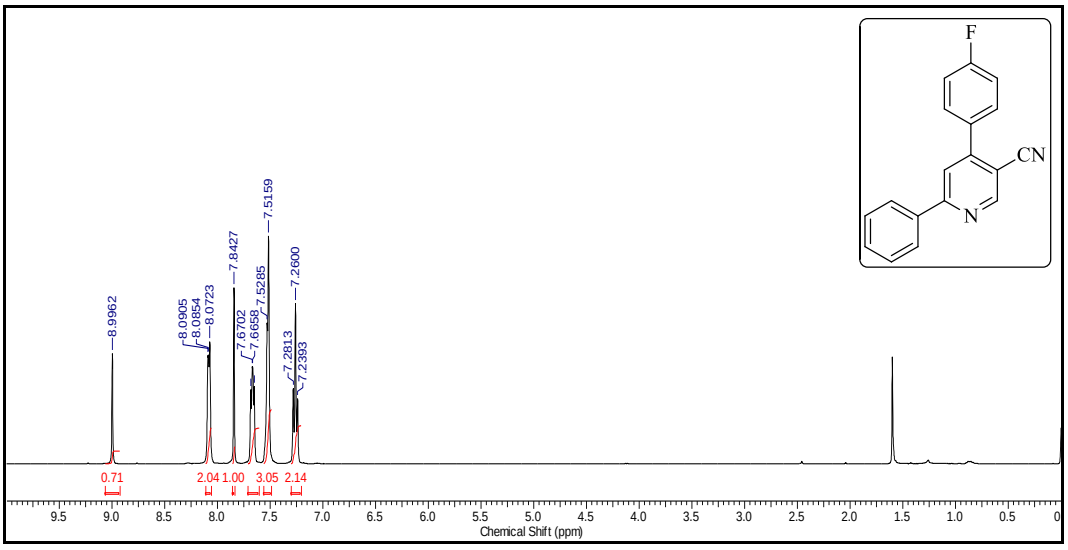


Figure 5.60 400 MHz ^{1}H NMR spectrum of **3ao** in $CDCl_3$

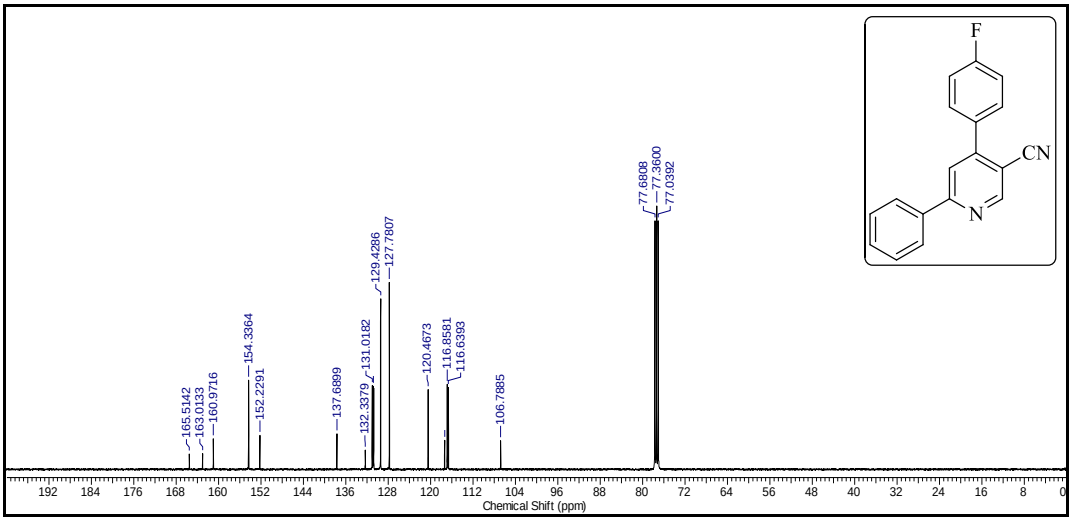


Figure 5.61 100 MHz ^{13}C NMR spectrum of **3ao** in $CDCl_3$

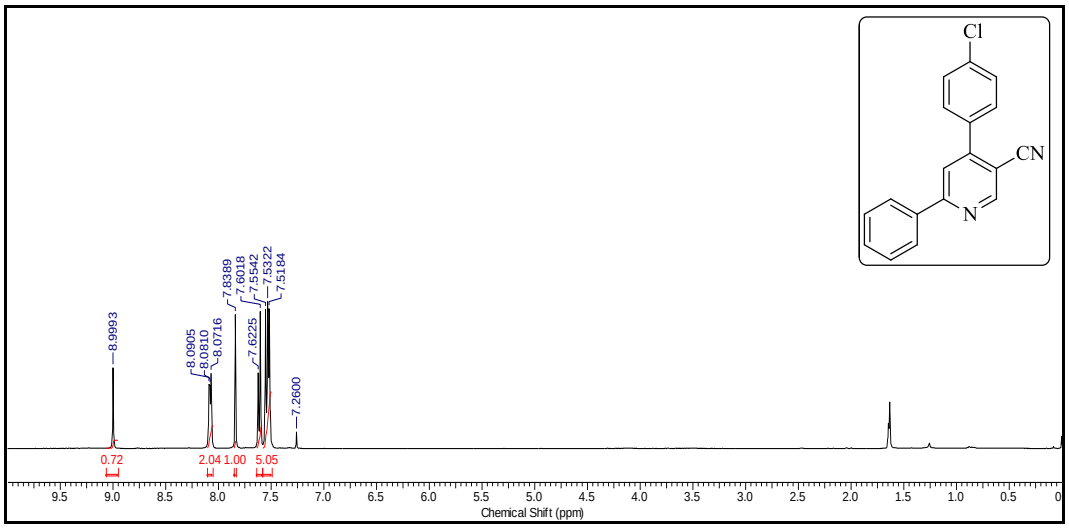


Figure 5.62 400 MHz ^{1}H NMR spectrum of **3ap** in $CDCl_3$

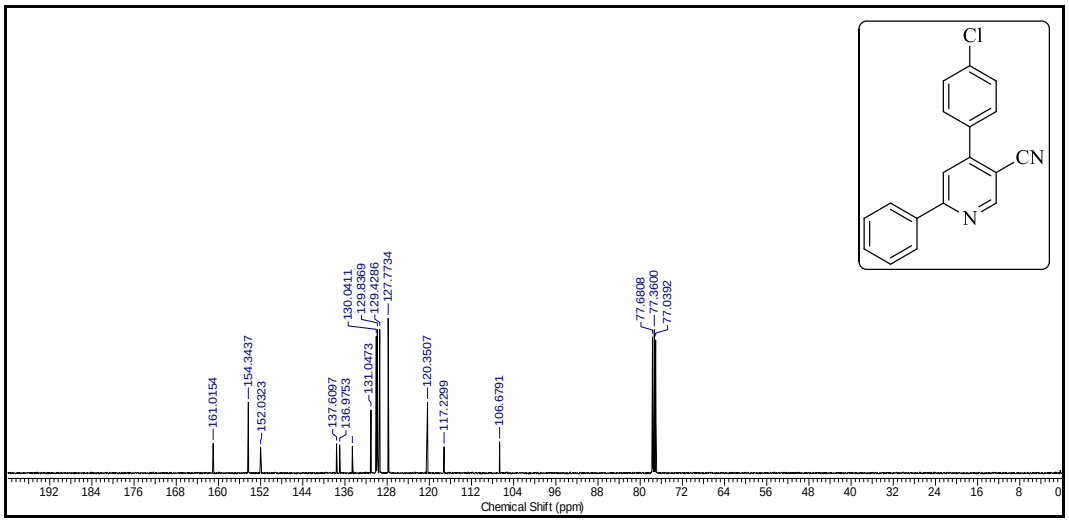


Figure 5.63 100 MHz ^{13}C NMR spectrum of **3ap** in $CDCl_3$

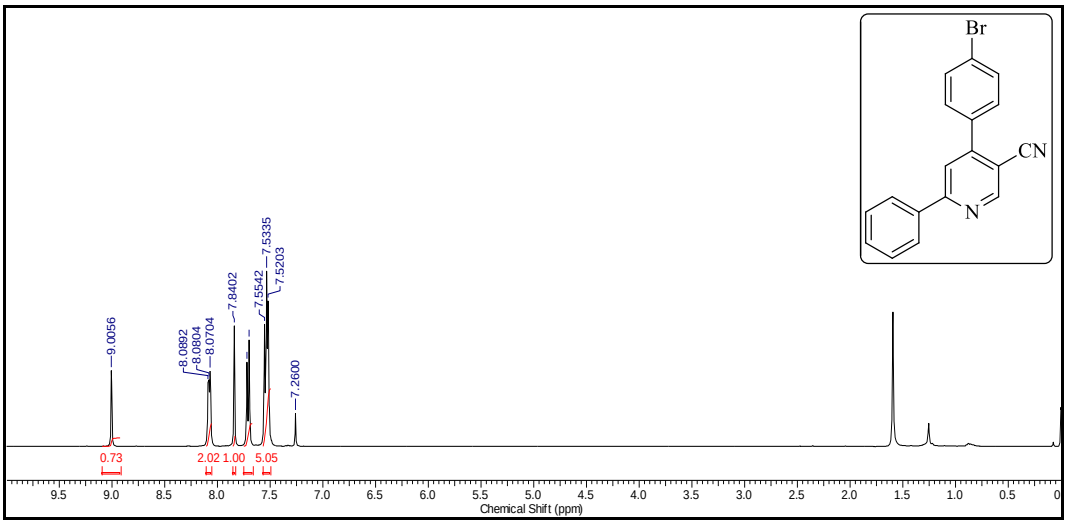


Figure 5.64 400 MHz ^{1}H NMR spectrum of **3aq** in $CDCl_3$

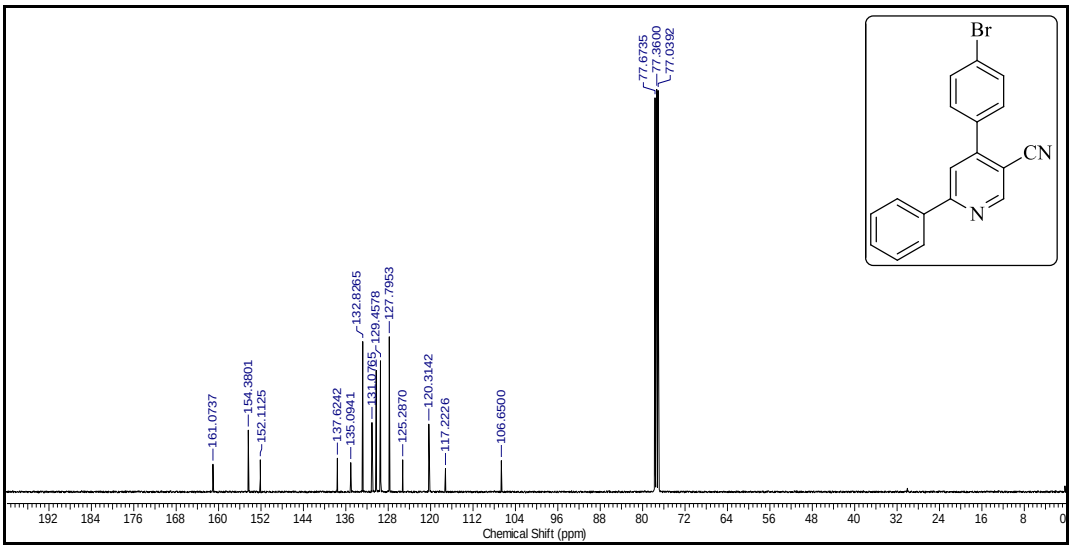


Figure 5.65 100 MHz ^{13}C NMR spectrum of **3aq** in $CDCl_3$

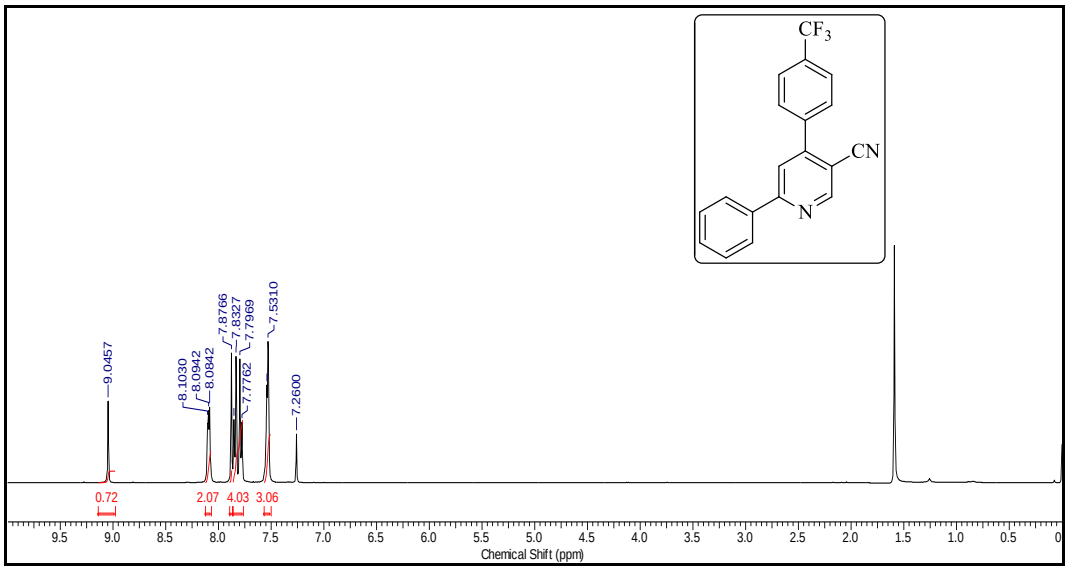


Figure 5.66 400 MHz ^{1}H NMR spectrum of **3ar** in $CDCl_3$

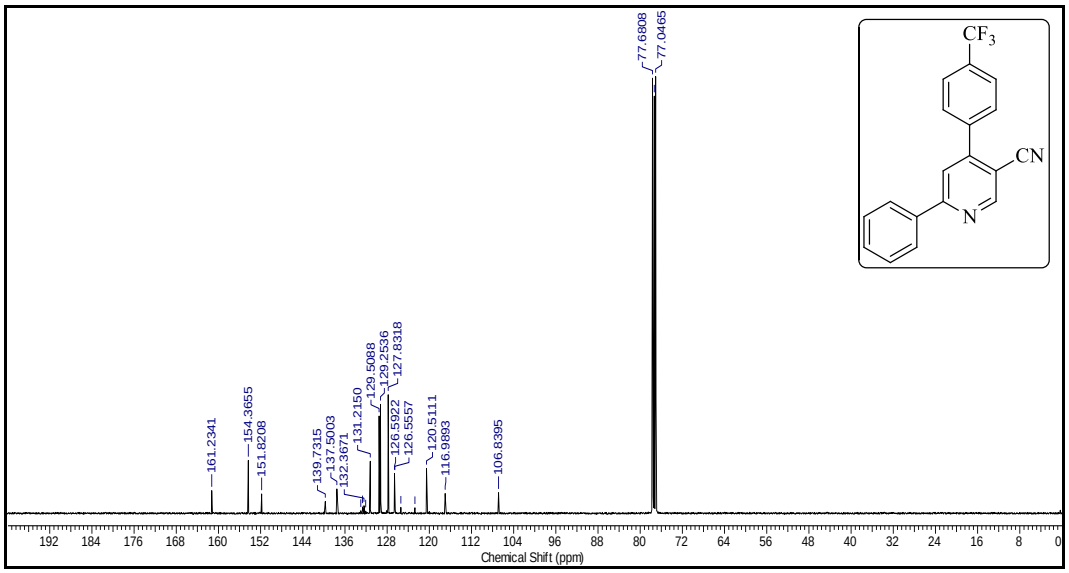


Figure 5.67 100 MHz ^{13}C NMR spectrum of **3ar** in $CDCl_3$

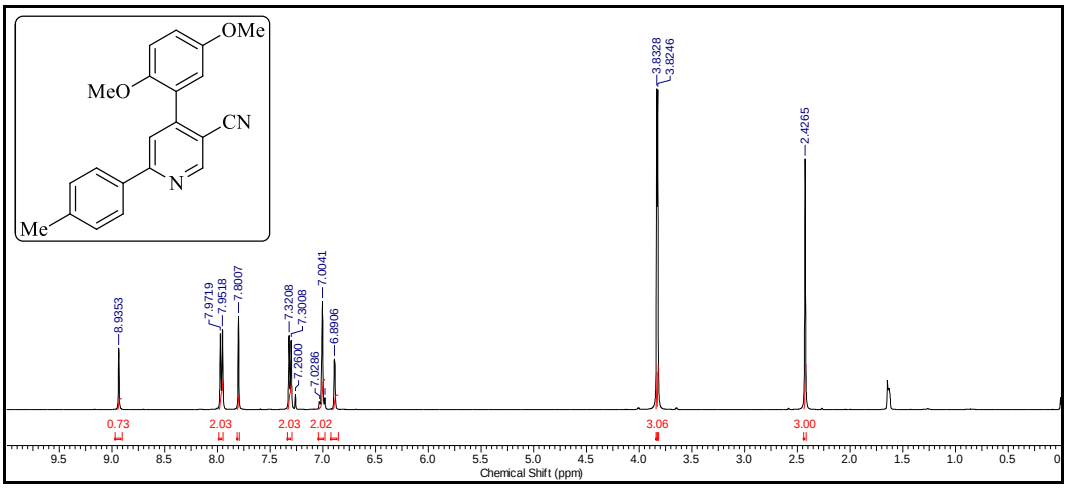


Figure 5.68 400 MHz ^{1}H NMR spectrum of **3bm** in $CDCl_3$

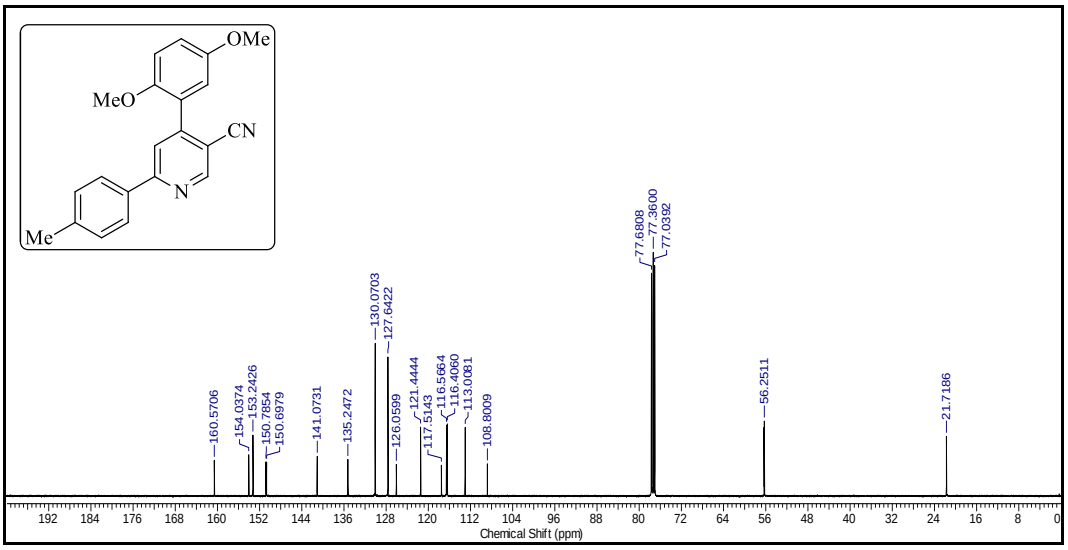


Figure 5.69 100 MHz ^{13}C NMR spectrum of **3bm** in $CDCl_3$

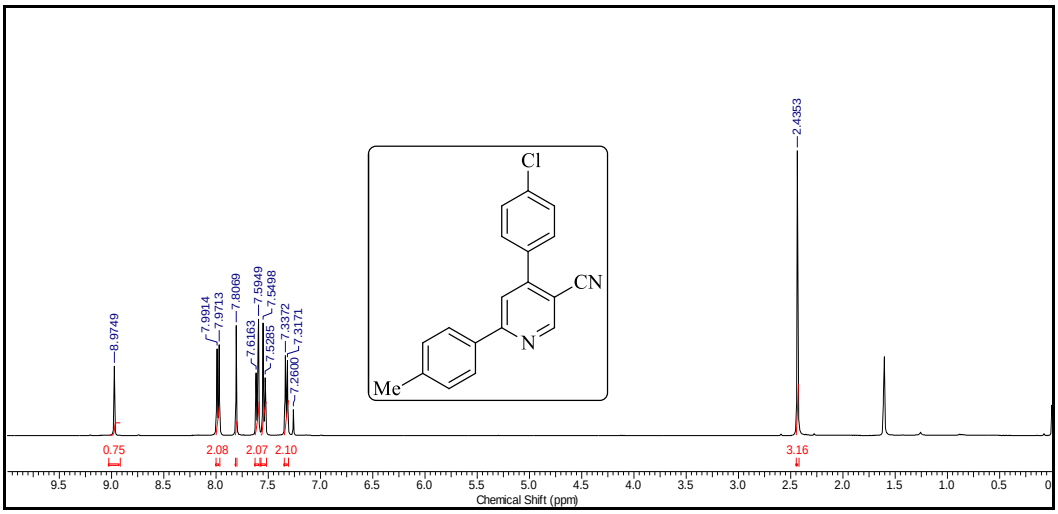


Figure 5.70 400 MHz ^{1}H NMR spectrum of **3bp** in $CDCl_3$

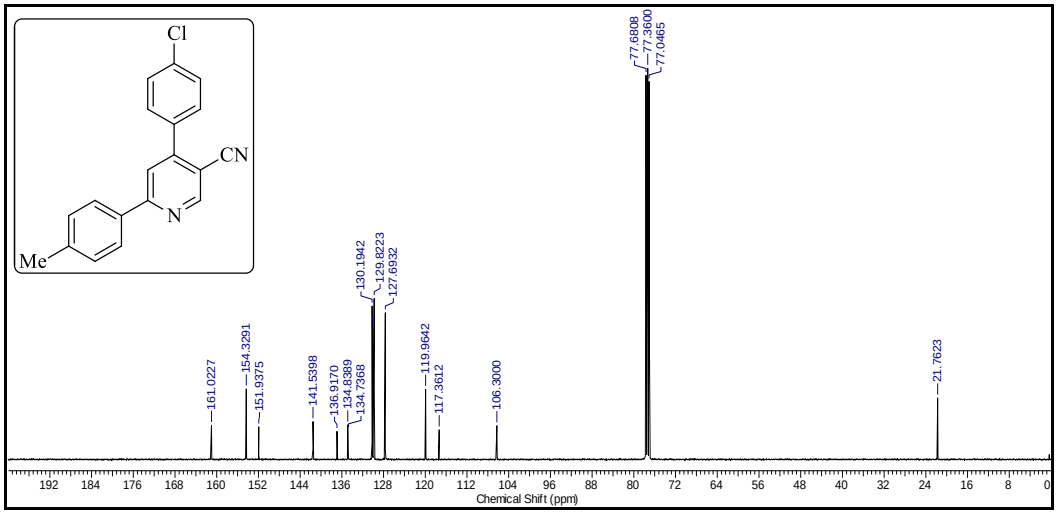


Figure 5.71 100 MHz ^{13}C NMR spectrum of **3bp** in $CDCl_3$

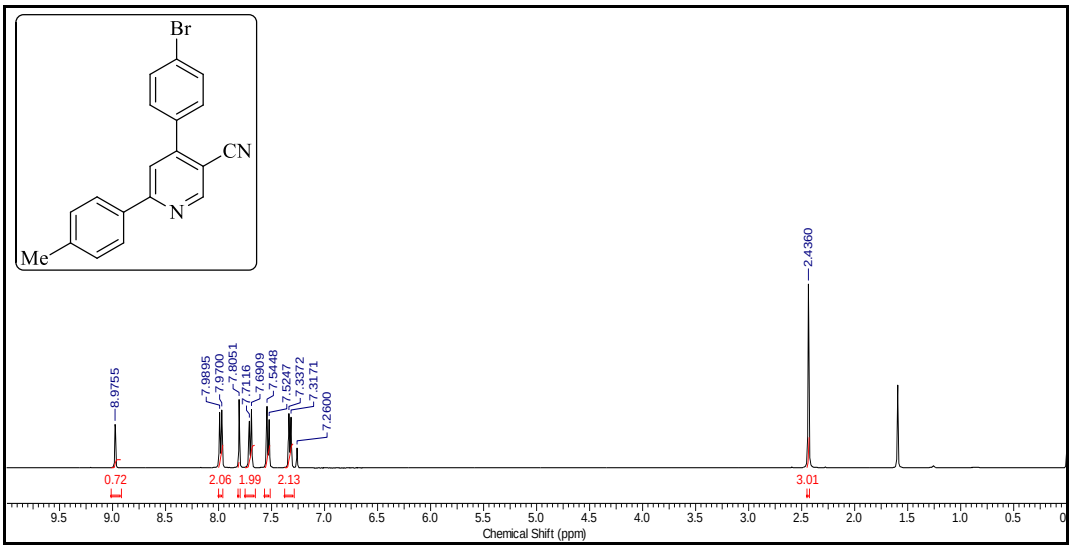


Figure 5.72 400 MHz ^{1}H NMR spectrum of **3bq** in $CDCl_3$

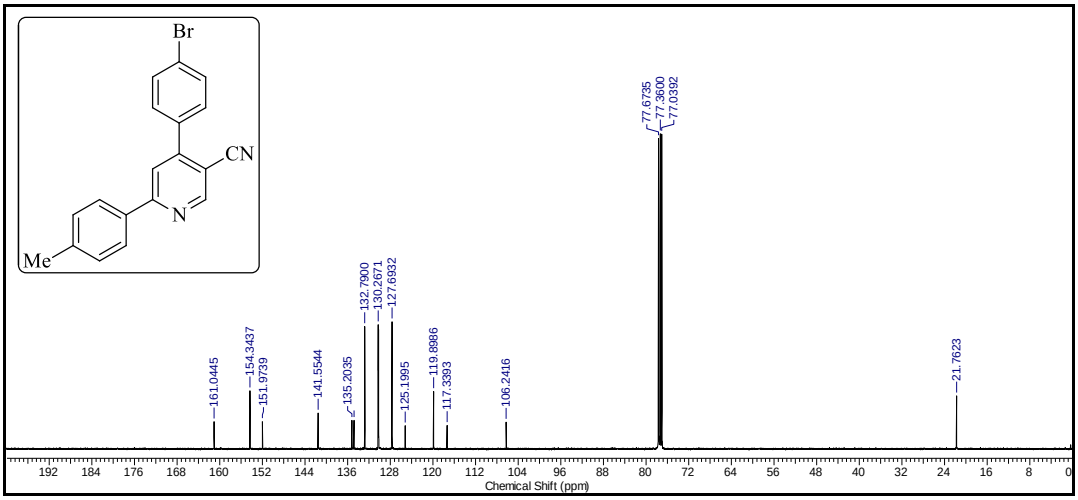


Figure 5.73 100 MHz ^{13}C NMR spectrum of **bq** in $CDCl_3$

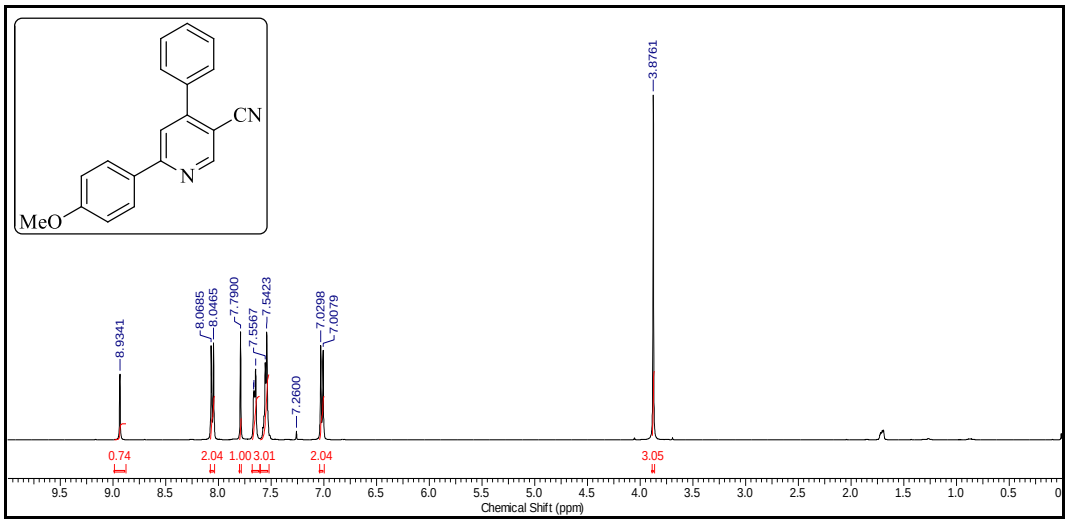


Figure 5.74 400 MHz ^{1}H NMR spectrum of **3ck** in $CDCl_3$

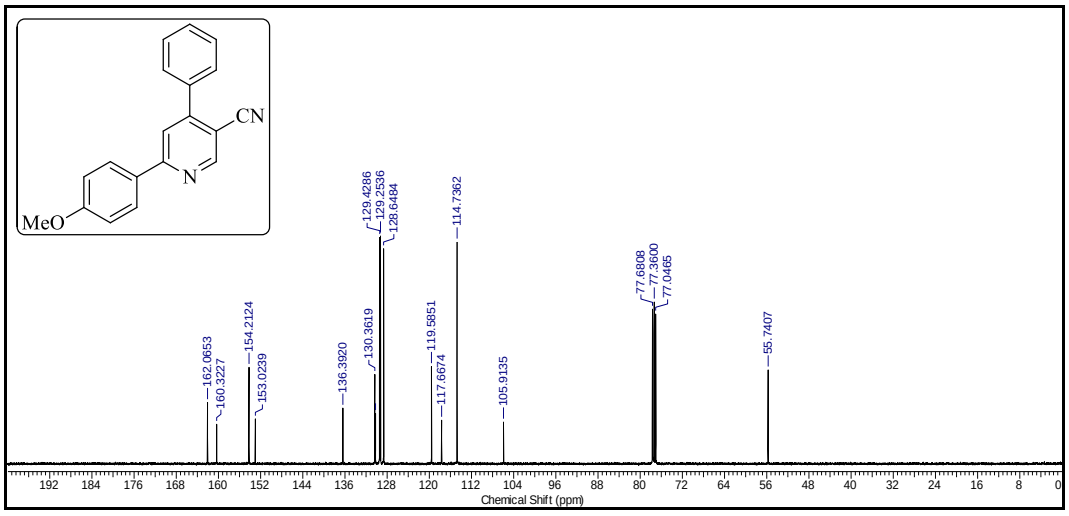


Figure 5.75 100 MHz ^{13}C NMR spectrum of **3ck** in $CDCl_3$

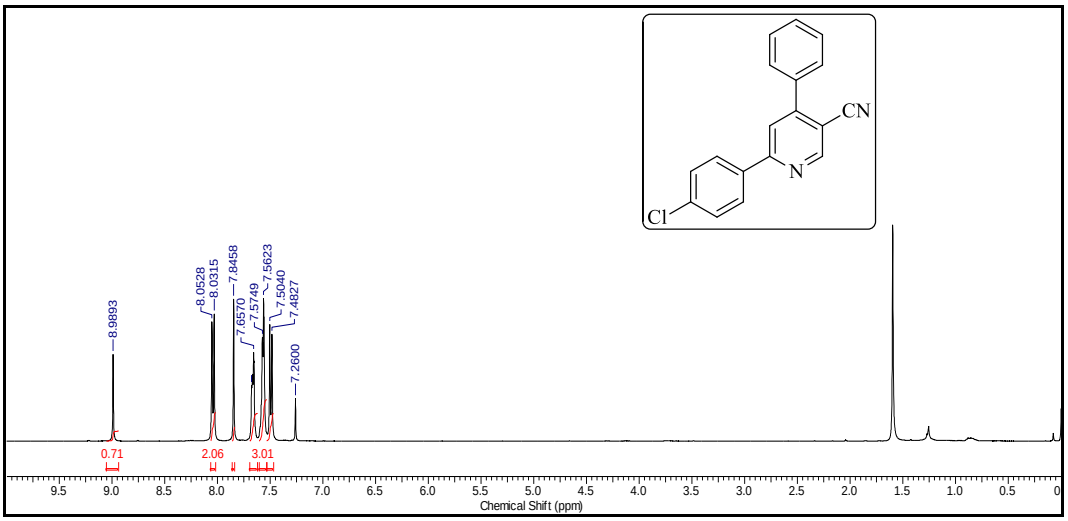


Figure 5.76 400 MHz ^{1}H NMR spectrum of **3fk** in $CDCl_3$

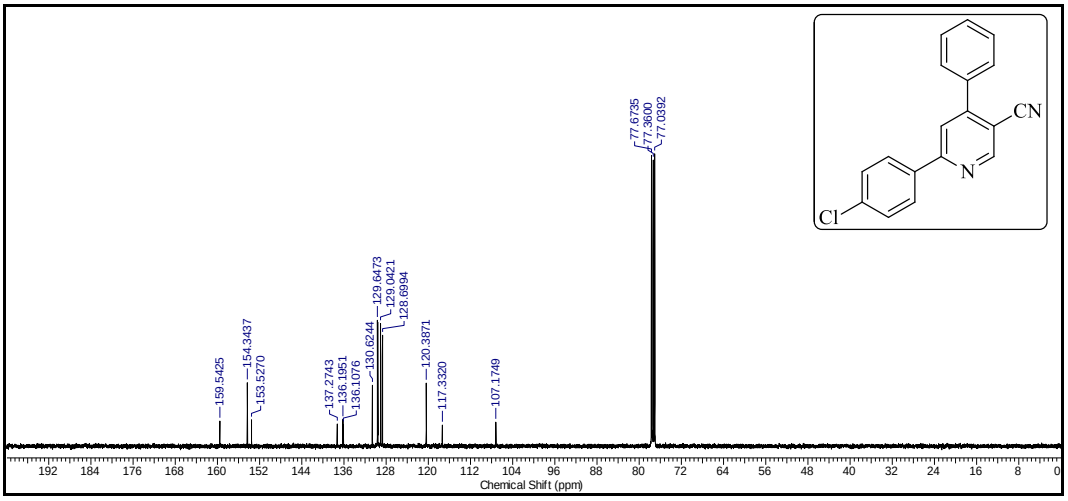


Figure 5.77 100 MHz ^{13}C NMR spectrum of **3fk** in $CDCl_3$

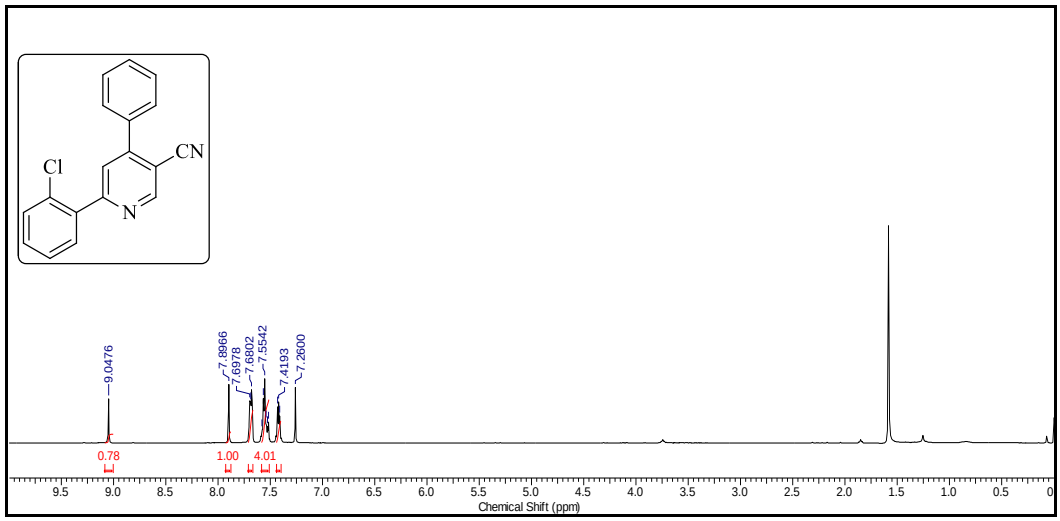


Figure 5.78 400 MHz ^{1}H NMR spectrum of **3gk** in $CDCl_3$

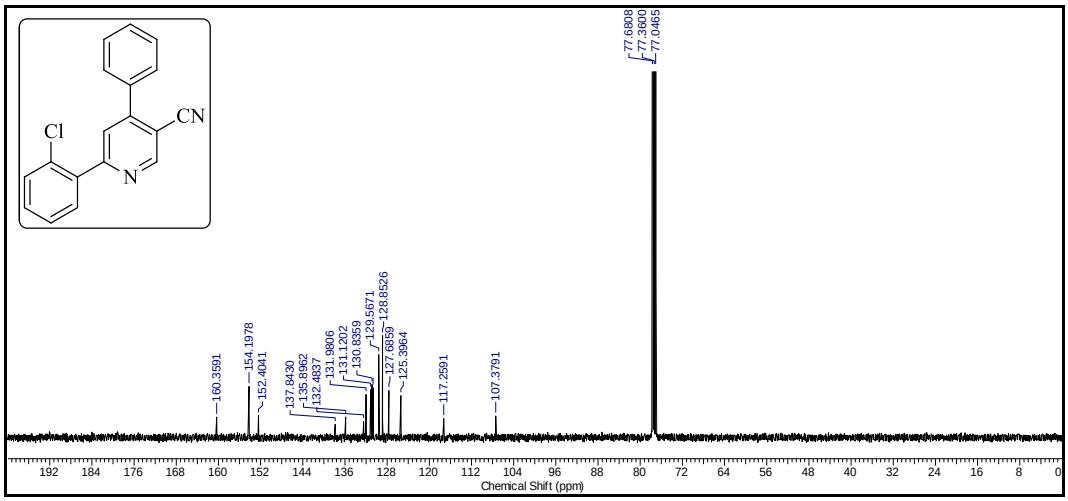


Figure 5.79 100 MHz ^{13}C NMR spectrum of **3gk** in $CDCl_3$

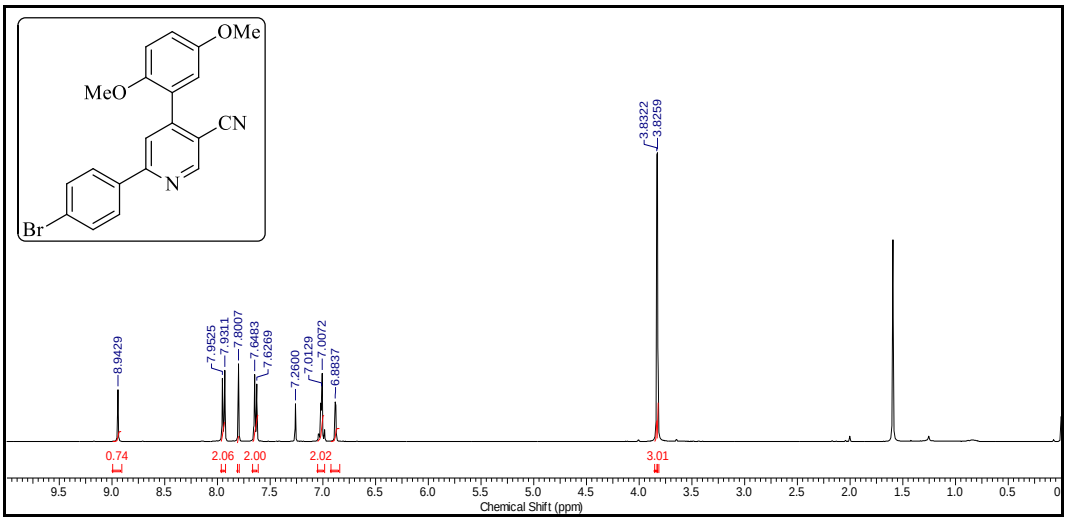


Figure 5.80 400 MHz ^{1}H NMR spectrum of **3hm** in $CDCl_3$

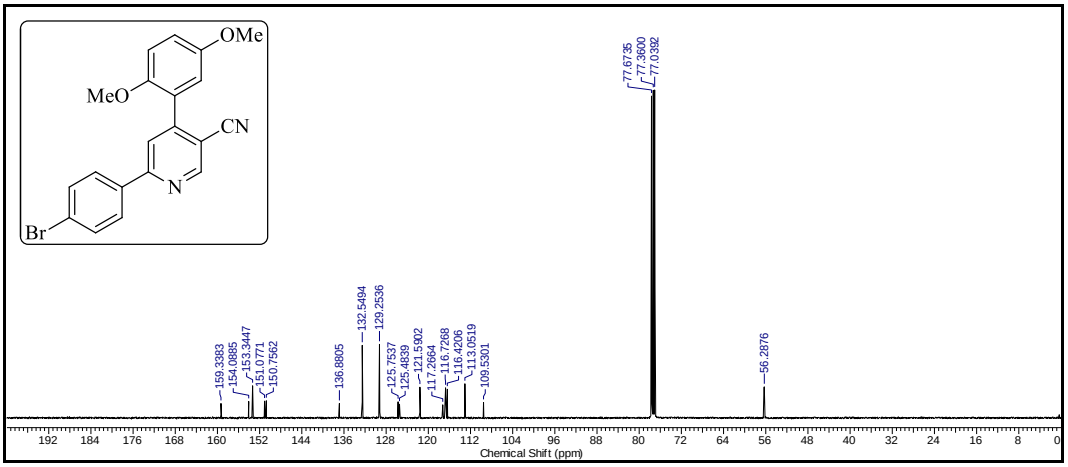


Figure 5.81 100 MHz ^{13}C NMR spectrum of **3hm** in $CDCl_3$

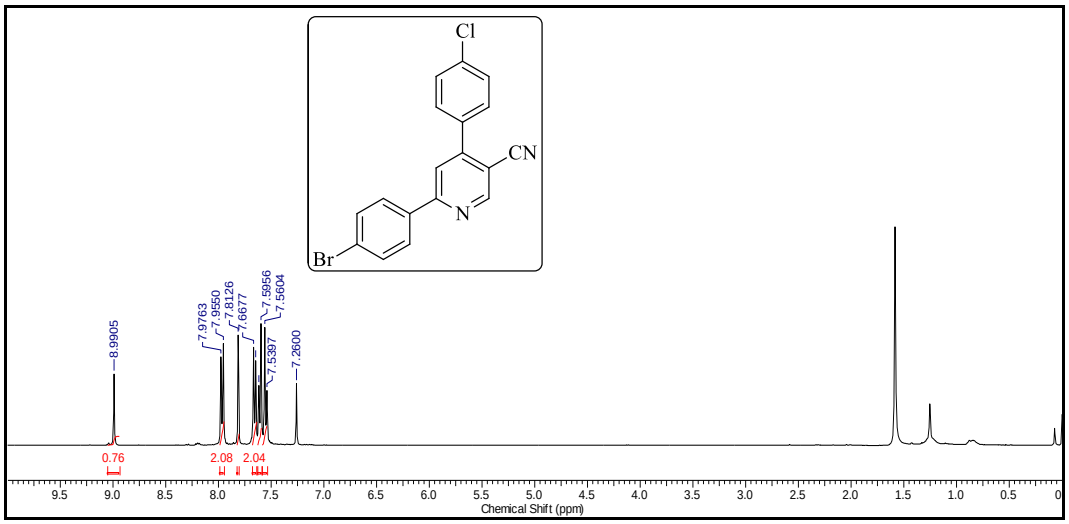


Figure 5.82 400 MHz ^{1}H NMR spectrum of **3hp** in $CDCl_3$

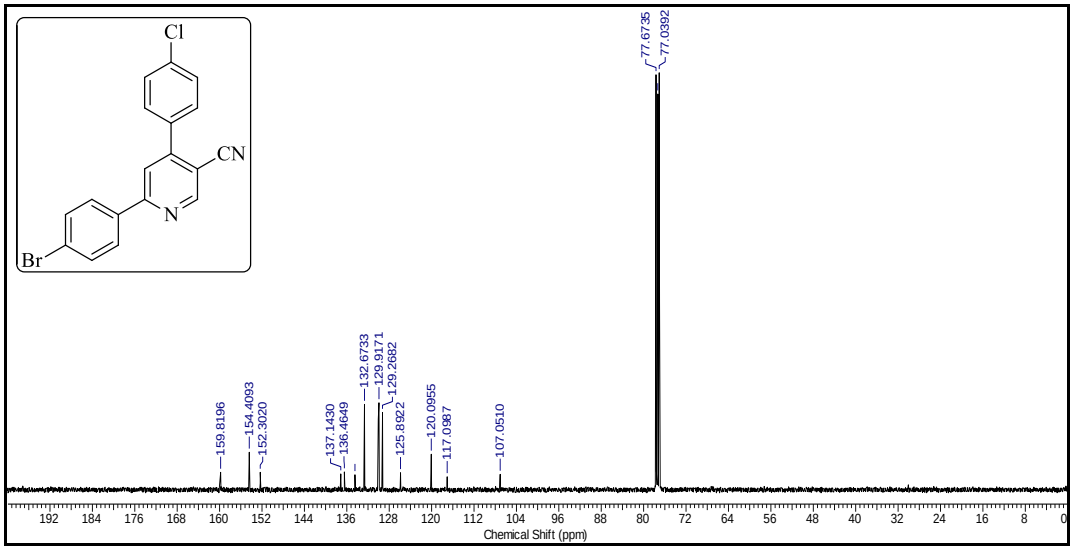


Figure 5.83 100 MHz ^{13}C NMR spectrum of **3hp** in $CDCl_3$

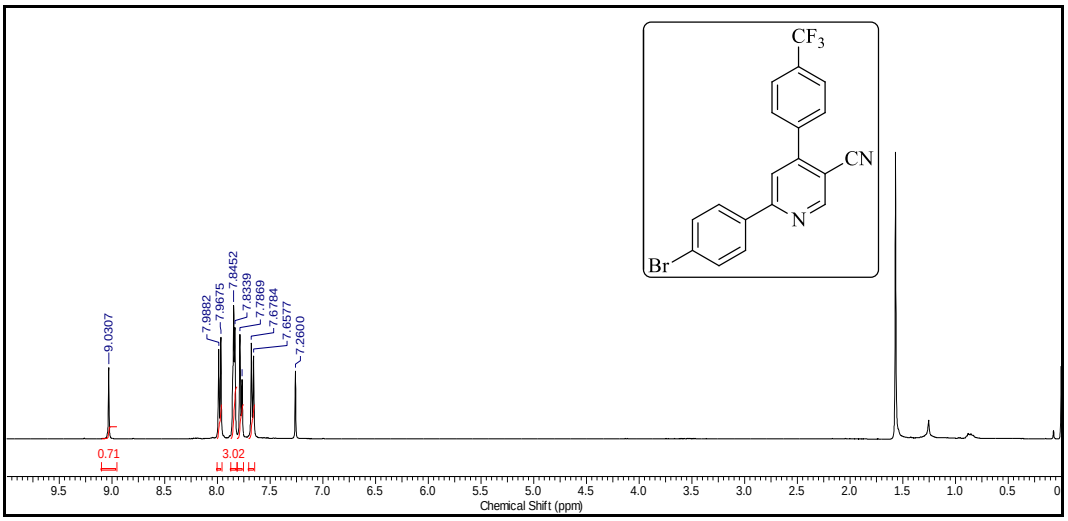


Figure 5.84 400 MHz ^{1}H NMR spectrum of **3hr** in $CDCl_3$

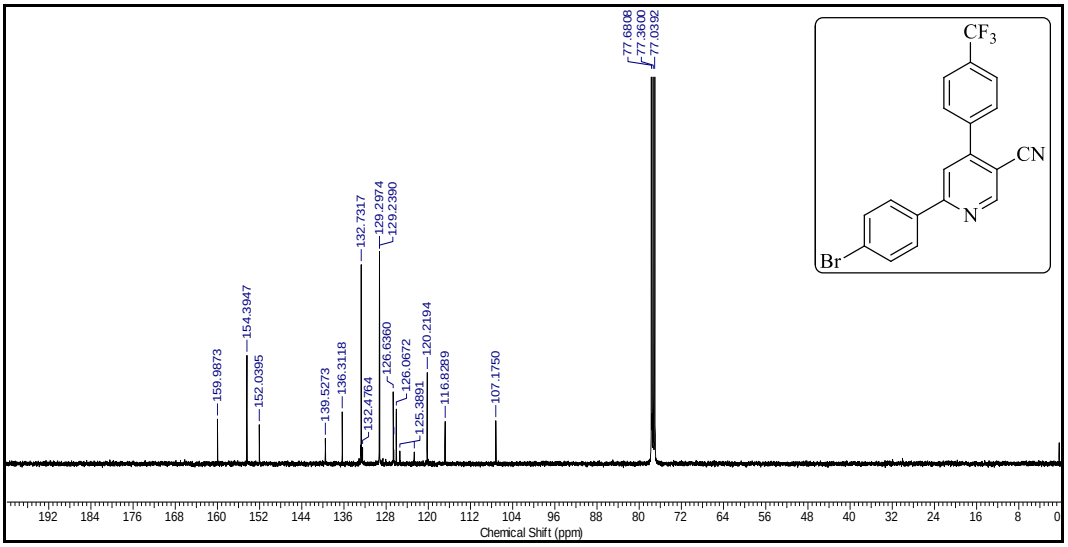


Figure 5.85 100 MHz ^{13}C NMR spectrum of **3hr** in $CDCl_3$

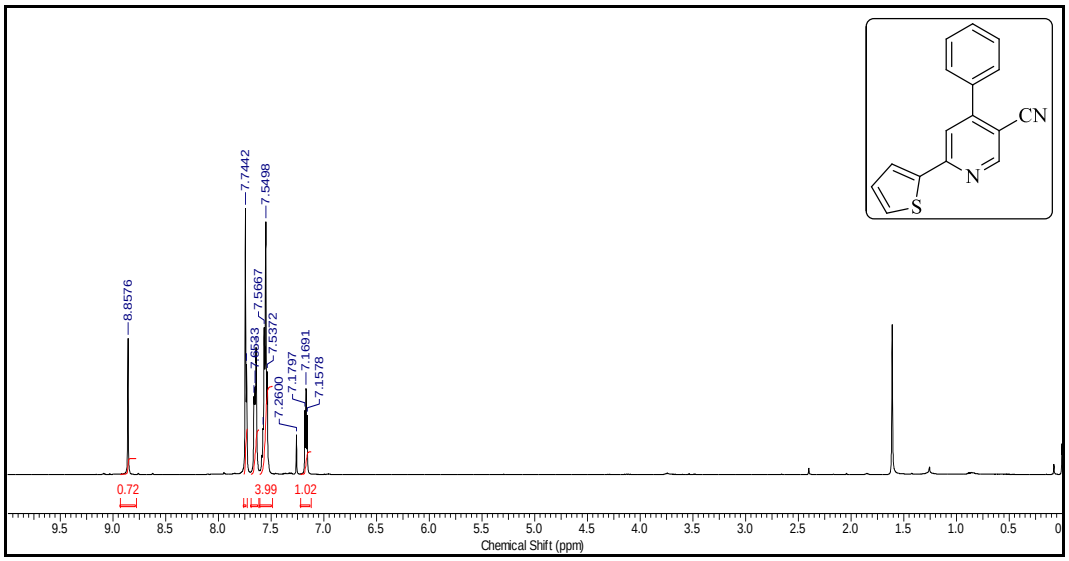


Figure 5.86 400 MHz ^{1}H NMR spectrum of **3ik** in $CDCl_3$

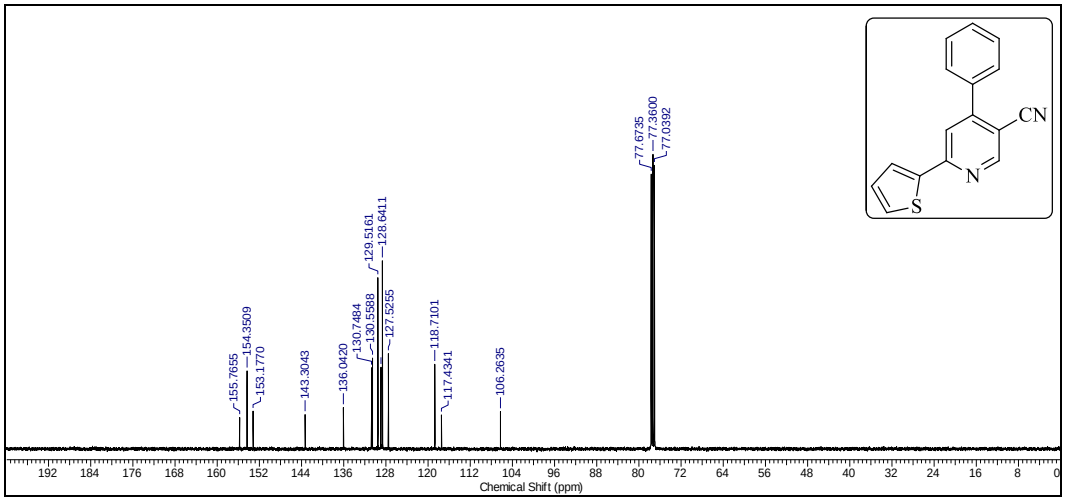


Figure 5.87 100 MHz ^{13}C NMR spectrum of **3ik** in $CDCl_3$

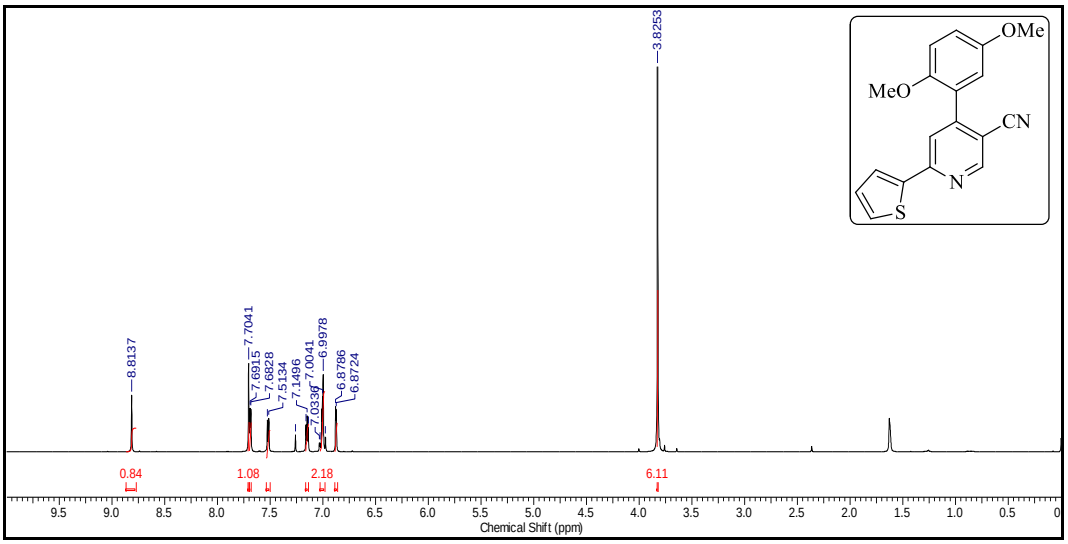


Figure 5.88 400 MHz ^{1}H NMR spectrum of **3im** in $CDCl_3$

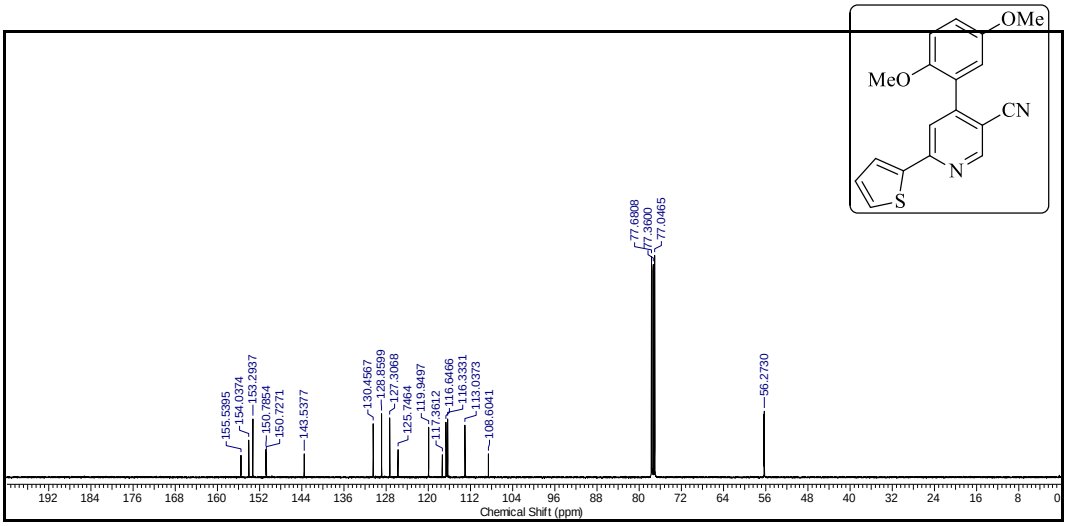


Figure 5.89 100 MHz ^{13}C NMR spectrum of **3im** in $CDCl_3$

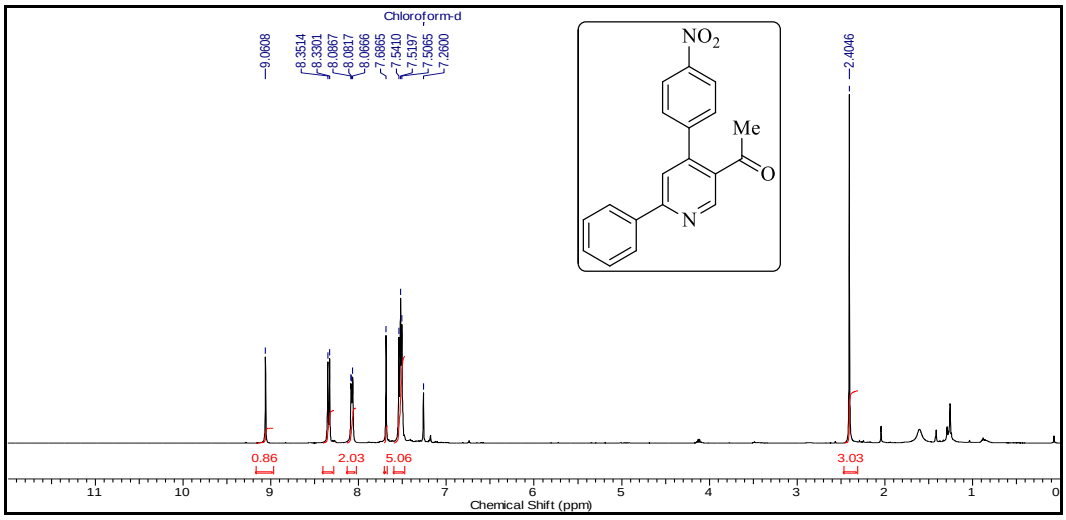


Figure 5.90 400 MHz ^{1}H NMR spectrum of **3as** in $CDCl_3$

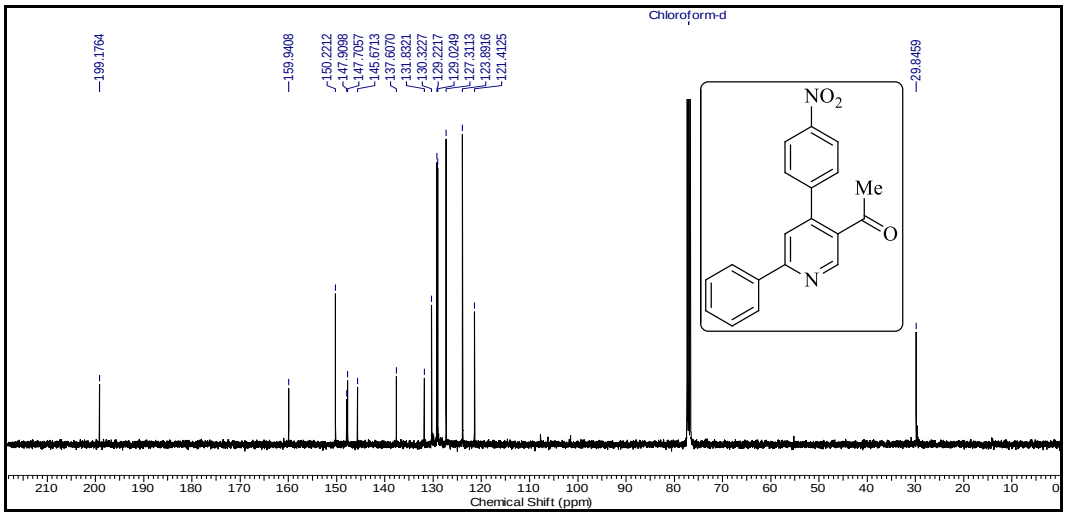


Figure 5.91 100 MHz ^{13}C NMR spectrum of **3as** in $CDCl_3$

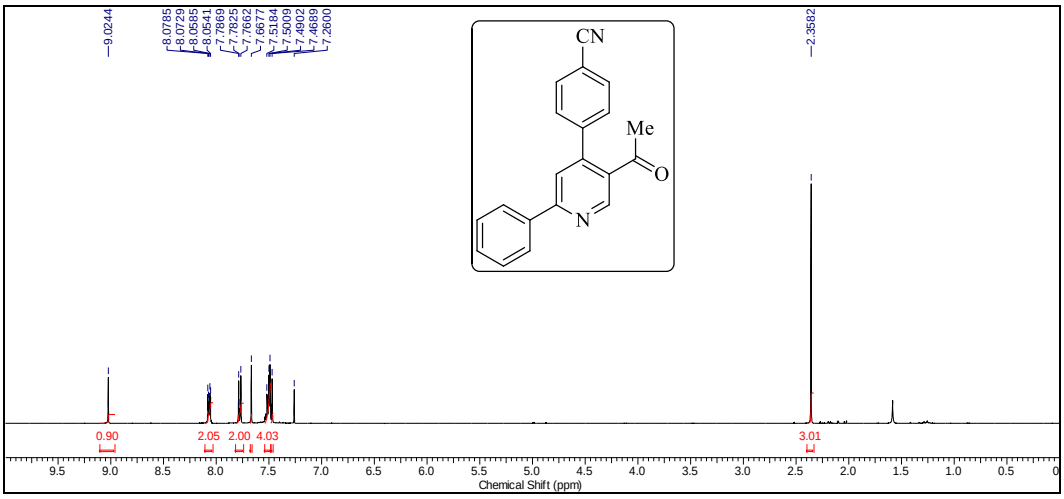


Figure 5.92 400 MHz ^{1}H NMR spectrum of **3at** in $CDCl_3$

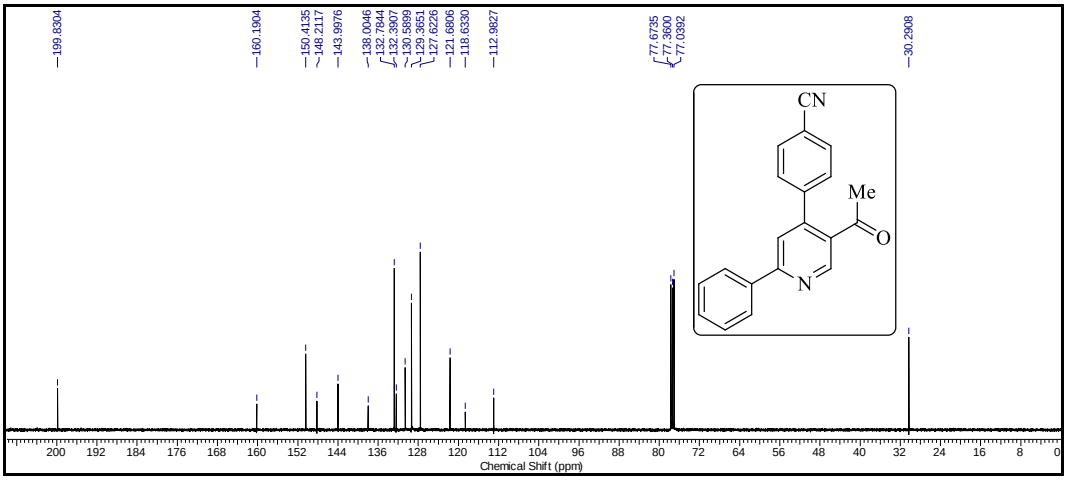


Figure 5.93 100 MHz ^{13}C NMR spectrum of **3at** in $CDCl_3$

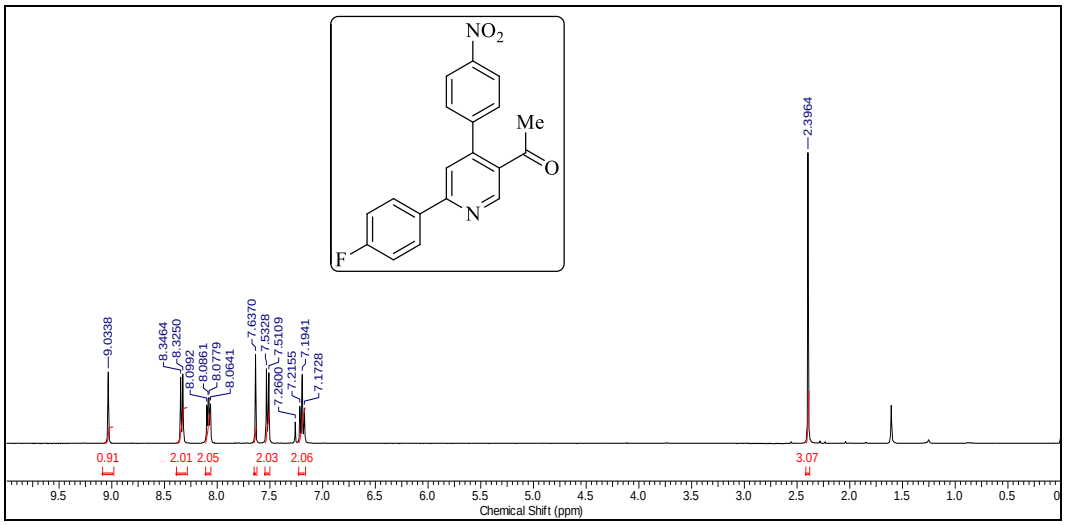


Figure 5.94 400 MHz ^{1}H NMR spectrum of **3es** in $CDCl_3$

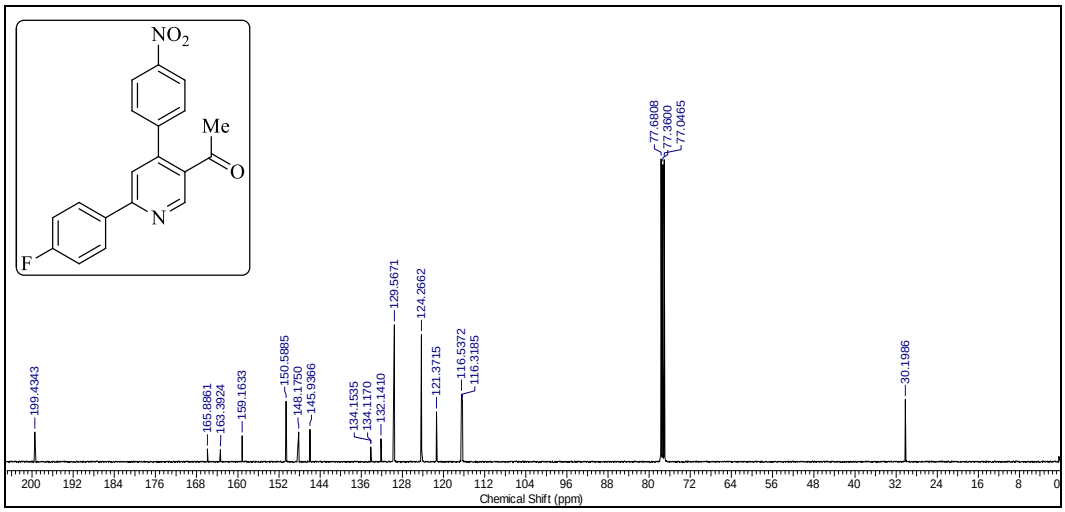


Figure 5.95 100 MHz ^{13}C NMR spectrum of **3es** in $CDCl_3$

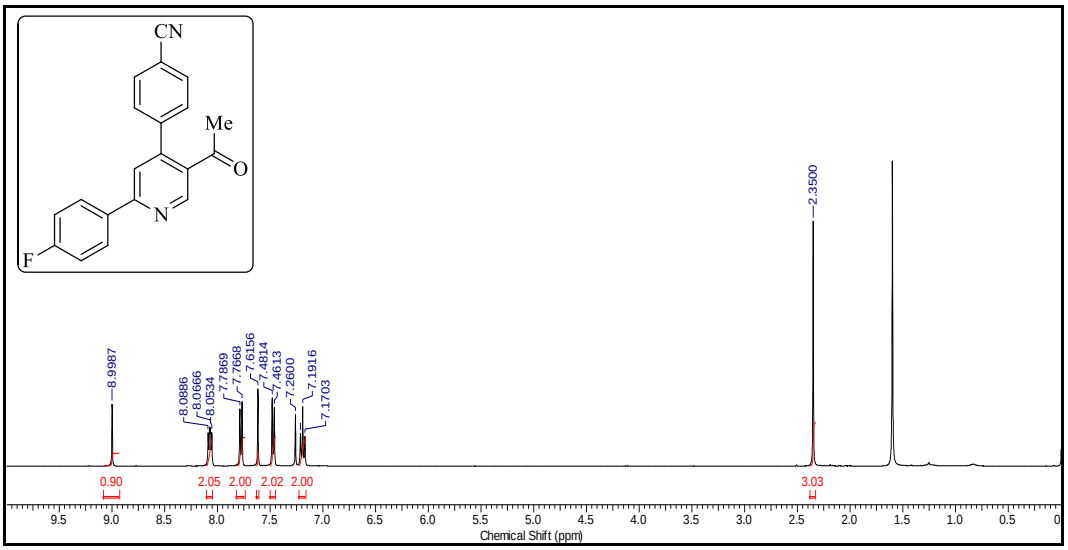


Figure 5.96 400 MHz ^{1}H NMR spectrum of **3et** in $CDCl_3$

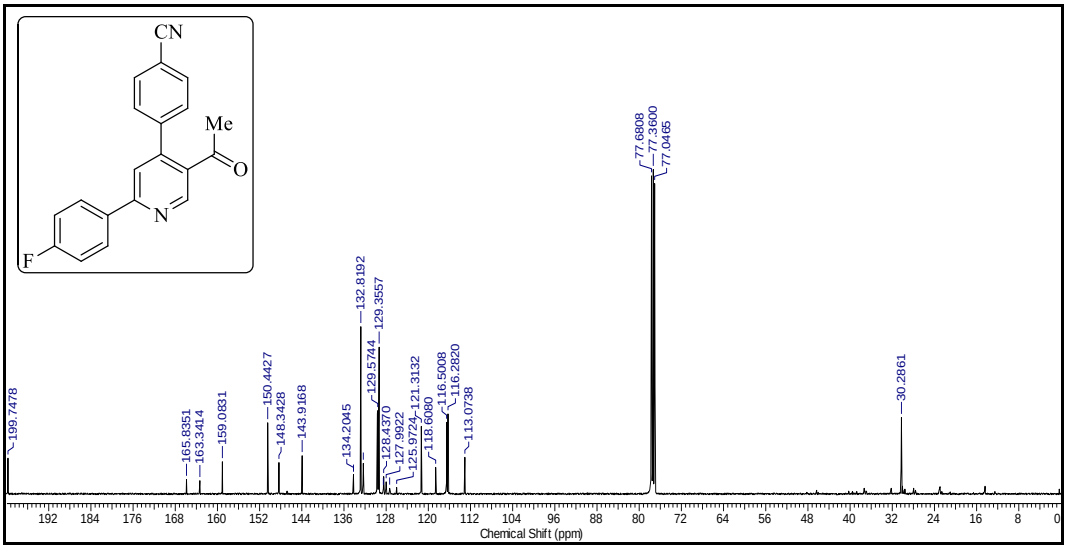


Figure 5.97 100 MHz ^{13}C NMR spectrum of **3et** in $CDCl_3$

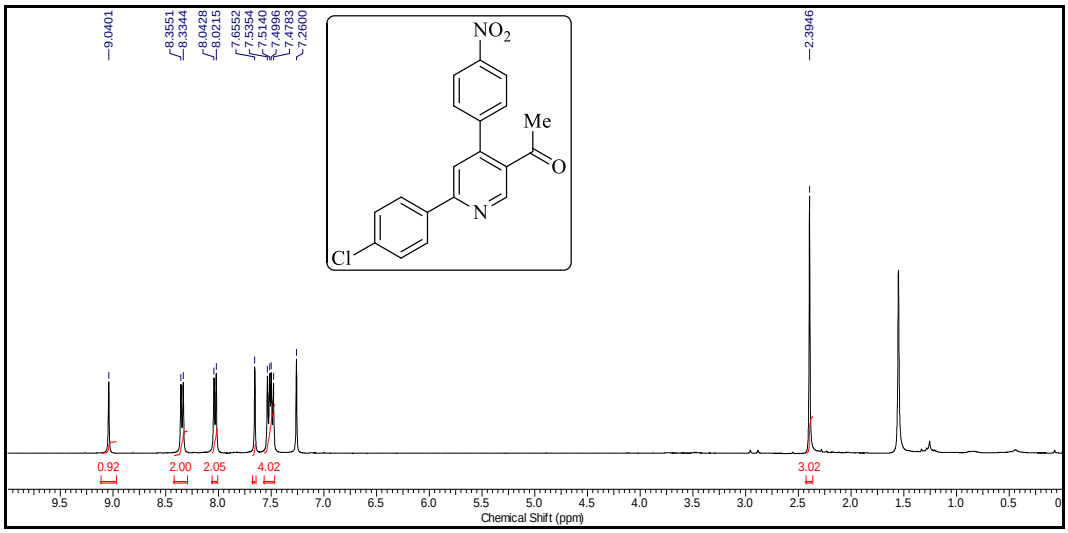


Figure 5.98 400 MHz ^{1}H NMR spectrum of **3fs** in $CDCl_3$

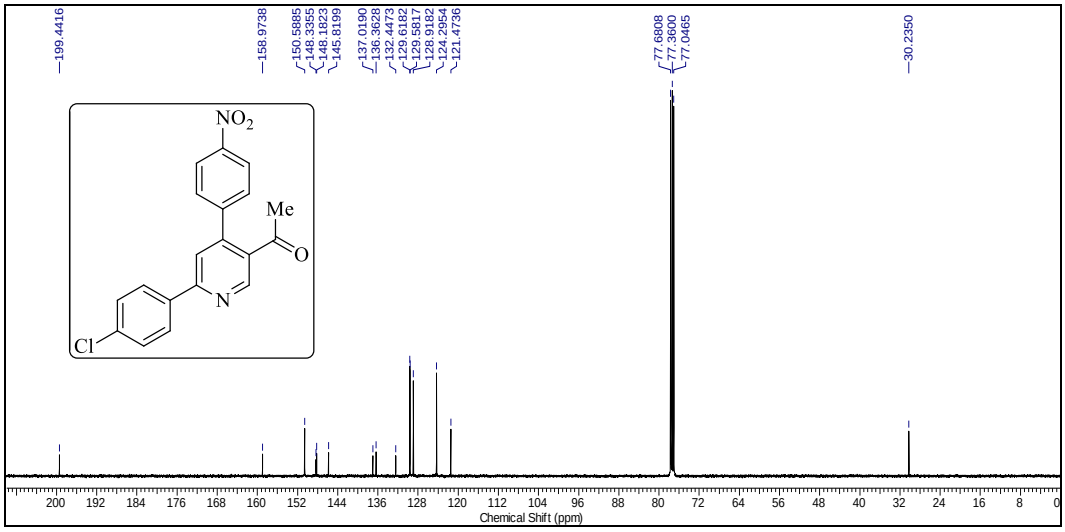


Figure 5.99 100 MHz ^{13}C NMR spectrum of **3fs** in $CDCl_3$

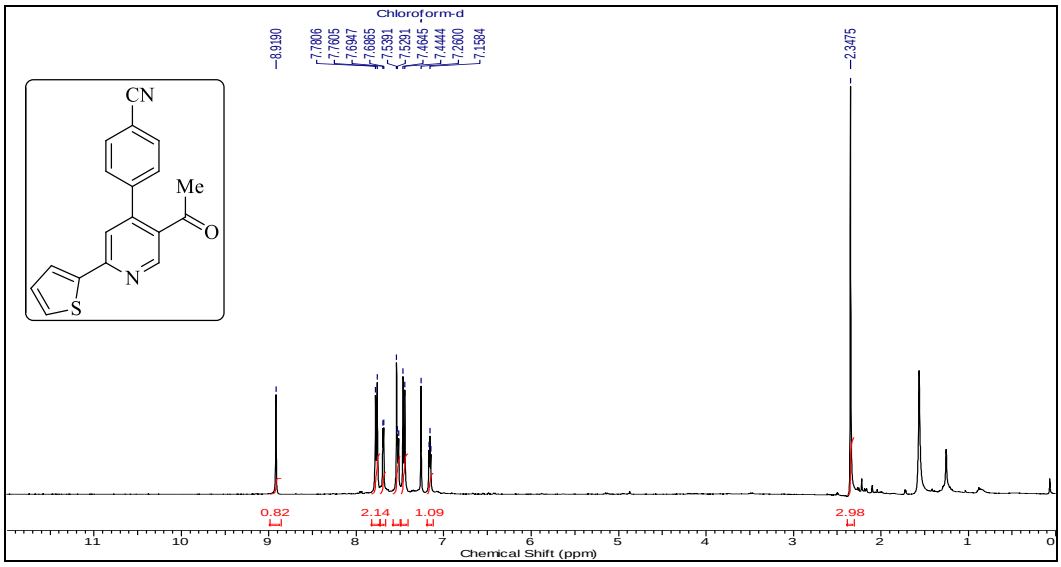


Figure 5.100 400 MHz ^{1}H NMR spectrum of **3it** in $CDCl_3$

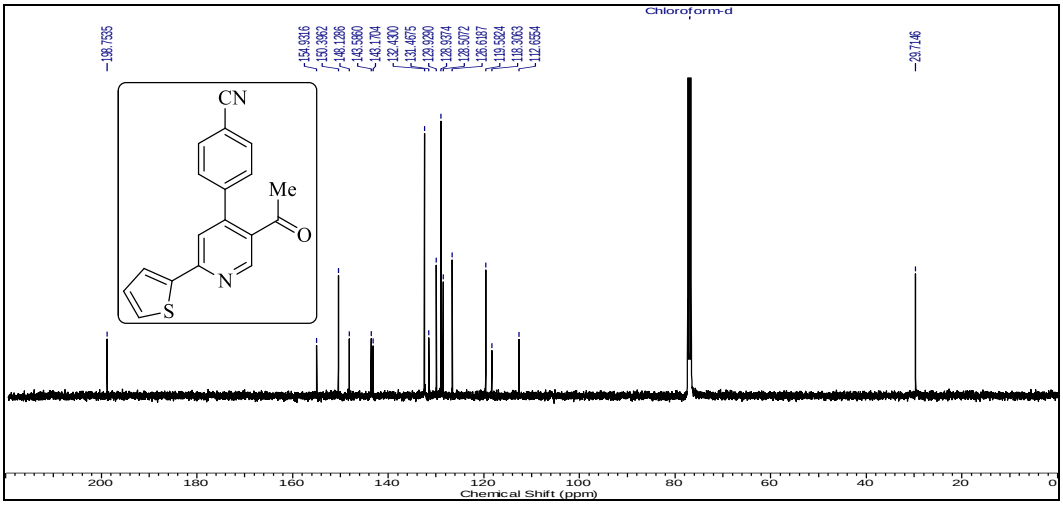


Figure 5.101 100 MHz ^{13}C NMR spectrum of **3it** in $CDCl_3$

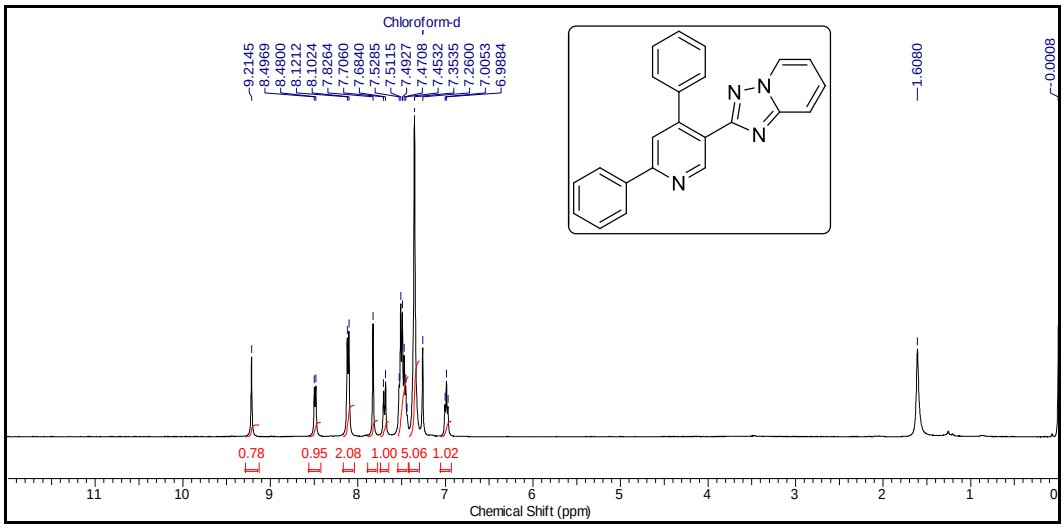


Figure 5.102 400 MHz ^{1}H NMR spectrum of **9** in $CDCl_3$

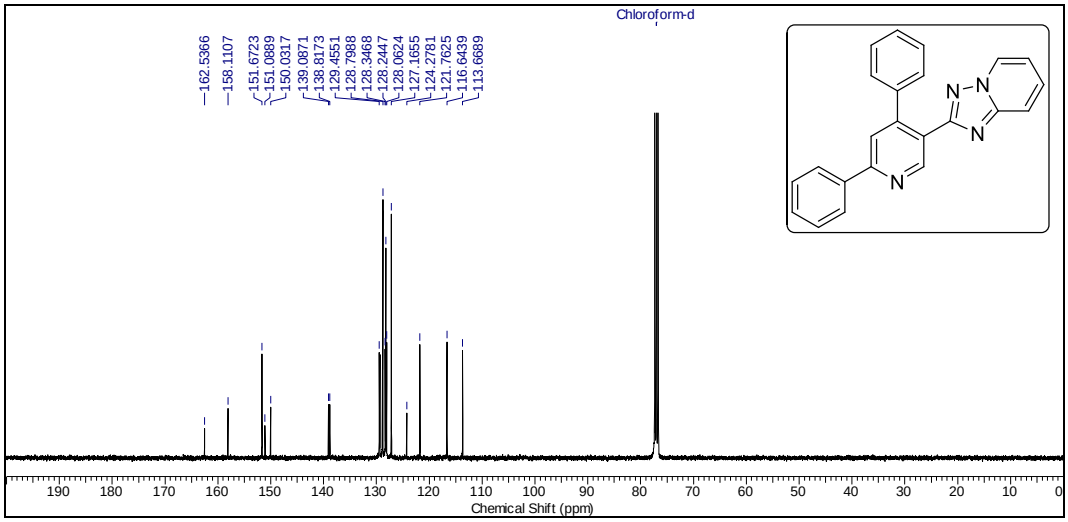


Figure 5.103 100 MHz ^{13}C NMR spectrum of **9** in $CDCl_3$

5.6 Reference

1. Fraser. H. L., Hopper. D. W., Kutterer. K. M. K., Crombie A. L. (2008) Progress in heterocyclic chemistry, G. W. Gribble and J. A. Joule, Eds., *Elsevier: Amsterdam*, 19, 314 (ISBN: 0081007558)
2. Baumann M., Baxendale I. R. (2013), An overview of the synthetic routes to the best selling drugs containing 6-membered heterocycles, *Beilstein J. Org. Chem.*, 9, 2265-2319 (DOI: 10.3762/bjoc.9.265)
3. Allais C., Grassot J.-M., Rodriguez J., Constantieux T. (2014), Metal-free multicomponent syntheses of pyridines, *Chem. Rev.*, 114, 10829-10868 (DOI: 10.1021/cr500099b)
4. Hill M. D. (2010), Recent strategies for the synthesis of pyridine derivatives, *Chem. Eur. J.*, 2010, 16, 12052-12062 (DOI: 10.1002/chem.201001100)
5. Longstreet A. R., Opalka S. M., Campbell B. S., Gupton B.F., McQuade D. T. (2013), Investigating the continuous synthesis of a nicotinonitrile precursor to nevirapine, *Beilstein J. Org. Chem*., 9, 2570-2578 (DOI: 10.3762/bjoc.9.292)
6. Sinthupoom. N., Prachayasittikul. V., Prachayasittikul. S., Ruchirawat. S., Prachayasittikul V. (2015) *Eur. Food Res. Technol*., 240, 1
7. Trist I. M. L., Nannetti G., Tintori C., Fallacara A. L., Deodato D., Mercorelli B., Palu G., Wijtmans M.l., Gospodova T., Edink E., Verheij M., de Esch I., Viteva L., Loregian A., Botta M. (2016), 4,6-diphenylpyridines as promising novel anti-influenza agents targeting the PA-PB1 protein-protein interaction: structure-activity relationships exploration with the aid of molecular modeling, *J. Med. Chem*., 59, 2688-2703 (DOI: 10.1021/acs.jmedchem.5b01935)
8. Guan A.-Y., Liu C.-L., Sun X.-F., Xie Y., Wang M.-A. (2016) Discovery of pyridine-based agrochemicals by using intermediate derivatization methods, *Bioorg. Med. Chem.*, 24, 342-353 (DOI: 10.1016/j.bmc.2015.09.031)

9. Henry G. D. (2004), *De novo* synthesis of substituted pyridines *Tetrahedron*, 60, 6043-6061 (DOI: 10.1016/j.tet.2004.04.043)
10. Müller T. J. J., Bunz U. H. F.(2007), Functional organic materials, ed., *Wiley-VCH, Weinheim*, (ISBN: 978-3-527-31302-0)
11. Sasabe H., Kido J. (2011), Multifunctional materials in high-performance OLEDs: Challenges for solid-state lighting, *Chem. Mater.*, 23, 621-630 (DOI: 10.1021/cm1024052)
12. Chan Y.-T., Moorefield C. N., Soler M., Newkome G. R. (2010), Unexpected isolation of a pentameric metallomacrocycle from the Fe^{II}-mediated complexation of 120° juxtaposed 2,2′:6′,2″-terpyridine ligands *Chem. Eur. J.*, 16, 1768-1771 (DOI: 10.1002/chem.200902988)
13. Bohlmann F., Rahtz D. (1957) On a new pyridine synthesis, *Chem. Ber.*, 90, 2265-2272 (DOI: 10.1002 / cber.19570901021)
14. Bagley M. C., Glover C., Merritt E. A. (2007) The Bohlmann-Rahtz pyridine synthesis: from discovery to applications, *Synlett*, 16, 2459-2482 (DOI: 10.1055/s-2007-986674)
15. Bagley M. C., Dale J. W., Bower J. (2002) A new one-pot three-component condensation reaction for the synthesis of 2,3,4,6-tetrasubstituted pyridines, *Chem. Commun.*, 2002, 1682-1683 (DOI:10.1039/B203900A)
16. Bagley M. C., Chapaneri K., Dale J. W., Xiong X., Bower J. (2005), One-pot multistep Bohlmann-Rahtz heteroannulation reactions: Synthesis of dimethyl sulfomycinamate, *J. Org. Chem.*, 70, 1389-1399 (DOI: 10.1021/jo048106q)
17. Blayo A.-L., Meur S. L., Grée D., Grée R. (2008), New enantioselective synthesis of monofluorinated pyridines designed for the preparation of chemical libraries, *Adv. Synth. Catal.*, 2008, 350, 471-476 (DOI: 10.1002/adsc.200700488)
18. Allais C., Constantieux T., Rodriguez J. (2009), Use of β,γ-unsaturated α-ketocarbonyls for a totally regioselective oxidative multicomponent

synthesis of polyfunctionalized pyridines, *Chem. Eur. J*., 2009, 15, 12945-12948 (DOI: 10.1002/chem.200902491)

19. Liéby-Muller F., Allais C., Constantieux T., Rodriguez J. (2008), Metal-free Michael addition initiated multicomponent oxidative cyclodehydration route to polysubstituted pyridines from 1,3-dicarbonyls, *Chem. Commun*., 2008, 4207-4209 (DOI:10.1039/B805680C)
20. Allais C., Liéby-Muller F., Rodriguez J., Constantieux T. (2013), Metal-free Michael-addition-initiated three-component reaction for the regioselective synthesis of highly functionalized pyridines: Scope, mechanistic investigations and applications, *Eur. J. Org. Chem.*, 2013, 4131-4145 (DOI: 10.1002/ejoc.201300246)
21. Gade N. R., Devendram V., Pal M., Iqbal J. (2013), IBX mediated reaction of β-enamino esters with allylic alcohols: a one pot metal free domino approach to functionalized pyridines, *Chem. Commun*., 2013, 49, 7926-7928 (DOI:10.1039/C3CC44274H)
22. Song Z., Huang X., Yi W., Zhang W. (2016), One-pot reactions for modular synthesis of polysubstituted and fused pyridines, *Org. Lett*., 18, 5640-5643 (DOI: 10.1021/acs.orglett.6b02883)
23. Wan J.-P., Jing Y., Hu C., Sheng S. (2016), Metal-free synthesis of fully substituted pyridines *via* ring construction based on the domino reactions of enaminones and aldehydes, *J. Org. Chem*., 2016, 81, 6826-6831 (DOI: 10.1021/acs.joc.6b01149)
24. Kumar S., Sawant A. A., Chikhale R. P. , Karanjai K., Thomas A. (2016), One-pot synthesis of highly substituted nicotinic acid derivatives based on a formylation strategy of enamino keto esters, *J. Org. Chem*., 2016, 81, 1645-1653 (DOI: 10.1021/acs.joc.5b02796)
25. Reddy C. R., Panda S. A., Reddy M. D. (2005), Aza-annulation of enynyl azides: A new approach to substituted pyridines, *Org. Lett*., 2015, 17, 896-899 (DOI: 10.1021/ol503752k)
26. Prechter A., Henrion G., dit Bel P. F., Gagosz, F. (2014), Gold-catalyzed synthesis of functionalized pyridines by using 2*H*-azirines as synthetic

equivalents of alkenyl nitrenes, *Angew. Chem., Int. Ed*., 53, 4959-4963 (DOI: 10.1002/anie.201402470)

27. Tejedor D., Méndez-Abt G., García-Tellado F. (2010), Microwave-assisted diversity-oriented domino synthesis of functionalized nicotinic acid derivatives, *Eur. J. Org. Chem.*, 6582-6587 (DOI: 10.1002/ejoc.201001067)
28. Tejedor D., Méndez-Abt G., García-Tellado F. (2010), A convenient domino Access to substituted alkyl 1,2-dihydropyridine-3-carboxylates from propargyl enol ethers and primary amines, *Chem. Eur. J*., 16, 428-431 (DOI: 10.1002/chem.200902140)
29. Jiang Y., Park C.-M., Loh T.-P., (2041), Transition-metal-free synthesis of substituted pyridines *via* ring expansion of 2-allyl-2*H*-azirines, *Org. Lett*., 16, 3432-3435 (**DOI:** 10.1021/ol501010k)
30. Jiang Y., Park C.-M., (2014), A catalyst-controlled selective synthesis of pyridines and pyrroles, *Chem. Sci*., 5, 2347-2351 (DOI:10.1039/C4SC00125G)
31. Robert N., Bonneau A.-L., Hoarau C., Marsais F. (2006), Unusual sterically controlled regioselective lithiation of 3-bromo-5-(4,4′-dimethyl)oxazolinylpyridine. straightforward access to highly substituted nicotinic acid derivatives, *Org. Lett*., 8, 6071-6074 (DOI: 10.1021/ol062556i)
32. Yu J., Kim K. H., Lee H. J., Kim J. N. (2013), An efficient synthesis of poly-substituted phenols and pyridines from Morita-Baylis-Hillman acetates and diethyl oxaloacetate, *Bull. Korean Chem. Soc*., 34, 3027-3032 (DOI : 10.5012/bkcs.2013.34.10.3027)
33. Kim K. H., Kim S.H., Lee H. J., Kim J. N. (2013), Palladium-catalyzed domino cyclization (5-exo/3-exo), ring- expansion by palladium rearrangement, and aromatization: An expedient synthesis of 4-arylnicotinates from Morita-Baylis-Hillman adducts, *Adv. Synth. Catal*., 355, 1977-1983 (DOI: 10.1002/adsc.201300211)

34. Neely J. M., Rovis T. (2104), Pyridine synthesis by [4 + 2] cycloadditions of 1-azadienes: hetero-Diels Alder and transition metal-catalysed approaches, *Org. Chem. Front.*, 1, 1010-1015 (DOI:10.1039/C4QO00187G)

35. Shimada K., Takata Y. , Osaki Y., Moro-oka A., Kogawa H. , Sakuraba M., Aoyagi S., Takikawa Y., Ogawa S. (2009), Regioselective synthesis of polysubstituted pyridines *via* hetero-Diels-Alder reaction of isotellurazoles with acetylenic dienophiles, *Tetrahedron Lett*., 2009, 50, 6651-6653 (DOI: 10.1016/j.tetlet.2009.09.060)
36. Krishnan V., Bhat A., Sachade N. (1994), Process for the preparation of pyridine and β-picoline in vapour phase *via* amorphous silica-alumina catalysts, Indian Patent IN 179244, Jan 25.
37. Stout D. M., Meyers A. I. (1982), Recent advances in the chemistry of dihydropyridines, *Chem. Rev*., 82, 223-243 (DOI: 10.1021/cr00048a004)
38. Bagley M. C., Dale J. W., Bower J. (2001), A new modification of the Bohlmann-Rahtz pyridine synthesis, *Synlett*, 1149-1151 (DOI: 10.1055/s-2001-15140)
39. Bagley M. C., Dale J. W., Hughes D. D., Ohnesorge M., Phillips N. G., Bower J., (2001), Synthesis of pyridines and pyrido[2,3-d]pyrimidines by the lewis acid catalysed Bohlmann-Rahtz heteroannulation reaction, *Synlett*, 10, 1523-1526 (DOI: 10.1055/s-2001-17447)
40. Bagley M. C., Dalea J. W., Bower J. (2002), A new one-pot three-component condensation reaction for the synthesis of 2,3,4,6-tetrasubstituted pyridines, *Chem. Commun*., 0, 1682-1683 (DOI:10.1039/B203900A)
41. Xiong X., Bagley M. C., Chapaneri K. (2004), A new mild method for the one-pot synthesis of pyridines, *Tetrahedron Lett*., 2004, 45, 6121-6124 (DOI: 10.1016/j.tetlet.2004.06.061)
42. Hirai S., Horikawa Y., Asahara H., Nishiwaki N. (2017), Tailor-made synthesis of fully alkylated/arylated nicotinates by $FeCl_3$-mediated

condensation of enamino esters with enones, *Chem. Commun.*, 2017, 53, 2390-2393 (DOI: 10.1039/c7cc00051k)

43. Jiang H. , Yang J., Tang X., Li J., Wu W., (2015), Cu-catalyzed three-component cascade annulation reaction: An entry to functionalized pyridines, *J. Org. Chem*., 80, 8763-8771 (DOI: 10.1021/acs.joc.5b01621)
44. Wu Q., Zhang Y., Cui S., (2014), Divergent syntheses of 2-aminonicotinonitriles and pyrazolines by copper-catalyzed cyclization of oxime ester, *Org. Lett.*, 16, 1350-1353 (DOI: 10.1021/ol500094w)
45. Majee D., Biswas S., Mobin S. M., Samanta S. (2016), Access to 4,6-diarylpicolinates *via* a domino reaction of cyclic sulfamidate imines with Morita-Baylis-Hillman acetates of nitroolefins/nitrodienes, *J. Org. Chem*., 2016, 81, 4378-4385 (DOI: 10.1021/acs.joc.6b00472)
46. Baidya M., Remennikov G. Y., Mayer P., Mayr H. (2010), S_N2' versus S_N2 reactivity: control of regioselectivity in conversions of Baylis-Hillman adducts, *Chem. Eur. J*., 16, 1365-1371 (DOI: 10.1002/chem.200902487)
47. Wei Y., Shi M. (2013), Recent advances in organocatalytic asymmetric Morita-Baylis-Hillman/aza-Morita-Baylis-Hillman reactions, *Chem. Rev.*, 113, 6659-6690 (DOI: 10.1021/cr300192h)
48. Hantzsch, A. (1881), Condensationsprodukte aus aldehydammoniak und ketonartigen verbindungen, *Ber. Dtsch. Chem. Ges*., 14, 1637-1638 (DOI: 10.1002/cber.18810140214)
49. Longstreet A. R., Rivalti D., McQuade D. T. (2015) Synthesis and reactivity profile of ylidenemalononitrile enamines and their ester analogs towards electrophiles and nucleophiles, *J. Org. Chem*., 80, 8583-8596 (DOI: 10.1021/acs.joc.5b01169)
50. Longstreet A. R., Campbell B. S., Gupton B. F., McQuade D. T. (2013), Improved synthesis of mono- and disubstituted 2-halonicotinonitriles from alkylidene malononitriles, *Org. Lett*., 15, 5298-5301 (DOI: 10.1021/ol4025265)

51. Liu C., Wang Q. (2016), Arylation, vinylation, and alkynylation of electron-deficient (hetero)arenes using iodonium salts, *Org. Lett*., 18, 5118-5121 (DOI: 10.1021/acs.orglett.6b02550)
52. Wu Q., Zhang Y., Cui S. (2014), Divergent syntheses of 2-aminonicotinonitriles and pyrazolines by copper-catalyzed cyclization of oxime ester, *Org. Lett*., 16, 1350-1353 (DOI: 10.1021/ol500094w)
53. Shi Z., Tong Q., Leong W. W. Y., Zhong G. (2012), [4+2] Annulation of vinyl ketones initiated by a phosphine-catalyzed aza-Rauhut-Currier reaction: A practical access to densely functionalized tetrahydropyridines, *Chem. Eur. J*., 18, 9802-9806 (DOI: 10.1002/chem.201201318)
54. Yamamoto S.-I., Okamoto K., Murakoso M., Kuninobu Y., Takai K. (2012), Rhenium-catalyzed regioselective synthesis of multisubstituted pyridines from β-enamino ketones and alkynes *via* C-C bond cleavage, *Org. Lett*., 14, 3182-3185 (DOI: 10.1021/ol301273j)
55. Manning J. R., Davies H. M. L., (2008), One-pot synthesis of highly functionalized pyridines *via* a Rhodium carbenoid induced ring expansion of isoxazoles, *J. Am. Chem. Soc.*, 130, 8602-8603 (DOI: 10.1021/ja803139k)
56. Ueda S., Nagasawa H. (2009), Facile synthesis of 1,2,4-triazoles *via* a copper-catalyzed tandem addition-oxidative cyclization, *J. Am. Chem. Soc*., 131, 15080-15081 (DOI: 10.1021/ja905056z)
57. Flohr A., Zbinden K.G., Koerner M. (2014), Triazolopyridine compounds. *US Patent*, 20140303141.
58. Wang Y.-Q., Yu C.-B., Wang D.-W., Wang X.-B., Zhou Y.-G., Enantioselective synthesis of cyclic sulfamidates *via* Pd-catalyzed hydrogenation, *Org. Lett*., 10, 2071-2074 (DOI: 10.1021/ol800591u)
59. Shi M., Jiang J.-K., Li C.-Q. (2002), Lewis base and l-proline co-catalyzed Baylis-Hillman reaction of arylaldehydes with methyl vinyl ketone, *Tetrahedron Lett*., 43, 127-130 (DOI: 10.1016/S0040-4039(01)02057-3)
60. Geesala R., Gangasani J. K. , Budde M., Balasubramanian S., Vaidya J. R., Das A. (2016), 2-Azetidinones: Synthesis and biological evaluation as

potential anti-breast cancer agents, *Eur. J. Med. Chem*., 124, 544-558 (DOI: 10.1016/j.ejmech.2016.08.041)

Chapter 5

Chapter 6

One-pot sequential reaction of cyclic sulfamidate imine with β-substituted acroleins to access 2,4-disubstituted pyridine by a metal-free new approach

6.1 Introduction

The journey of pyridine starts in 1846 when the Scottish chemist Thomas Anderson first discovered 'Picoline' as the first known pyridine derivative from bone oil,[1] but the correct structure of pyridine was proposed independently by Körner (1869)[2] and Dewar (1871).[3] With the understanding of the structure of pyridine in 1876, William Ramsay[4] combined acetylene and hydrogen cyanide to synthesize pyridine in a red-hot iron-tube furnace and the chemistry of the evergreen azaheterocycles starts.

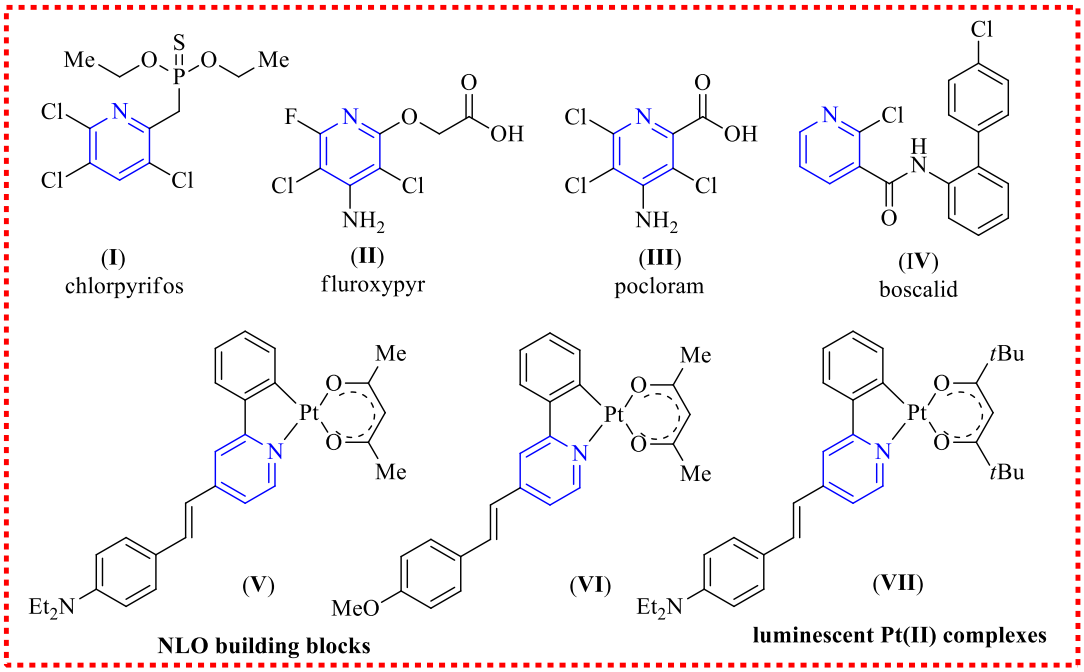


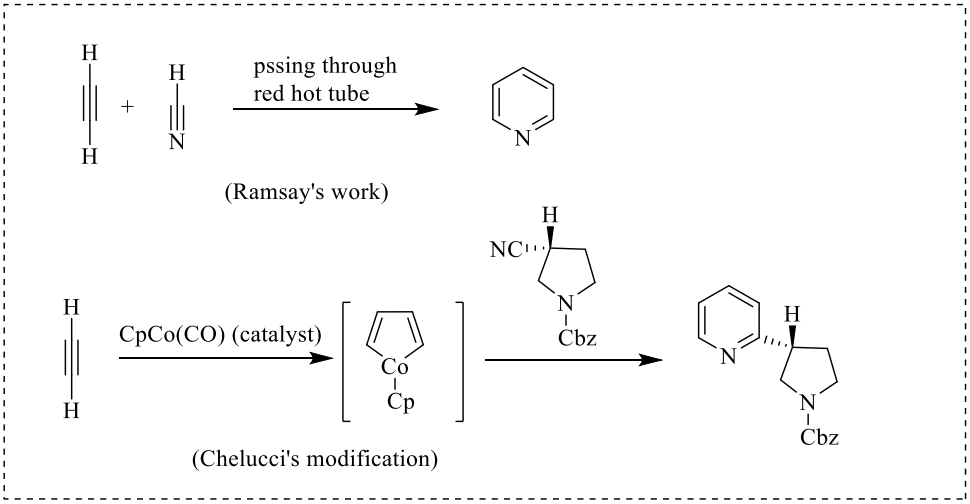
Figure 6.1 Representative molecules containing pyridine moiety

Pyridine and its functionalized forms have been recognized as one of the most extensively studied heterocyclic molecules,[5-7] Importantly, these aza-heterocyclic scaffolds constitute the core of a large number of top selling marketable drugs,[8-9] natural products,[10] pharmaceuticals,[11-12] agrochemicals,[13] advanced functional materials,[14] inorganic complexes.[15-16] Some of the important examples are shown in **Figure 6.1**.

Due to the various applications in several fields, intense efforts have been devoted since 19th century towards the efficient access to both symmetrical and unsymmetrical substituted pyridines through various novel methods such as one-pot multicomponent reaction,[17] condensation reaction of reactive carbonyl compounds with various forms of amines,[18] 6-π-electrocyclization,[19] transition-metal catalyzed [4+2][20]/ [2+2+2][21] cycloaddition reactions of alkynes with α,β-unsaturated oximes/enamides/nitriles, and direct C-H functionalization on the pyridines.[22] Some of the important reports related to the synthesis of 2,4-disubstituted pyridines are included in the review **Section 6.2**.

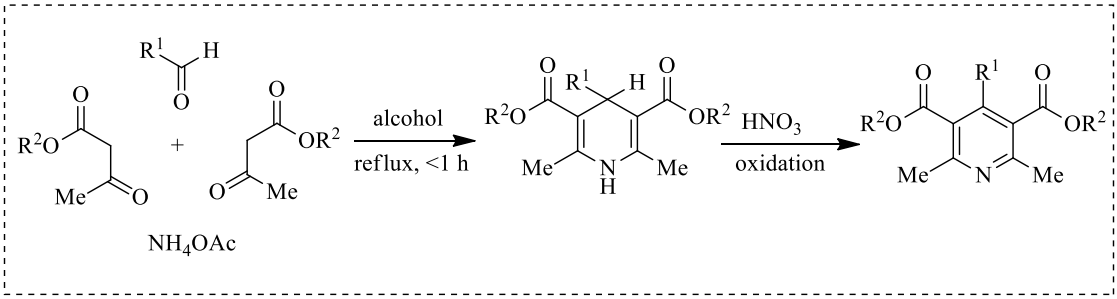
6.2 Review work

The synthesis of pyridine was developed for the first time by Ramsay[4] in 1876 by passing the mixture of acetylene and hydrogen cyanide through a red hot tube. Later, in 1990, Chelucci and co-workers modified this procedure by using cobalt (I) catalyzed variant which is a good commercial source of alkylpyridines.[23]



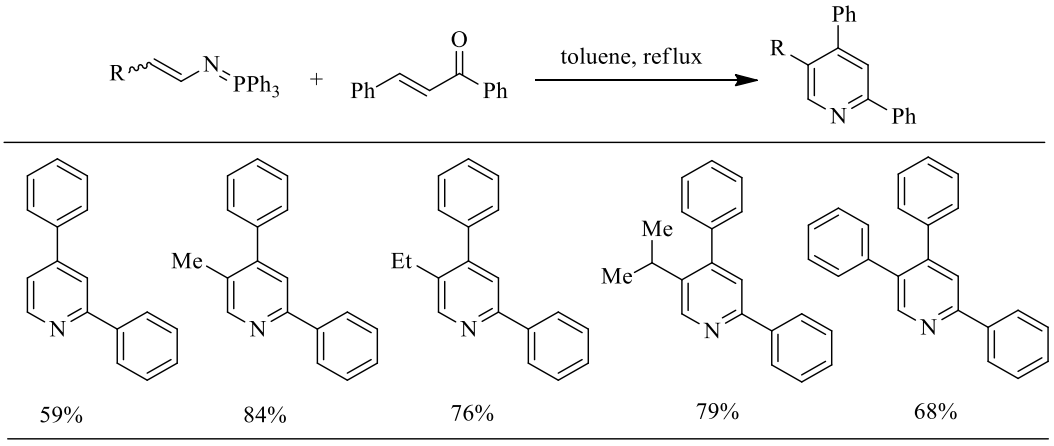
Scheme 6.1 Synthesis of pyridine by Ramsay and Chelucci

In 1881, Prof. Arthur Rudolf Hantzsch discovered the synthesis of highly substituted symmetrical dehydro pyridines by a pseudo four-component reaction by taking an aldehyde, β-keto ester (2.0 equiv) and ammonium acetate or ammonia in alcoholic solvent. Next DHP moiety was oxidized by HNO_3 oxidation of corresponding substituted pyridine moiety.[18]



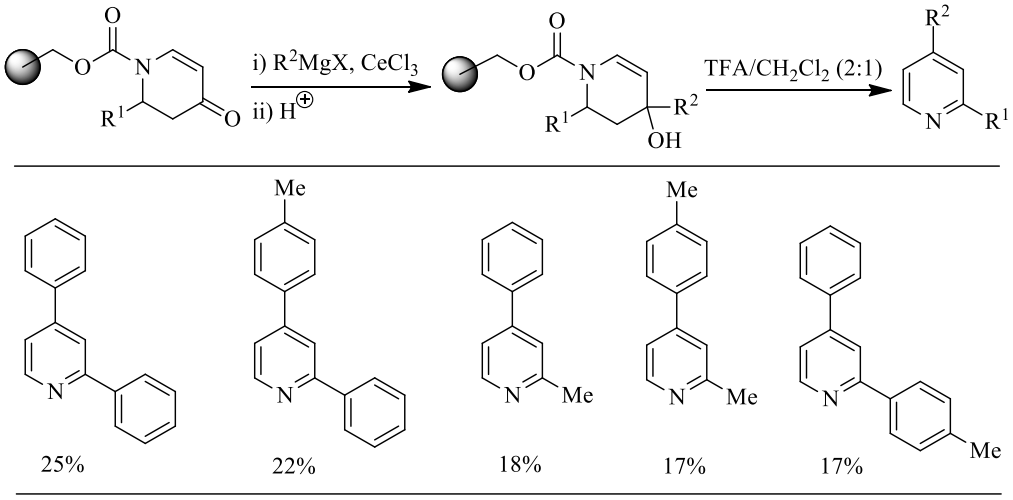
Scheme 6.2 Classical Hantzsch synthesis for the symmetrical pyridine

The cyclization reaction was carried out with (*N*-vinylimino)phosphoranes and an excess amount of chalcone in toluene under refluxing conditions to obtain 2,4-diphenyl pyridines in good yields as reported by Katritzky *et al.* in 1994 (**Scheme 6.3**).[24]



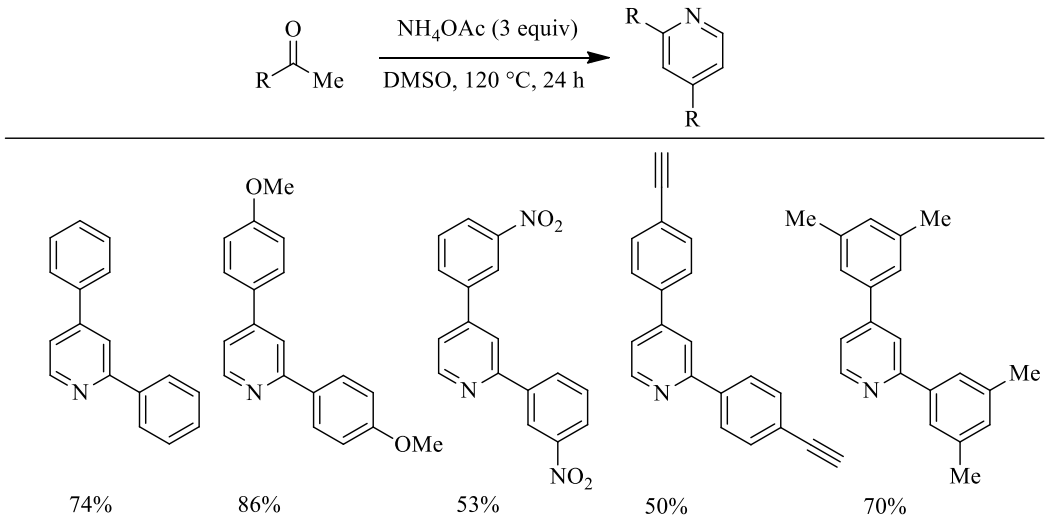
Scheme 6.3 One-pot synthesis of 2,4-diphenylpyridines form (*N*-vinyimino)-phosphoranes

The conversion of dihydropyridones to tetrahydropyrid-4-ols by Grignard reagents in the presence of cerium chloride followed by acidic cleavage using TFA/CH_2Cl_2 gave the 2,4-disubstituted pyridines as major products in poor yields as published by Munoz *et al.* in 1998. Some of the promising results are summarized in **Scheme 6.4**.[25]



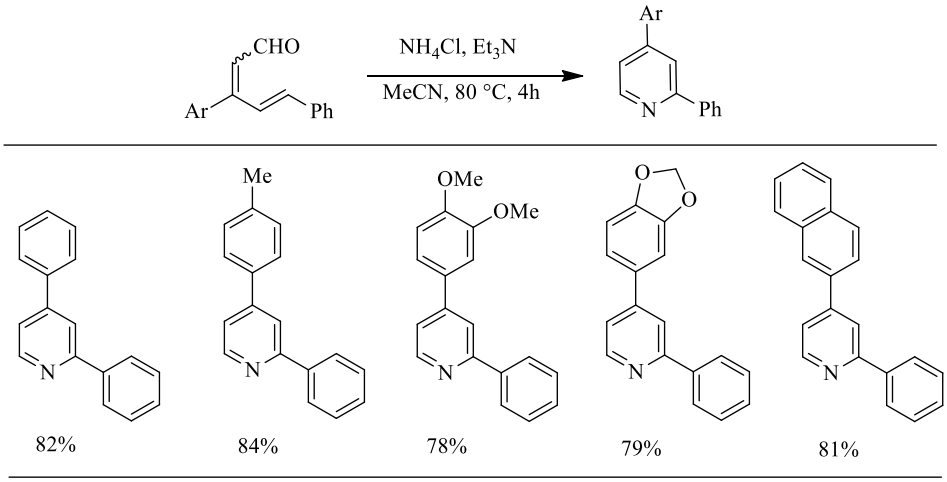
Scheme 6.4 Solid support synthesis of 2,4-disubstituted pyridines

In 2010, Huang and his co-workers discovered an easy, efficient one-pot route for the access of 2,4-diarylpyridines through a condensation reaction of aromatic ketones with ammonium acetate in DMSO at 120 °C for 24 h as described in **Scheme 6.5**.[26]



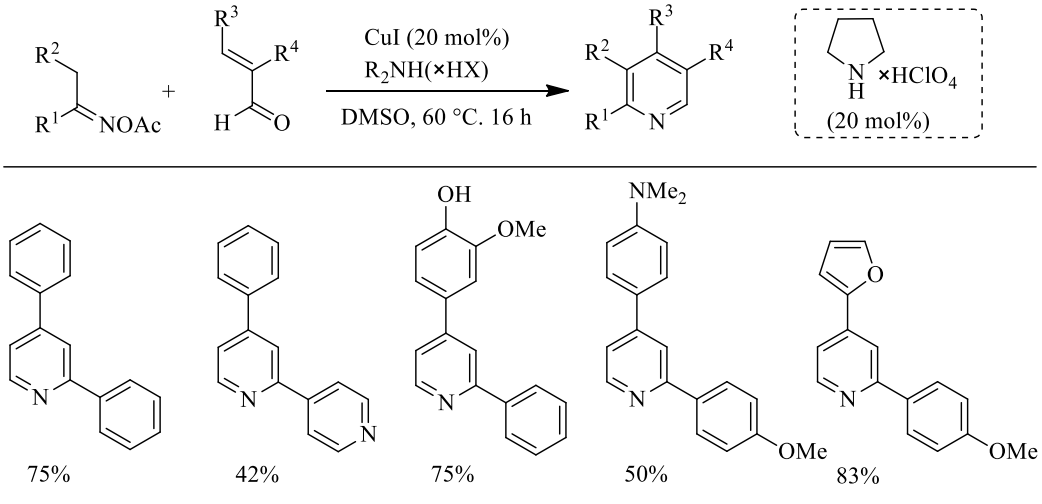
Scheme 6.5 Synthesis of 2,4-diarylpyridines from 1-substituted ethanones

In 2013, Ray group discovered a very interesting and mild procedure for the synthesis of 2,4-disubstituted pyridine in good yields by heating α,β,γ,δ-unsaturated aldehydes with NH_4Cl in presence of mild base Et_3N in refluxing condition for 4 h in MeCN. Some of the examples are summarized in **Scheme 6.6**.[27]



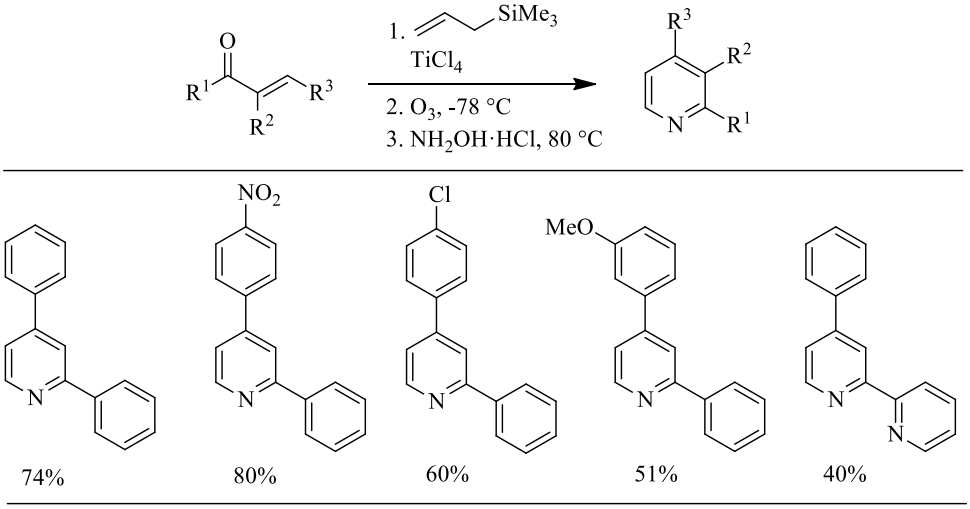
Scheme 6.6 Synthesis of 2,4-diaryl pyridines from α,β,γ,δ-unsaturated aldehydes

A [3+3]-type cyclization of *O*-acetyl ketoximes with α,β-unsaturated aldehydes catalyzed by the combination of a copper(I) salt and secondary amine salt was presented in 2013 by Yoshikai *et al.* This one-pot method delivers 2,4-disubstituted pyridines in satisfactory level of yields with a broad range of functional group. Some of the examples are depicted in **Scheme 6.7**.[28]



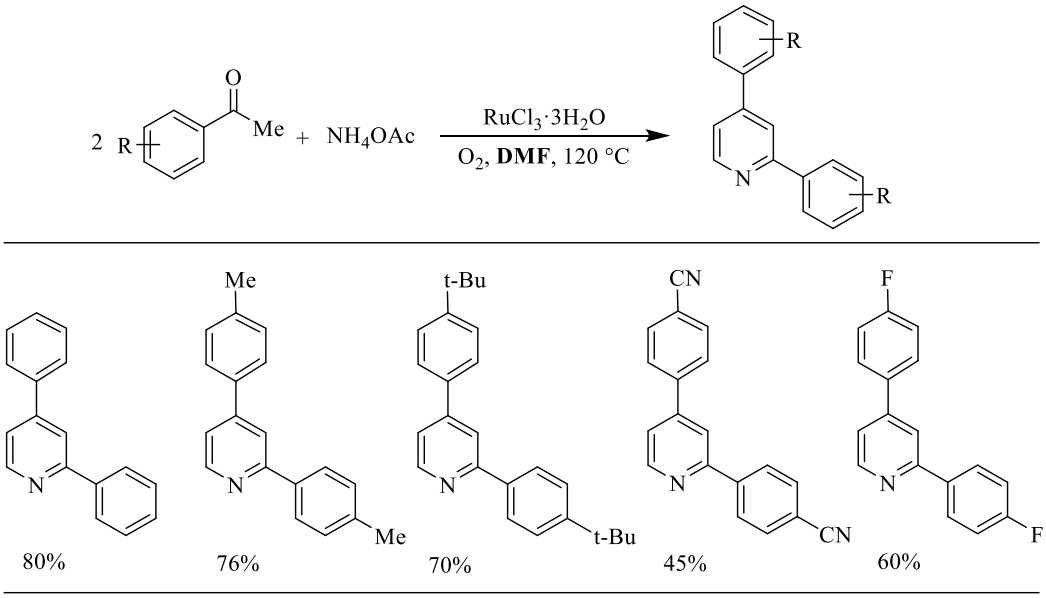
Scheme 6.7 Synthesis of 2,4-substituted pyridines by [3+3] cyclization of oximes and enals

In 2016, a robust method to access highly substituted pyridines by performing the Hosomi-Sakurai reaction between enone and allyltrimethylsilane promoted by $TiCl_4$ followed by ozonolysis to form 1,5-diketones which subsequently reacted with hydroxylamine hydrochloride in MeCN at 80 °C as described by Rychnovsky *et al.* **Scheme 6.8**.[29]



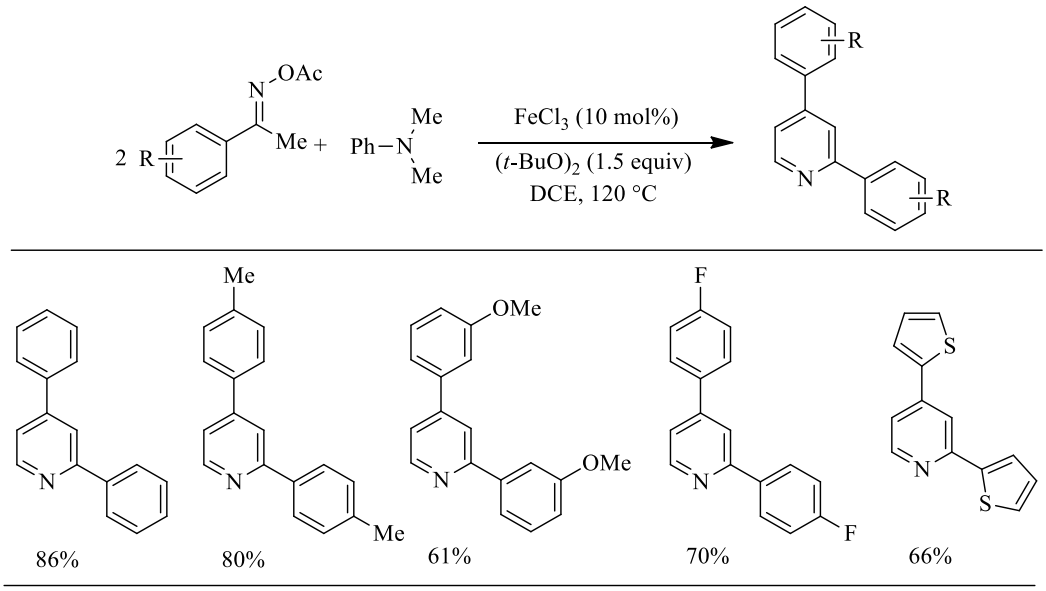
Scheme 6.8 Scope of 2,4- substituted pyridines by the reaction between enone and allyltrimethylsilane

A Ru-catalyzed one-pot pseudo four component reaction of acetophenone, ammonium acetate in DMF (solvent as well as reagent) under oxygen atmosphere at 120 ºC for the synthesis of 2,4-diarylsubstituted pyridine derivatives in satisfactory yields was reported by Deng and his associates in 2015 as described in **Scheme 6.9**.[30]



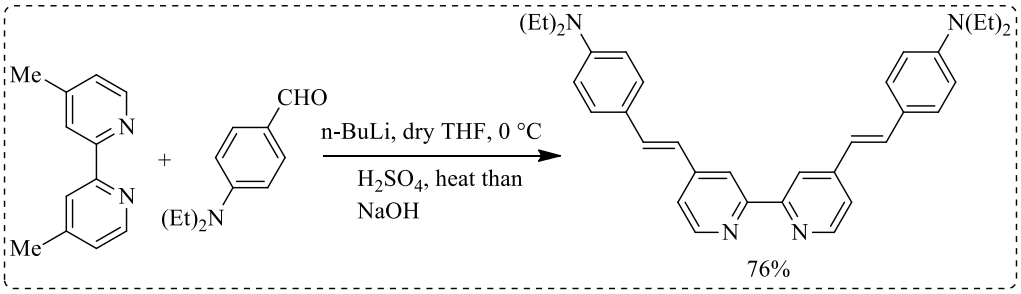
Scheme 6.9 Ru-catalyzed synthesis of 2,4-diarylpyridines

In 2016, Guan *et al.* prepared 2,4-disubstituted pyridine in good to excellent yields by a mild and efficient iron-catalyzed cyclization of ketoximes with N,N-dimethyl anilines as described in **Scheme 6.10**.[31]



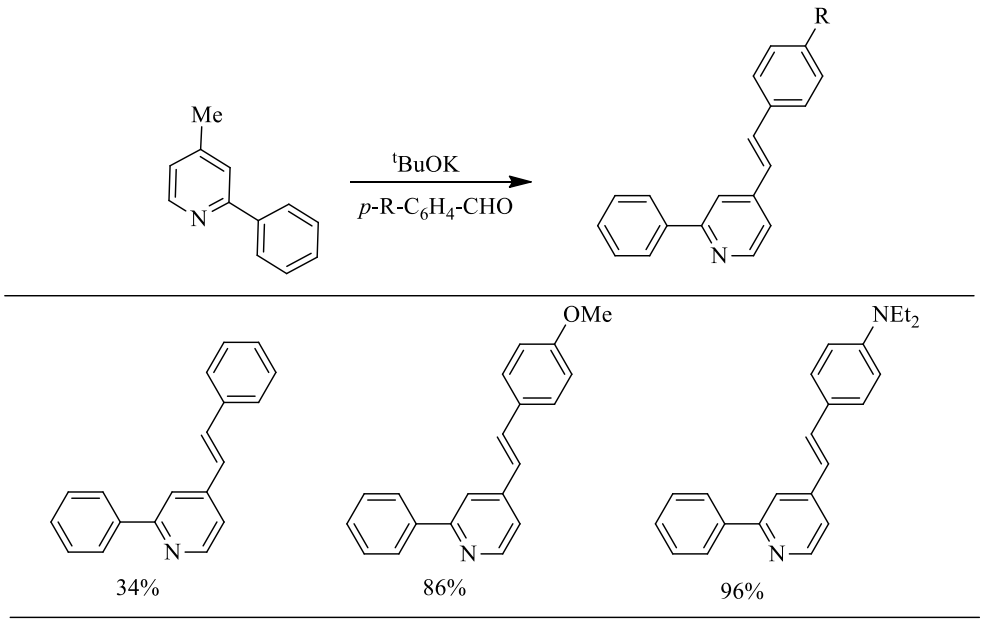
Scheme 6.10 Fe catalyzed cyclization of ketooxime acetates and *N,N*-dimethyl aniline

In 1988, Juris *et al.* synthesized styryl substituted bipyridine by the condensation reaction of methyl substituted bipyridine and corresponding aldehydes in presence of *n*-Butyl lithium in dry THF at 0 ºC as described in **Scheme 6.11**.[32]



Scheme 6.11 Synthesis of styryl bipyridine ligand

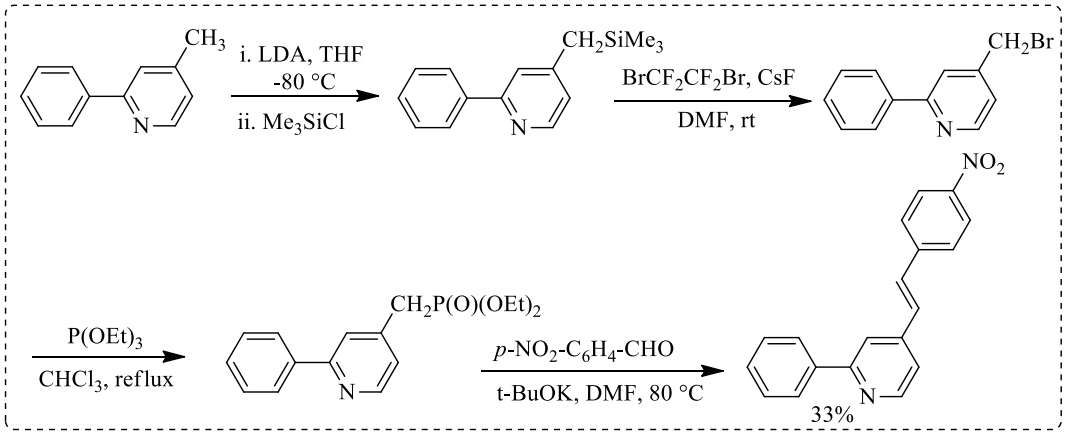
In 2007, Guerchais *et al.* prepared 2-aryl-4-styryl pyridines by the condensation reaction of 2-aryl-4-picoline and aromatic aldehydes promoted by ^{t}BuOK as described in **Scheme 6.12**.[33]



Scheme 6.12 Preparation of substituted or electron donating substituted styryl pyridine

For the preparation of electron withdrawing group substituted styryl pyridines they gone through Wadsworth–Emmons procedure by reacting *p*-

nitrobenzaldehyde and (diethylphosphoryl)methyl-2 phenylpyridine which was prepared by the following procedure of **Scheme 6.13**.



Scheme 6.13 Preparation of electron withdrawing substituted styryl pyridine

6.2.1 Conclusion

From the above discussion it is indicated that although a quite number of methods have been developed for the preparation of 2,4-disubstituted pyridine. However, a metal free, one-pot synthesis of 2,4-disubstituted pyridines especially 2-aryl-4-styrylsubstituted pyridines has been less explored despite its great applications in organometallic chemistry and optical materials. Moreover, the preparation of 2-aryl-4-styrylpyridine derivative starting from 2-aryl-4-methylpyridine still requires multistep operations (**Scheme 6.13**).[33] Besides, the existing methods suffer several drawbacks such as limited substrate scope, higher temperature, lower yield, use of costly metal salts. Therefore, it is of great interest to develop a new, convenient, metal-free based high yielding one-pot method that may provide a series of 2-aryl-4-styrylpyridines/2,4-diarylpridines in an efficient manner.

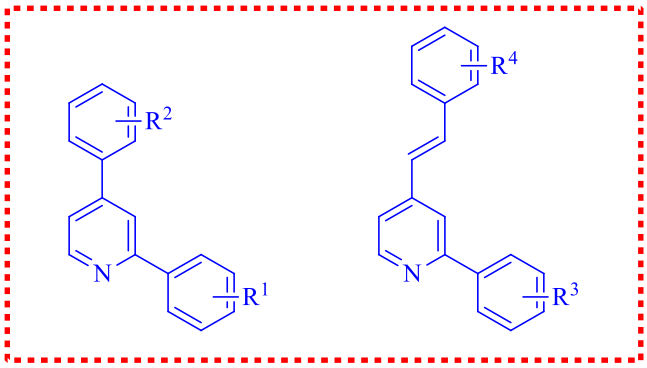
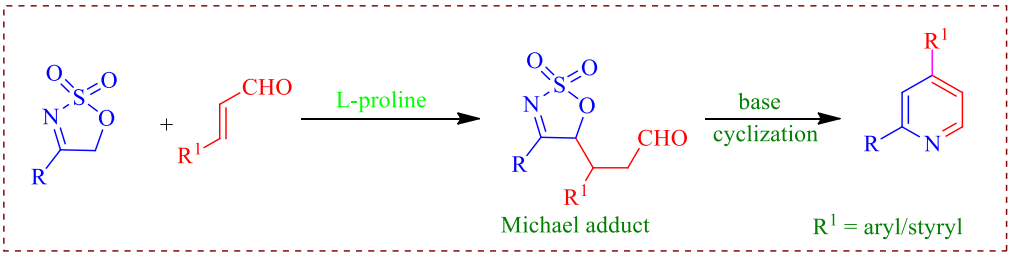


Figure 6.2 2,4-diaryl/2-aryl-4-styrylpyridine derivatives

6.3 Present work

Owing to the great demand and potential utility of substituted pyridines, a new synthetic method for the synthesis of functionalized pyridines under metal-free conditions is still a prime research area in synthetic organic and medicinal chemistry. In this context, we have observed that 5-membered cyclic sulfamidate imines can act as efficient nucleophiles[34-36] to construct functionalized *spiro*-sulfamidate imine fused δ-lactones[35] when α, β-unsaturated aldehydes were used as Michael acceptors. With this understanding, we envisaged that the Michael addition reaction between α,β unsaturated or α,β,γ,δ-unsaturated aldehydes and cyclic sulfamidate imines may react with at the β-position in the presence of L-proline to form β-styryl-substituted Michael adduct which may be converted in to 4-styrylpyridine under basic conditions (**Scheme 6.14**).



Scheme 6.14 Preparation of functionalized 2-aryl-4-(*E*)-aryl/styrylpyridines using cyclic sulfamidate imine as precursor

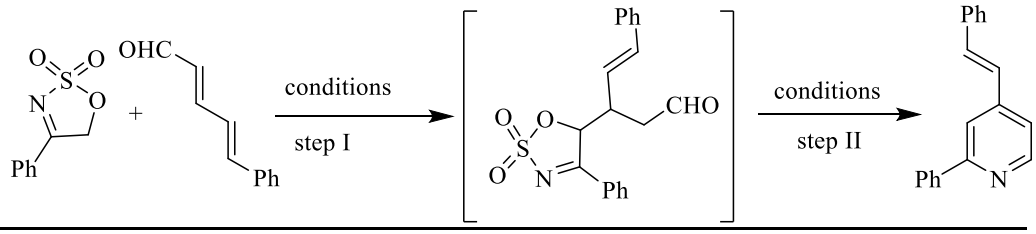
6.3.1 Results and discussion

6.3.1.1 Screening of solvents and catalysts/bases

By using 4-phenyl-5*H*-1,2,3-oxathiazole 2,2-dioxide (**1a**) and (2*E*,4*E*)-5-phenylpenta-2,4-dienal (**2a**) as test substrate, the initial reaction was performed in MeOH at room temperature using 20 mol% L-proline as an effective organocatalyst. After 24 h, we have isolated the Michael adduct **3aa′** in 73% yield with a non-separable mixture of disatereomer (dr 9:1). Next, the obtained Michael adduct **3aa′** was treated with DABCO (1.5 equiv.) in THF at room temperature. After 12 h, we have isolated the product **3aa** in 39% (two steps, entry 1, **Table 6.1**) overall yield. The product **3aa** was fully characterized by its spectroscopic data (IR, ^{1}H, ^{13}C and HRMS). ^{1}H NMR spectrum shows that all peaks are in aromatic region 7.10-8.66 ppm which indicates the formation of fully aromatic moiety. Furthermore, the coupling constant of vicinal protons of double bond is 16.3 Hz at δ 7.10 ppm which indicates the orientation of double bond protons is *trans* to each other. In addition, the total number carbon peaks in ^{13}C NMR spectrum are 15 which belong to the desired 2-phenyl-4-styrylpyridine (**3aa**)**.** The HRMS spectrum shows the presence of molecular ion peak $[M+H]^{+}$: 258.1271 which corresponds to the molecular weight of product of **3aa**. Pleasantly, 70% yield of **3aa** occurred when the second step was performed at 40ºC instead of room temperature. In order to avoid the isolation and characterization processes of Michael adduct, we performed the reaction in one-pot manner by adding DABCO directly into the reaction mixture. However, after 12 h, a negligible (9%) (entry **3**) yield of desired compound **3aa** was isolated. Interestingly, a better yield (42%) of **3aa** was obtained when both the steps were conducted in THF instead of MeOH. Further screening of common organic solvents showed that polar solvents like EtOH and DMF provided much lower yields (10-21%) (entries **5,6** of **Table 6.1**) as compared to non-polar ones (68-71%)(entry in table). All the results summarized in **Table 6.1**. Considering the yield of **3aa,** toluene was chosen as best solvent for this sequential reaction (entry **7**). After finding the best solvent, we turned our attention to know the effects of bases for the cyclization process

(step **II**). We performed the same reactions by using several common organic bases namely DBU, DMAP and Et_3N under same conditions but all these bases produced lower yields of **3aa** (5-63%) (entries **9-11**) as compared to DABCO. It is noted that Michael reaction did not proceed at all when only DABCO was used (entry **12**).

Table 6.1 Optimization of the reaction conditions[a,e]



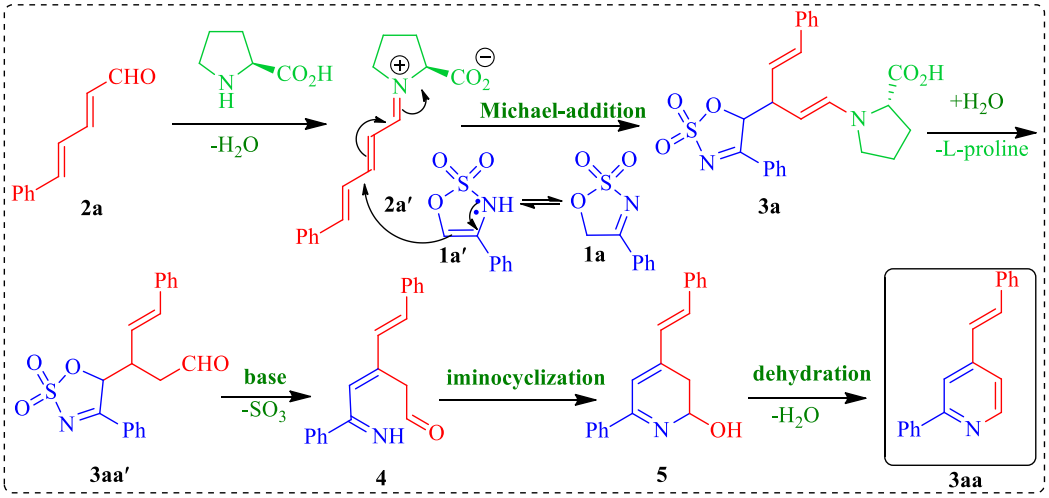
entry	conditions of step I and II	yield (%)[c]
1.	I[a] L-proline, MeOH, rt, 24h II[b] DABCO, THF, rt, 12h	39
2.	I[a] L-proline, MeOH, rt, 24h II[d] DABCO, THF, 40 ºC, 12h	70
3.	I[a] L-proline, MeOH, rt, 24h II[e] DABCO, 40 ºC, 12h	9
4.	I[a] L-proline, MeOH, rt, 24h II[e] DABCO, 40 ºC, 12h	42
5.	I[a] L-proline, EtOH, rt, 24h II[e] DABCO, 40 ºC, 12h	10
6.	I[a] L-proline, DMF, rt, 24h II[e] DABCO, 40 ºC, 12h	21
7.	I[a] L-proline, CH_2Cl_2, rt, 24h II[e] DABCO, 40 ºC, 12h	68
8.	I[a] L-proline, toluene, rt, 24h II[e] DABCO, 40 ºC, 12h	71
9.	I[a] L-proline, toluene, rt, 24h II[b] DBU, 40 ºC, 12h	63
10.	I[a] L-proline, toluene, rt, 24h II[e] DMAP, 40 ºC, 18h	11
11.	I[a] L-proline, toluene, rt, 24h II[e] Et_3N, 40 ºC, 18h	5
12.	I[f] DABCO, toluene, rt, 18h	ND

[a]Unless otherwise specified, all the reactions were conducted with cyclic sulfamidate imine **1a** (0.2 mmol), **2a** (0.24 mmol) and L-proline (0.05 mmol, 20 mol%) in the specified solvent (1.0 mL) for 24h at room temperature under nitrogen atmosphere. [b]Isolated Michael adduct was treated with DABCO (0.3 mmol) in THF (1.0 mL) at room temperature for 12h. [c]Yield of isolated product after column chromatography. [d]Step-II was carried out at 40 °C. [e]After

completion of step I, base (0.3 mmol) was added directly to the reaction mixture. [f]DABCO (1.5 equiv) was used. [g]ND = not detected

6.3.1.2 Plausible mechanism

On the basis of above results, we proposed a plausible mechanism for this sequential reaction as depicted in **Scheme 6.15**. For the synthesis of compound **3aa**, L-proline may react with α,β,γ,δ-unsaturated aldehyde to form a reactive iminium ion intermediate **2a′.** Afterwards, cyclic sulfamidate imine **1a** may nucleophilic attack exclusively at the β-carbon center of **2a′** to form an isolable Michael adduct **3aa′** via a hydrolysis of **3a**. Finally, the styrylpyridine **3aa** is generated from **3aa′** via an elimination of SO_3 under the influence of base, followed by iminocyclization-dehydration process of **4**.



Scheme 6.15 Plausible mechanism for the formation of 2-aryl-4-(*E*)-styrylpyridine

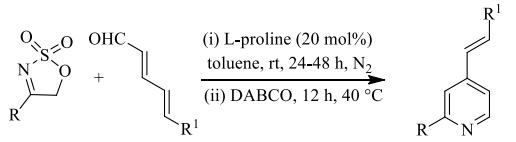
6.3.1.3 Generality and substrate scope

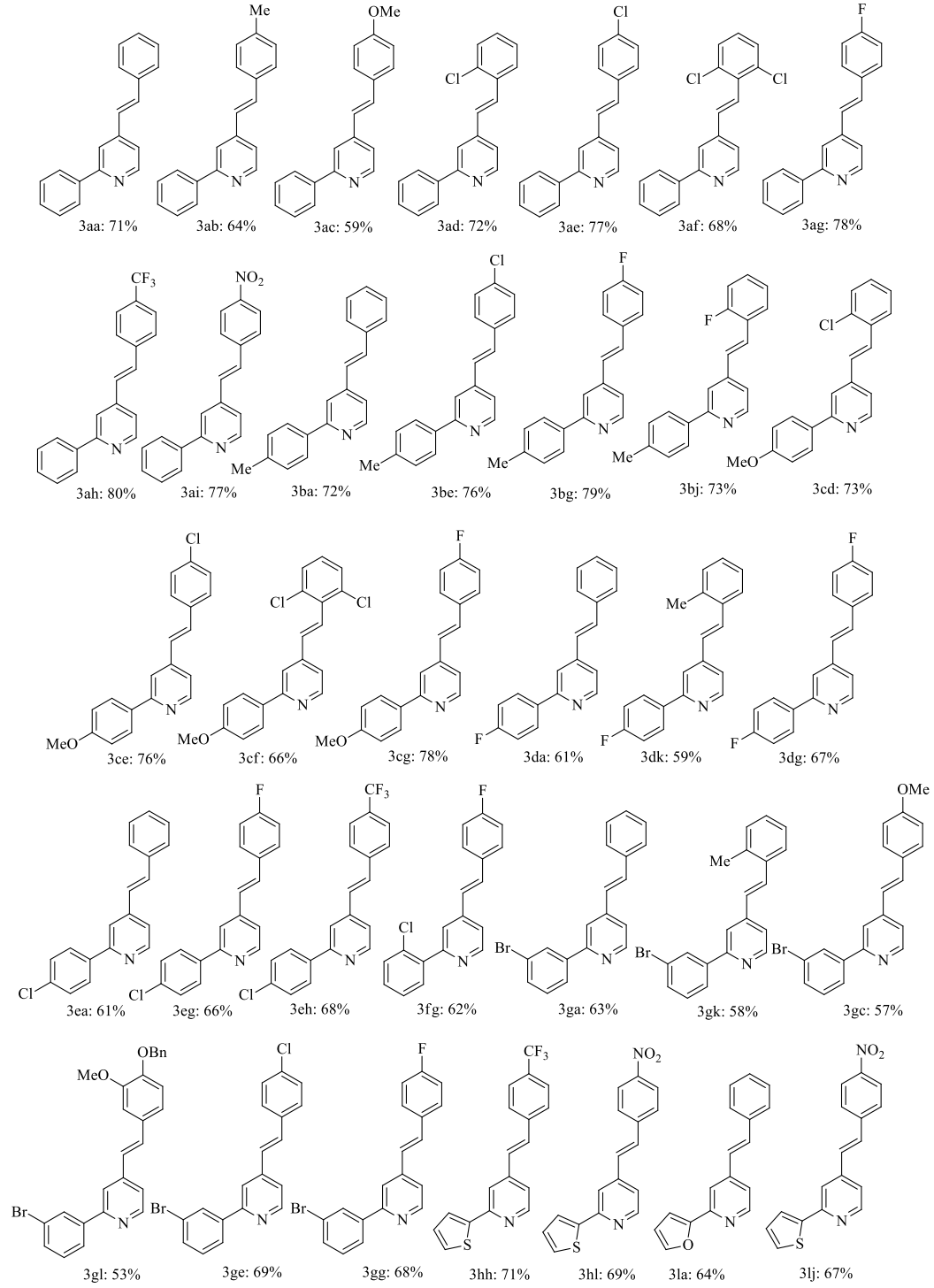
With these promising results in hand, , we proceeded to examine the scope and generality of this sequential reaction by employing several aryl/heteroaryl-substituted 5-membered cyclic sulfamidate imines and a wide range of α,β,γ,δ-unsaturated aldehydes as challenging electrophiles under imposed reaction conditions (entry **8**, Table **6.2**). The results have been included systematically in

Table 6.2. It is evident from Scheme 3, γ-aryl-substituted α,β,γ,δ-unsaturated aldehydes bearing electron withdrawing substituents (Cl, F, CF_3, NO_2) at C-2, C-4, C-6 positions on the aryl-rings coupled smoothly with cyclic imine **1a** to afford corresponding 2-phenyl-4-styrylpyridines (**3ad**-**3ai**) with slightly higher yields in comparison to electron donating ones (**3ab**-**3ac**) under similar reaction conditions (68-80% vs 59-64%). In contrast, attaching with electron withdrawing substituents F, Cl, Br at different positions of benzene rings of cyclic imines (**1d-1g**) obviously reduced their reactivities towards several substituted β-styrylacroleins as compared to electron releasing ones (**1b-1c**), resulting in 10-12% lower yields of desired pyridines (e.g. **3da**-**3gg** vs **3ba**-**3cf**; 53-69% vs 66-79%).

Pleasantly, 4-heteroaryl-substituted cyclic sulfamidate imines (**1h**-**1i**) were found to be suitable Michael donors for this reaction, while reacting with **2a**, **2h**, **2i** and **2j** as acceptors to give the desired 2-thiophenyl/furyl-4-styrylpyridine derivatives (**3hh**-**3ij**) in 64-71% yields. This pyridine-forming protocol is enough mild to bear several relevant functional groups including Me, MeO, OBn, F, Cl, Br, CF_3, NO_2, C=C, thiophene, furan, etc.

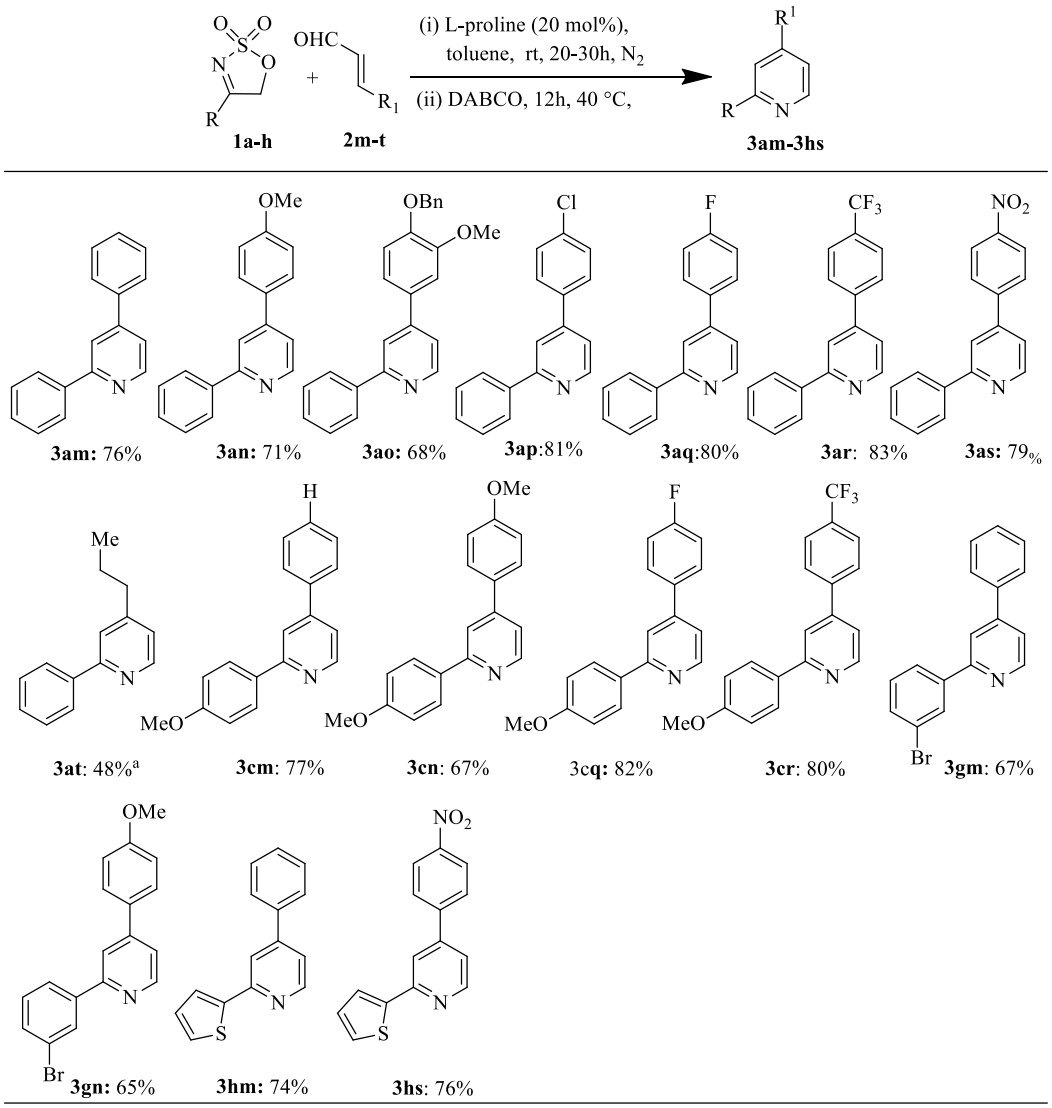
Table 6.2 One-pot synthesis of 2-aryl-4-styrylpyridines (**3aa-3ij**)





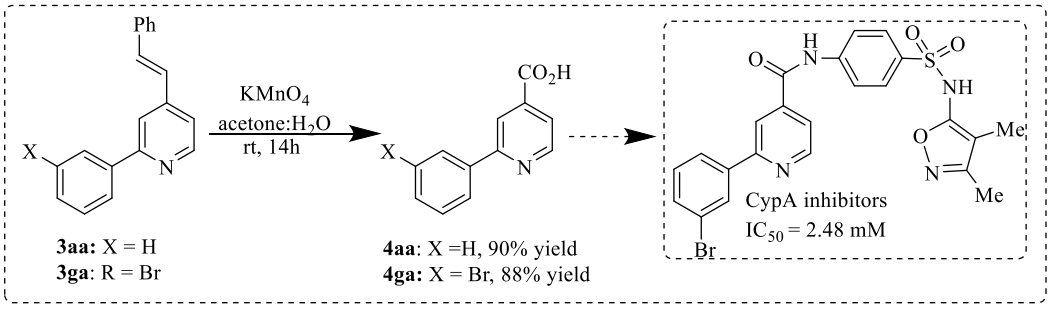
Next, we focused our efforts towards the facile creation of functionalized 2,4-diarylpyridines by involving several β-aryl-substituted acroleins as well-known Michael acceptors in the place of β-styryl-substituted acroleins in our established conditions (**Table 6.3**). It was witnessed that cyclic imine **1a** efficiently participated in the Michael reaction with a range of α,β-unsaturated aldehydes (**2m**-**2s**) bearing electron-donating (OMe, OBn) and electron-withdrawing (Cl, F, CF_3, NO_2) substituents on the benzene rings catalyzed by L-proline. As a consequence, all of the reactions led to the satisfactory to high yields (68-83%) of the corresponding 2-phenyl-4-arylpyridines (**3am**-**3as**) as these frameworks are widely used in the transition-metal catalyzed C-H functionalization reactions as well as preparation of a highly photoluminescent transition-metal complexes. Similarly, not only aryl-substituted cyclic imines (**1c** and **1g**) with MeO and Br groups on the aryl rings but also hetero-substituted cyclic imine **1h** underwent spotless reaction with a number of aryl-substituted acroleins by this procedure to produce the corresponding 2-aryl/heteroaryl-4-arylpyridines (**3cm**-**3hs**) in 65-82% yields. Most importantly, alkyl-substituted β-acrolein **2t** as a well-known poor Michael acceptor was also allowed to react with a cyclic imine **1a**, leading to the 4-alkylpyridine (**3at**) in a mediocre yield 48% after 72h (overall time). Therefore, this one-pot metal-free process certainly offers a good alternative procedure for making unsymmetrical 2,4-disubstituted pyridines under mild conditions (lower reaction temperature).

Table 6.3 Synthesis of 2,4-disubstitutedpyridines (**3am-3hs**)



6.3.1.4 Synthesis of 2-arylisonicotinic acid derivatives

In order to evaluate the synthetic application of our prepared compounds, the oxidation reactions of alkene double bonds of pyridines **3aa** and **3ga** have been performed in acetone by using $KMnO_4$ as a strong oxidising agent at room temperature for 14h to give commercially available 2-arylisonicotinic acids (**4aa-4ga**, 88-90%, **Scheme 6.16**) as useful intermediates for the synthesis of highly active CypA inhibitors.[37]



Scheme 6.16 Synthesis of 2-arylisonicotinic acid derivatives

6.4 Conclusion

Our current procedure is a unique, convenient, general metal-free based one-pot two-step sequential approach for the synthesis of an important category of a series of 2-aryl/heteroaryl-4-styryl/aryl/alkylpyridines *via* a regioselective Michael addition of a variety of aryl/heteroaryl-substituted cyclic sulfamidate imines with several β-styryl/aryl/alkyl-substituted acroleins using L-proline (20 mol%) as an organocatalyst, followed by elimination/cyclization/dehydration reaction of generated Michael adducts in the presence of DABCO. This unprecedented sequential reaction affords good to high yields of the title aza-heterocycles under mild conditions with tolerance of a several compatible functional groups. Furthermore, a practical synthesis of medicinally relevant 2-arylisonicotinic acids has been obtained through our developed method.

6.5 Experimental section

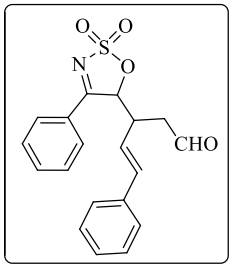
6.5.1 General Information

All the reactions were carried out either under inert atmosphere or air and monitored by TLC using Merck 60 F_{254} pre coated silica gel plates (0.25 mm thickness) and the products were visualized by UV detection. Flash chromatography was carried out with silica gel (200-300 mesh). ^{1}H and ^{13}C NMR spectra were recorded on a Bruker Avance (III) 400 MHz spectrometer. Data for ^{1}H NMR are reported as a chemical shift (δ ppm), multiplicity (s = singlet, d = doublet, q = quartet, m = multiplet), coupling constant *J* (Hz), integration, and assignment, data for ^{13}C are reported as a chemical shift. High resolutions mass spectral analyses (HRMS) were carried out using ESI-TOF-MS.

6.5.2 Materials

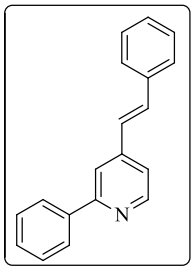
Cyclic sulfamidate imines **1a-i**[38,39] and β-substituted acroleins were either purchased from commercial sources or synthesized by literature known procedures. L-proline and bases were purchased from Sigma Aldrich.

Michael adduct 3aa′: **^{1}H NMR** (400 MHz, $CDCl_3$): δ 9.89 (s, 1H), 8.02 (d, *J* = 7.6 Hz, 2H), 7.71-7.75 (m, 1H), 7.57-7.61 (m, 2H), 8.18-7.27 (m, 5H), 6.21 (s, 1H), 5.90-6.02 (m, 2H), 3.53 (t, *J* = 8.8 Hz, 1H), 3.22 (m, 1H), 2.80-2.86 (m,1H); **^{13}C NMR** (100 MHz, $CDCl_3$): δ 200.1, 178.0, 135.6, 135.2, 135.0, 129.7, 129.6, 128.5, 128.2, 127.4, 126.5, 121.9, 89.1, 45.7, 40.6; **HRMS** (ESI) m/z calculated for $C_{19}H_{17}NO_4S$ $[M+Na]^+$: 378.0770, found 378.0758.



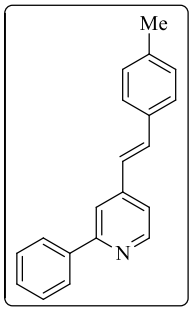
General experimental procedure for the synthesis of 2,4-disubstituted pyridine:

A mixture of cyclic sulfamidate imine (**1**, 0.2 mmol) and β-substituted acrolein (**2**, 0.24 mmol) in toluene (1.0 mL) was added L-proline (20 mol%, 11.5 mg) under N_2 atmosphere. The reaction mixture was allowed to stir at room temperature until complete consumption of the cyclic imine (monitored by TLC). Afterwards, DABCO (1.5 equiv) was added to the above reaction mixture at 40 °C for 12-16h. After completion of the reaction, the reaction mixture was extracted with EtOAc (3 × 10 mL), washed with brine and dried Na_2SO_4. The evaporation of organic solvent left the crude residue which was purified by column chromatography over silica-gel with hexane/ethyl acetate mixture as an eluent to deliver a pure 2,4-disubstitutedpyridine derivative. The product was characterized by ^1H, ^{13}C NMR and HRMS data. It should be noted that in some case the desired product was merged with an aldehyde spot. For this purpose, the crude reaction mixture was treated with $NaBH_4$ in MeOH at 0 °C, followed by usual work-up to give the crude mass. After that, product was purified by the above described method.

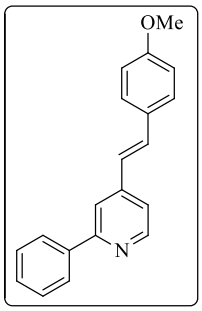


(*E*)-2-Phenyl-4-styrylpyridine (3aa):[40] (36.5 mg, 71%); **^{1}H NMR** (400 MHz, $CDCl_3$): δ 8.66 (d, *J* = 5.0 Hz, 1H), 8.03 (d, *J* = 7.5 Hz, 2H), 7.79 (s, 1H), 7.57 (d, *J* = 7.8 Hz, 2H), 7.50 (t, *J* = 7.2 Hz, 2H), 7.39-7.45 (m, 3H), 7.33-7.34 (m, 3H), 7.10 (d, *J* = 16.3 Hz, 1H); **^{13}C NMR** (100 MHz, $CDCl_3$): δ 158.4, 150.3, 145.8, 139.8, 136.5, 133.4, 129.3, 129.2, 129.0 (2C), 127.3, 127.3, 126.6, 119.5, 118.4; **HRMS** (ESI) m/z calculated for $C_{19}H_{15}N[M+H]^+$: 258.1277, found 258.1271.

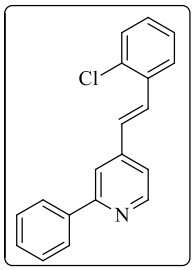
(*E*)-2-Phenyl-4-(4-methylstyryl)pyridine (3ab): (34.6 mg, 64%); **^{1}H NMR** (400 MHz, $CDCl_3$): δ 8.64 (d, *J* = 5.0 Hz, 1H), 8.02 (d, *J* = 7.2 Hz, 2H), 7.77 (s, 1H), 7.41-7.51 (m, 5H), 7.32-7.36 (m, 2H), 7.21 (d, *J* = 7.8 Hz, 2H), 7.05 (d, *J* = 16.3 Hz, 1H), 2.38 (s, 3H); **^{13}C NMR** (100 MHz, $CDCl_3$): δ 158.4, 150.3, 146.0, 139.9, 139.2, 133.8, 133.4, 129.9, 129.3, 129.0, 127.3, 127.3, 125.6, 119.4, 118.3, 22.0; **HRMS** (ESI) m/z calculated for $C_{20}H_{17}N[M+H]^+$: 272.1434, found 272.1432.



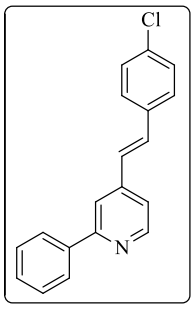
(*E*)-2-Phenyl-4-(4-methoxystyryl)pyridine (3ac):[40] (33.9 mg, 59%); **^{1}H NMR** (400 MHz, $CDCl_3$): δ 8.63 (d, *J* = 4.8 Hz, 1H), 8.02 (d, *J* = 7.2 Hz, 2H), 7.76 (s, 1H), 7.48-7.52 (m, 4H), 7.41-7.45 (m, 1H), 7.30-7.34 (m, 2H), 6.92-6.98 (m, 3H); **^{13}C NMR** (100 MHz, $CDCl_3$): δ 160.5, 158.1, 150.0, 146.3, 139.6, 133.1, 129.3, 129.2, 129.0, 128.7, 127.3, 124.3, 119.3, 118.2, 114.6, 55.7; **HRMS** (ESI) m/z calculated for $C_{20}H_{17}NO[M+H]^+$: 288.1383, found 288.1379.



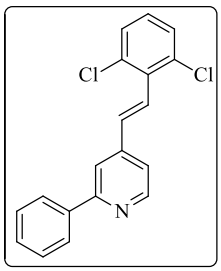
(*E*)-2-Phenyl-4-(2-chlorostyryl)pyridine (3ad): (41.9 mg, 72%); **^{1}H NMR** (400 MHz, $CDCl_3$): δ 8.68 (d, *J* = 5.0Hz, 1H), 8.02 (d, *J* = 8.7 Hz, 2H), 7.80 (s, 1H), 7.77 (d, *J* = 16.3 Hz, 1H), 7.70-7.73 (m, 1H), 7.50 (t, *J* = 7.0 Hz, 2H), 7.41-7.45 (m, 2H), 7.36-7.38 (m, 1H), 7.25-7.33 (m, 2H), 7.07 (d, *J* = 16.0 Hz, 1H); **^{13}C NMR** (100 MHz, $CDCl_3$): δ 158.5, 150.4, 145.4, 139.7, 134.7, 134.3, 130.3, 129.9, 129.5, 129.4, 129.2, 129.1, 127.4, 127.3, 127.2, 119.7, 118.7; **HRMS** (ESI) m/z calculated for $C_{19}H_{14}ClN[M+H]^+$: 292.0888, found 292.0892.



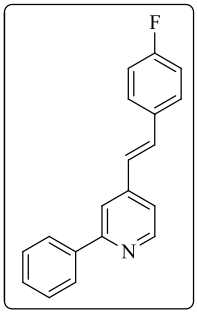
(*E*)-2-Phenyl-4-(4-chlorostyryl)pyridine (3ae): (44.8 mg, 77%); **^{1}H NMR** (400 MHz, $CDCl_3$): δ 8.66 (d, *J* = 5.0 Hz, 1H), 8.01 (d, *J* = 7.5 Hz, 2H), 7.77 (s, 1H), 7.48-7.50 (m, 4H), 7.41-7.45 (m, 1H), 7.37 (d, *J* = 8.2 Hz, 2H), 7.29-7.32 (m, 2H), 7.07 (d, *J* = 16.3 Hz, 1H); **^{13}C NMR** (100 MHz, $CDCl_3$): δ 158.5, 150.4, 145.4, 139.7, 135.0, 134.8, 132.1, 129.4, 129.4, 129.1, 128.5, 127.3, 127.2, 119.5, 118.4; **HRMS** (ESI) m/z calculated for $C_{19}H_{14}ClN[M+H]^+$: 292.0888, found 292.0873.



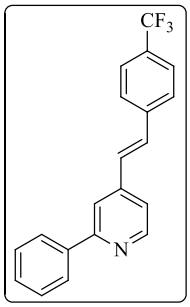
(*E*)-2-Phenyl-4-(2,6-dichlorostyryl)pyridine (3af): (44.3 mg, 68%); **^{1}H NMR** (400 MHz, $CDCl_3$): δ 8.70 (d, *J* = 5.04 Hz, 1H), 8.02 (d, *J* = 7.5 Hz, 2H), 7.80 (s, 1H), 7.49 (t, *J* = 7.2 Hz, 2H), 7.35-7.45 (m, 5H), 7.15-7.20 (m, 2H); **^{13}C NMR** (100 MHz, $CDCl_3$): δ 158.6, 150.4, 145.2, 139.7, 135.1, 135.0, 133.9, 129.4, 129.2, 129.1, 129.0, 127.3, 127.3, 119.6, 118.7; **HRMS** (ESI) m/z calculated for $C_{19}H_{13}Cl_2N[M+H]^+$: 326.0498, found 326.0495.



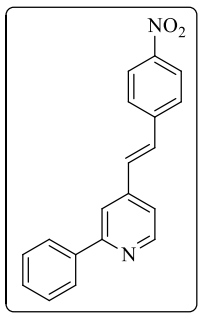
(*E*)-2-Phenyl-4-(4-fluorostyryl)pyridine (3ag): (43.0 mg, 78%); **^{1}H NMR** (400 MHz, $CDCl_3$): δ 8.66 (*J* = 5.2 Hz, 1H), 8.02 (d, *J* = 7.2 Hz, 2H), 7.77 (s, 1H), 7.48-7.55 (m, 4H), 7.41-7.45 (m, 1H), 7.30-7.34 (m, 2H), 7.09 (t, *J* = 8.5 Hz, 2H), 7.01 (d, *J* = 16.3 Hz, 1H); **^{13}C NMR** (100 MHz, $CDCl_3$): δ 163.3 (J_{C-F} = 247.1 Hz), 158.4, 150.3, 145.6, 139.7, 132.7 (J_{C-F} = 2.9 Hz), 132.1, 129.3, 129.1, 128.9 (J_{C-F} = 8.0 Hz), 127.3, 126.4 (J_{C-F} = 2.1 Hz), 119.4, 118.3, 116.2 (J_{C-F} = 21.8 Hz); **HRMS** (ESI) m/z calculated for $C_{19}H_{14}FN[M+H]^+$: 276.1183, found 276.1187.



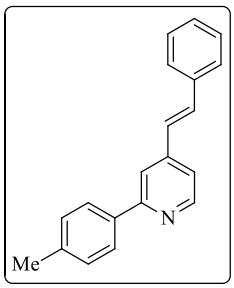
(*E*)-2-Phenyl-4-[4-(trifluoromethyl)styryl]pyridine (3ah): (52.0 mg, 80%); **^{1}H NMR** (400 MHz, $CDCl_3$): δ 8.69 (d, *J* = 5.0 Hz, 1H), 8.03 (d, *J* = 7.5 Hz, 2H), 7.80 (s, 1H), 7.66 (s, 4H), 7.48-7.52 (m, 2H), 7.42-7.46 (m, 1H), 7.34-7.39 (m, 2H), 7.18 (d, *J* = 16.2 Hz, 1H); **^{13}C NMR** (100 MHz, $CDCl_3$): δ 158.6, 150.5, 145.0, 140.0, 139.6, 131.8, 130.8, 130.5, 129.4, 129.2, 129.1, 127.4, 127.3, 126.1 (q, *J* = 3.6 Hz), 119.6, 118.5; **HRMS** (ESI) m/z calculated for $C_{20}H_{14}F_3N[M+H]^+$: 326.1151, found 326.1174.



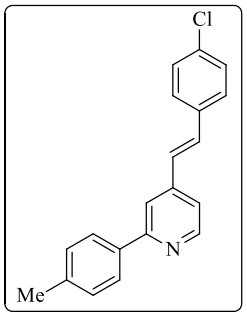
(*E*)-2-phenyl-4-(4-nitrostyryl)pyridine (3ai):[40](46.5 mg, 77%); **^{1}H NMR** (400 MHz, $CDCl_3$): δ 8.70 (d, *J* = 4.5 Hz, 1H), 8.25 (d, *J* = 8.2 Hz, 2H), 8.01 (d, *J* = 7.2 Hz, 2H), 7.80 (s, 1H), 7.68 (d, *J* = 8.2 Hz, 2H), 7.34-7.51 (m, 5H), 7.21-7.26 (m, 1H); **^{13}C NMR** (100 MHz, $CDCl_3$): δ 158.7, 150.6, 147.8, 144.5, 142.8, 139.4, 131.1, 130.9, 129.5, 129.1, 127.8, 127.3, 124.5, 119.6, 118.6; **HRMS** (ESI) m/z calculated for $C_{19}H_{14}N_2O_2[M+H]^+$: 303.1128, found 303.1123.



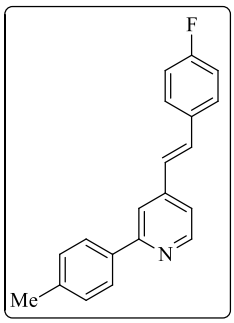
(*E*)-2-(4-Methylphenyl)-4-styrylpyridine (3ba): (39.0 mg, 72%); **^{1}H NMR** (400 MHz, $CDCl_3$): δ 8.64 (d, *J* = 5.0 Hz, 1H), 7.94 (d, *J* = 7.8 Hz, 2H), 7.75 (s, 1H), 7.56 (d, *J* = 7.5 Hz, 2H), 7.40 (t, *J* = 7.2 Hz, 2H), 7.35-7.36 (m, 1H), 7.30-7.32 (m, 4H), 7.08 (d, *J* = 16.3 Hz, 1H), 2.42 (s, 3H); **^{13}C NMR** (100 MHz, $CDCl_3$): δ 158.3, 150.2, 145.6, 139.2, 136.9, 136.5, 133.2, 129.7, 129.1, 128.9, 127.3, 127.1, 126.6, 119.1, 118.0, 21.5; **HRMS** (ESI) m/z calculated for $C_{20}H_{17}N[M+H]^+$: 272.1434, found 272.1434.



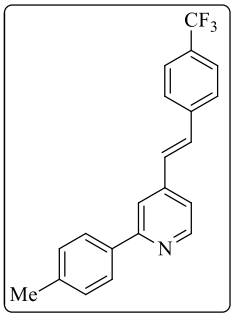
(*E*)-2-(4-Methylphenyl)-4-(4-chlorostyryl)pyridine (3be): (46.3 mg, 76%); **^{1}H NMR** (400 MHz, $CDCl_3$): δ 8.63 (d, *J* = 5 Hz, 1H), 7.91 (d, *J* = 8.0 Hz, 2H), 7.74 (s, 1H), 7.48 (d, *J* = 8.5 Hz, 2H), 7.36 (d, *J* = 8.5 Hz, 2H), 7.27-7.30 (m, 4H), 7.05 (d, *J* = 16.3 Hz, 1H), 2.41 (s, 3H); **^{13}C NMR** (100 MHz, $CDCl_3$): δ 158.4, 150.3, 145.3, 139.4, 136.8, 135.1, 134.7, 131.9, 129.8, 129.3, 128.5, 127.3, 127.1, 119.1, 118.1, 21.6; **HRMS** (ESI) m/z calculated for $C_{20}H_{16}ClN[M+H]^+$: 306.1044, found 306.1046.

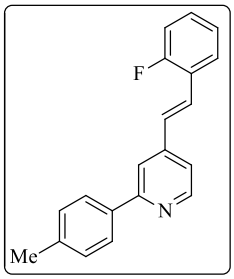


(*E*)-2-(4-Methylphenyl)-4-(4-fluorostyryl)pyridine (3bg): (45.6 mg, 79%); **^{1}H NMR** (400 MHz, $CDCl_3$): δ 8.63 (d, *J* = 5.2 Hz, 1H), 7.92 (d, *J* = 8.0 Hz, 2H), 7.74 (s, 1H), 7.52-7.55 (m, 2H), 7.29-7.33 (m, 4H), 7.09 (t, *J* = 8.2 Hz, 2H), 7.00 (d, *J* = 16.2 Hz, 1H), 2.42 (s, 3H); **^{13}C NMR** (100 MHz, $CDCl_3$): δ 163.2 (J_{C-F} = 247.9 Hz), 158.4, 150.3, 145.5, 139.3, 136.9, 132.8 (J_{C-F} = 2.9 Hz), 132.0, 129.8, 128.9 (J_{C-F} = 8.7 Hz), 127.1, 126.5 (J_{C-F} = 2.1 Hz), 119.1, 118.0, 116.2 (J_{C-F} = 21.8 Hz), 21.6; **HRMS** (ESI) m/z calculated for $C_{20}H_{16}FN[M+H]^+$: 290.1340, found 290.1332.

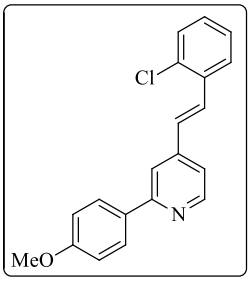


(*E*)-2-(4-Methylphenyl)-4-[4-trifluoromethylstyryl]pyridine (3bh): (52.7 mg, 78%); **^{1}H NMR** (400 MHz, $CDCl_3$): δ 8.66 (d, *J* = 5.2 Hz, 1H), 7.93 (d, *J* = 8.0 Hz, 2H), 7.77 (s, 1H), 7.65 (s, 4H), 7.29-7.38 (m, 4H), 7.17 (d, *J* = 16.3 Hz, 1H), 2.42 (s, 3H); **^{13}C NMR** (100 MHz, $CDCl_3$): δ 158.5, 150.4, 144.9, 140.0, 139.5, 136.8, 131.6, 130.8, 130.4, 129.8, 129.3, 127.4, 127.1, 126.1 (q, J_{C-F} = 3.6 Hz), 119.3, 118.2, 21.6 ; **HRMS** (ESI) m/z calculated for $C_{21}H_{16}F_3N[M+H]^+$: 340.1308, found 340.1300.

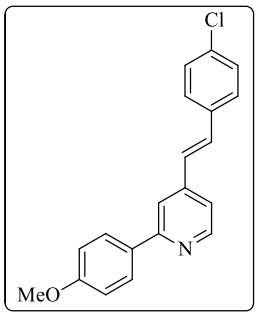


(*E*)-2-(4-Methylphenyl)-4-[2-fluorostyryl]pyridine (3bj): (42.1 mg, 73%); 

^{1}H NMR (400 MHz, $CDCl_3$): δ 8.65 (d, *J* = 4.5 Hz, 1H), 7.93 (d, *J* = 7.5 Hz, 2H), 7.77 (s, 1H), 7.63 (t, *J* = 7.2 Hz, 1H), 7.50 (d, *J* = 16.3 Hz), 7.29-7.31(m, 4H), 7.09-7.19 (m, 3H), 2.42 (s, 3H); **^{13}C NMR** (100 MHz, $CDCl_3$): δ 161.0 (d, J_{C-F} = 249.3 Hz), 158.4, 150.2, 145.5, 139.3, 136.9, 130.2 (d, J_{C-F} = 8.0 Hz), 129.8, 129.0 (d, J_{C-F} = 5.1 Hz), 127.9 (d, J_{C-F} = 2.9 Hz), 127.1, 125.6 (d, J_{C-F} = 3.4 Hz), 124.7 (d, J_{C-F} = 2.9 Hz), 124.5 (d, J_{C-F} = 11.6 Hz), 119.2, 118.2, 116.3 (d, J_{C-F} = 21.8 Hz), 21.6; **HRMS** (ESI) m/z calculated for $C_{20}H_{16}FN[M+Na]^+$: 290.1340, found 290.1338.

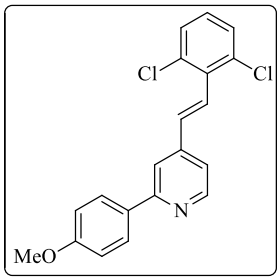
(*E*)-2-(4-Methoxyphenyl)-4-(2-chlorostyryl)pyridine (3cd): (46.8 mg, 73%); 

^{1}H NMR (400 MHz, $CDCl_3$): δ 8.56 (d, *J* = 5 Hz, 1H), 7.90 (d, *J* = 8.8 Hz, 2H), 7.63-7.66 (m, 3H), 7.35 (d, *J* = 7.5 Hz, 1H), 7.20-7.25 (m, 3H), 6.93-7.00 (m, 3H); **^{13}C NMR** (100 MHz, $CDCl_3$): δ 160.9, 158.1, 150.2, 145.4, 134.7, 134.2, 132.2, 130.3, 129.9, 129.3, 129.3, 128.6, 127.4, 127.1, 119.0, 118.0, 114.4, 55.7; **HRMS** (ESI) m/z calculated for $C_{20}H_{16}ClNO[M+H]^+$: 322.0993, found 322.0976.

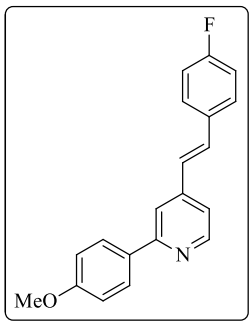
(*E*)-2-(4-Methoxyphenyl)-4-(4-chlorostyryl)pyridine (3ce): (48.4 mg, 76%); 

^{1}H NMR (400 MHz, $CDCl_3$): δ 8.56 (d, *J* = 5 Hz, 1H), 7.93 (d, *J* = 8.5 Hz, 2H), 7.65 (s, 1H), 7.43 (d, *J* = 8.2 Hz, 2H), 7.31 (d, *J* = 8.2 Hz, 2H), 7.21 (s, 2H), 6.95-7.02 (m, 3H), 3.82 (s, 3H); **^{13}C NMR** (100 MHz, $CDCl_3$): δ 160.8, 158.1, 150.2, 145.3, 135.1, 134.7, 132.2, 131.9, 129.3, 128.5, 128.4, 127.3, 118.7, 117.7, 114.4, 55.7; **HRMS** (ESI) m/z calculated for $C_{20}H_{16}ClNO[M+H]^+$: 322.0993, found 322.0987.

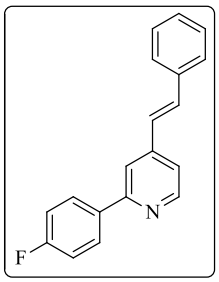
(*E*)-2-(4-Methoxyphenyl)-4-(2,6-dichlorostyryl)pyridine (3cf): (46.8 mg, 66%); **^{1}H NMR** (400 MHz, $CDCl_3$): δ 8.72 (d, *J* = 4.2 Hz, 1H), 8.06 (d, *J* = 7.2 Hz, 2H), 7.81 (s, 1H), 7.45 (d, *J* = 8 Hz, 2H), 7.39-7.42 (m, 1H), 7.33 (s, 1H), 7.21-7.26 (m, 2H), 7.08 (d, *J* = 7.5 Hz, 2H), 3.94 (s, 3H); **^{13}C NMR** (100 MHz, $CDCl_3$): δ 160.9, 158.2, 150.3, 145.1, 135.2, 135.0, 134.0, 132.2, 135.0, 134.0, 132.2, 129.1, 129.0, 128.6, 127.1, 118.9, 118.0, 114.4, 55.7; **HRMS** (ESI) m/z calculated for $C_{20}H_{15}Cl_2NO[M+H]^+$: 356.0603, found 356.0596.



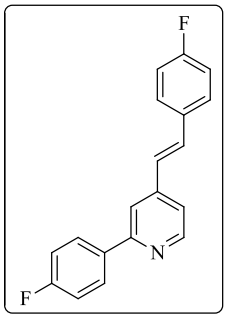
(*E*)-2-(4-Methoxyphenyl)-4-(4-fluorostyrylpyridine (3cg): (47.5 mg, 78%); **^{1}H NMR** (400 MHz, $CDCl_3$): δ 8.61 (d, *J* = 5.0 Hz, 1H), 7.97 (d, *J* = 8.8 Hz, 2H), 7.70 (s, 1H)7.52-7.55 (m, 2H), 7.26-7.32 (m, 2H), 7.09 (t, *J* = 8.5 Hz, 2H), 6.98-7.02 (m, 3H), 3.87 (s, 3H); **^{13}C NMR** (100 MHz, $CDCl_3$): δ 163.3 (J_{C-F} = 247.1 Hz), 160.8, 158.0, 150.1, 145.5, 132.8 (J_{C-F} = 3.6 Hz), 132.3, 132.0, 129.0 (J_{C-F} = 8.0 Hz), 128.6, 126.5 (J_{C-F} = 2.9 Hz), 118.7, 117.7, 116.2 (J_{C-F} = 21.1 Hz), 114.4, 55.7; **HRMS** (ESI) m/z calculated for $C_{20}H_{16}FNO[M+H]^+$: 306.1289, found 306.1291.



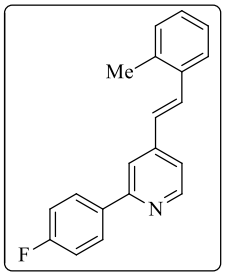
(*E*)-2-(4-Fluorophenyl)-4-styrylpyridine (3da): (33.5 mg, 61%); **^{1}H NMR** (400 MHz, $CDCl_3$): δ 8.63 (d, *J* = 4.5 Hz, 1H), 8.01 (t, *J* = 6.2 Hz, 2H), 7.73 (s, 1H), 7.56 (d, *J* = 7.2 Hz, 2H), 7.38-7.42 (m, 2H), 7.32-7.35 (m, 3H), 7.17 (t, *J* = 8.0 Hz, 2H), 7.09 (d, *J* = 16.0 Hz, 1H); **^{13}C NMR** (100 MHz, $CDCl_3$): δ 163.8 (J_{C-F} = 247.1 Hz), 157.4, 150.3, 145.8, 136.2 (J_{C-F} = 51.7 Hz), 135.5, 129.2, 129.1, 129.1, 129.0, 127.3, 126.5, 119.4, 118.0, 115.9 (J_{C-F} = 21.1 Hz); **HRMS** (ESI) m/z calculated for $C_{19}H_{14}FN[M+H]^+$: 276.1183, found 276.1190.



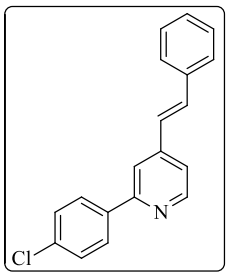
(*E*)-2-(4-Fluorophenyl)-4-(4-fluorostyryl)pyridine (3dg): (39.2 mg, 67%); **^{1}H NMR** (400 MHz, $CDCl_3$): δ 8.56 (d, *J* = 5.0 Hz, 1H), 7.91-7.95 (m, 2H), 7.64 (s, 1H), 7.44-7.48 (m, 2H), 7.22-7.26 (m, 2H), 7.10 (t, *J* = 8.5 Hz, 2H), 7.02 (t, *J* = 8.5 Hz, 2H), 6.93 (*J* = 16.2 Hz, 1H); **^{13}C NMR** (100 MHz, $CDCl_3$): δ 164.8 (J_{C-F} = 56.8 Hz),162.3 (J_{C-F} = 57.6 Hz), 157.4, 150.3, 145.7, 135.8 (J_{C-F} = 3.6 Hz), 132.7 (J_{C-F} = 3.6 Hz), 132.3, 129.1 (J_{C-F} = 8.7 Hz), 128.9 (J_{C-F} = 8.0 Hz), 126.3 (J_{C-F} = 2.1 Hz), 119.4, 118.0, 116.2 (J_{C-F} = 21.1 Hz), 116.0 (J_{C-F} = 21.1 Hz); **HRMS** (ESI) m/z calculated for $C_{19}H_{13}F_2N[M+H]^+$: 294.1089, found 294.1081.



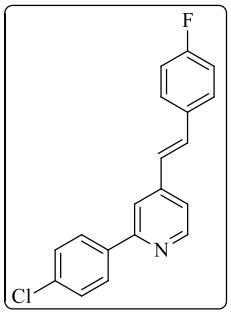
(*E*)-2-(4-Fluorophenyl)-4-(2-methylstyryl)pyridine (3dk): (34.0 mg, 59%); **^{1}H NMR** (400 MHz, $CDCl_3$): δ 8.63 (d, *J* = 5.0 Hz, 1H), 7.99-8.02 (m, 2H), 7.71 (s, 1H), 7.57-7.63 (m, 2H), 7.33(d, *J* = 5.0 Hz, 1H), 7.21-7.26 (m, 3H), 7.17 (t, *J* = 8.7 Hz, 2H), 6.98 (d, *J* = 16.0 Hz, 1H), 2.46 (s, 3H); **^{13}C NMR** (100 MHz, $CDCl_3$): δ 165.1, 162.6, 157.4, 150.3, 146.1, 136.7, 135.9, 135.9, 135.6, 131.3, 130.9, 129.1, 129.0, 128.9, 127.8, 126.7, 126.0, 119.4, 118.2, 116.0, 115.8, 20.2 ; **HRMS** (ESI) m/z calculated for $C_{20}H_{16}FN[M+H]^+$: 290.1340, found 290.1345.



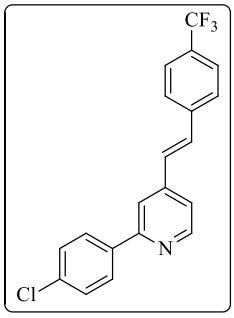
-2-(4-Chlorophenyl)-4-styrylpyridine (3ea): (35.5 mg, 61%); **^{1}H NMR** (400 MHz, $CDCl_3$): δ 8.64 (d, *J* = 5.2 Hz, 1H), 7.98 (d, *J* = 8.5 Hz, 2H), 7.75 (s, 1H), 7.56 (d, *J* = 7.2 Hz, 2H), 7.45-7.47 (m, 2H), 7.38-7.42 (m, 2H), 7.34-7.35 (m, 3H), 7.09 (d, *J* = 16.3 Hz, 1H); **^{13}C NMR** (100 MHz, $CDCl_3$): δ 157.1, 150.4, 145.9, 138.2, 136.4, 135.4, 133.6, 129.2, 129.2, 129.1, 128.6, 127.4, 126.4, 119.7, 118.1; **HRMS** (ESI) m/z calculated for $C_{19}H_{14}ClN[M+H]^+$: 292.0888, found 292.0902.



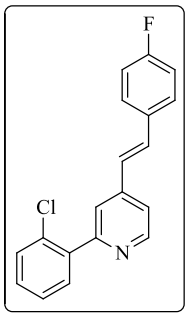
(*E*)-2-(4-Chlorophenyl)-4-(4-fluorostyryl)pyridine (3eg): (40.7 mg, 66%); **^{1}H NMR** (400 MHz, $CDCl_3$): δ 8.64 (d, *J* = 5.0 Hz, 1H), 7.97 (d, *J* = 8.2 Hz, 2H), 7.73 (s, 1H), 7.53 (t, *J* = 7.5 Hz, 2H), 7.45 (d, *J* = 8.0 Hz, 2H), 7.29-7.33 (m, 2H), 7.09 (t, *J* = 8.2 Hz, 2H), 6.99 (d, *J* = 16.3 Hz, 1H); **^{13}C NMR** (100 MHz, $CDCl_3$): δ 163.3 (d, J_{C-F} = 247.9 Hz), 157.2, 150.4, 145.7, 138.1, 135.5, 132.6 (d, J_{C-F} = 2.9 Hz), 129.2, 129.0 (d, J_{C-F} = 8.7 Hz), 128.5, 126.2, 126.2, 119.6, 118.0, 116.2 (d, J_{C-F} = 21 Hz); **HRMS** (ESI) m/z calculated for $C_{19}H_{13}ClFN[M+H]^+$: 310.0793, found 310.0793.



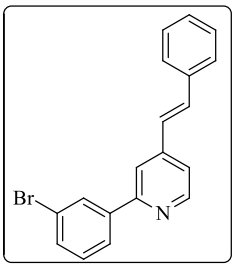
(*E*)-2-(4-Chlorophenyl)-4-(4-(trifluoromethyl)styryl)pyridine (3eh): (48.8 mg, 68%); **^{1}H NMR** (400 MHz, $CDCl_3$): δ 8.66 (d, *J* = 5.0 Hz, 1H), 7.97 (d, *J* = 8.2 Hz, 2H), 7.75 (s, 1H), 7.65 (s, 4H), 7.45 (d, *J* = 8.2 Hz, 2H), 7.33-7.37 (m, 2H), 7.15 (d, *J* = 16.3 Hz, 1H); **^{13}C NMR** (100 MHz, $CDCl_3$): δ 157.3, 150.5, 145.1, 139.8, 138.0, 135.6, 131.9, 129.2, 128.9, 128.5, 127.4, 126.1 (q, J_{C-F} = 3.6 Hz), 125.7, 123.0, 119.8, 118.2; **HRMS** (ESI) m/z calculated for $C_{20}H_{13}ClF_3N[M+H]^+$: 360.0761, found 360.0767.



(*E*)-2-(2-Chlorophenyl)-4-(4-fluorostyryl)pyridine (3fg): (38.3 mg, 62%); **^{1}H NMR** (400 MHz, $CDCl_3$): δ 8.67 (d, *J* = 4.7 Hz, 1H), 7.69 (s, 1H), 7.61 (d, *J* = 6.7 Hz, 1H), 7.48-7.53 (m, 3H), 7.27-7.39 (m, 4H), 7.08 (t, *J* = 8.0 Hz, 2H), 6.99 (d, *J* = 16.2 Hz, 1H) ; **^{13}C NMR** (100 MHz, $CDCl_3$): δ 163.3 (d, J_{C-F} = 247.1Hz), 157.7, 150.2, 144.8, 139.5, 132.7 (d, J_{C-F} = 2.9 Hz), 132.4, 131.8, 130.4, 129.9, 129.0, 128.9, 127.3, 126.1 (d, J_{C-F} = 2.1 Hz), 122.3, 119.8, 116.2 (d, J_{C-F} = 21.8 Hz); **HRMS** (ESI) m/z calculated for $C_{19}H_{13}ClFN$ $[M+H]^+$: 310.0793, found 310.0794.

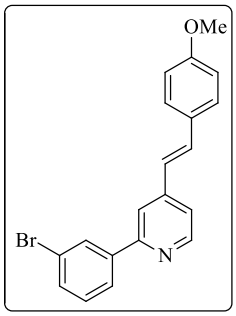


(*E*)-2-(3-Bromophenyl)-4-styrylpyridine (3ga): (42.3 mg, 63%); **^{1}H NMR** (400



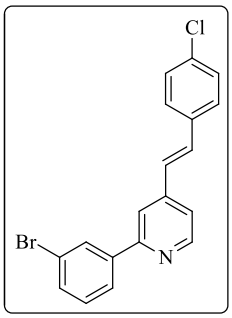
MHz, $CDCl_3$): δ 8.65 (d, *J* = 4.7 Hz, 1H), 8.20 (s, 1H), 7.95 (d, *J* = 7.5 Hz, 1H), 7.75 (s, 1H), 7.54-7.58 (m, 3H), 7.34-7.43 (m, 6H), 7.08 (d, *J* = 16.2 Hz, 1H); **^{13}C NMR** (100 MHz, $CDCl_3$): δ 156.7, 150.4, 145.9, 141.8, 136.4, 133.7, 132.2, 130.5, 130.3, 129.2, 129.1, 127.4, 126.3, 125.8, 123.3, 120.0, 118.3; **HRMS** (ESI) m/z calculated for $C_{19}H_{14}{}^{79}BrN[M+H]^+$: 336.0382, found 336.0383. $C_{19}H_{14}{}^{81}BrN[M+H]^+$: 338.0363, found 338.0365.

(*E*)-2-(3-Bromophenyl)-4-(4-methoxystyryl)pyridine (3gc): (41.7 mg, 57%) ;



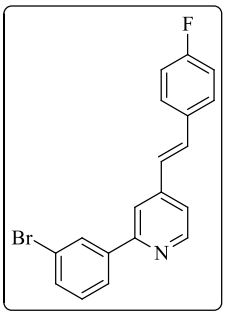
^{1}H NMR (400 MHz, $CDCl_3$): δ 8.61 (d, *J* = 5.0 Hz, 1H), 8.19 (s, 1H), 7.94 (d, *J* = 7.5 Hz, 1H), 7.71 (s, 1H), 7.49-7.55 (m, 3H), 7.29-7.36 (m, 3H), 6.92-6.95 (m, 3H), 3.84 (s, 3H); **^{13}C NMR** (100 MHz, $CDCl_3$): δ 160.5, 156.6, 150.3, 146.3, 141.9, 133.2, 132.1, 130.5, 130.3, 129.1, 128.7, 125.8, 124.0, 123.3, 119.8, 118.1, 114.6, 55.6; **HRMS** (ESI) m/z calculated for $C_{20}H_{16}{}^{79}BrNO[M+H]^+$: 366.0448, found 366.0490; $C_{20}H_{16}{}^{81}BrNO[M+H]^+$: 368.0468, found 368.0471.

(*E*)-2-(3-Bromophenyl)-4-(4-chlorostyryl)pyridine (3ge): (51.1 mg, 69%); **^{1}H**

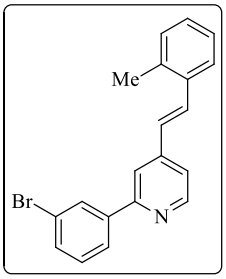


NMR (400 MHz, $CDCl_3$): δ 8.65 (d, *J* = 4.2 Hz, 1H), 8.18 (s, 1H), 7.94 (d, *J* = 7.7 Hz, 1H), 7.73 (s, 1H), 7.55 (d, *J* = 7.7 Hz, 1H), 7.48 (d, *J* = 7.8 Hz, 2H), 7.28-7.38 (m, 5H), 7.04 (d, *J* = 16.2 Hz, 1H); **^{13}C NMR** (100 MHz, $CDCl_3$): δ 156.8, 150.5, 145.6, 141.7, 134.9, 134.8, 132.3, 132.2, 130.5, 130.3, 129.4, 128.5, 126.9, 125.8, 123.3, 120.0, 118.3; **HRMS** (ESI) m/z calculated for $C_{19}H_{13}{}^{79}BrClN[M+H]^+$: 369.9993, found 369.9991, $C_{19}H_{13}{}^{81}BrClN[M+H]^+$: 371.9972, found 371.9968.

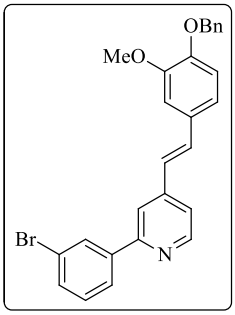
(*E*)-2-(3-Bromophenyl)-4-(4-fluorostyryl)pyridine (3gg): (48.1 mg, 68%); **^{1}H NMR** (400 MHz, $CDCl_3$): δ 8.65 (d, *J* = 4.5 Hz, 1H), 8.19 (s, 1H), 7.95 (d, *J* = 7.7 Hz, 2H), 7.74 (s, 1H), 7.53-7.56 (m, 3H), 7.31-7.38 (m, 3H), 7.10 (t, *J* = 8.2 Hz, 2H), 7.00 (d, *J* = 16.3 Hz, 1H); **^{13}C NMR** (100 MHz, $CDCl_3$): δ 163.3(J_{C-F} = 247.1 Hz), 156.8, 150.4, 145.9, 141.7, 132.6 (J_{C-F} = 2.9 Hz), 132.5, 132.3, 130.6, 130.4, 129.0 (J_{C-F} = 8.0 Hz), 126.1(J_{C-F} = 2.1 Hz), 125.8, 123.3, 120.0, 118.3, 116.3 (J_{C-F} = 21.1 Hz); **HRMS** (ESI) m/z calculated for $C_{19}H_{13}{}^{79}BrFN[M+H]^+$: 354.0288, found 354.0279; $C_{19}H_{13}{}^{81}BrFN[M+H]^+$: 356.0268, found 356.0260.



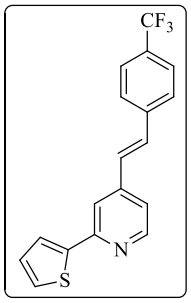
(*E*)-2-(3-Bromophenyl)-4-(2-methylstyryl)pyridine (3gk): (40.6 mg, 58%); **^{1}H NMR** (400 MHz, $CDCl_3$): δ 8.58 (d, *J* = 3.5 Hz, 1H), 8.11 (s, 1H), 7.86 (d, *J* = 7.5 Hz, 1H), 7.65 (s, 1H), 7.46-7.54 (m, 3H), 7.28 (d, *J* = 6.2 Hz, 2H), 7.16-7.17 (m, 3H), 6.90 (d, *J* = 16.0 Hz, 1H); **^{13}C NMR** (100 MHz, $CDCl_3$): δ 155.7, 149.3, 145.3, 140.7, 135.7, 134.5, 131.2, 130.5, 129.9, 129.5, 129.4, 128.0, 126.6, 125.7, 125.0, 124.8, 122.3, 119.0, 117.6, 19.2; **HRMS** (ESI) m/z calculated for $C_{20}H_{16}{}^{79}BrN[M+H]^+$: 350.0539, found 350.0530; $C_{20}H_{16}{}^{81}BrN[M+H]^+$: 352.0519, found 352.0513.



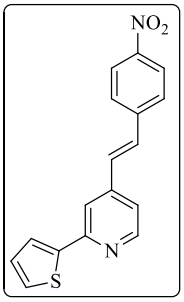
(*E*)-2-(3-bromophenyl)-4-(4-(benzyloxy)-3-methoxystyryl)pyridine (3gl): (50.0 mg, 53%); **^{1}H NMR** (400 MHz, $CDCl_3$): δ 8.61 (d, *J* = 4.8 Hz, 1H), 8.18 (s, 1H), 7.94 (d, *J* = 7.7 Hz, 1H), 7.71 (s, 1H), 7.54 (d, *J* = 7.7 Hz, 1H), 7.43-7.45 (m, 2H), 7.25-7.39 (m, 6H), 7.12 (s, 1H), 7.04 (d, *J* = 8.0 Hz, 1H), 6.88-6.95 (m, 2H), 5.19 (s, 2H), 3.96 (s, 3H); **^{13}C NMR** (100 MHz, $CDCl_3$): δ 156.6, 150.3, 150.2, 149.4, 146.2, 141.8, 137.1, 133.4, 132.1, 130.5, 130.3, 129.9, 128.9, 128.2, 127.5, 125.8, 124.4, 123.3, 121.0, 119.8, 118.1, 114.1, 110.0, 71.2, 56.3; **HRMS** (ESI) m/z calculated for $C_{27}H_{22}{}^{79}BrNO_2[M+H]^+$: 472.0907, found 472.0912; $C_{27}H_{22}{}^{81}BrNO_2[M+H]^+$: 474.0888, found 474.0889.



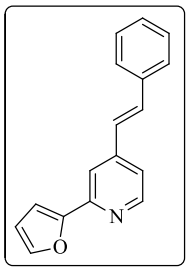
(*E*)-2-(Thiophen-2-yl)-4-[4-(trifluoromethyl)styryl]pyridine (3hh): (47.0 mg, 71%); **^{1}H NMR** (400 MHz, $CDCl_3$): δ 8.56 (d, *J* = 5.0 Hz, 1H), 7.72 (s, 1H), 7.65 (s, 5H), 7.42 (d, *J* = 4.7 Hz, 1H), 7.35 (d, *J* = 16.3 Hz, 1H), 7.26-7.27 (m, 1H), 7.12-7.16 (m, 2H); **^{13}C NMR** (100 MHz, $CDCl_3$): δ 153.5, 150.3, 150.1, 144.9, 139.9, 131.9, 129.4, 128.9, 128.4, 128.3, 128.1, 127.5, 126.1 (q, $J_{C\text{-}F}$ = 3.6 Hz), 125.0, 119.3, 116.7; **HRMS** (ESI) m/z calculated for $C_{18}H_{12}F_3NS[M+H]^+$ 332.0715, found 332.0711.



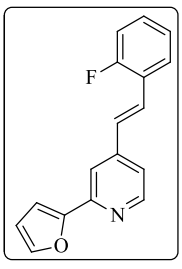
(*E*)-2-(Thiophen-2-yl)-4-(4-nitrostyryl)pyridine (3hi): (42.5 mg, 69%); **^{1}H NMR** (400 MHz, $CDCl_3$): δ 8.58 (d, *J* = 4.2 Hz), 8.26 (d, *J* = 8.0 Hz, 2H), 7.66-7.73 (m, 4H), 7.35-7.43 (m, 2H), 7.14-7.28 (m, 3H); **^{13}C NMR** (100 MHz, $CDCl_3$): δ 153.7, 150.4, 147.9, 144.8, 144.5, 142.8, 131.0, 130.8, 128.4, 128.2, 127.8, 125.1, 124.6, 119.3, 116.8; **HRMS** (ESI) m/z calculated for $C_{17}H_{12}N_2O_2S[M+H]^+$: 309.0692, found 309.0692.



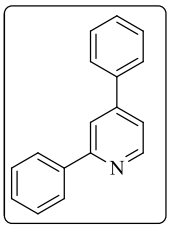
(*E*)-2-(Furan-2-yl)-4-styrylpyridine (3ia)*:* (31.6 mg, 64%); **^{1}H NMR** (400 MHz, $CDCl_3$): δ 8.56 (d, *J* = 5.0 Hz, 1H), 7.79 (s, 1H), 7.56-7.58 (m, 3H), 7.32-7.43 (m, 4H), 7.24-7.27 (m, 1H), 7.05-7.09 (m, 2H), 6.56 (s, 1H); **^{13}C NMR** (100 MHz, $CDCl_3$): δ 153.9, 150.3, 150.1, 145.7, 143.6, 136.5, 133.6, 129.2, 129.1, 127.4, 126.4, 119.4, 116.1, 112.4, 109.0; **HRMS** (ESI) m/z calculated for $C_{17}H_{13}NO[M+H]^+$: 248.1070, found 248.1062.



(*E*)-2-(Furan-2-yl)-4-(2-fluorostyryl)pyridine (3ij): (35.5 mg, 67%); **^{1}H NMR** (400 MHz, $CDCl_3$): δ 8.63 (d, *J* = 4.5 Hz, 1H), 7.85 (s, 1H), 7.68 (t, *J* = 7.5 Hz, 1H), 7.55-7.62 (m, 2H), 7.16-7.37 (m, 7 H), 6.61 (s, 1H); **^{13}C NMR** (100 MHz, $CDCl_3$): δ 161.0 ($J_{C\text{-}F}$ = 250.1 Hz), 153.8, 150.3, 150.2, 145.6, 143.6, 130.3 ($J_{C\text{-}F}$ = 8.7 Hz), 128.6 ($J_{C\text{-}F}$ = 5.1 Hz), 127.9 ($J_{C\text{-}F}$ = 2.9 Hz) 126.0 ($J_{C\text{-}F}$ = 3.6 Hz), 124.7 ($J_{C\text{-}F}$ = 3.6 Hz), 124.4 ($J_{C\text{-}F}$ = 11.6 Hz), 119.4, 116.4, 116.2, 112.4, 109.1; **HRMS** (ESI) m/z calculated for $C_{17}H_{12}FNO[M+H]^+$: 266.0976, found 266.0978.

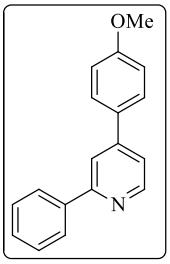


2,4-Diphenylpyridine (3am):[41] (35.1 mg, 76%); **^{1}H NMR** (400 MHz, $CDCl_3$): δ



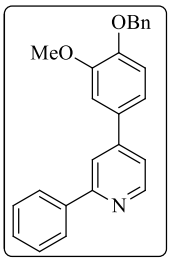
8.75 (d, *J* = 5 Hz, 1H), 8.09 (d, *J* = 7.2 Hz, 2H), 7.94 (s, 1H), 7.69 (d, *J* = 7.2 Hz, 2H), 7.43-7.51 (m, 7H); **^{13}C NMR** (100 MHz, $CDCl_3$): δ 158.3, 150.3, 149.4, 139.7, 138.7, 129.3, 129.2, 129.0(2C), 127.3, 127.2, 120.4, 118.9; **HRMS** (ESI) m/z calculated for $C_{17}H_{13}N[M+H]^+$: 232.1121, found 232.1134.

2-Phenyl-4-(4-methoxyphenyl)pyridine (3an):[41] (37.0 mg, 71%);**^{1}H NMR**



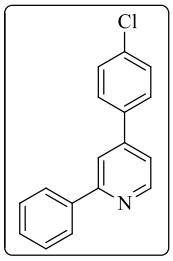
(400 MHz, $CDCl_3$): δ 8.70 (d, *J* = 5.0 Hz, 1H), 8.04 (d, *J* = 7.5 Hz, 2H), 7.89 (s, 1H), 7.66 (d, *J* = 8.0 Hz, 2H), 7.49 (t, *J* = 7.0 Hz, 2H), 7.41-7.45 (m, 2H), 7.03 (d, *J* = 8.0 Hz, 2H), 3.88 (s, 3H); **^{13}C NMR** (100 MHz, $CDCl_3$): δ 160.8, 158.4, 150.3, 149.1, 140.0, 131.1, 129.3, 129.1, 128.5, 127.3, 120.0, 118.5, 114.9, 55.7; **HRMS** (ESI) m/z calculated for $C_{18}H_{15}NO[M+H]^+$: 262.1226, found 262.1226.

2-Phenyl-4-(4-benzyloxy-3-methoxyphenyl)pyridine (3ao): (49.9 mg, 68%);



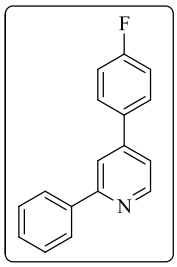
^{1}H NMR (400 MHz, $CDCl_3$): δ 8.58 (d, *J* = 4.4 Hz, 1H), 7.92 (d, *J* = 7.2 Hz, 2H), 7.75 (s, 1H), 7.32-7.40 (m, 5H), 7.26-7.28 (m, 3H), 7.21-7.22 (m, 1H), 7.08-7.09 (m, 2H), 6.88 (d, *J* = 8.0 Hz, 1H), 5.11 (s, 2H), 3.86 (s, 3H); **^{13}C NMR** (100 MHz, $CDCl_3$): δ 158.3, 150.3, 150.3, 149.4, 149.3, 139.8, 137.1, 131.9, 129.3, 129.0, 128.9, 128.2, 127.5, 127.3, 120.2, 119.9, 118.6, 114.4, 110.9, 71.3, 56.5; **HRMS** (ESI) m/z calculated for $C_{25}H_{21}NO_2[M+H]^+$: 368.1645, found 368.1643.

2-Phenyl-4-(4-chlorophenyl)pyridine (3ap):[29] (42.9 mg, 81%); **^{1}H NMR** (400

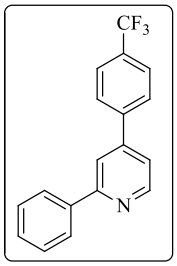


MHz, $CDCl_3$): δ 8.74 (d, *J* = 4.8 Hz, 1H), 8.04 (d, *J* = 7.2 Hz, 2H), 7.88 (s, 1H), 7.62 (d, *J* = 8.0 Hz, 2H), 7.44-7.52 (m, 5H), 7.40 (d, *J* = 4.5 Hz, 1H); **^{13}C NMR** (100 MHz, $CDCl_3$): δ 158.6, 150.5, 148.3, 139.6, 137.3, 135.6, 129.6, 129.4, 129.1, 128.6, 127.3, 120.3, 118.8; **HRMS** (ESI) m/z calculated for $C_{17}H_{12}ClN[M+H]^+$: 266.0731, found 266.0751.

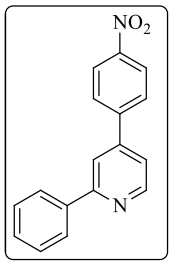
2-Phenyl-4-(4-fluorophenyl)pyridine(3aq):[41] (39.8 mg, 80%); **^{1}H NMR** (400 MHz, $CDCl_3$): δ 8.73 (d, *J* = 4.2 Hz, 1H), 8.04 (d, *J* = 7.2 Hz, 2H), 7.88 (s, 1H), 7.67 (t, *J* = 6.0 Hz, 2H), 7.39-7.52 (m, 4H), 7.20 (t, *J* = 8.0 Hz, 2H); **^{13}C NMR** (100 MHz, $CDCl_3$): δ 163.7 (d, J_{C-F} = 247.9 Hz), 158.5, 150.5, 148.5, 139.7, 135.0 (d, J_{C-F} = 2.9 Hz), 129.4, 129.2, 129.1, 127.3, 120.3, 118.8, 116.4 (d, J_{C-F} = 21.1 Hz); **HRMS** (ESI) m/z calculated for $C_{17}H_{12}FN[M+H]^+$: 250.1027, found 250.1026.



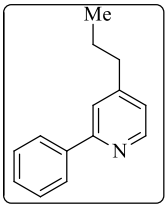
2-Phenyl-4-(4-trifluoromethylphenyl)pyridine (**3ar**): (49.6 mg, 83%); **^{1}H NMR** (400 MHz, $CDCl_3$): δ 8.77 (d, *J* = 4.7 Hz, 1H), 8.06 (d, *J* = 7.2 Hz, 2H), 7.91 (s, 1H), 7.76 (s, 4H), 7.51 (t, *J* = 7.2 Hz, 2H), 7.46 (d, *J* = 6.8 Hz, 1H), 7.42 (d, *J* = 5.0 Hz, 1H); **^{13}C NMR** (100 MHz, $CDCl_3$): δ 157.6, 149.6, 147.1, 141.4, 138.4, 128.5, 128.1, 126.8, 126.3, 125.3 (q, J_{C-F} = 3.6 Hz), 124.6, 121.9, 119.5, 118.0 ; **HRMS** (ESI) m/z calculated for $C_{18}H_{12}F_3N[M+H]^+$: 300.0995, found 300.0985.

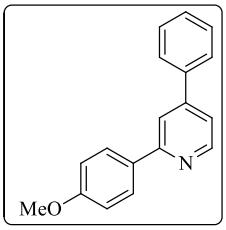


2-Phenyl-4-(4-nitrophenyl)pyridine (3as):[41] (43.6 mg, 79%); **^{1}H NMR** (400 MHz, $CDCl_3$): δ 8.81 (s, 1H), 8.36 (d, *J* = 7.7 Hz, 2H), 8.05 (d, *J* = 7.0 Hz, 2H), 7.92 (s, 1H), 7.84 (d, *J* = 8.0 Hz, 2H), 7.46-7.53 (m, 4H); **^{13}C NMR** (100 MHz, $CDCl_3$): δ 158.9, 150.8, 148.5, 147.2, 145.2, 139.2, 129.7, 129.2, 128.4, 127.3, 124.7, 120.5, 119.0; **HRMS** (ESI) m/z calculated for $C_{17}H_{12}N_2O_2[M+H]^+$: 277.0972, found 277.0971.

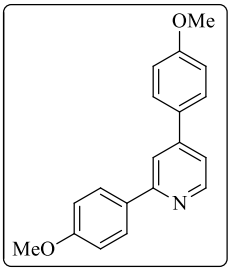


2-Phenyl-4-propylpyridine (3at):[41] (19.0 mg, 48%); **^{1}H NMR** (400 MHz, $CDCl_3$): δ 8.57 (d, *J* = 5.0 Hz, 1H), 7.98 (d, *J* = 7.5 Hz, 2H), 7.54 (s, 1H), 7.47 (t, *J* = 7.2 Hz, 2H), 7.41 (d, *J* = 7.2 Hz, 1H), 7.05 (d, *J* = 4.7 Hz, 1H), 2.64 (t, *J* = 7.5 Hz, 2H), 1.66-1.75 (m, 2H), 0.98 (t, *J* = 7.2 Hz, 3H); **^{13}C NMR** (100 MHz, $CDCl_3$): δ 157.7, 152.5, 149.8, 139.9, 129.1, 129.0, 127.2, 122.7, 121.2, 37.8, 23.9, 14.0 ; **HRMS** (ESI) m/z calculated for $C_{14}H_{15}N[M+H]^+$: 198.1277, found 198.1275.

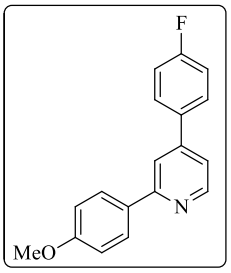


2-(4-Methoxyphenyl)-4-phenylpyridine (3cm):[41] (40.2 mg, 77%); **^{1}H NMR** 

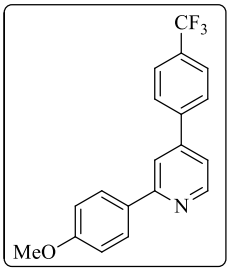
(400 MHz, $CDCl_3$): δ 8.69 (d, *J* = 4.7 Hz, 1H), 8.01 (d, *J* = 8.2 Hz, 2H), 7.87 (s, 1H), 7.69 (d, *J* = 7.5 Hz, 2H), 7.45-7.52 (m, 3H), 7.39 (d, *J* = 5.0 Hz, 1H), 7.01 (d, *J* = 8.0 Hz, 2H), ; **^{13}C NMR** (100 MHz, $CDCl_3$): δ 160.8, 158.0, 150.3, 149.5, 139.0, 132.4, 129.4, 129.3, 128.6, 127.4, 119.9, 118.3, 114.4, 55.7; **HRMS** (ESI) m/z calculated for $C_{18}H_{15}NO[M+H]^+$: 262.1226, found 262.1236.

2-(4-Methoxyphenyl)-4-(4-methoxyphenyl)pyridine (3cn):[31] (39.0 mg, 67%); 

^{1}H NMR (400 MHz, $CDCl_3$): δ 8.65 (d, *J* = 4.2 Hz, 1H), 8.00 (d, *J* = 8 Hz, 2H), 7.83 (s, 1H), 7.64 (d, *J* = 7.7 Hz, 2H), 7.35 (d, *J* = 3.0Hz, 1H), 7.02 (s, 4H), 3.87 (s, 6H); **^{13}C NMR** (100 MHz, $CDCl_3$): δ 160.8, 158.0, 150.2, 148.9, 132.6, 131.2, 128.6, 128.5(2C), 119.4, 117.7, 114.8, 114.4, 55.7, 55.7; **HRMS** (ESI) m/z calculated for $C_{19}H_{17}NO_2[M+H]^+$: 292.1332, found 292.1336.

2-(4-Methoxyphenyl)-4-(4-fluorophenyl)pyridine (3cq): (45.7 mg, 82%); **^{1}H** 

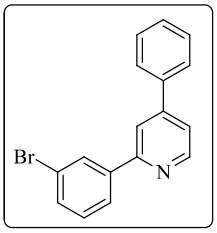
NMR (400 MHz, $CDCl_3$): δ 8.68 (d, *J* = 4.7 Hz, 1H), 8.00 (d, *J* = 8.0 Hz, 2H), 7.81 (s, 1H), 7.66 (t, *J* = 6.2 Hz, 2H), 7.34 (d, *J* = 4.7 Hz, 1H), 7.19 (t, *J* = 8.2 Hz, 2H), 7.01 (d, *J* = 7.8 Hz, 2H), 3.87 (s, 3H); **^{13}C NMR** (100 MHz, $CDCl_3$): δ 163.7 (d, J_{C-F} = 247.1 Hz), 160.9, 158.1, 150.3, 148.5, 135.1 (d, J_{C-F} = 2.9 Hz), 132.3, 129.1 (d, J_{C-F} = 8.0 Hz), 128.6, 119.7, 118.1, 116.4 (d, J_{C-F} = 21.8 Hz), 114.5, 55.7; **HRMS** (ESI) m/z calculated for $C_{18}H_{14}FNO[M+H]^+$: 280.1132, found 280.1158.

2-(4-Methoxyphenyl)-4-(4-trifluoromethylphenyl)pyridine (3cr): (52.6 mg, 

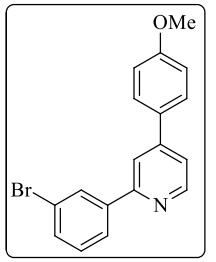
80%); **^{1}H NMR** (400 MHz, $CDCl_3$): δ 8.73 (d, *J* = 4.7 Hz, 1H), 8.01 (d, *J* = 7.8 Hz, 2H), 7.85 (s, 1H), 7.76 (s, 4H), 7.37 (d, *J* = 4.7 Hz, 1H), 7.02 (d, *J* = 8.0 Hz, 2H), 3.87 (s, 3H); **^{13}C NMR** (100 MHz, $CDCl_3$): δ 161.0, 158.3, 150.5, 148.0, 142.6, 132.0, 128.6, 127.8, 126.38 (d, J_{C-F} = 14.5 Hz), 119.9,

118.3, 114.5, 55.7 ; **HRMS** (ESI) m/z calculated for $C_{19}H_{14}F_3NO[M+H]^+$: 330.1100, found 330.1103.

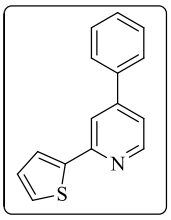
2-(3-Bromophenyl)-4-phenylpyridine (3gm):[41] (41.5 mg, 67%); **^{1}H NMR** (400 MHz, $CDCl_3$): δ 8.73 (d, *J* = 4.7 Hz, 1H), 8.22 (s, 1H), 7.97 (d, *J* = 7.7 Hz, 2H), 7.90 (s, 1H), 7.45-7.57 (m, 5H), 7.36 (t, *J* = 7.8 Hz, 1H); **^{13}C NMR** (100 MHz, $CDCl_3$): δ 156.8, 150.5, 149.9, 141.8, 138.6, 132.3, 130.6, 130.4, 129.5, 129.5, 127.4, 125.9, 123.4, 121.1, 119.1; **HRMS** (ESI) m/z calculated for $C_{17}H_{12}{}^{79}BrN[M+H]^+$: 310.0226, found 310.0223, $C_{17}H_{12}{}^{81}BrN[M+H]^+$: 312.0206, found 312.0205.



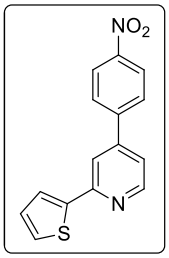
2-(3-Bromophenyl)-4-(4-methoxyphenyl)pyridine (3gn): (44.2 mg, 65%); **^{1}H NMR** (400 MHz, $CDCl_3$): δ 8.69 (d, *J* = 5.0 Hz, 1H), 8.21 (s, 1H), 7.96 (d, *J* = 7.7 Hz, 2H), 7.85 (s, 1H), 7.65 (d, *J* = 8.2 Hz, 2H), 7.55 (d, *J* = 8.0 Hz, 1H), 7.43 (d, *J* = 5.0 Hz, 1H), 7.35 (t, *J* = 7.8 Hz, 1H), 7.03 (d, *J* = 8.2 Hz, 2H) ; **^{13}C NMR** (100 MHz, $CDCl_3$): δ 160.9, 156.7, 150.4, 149.3, 142.0, 132.2, 130.8, 130.5, 130.4, 128.5, 125.8, 123.3, 120.5, 118.5, 114.9, 55.7 ; **HRMS** (ESI) m/z calculated for $C_{18}H_{14}{}^{79}BrNO[M+H]^+$: 340.0332, found 340.0339, $C_{18}H_{14}{}^{81}BrNO\ [M+H]^+$: 342.0312, found 342.0322.



2-(2-Thiophenyl)-4-phenylpyridine (3hm):[41] (35.0 mg, 74%); **^{1}H NMR** (400 MHz, $CDCl_3$): δ 8.61 (d, *J* = 4.2 Hz,1H), 7.85 (s, 1H), 7.66-7.68 (m, 3H), 7.46-7.53 (m, 3H), 7.35-7.42 (m, 2H), 7.13 (s, 1H); **^{13}C NMR** (100 MHz, $CDCl_3$): δ 153.4, 150.3, 149.6, 145.1, 138.6, 129.4, 128.3, 127.9, 127.3, 124.9, 120.4, 117.2; **HRMS** (ESI) m/z calculated for $C_{15}H_{11}NS[M+H]^+$: 238.0685, found 238.0711.



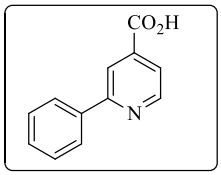
2-(Thiophen-2-yl)-4-(4-nitrophenyl)-pyridine (3hs): (42.8 mg), 76%; **^{1}H NMR (400 MHz, $CDCl_3$)** δ 8.67 (d, *J* = 4.7 Hz, 1H), 8.36 (d, *J* = 8.0 Hz, 2H), 7.81-7.83 (m, 3H), 7.68 (s, 1H), 7.45 (d, *J* = 4.5 Hz, 1H), 7.36 (d, *J* = 4.7 Hz, 1H), 7.15 (s, 1H) ; **^{13}C NMR (100 MHz, $CDCl_3$)** δ 153.9, 150.7, 148.5, 147.2, 145.0, 144.6, 128.5, 128.5, 128.4, 125.4, 124.7, 120.3, 117.1; **HRMS** (ESI) m/z calculated for $C_{15}H_{10}N_2O_2S[M+H]^+$ 283.0536, found 283.0534.



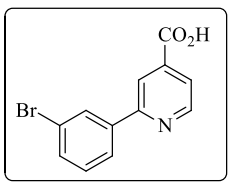
Preparation of 2-phenylisonicotinic acid (4aa):

To a stirred solution of compound **3aa** (0.1 mmol) in acetone/H_2O (5.0 mL, 9:1) was added $KMnO_4$ (3.0 equiv) at room temperature for 14h. After that, reaction mixture was concentrated under reduced pressure before being quenched with AcOH (0.1 mL) to provide crude mass. It was directly purified by column chromatography over silica-gel using ethyl acetate as an eluent to give the pure acid **4aa** in 90% yield. The product was characterized by its spectroscopic data which was good agreement with reported data.

2-Phenylisonicotinic acid (4aa):[42] (18.0 mg, 90%);**^{1}H NMR** (400 MHz, DMSO-d_6): δ 8.80 (d, *J* = 4.7 Hz, 1H), 8.28 (s, 1H), 8.10 (d, *J* = 7.5 Hz, 2H), 7.76 (d, *J* = 4.7 Hz, 1H), 7.43-7.52 (m, 3H); **^{13}C NMR** (100 MHz, DMSO-d_6): δ 166.6, 156.8, 150.3, 141.1, 138.1, 129.3, 128.8, 126.6, 121.5, 119.0; **HRMS** (ESI) m/z calculated for $C_{12}H_9NO_2[M+H]^+$: 200.0706, found 200.0709.



2-(3-Bromophenyl)isonicotinic acid (4ga): (22.2 mg, 88%); **^{1}H NMR** (400 MHz, DMSO-d_6): δ 8.82 (d, *J* = 4.2 Hz, 1H), 8.30 (d, *J* = 10.56 Hz, 2H), 8.10 (d, *J* = 7.7 Hz, 1H), 7.79 (d, *J* = 4Hz, 1H), 7.65 (d, *J* = 7.8 Hz, 1H), 7.46 (t, *J* = 7.8 Hz, 1H); **^{13}C NMR** (100 MHz, DMSO-d_6): δ 166.3, 155.1, 150.5, 141.1, 140.3, 132.0, 131.0, 129.2, 125.6, 122.3, 122.2, 119.4; **HRMS** (ESI) m/z calculated for $C_{12}H_8{}^{79}BrNO_2[M+H]^+$: 277.9811, found 277.9808, calculated for $C_{12}H_8{}^{81}BrNO_2[M+H]^+$: 279.9791, found 279.9805.



6.6 Copies of ^{1}H and ^{13}C NMR spectra of some important compounds described in Chapter 6

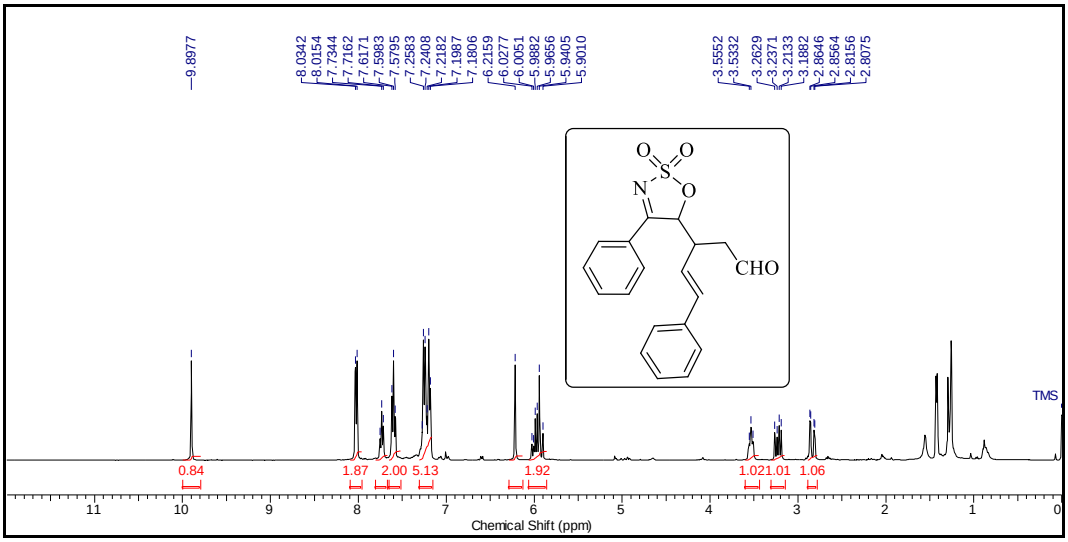


Figure 6.3 400 MHz ^{1}H NMR spectrum of **3aa'** in $CDCl_3$

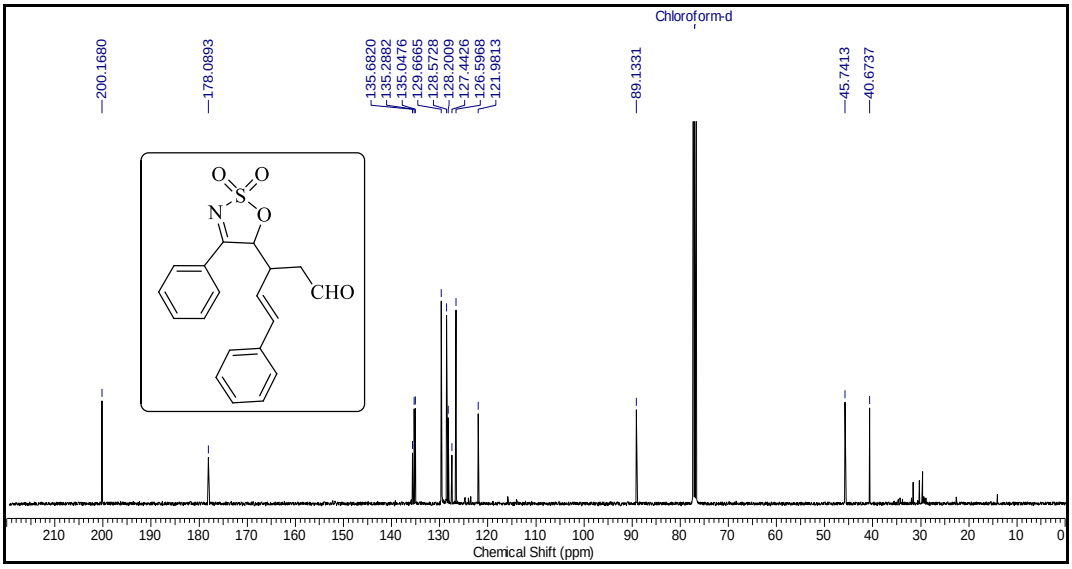


Figure 6.4 100 MHz ^{13}C NMR spectrum of **3aa'** in $CDCl_3$

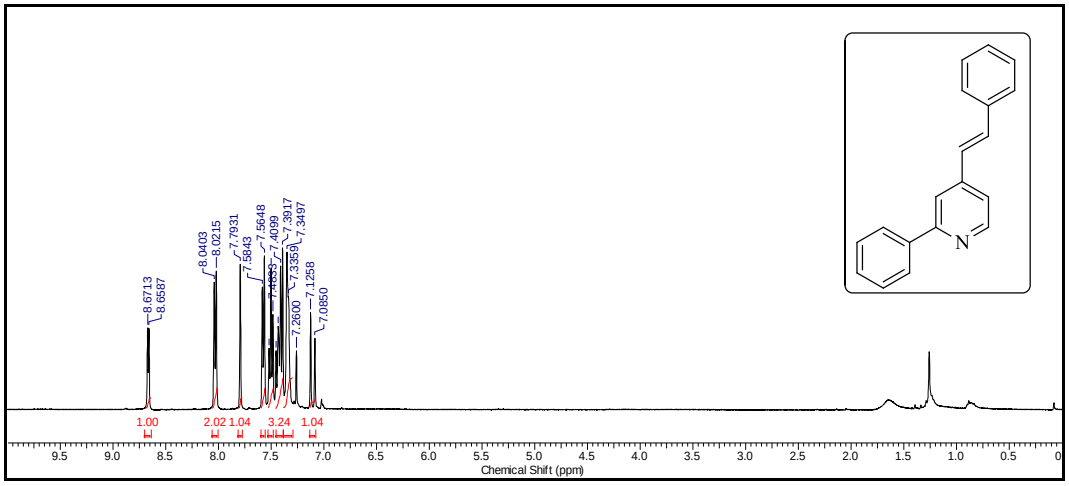


Figure 6.5 400 MHz ^{1}H NMR spectrum of **3aa** in $CDCl_3$

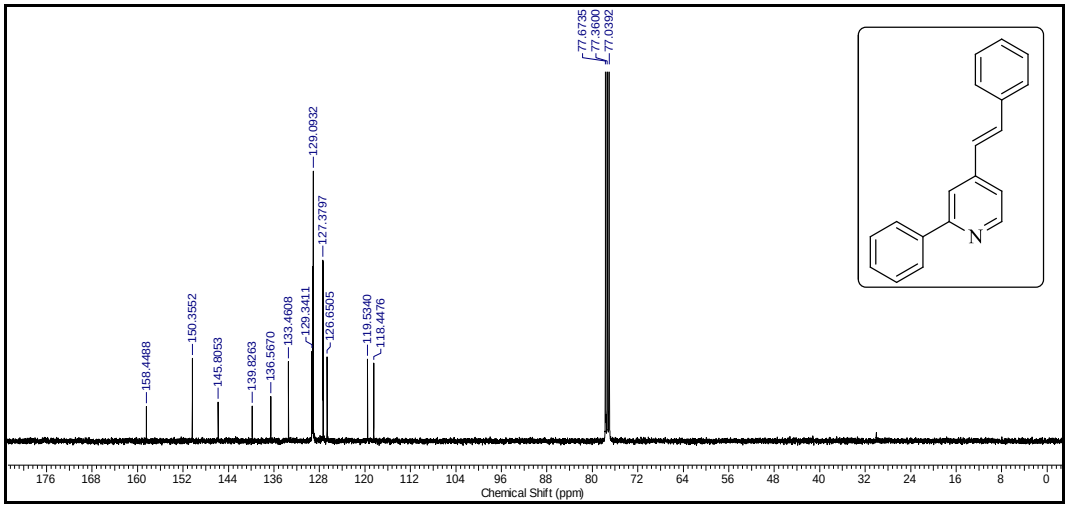


Figure 6.6 100 MHz ^{13}C NMR spectrum of **3aa** in $CDCl_3$

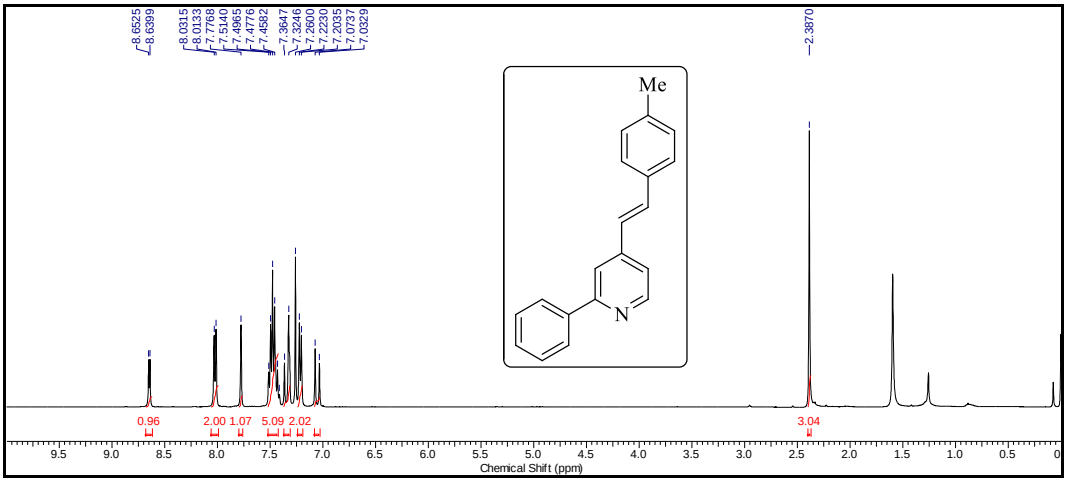


Figure 6.7 400 MHz ^{1}H NMR spectrum of **3ab** in $CDCl_3$

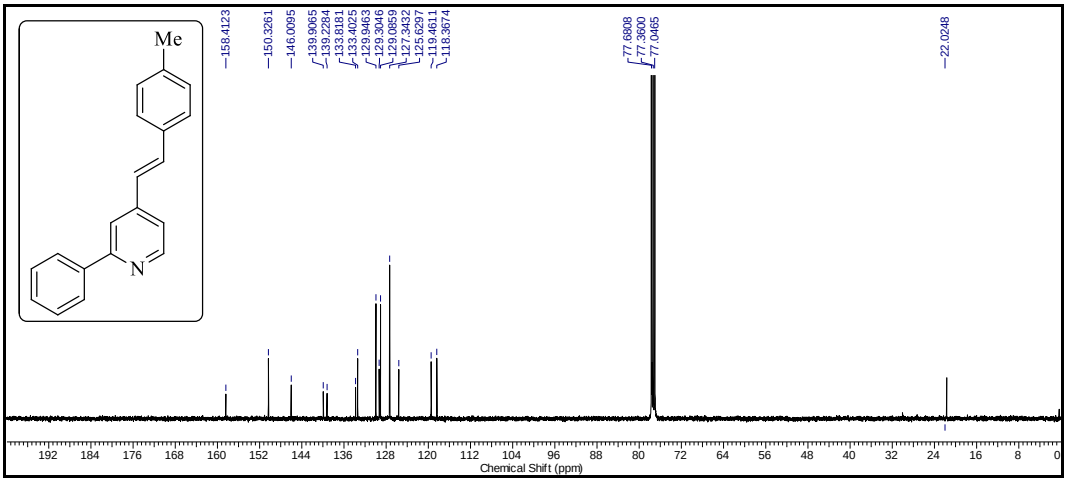


Figure 6.8 100 MHz ^{13}C NMR spectrum of **3ab** in $CDCl_3$

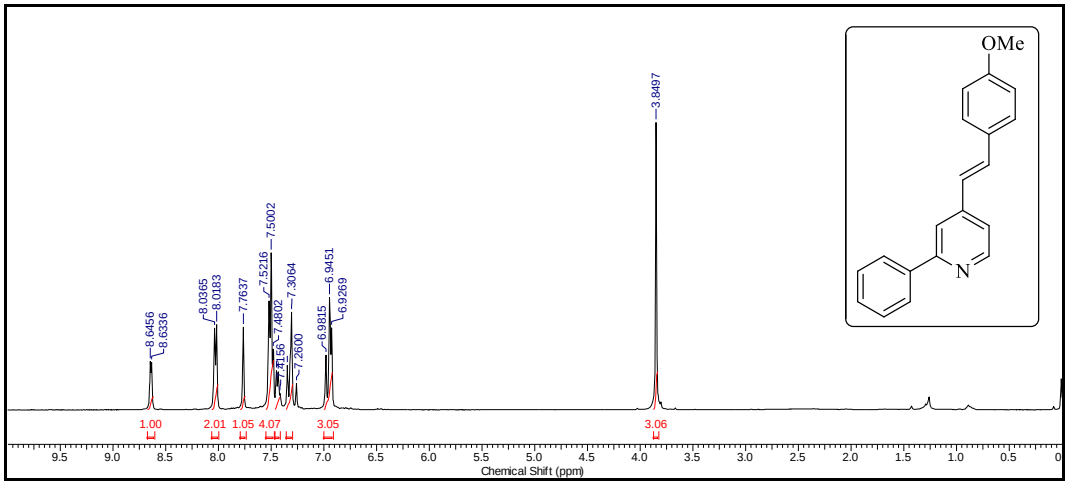


Figure 6.9 400 MHz ^{1}H NMR spectrum of **3ac** in $CDCl_3$

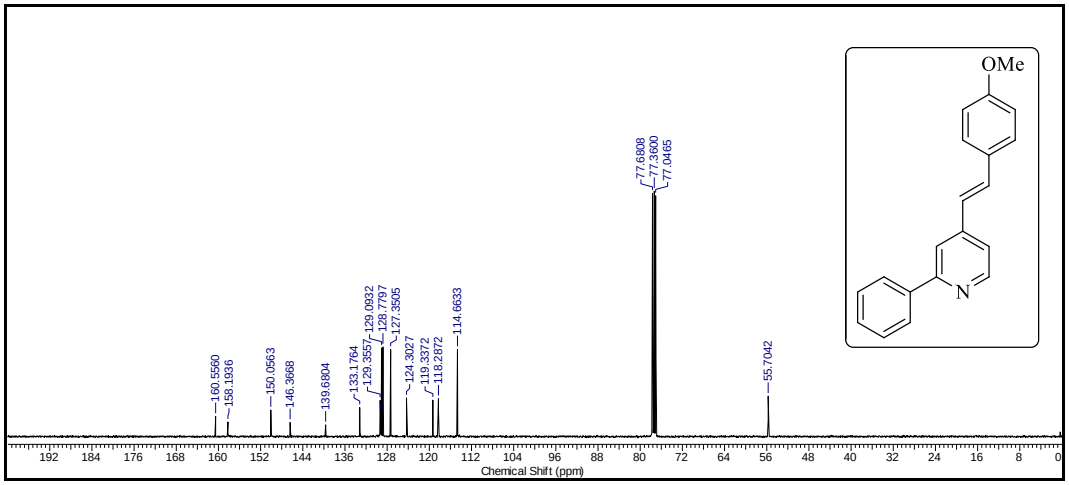


Figure 6.10 100 MHz ^{13}C NMR spectrum of **3ac** in $CDCl_3$

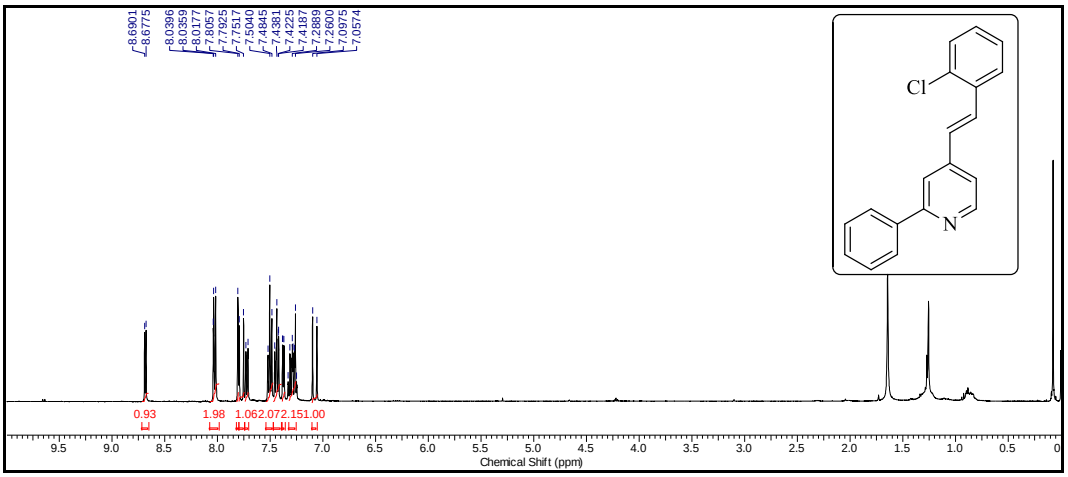


Figure 6.11 400 MHz ^{1}H NMR spectrum of **3ad** in $CDCl_3$

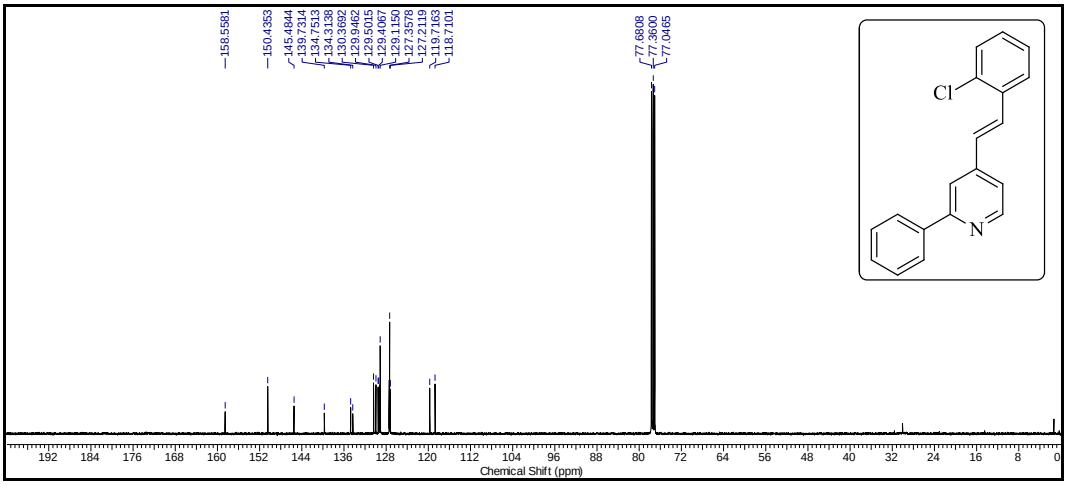


Figure 6.12 100 MHz ^{13}C NMR spectrum of **3ad** in $CDCl_3$

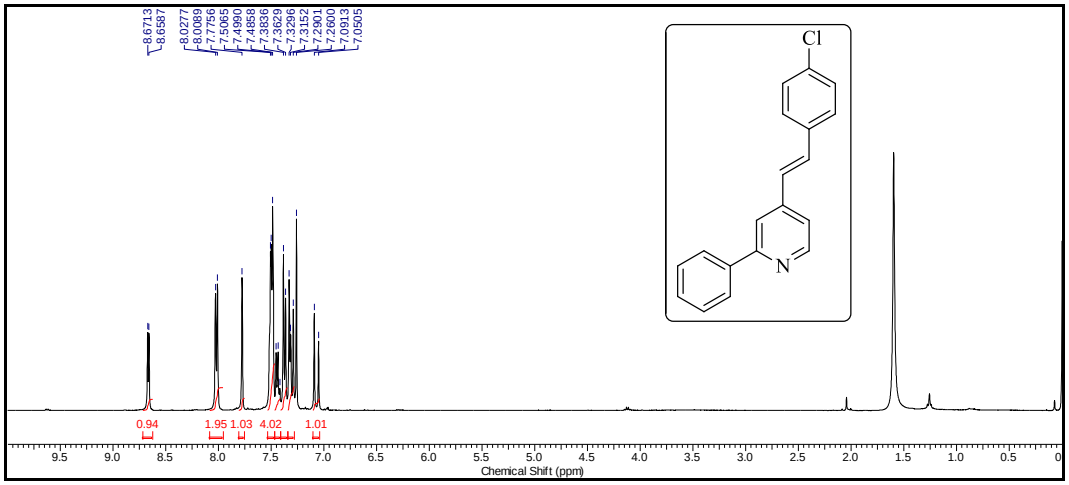


Figure 6.13 400 MHz ^{1}H NMR spectrum of **3ae** in $CDCl_3$

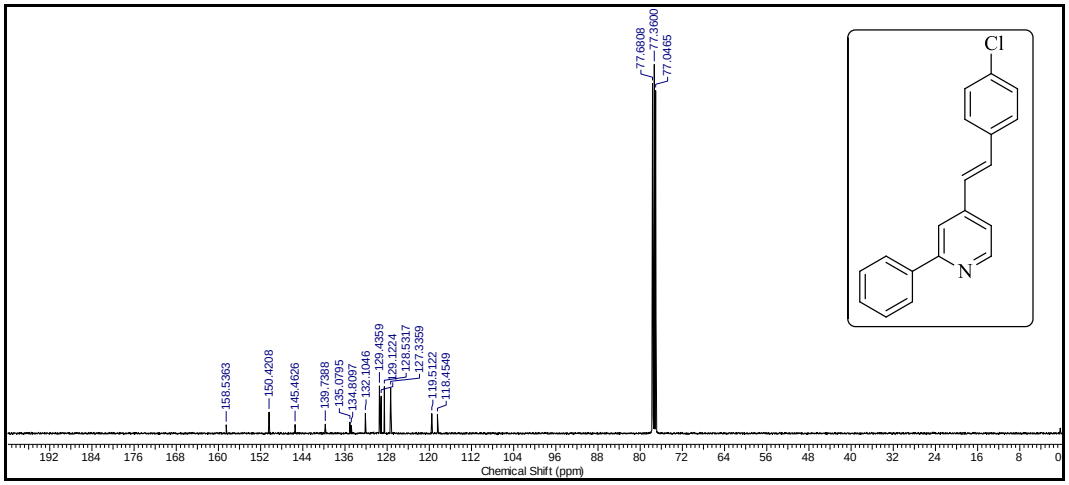


Figure 6.14 100 MHz ^{13}C NMR spectrum of **3ae** in $CDCl_3$

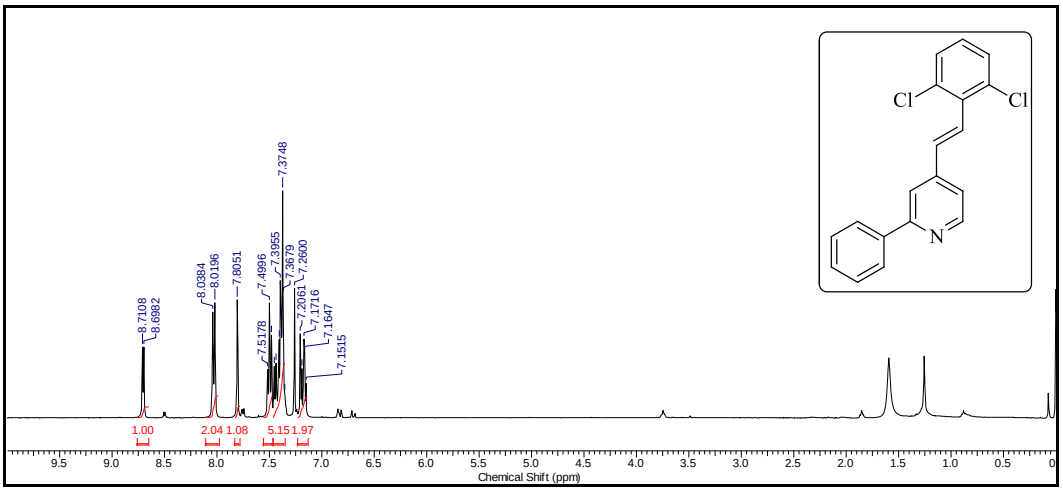


Figure 6.15 400 MHz ^{1}H NMR spectrum of **3af** in $CDCl_3$

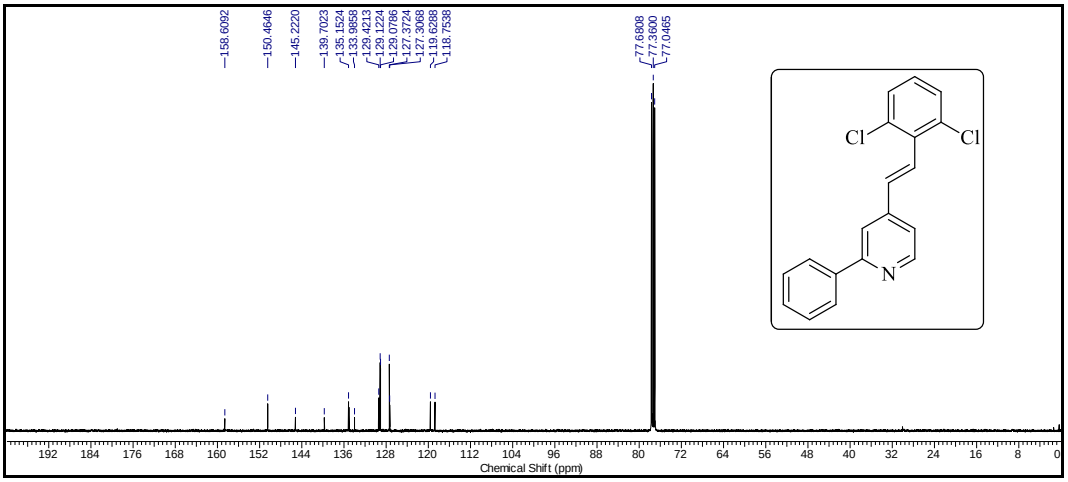


Figure 6.16 100 MHz ^{13}C NMR spectrum of **3af** in $CDCl_3$

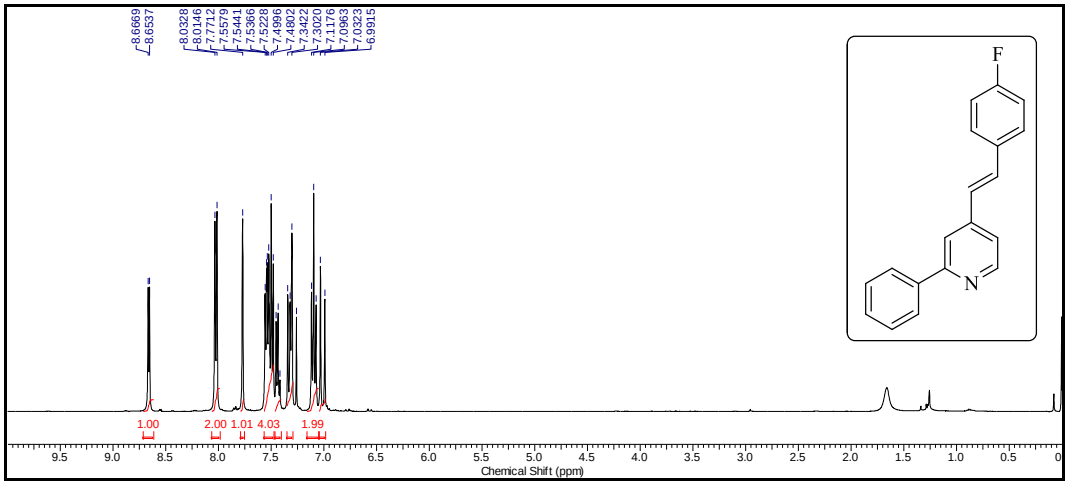


Figure 6.17 400 MHz ^{1}H NMR spectrum of **3ag** in $CDCl_3$

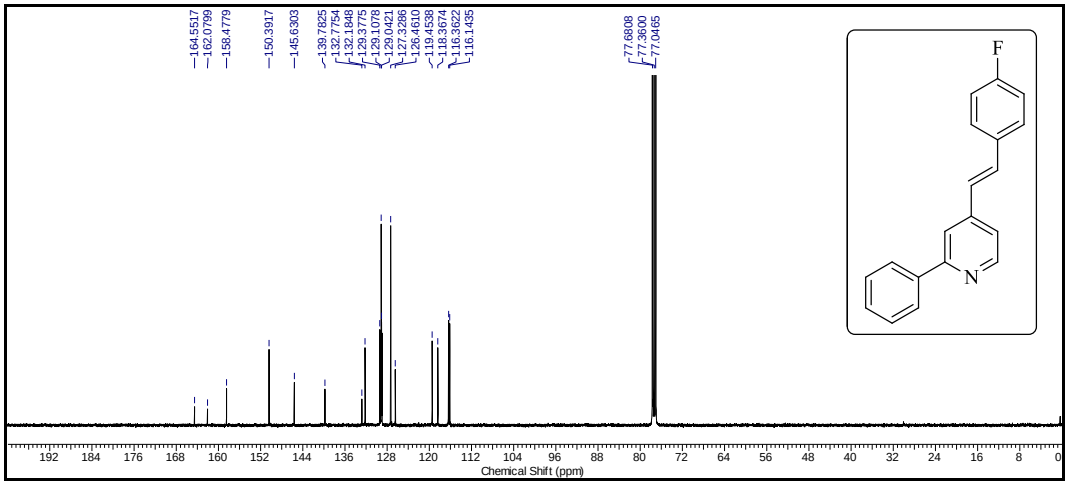


Figure 6.18 100 MHz ^{13}C NMR spectrum of **3ag** in $CDCl_3$

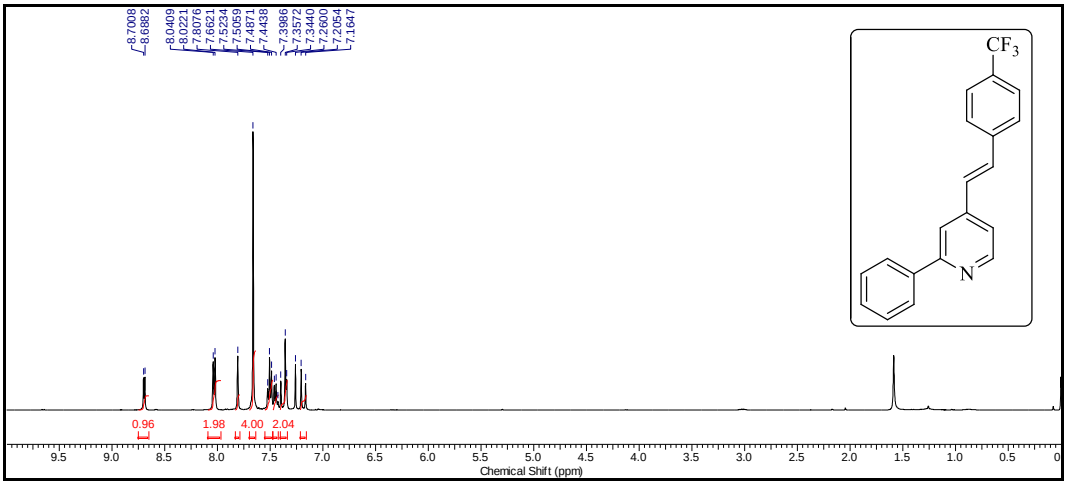


Figure 6.19 400 MHz ^{1}H NMR spectrum of **3ah** in $CDCl_3$

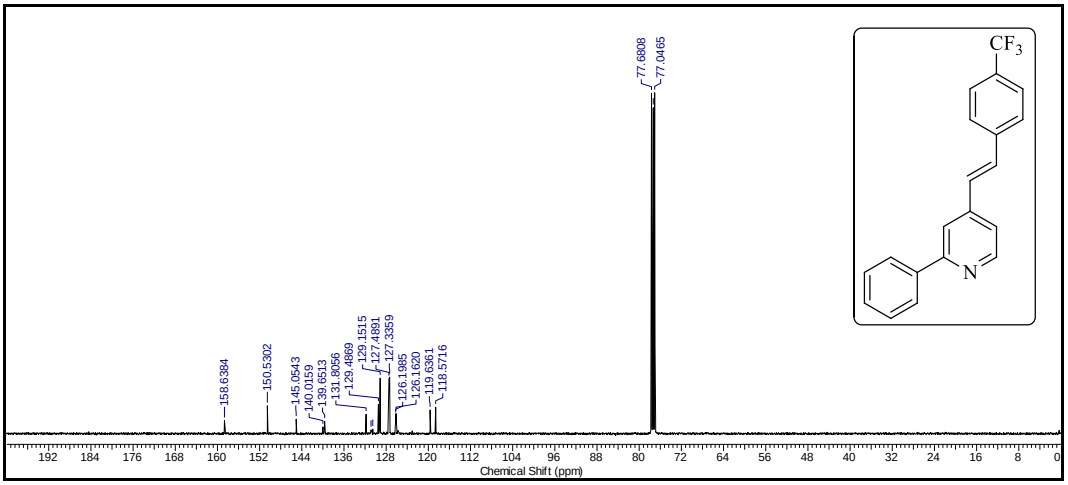


Figure 6.20 100 MHz ^{13}C NMR spectrum of **3ah** in $CDCl_3$

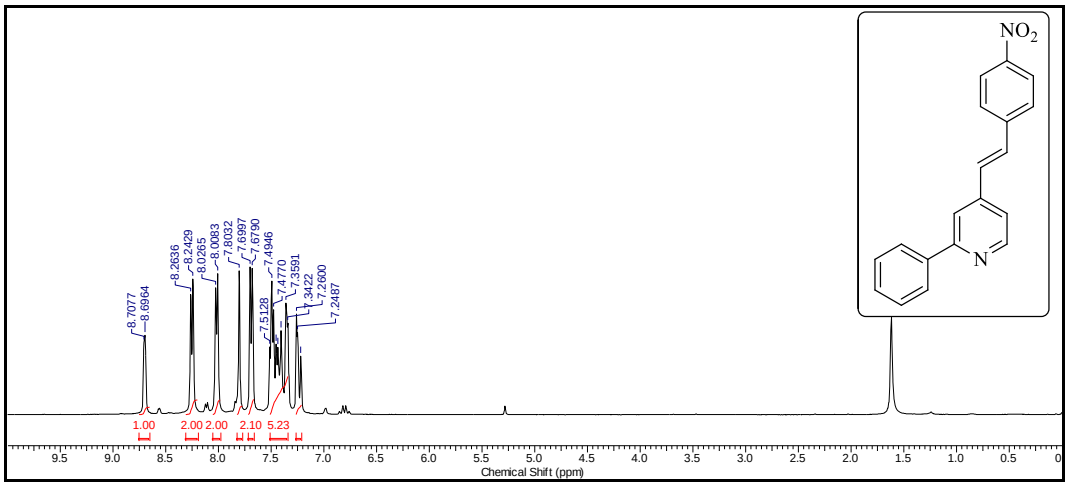


Figure 6.21 400 MHz ^{1}H NMR spectrum of **3ai** in $CDCl_3$

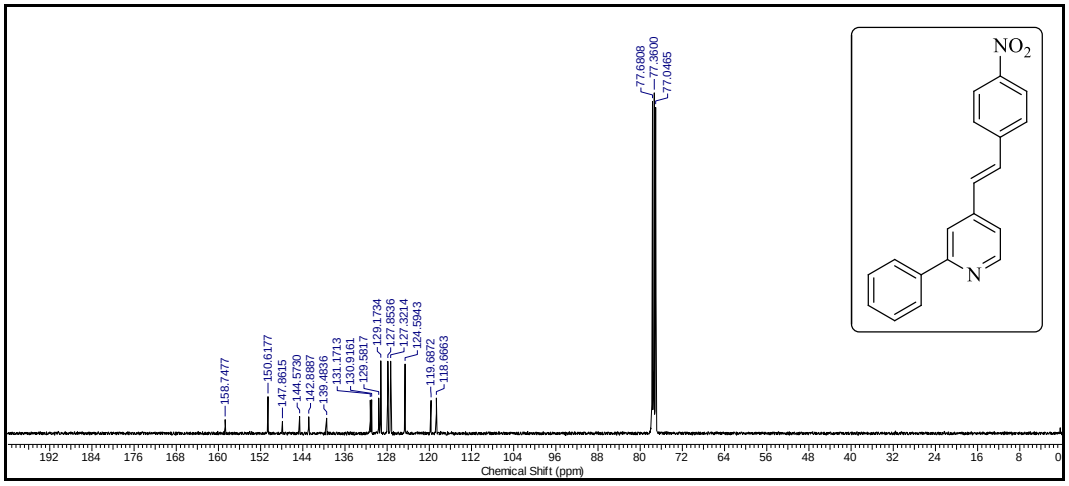


Figure 6.22 100 MHz ^{13}C NMR spectrum of **3ai** in $CDCl_3$

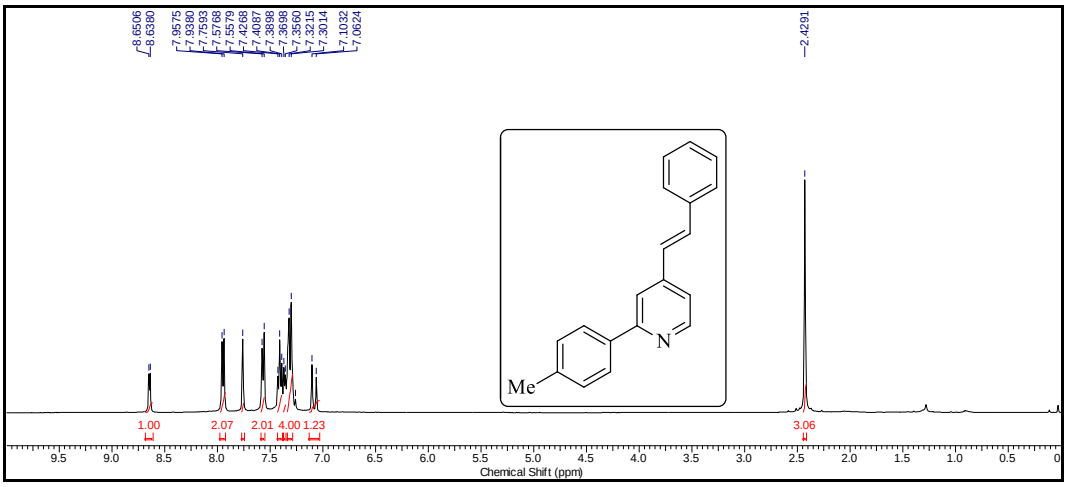


Figure 6.23 400 MHz ^{1}H NMR spectrum of **3ba** in $CDCl_3$

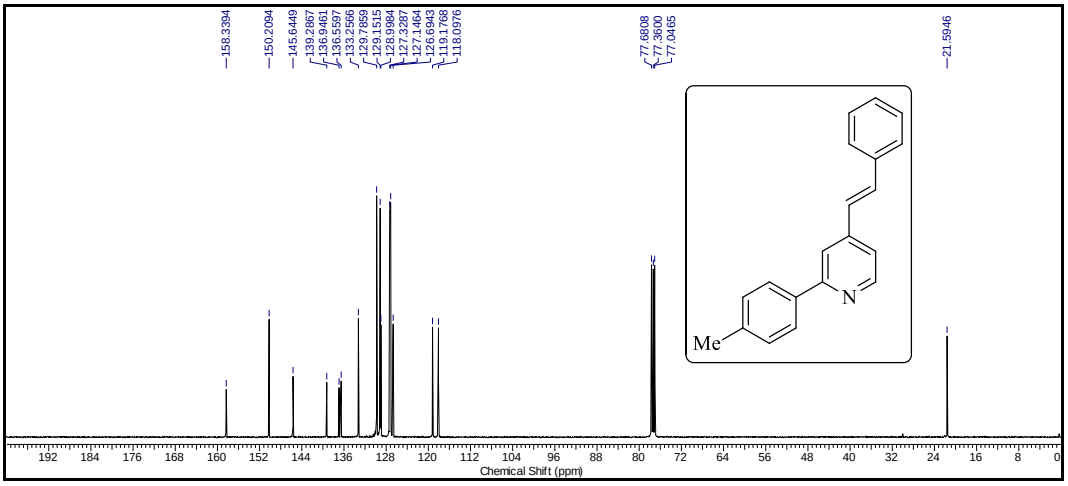


Figure 6.24 100 MHz ^{13}C NMR spectrum of **3ba** in $CDCl_3$

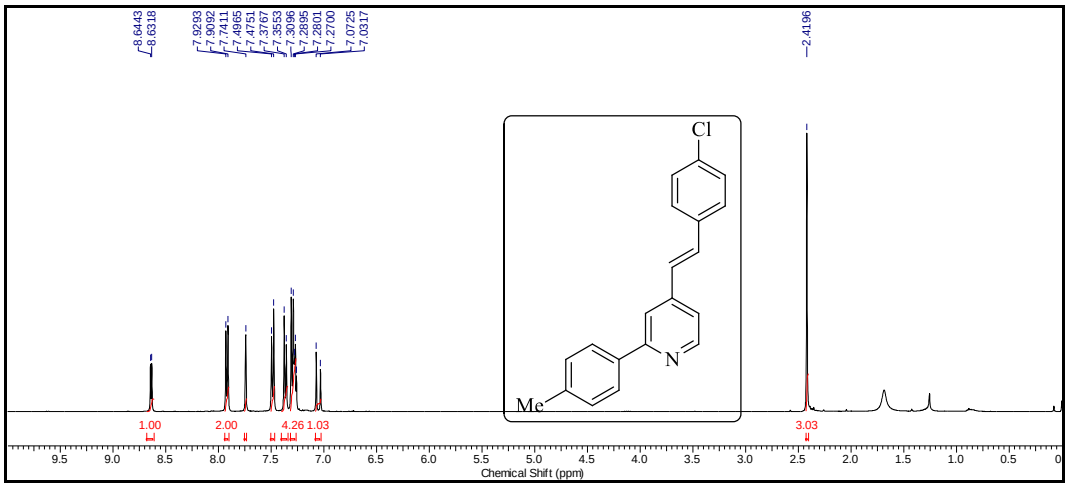


Figure 6.25 400 MHz ^{1}H NMR spectrum of **3be** in $CDCl_3$

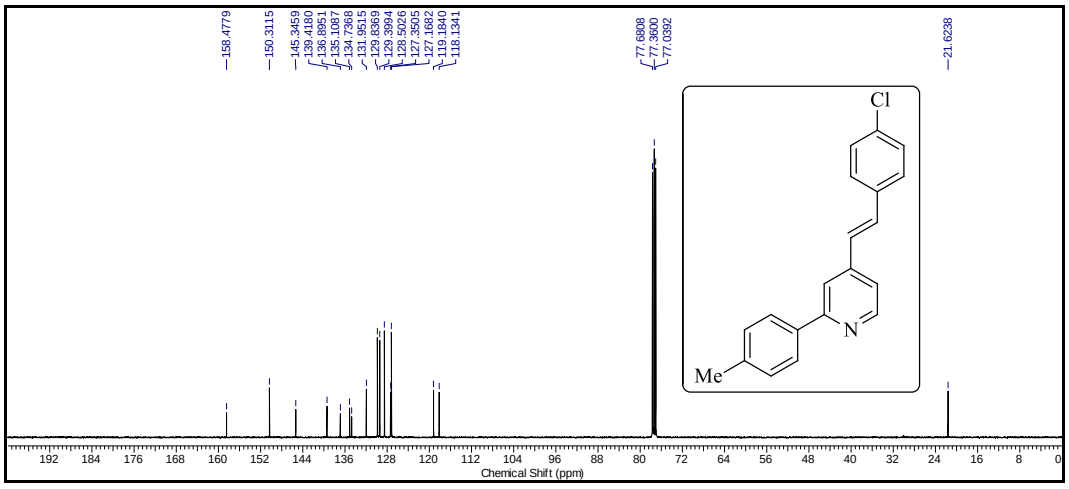


Figure 6.26 100 MHz ^{13}C NMR spectrum of **3be** in $CDCl_3$

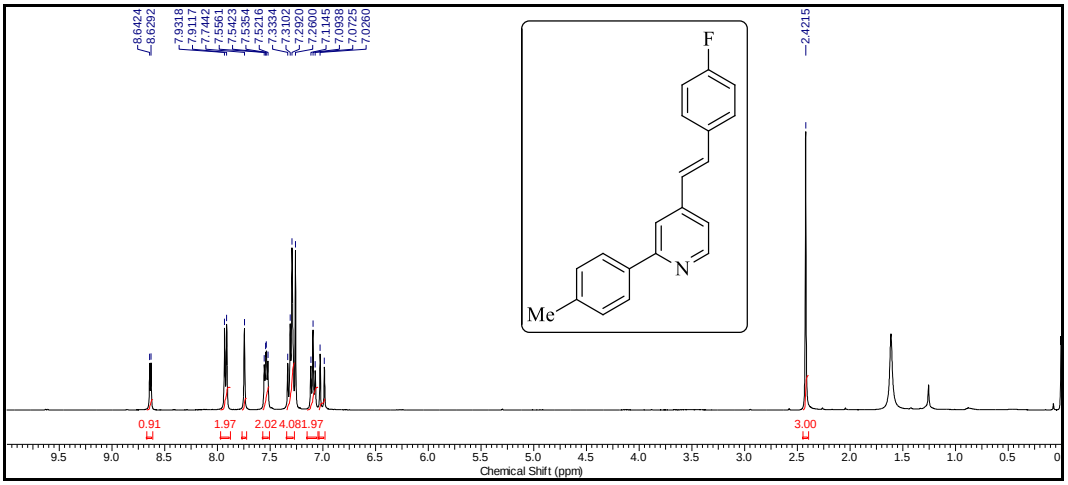


Figure 6.27 400 MHz ^{1}H NMR spectrum of **3bg** in $CDCl_3$

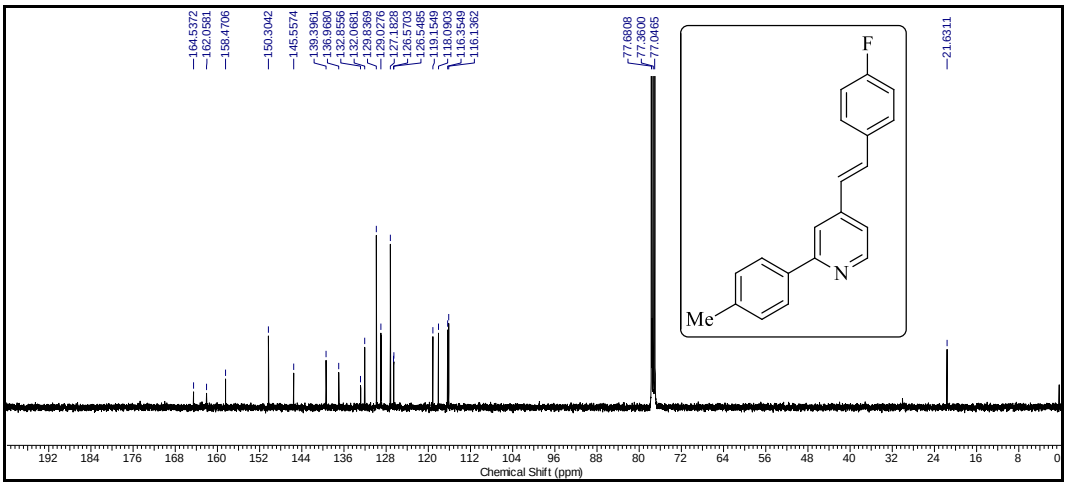


Figure 6.28 100 MHz ^{13}C NMR spectrum of **3bg** in $CDCl_3$

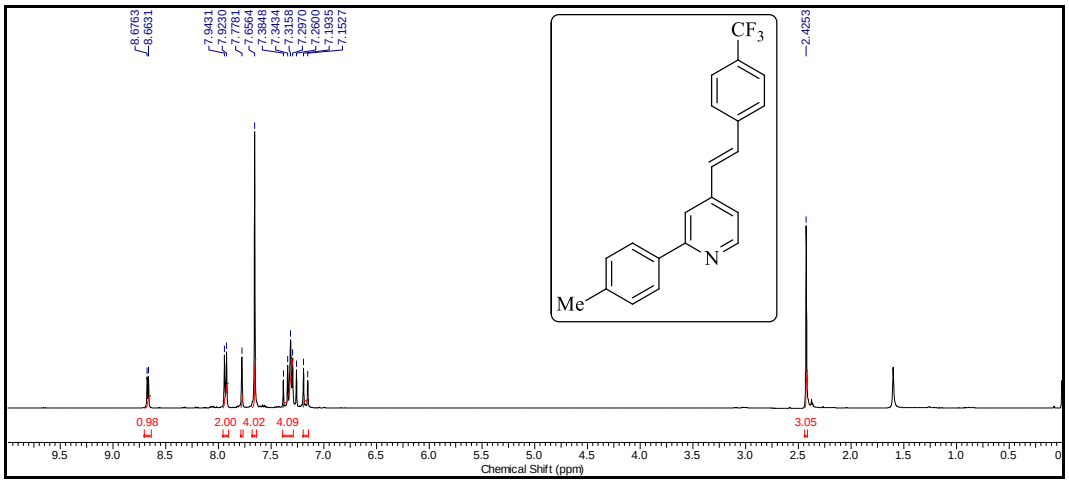


Figure 6.29 400 MHz ^{1}H NMR spectrum of **3bh** in $CDCl_3$

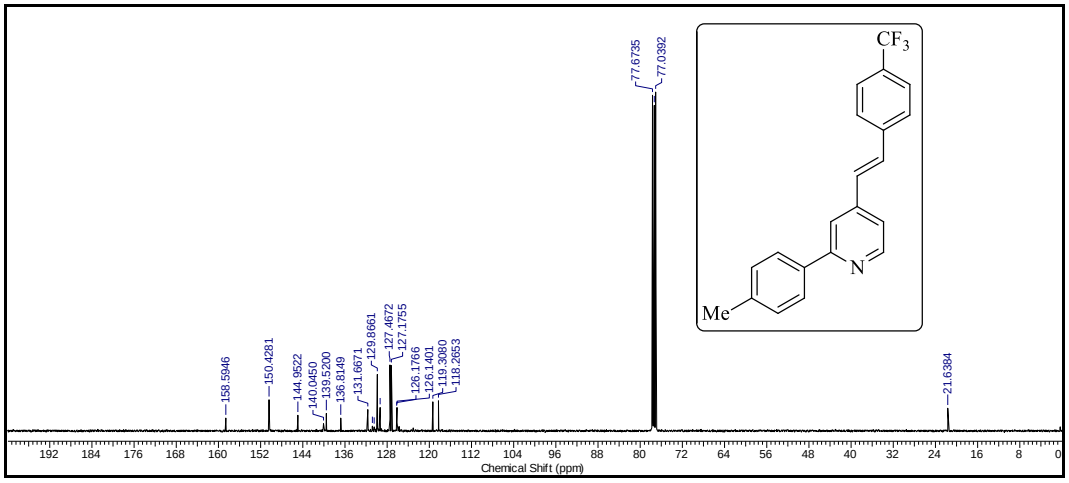


Figure 6.30 100 MHz ^{13}C NMR spectrum of **3bh** in $CDCl_3$

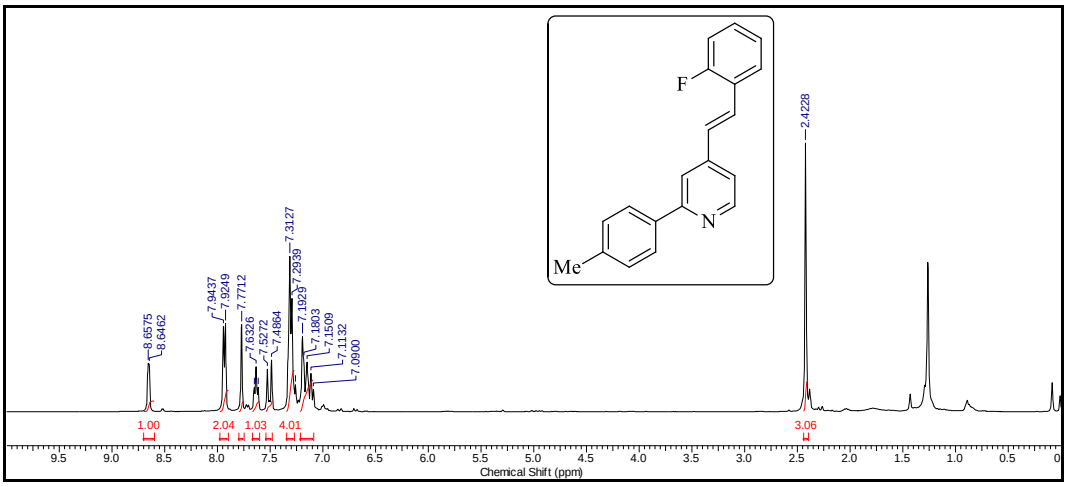


Figure 6.31 400 MHz ^{1}H NMR spectrum of **3bj** in $CDCl_3$

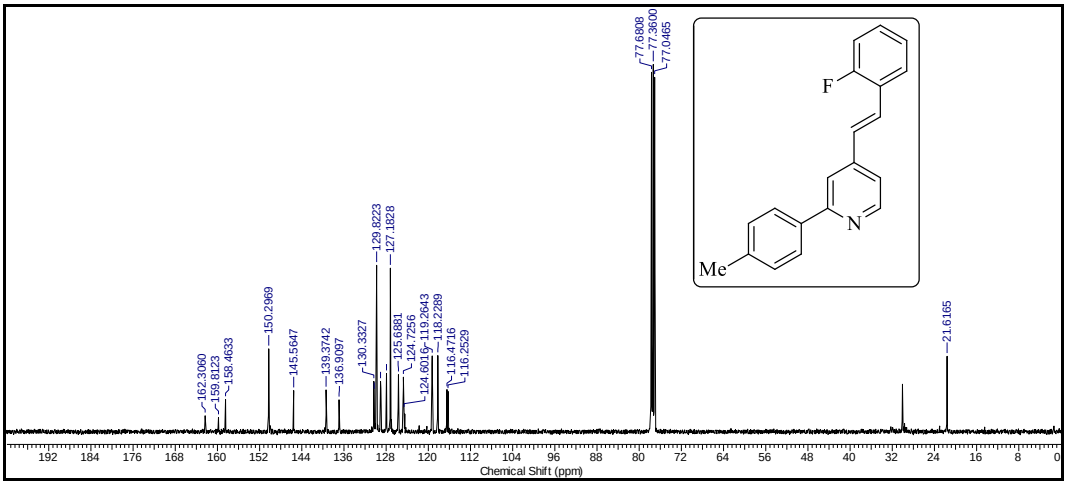


Figure 6.32 100 MHz ^{13}C NMR spectrum of **3bj** in $CDCl_3$

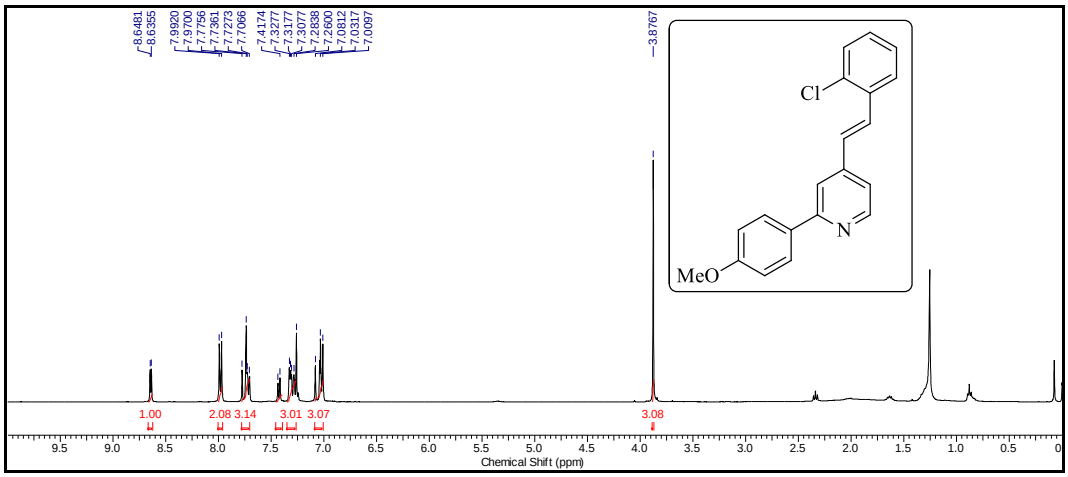


Figure 6.33 400 MHz ^{1}H NMR spectrum of **3cd** in $CDCl_3$

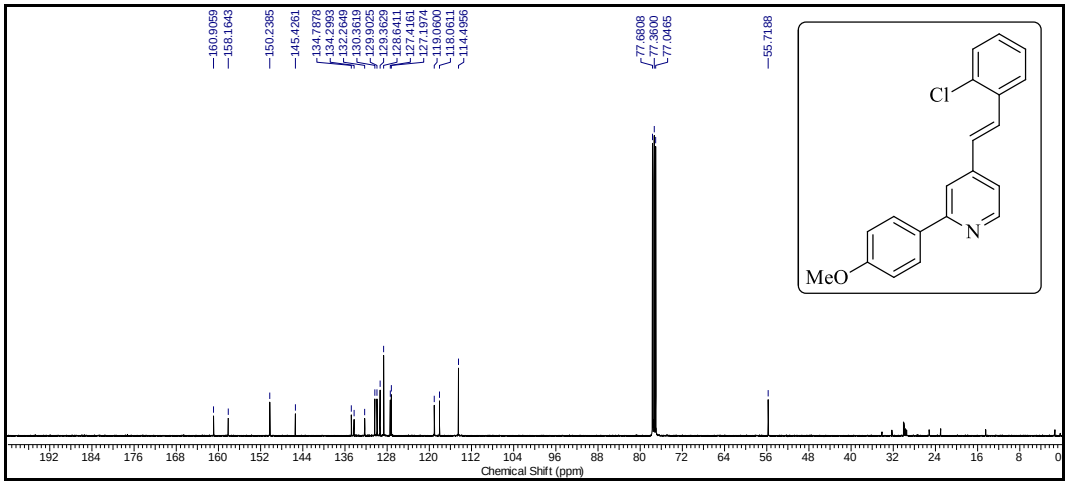


Figure 6.34 100 MHz ^{13}C NMR spectrum of **3cd** in $CDCl_3$

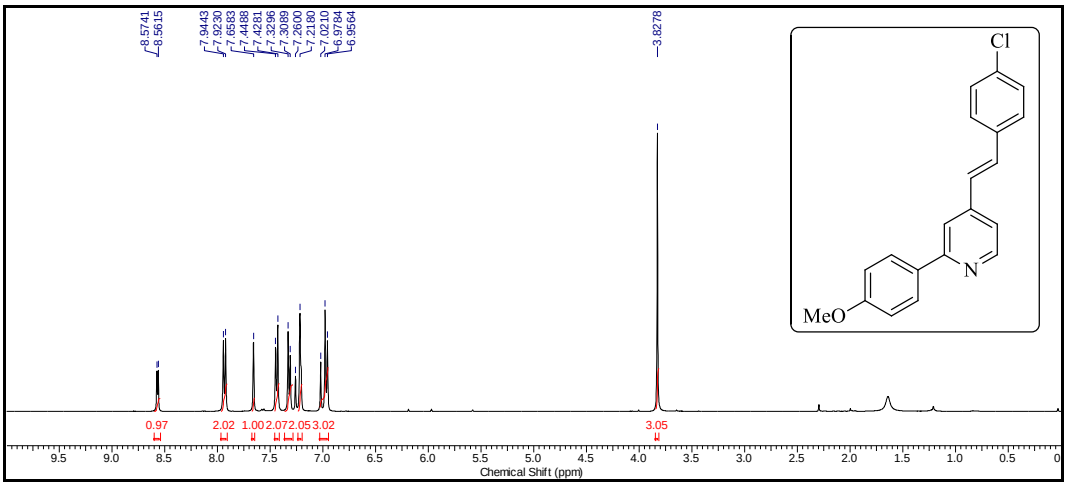


Figure 6.35 400 MHz ^{1}H NMR spectrum of **3ce** in $CDCl_3$

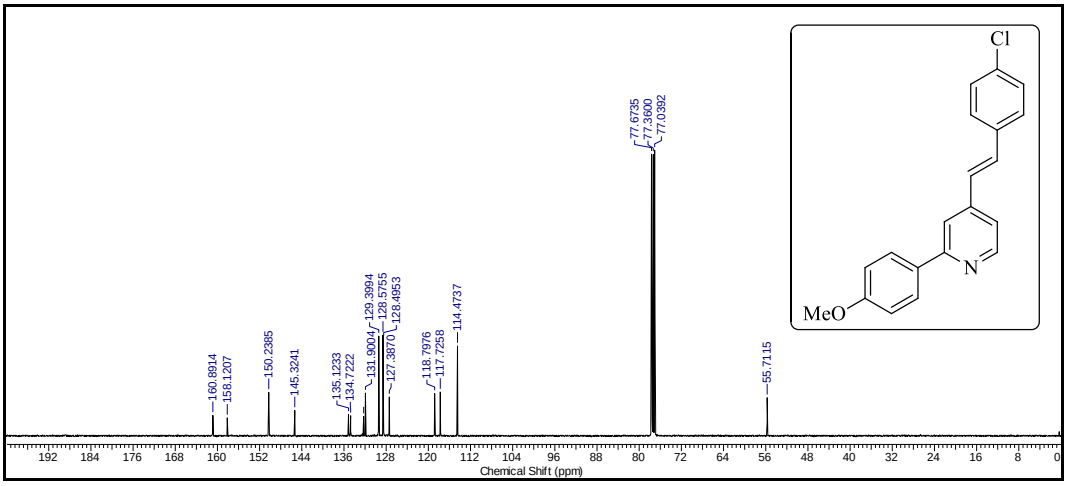


Figure 6.36 100 MHz ^{13}C NMR spectrum of **3ce** in $CDCl_3$

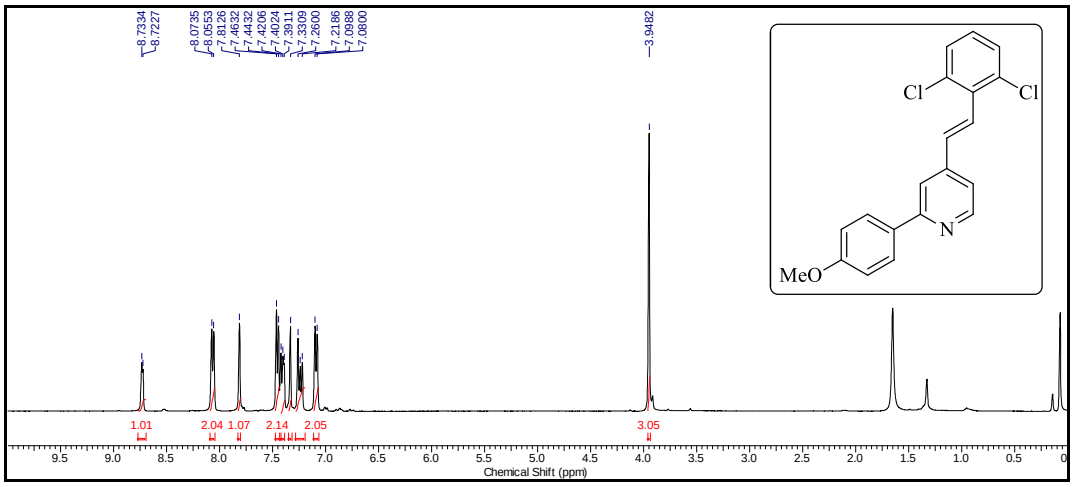


Figure 6.37 400 MHz ^{1}H NMR spectrum of **3cf** in $CDCl_3$

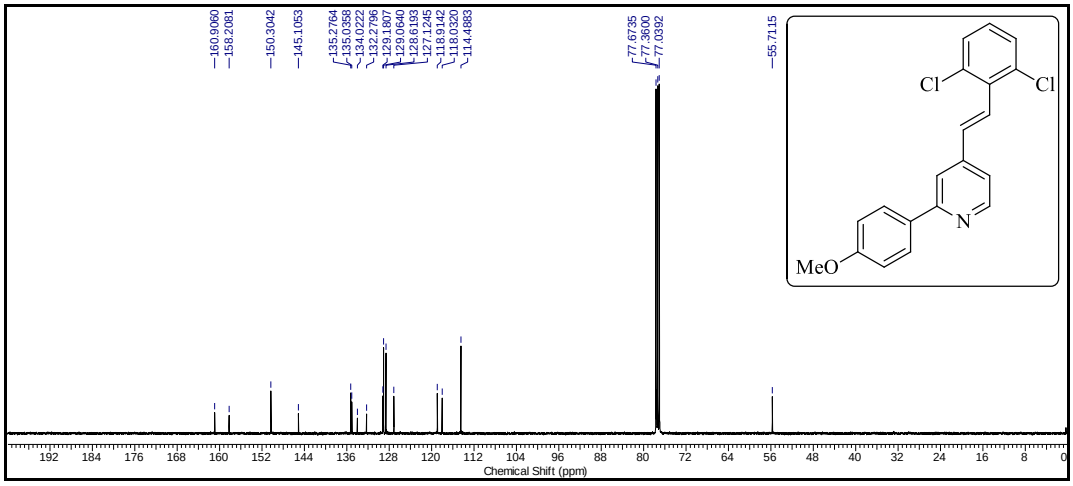


Figure 6.38 100 MHz ^{13}C NMR spectrum of **3cf** in $CDCl_3$

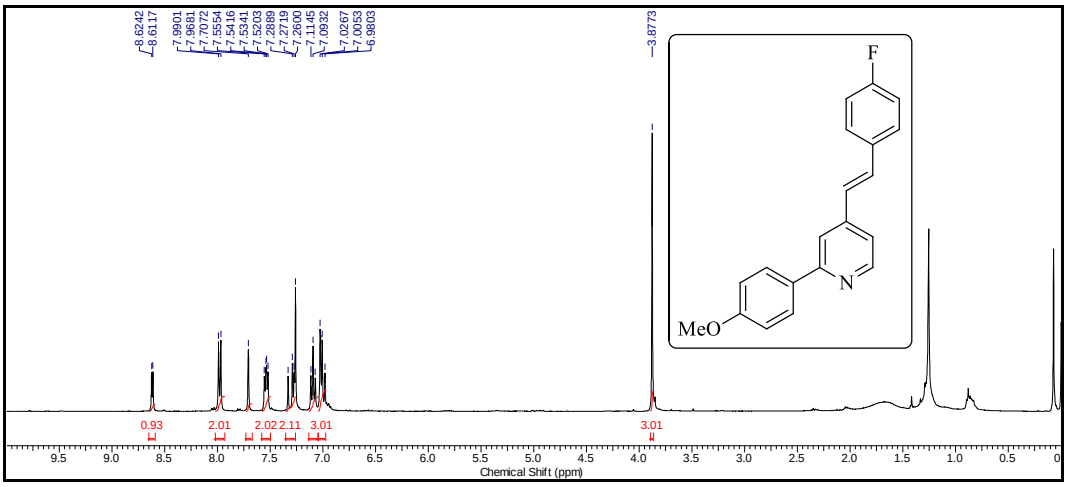


Figure 6.39 400 MHz ^{1}H NMR spectrum of **3cg** in $CDCl_3$

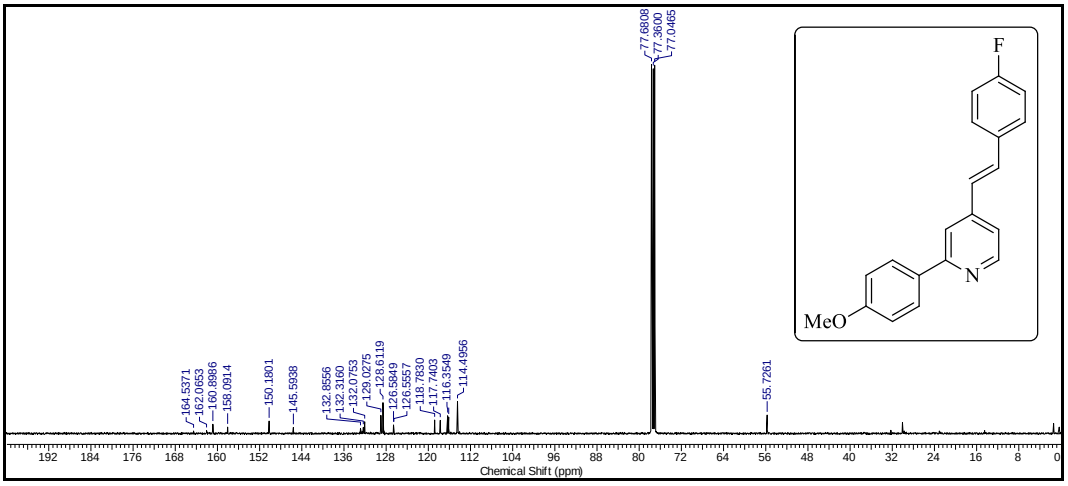


Figure 6.40 100 MHz ^{13}C NMR spectrum of **3cg** in $CDCl_3$

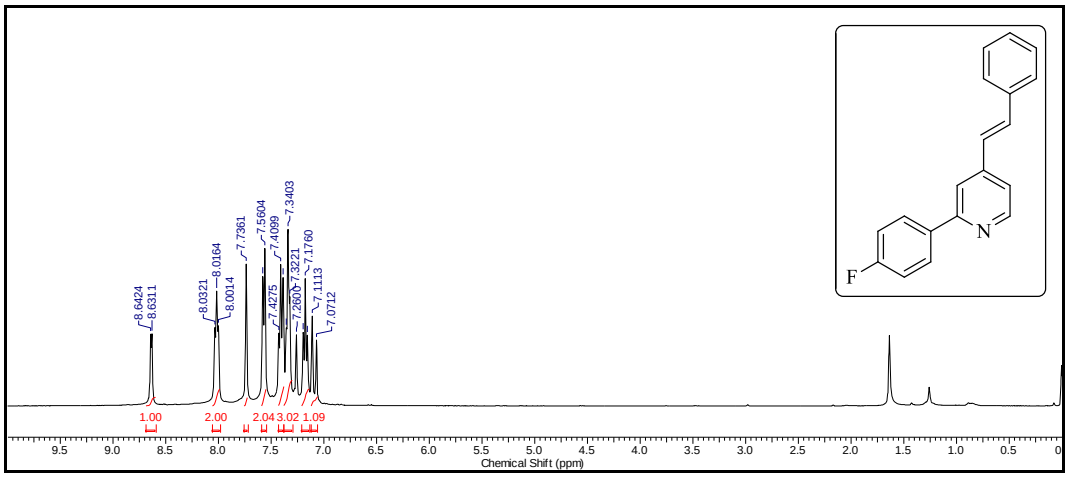


Figure 6.41 400 MHz ^{1}H NMR spectrum of **3da** in $CDCl_3$

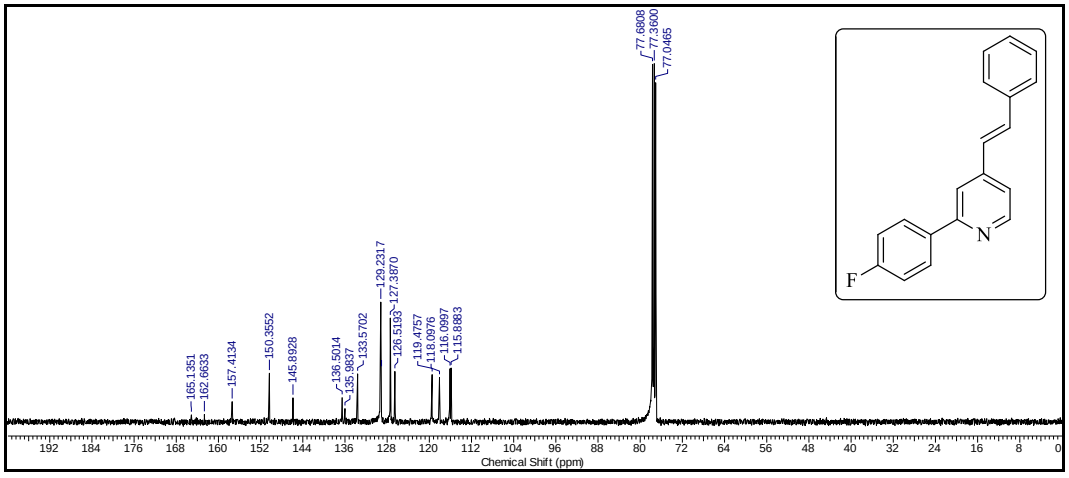


Figure 6.42 100 MHz ^{13}C NMR spectrum of **3da** in $CDCl_3$

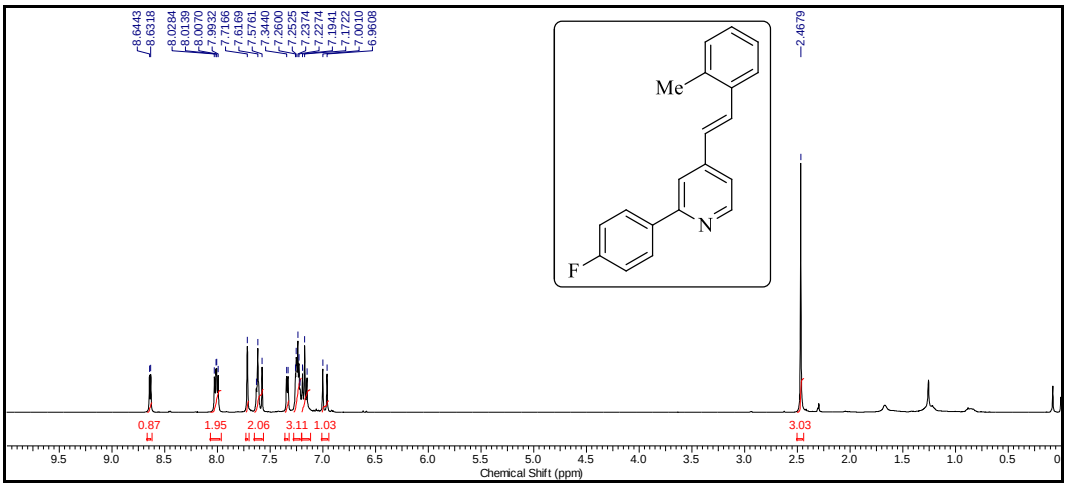


Figure 6.43 400 MHz ^{1}H NMR spectrum of **3dk** in $CDCl_3$

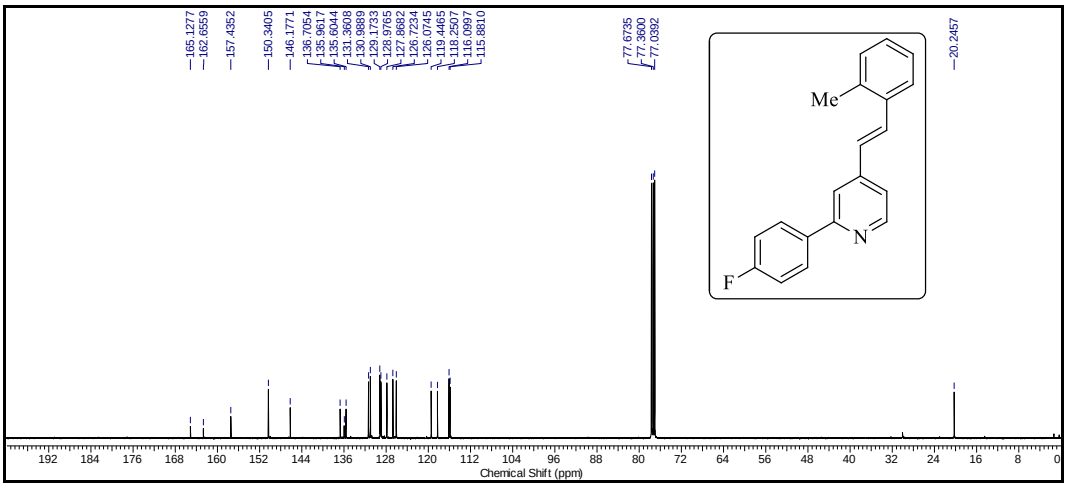


Figure 6.44 100 MHz ^{13}C NMR spectrum of **3dk** in $CDCl_3$

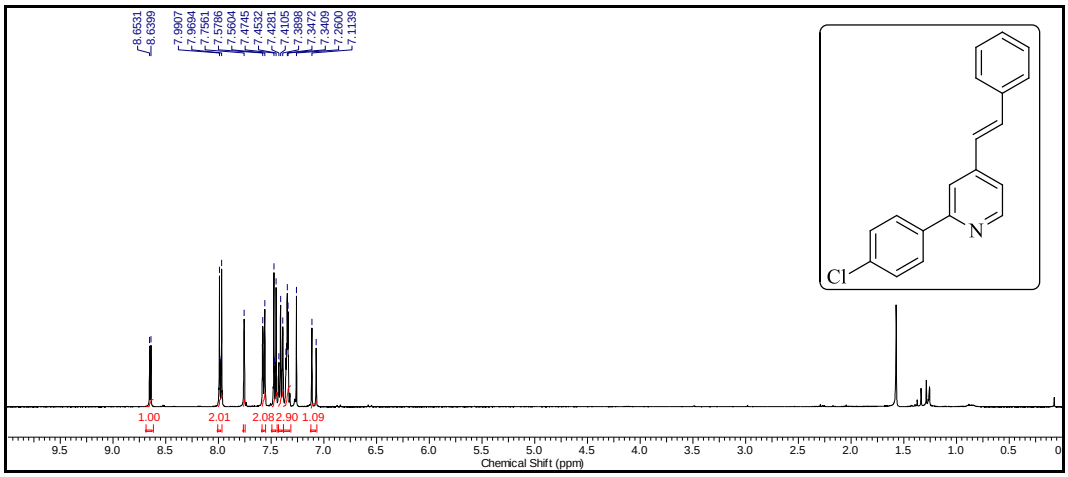


Figure 6.45 400 MHz ^{1}H NMR spectrum of **3ea** in $CDCl_3$

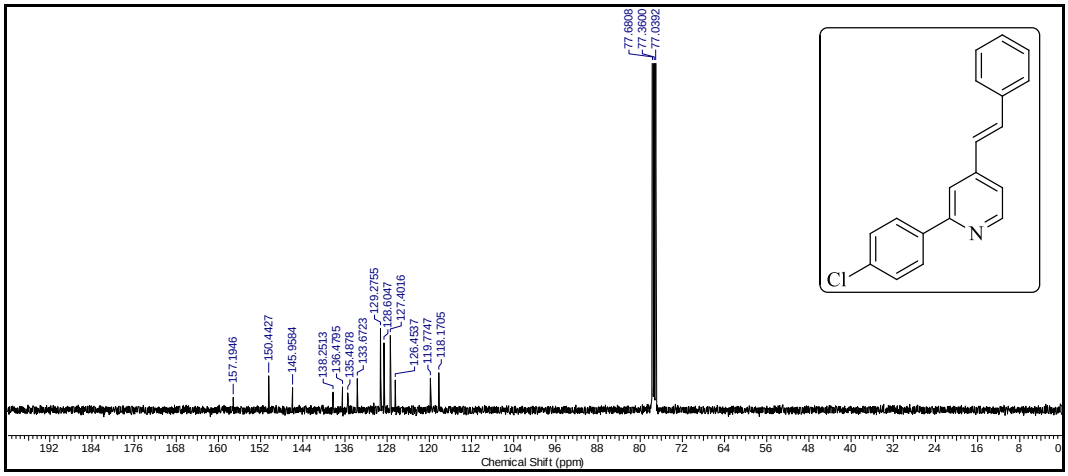


Figure 6.46 100 MHz ^{13}C NMR spectrum of **3ea** in $CDCl_3$

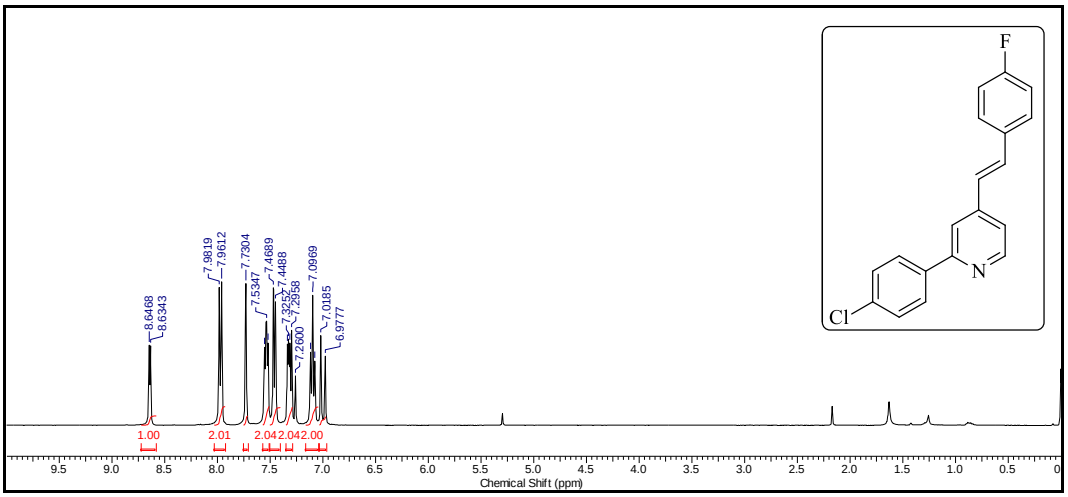


Figure 6.47 400 MHz ^{1}H NMR spectrum of **3eg** in $CDCl_3$

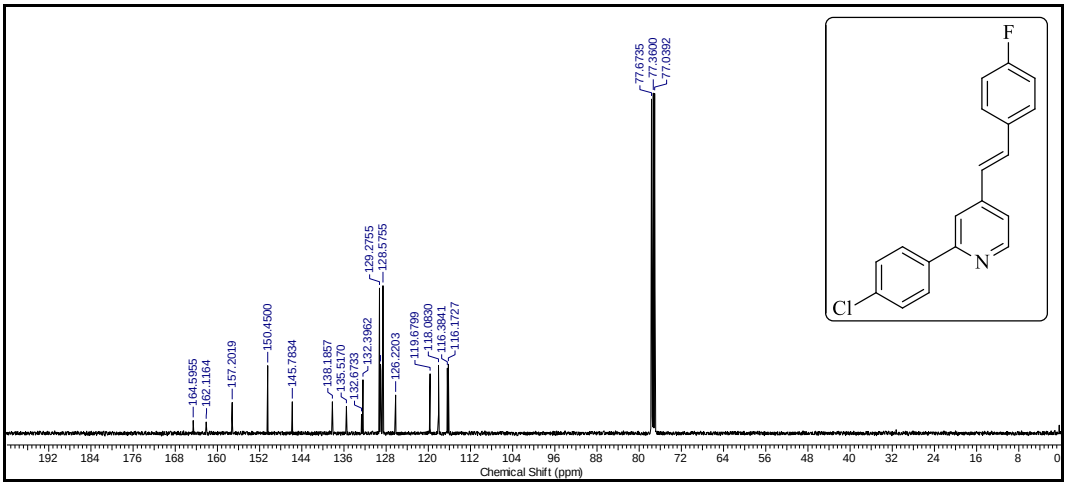


Figure 6.48 100 MHz ^{13}C NMR spectrum of **3eg** in $CDCl_3$

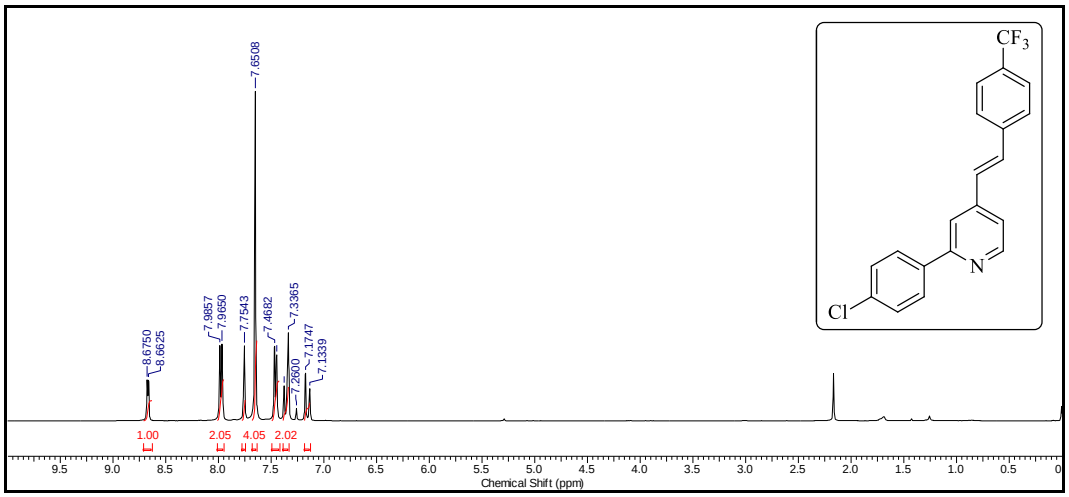


Figure 6.49 400 MHz ^{1}H NMR spectrum of **3eh** in $CDCl_3$

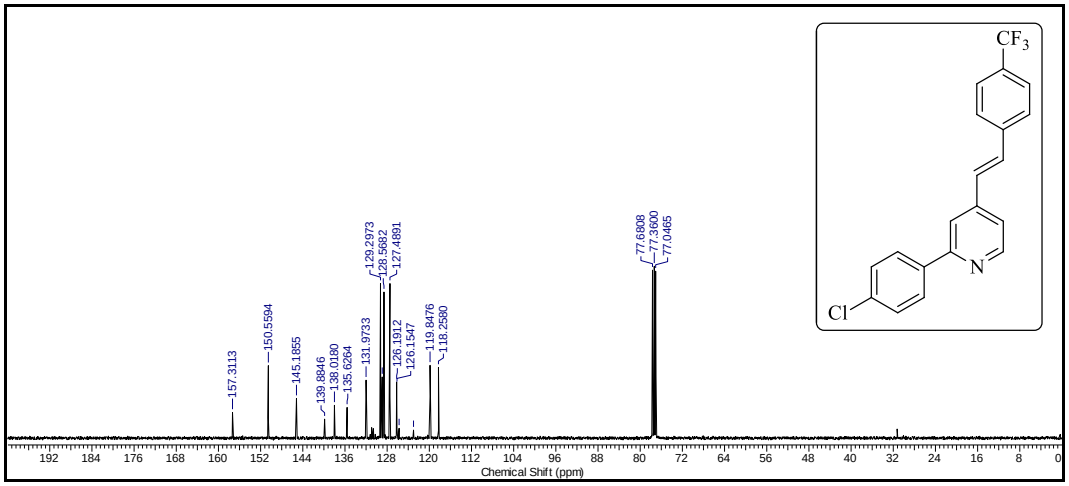


Figure 6.50 100 MHz ^{13}C NMR spectrum of **3eh** in $CDCl_3$

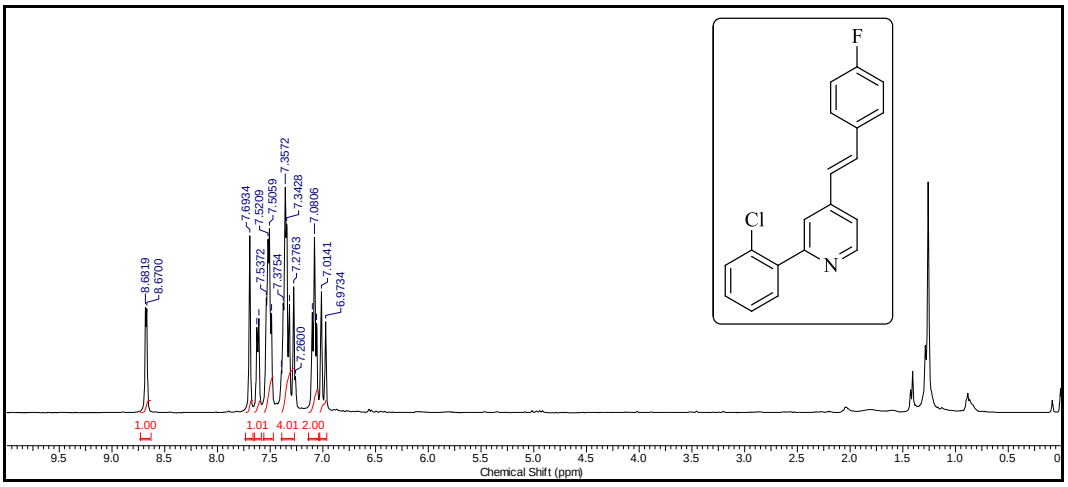


Figure 6.51 400 MHz ^{1}H NMR spectrum of **3fg** in $CDCl_3$

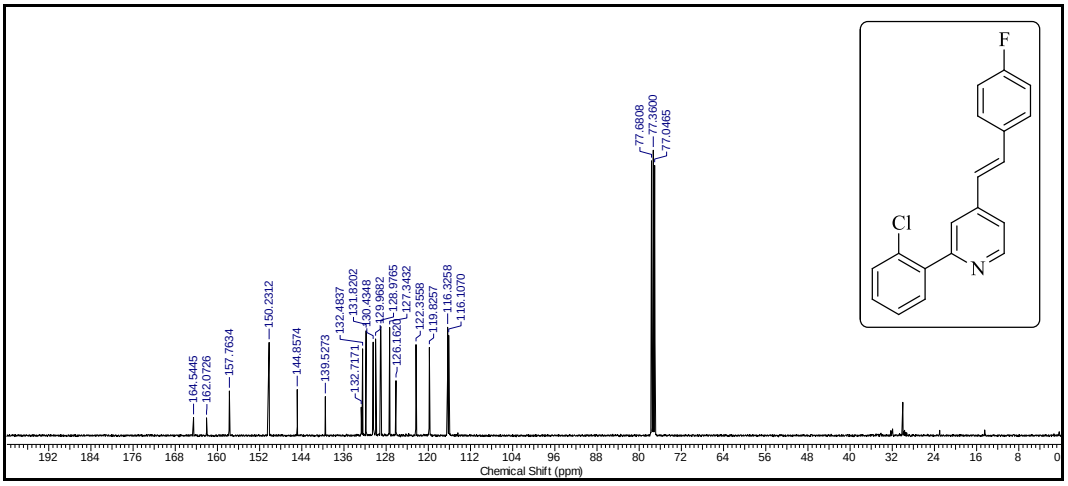


Figure 6.52 100 MHz ^{13}C NMR spectrum of **3fg** in $CDCl_3$

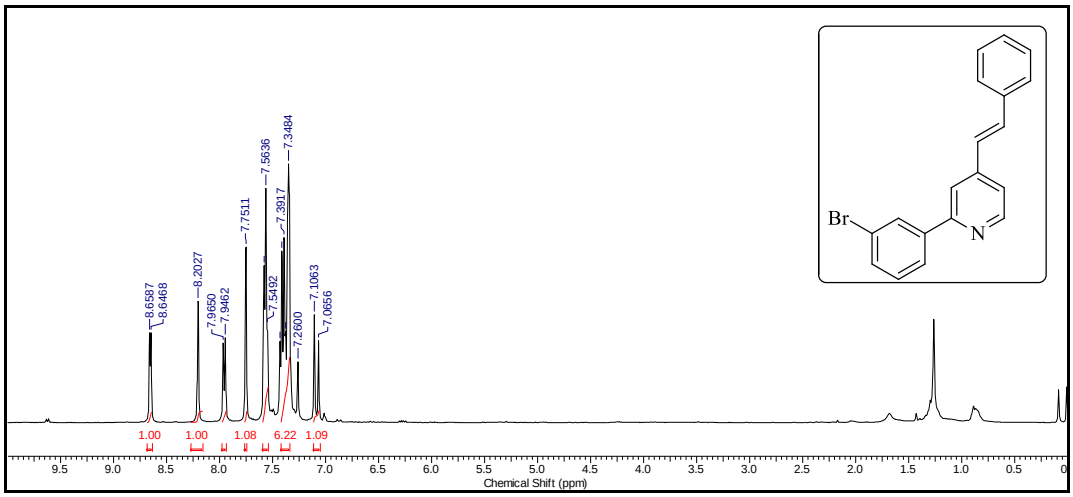


Figure 6.53 400 MHz ^{1}H NMR spectrum of **3ga** in $CDCl_3$

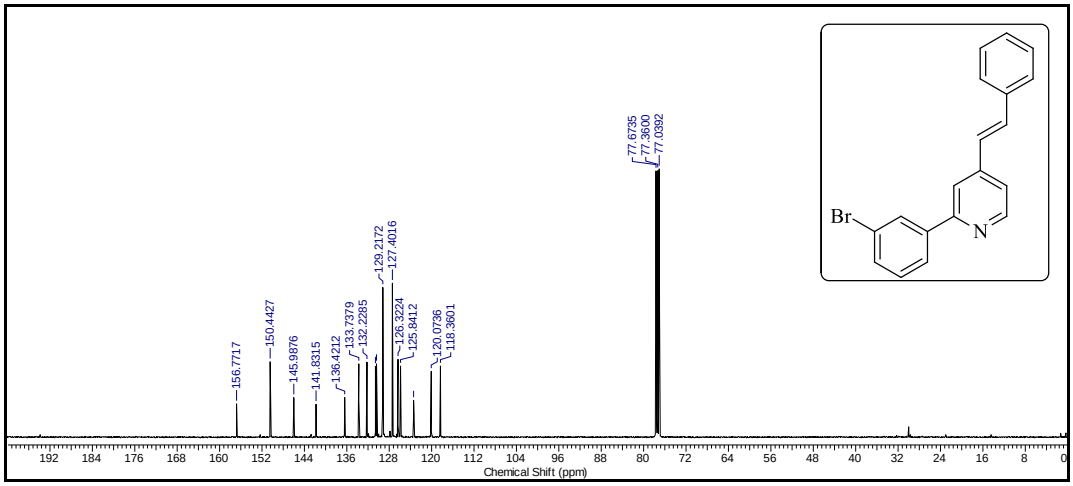


Figure 6.54 100 MHz ^{13}C NMR spectrum of **3ga** in $CDCl_3$

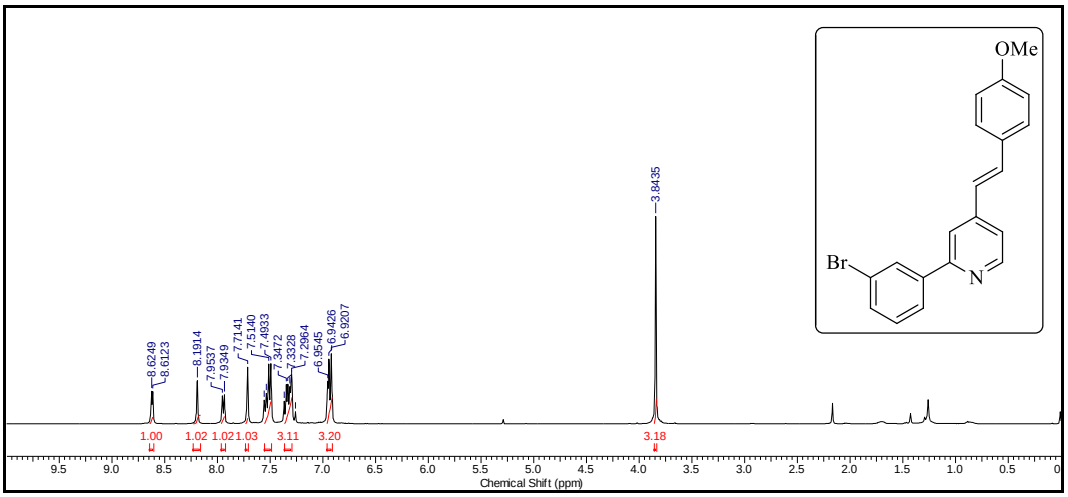


Figure 6.55 400 MHz ^{1}H NMR spectrum of **3gc** in $CDCl_3$

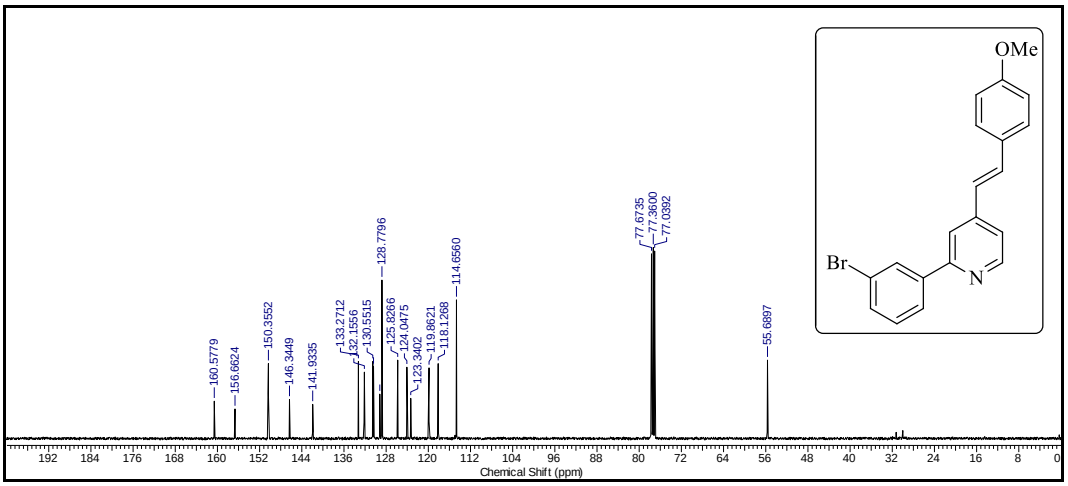


Figure 6.56 100 MHz ^{13}C NMR spectrum of **3gc** in $CDCl_3$

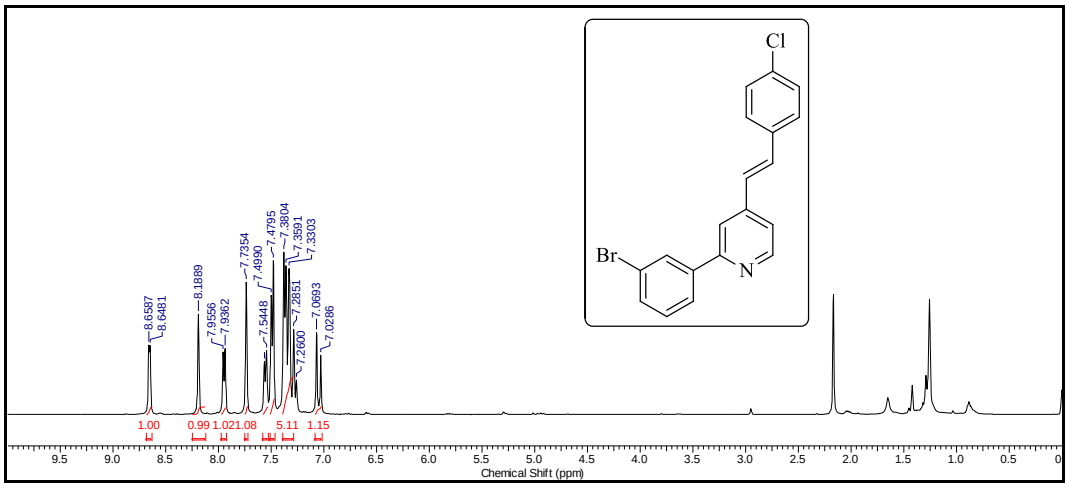


Figure 6.57 400 MHz ^{1}H NMR spectrum of **3ge** in $CDCl_3$

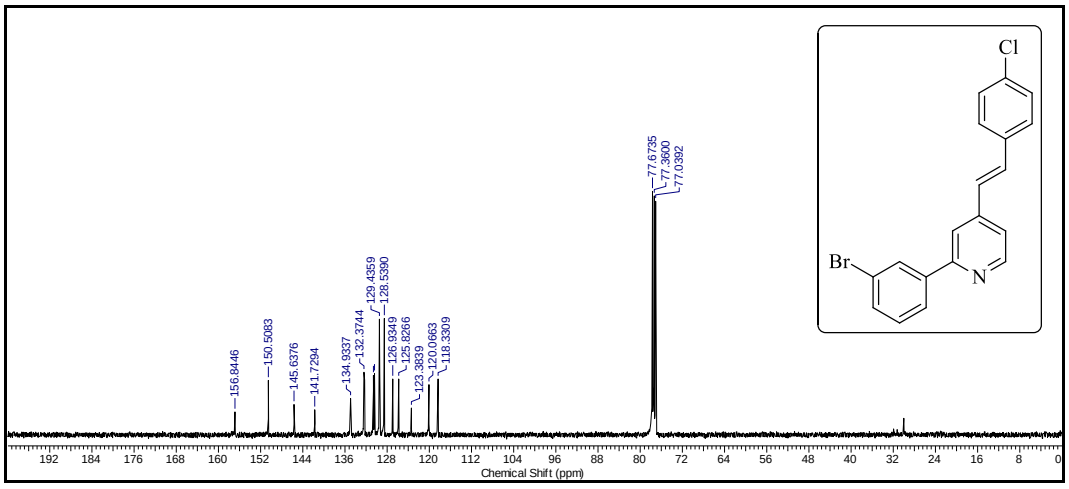


Figure 6.58 100 MHz ^{13}C NMR spectrum of **3ge** in $CDCl_3$

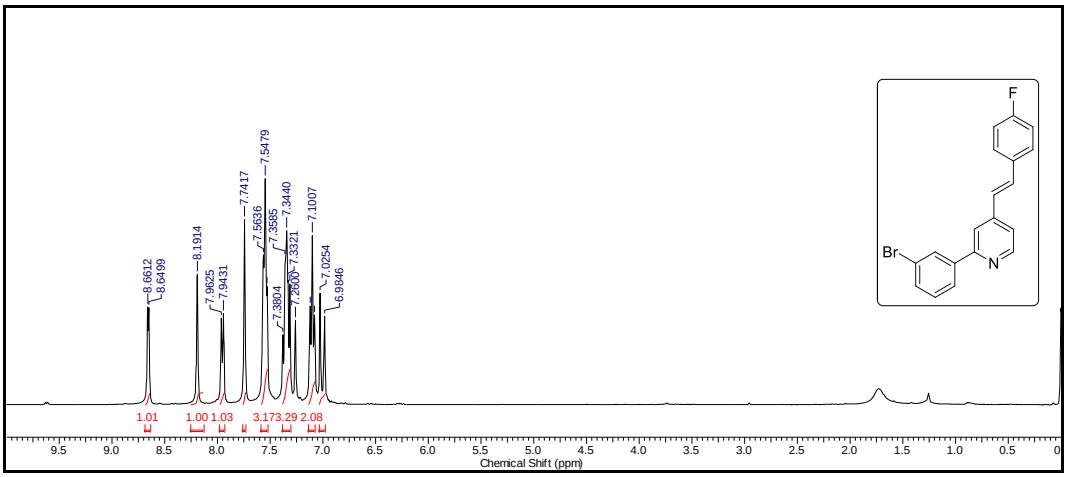


Figure 6.59 400 MHz ^{1}H NMR spectrum of **3gg** in $CDCl_3$

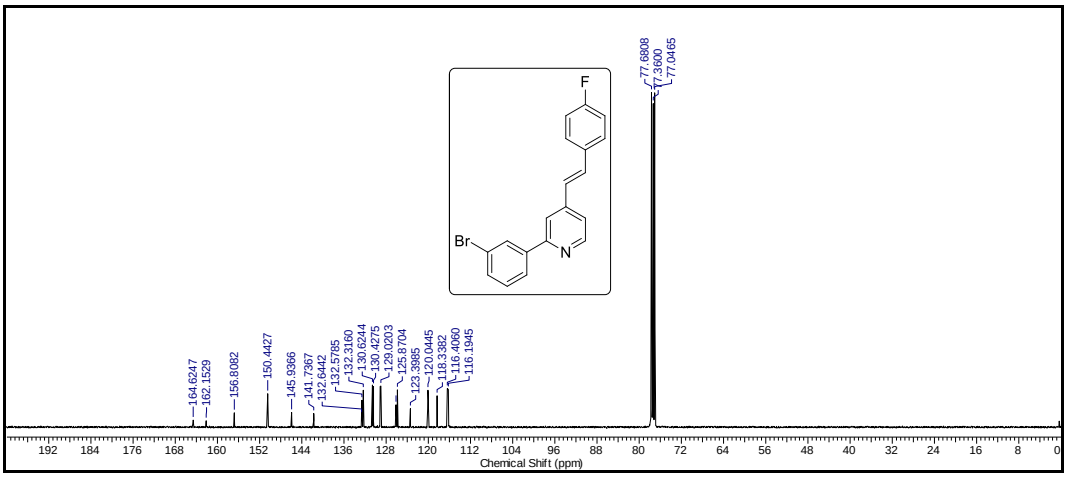


Figure 6.60 100 MHz ^{13}C NMR spectrum of **3gg** in $CDCl_3$

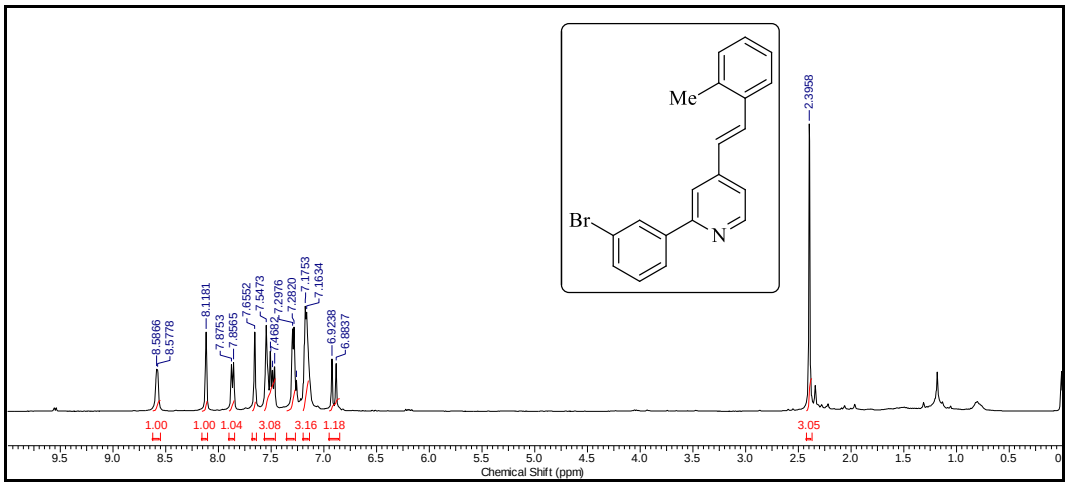


Figure 6.61 400 MHz ^{1}H NMR spectrum of **3gk** in $CDCl_3$

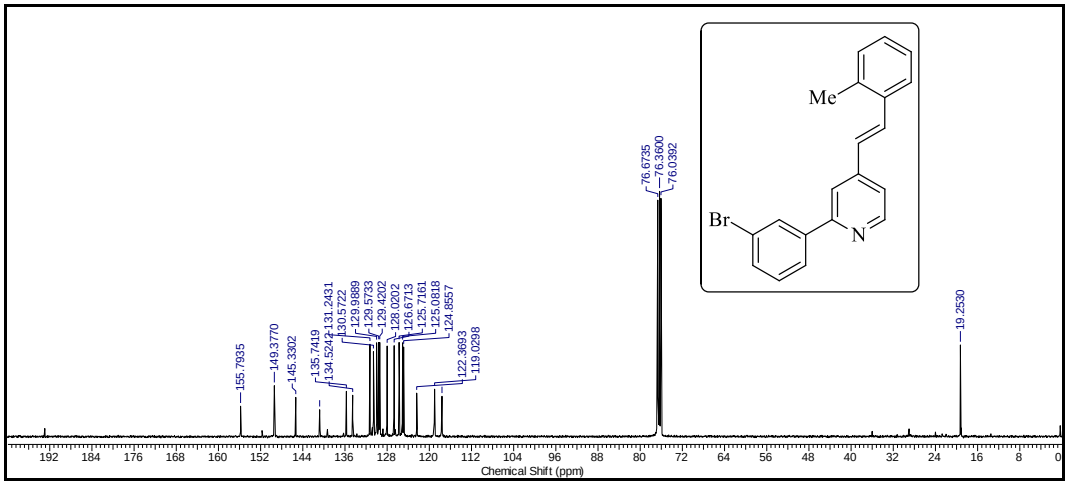


Figure 6.62 100 MHz ^{13}C NMR spectrum of **3gk** in $CDCl_3$

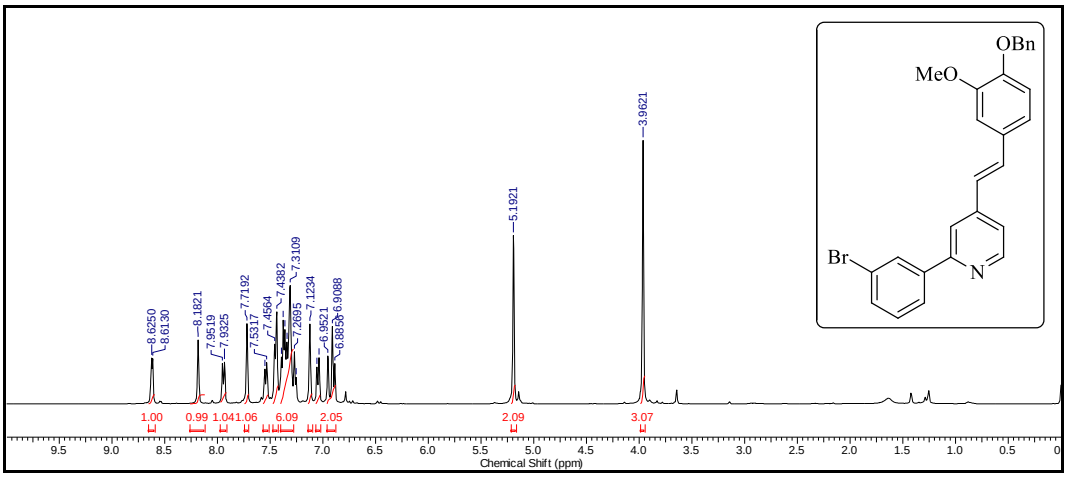


Figure 6.63 400 MHz ^{1}H NMR spectrum of **3gl** in $CDCl_3$

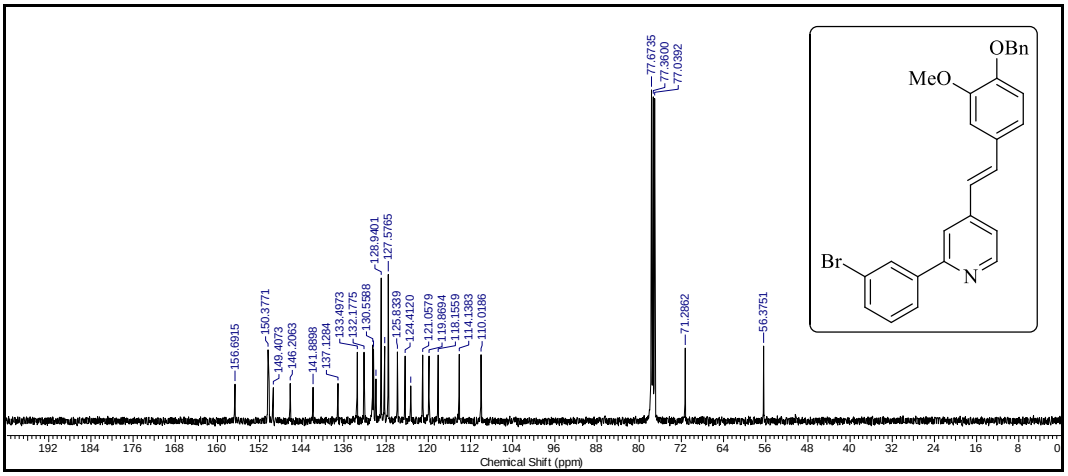


Figure 6.64 100 MHz ^{13}C NMR spectrum of **3gl** in $CDCl_3$

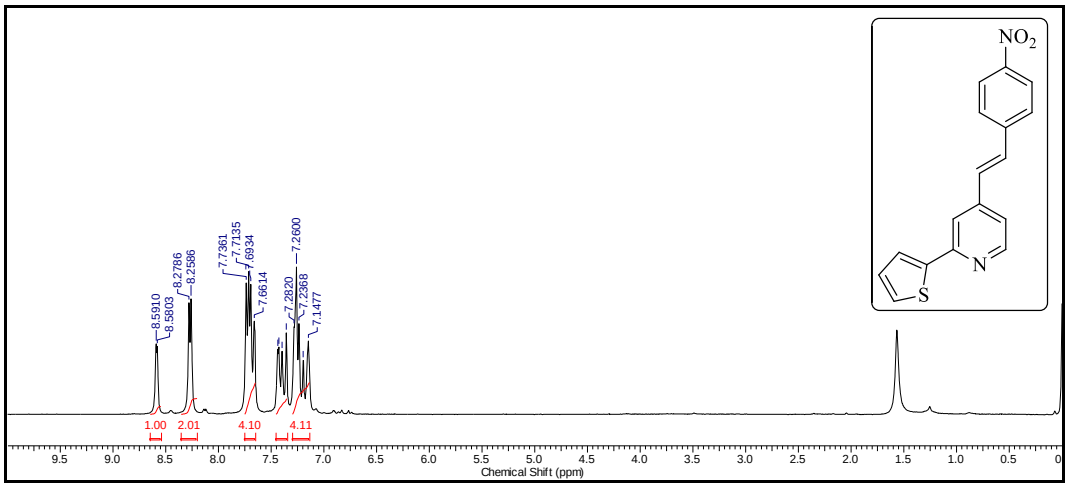


Figure 6.65 400 MHz ^{1}H NMR spectrum of **3hi** in $CDCl_3$

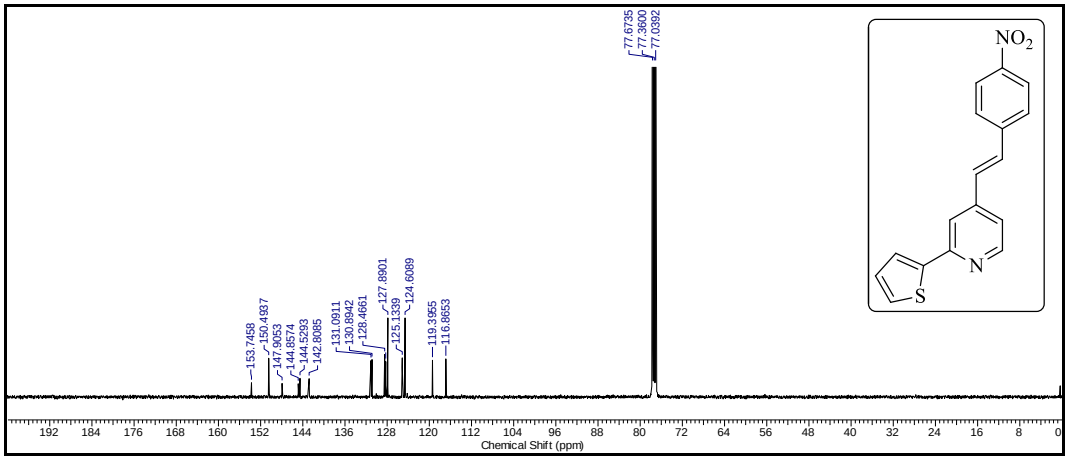


Figure 6.66 100 MHz ^{13}C NMR spectrum of **3hi** in $CDCl_3$

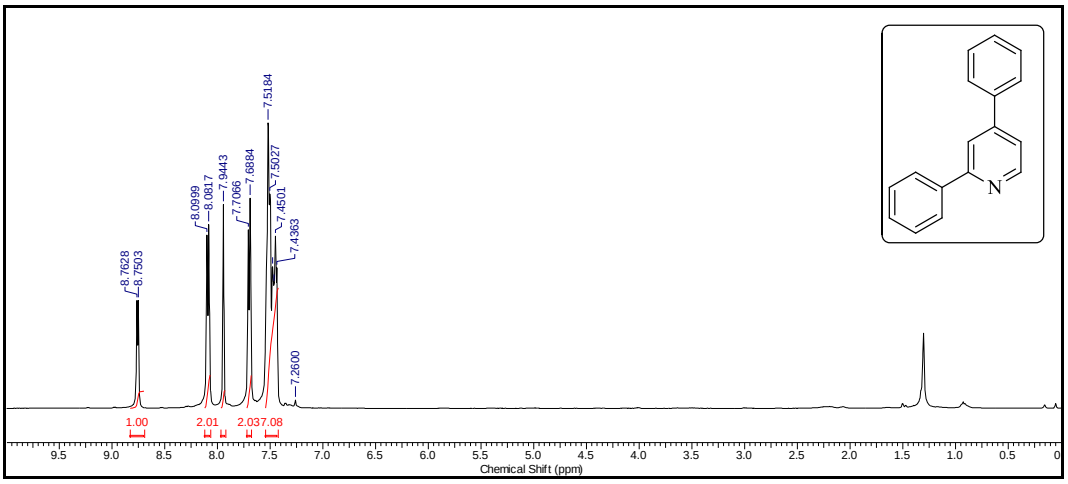


Figure 6.67 400 MHz ^{1}H NMR spectrum of **3am** in $CDCl_3$

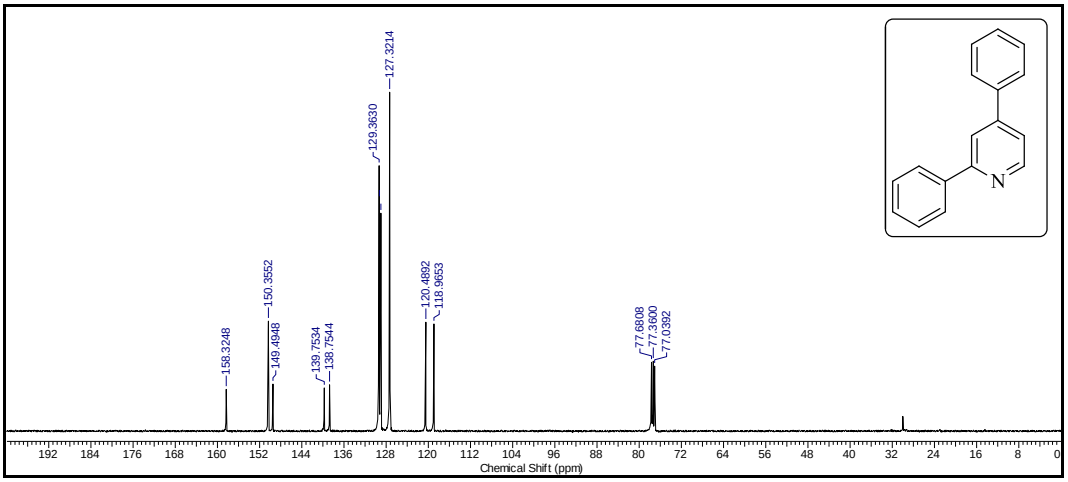


Figure 6.68 100 MHz ^{13}C NMR spectrum of **3am** in $CDCl_3$

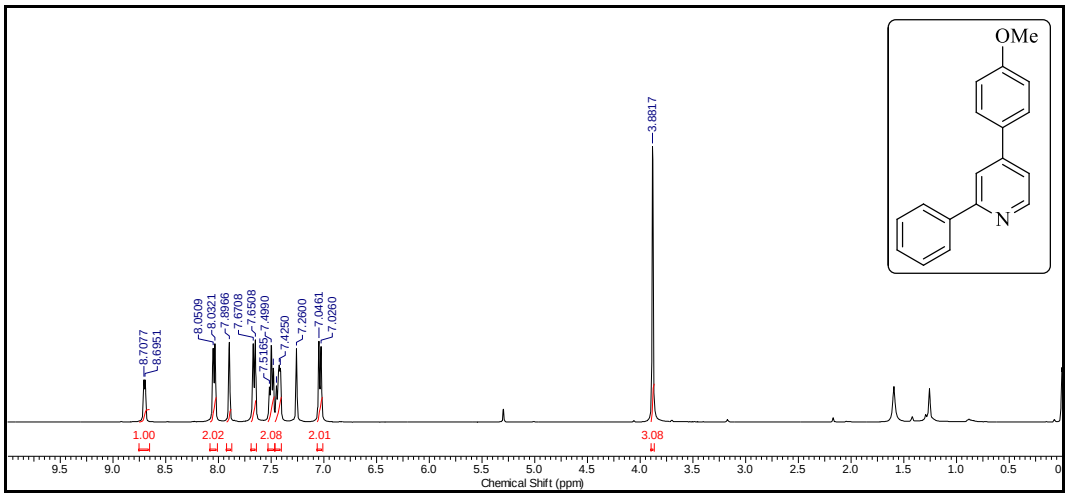


Figure 6.69 400 MHz ^{1}H NMR spectrum of **3an** in $CDCl_3$

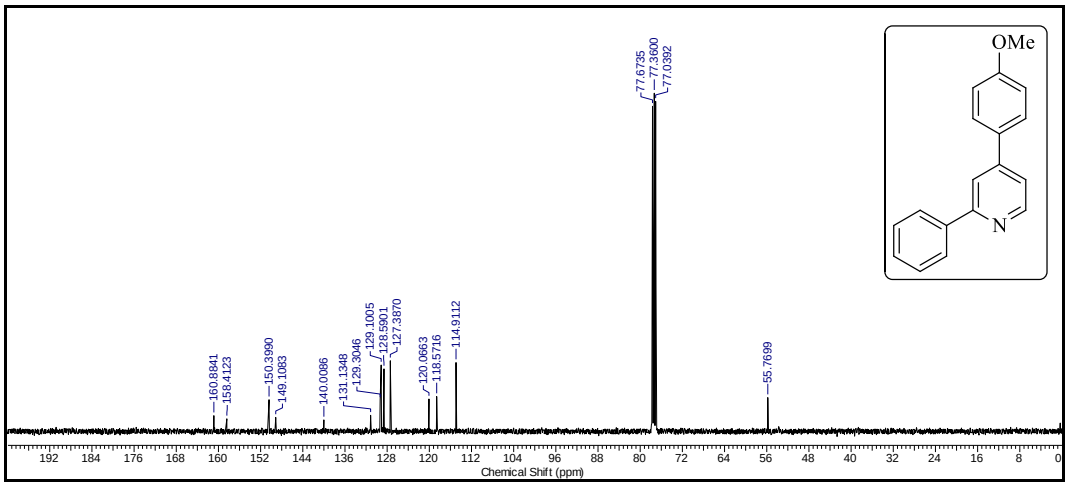


Figure 6.70 100 MHz ^{13}C NMR spectrum of **3an** in $CDCl_3$

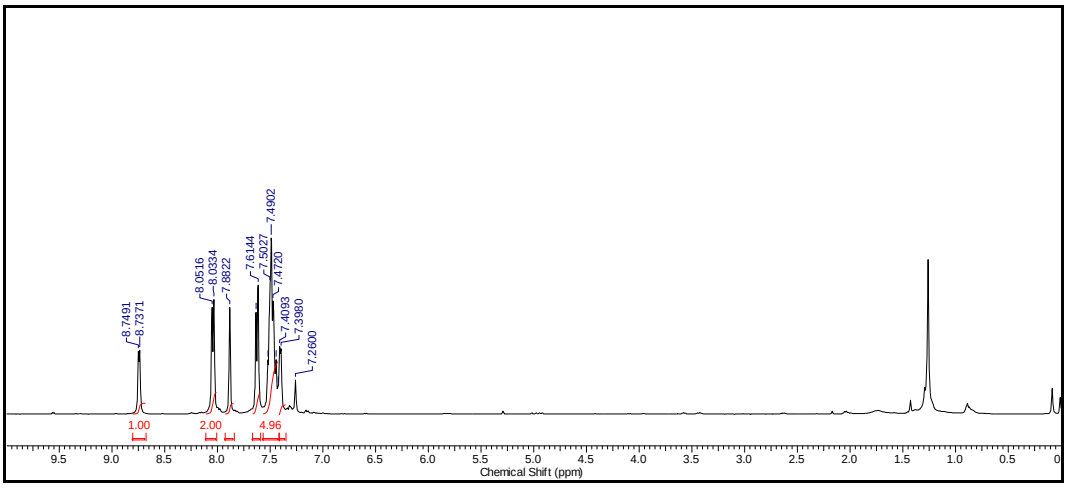


Figure 6.71 400 MHz ^{1}H NMR spectrum of **3ap** in $CDCl_3$

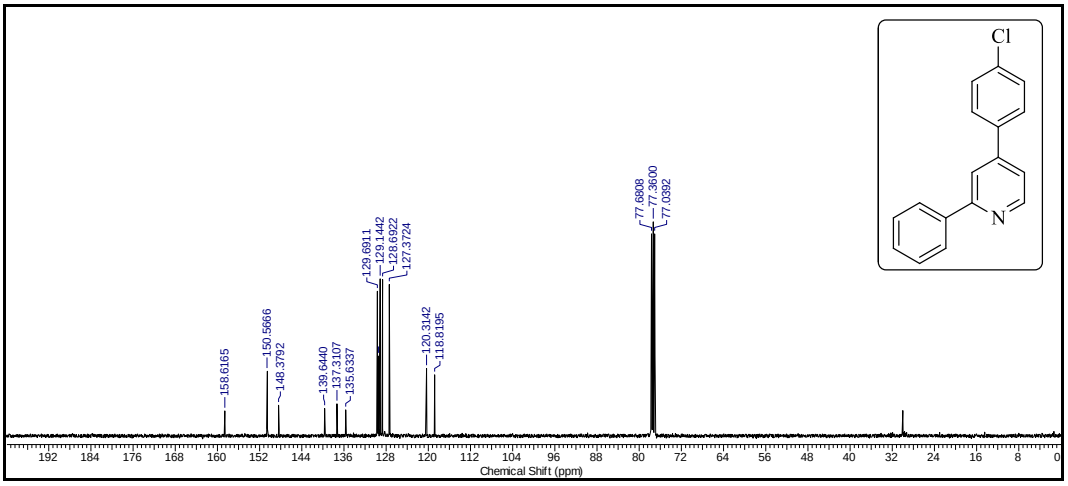


Figure 6.72 100 MHz ^{13}C NMR spectrum of **3ap** in $CDCl_3$

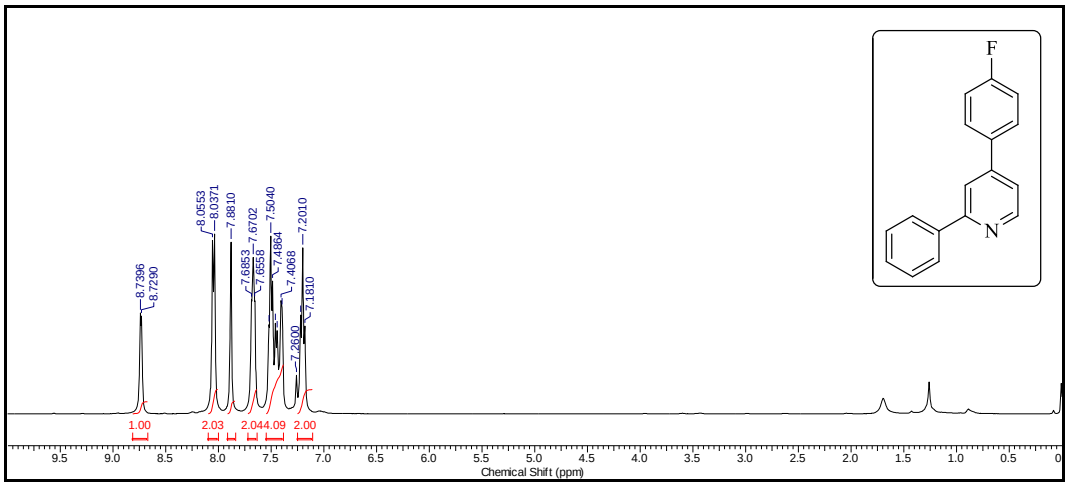


Figure 6.73 400 MHz ^{1}H NMR spectrum of **3aq** in $CDCl_3$

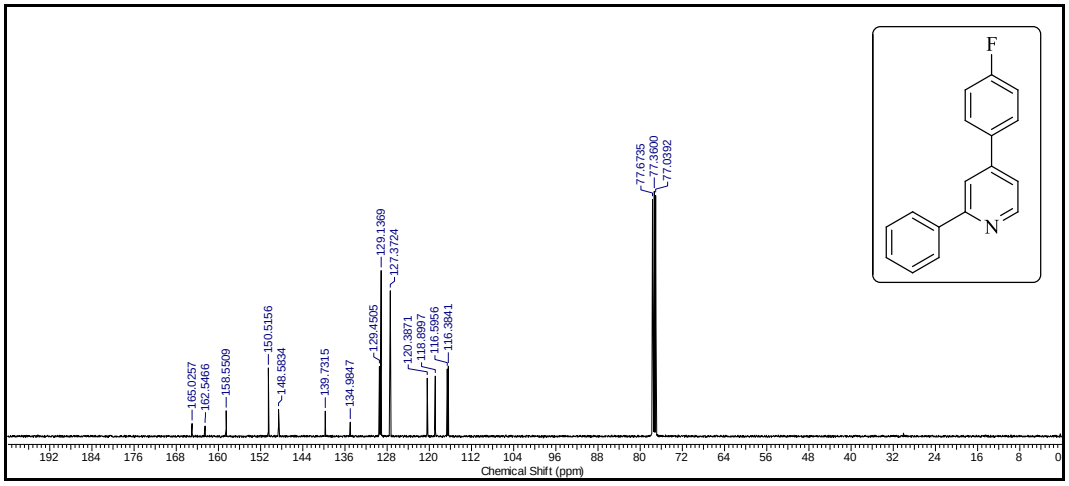


Figure 6.74 100 MHz ^{13}C NMR spectrum of **3aq** in $CDCl_3$

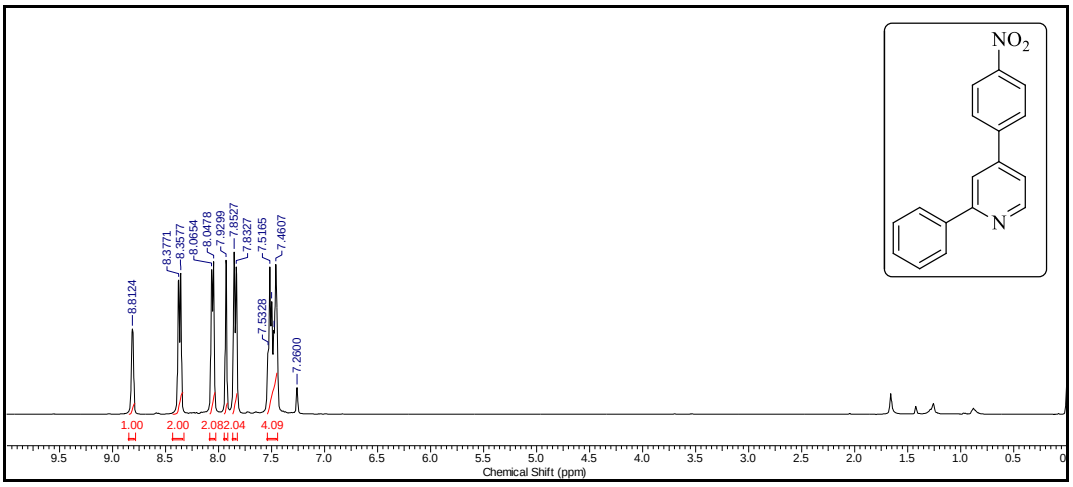


Figure 6.75 400 MHz ^{1}H NMR spectrum of **3as** in $CDCl_3$

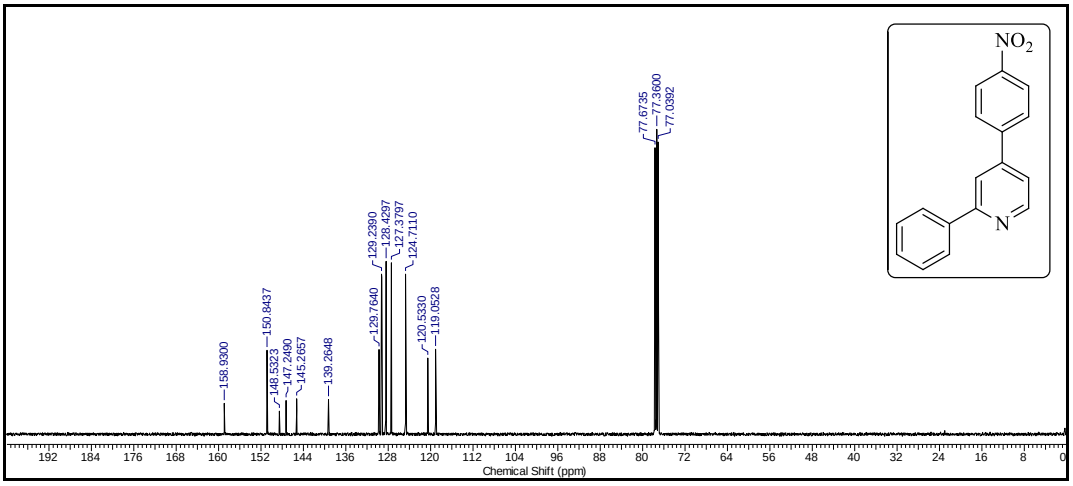


Figure 6.76 100 MHz ^{13}C NMR spectrum of **3as** in $CDCl_3$

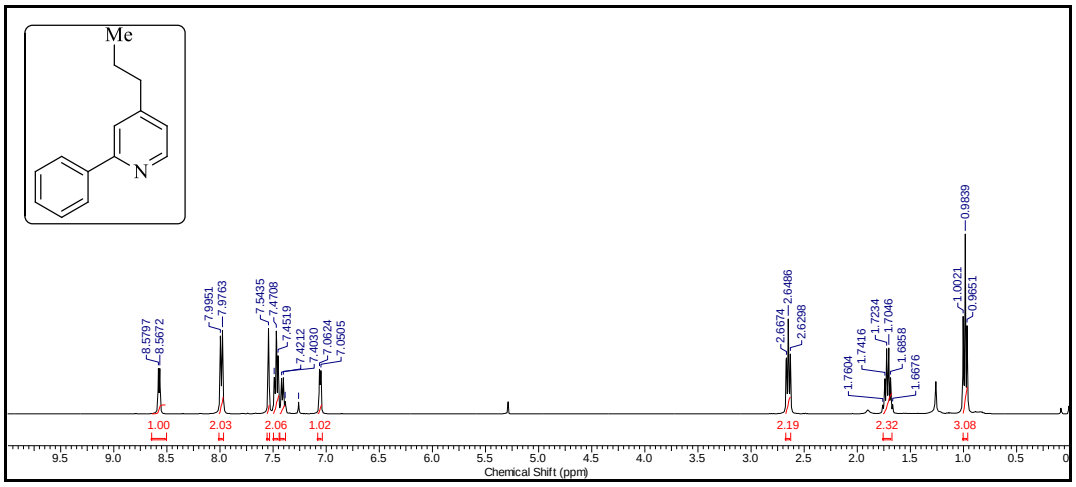


Figure 6.77 400 MHz ^{1}H NMR spectrum of **3at** in $CDCl_3$

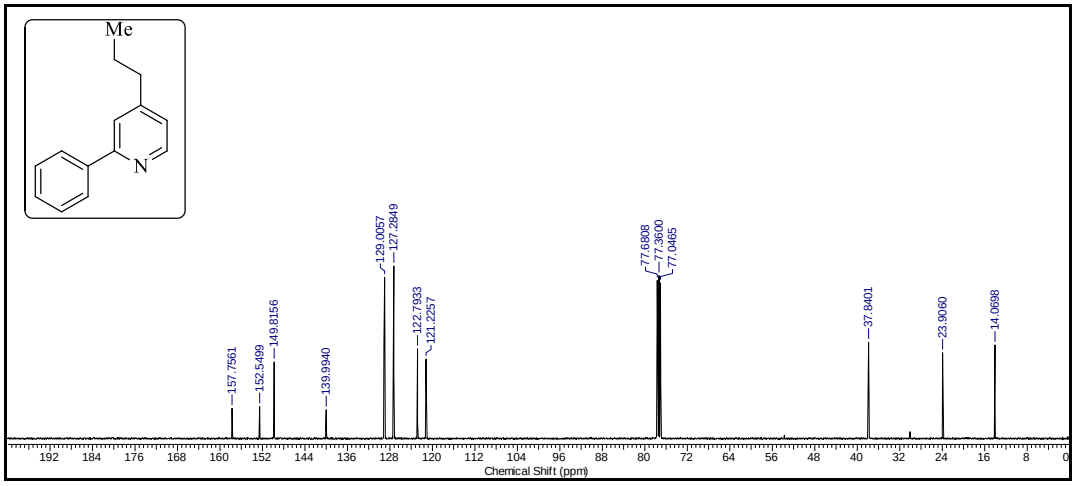


Figure 6.78 100 MHz ^{13}C NMR spectrum of **3at** in $CDCl_3$

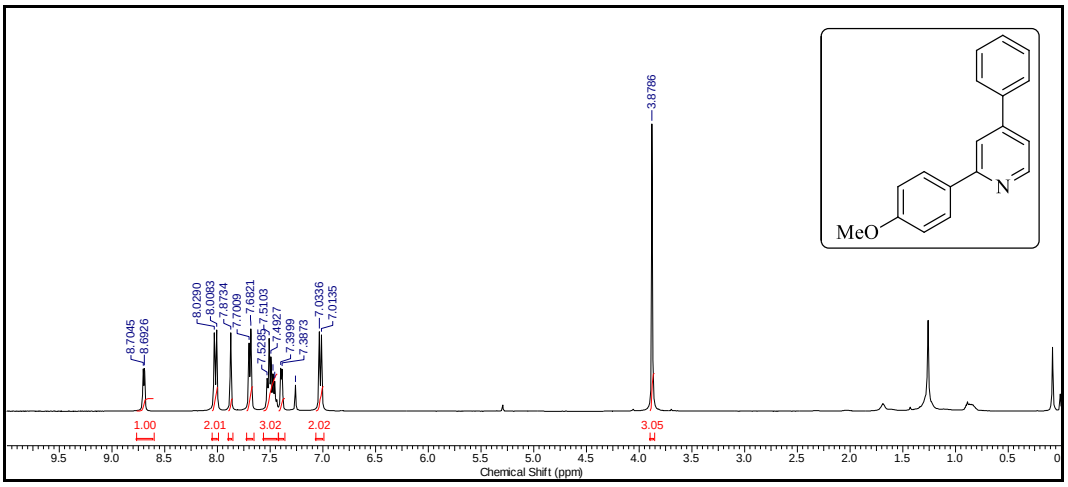


Figure 6.79 400 MHz ^{1}H NMR spectrum of **3cm** in $CDCl_3$

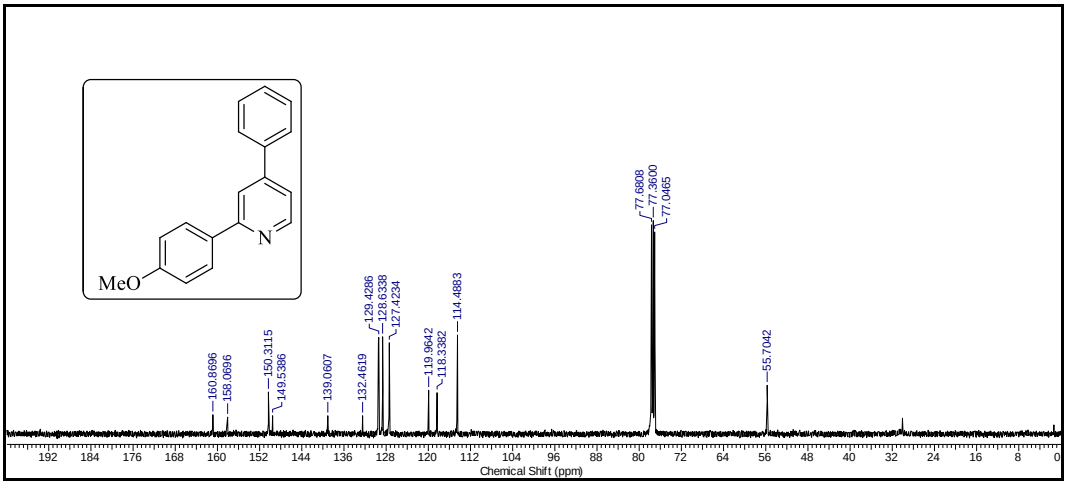


Figure 6.80 100 MHz ^{13}C NMR spectrum of **3cm** in $CDCl_3$

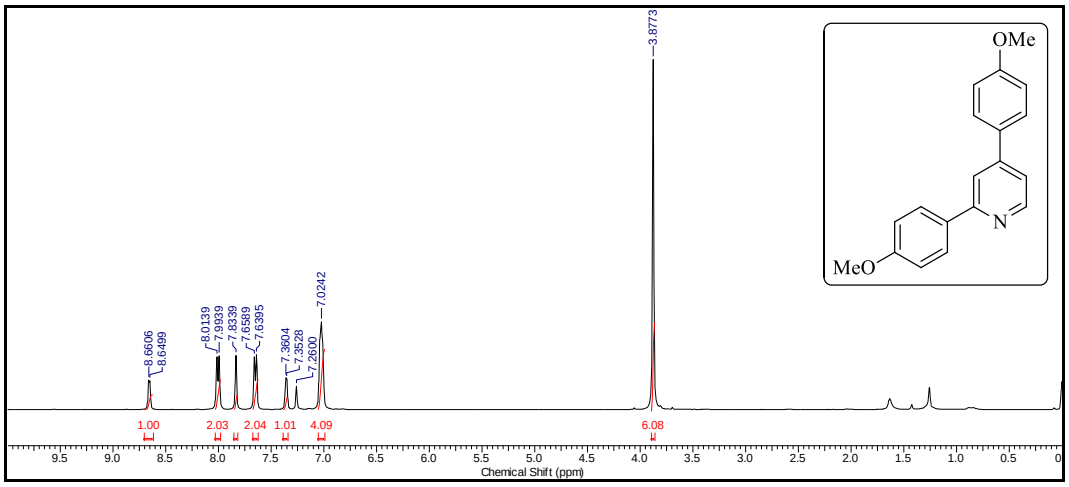


Figure 6.81 400 MHz ^{1}H NMR spectrum of **3cn** in $CDCl_3$

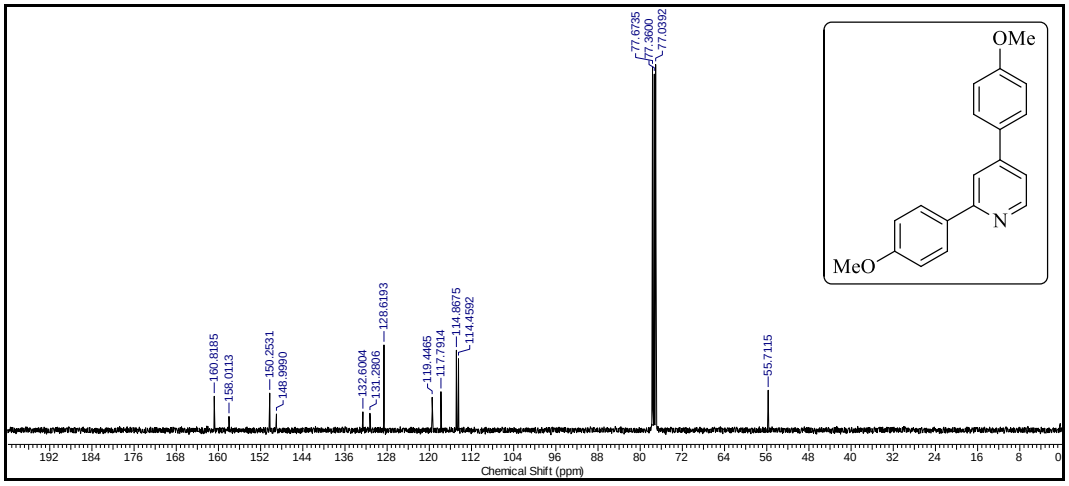


Figure 6.82 100 MHz ^{13}C NMR spectrum of **3cn** in $CDCl_3$

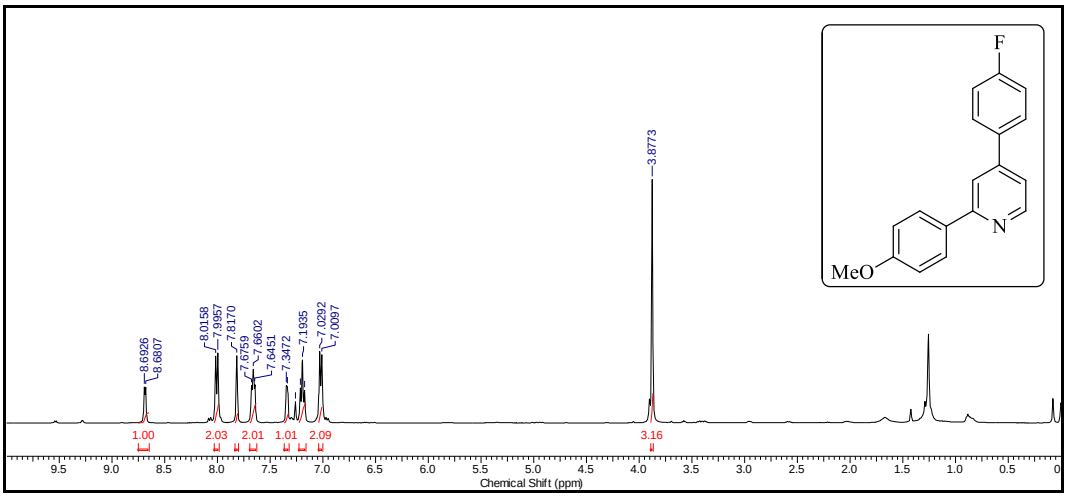


Figure 6.83 400 MHz ^{1}H NMR spectrum of **3cq** in $CDCl_3$

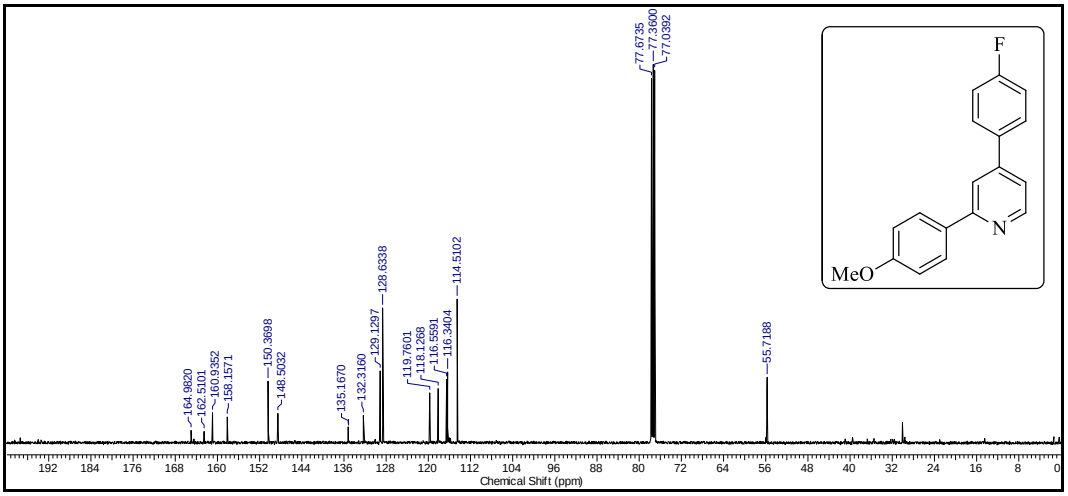


Figure 6.84 100 MHz ^{13}C NMR spectrum of **3cq** in $CDCl_3$

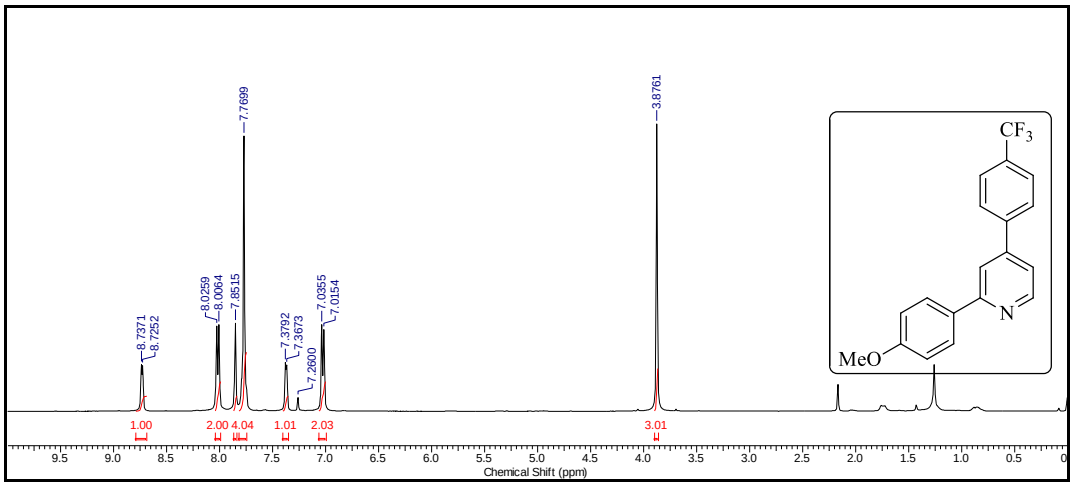


Figure 6.85 400 MHz ^{1}H NMR spectrum of **3cr** in $CDCl_3$

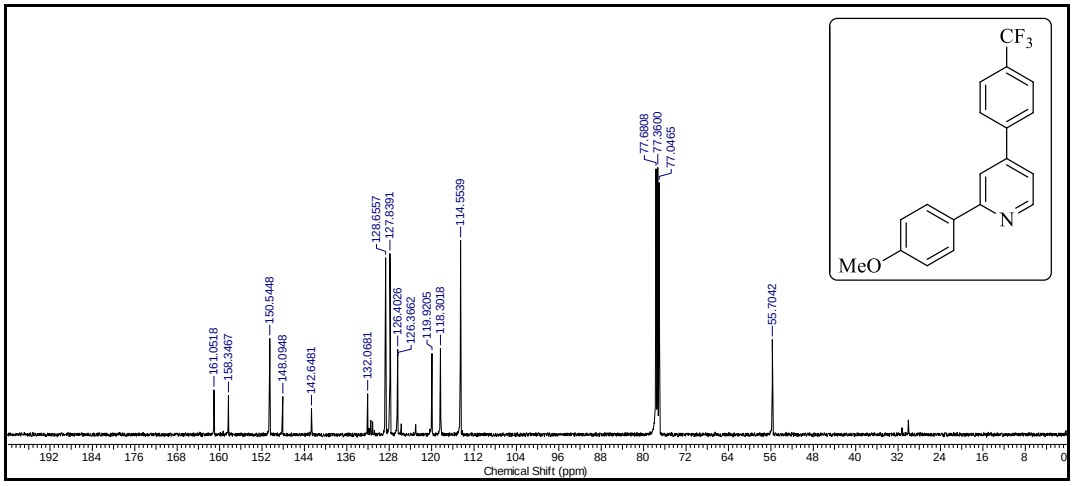


Figure 6.86 100 MHz ^{13}C NMR spectrum of **3cr** in $CDCl_3$

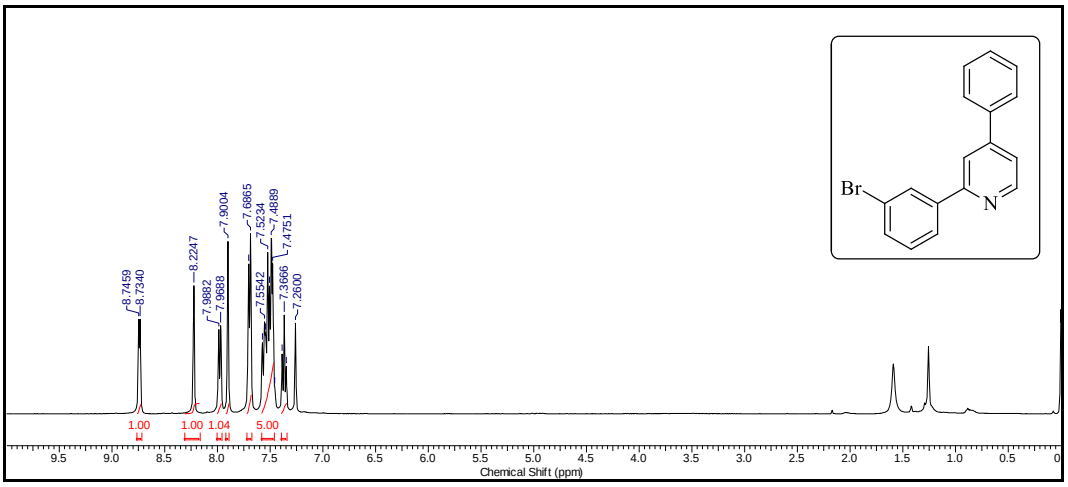


Figure 6.87 400 MHz ^{1}H NMR spectrum of **3gm** in $CDCl_3$

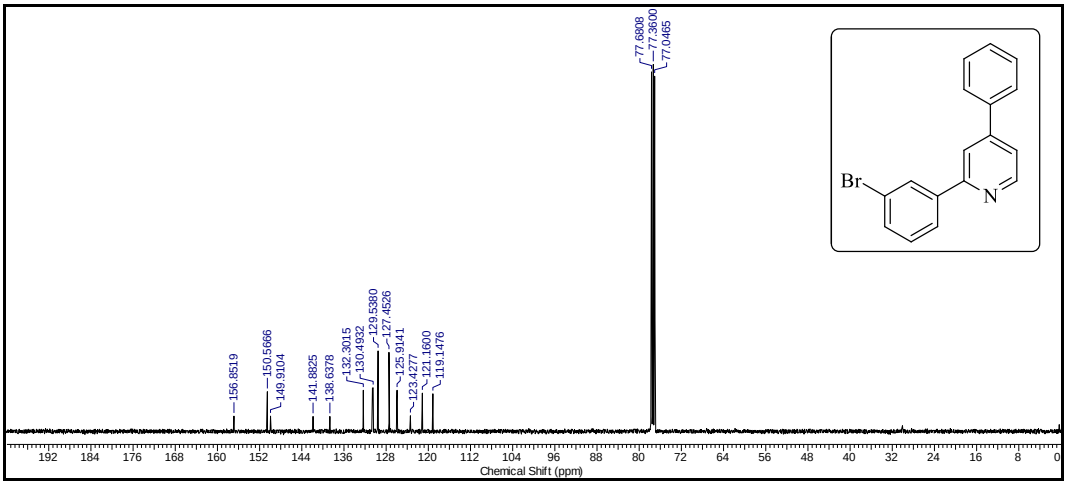


Figure 6.88 100 MHz ^{13}C NMR spectrum of **3gm** in $CDCl_3$

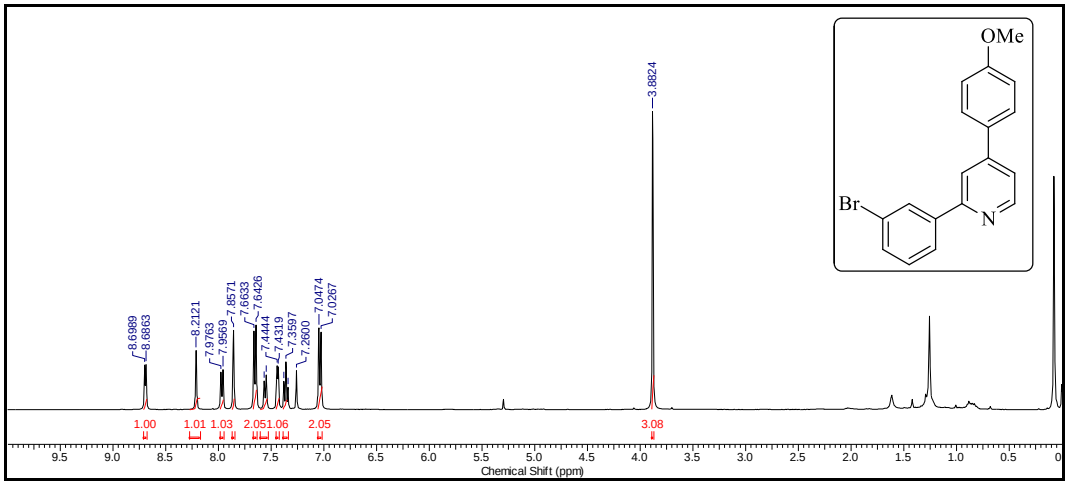


Figure 6.89 400 MHz ^{1}H NMR spectrum of **3gn** in $CDCl_3$

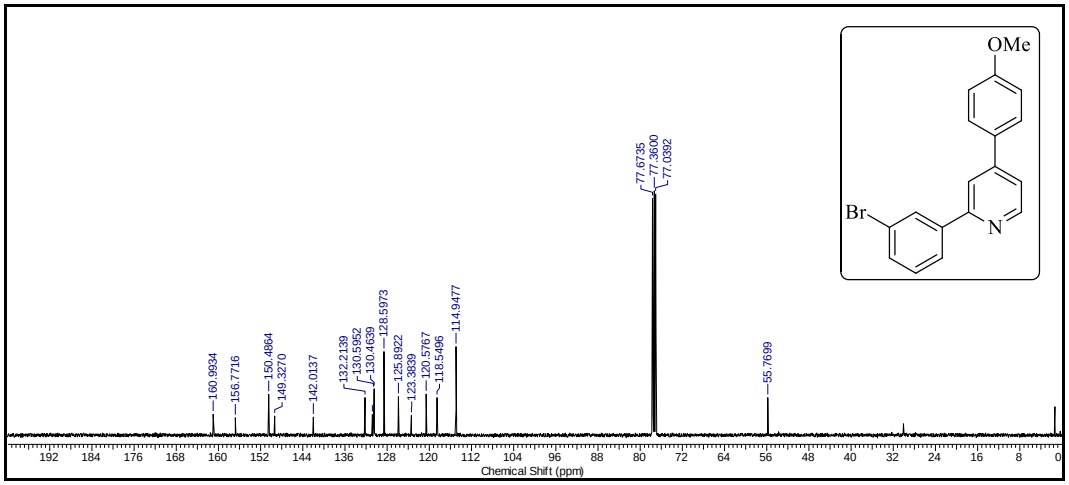


Figure 6.90 100 MHz ^{13}C NMR spectrum of **3gn** in $CDCl_3$

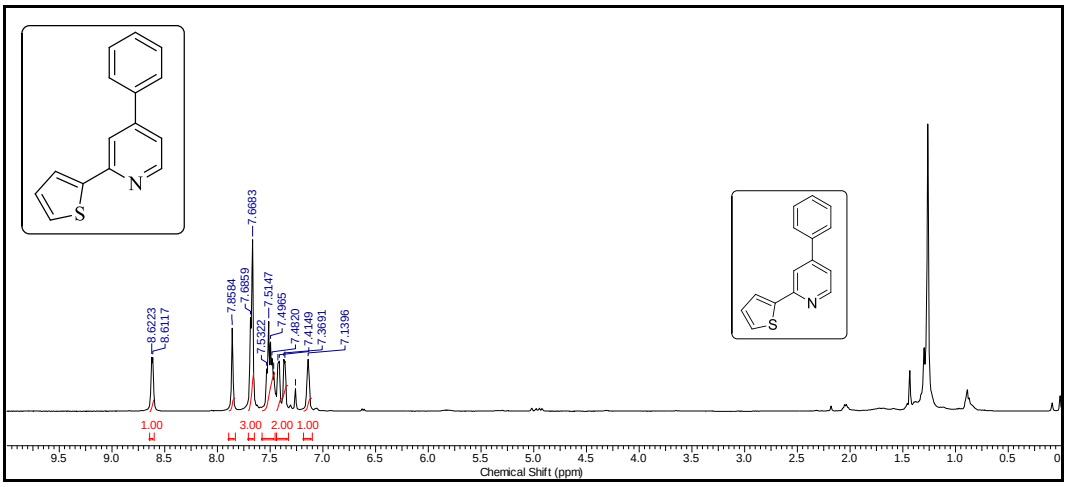


Figure 6.91 400 MHz ^{1}H NMR spectrum of **3hm** in $CDCl_3$

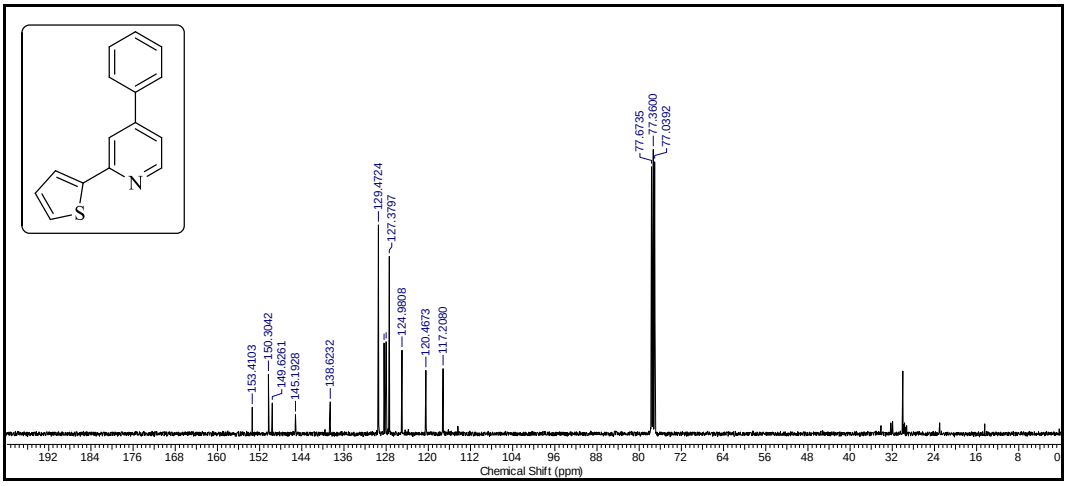


Figure 6.92 100 MHz ^{13}C NMR spectrum of **3hm** in $CDCl_3$

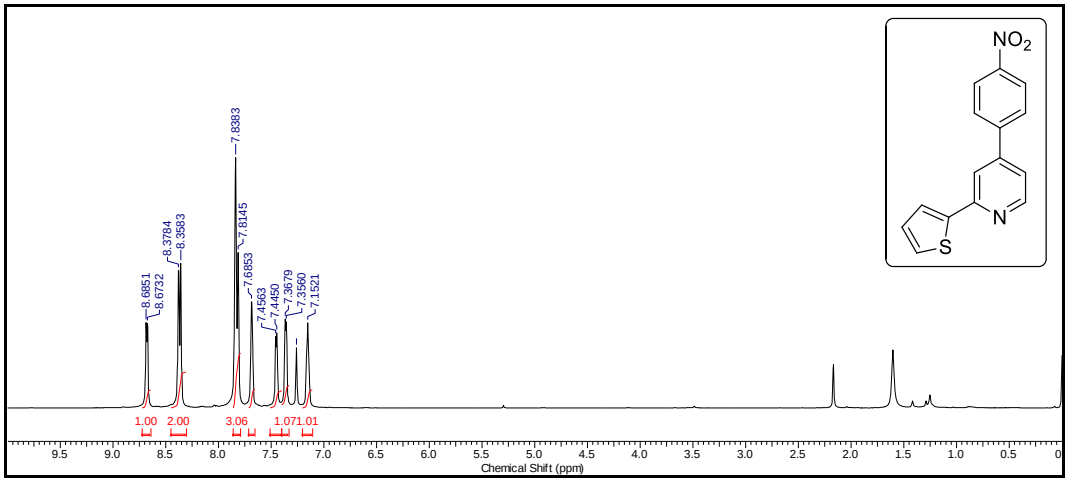


Figure 6.93 400 MHz ^{1}H NMR spectrum of **3hs** in $CDCl_3$

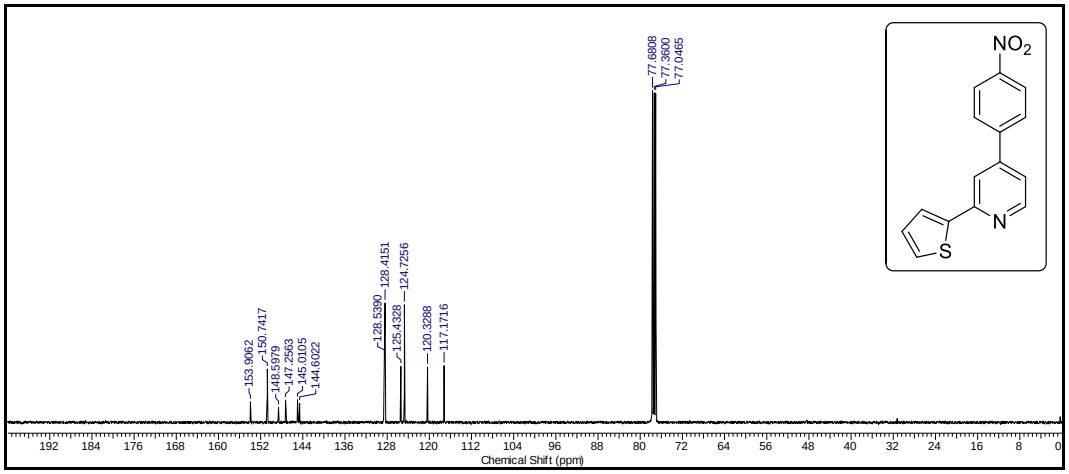


Figure 6.94 100 MHz ^{13}C NMR spectrum of **3hs** in $CDCl_3$

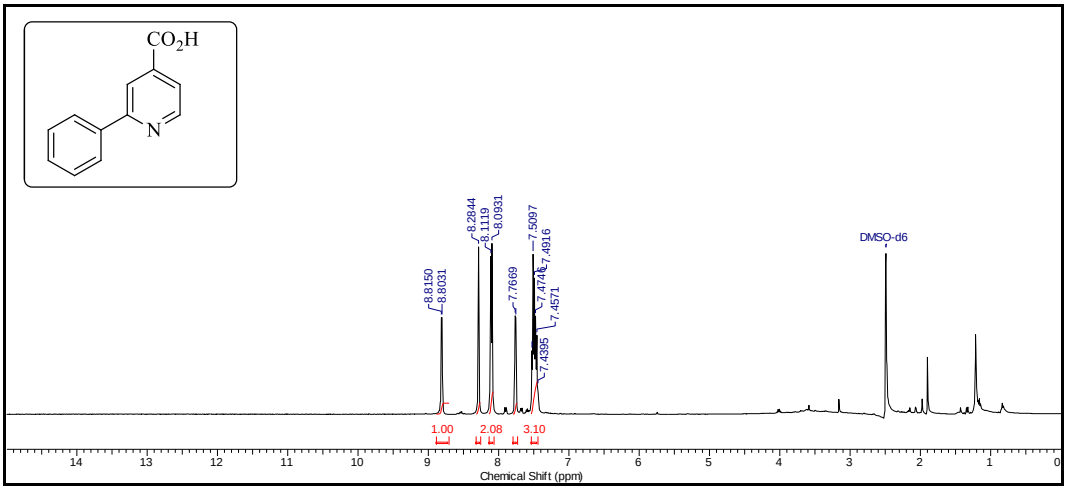


Figure 6.95 400 MHz ^{1}H NMR spectrum of **4aa** in DMSO-d_6

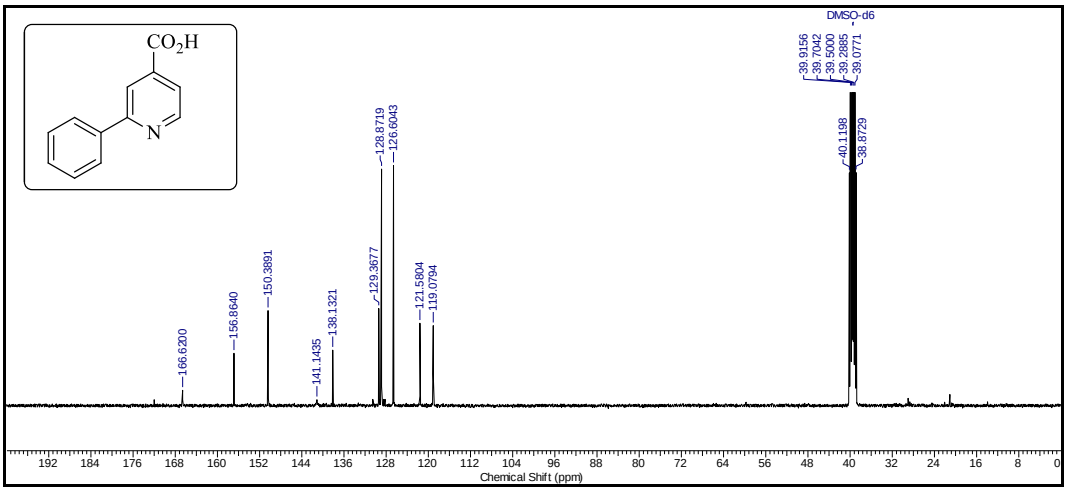


Figure 6.96 100 MHz ^{13}C NMR spectrum of **4aa** in DMSO-d_6

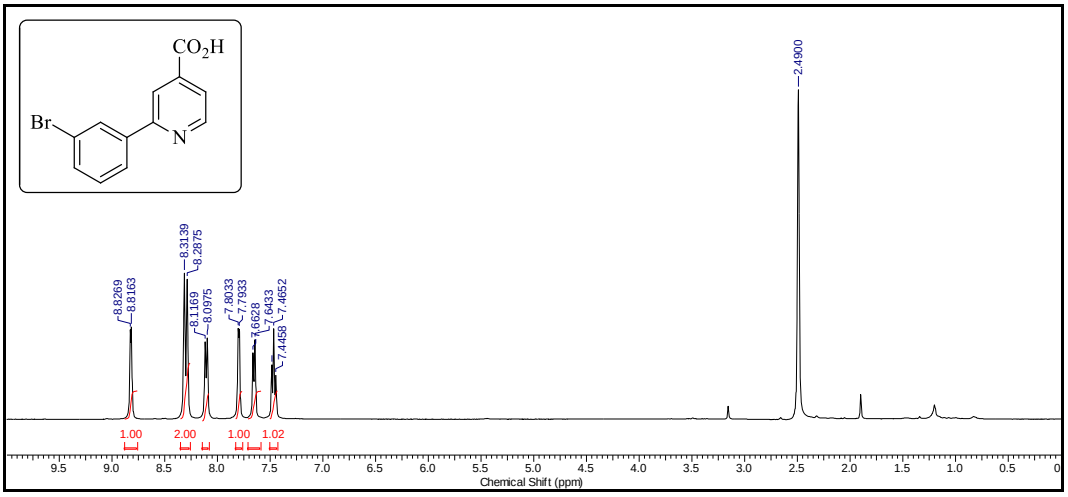


Figure 6.97 400 MHz ^{1}H NMR spectrum of **4ga** in DMSO-d_6

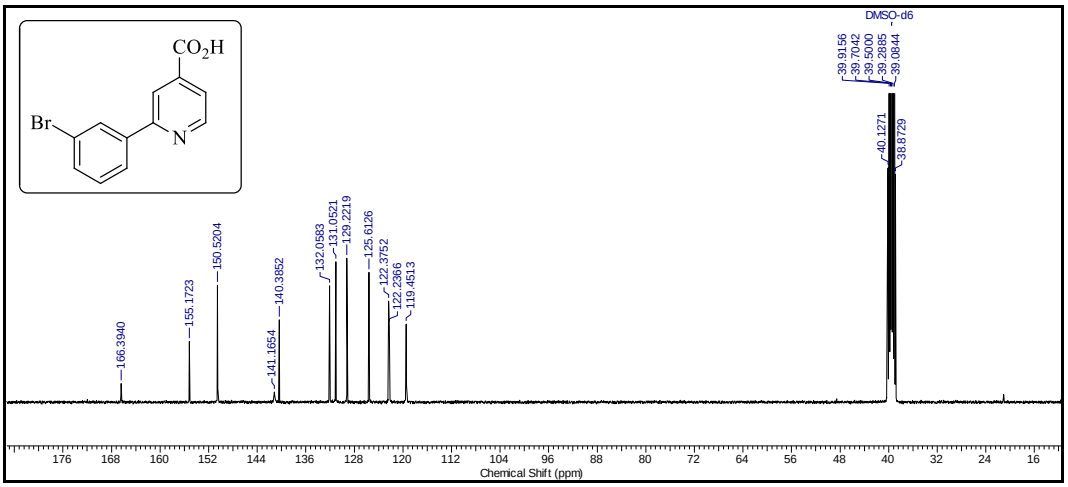


Figure 6.98 100 MHz ^{13}C NMR spectrum of **4ga** in DMSO-d_6

6.7 References

1. Anderson T. V. (1849) "Producte der trocknen Destillation thierischer Materien" [Products of the dry distillation of animal matter], *Annalen der Chemie und Pharmacie.,* 70, 32-38 (DOI: 10.1002/jlac.18490700105)
2. Körner W. (1869) *Giornale academico di Palermo.* 5
3. Dewar J. (1871) *Chemical News.* 23, 38
4. Henninger A. (1877) Berichte der deutschen chemischen Gesellschaft (Correspondence). *Eur. J. Inorg. Chem.* 10, 727-737 (DOI: 10.1002/cber.187701001202)
5. Gribble, G. W., Joule, J. A. (2015), Progress in heterocyclic chemistry, *Elsevier: Amsterdam*, 19, 314-352 (ISBN: 9780081000243)
6. Heller B., Hapke M., (2007), The fascinating construction of pyridine ring systems by transition metalcatalysed [2 + 2 + 2] cycloaddition reactions, *Chem. Soc. Rev.*,36, 1085-1094 (DOI: 10.1039/b607877j)
7. Allais C., Grassot J. M., Rodriguez J., Constantieux T. (2014), Metal-free multicomponent syntheses of pyridines, *Chem. Rev.*, 114, 10829-10868 (DOI: 10.1021/cr500099b)
8. Baumann M., Baxendale I. R. (2013), An overview of the synthetic routes to the best selling drugs containing 6-membered heterocycles, *Beilstein J.Org. Chem.*, 9, 2265-2319 (DOI:10.3762/bjoc.9.265)
9. Longstreet A. R., Opalka S. M., Campbell B. S., Gupton B. F., McQuade D. T. (2013), Investigating the continuous synthesis of a nicotinonitrile precursor to nevirapine, *Beilstein J. Org. Chem.*, , 9, 2570-2578 (DOI: 10.3762/bjoc.9.292)
10. Michael J. P., (2005), Quinoline, quinazoline and acridone alkaloids, *Nat. Prod. Rep*., *22*, 627-646 (DOI:10.1039/B413750G)
11. Sinthupoom N., Prachayasittikul V., Prachayasittikul S., Ruchirawat S., Prachayasittikul V. (2015), Nicotinic acid and derivatives as multifunctional pharmacophores for medical applications, *Eur. Food Res. Technol.*, 240, 1-17 (DOI: 10.1007/s00217-014-2354-1)

12. Trist I. M. L., Nannetti G., Tintori C., Fallacara A. L., Deodato D., Mercorelli B., Palu G., Wijtmans M.l., Gospodova T., Edink E., de Esch M., Verheij I., Viteva L., Loregian A., Botta M. (2016), 4,6-diphenylpyridines as promising novel anti-influenza agents targeting the PA-PB1 protein-protein interaction: structure-activity relationships exploration with the aid of molecular modeling, *J. Med. Chem.*, 59, 2688-2703
13. Guan A.-Y., Liu C.-L., Sun X.-F., Xie Y., Wang M.-A. (2016), Discovery of pyridine-based agrochemicals by using intermediate derivatization methods, *Bioorg. Med. Chem.*, 24, 342-353 (DOI: 10.1016/j.bmc.2015.09.031)
14. Sasabe H., Kido J. (2011), Multifunctional materials in high-performance OLEDs: challenges for solid-state lighting, *Chem. Mater.*, 23, 621-630 (DOI: 10.1021/cm1024052)
15. Tomasik P., Ratajewicz Z., Newkome G. R., Strekowski L. (1985), σ-pyridine coordination compounds with transition metals, in chemistry of heterocyclic compounds: pyridine metal complexes, *John Wiley & Sons, Inc.*, 6, 14, 186-2067
16. Suhr K. J., Bastatas L. D., Shen Y., Mitchell L. A., Frazier G. A., Taylor D. W., Slinker J. D., Holliday B. J. (2016), Phenyl substitution of cationic bis-cyclometalated iridium(III) complexes for iTMC-LEECs, *Dalton Trans.*, 45, 17807-17823 (DOI: 10.1039/C6DT03415B)
17. Jiang H., Yang J., Tang X., Li J., Wu W. (2015), Cu-catalyzed three-component cascade annulation reaction: an entry to functionalized pyridines, *J. Org. Chem.*, 80, 8763-877 (DOI: 10.1021/acs.joc.5b01621)
18. Hantzsch A. (1881), Condensationsprodukte aus aldehydammoniak und ketonartigen verbindungen, *Ber. Dtsch. Chem. Ges.*,14, 1637-1638 (DOI: 10.1002/cber.18810140214)
19. Nakamura I., Oyama Y., Zhang D., Terada M. (2017), Efficient synthesis of multisubstituted 2-alkenylpyridines via 2,3-rearrangement of

O-homoallenylic oximes, *Org. Chem. Front.*, (DOI: 10.1039/C6QO00703A)

20. Zhang Q.-R., Huang J.-R., Zhang W., Dong L. (2014), Highly functionalized pyridines synthesis from *N*-sulfonyl ketimines and alkynes using the N-S bond as an internal oxidant, *Org. Lett.*, 16, 1684-1687 (DOI: 10.1021/ol500345n)
21. Goswami A., Ohtaki K., Kase K., Ito T., Okamoto S. (2008), Synthesis of substituted 2,2′-bipyridines and 2,2′:6′,2″-terpyridines by cobalt-catalyzed cycloaddition reactions of nitriles and α,ω-diynes with exclusive regioselectivity, *Adv. Synth. Catal.* 2008, 350, 143-152 (DOI: 10.1002/adsc.200700380)
22. Mai D. N., Baxter R. D. (2016), Unprotected amino acids as stable radical precursors for heterocycle C-H functionalization, *Org. Lett.*, 18, 3738-3741 (DOI: 10.1021/acs.orglett.6b01754)
23. Chelucci, G., Faloni, M., Giacomelli, G. (1990), Synthesis of 1-substituted 2-[(2*S*)-2-pyrrolidinyl]pyridine from L-proline, *Synthesis*, 12, 1121-1122 (DOI: 10.1055/s-1990-27109)
24. Katritzky A. R., Abdel-Fattah A. A. A., Tymoshenko D. O., Essawy S. A. (1999), A novel and efficient 2,4,6-trisubstituted pyridine ring synthesis via α-benzotriazolyl ketones, *Synthesis*, 1999, 12, 2114-2118 (DOI: 10.1055/s-1999-3637)
25. Chen C, Munoz B. (1998), Solid phase synthesis of 2,4-disubstituted pyridine and tetrahydropyridine derivatives: Resin activation/capture approach/REACAP technology, *Tetrahedron Letters*, 39, 3401-3404 (DOI: 10.1016/S0040-4039(98)00533-4)
26. Liu J., Wang C., Wu L., Liang F., Huang G., (2010), Simple selective synthesis of 2,4- and 2,6-diarylpyridines through metal-free cyclocondensation of aromatic ketones with ammonium acetate, *Synthesis*, 24, 4228-4234 (DOI: 10.1055/s-0030-1258274)

27. Singha R., Dhara S., Ray J. K. (2013), A modular approach toward the synthesis of 2,4-disubstituted pyridines, *Tetrahedron Lett.*, 54, 4841-4843 (DOI: 10.1016/j.tetlet.2013.06.092)
28. Wei Y., Yoshikai N. (2013), Modular pyridine synthesis from oximes and enals through synergistic copper/iminium catalysis, *J. Am. Chem. Soc.*, 135, 3756-3759 (DOI: 10.1021/ja312346s)
29. Hilf J. A., Holzwarth M. S., Rychnovsky S. D. (2016), Route to highly substituted pyridines, *J. Org. Chem.*, 81, 10376-10382 (DOI: 10.1021/acs.joc.6b01370)
30. Bai Y., Tang L., Huang H., Deng G.-J. (2015), Synthesis of 2,4-diarylsubstituted-pyridines through a Ru-catalyzed four component reaction, *Org. Biomol. Chem.*, 13, 4404-4407 (DOI: 10.1039/C5OB00162E)
31. Zhao M.-N., Ren Z.-H., Yu L., Wang Y.-Y., Guan Z.-H. (2016), Iron-catalyzed cyclization of ketoxime carboxylates and tertiary anilines for the synthesis of pyridines, *Org. Lett.*, 18, 1194-1197. (DOI: 10.1021/acs.orglett.6b00326)
32. Juris A., Campagna S., Bidd I., Lehn J. M., Ziessel R. (1988), Synthesis and photophysical and electrochemical properties of new halotricarbonyl(polypyridine)rhenium(I) complexes, *Inorg. Chem.*, 27, 4007-4011 (DOI: 10.1021/ic00295a022)
33. Lepeltier M., Lee T. K-M., Lo K. K.-W., Toupet L., Bozec H. L., Guerchais V. (2007), Synthesis and photophysical properties of bis-cyclometallated Iridium(III)-styryl complexes and their saturated analogues, *Eur. J. Inorg. Chem.*, 2734-2747 (DOI: 10.1002/ejic.200700042)
34. Majee D., Srivastava A., Mobin S. M., Samanta S. (2013), L-proline catalyzed highly efficient synthesis of *Z*-5-alkylidene cyclic sulfamidate imines: an easy access to 5-alkyl-substituted cyclic sulfamidate imines, *RSC Adv.*, *3*, 11502-11506 (DOI:10.1039/C3RA40299A)

35. Majee D., Biswas S., Mobin S. M., Samanta S. (2014), An expedient one-pot sequential three-component reaction for the stereoselective synthesis of functionalized spiro-sulfamidate imine fused δ-lactone scaffold, *Tetrahedron Lett.*, *55*, 4553-4558 (DOI: 10.1016/j.tetlet.2014.06.088)
36. Majee D., Biswas S., Mobin S. M., Samanta S. (2016), Access to 4,6-diarylpicolinates via a domino reaction of cyclic sulfamidate imines with Morita-Baylis-Hillman acetates of nitroolefins/nitrodienes, *J. Org. Chem.*, 81, 4378-4385 (DOI: 10.1021/acs.joc.6b00472)
37. Li J., Chen J., Gui C., Zhang L., Qin Y., Xu Q., Zhang J., Liu H., Shena X., Jianga H. (2006), Discovering novel chemical inhibitors of human cyclophilin A: Virtual screening, synthesis, and bioassay, *Bioorg. Med. Chem.*, 14, 2209–2224 (DOI: 10.1016/j.bmc.2005.11.006)
38. Wang Y.-Q., Yu C.-B., Wang D.-W., Wang X.-B., Zhou Y.-G. (2008), Enantioselective synthesis of cyclic sulfamidates *via* Pd-catalyzed hydrogenation, *Org. Lett*., 2008, 10, 2071-2074 (DOI: 10.1021/ol800591u)
39. Reddy R. J., Chen K. (2011), Highly efficient organocatalytic kinetic resolution of activated nitroallylic acetates with aldehydes via conjugate addition-elimination, *Org. Lett.*, 2011, 13, 1458-1461 (DOI: 10.1021/ol200133y)
40. Lepeltier M., Lee T. K-M., Lo K. K.-W., Toupet L., Bozec H. L., Guerchais V. (2007), Synthesis and photophysical properties of bis-cyclometallated Iridium(III)-styryl complexes and their saturated analogues, *Eur. J. Inorg. Chem*., 2007, 2734-2747 (DOI: 10.1002/ejic.200700042)
41. Huang H., Cai J., Tang L., Wang Z., Li F., Deng G.-J. (2016), Metal-free assembly of polysubstituted pyridines from oximes and acroleins, *J. Org. Chem*., 2016, 81, 1499-1505 (DOI: 10.1021/acs.joc.5b02624)
42. Jansen K., Heirbaut L., Verkerk R., Cheng J. D., Joossens J., Cos P., Maes L., Lambeir A.-M., De Meester I., Augustyns K., Van der Veken P. (2014), Extended structure-activity relationship and pharmacokinetic

investigation of (4-quinolinoyl)glycyl-2-cyanopyrrolidine inhibitors of fibroblast activation protein (FAP), *J. Med. Chem.* 57, 3053-3074 (DOI: 10.1021/jm500031w)

Chapter 7

Conclusion and future outlook

The research work as reported in this thesis embodies the development of atom-economical, cost-effective, efficient, metal-free based synthetic protocols for the development of new synthetic procedure for the preparations of 5-alkylidine/alkyl-substituted cyclic sulfamidate imines, spiro-fused-δ-lactone, 2,4-disubstutedpyridines/picolinates/nicotinates by involving 5-membered cyclic sulfamidate imines as valuable raw materials. The current methodologies provide good to excellent yields of the corresponding heterocyclic derivatives with high to excellent yields and tolerate a wide range of synthetically valuable functional groups under optimal reaction conditions. Moreover, the biologically interesting imidazo[1,2-*a*]pyridine (alpidem derivative) has been prepared in high chemical yield through a unique procedure.

It should be noted that all the aforementioned procedures avoid the use of costly metals or their salts, minimize the use of organic solvents, prevent a tedious workup, offer the possible advantage of significantly lower costs, and mitigate the environmental burden of their manufacturing processes. Therefore, we believe that all the described methods in this thesis will offer great importance in synthetic organic as well as medicinal chemistry as powerful tactics for the efficient access to the aforesaid heterocyclic compounds in an environmentally friendly manner.

As a future prospect of the developments as reported in this thesis, many effective methods can be designed for the development of various heterocyclic scaffolds involving cyclic sulfamidate imines as powerful nucleophiles taking several readily available starting materials.